ENERGY-SAVING DATA ABSTRACTION AND REFORMATION SCHEMES FOR WIRELESS SENSOR NETWORKS

By

TONI

A dissertation submitted to the Department of Computer and Communication Technology,
Faculty of Information and Communication Technology,
Universiti Tunku Abdul Rahman,
in partial fulfillment of the requirements for the degree of
Master of Computer Science
February 2017

ABSTRACT

ENERGY-SAVING DATA ABSTRACTION AND REFORMATION SCHEMES FOR WIRELESS SENSOR NETWORKS

Toni

Wireless Sensor Network (WSN) is comprising of sensor nodes that are able to collect sensor readings and co-operatively send the readings to a base station through multi-hop communication. In general, sensor nodes have limited energy resource due to they are built small in size with inexpensive components. Therefore, efficiency in collecting the data is one of the key factors that determines the lifetime of WSN. If sensor nodes have the capability to select only significant values to transmit, the number of transmissions and the amount of energy consumption in the radio can be greatly reduced in overall. This mechanism is referred as data abstraction. On the other hand, a corresponding reformation scheme is required at a base station so that the complete set of data can be reconstructed accurately with the partially received data. This work introduces the zeroth-, first-, and second-order data abstraction and reformation (DAR) schemes and their applications in WSN. Through performance studies in applications with low and high changing rate, the data transmission can be significantly reduced with a proper selection of DAR schemes, and yet the data can be reformed at the base station with acceptable accuracy.

ACKNOWLEDGEMENTS

I would first like to thank my supervisor Dr Liew Soung Yue and Dr Goh Hock Guan of the Faculty of Information and Communication Technology at Universiti Tunku Abdul Rahman. The doors to their office were always open whenever I ran into a trouble spot or had a question about my research or writing. They consistently allowed this paper to be my own work, but steered me in the right direction whenever they thought I needed it.

Finally, I must express my very profound gratitude to my church mates at Hope Kampar, to my friends at Westlake International School, to my parents and to my partner for providing me unfailing support and continuous encouragement throughout my years of study and through the process of researching and writing this dissertation. This accomplishment would not have been possible without them. Thank you.

Author

Toni

APPROVAL SHEET

This dissertation entitled "**<u>ENERGY-SAVING DATA ABSTRACTION AND REFORMATION SCHEMES FOR WIRELESS SENSOR NETWORKS</u>**" was prepared by TONI and submitted as partial fulfillment of the requirements for the degree of Master of Computer Science at Universiti Tunku Abdul Rahman.

Approved by:

____
(Dr. Liew Soung Yue) Date
Supervisor
Department of Computer and Communication Technology
Faculty of Information and Communication Technology
Universiti Tunku Abdul Rahman

____
(Dr. Goh Hock Guan) Date
Co-supervisor
Department of Computer and Communication Technology
Faculty of Information and Communication Technology
Universiti Tunku Abdul Rahman

FACULTY OF INFORMATION AND COMMUNICATION TECHNOLOGY

UNIVERSITI TUNKU ABDUL RAHMAN

Date: ____________________

SUBMISSION OF DISSERTATION

It is hereby certified that **Toni** (ID No: **11ACM06191**) has completed this dissertation entitled "ENERGY-SAVING DATA ABSTRACTION AND REFORMATION SCHEMES FOR WIRELESS SENSOR NETWORKS" under the supervision of Dr. Liew Soung Yue (Supervisor) from the Department of Computer and Communication Technology, Faculty of Information and Communication Technology, and Dr. Goh Hock Guan (Co-Supervisor) from the Department of Computer and Communication Technology, Faculty of Information and Communication Technology.

I understand that the University will upload softcopy of my dissertation in pdf format into UTAR Institutional Repository, which may be made accessible to UTAR community and public.

Yours truly,

____

(Toni)

DECLARATION

I Toni hereby declare that the dissertation is based on my original work except for quotation and citations which have been duly acknowledged. I also declare that it has not been previously or concurrently submitted for any other degree at UTAR or other institutions.

____

(TONI)

Date ____________________

TABLE OF CONTENTS

LIST OF TABLES

LIST OF FIGURES

LIST OF ABBREVIATIONS

0A0R	Zeroth-order data abstraction & zeroth-order data reformation
0A1R	Zeroth-order data abstraction & first-order data reformation
0A2R	Zeroth-order data abstraction & second-order data reformation
1A0R	First-order data abstraction & zeroth-order data reformation
1A1R	First-order data abstraction & first-order data reformation
1A2R	First-order data abstraction & second-order data reformation
2A0R	Second-order data abstraction & zeroth-order data reformation
2A1R	Second -order data abstraction & first-order data reformation
2A2R	Second -order data abstraction & second-order data reformation
ADC	Analog-to-digital converters
AODV	Ad-hoc on-demand distance vector
ARR	Abstract reporting and reformation
CMOS	Complementary metal-oxide-semiconductor
CO_2	Carbon dioxide
CS	Compressed sensing
DAR	Data abstraction and reformation
DARPA	Defense advanced research project agency
DO	Dissolved oxygen
emSWAB	Embedded sliding window and bottom-up
GAF	Geographic adaptive fidelity
GPS	Global positioning system
GSM	Global system for mobile communications
HT	Hard threshold
IEEE	Institute of electrical and electronics engineers

INS	Inertial navigation system
IR	Infrared
ISM	Industrial, scientific and medical
MAPE	Mean absolute percentage error
MEWIN	Multi-environmental wireless node
MPU	Microprocessor unit
NoDT	Number of data transmitted
NoPT	Number of packet transmissions
OS	Operating system
PA	Precision agriculture
PAR	Photosynthetic active radiation
PC	Personal computer
pH	Potential hydrogen
PIR	Passive infrared sensor
RMSE	Root mean square error
SAR	Sequential assignment routing
SBC	Single board computer
SoC	System-on chip
SPIN	Sensor protocol for information via negotiation
ST	Soft threshold
TEEN	Threshold sensitive energy efficient sensor network
WEAMR	Weighted energy aware multipath reliable
WSN	Wireless sensor network

CHAPTER 1

INTRODUCTION

This chapter gives an overview of the research starting with the motivation and the problem statements. Objectives and main contributions are defined to solve the problems highlighted. The organisation of the Dissertation is outlined. Finally, a list of publications is attached.

1.1. Motivation

Wireless sensor network (WSN) is a network that consists of nodes with sensors able to sense the environmental attributes and transceivers able to communicate with each other through radio in certain frequency range (Damaso et al., 2013). In WSN, there is always at least one sink node or base station. Base station is a special node for which the collected data is destined. That is, the sensed data of a node can be relayed in a multi-hop manner through other sensor nodes to the base station, as shown in Figure 1.1. Due to high cost of production and market demand, the industrial, scientific and medical (ISM) frequency bands are used by the transceivers to perform data transmission.

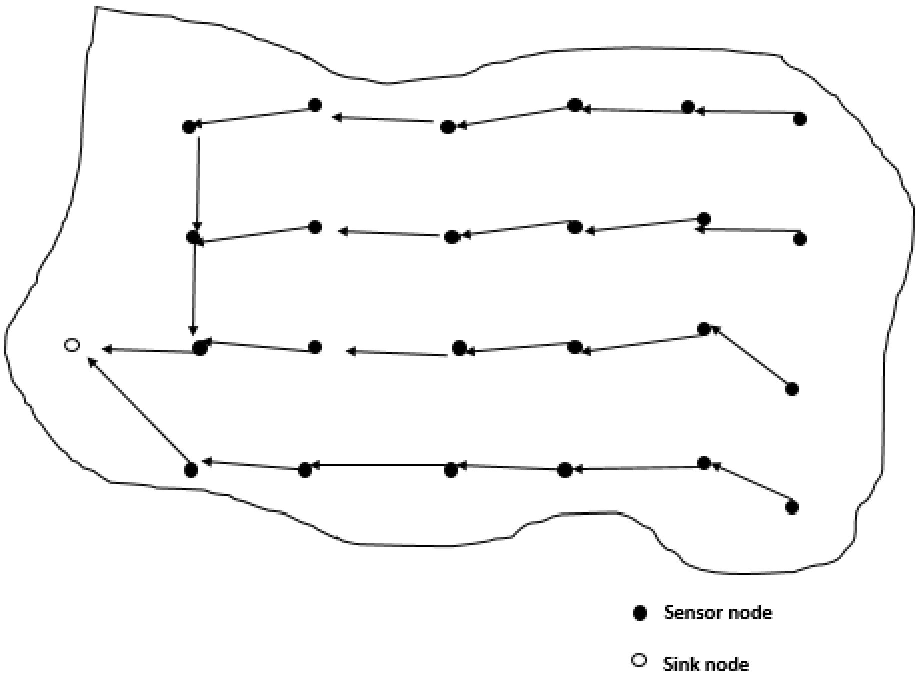

Figure 1.1: WSN architecture

A wireless sensor node consists of four basic elements as shown in Figure 1.2. They are power supply, sensors, processing unit, and transceiver for communication. The power supply is an element that provides energy for the entire sensor node for its operations. The sensors, or collectively called the sensing unit, are used to sense the environment attributes and convert the analogue signals into digital data for collection. The processing unit is an element that consists of microprocessor and memory, which are used to process the sensed data. The transceiver consists of transmitter and receiver, which are used for communications.

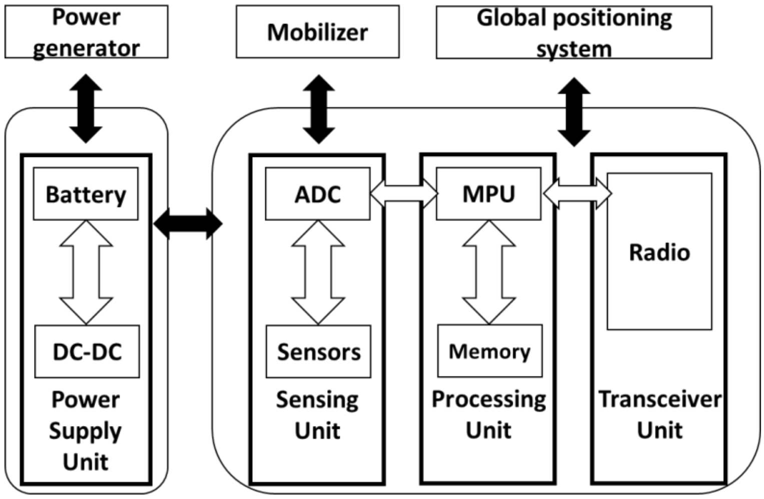

Figure 1.2: Wireless sensor node architecture

The advantages of using WSN are the small size of nodes, low energy consumption, and expandability. However, the sensor node usually employs batteries as the power source. This will cause the limitation in the lifetime of the sensor node as all its operations requires the power from the power unit. In addition to the capacity of the power source, lifetime of a sensor node on the other hand depends also on the application's duty and reporting strategy. For instance, if data are reported too frequently then the power consumption would be very high, but on the contrary too infrequent data reporting may make the collected data inaccurate. Therefore, the best practices need to be approached to reduce the power consumption yet preserving the data accuracy. Evaluation of power consumption should be done before the real deployment. Through the evaluation, factors that determine the lifetime of sensor node could be identified. Compared among the operations, communication consumes the highest energy consumption (Lajara et al., 2010). Thus, the efficient way to reduce the power consumption is by minimizing the communication. Several approaches have been studied and implemented to extend the lifetime of WSN. Some of them are through routing protocol, external power source, data aggregation, data abstraction, etc.

A routing protocol in WSN can be defined as the way how sensor nodes forward packets through some routing paths to the destination, or sink. As mentioned earlier that communication of sensor nodes consumes the most power consumption, studies have been done to have efficient and effective routing protocol in WSN. One of the routing protocols that have been proposed is Ad-hoc On-demand Distance Vector (AODV) (Booranawong et al., 2013). AODV is a routing protocol that establishes shortest route for data transmission. In order to avoid the high traffic load, AODV utilizes a pre-defined threshold of delay time to choose the possible routes. If the delay time of a route exceeds the pre-defined threshold of delayed time, the route will be considered as congested. The predefined threshold of delay time is the average delay of routing data transmission in the IEEE 802.15.4 wireless network. Through the proposed routing protocol, the data transmission can be delivered through the shortest path and lowest traffic load. Therefore, AODV will solve the failure of path-setup and data loss due to the network congestion.

Another instance of routing protocol is Weighted Energy Aware Multipath Reliable (WEAMR) (Tufail et al., 2013). WEAMR is the extension of AODV that utilizes multipath routing protocol. When a sensor node wants to send a data packet, the sensor node needs to check the existence of valid path in the routing table. If there is no valid path, the sensor node will discover two best low cost paths by using AODV approach. If there are valid paths, the sensor node will select the best path from the two paths discovered in the route discovery process. Upon receiving the data packet, the receiving sensor node will decrement the local energy value. Then, the receiving sensor node will forward the data packet to the next sensor nodes or base station. Through multipath communication, load-balancing mechanism is applied in order to extend the lifetime of WSN.

A self-optimizing scheme for energy balanced routing in wireless sensor networks using SensorAnt is another instance of routing protocol method (Saleh et al., 2012). In the initialization process of this method, a source node will check the Routing Table and Generated Ant-Forward. If the Routing Table has the Destination Address, the source node will transmit Ants by unicast. If Routing Table does not have the Destination Address, the source node will transmit Ants by broadcast. After the check of routing process in the sensor node, the sensor node will transmit the Ant-Forward to the intermediate node. Upon receiving the Ant-Forward, intermediate node will add local information to the Ant and calculate the probability of choose next hop based on routing table of hop and path assessment functions. Upon receiving the Ant-Forward, the sink node will generate Ant-Backward as an acknowledgement by using unicast. Then, the sink node will discard the Ant-Forward. After the intermediate node receive the Ant-Backward, the intermediate node will update the routing table based on the hop and path assessment functions in routing table. Afterward, the intermediate node will transmit the Ant-Backward to the source node. Upon receiving the Ant-Backward, the source node will update the routing table based on hop and path assessment functions as well. Then, the source node will remove the Ant-Backward. After the initialization process is finished, the source node will start transmit data via the selected route to the sink node.

Although the routing protocol approaches have been proposed, the communication activity still can be further reduced with a complementary approach, such as data abstraction scheme, to minimize the energy consumption, and thus extend the lifetime of WSN.

Besides routing protocol, external power sources have been studied, such as solar powered, wind powered, hydroelectricity, etc. Generally, external power sources need additional equipment based on the power source. The instance of wind-powered application is a tree movement energy-harvesting device (McGarry and Knight, 2012). Naturally, branch of a tree is shaken if there wind blows. The author uses this mechanism to generate the electricity.

Another approach of external power source is solar powered which is using the concept of photovoltaic that convert the solar radiation to electricity. The instance of solar powered application is wEcoValve mote (Lajara et al., 2011). wEcoValve is an irrigation system that is solar energy powered. A rechargeable battery will be used as a power source and it will be continuously charged by using solar panel. When the sunshine is available, the converted electricity will be used to power up the sensor node and to charge the rechargeable battery. However, if the sunshine is not available, the sensor node will use the energy from the rechargeable battery.

Hydroelectric power source is another instance of external power source in WSN. By using the continuous flowing water, hydro turbine can be used to generate an electricity (Azevedo and Santos, 2012). In the real experiment, hydroelectric power source only can be implemented in the indoor application. At outdoor application, hydroelectric power source mostly will be implemented where sunshine is rarely available and there is a continuous flowing water, for example waterfall.

However, the external power sources have an essential requirement where the resources such as wind, solar radiation, and water must be available continuously to do the battery charging. Besides, external power sources require additional equipment that resulted in additional space is needed as well. The typical external power source schematic is shown in Figure 1.3.

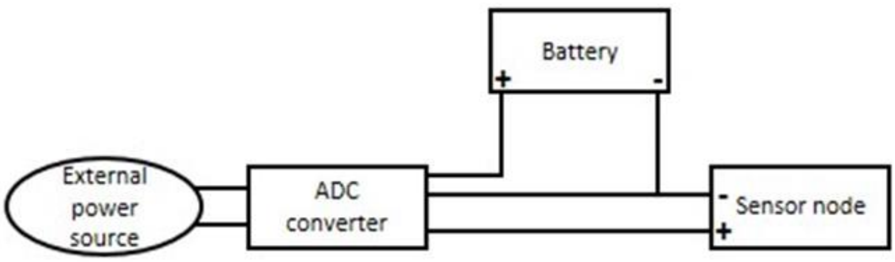

Figure 1.3: Typical schematic of external power source

Since there are limitations by using routing protocols to save energy or by employing renewable energy sources to generate extra energy, there is a need for a more efficient way to reduce the communication requirement among the sensor nodes to save energy. One of the simple ways of reducing the number of transmissions is by selecting only a subset of sensed data to report to the base station rather than sending all of them. However, if not carefully designed, such a simple approach will suffer from the accuracy of the data collected in the base station, as not all the sensed data will be reported. Through the proposed Data Abstraction and Reformation (DAR) schemes, only significant data will be reported to the base station and the non-reported data will be reformed without compromising the quality of the information. Data abstraction is a data filtration scheme whereby each sensed data is evaluated based on certain criteria to determine whether the data should be reported to a base station. Data reformation is data interpolation that reconstructs the non-received data based on the received data.

1.2. Objectives

The energy source of WSN is mostly consumed by the data communication or transmission. A WSN with an application that has a lot of data transmission will have a shorter lifetime. Several questions arise related to this issue:

1. What can be done to reduce the number of transmissions thus the energy can be conserved?

2. What is the solution to keep the accuracy of the information if not all of the sensed values are reported because of the reduced transmission?
3. What is the performance of the proposed solution?

In order to provide solutions to the risen questions, the objectives of the study are:

1. To propose Data Abstraction scheme at sensor nodes that can efficiently filter significant data for transmission in order to minimize communications in the network.
2. To propose Data Reformation scheme at the base station that can effectively reconstruct the full set of data without compromising the quality of information.
3. To evaluate the performance of different combinations of DAR.

1.3. Main Contributions

The main contributions of the research are:

1. Proposed a data abstraction as part of DAR schemes that able to minimize the energy usage by reducing the number of transmission. Data transmission is part of communication operations that consume most of the energy. Thus, by reducing the number of transmission, energy can be conserved and sensor nodes able to operate for longer period.
2. Proposed a data reformation as part of DAR schemes that able to reconstruct the non-reported values at the base station. Data

reformation is important, thus the data information accuracy will not be greatly affected by the data abstraction.

3. Design several orders of DAR schemes in several conditions. DAR schemes have been applied in application/attribute with different sampling rate. They are application/attribute with low sampling rate which represented by temperature monitoring and application/attribute with abrupt sampling rate which represented by accelerometer monitoring.
4. Validate the performance of DAR schemes. The Dissertation verifies the performance of the DAR schemes in terms of number of data transmitted, number of packet transmissions, and Root Mean Square Error (RMSE).

1.4. Organisation of the Dissertation

The Dissertation is organised as follows. A review of the literature on the ways to conserve energy by routing protocol and external power sources are presented in Chapter 1. In Chapter 2, literature reviews about wireless sensor network (WSN) are presented. In Chapter 3, the DAR schemes are presented. In Chapter 4, experiment design and settings are explained and in Chapter 5, the results of DAR schemes are presented. Finally, the Dissertation draws conclusions on the research and presents suggestions for future improvement and research in Chapter 6.

CHAPTER 2

LITERATURE REVIEW

This chapter gives an overview of the research starting with the overview of wireless sensor network (WSN). Data collection method in WSN also will be briefly discussed.

2.1 Wireless Sensor Network

Wireless Sensor Network (WSN) is an Ad-hoc networks that sensors are able to sense, process, store and communicate the sensed data (Lotf et al., 2011). According to Potdar et al. (2009), the characteristic requirements of a system to be called as wireless sensor nodes are:

1. Fault tolerant: the system should be robust to node failure and able to indicate that the node is not functioning properly.
2. Scalable: the system should be able to support a large number of sensor nodes.
3. Long life: the system should be able to have long life, as the replacement of batteries in sensor node is difficult. Therefore, the node's operations should be energy efficient.
4. Programmable: the sensor nodes should be able to be reprogrammed to achieve specific purpose of an application.
5. Secure: the sensor nodes should support the access control, message integrity, confidentiality and replay protection.
6. Affordable: the system should use low cost devices as the network comprised of large number of sensor nodes.

2.1.1 Applications of Wireless Sensor Network

The history of sensor networks started during the cold war era (mid-1950s decade), where United States used the system to track Soviet Union submarines. And later, the US ministry of Defense, Defense Advanced Research Project Agency (DARPA) continued to use the innovation of sensor network as research topics in universities. Nowadays, the usage of WSN is not only located in military applications, but also in many applications in human daily life.

The classifications of wireless sensor network's applications in this dissertation are focused on three applications. The applications are monitoring, healthcare, and military applications.

1. Monitoring applications

   There are a lot of monitoring applications that use wireless sensor network as the platform, such as:

   1) Water monitoring applications

      Xue et al. (2010) propose a two-layer sensor network based on real-time underground water analysis in Nebraska. The first-layer provides the reliable communication for monitoring sites. The second-layer provides the groundwater measurement systems. The wireless sensor nodes were based on Crossbow IRIS mote and MIB510 gateway.

Nasirudin et al. (2011) propose fresh water real-time monitoring system based on wireless sensor network and global system for mobile communications (GSM). The system will determine the freshness of water by monitoring the water temperature, pH, turbidity and dissolved oxygen. The wireless sensor nodes were based on Microchip PIC16F886 and Xbee transceiver.

Hormann et al. (2010) proposed a river monitoring application using energy harvesting. This application used MSP430F1611 microcontroller and 820.15.4 transceiver. This application is used to measure the water level of a river by using pressure transducer, ultrasonic measurement and global positioning system (GPS) coordinates.

Xiao-peng, H. and Xiao-liang, H. (2011) proposed a river flow velocity monitoring system. This application is used to investigate the bail swing angle. The wireless sensor nodes were based on MSP430F1612 microcontroller, CC2420 IEEE (Institute of electrical and electronics engineers) 802.15.4 transmitter and the MMA72609 accelerator.

Jin et al. (2010) proposed a water monitoring application that measures temperature, dissolved oxygen, pH (potential hydrogen) and salinity. The sensor nodes were based on

Toroidal Conductivity Datastick (RS-485), Texas Instruments CC2430 System-on Chip (SoC), MAX3485 converter and RS-232.

O'Connor et al. (2011) proposed a river and coaster marine monitoring application equipped with visual sensors, i.e. cameras and satellite imaging systems to improve the detection and tracking capabilities of the application. The sensor nodes were based on Programmable SoC, WQ101 Submersible Temperature Meter, WQ201 Water pH Meter, WQ301 Water Conductivity Meter, WQ401 Dissolved Oxygen Sensor, WQ701 Water Turbidity Meter, WL400 Water Level Meter, and AXI PTZ camera.

Lee et al. (2010) proposed a multifunctional wireless sensor for debris flow monitoring. This application is used to estimate the speed and tendency of the river stream. The sensor nodes were based on MSP430, a ZigBee transceiver (CC2420), ADXC330 and ADCS78.

Perez et al. (2011) proposed a marine monitoring application that measures current velocity, depth, salinity, temperature, turbidity, DO (dissolved oxygen), chlorophyll and nitrates probes. The sensor nodes were based on Multi-Environmental Wireless Node Main board (MEWIN).

Herlien et al. (2010) proposed an ocean observatory sensor network application that studying the effect of pH changes when CO_2 (carbon dioxide) is injected in seawater. It measures pH, salinity, temperature, and velocity.

2) Water monitoring applications

Sanchez-Azofeifa et al. (2011) proposed two different sensor network based on tropical forest monitoring. The first deployment of the application monitors the leaf temperature of a tree and the second deployment monitors the fraction of Photosynthetic Active Radiation (PAR) absorbed by a plant canopy. The sensor nodes were based on Olsonet communications motes, Apoge PAR SQ-110 and SP-110 solar radiation sensors.

3) Agriculture monitoring applications

Chebbi et al. (2011) proposed a sensor network for precision agriculture (PA) in order to limit the water consumption. This application measures the water soil moisture, air temperature/humidity, solar radiation, precipitation, wind speed and direction. The sensor nodes were based on Watermark, SHT75, Davis, ADS, Microchip PIC18F2620 and Xbee transceiver.

Sang and Song (2010) proposed a system for vineyard monitoring. This application measures the temperature, humidity and pH. The sensor nodes were based on CC2430 SoC and Intel PXA270 microprocessor.

Vijayakumar and Rosario (2011) proposed an automatic irrigation system. This application was integrated with MICAz nodes and pH sensors in order to measure the soil humidity and the quantity of fertilizer. The sensor nodes were based on MICAz nodes, MDA300CA, Irrometer, MPX4115A, MIB510 and RS-232.

Wei et al. (2011) proposed monitoring water resources for agriculture applications (irrigation). This application measures the wind speed, atmospheric temperature, air and soil humidity sensors, and solar radiation.

4) Wildlife monitoring applications

Huang et al. (2010) proposed a sensor network system to study wildlife. This application was based on Taroko (Telos node) and GPS. It measures the light, humidity, temperature and acceleration.

Sieber et al. (2011) proposed a Hermit beetle behaviour to indicate the status of a forest. The sensor nodes were based on

EZ-430 Chronos and Sensirion SHT71 to measure the temperature and humidity.

Bagree et al. (2010) proposed a sensor network system to monitor tiger movement. The sensor nodes were based on passive infrared sensor (PIR), CMOS (complementary metal-oxide-semiconductor) sensor, Xbee Pro transceiver and ATMega 128 microcontroller. This application able to detect the route of tigers and took a photograph.

5) Disaster monitoring application

Zhuang et al. (2011) proposed a flood monitoring system based on sensor network. Besides, it also monitors the state of electrical distribution boxes during floods. The sensor nodes were based on water level sensors, 8051-based microprocessor and Xbee transceiver.

6) Urban monitoring application

Renterghem et al. (2010) proposed a sensor network system to monitor noise and black carbon pollution. The sensor nodes were based on ALIC Single Board Computer (SBC) and it measures the acoustic noise, CO_2 levels and black carbon.

2. Healthcare application

The usage of WSN technologies in healthcare application is increased. One example of healthcare applications is ANT. ANT is a sensor network technology system that used to detect heart rate, step count, running/walking speed, activity, position, personal fall and emergency response alert, temperature and weight (Dynastream Innovations, Inc., 2014). It can be integrated with watch, smartphone and computer.

3. Military applications

de Bree and Wind (2011) proposed an acoustic vector sensors to measure the pressure and the particle velocity. The measurements are furthermore to detect and localize transient signals from mortars, artillery and small arms fire.

Naz et al. (2012) proposed a sensor network system for soldier detection. This application utilized unattended acoustic and seismic sensors to detect the specific point of individual enemy soldier.

Dulski et al. (2011) proposed a multisensory system for perimeter protection. This application utilized the day/night camera, IR (infrared) uncooled thermal cameras, millimetre-wave radars to detect radiation reflected from target.

Baine et al. (2011) proposed an inertial navigation system (INS) aided by an acoustic WSN and magnetometer. Magnetometer data able to provide the information of vehicle's direction and improves orientation estimation.

2.1.2 Hardware

According to Chien et al. (2012), a wireless sensor node consists of four main components as shown in Figure 2.1, which are radio transceiver, microcontroller, sensors, and power.

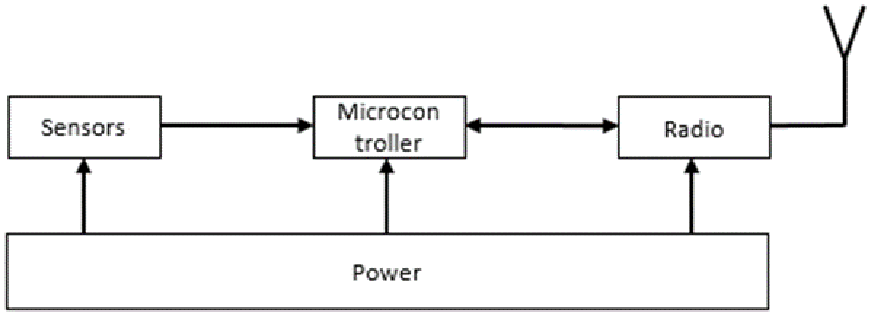

Figure 2.1: Main components of wireless sensor node

1. Radio transceiver

   This component enables a wireless sensor node to communicate within its network. It will be equipped with antenna to have a wider area coverage. Radio transceiver consumes the most power due to its processing in modulation and demodulation.

2. Microcontroller

   This component enables a wireless sensor node to connect external devices such as sensors and radio transceivers. Microcontroller is a microprocessor with built-in memory, timers and hardware. Typically, a microcontroller in wireless sensor node has a smaller capabilities compared with a microcontroller in a general personal computer (PC).

3. Sensors

   This component enables a wireless sensor node to interact with its environment. This component has a variety type based on its purpose, such as temperature sensor, humidity sensor, light sensor, etc.

4. Power source

   This component enables a wireless sensor node to operate its other components. Batteries are the most common power source for wireless sensor node.

Hardware in wireless sensor node can be categorized into two platforms based on their capabilities and usage. The two platforms are as the following.

1. Low-end platform

   Low-end platform is characterized by its limited capabilities in terms of processing, memory, and communication. The low-end platform that commonly used recently is as the following.

   1) MICA platform

MICA platform consists of MICA2, MICA2DOT, MICAz, and IRIS. The nodes are shown in the Figure 2.2.

(a) MICA2 (Crossbow Technology, Inc., n.d.)

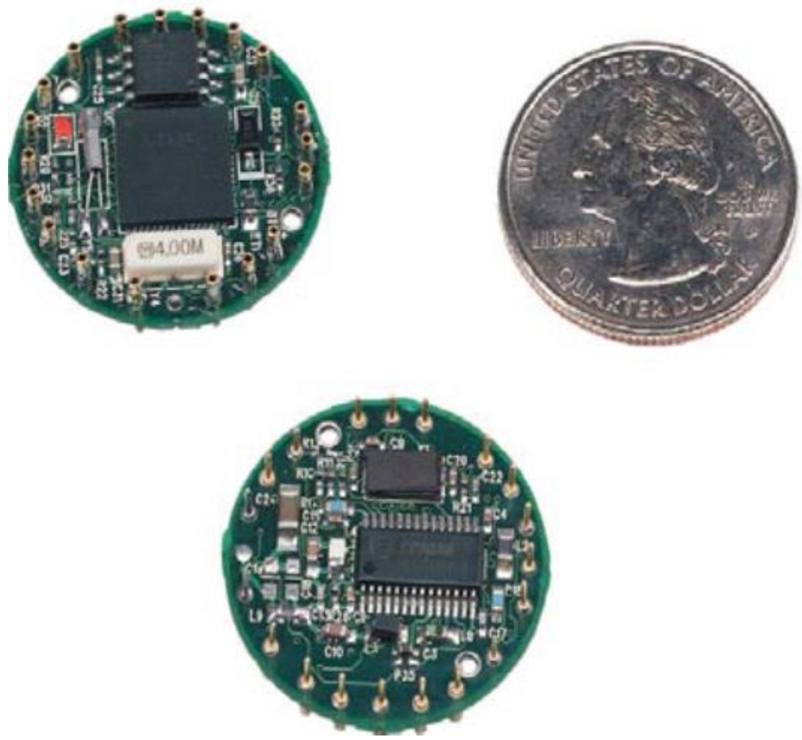

(b) MICA2DOT (Crossbow Technology, Inc., n.d.)

(c) MICAz (Crossbow Technology, Inc., n.d.)

(d) IRIS (MEMSIC Inc., n.d.)

Figure 2.2: MICA platform

The summary characteristics of MICA platform are shown in Table 2.1.

Table 2.1: Summary Characteristics of MICA Platform (Chien et al., 2012)

Platform	Microcontroller/Processor	Radio Transceiver	Centre Frequency	Operating System
MICA2	ATMega 128L, 8bit, 128KB program memory, 4KB SRAM	Chipcon CC1000	315/433/868/916 MHz	TinyOS, SOS, Mantis
MICA2DOT	ATMega 128L, 8bit, 128KB program memory, 4KB SRAM	Chipcon CC1000	315/433/868/916 MHz	TinyOS, SOS, Mantis
MICAz	ATMega 128L, 8bit, 128KB program memory, 4KB SRAM	Chipcon CC2420	2.4 GHz	TinyOS, SOS, Mantis, Nano-PK, RETOS, LiteOS
IRIS	ATMega 1281, 8bit, 128KB program memory, 8KB SRAM	Atmel AT86RF230	2.4 GHz	TinyOS, LiteOS

2) TelosB & Tmote Sky

TelosB & Tmote Sky nodes are shown in Figure 2.3 and 2.4 respectively.

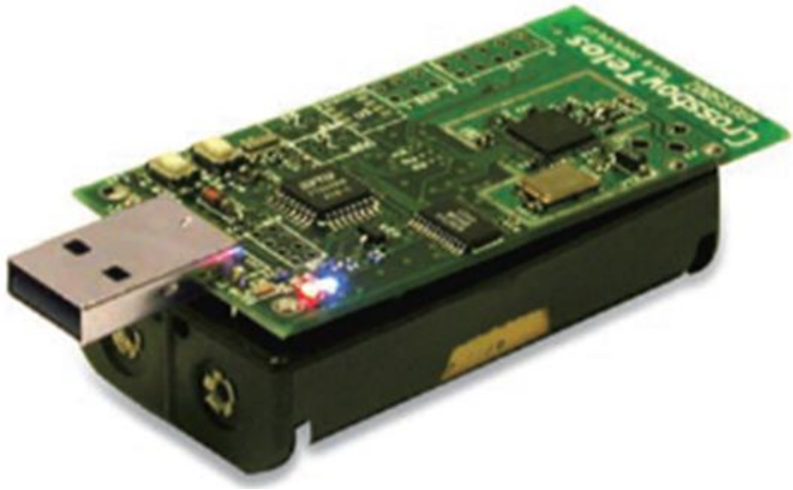

Figure 2.3: TelosB (Crossbow Technology, Inc., n.d.)

Figure 2.4: Tmote Sky (Moteiv Corporation., 2006)

The summary characteristics of TelosB & Tmote Sky are shown in Table 2.2.

Table 2.2: Summary Characteristics of TelosB & Tmote Sky (Chien et al., 2012)

Platform	Microcontroller/Processor	Radio Transceiver	Centre Frequency	Operating System
TelosB	TI MSP430F1611, 16bit, 48KB program memory, 10KB RAM	Chipcpn CC2420	2.4 GHz	Contiki, TinyOS, SOS, RETOS
Tmote Sky	TI MSP430F1611, 16bit, 48KB program memory, 10KB RAM	Chipcpn CC2420	2.4 GHz	Contiki, TinyOS, SOS, RETOS

3) Eyes platform

Eyes platform consists of Eyes, EyesIFX v1, and EyesIFX v2. EyesIFX v2 is shown in Figure 2.5.

Figure 2.5: EyesIFX v2 ((Handziski, 2005)

The summary characteristics of Eyes are shown in Table 2.3.

Table 2.3: Summary Characteristics of Eyes Platforms

(Chien et al., 2012)

Platform	Microcontroller/Processor	Radio Transceiver	Centre Frequency	Operating System
Eyes	MSP430F149, 16bit, 60KB program memory, 2KB SRAM	RFM TR1001	868 MHz	TinyOS, PEEROS
EyesIFX v1	MSP430F149, 16bit, 60KB program memory, 2KB SRAM	Infineon TDA5250	868 MHz	TinyOS
EyesIFX v2	MSP430F1611, 16bit, 48KB program memory, 10KB RAM	Infineon TDA5250	868 MHz	TinyOS

4) V-Link, TEHU-1121, and NI WSN-3202

V-Link, TEHU-1121, and NI WSN-3202 nodes are shown in Figure 2.6, 2.7 and 2.8 respectively.

Figure 2.6: V-Link (LORD Corporation, 2013)

Figure 2.7: TEHU-1121 (Sensicast Systems, Inc, 2006)

Figure 2.8: NI WSN-3202 (National Instruments Corporation, 2010)

The summary characteristics of V-Link, TEHU-1121 and NI WSN-3202 are shown in Table 2.4.

Table 2.4: Summary Characteristics of V-Link, TEHU-1121 and NI WSN-3202 (Chien et al., 2012)

Platform	Microcontroller/Processor	Radio Transceiver	Centre Frequency	Operating System
V-Link	Not specified	IEEE 802.15.4 compliant RF transceiver	2.4 GHz	Not specified
TEHU-1121	Not specified	IEEE 802.15.4 compliant RF transceiver	2.4 GHz	Not specified
NI WSN-3202	Not specified	IEEE 802.15.4 compliant RF transceiver	2.4 GHz	Not specified

2. High-end platform

High-end platform is characterized by its high capabilities in terms of processing, memory, communication, and network management. The high-end platform that commonly used recently is as the following.

1) Stargate platform

Stargate platform consists of Stargate and Stargate NetBridge. The nodes are shown in the Figure 2.9 and 2.10 respectively.

Figure 2.9: Stargate (Crossbow Technology, Inc., n.d.)

Figure 2.10: Stargate NetBridge (Crossbow Technology, Inc., 2007)

The summary characteristics of Stargate platform are shown in Table 2.5.

Table 2.5: Summary Characteristics of Stargate Platform (Chien et al., 2012)

Platform	Processor	Memory	Mote/Board Connectors	Operating System
Stargate	Intel PXA255 Processor, 400 MHz	64MB SDRAM, 32MB Flash	PCMCIA and compact flash connector, 51-pin expansion Connector for MICA2 Motes; Ethernet, RS232 Serial, JTAG, USB Connector via 51-pin Daughter Card Interface	Embedded Linux
Netbridge NB-100	Intel IXP420 Xscale Processor, 266 MHz	32MB RAM, 8MB Flash, 2GB USB Flash Disk	MICA2, MICAz, IRIS, Telos Connector Ethernet, USB connector	Debian Linux

2) Imote platform

Imote platform consists of Imote and Imote2. The nodes are shown in the Figure 2.11.

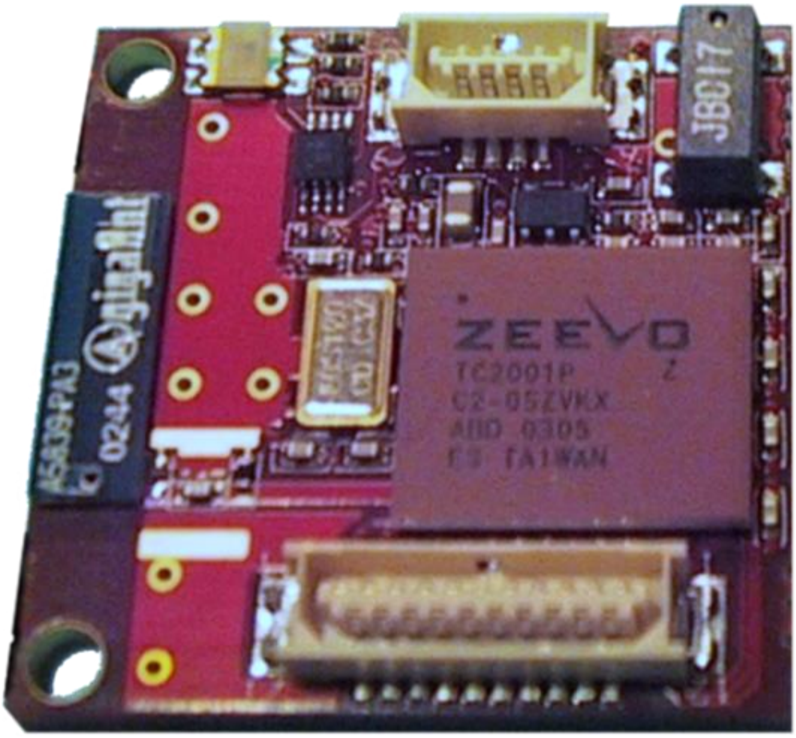

(a) Imote (Nachman, n.d.)

(b) Imote2 (Nachman, n.d.)

Figure 2.11: Imote platform

The summary characteristics of Imote platform are shown in Table 2.6.

Table 2.6: Summary Characteristics of Imote Platform (Chien et al., 2012)

Platform	Processor	Memory	Mote/Board Connectors	Operating System
Imote	ARM7 processor, 12MHz	64KB SRAM, 512KB Flash	I2C, UART, USB, JTAG connector	TinyOS
Imote2	Marvell PXA271 Xscale Processor, 13 - 416MHz	256KB SRAM, 32MB SDRAM, 32MB Flash Memory	Integrated 802.15.4 radio, support for external radio through SDIO, and UART; USB client and host, 2xSPI, 3xUART, Camera, I2C, I2S, GPIO, AC97 connector	TinyOS, Linux, SOS

2.1.3 Software

According to Faaroq and Kunz (2011), the major characteristics of WSN Operating System (OS) are as the following.

1. Architecture

   The architecture of an Operating System influences the size of the OS kernel. Some of the famous OS architectures are monolithic architecture, microkernel architecture, virtual machine architecture and layered OS architecture. OS architecture descriptions are shown in Table 2.7.

Table 2.7: OS Architectures

Architecture	Description	Advantages	Disadvantages
Monolithic	• Does not have any structure • Services provided are applied independently • Every services deliver an interface for other services • Permits bundling of all the essential service together into a lone method image • Smaller OS memory footprint	• The module interaction costs are low	• The system is hard to understand and modify, unreliable, and difficult to maintain
Microkernel	• Providing minimum functionality • Kernel size is significantly condensed • OS functionality is delivered through user-level servers. If a server flops, entire system does not crash	• Delivers improved dependability, ease of addition also customization	• Bad presentation because of common user to kernel borderline overpasses
Virtual machine	• Transfer simulated mechanisms to employer programs, which resemble hardware	• Moveable	• Typically a poor system performance
Layered OS	• Implement services in the form of layers	• Manageable • Easy to understand • Reliable	• Not a flexible architecture from an OS design perspective

2. Programming model

The programming model of an OS influences the application development. Some of the well-known programming model are event-driven programming and multithreaded programming. Programming model descriptions are shown in Table 2.8.

Table 2.8: OS Programming Model

Programming Model	Advantages	Disadvantages
Event driven	• More valuable for figuring devices armed with rare source	• Not measured suitable for old-style application designers.
Multithreaded	• Application expansion model most familiar to programmer	• Its factual logic rather source thorough. • Not deliberate well appropriate for source restriction devices.

3. Scheduling

Scheduling of an OS influences the order in which tasks are executed. There are two types of scheduling, which are real-time and non-real-time. For applications with real-time necessities, real-time scheduling algorithms must be used and for applications with non-real-time necessities, non-real-time scheduling is sufficient.

4. Memory management

Memory management of an OS influences the way used to assign and de-assign memory for dissimilar processes and threads. Two types of memory management are static memory management and dynamic memory management. Memory management models are described in Table 2.9.

Table 2.9: Memory Management Model

Memory Management Model	Advantages	Disadvantages
Static	• Simple • Useful technique to deal with scare memory resources	• Uncompromising systems because run-time memory distribution cannot happen.
Dynamic	• More elastic system because memory can be assigned and de-assigned at run-time	• Complex

5. Communication protocol support

   Communication protocol support of an OS influences the inter-process communication among the system also with other devices in the network. There are two types of communication protocol support in WSN. The types of communication are heterogeneous sensor nodes and network-based communication. For heterogeneous sensor devices, the communication procedure delivered by OS must be heterogeneity where for network-based communication; the OS should deliver transport, network, and MAC layer protocol executions.

6. Resource sharing

   The resource sharing of an OS influences the behaviour when several programs are synchronously performing. Most of the OS nowadays deliver a multithreading, which demanding a resource sharing mechanism.

Some of well-known OS in WSN are described in Table 2.10.

Table 2.10: OS in WSN (Faaroq and Kunz, 2011)

OS	Architecture	Programming model	Scheduling	Memory management and protection	Communication protocol support	Resource sharing	Support for real-time applications
TinyOS	Monolithic	Mainly event driven, support for TOS thread has been added	FIFO	Static Memory Management with memory safety	Active Message	Virtualization and Conclusion Events	No
Contiki	Modular	Proto threads and events	Events are executed as they happen. Intrudes performed based on urgency	Dynamic memory administration and linking. No procedure address space safety.	*u*IP and Rime	Serialized Access	No
MANTIS	Layered	Threads	Five significance programs and additional urgencies in all priority class.	Dynamic memory management supported but use id discouraged, no memory safety	At Kernel Level COMM layer. Networking Layer is at user level. Application is allowed to use custom routing protocols	Through Semaphores	To some degree at procedure arrangement level (Execution of priority scheduling among dissimilar processes types)

Table 2:10 continued

OS	Architecture	Programming model	Scheduling	Memory management and protection	Communication protocol support	Resource sharing	Support for real-time applications
Nano-RK	Monolithic	Threads	Rate Monotonic and rate harmonized arrangement	Static Memory Management and no memory safety	Socket like abstraction for networking	Serialized access through mutexes and semaphores. Deliver an execution of Priority Ceiling Algorithm for priority overturn	Yes
LiteOS	Modular	Threads and events	Priority based on Round Robin Scheduling	Dynamic memory management and it provides memory safety to processes	File based communication	Through harmonization primitives	No

2.2 Data Collection Method

Data collection method in WSN is the routing layer protocols about how the data transmitted to the base station (Wang, 2012). Patil and Biradar (2012) presented taxonomy of routing protocols for WSNs based on various classification criteria such as data centric, hierarchical, location based, negotiation, multipath, quality of service based and mobility based.

The objective of the taxonomy is: (1) to provide a framework WSN in which routing and data dissemination protocols for WSNs can be examined and compared; and (2) to gain new insights into the routing and data dissemination protocols and thereby suggests avenues for future research.

2.2.1 Data Centric Routing

In data centric routing, the properties of data are based on the attribute. One example of data centric routing is directed diffusion. The schematic protocol of directed diffusion is shown at Figure 2.12.

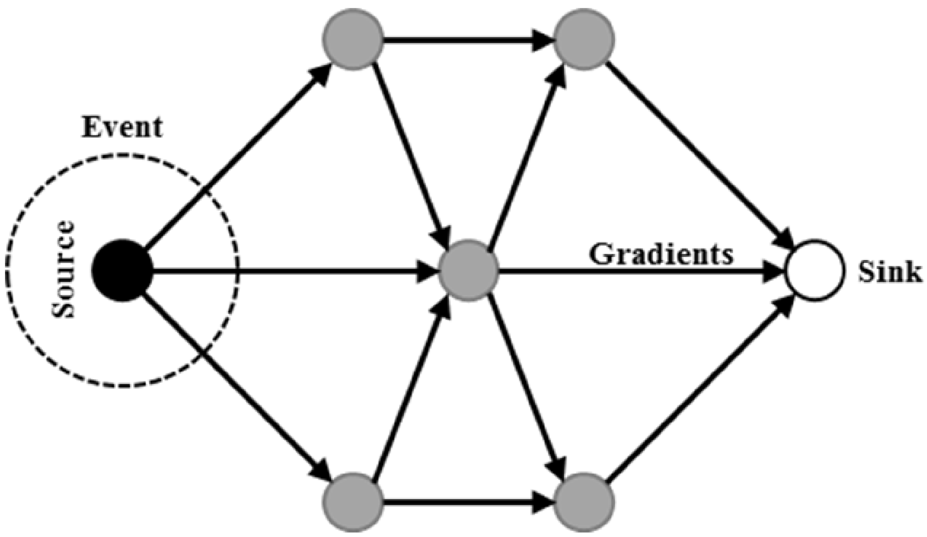

(a) Interest propagation

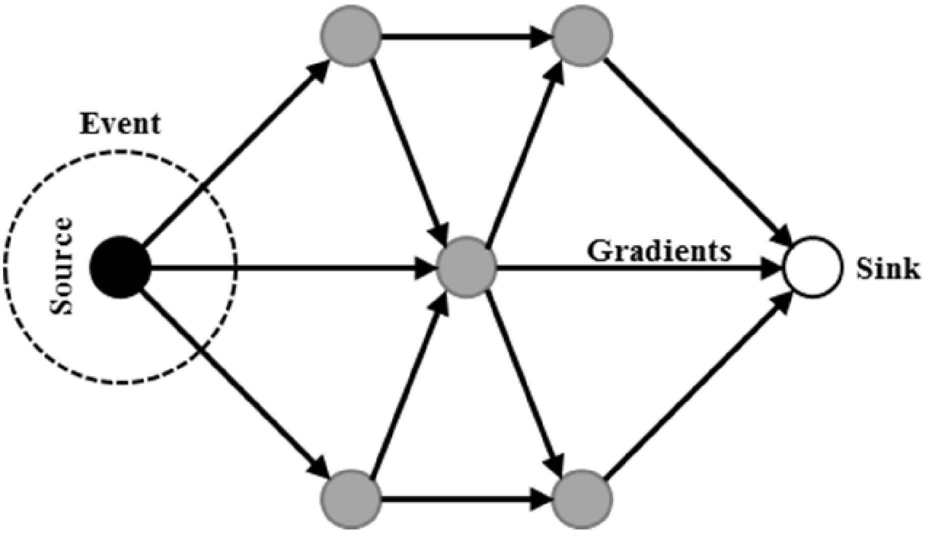

(b) Initial gradients setup

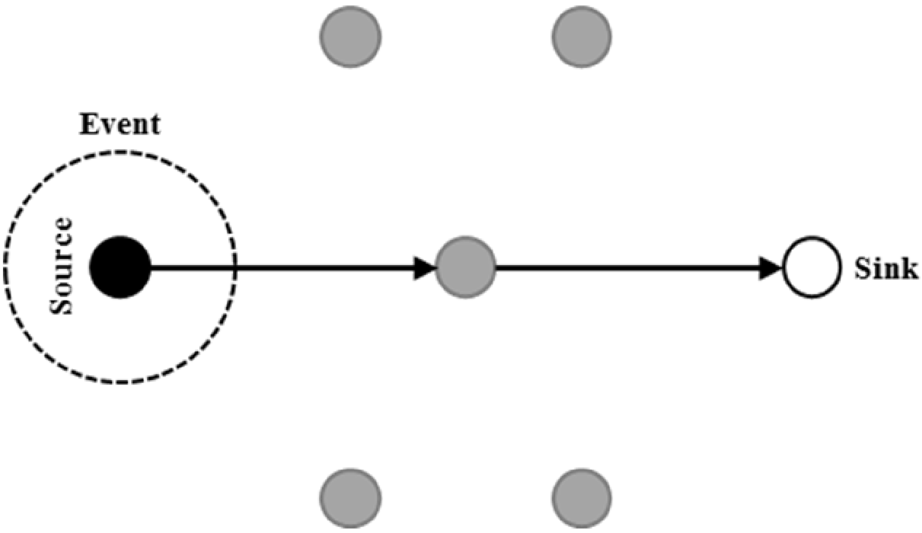

(c) Data delivery reinforced

Figure 2.12: Directed diffusion protocol description

The advantages of directed diffusion are the communication between neighbour-to-neighbour and on demand with no need for node addressing mechanism; and it is energy efficient and delay minimum. The disadvantage is applications that require continuous data delivery to the sink will not work efficiently with such a query-driven on demand data model (Patil and Biradar, 2012).

2.2.2 Hierarchical Routing

In hierarchical routing, sensor nodes are formed into clusters and higher energy node can be selected as a cluster head to aggregate data and send it to the sink node; and lower energy node to sense and send it to the cluster head. One example of hierarchical routing is Threshold Sensitive Energy Efficient Sensor Network Protocol (TEEN). The schematic protocol of TEEN is shown at Figure 2.13.

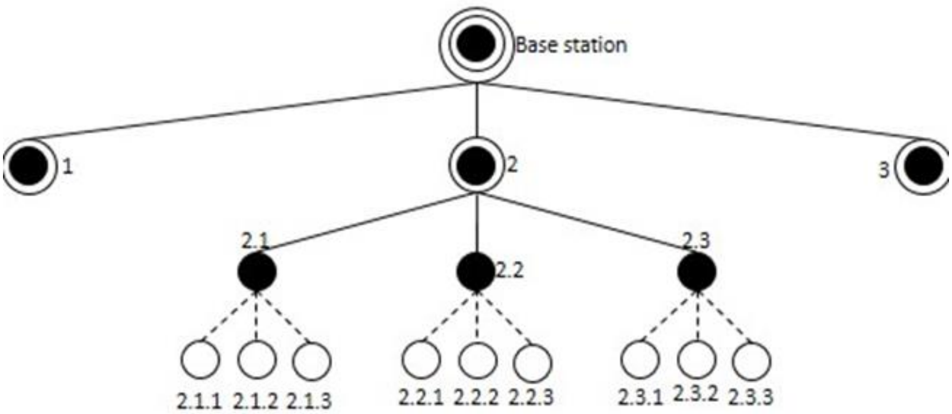

Figure 2.13: TEEN protocol description

There are two types of threshold value in TEEN protocol, which are hard threshold (HT) and soft threshold (ST). HT will enable a sensor to turn on the transmitter and report the sensed data to the cluster head after beyond the threshold, whereby ST will enable a sensor to turn on the transmitter and report the sensed data to the cluster head to indicate small changes in the sensed attribute. The advantage of TEEN protocol is the HT and ST can be adjusted in order to control the number of transmissions. However, it is not suitable for periodic data reporting applications. Moreover, the overhead and complexity of forming clusters in multiple levels, implementing threshold-based function and dealing with attribute-based naming of queries are its main drawbacks (Patil and Biradar, 2012).

2.2.3 Location Based Routing

In location based routing, the distance between two sensor-nodes needs to be calculated to estimate the energy consumption. One example of location based routing is Geographic Adaptive Fidelity (GAF). The state transition diagram of GAF is shown at Figure 2.14.

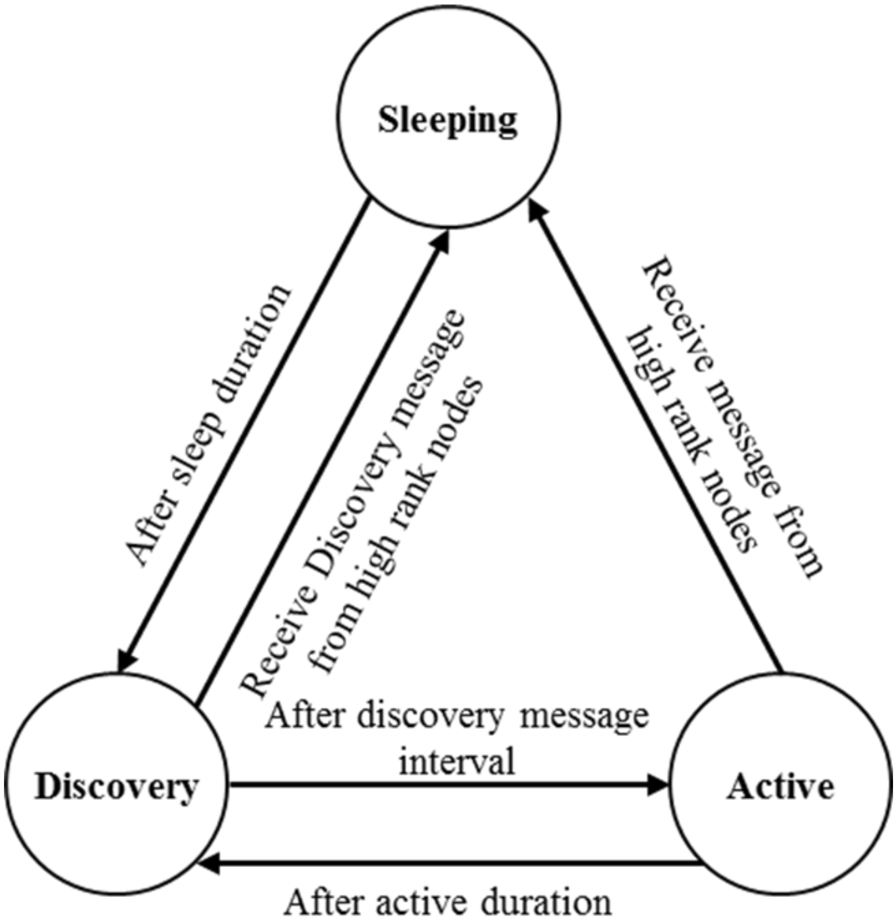

Figure 2.14: State transition diagram for GAF

The advantage of GAF protocol is the minimum amount of energy consumption due to large number of sleeping nodes. However, GAF uses extra hardware for finding the location of the sensor nodes (Patil and Biradar, 2012).

2.2.4 Negotiation Based Routing

The special characteristic of this routing protocol is its metadata to avoid redundant data transmission. One example of negotiation based routing is Sensor Protocol for Information via Negotiation (SPIN). The schematic protocol of SPIN is shown at Figure 2.15.

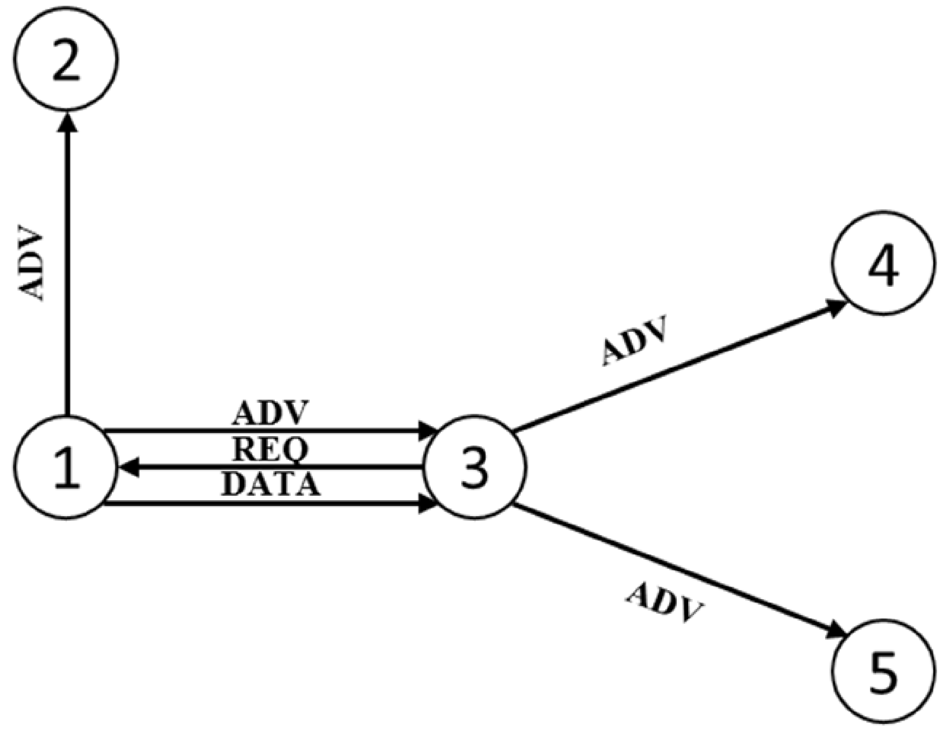

Figure 2.15: SPIN protocol description

The advantage of SPIN protocol is each node only needs to know its neighbours. However, the data advertisement cannot guarantee data delivery if the nodes between the source and destination are not interested in the data. Besides, the metadata adds the cost for storage, retrieval and management (Patil and Biradar, 2012).

2.2.5 Multipath Based Routing

The advantage of multipath based routing is its fault tolerance. One example of multipath based routing is disjoint path routing as described in Figure 2.16.

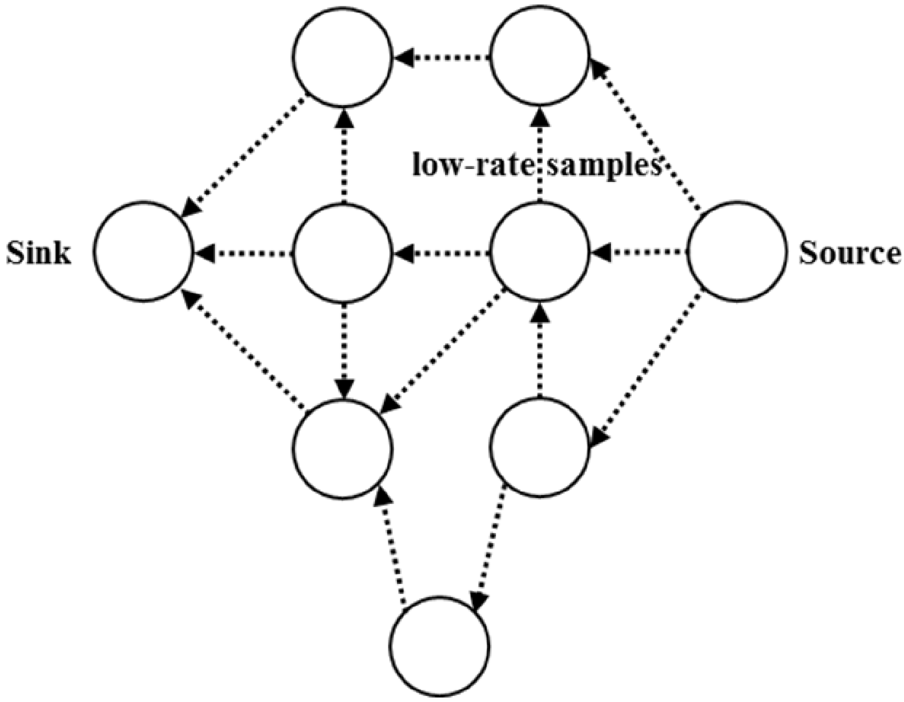

(a) Low-Rate sample

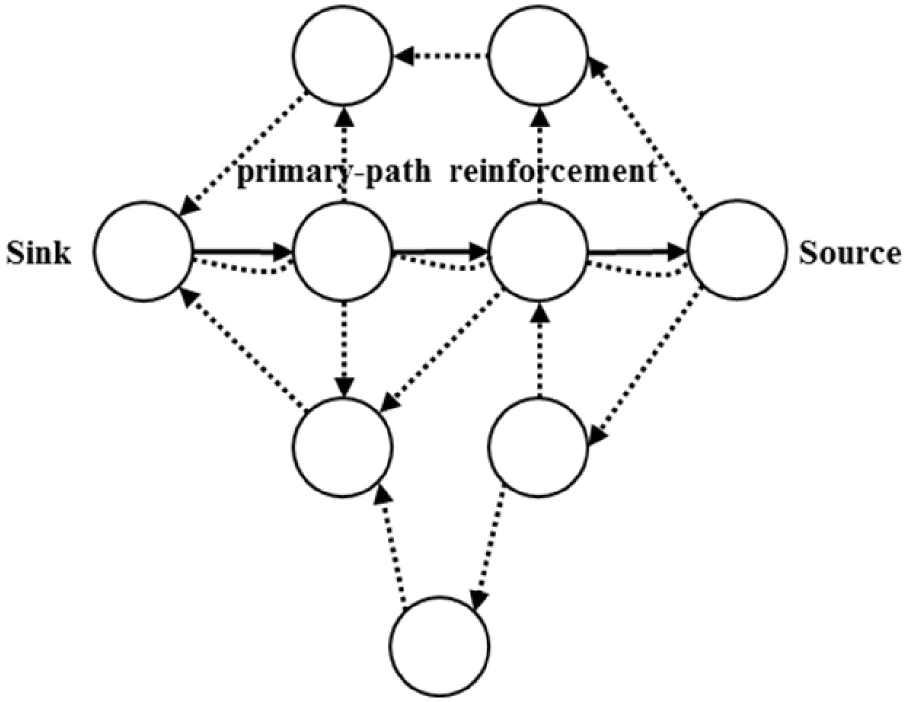

(b) Primary-Path *P*

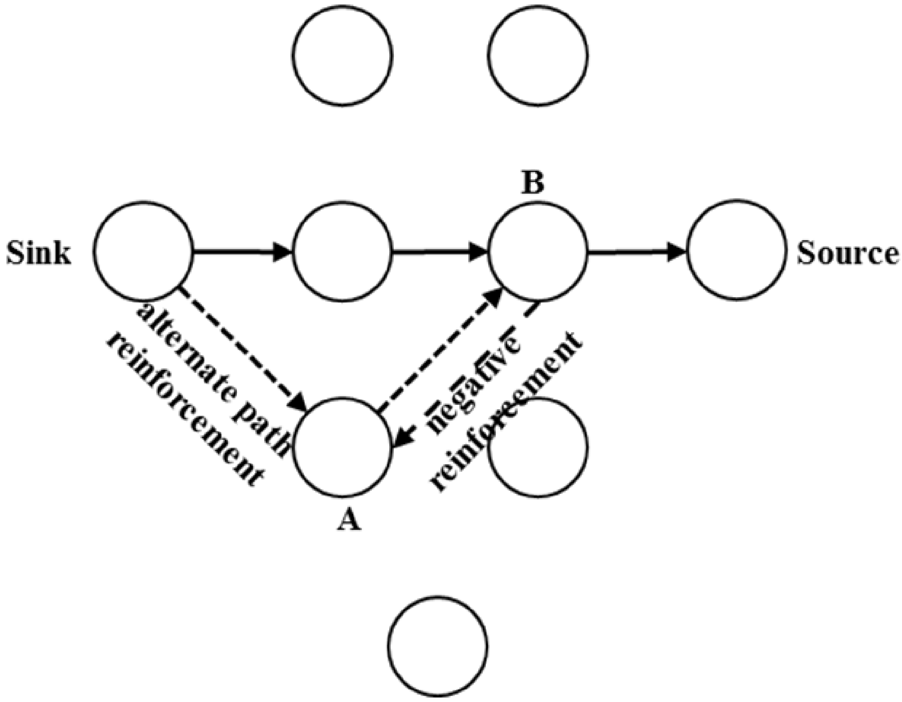

(c) Alternate-Path – Negative Reinforcement

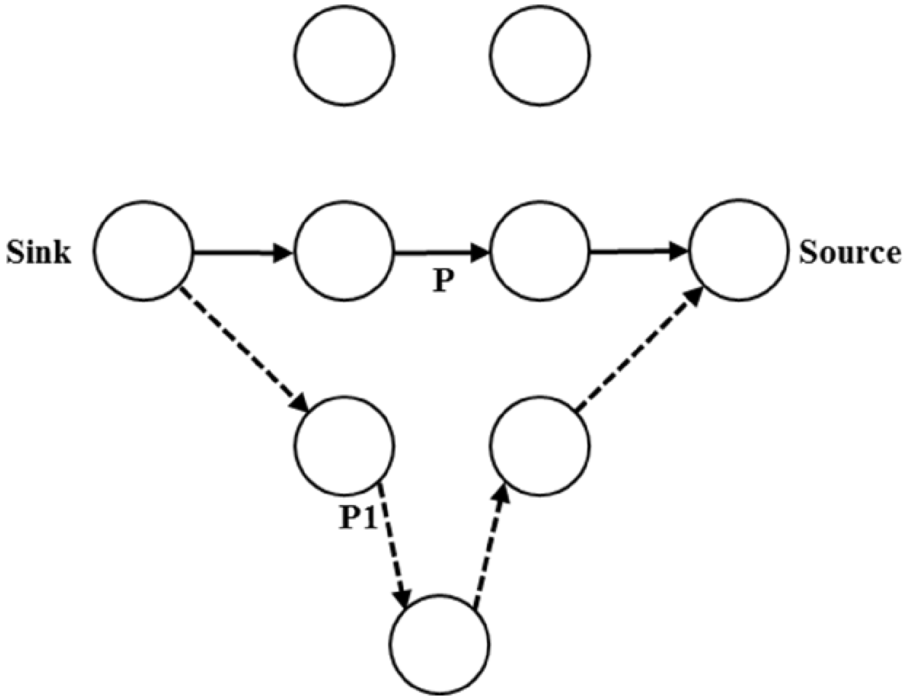

(d) Alternate-Path *P₁*

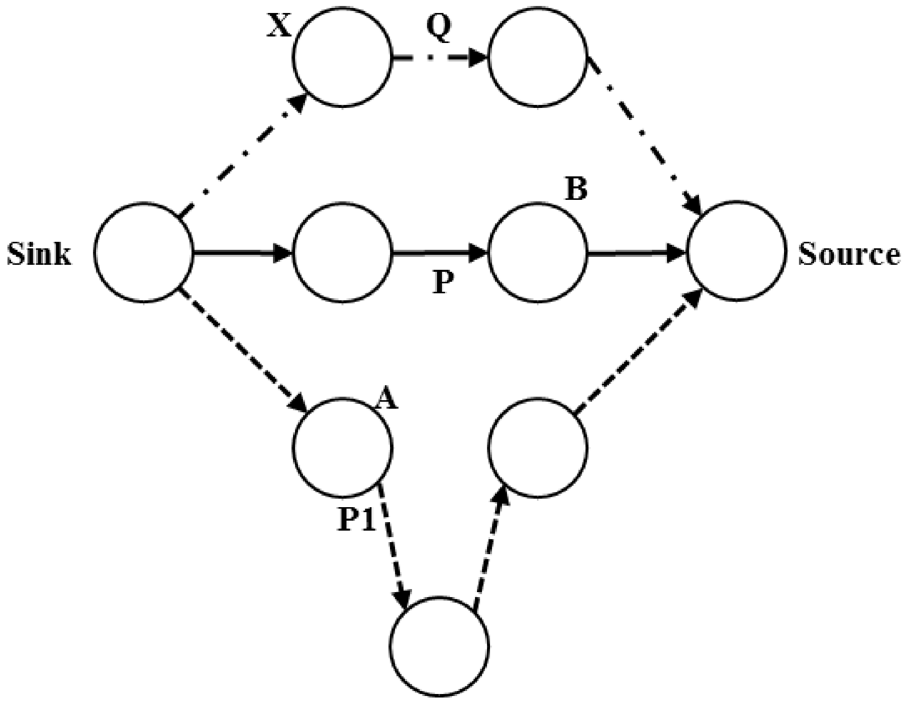

(e) Caveat

Figure 2.16: Disjoint path routing protocol description

Multipath routing is effective to improve the robustness in case of path failures. Besides, it recovers the path from sink to source and provide necessary resilience to the network at the cost of excessive redundancy and traffic generation (Patil and Biradar, 2012). However, it introduces some overhead and consumes more energy.

2.2.6 QoS Based Routing

QoS based routing emerges to minimize the energy consumption in network. One example of QoS based routing is Sequential Assignment Routing (SAR) as described in Figure 2.17.

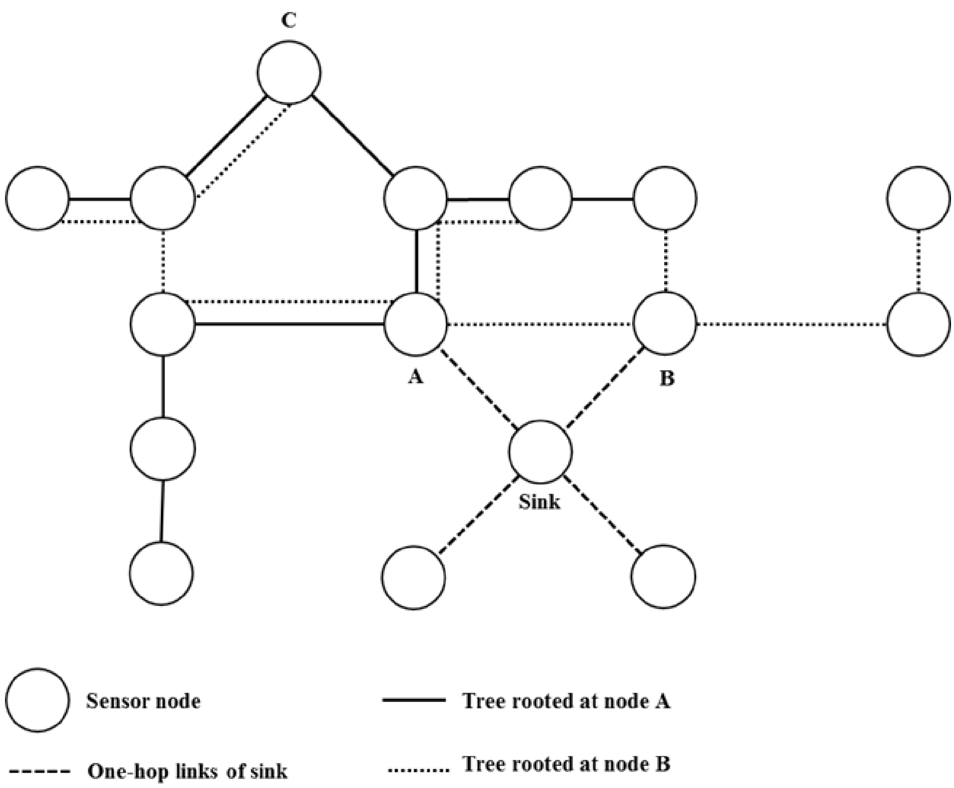

Figure 2.17: Sequential assignment routing protocol description

The advantage of SAR is it consumes less power than the minimum-energy metric algorithm that does not consider the packet priority. However, it suffers overhead in maintaining the tables and states at each node especially when the number of nodes is huge (Patil and Biradar, 2012).

2.2.7 Mobility Based Routing

Some application requires a node to mobile to do its task. It increases in the complexity of energy consumption and routing protocol. One example of mobility based routing is Joint Mobility and Routing Protocol (Patil and Biradar, 2012). The disadvantage of mobility based routing is its shorter lifetime because the mobility of sensor node consumes more power compared to static sensor node.

2.3 Why Data Abstraction and Reformation Schemes?

Data Abstraction and Reformation (DAR) schemes are the proposed schemes to solve energy consumption and accuracy of data reformation issues. DAR schemes contain of Data Abstraction and Data Reformation schemes. Data abstraction is a data filtration scheme whereby each sensed data is evaluated based on certain criteria to determine whether the data should be reported to a base station. Data reformation is data interpolation that reconstructs the non-received data based on the received data.

There are many approaches to conserve energy consumption, such as routing protocol, external power source, and data aggregation. Compared to data abstraction, routing protocol approach will resulted in extra overhead. This overhead will resulted in ineffective data transmission because the sensor nodes need to process the extra overhead before they process the data. With external power source approach, the sensor node will have longer lifetime because of external source. However, this approach requires a larger site compare to battery-powered sensor node. This is because the external hardware required, e.g. solar panel, dynamo, and turbine. The last approach is data aggregation approach. This approach does minimize the number of data transmission; however, it is suitable only for delay-tolerant applications, such as temperature monitoring. Whereby, with data abstraction, the number of data transmission will be reduced and it is suitable for both delay-tolerant and non-delay-tolerant applications, such as patient monitoring. However, in data abstraction, not all of the sensed data will be reported. Therefore, it requires extra processing, so called data reformation to reconstruct the whole data.

There are two types of reporting scheme in order to reduce the number of transmission. Firstly, static interval data abstraction, which is a common method that will subsample a set of value with fixed time interval. For example, data abstraction that applied in the sensor node has the value of fixed interval of n seconds. It means the sensor node will send the sensed value every n seconds. However, the weakness of this approach is a possibility of significant sensed value within the n second that will affect the value of the data information. Besides, there might be no significant data within the n second, thus the number of transmission still can be reduced. Based on the weakness of first approach, dynamic interval data abstraction has been implemented, where the data transmission is determined by the sensed value instead of time interval. The data transmission in second approach only will happened when there is a worth-noting sensed value.

Yang et al. (2009) considered that the WSN is divided into clusters, each with a cluster head. A cluster head is responsible for gathering data from the sensor nodes within the cluster, and then compiling and transmitting the data to the sink node of the WSN when necessary. With such a scenario, the authors further proposed that the sink node and each of the cluster heads share a similar data prediction model by the use of regression. Every time when the cluster head receives data from sensor nodes, it will compare it with the data generated from the prediction model. If the error between the collected data and predicted data is smaller than the error threshold, the cluster head will keep silent without sending anything to the sink node; otherwise, it will send the data to the sink node for necessary updating. Meanwhile, if the sink node does not receive any data from a certain cluster head, it will predict the data value by using the same prediction model. This model will only be updated if the amount of incoming data from the cluster head is more than a pre-set value. Once the model is updated, the sink node will send the prediction model to the cluster head in order to synchronize the prediction model. With the prediction model, the number of transmissions between the cluster heads and sink node can be reduced. However, there could still be frequent communication between the cluster heads and sensor nodes, because the prediction model only shared between cluster heads and sink node. Nevertheless, the sensor nodes still send the whole data to the cluster heads to be processed, which may not be efficient in terms of saving the transmission energy.

Another instance of data abstraction is emSWAB (embedded Sliding Window And Bottom-up) (Berlin and Larrhoven, 2010). The emSWAB will abstract the data based on the slope's sign changes between positive and negative, or zero. If the slope's sign changes positive and negative, or zero, the current sensed value will be reported to the base station, else it will wait until the slope's sign changes. The reformation of emSWAB is by joining the previous received value and the next receive value with linear line. Similar to the ARR approach, where the number of data transmission is successfully reduced, but the accuracy of the reformation method still can be improved.

Raza et al. (2012) proposed a method where the data will not be reported to the base station if the sensed data is between the maximum relative and absolute errors acceptable. However, when the time tolerance of not reporting the data reached, the data will be reported to the base station. The prediction model at the base station is based on derivative-based prediction by piece-wise linear line. However, this approach has a drawback where the data may not be significant enough to be reported.

Aderohunmu et al. (2015) proposed SWIFTNET where transmission of a sensed value will be determined by two algorithm, which are compressed sensing (CS) and adaptive prediction algorithm. Fixed threshold (ρ) is presented to switch between CS and adaptive prediction algorithm dynamically. When sensed data is below ρ, the sensor node will report the sensed data based on fixed sample interval β, which means the sensed data will be reported every time β. When sensed data is above ρ, the sensor node will report the data based on error bound $\in_{max}$ if the difference between the sensed data and predicted data is larger than $\in_{max}$. When sensed data fulfil the criteria of above ρ and larger than $\in_{max}$, the sensed data will be reported to the base station. In the prediction model, the author considers na ïve prediction (non-reported data equals to last reported data), fixed Weighted Moving Average, which is

$$\hat{P}_{t+1} = P_t + \frac{1}{n} \times \sum_{i=1}^{n-1} (P_{t-i+1} - P_{t-i}) \times \omega_i$$

where P_t is the last reported data, n is the set moving window at P_t and ω_i is fixed weight where the sum of the weights should be approximately one. SWIFTNET also considers Least-Mean-Square, and ARIMA model (Aderohunmu et al., 2013) as its prediction model in the sink node. SWIFTNET successfully reduces the number of data transmission. However, the vast number of prediction models will create a problem for the user to determine the best prediction model.

Goh et al. (2011: 69) proposed Abstract Reporting and Reformation (ARR) scheme where the transmission of a sensed value will be determined by a threshold, which is

$$th_n = a + (n - 1)s$$

where a is a value assigned based on degree of sensor sensitivity, s is the sensor sensitivity value achieved from its datasheet and n is a variable incremented by 1 after each threshold comparison. The value of n will be reset to 0 where if it reaches the maximum value of 10 and the sensed value will be sent or a sensed value is reported before n reaches the maximum value. Let x_0 be the previous reported sensed value and x_i be the current sensed value, if the difference of x_0 and x_i exceeds the threshold value, the current sensed value will be transmitted. In other words, if $|x_i - x_0| \geq th_n$, the sensor node will send the value of x_i. The scheme to be applied to determine whether to report a value:

increase i by 1

$n \leftarrow \min\,(i, n_{max})$

$th_n \leftarrow a + (n-1)s$

if $(|x_i - x_0|) \geq th_n$ then

report the values of i and x_i

$x_0 \leftarrow x_i$

i reset to 0

Example of ARR scheme is shown in Table 2.11.

Table 2.11: Example of ARR Scheme

i	1	2	3	…	30	1	2	3	1	2	…
n	1	2	3		10	1	2	3	1	2	
th	0.1	0.2	0.3		1.0	0.1	0.2	0.3	0.1	0.2	
x_0	22.3	22.3	22.3		22.3	23.5	23.5	23.5	23.1	23.1	
x	22.3	22.3	22.2		23.5	23.5	23.1	23.1	23.1	23.0	
$\|x - x_0\|$	0	0	0.1		1.2	0	0.4	0.4	0	0.1	
report	N	N	N		Y	N	Y	Y	N	N	

When the abstracted data reached the base station, the non-received value will be reformed with the previous received data. Let x_0 be the last received value and $\hat{x}_j$ be the non-received value that will be reformed, thus

$$\hat{x}_j = x_0$$

The abstraction method that was introduced in ARR successfully reduce the number of data transmission. However, the accuracy of the reformation method is not well considered.

2.4 Summary

The usage of WSN is commonly nowadays. It can be used at industry, school or university and even at home. However, the lifetime of sensor node depends on the application's operation and mostly it is consumed by its communication or data transmission. Therefore, the conservation of energy consumption in wireless sensor node is important to prolong the lifetime of the network. The motivation of choosing data abstraction approach was explained earlier in Section 2.3.

CHAPTER 3

DATA ABSTRACTION AND REFORMATION SCHEMES

Based on Abstract Reporting and Reformation (ARR) scheme, a new scheme called Data Abstraction and Reformation (DAR) schemes will be proposed to solve the energy consumption and the accuracy of data reformation issues. DAR schemes consist of data abstraction and data reformation. Data abstraction in sensor node is a data filtration scheme whereby each sensed data is evaluated based on certain criteria to determine whether the data should be reported to a base station. Data reformation in base station or server is data interpolation that reconstructs the non-received data based on the received data. The details of DAR schemes will be explained in the following.

3.1 Data Abstraction

Data abstraction, as shown in the Figure 3.1, is a data filtration scheme whereby each sensed data is evaluated based on certain criteria to determine whether the data should be reported to a base station.

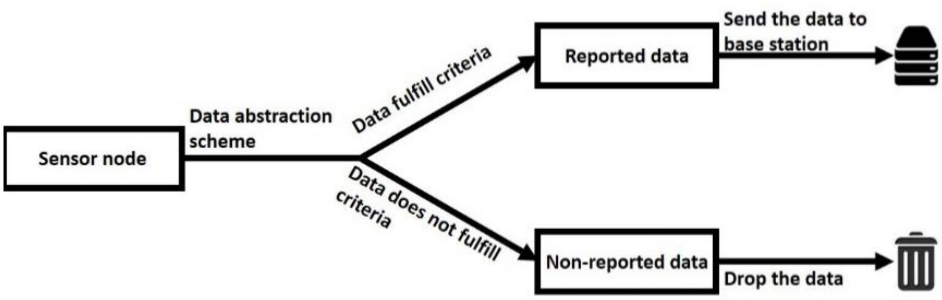

Figure 3.1: Illustration of data abstraction

For example, with refer to Figure 3.2, data are sensed in time 1, 2, 3, …, 10. However, data are only reported at time 1, 4, and 9. Let i denote a sequence number of the i^{th} sensed data, j denote a sequence number of the

j^{th} reported data, and t_j denote the timestamp of the j^{th}reported data. Thus, the reported data are to be at t_1 = 1, t_2 = 4, and t_3 = 9.

Data	●	○	○	●	○	○	○	○	●	○
i	1	2	3	4	5	6	7	8	9	10
j	1			2					3	
t_j	1			4					9	

● Data sensed and reported
○ Data sensed but not reported

Figure 3.2: Example of data abstraction

Data abstraction can be defined to have different orders. In this study, we focus only on zeroth-, first-, and second-order data abstraction.

In the zeroth-order data abstraction, the sensed data is compared with a pre-fixed threshold value, denotes as th_{value}. Let a_i denote the sensed data at time i, where $i \geq 1$. In this scheme, a_i is reported to the base station if the data of a_i is larger than or equal to th_{value}. That is

$$a_i \geq th_{value}$$

Note that when $i = 1$, a_1 has to be sent to the base station as the first reference data of the completion of the scheme for reformation, which will be discussed in the section 3.2. If the total number of data is pre-determined (n), a_n need to be sent to the base station as the last reference data of the completion of the scheme for reformation. For instance, a set of data are shown in Table 3.1 with $th_{value} = 22.2$.

Table 3.1: Example of Zeroth-Order Data Abstraction

	a_i	Report
a_1	22.313	Yes
a_2	22.313	Yes
a_3	22.313	Yes
a_4	22.250	Yes
a_5	22.250	Yes
a_6	22.250	Yes
a_7	22.250	Yes
a_8	22.188	No
a_9	22.188	No
a_{10}	22.188	yes

Let b_j denote the reported sensed data. Therefore, from Table 3.1, the reported data will be denoted as $b_1 = a_1 = 22.313$, $b_2 = a_2 = 22.313$, $b_3 = a_3 = 22.313$, $b_4 = a_4 = 22.250$, $b_5 = a_5 = 22.250$, $b_6 = a_6 = 22.250$, $b_7 = a_7 = 22.250$,and $b_8 = a_{10} = 22.188$. Typically, there is only one value to be reported in one time of data transmission.

In the first-order data abstraction, the changing of the sensed data is monitored and compared with the pre-fixed threshold of rate, denotes as th_{rate}. Let a_{t_j} denote the last reported data at time t_j, where $j \geq 1$. In this scheme, for any $i > t_j$, a_i, and $a_{i-1}$are reported to the base station if the difference of a_i and a_{t_j}, denotes as Δa_i, is larger than or equal to th_{rate}. That is

$$\Delta a_i = \left| a_i - a_{t_j} \right| \geq th_{rate}$$

Note that when $i = 1$, a_1 has to be sent to the base station as the first reference data of the completion of the scheme for reformation. Moreover, if at time $i > t_j$, data (i.e., a_i and a_{i-1}) are reported, we will then set

$t_{j+1} = i$, and this timestamp will become the last reporting time for the subsequent evaluation of the data. Again, if the total number of data is pre-determined (n), a_n need to be sent to the base station as the last reference data of the completion of the scheme for reformation. For instance, a set of data are shown in Table 3.2 with $th_{rate} = 0.1$.

Table 3.2: Example of First-Order Data Abstraction

	a_i	a_{t_j}	$\lvert\Delta a_i\rvert$	Report
a_1	22.313	-	-	Yes
a_2	22.313	22.313	0	No
a_3	22.313	22.313	0	No
a_4	22.250	22.313	0.063	no
a_5	22.250	22.313	0.063	no
a_6	22.250	22.313	0.063	no
a_7	22.250	22.313	0.063	yes
a_8	22.188	22.313	0.125	
a_9	22.188	22.188	0	no
a_{10}	22.188	22.188	0	yes

Let b_j denote the reported sensed data. Therefore, from Table 3.2, the reported data will be denoted as $b_1 = a_1 = 22.313$; b_2 contains of a_7 and $a_8 = 22.250$ and 22.188; and b_3 contains of $a_{10} = 22.188$. Typically, there are two data to be reported in one time of data transmission.

In the second-order data abstraction, the acceleration of the data is monitored and compared with the pre-fixed threshold of acceleration, denotes as th_{accel}. In this scheme, for any $i > t_j$, a_i, a_{i-1}, and a_{i-2} are reported to the base station if the second-order difference of the data of a_i, a_{i-1}, and a_{t_j}, denotes as $\Delta^2 a_i$ is larger than or equal to th_{accel}. That is

$$\Delta^2 a_i = \left| a_i - 2a_{i-1} + a_{t_j} \right| \geq th_{accel}$$

Note that when $i = 1$ and 2, a_1 and a_2 have to be sent to the base station as the first two reference data of the completion of the scheme for reformation. Moreover, if at time $i > t_j$, data (i.e., a_i, a_{i-1} and a_{i-2}) are reported, we will then set $t_{j+1} = i$, and this timestamp will become the last reporting time for the subsequent evaluation of the data. Again, if the total number of data is pre-determined (n), a_n need to be sent to the base station as the last reference data of the completion of the scheme for reformation. For instance, a set of data are shown in Table 3.3 with $th_{accel} = 1$.

Table 3.3: Example of Second-Order Data Abstraction

<table>
<tr><th></th><th>a_i</th><th>a_{i-1}</th><th>a_{t_j}</th><th>$\left|\Delta^2 a_i\right|$</th><th>report</th></tr>
<tr><td>a_1</td><td>22.313</td><td>-</td><td>-</td><td>-</td><td>yes</td></tr>
<tr><td>a_2</td><td>22.313</td><td>22.313</td><td>-</td><td>-</td><td>yes</td></tr>
<tr><td>a_3</td><td>22.313</td><td>22.313</td><td>22.313</td><td>0</td><td>no</td></tr>
<tr><td>a_4</td><td>22.250</td><td>22.313</td><td>22.313</td><td>0.063</td><td>no</td></tr>
<tr><td>a_5</td><td>22.250</td><td>22.250</td><td>22.313</td><td>0.063</td><td>no</td></tr>
<tr><td>a_6</td><td>22.250</td><td>22.250</td><td>22.313</td><td>0.063</td><td>no</td></tr>
<tr><td>a_7</td><td>22.250</td><td>22.250</td><td>22.313</td><td>0.063</td><td rowspan="3">yes</td></tr>
<tr><td>a_8</td><td>22.188</td><td>22.250</td><td>22.313</td><td>0.001</td></tr>
<tr><td>a_9</td><td>22.188</td><td>22.188</td><td>22.313</td><td>0.125</td></tr>
<tr><td>a_{10}</td><td>22.188</td><td>22.188</td><td>22.188</td><td>0</td><td>yes</td></tr>
</table>

Let b_j denote the reported sensed data. Therefore, from Table 3.3, the reported data will be denoted as $b_1 = a_1 = 22.313$, $b_2 = a_2 = 22.313$, b_3 contains of a_7, a_8, and $a_9 = 22.250$, 22.188, and 22.188; and $b_4 = a_{10} = 22.188$. Typically, there are three data to be reported in one time of data transmission.

3.2 Data Reformation

Data reformation, as shown in Figure 3.3, is in fact data interpolation that reconstructs the non-received data based on the received data. Similar to the data abstraction, data reformation scheme may have different orders, but in this paper focus only on zeroth-, first-, and second-order data reformation.

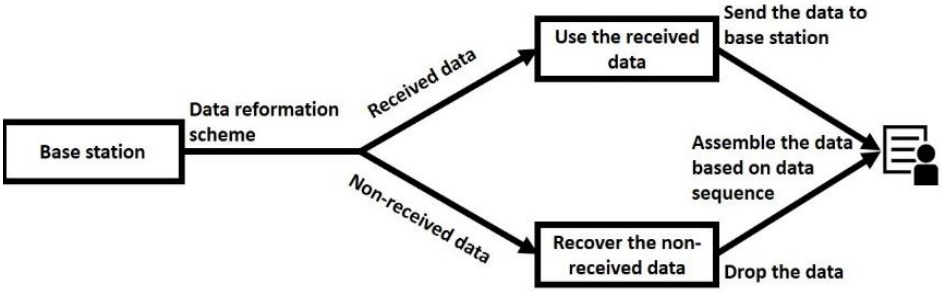

Figure 3.3: Illustration of data reformation

For $j \geq 1$and $t_j \leq i < t_{j+1}$, let $\hat{a}_i$ represent the reconstructed data of a_i at the base station after $a_{t_{j+1}}$ have been received. Note that we have

$$\hat{a}_{t_j} = a_{t_j} \text{and } \hat{a}_{t_{j+1}} = a_{t_{j+1}}$$

However, for any $i \notin \{t_j \mid j \geq 1\}$, $\hat{a}_i$ are not defined, and thus they need to be reformed. In the zeroth-order data reformation attempts to recover the non-received data by piece-wise constant data; the first-order the piece-wise linear lines; where the second-order the piece-wise parabolic curves. These schemes are shown in Table 3.4.

Table 3.4: Data Reformation Schemes

Order of Data Reformation	Scheme
Zeroth	$\hat{a}_i = a_{t_j}$, for $t_j \le i \le t_{j+1}$
First	$\hat{a}_i = \frac{(i - t_{j+1})}{(t_j - t_{j+1})} a_{t_j} + \frac{(i - t_j)}{(t_{j+1} - t_j)} a_{t_{j+1}}$, for $t_j \le i \le t_{j+1}$
Second	$\hat{a}_i = \frac{(i - t_j)(i - t_{j+1})}{(t_{j-1} - t_j)(t_{j-1} - t_{j+1})} a_{t_{j-1}} + \frac{(i - t_{j-1})(i - t_{j+1})}{(t_j - t_{j-1})(t_j - t_{j+1})} a_{t_j} + \frac{(i - t_{j-1})(i - t_j)}{(t_{j+1} - t_{j-1})(t_{j+1} - t_j)} a_{t_{j+1}}$, for $t_j \le i \le t_{j+1}$

For instance, the reported data in Table 3.3 are reformed with zeroth-, first-, and second-order data reformation. The results of the reformed data are shown respectively in Table 3.5 - 3.7.

Table 3.5: Example of Zeroth-order Data Reformation

	a_{t_j}	$\hat{a}_i$
a_{t_1}	22.313	22.313
a_{t_2}	22.313	22.313
a_{t_3}	-	22.313
a_{t_4}	-	22.313
a_{t_5}	-	22.313
a_{t_6}	-	22.313
a_{t_7}	22.250	22.250
a_{t_8}	22.188	22.188
a_{t_9}	22.188	22.188
$a_{t_{10}}$	22.188	22.188

Table 3.6: Example of First-Order Data Reformation

	a_{t_j}	$\hat{a}_i$
a_{t_1}	22.313	22.313
a_{t_2}	22.313	22.313
a_{t_3}	-	22.300
a_{t_4}	-	22.288
a_{t_5}	-	22.275
a_{t_6}	-	22.263
a_{t_7}	22.250	22.250
a_{t_8}	22.188	22.188
a_{t_9}	22.188	22.188
$a_{t_{10}}$	22.188	22.188

Table 3.7: Example of Second-Order Data Reformation

	a_{t_j}	$\hat{a}_i$
a_{t_1}	22.313	22.313
a_{t_2}	22.313	22.313
a_{t_3}	-	22.309
a_{t_4}	-	22.300
a_{t_5}	-	22.288
a_{t_6}	-	22.271
a_{t_7}	22.250	22.250
a_{t_8}	22.188	22.188
a_{t_9}	22.188	22.188
$a_{t_{10}}$	22.188	22.188

3.3 Concluding Remarks

In conclusion, by implementing DAR schemes, the data abstraction will reduce the number of packet transmissions or the number of data transmitted of a wireless sensor node. Because not all of the data is transmitted, the information's accuracy of the collected data in sink node or base station will be affected. As part of DAR schemes, data reformation will reconstruct the non-received data to ensure that the accuracy of the information does not greatly affected by the data abstraction.

CHAPTER 4

EXPERIMENT DESIGN & SETTINGS

In most WSN applications, sensors sense data regularly and these sensed data are supposed to be sent to the base station for processing and analysis. If the whole set of data is sent, the accuracy of the information will be excellent, but it will consume a lot of energy. In order to conserve the energy, it is necessary to reduce the number of transmissions by using the data abstraction schemes as proposed in Chapter 3. On the other hand, once the selected data have been received by the base station, the whole set of data can then be accurately reformed by using the data reformation scheme proposed in Chapter 3. In this Chapter, experiment design and setting that verifies our proposed DAR schemes will be discussed.

Experiment design and settings in this study are applied into two major categories, which are application/attribute with low sampling rate and application/attribute with abrupt sampling rate. Application/attribute with low sampling rate in this study is defined as an application that sample at < 10 Hz, for example temperature monitoring, pH monitoring, and etc.; where application/attribute with abrupt sampling rate is defined as an application that sample within 10 Hz – 1 kHz (Cosar, 2009), for example vibration monitoring, acceleration monitoring and etc.

4.1 Application/Attribute with Low Sampling Rate

An experiment to capture the temperature as in Goh et al. (2011) had been done as the application/attribute with low sampling rate. A sensor node with temperature sensor was configured to sample at 4 Hz until it reached 600 samples of value. There were three sensor data patterns designated as burst, incremental and decremental, and random data. The results of the experiment are shown in the followings.

4.1.1 Burst Temperature Data

The sensor was tested with a setting to achieve burst temperature data where a temperature increased in a short time. The result of the experiment is shown in Figure 4.1.

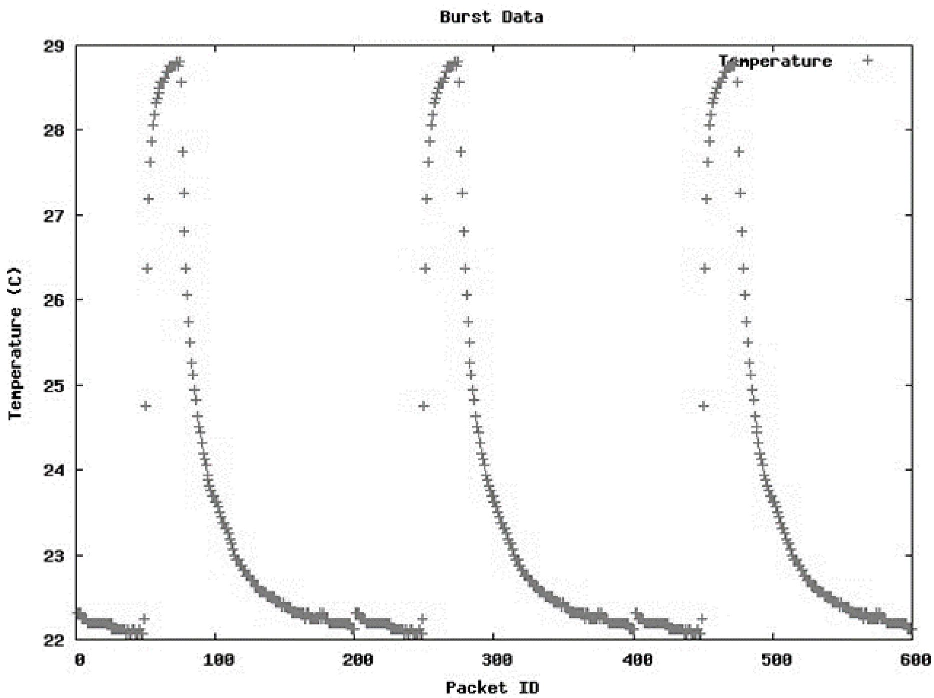

Figure 4.1: Burst temperature data

4.1.2 Incremental and Decremental Temperature Data

The sensor was tested with a setting to achieve incremental and decremental temperature data where a temperature increased in a short time. The result of the experiment is shown in Figure 4.2.

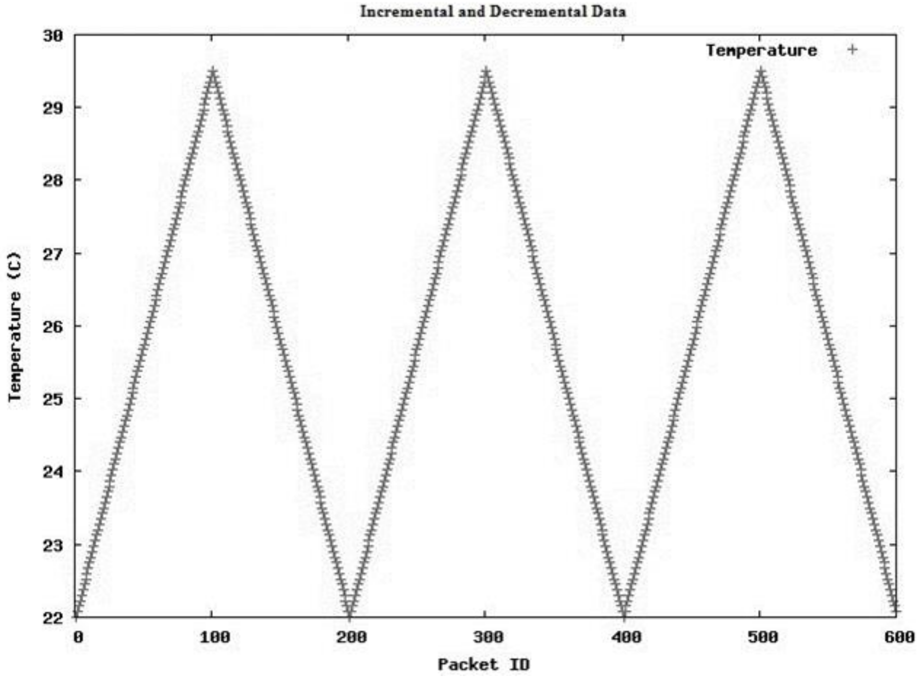

Figure 4.2: Incremental and decremental temperature data

4.1.3 Random Temperature Data

The sensor was tested with a setting to achieve random temperature data of an object. The result of the experiment is shown in Figure 4.3.

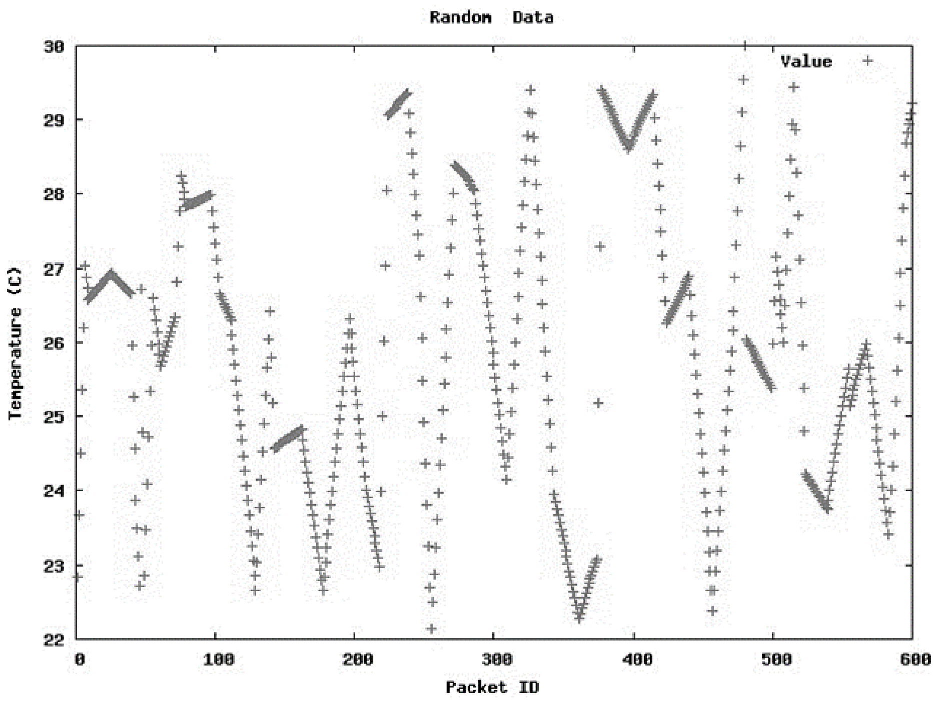

Figure 4.3: Random temperature data

4.2 Application/Attribute with Abrupt Sampling Rate

A sensor node with accelerometer sensor was configured to sample at 16 Hz until it reaches 3000 samples of value. The accelerometer used to capture the movement of an object (Arima et al., 2012). In this research, the accelerometer that was used is KXSD9 3-axis Accelerometer (Kionix, Inc., 2013). The object was a human that did four movements, which are sitting, standing, walking, and running movements. The sensor was placed in the middle of the body as shown in Figure 4.4. The results of the experiment are shown in the followings.

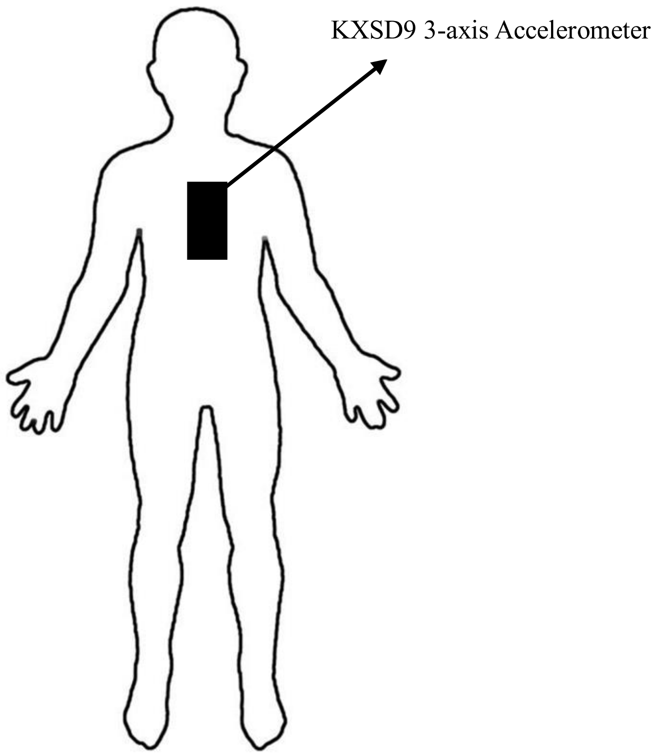

Figure 4.4: Placement of the KXSD9 3-axis Accelerometer sensor

4.2.1 Sitting Accelerometer Data

The sensor node was tested under different sitting movements designated as shown in Table 4.1 and Figure 4.5.

Table 4.1: Packet ID in Sitting Movements

Packet ID	Movement
1 - 225	Normal sitting position
226 - 450	Sit turning left 90°
451 - 675	Back to normal sitting position
676 - 900	Sit turning right 90°
901 - 1125	Back to normal sitting position
1126 - 1350	Sit laying back
1351 - 1575	Back to normal sitting position
1576 - 1800	Sit laying front
1801 - 2025	Back to normal sitting position
2026 - 2250	Standing up
2251 - 3000	Back to normal sitting position

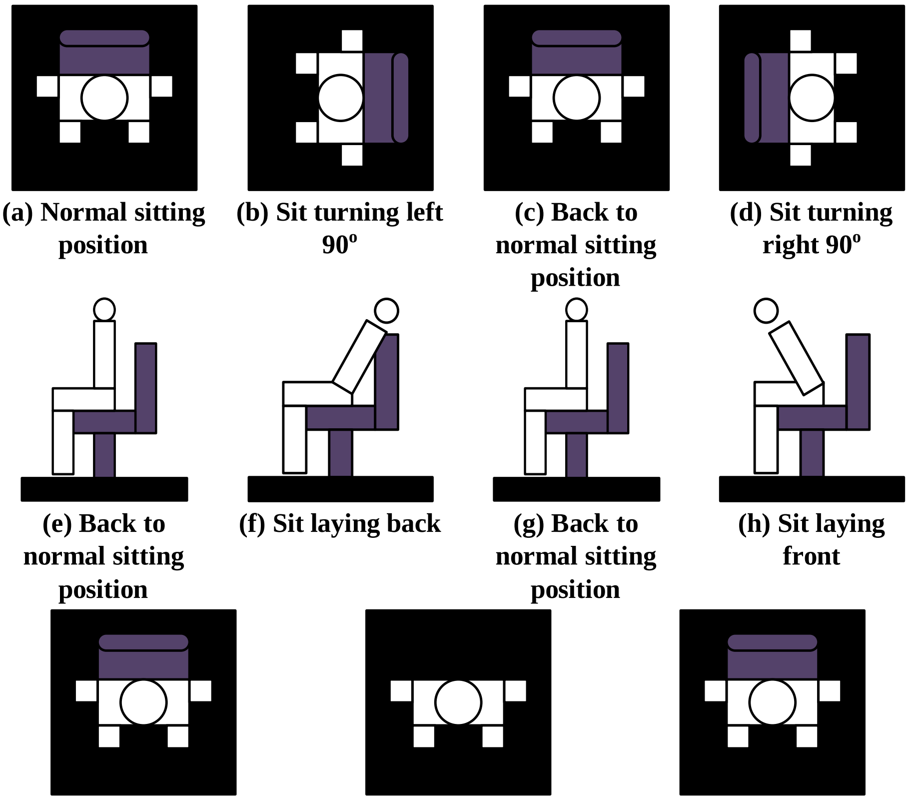

(a) Normal sitting position
(b) Sit turning left 90°
(c) Back to normal sitting position
(d) Sit turning right 90°
(e) Back to normal sitting position
(f) Sit laying back
(g) Back to normal sitting position
(h) Sit laying front
(i) Back to normal sitting position
(j) Standing up
(k) Back to normal sitting position

Figure 4.5: Sitting movements

Results of the experiment are shown in Figure 4.6.

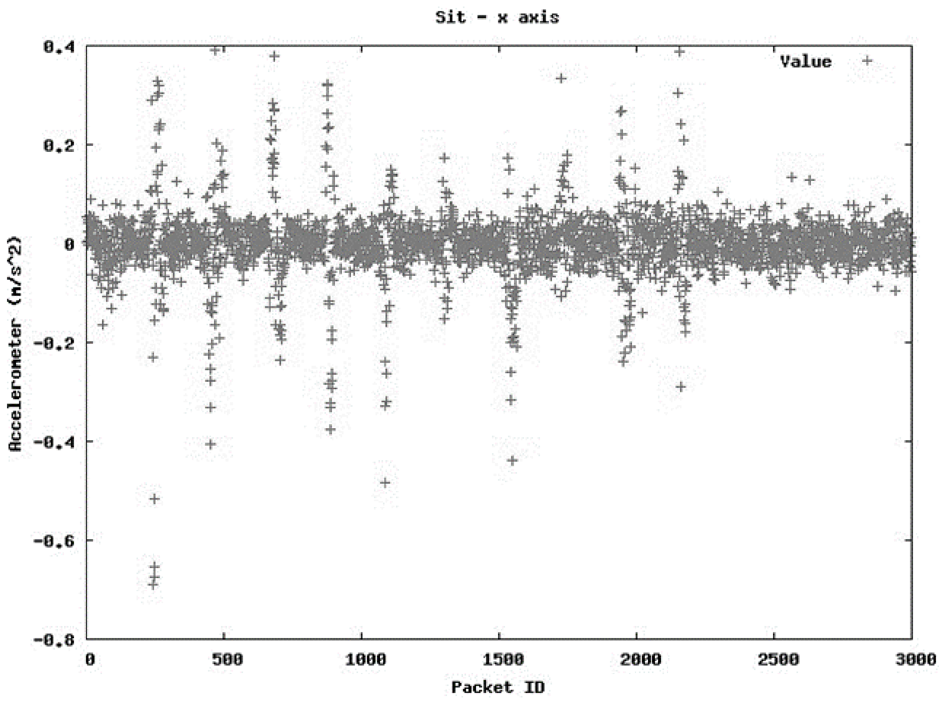

(a) x-axis

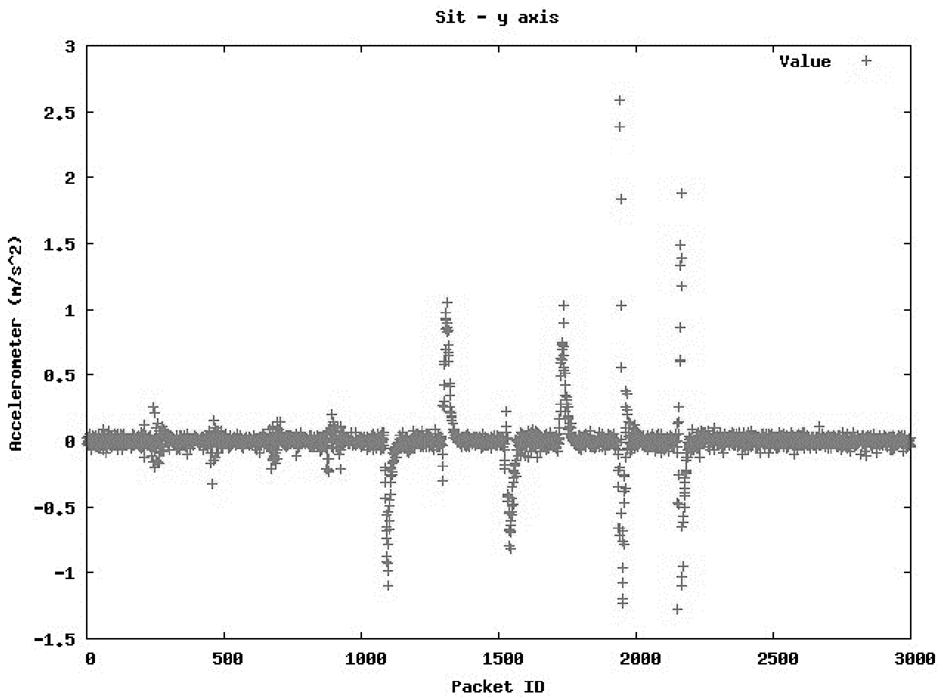

(b) y-axis

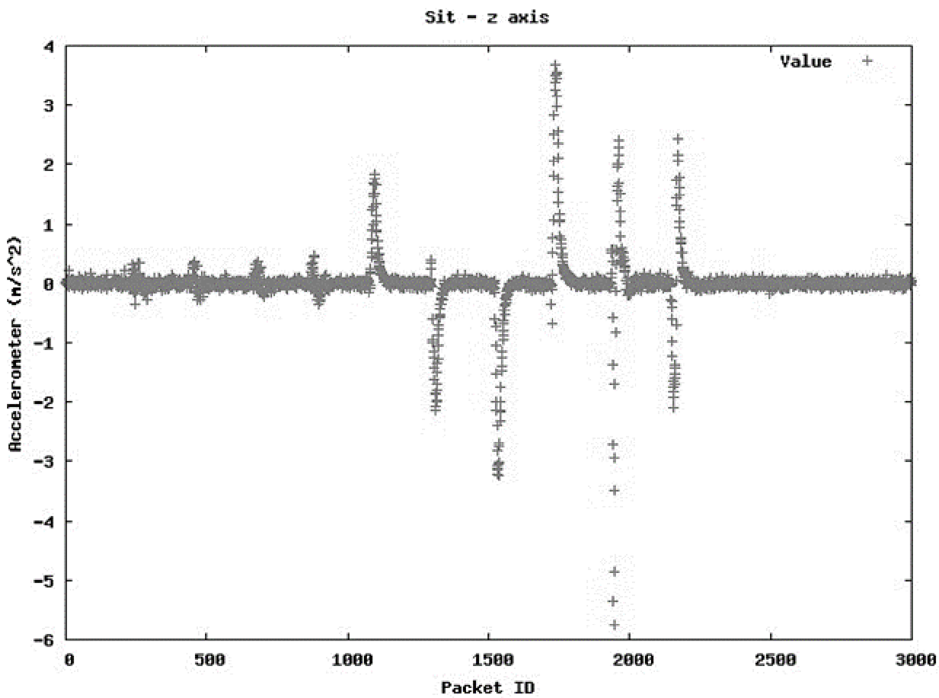

(c) z-axis

Figure 4.6: Sitting accelerometer data

4.2.2 Standing Accelerometer Data

The sensor node was tested under different standing movements designated as shown in Table 4.2 and Figure 4.7.

Table 4.2: Packet ID in Standing Movements

Packet ID	Movements
1-225	Standing still
226 - 450	Stand turning left 90º
451-675	Back to standing still
676-900	Stand turning right 90º
901-1125	Back to standing still
1126-1350	Sitting down
1351-3000	Back to standing still

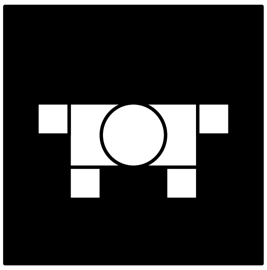

(a) Standing still

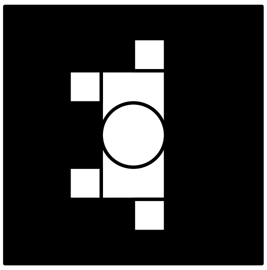

(b) Stand turning left 90^o

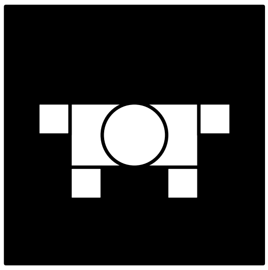

(c) Back to standing still

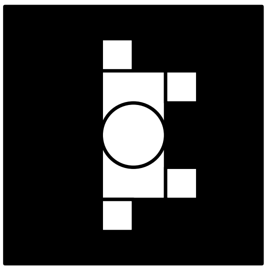

(d) Stand turning right 90^o

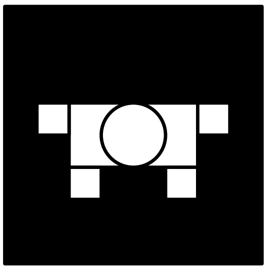

(e) Back to standing still

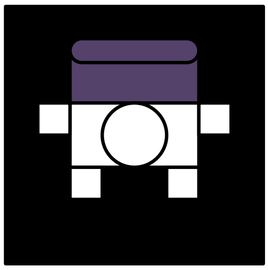

(f) Sitting down

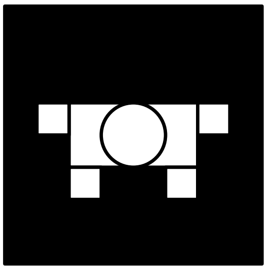

(g) Back to standing still

Figure 4.7: Standing movements

The results of the experiment are shown in Figure 4.8.

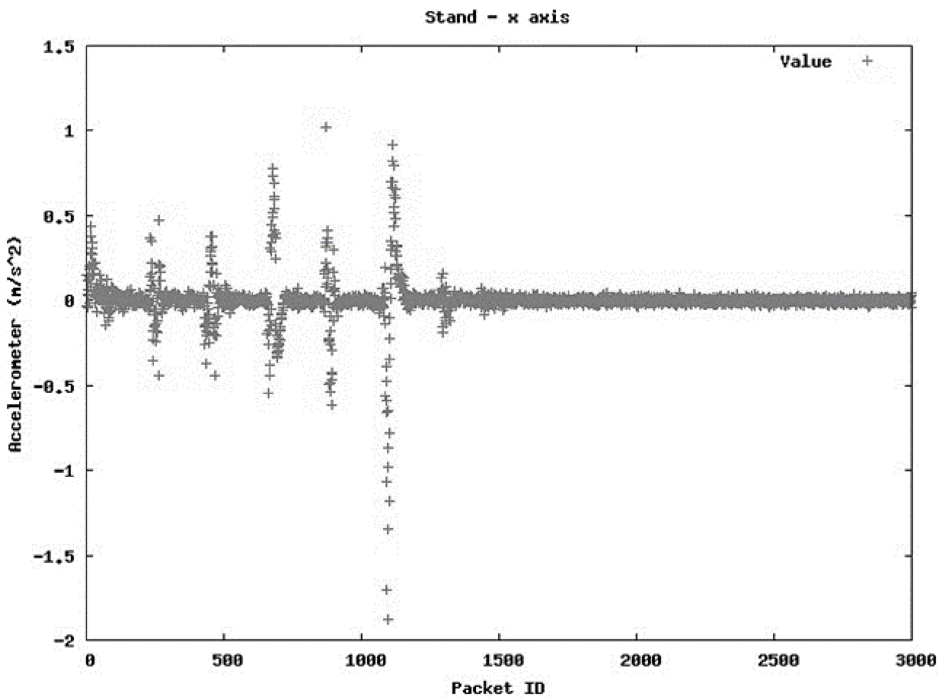

(a) x-axis

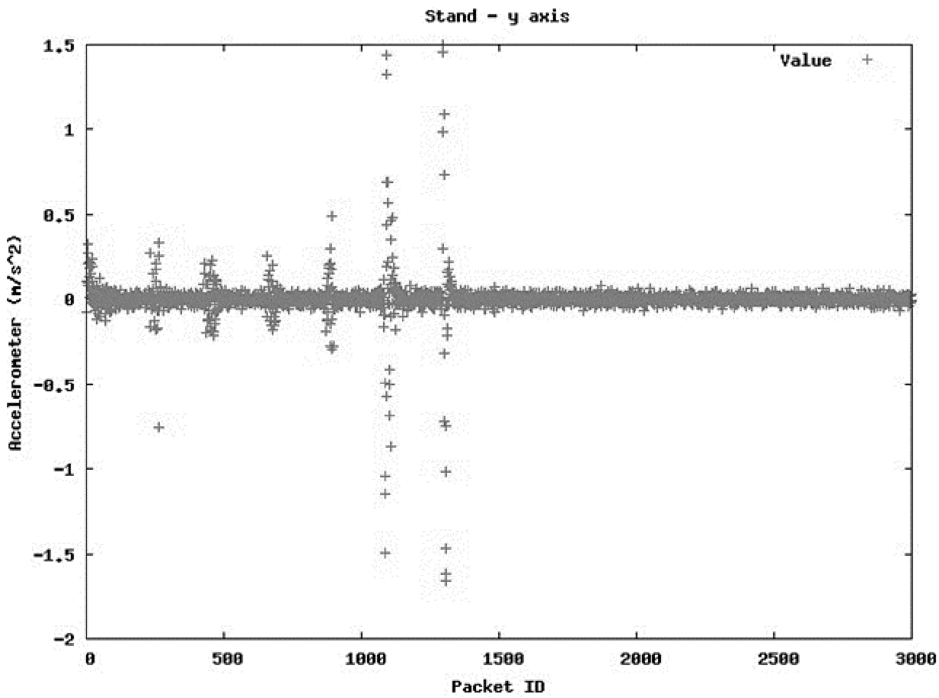

(b) y-axis

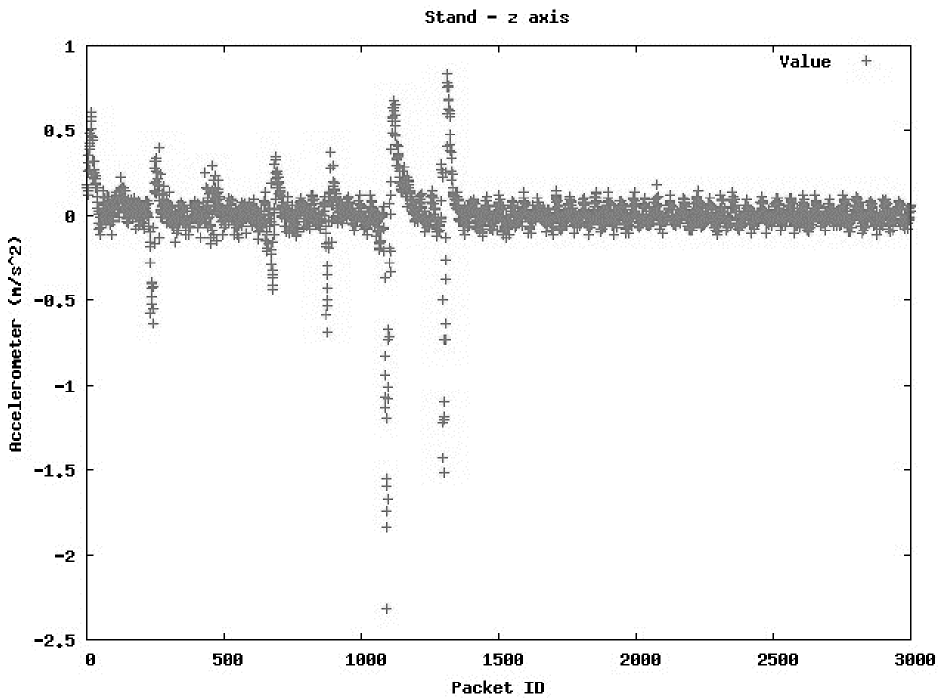

(c) z-axis

Figure 4.8: Standing accelerometer data

4.2.3 Walking Accelerometer Data

The sensor node was tested under different walking movements designated as shown in Table 4.3 and Figure 4.9.

Table 4.3: Packet ID in Walking Movements

Packet ID	Movements
1 - 150	Walking straight
151 - 450	Turning left 90º, walking straight
451 - 600	Turning left 90º, walking straight
601 - 900	Turning left 90º, walking straight
901 - 1200	Turning right 180º, walking straight
1201 - 1350	Turning right 90º, walking straight
1351 - 1650	Turning right 90º, walking straight
1651 - 1800	Turning right 90º, walking straight
1801 - 1950	Turning left 180º, walking straight
1951 - 2250	Turning left 90º, walking straight
2251 - 2400	Turning left 90º, walking straight
2401 - 2700	Turning left 90º, walking straight
2701 - 3000	Turning right 180º, walking straight

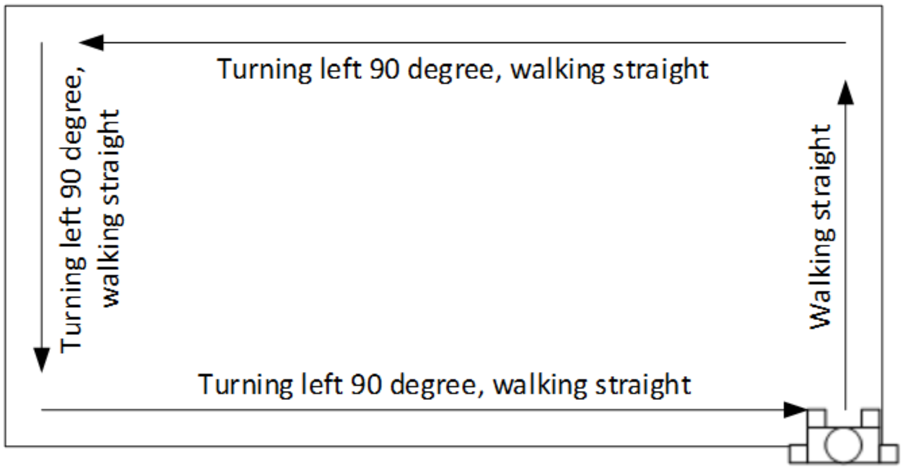

(a) Walking movements in Packet ID 1-900

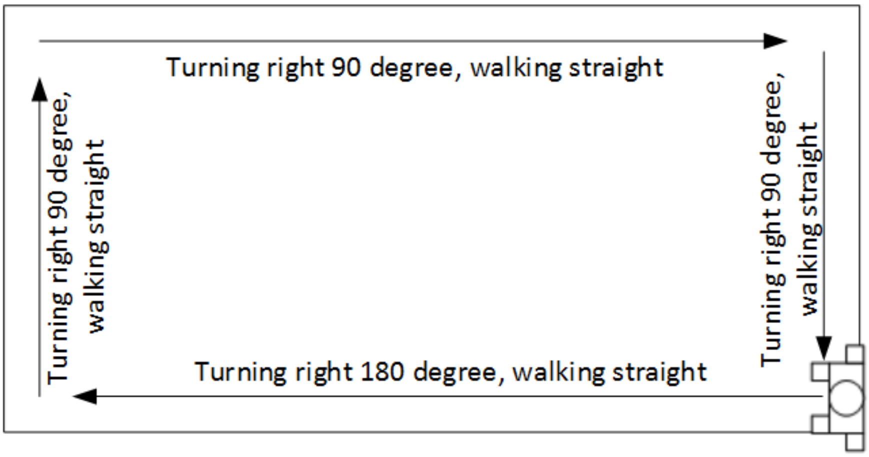

(b) Walking movements in Packet ID 901-1800

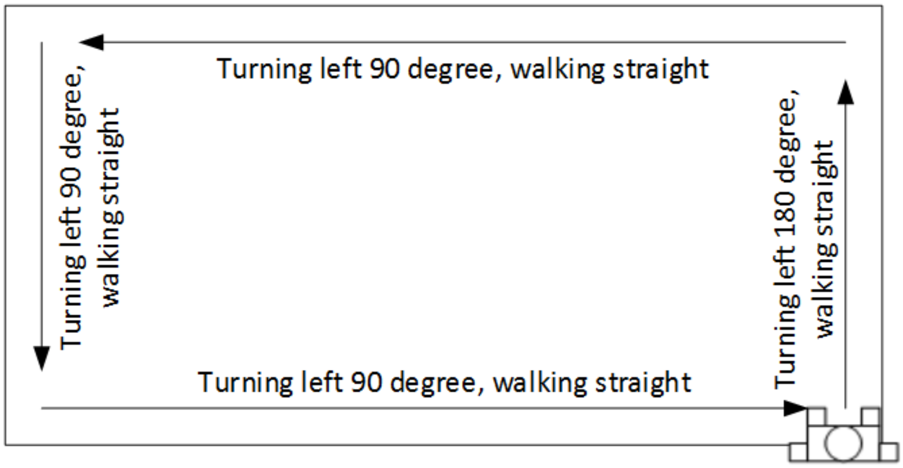

(c) Walking movements in Packet ID 1801-2700

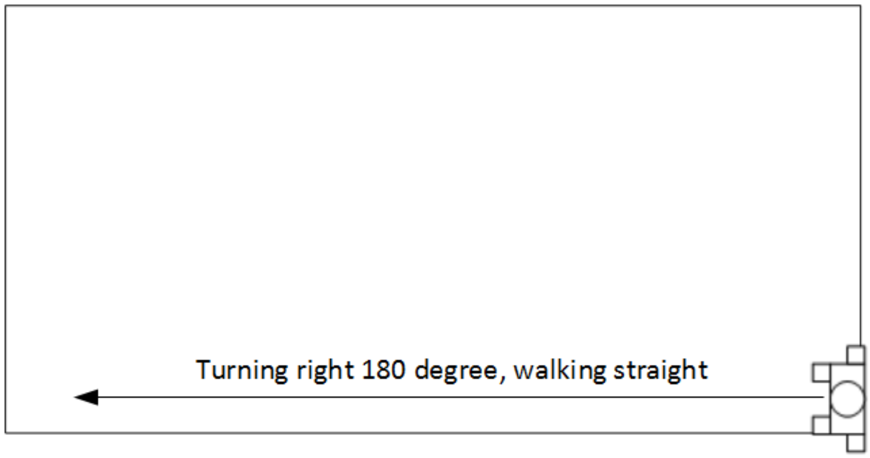

(d) Walking movements in Packet ID 2701-3000

Figure 4.9: Walking movements

The results of the experiment are shown in Figure 4.10.

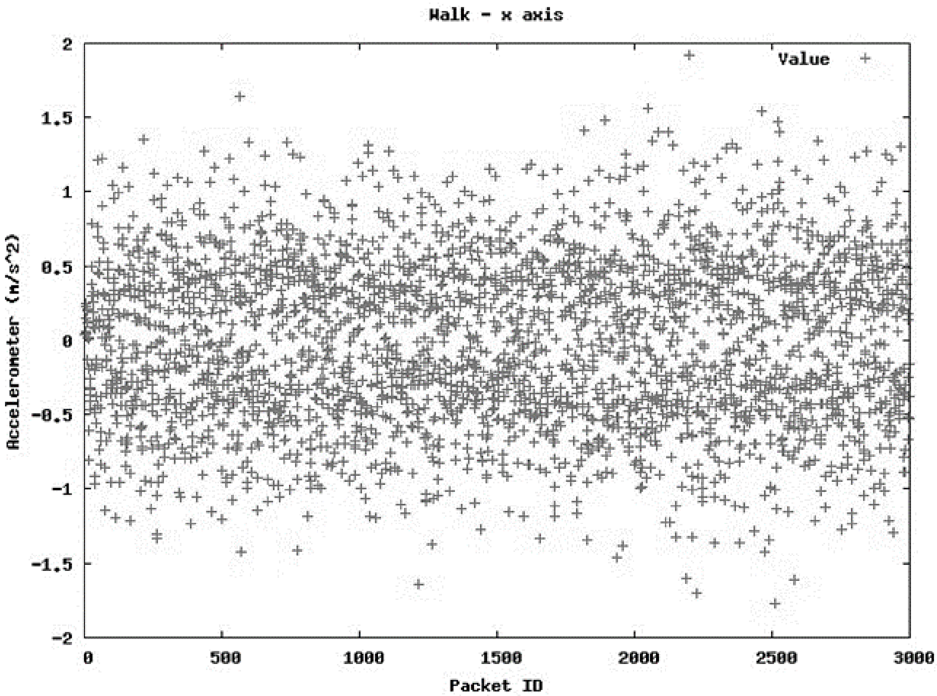

(a) x-axis

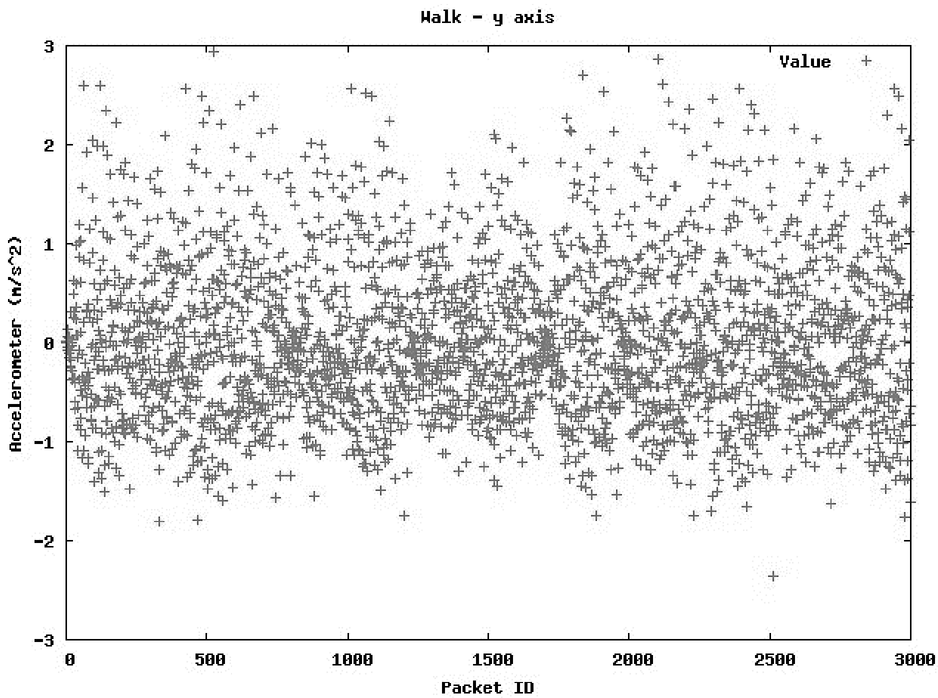

(b) y-axis

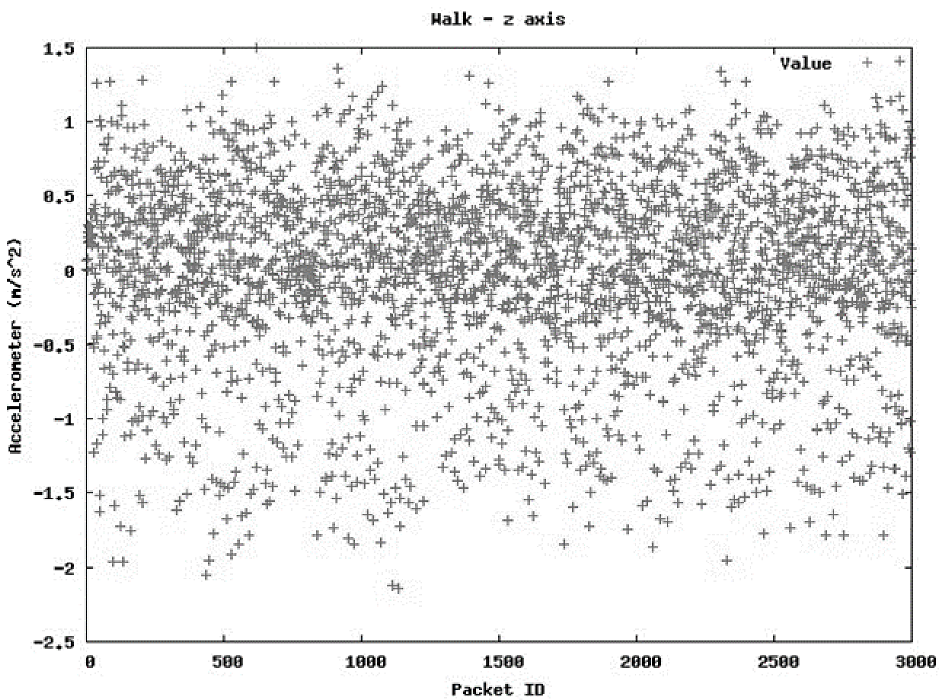

(c) z-axis

Figure 4.10: Walking accelerometer data

4.2.4 Running Accelerometer Data

The sensor node was tested under different running movements designated as shown in Table 4.4 and Figure 4.11.

Table 4.4: Packet ID in Running Movements

Packet ID	Activity
1 - 75	Running straight
76 - 225	Turning left 90º, running straight
226 - 300	Turning left 90º, running straight
301 - 450	Turning left 90º, running straight
451 - 600	Turning right 180º, running straight
601 - 675	Turning right 90º, running straight
676 - 825	Turning right 90º, running straight
826 - 900	Turning right 90º, running straight
901 - 975	Turning left 180º, running straight
976 - 1125	Turning left 90º, running straight
1126 - 1200	Turning left 90º, running straight
1201 - 1350	Turning left 90º, running straight
1351 - 1500	Turning right 180º, running straight
1501 - 1575	Turning right 90º, running straight
1576 - 1725	Turning right 90º, running straight
1726 - 1800	Turning right 90º, running straight
1801 - 1875	Turning left 180º, running straight
1876 - 2025	Turning left 90º, running straight
2026 - 2100	Turning left 90º, running straight
2101 - 2250	Turning left 90º, running straight
2251 - 2400	Turning right 180º, running straight
2401 - 2475	Turning right 90º, running straight
2476 - 2625	Turning right 90º, running straight
2626 - 2700	Turning right 90º, running straight
2701 - 2775	Turning left 180º, running straight
2776 - 2925	Turning left 90º, running straight
2926 - 3000	Turning left 90º, running straight

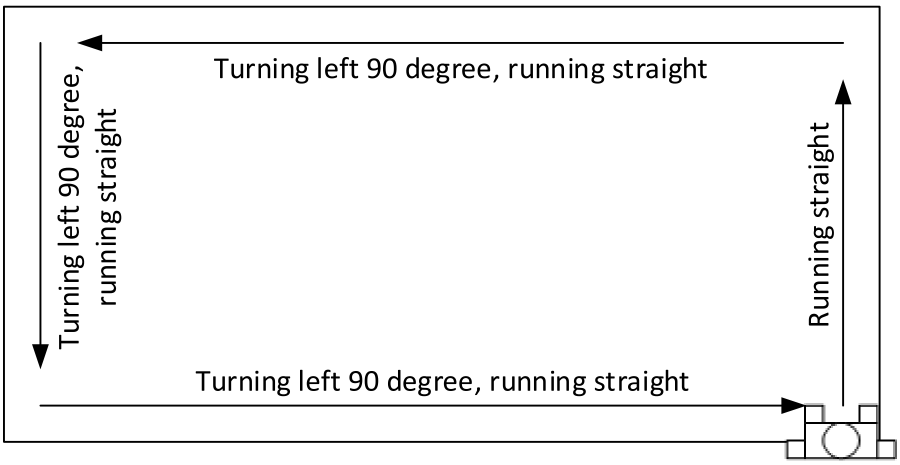

(a) Running movements in Packet ID 1-450

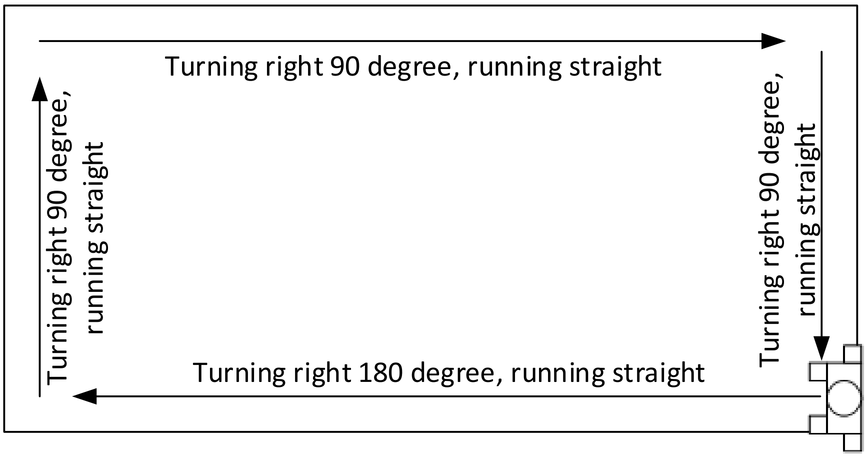

(b) Running movements in Packet ID 451-900

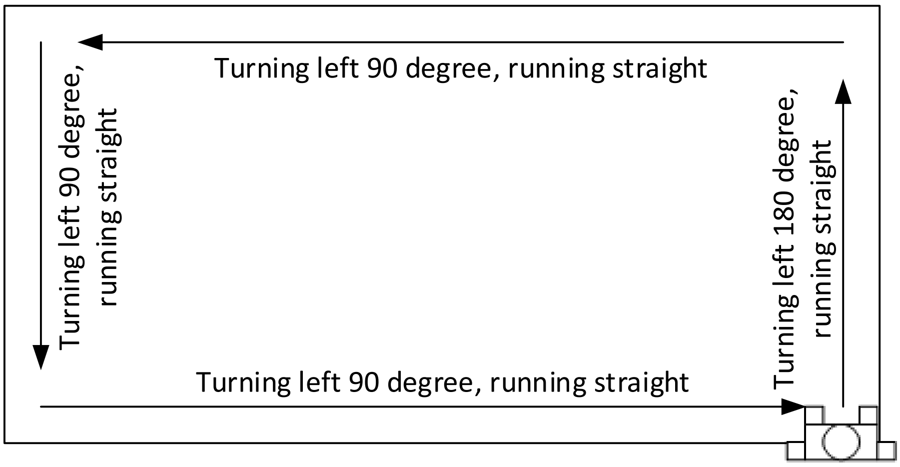

(c) Running movements in Packet ID 901-1350

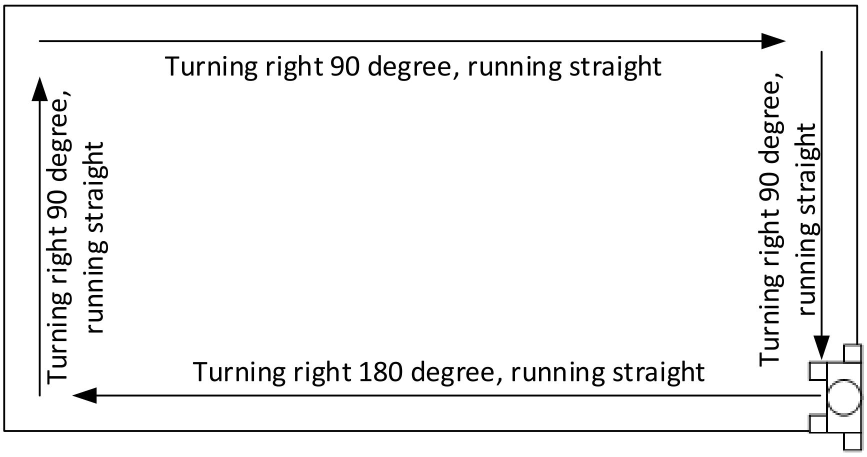

(d) Running movements in Packet ID 1351-1800

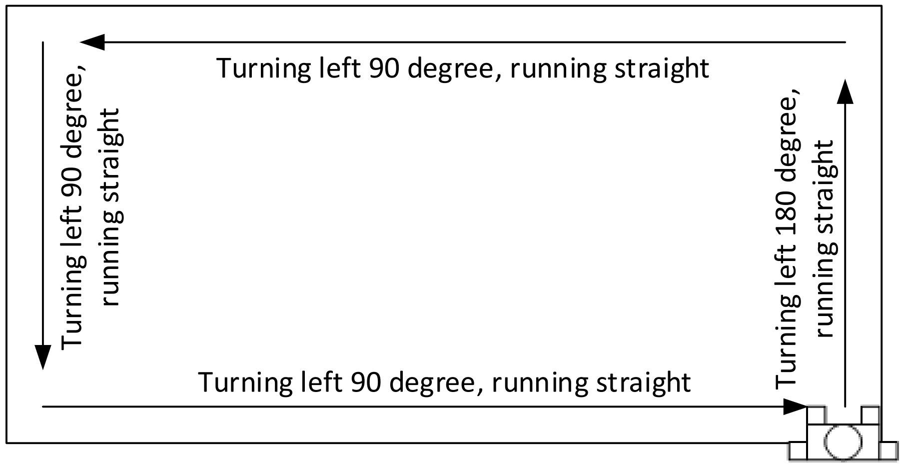

(e) Running movements in Packet ID 1801-2250

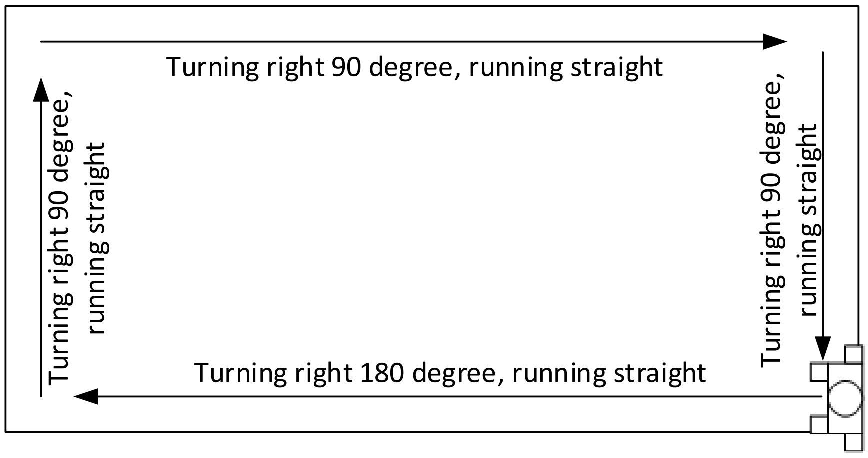

(f) Running movements in Packet ID 2251-2700

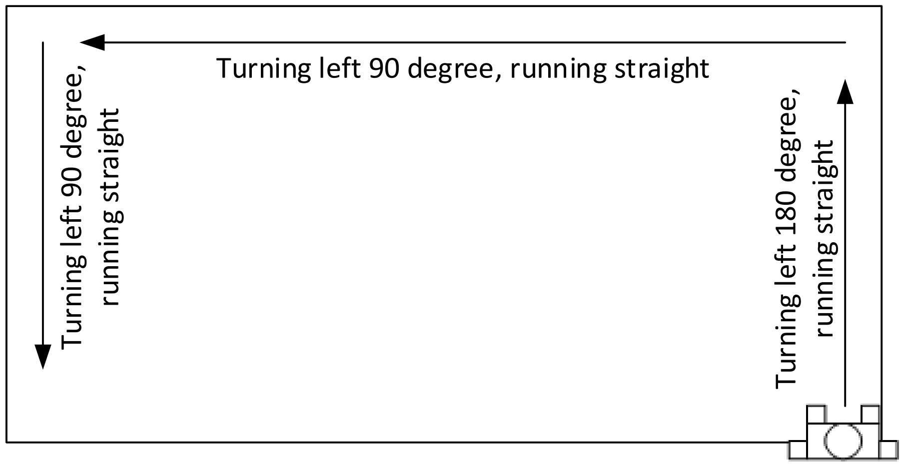

(g) Running movements in Packet ID 2701-3000

Figure 4.11: Running movements

The results of the experiment are shown in Figure 4.12.

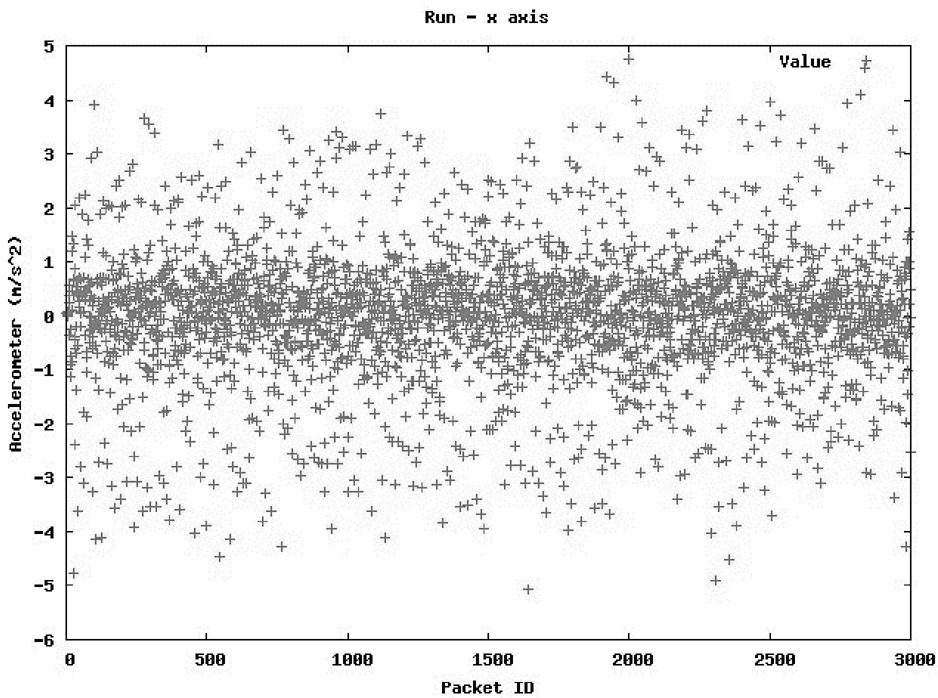

(a) x-axis

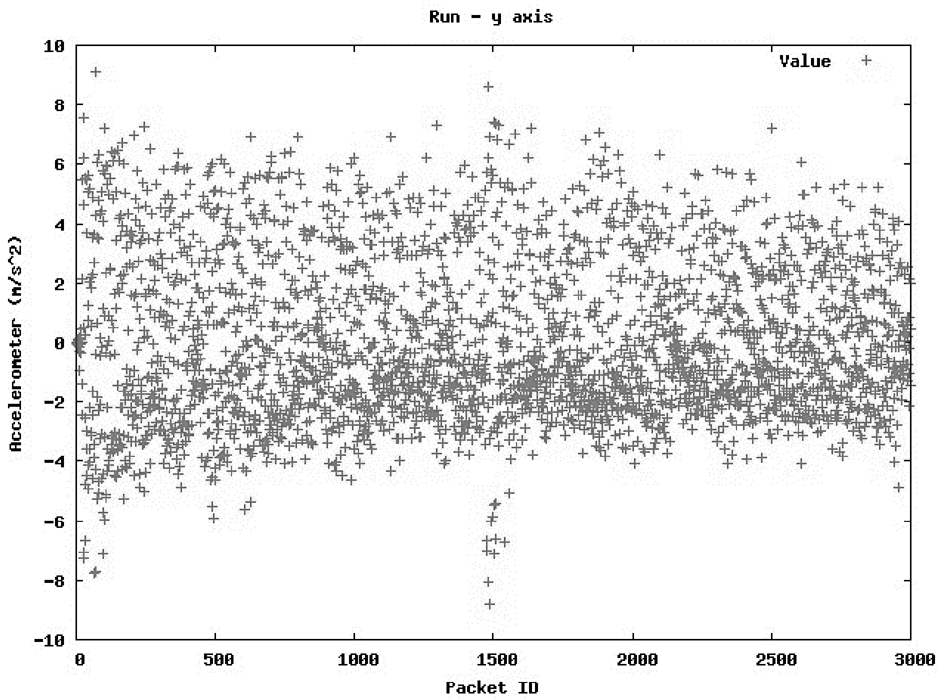

(b) y-axis

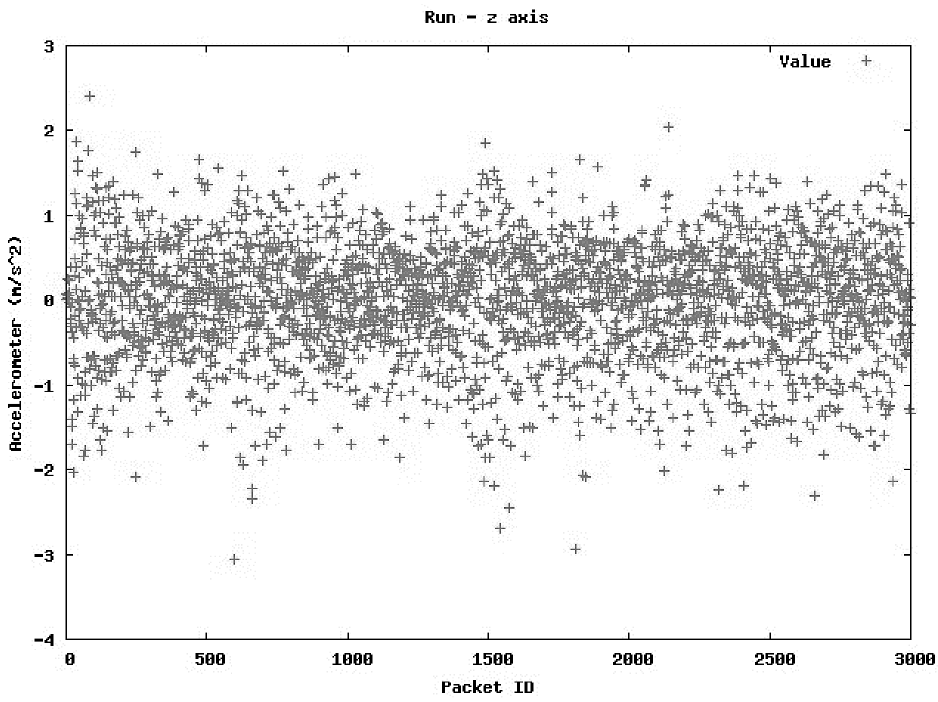

(c) z-axis

Figure 4.12: Running accelerometer data

4.3 Concluding Remarks

In conclusion, experiments had been done to collect the necessary data. Two experiments on each categories of application, which are application/attribute with low sampling rate and application/attribute with abrupt sampling rate had been done. Generally, each of the sensed data will be reported to the base station and the information's accuracy of the collected data is very reliable (100%). Therefore, Data Abstraction and Reformation (DAR) schemes are proposed to reduce the number of communications without greatly affecting the information's accuracy.

CHAPTER 5

EXPERIMENT RESULTS

Four parameters are introduced to quantify the performance of the proposed scheme. They are the number of packet transmission, number of data transmitted, root mean square error ($RMSE$) (Reyes et al., 2010), and mean absolute percentage error ($MAPE$) (Stellwagen. E., 2010).

Number of packet transmission is the total number of packet transmission from a sensor node to a base station whereby number of data transmitted is percentage number of data transmitted over the total number of data sensed from a sensor node to a base station. It is not necessary that the number of packet transmission equals to the number of data transmitted.

$RMSE$ is used to measure the difference between the sensed value and the reformed value. The best performance in $RMSE$ is when the $RMSE$ equals to 0.

$$RMSE = \sqrt{\frac{\sum(y_i - \hat{y}_i)^2}{n}}$$

where y_i is the sensed value, $\hat{y}_i$ is the reformed value and n is the total number of data sampling.

$MAPE$ is used to measure the unsigned percentage of error between the sensed value and the reformed value. The best performance in $MAPE$ is when the $MAPE$ equals to 0%.

$$MAPE = \frac{\sum_{i=1}^{n} \frac{|y_i - \hat{y}_i|}{|y_i|}}{n} \times 100\%$$

where y_i is the sensed value, $\hat{y}_i$ is the reformed value and n is the total number of data sampling.

The performance of the data abstraction will be quantified by the number of packet transmissions and number of data transmitted; and the performance of data reformation will be quantified by the value of $RMSE$ and $MAPE$.

5.1 Application/Attribute with Low Sampling Rate

In temperature-sensed values, there is only a temperature value. Therefore, in order to determine the transmission of values, the temperature value will be directly compared with a threshold value. In the following section, the performance of DAR schemes in temperature sensor in different patterns of data will be discussed.

5.1.1 Burst Temperature Data

In this experiment, the number of the packets of data is 600. The results of implementation of the DAR schemes in the terms of data abstraction (number of packet transmissions and number of data transmitted) and data reformation ($RMSE$ and $MAPE$) are as follows.

1. Number of Packet Transmissions

   Number of packet transmissions of burst temperature data in different orders of data abstraction are shown in Figure 5.1.

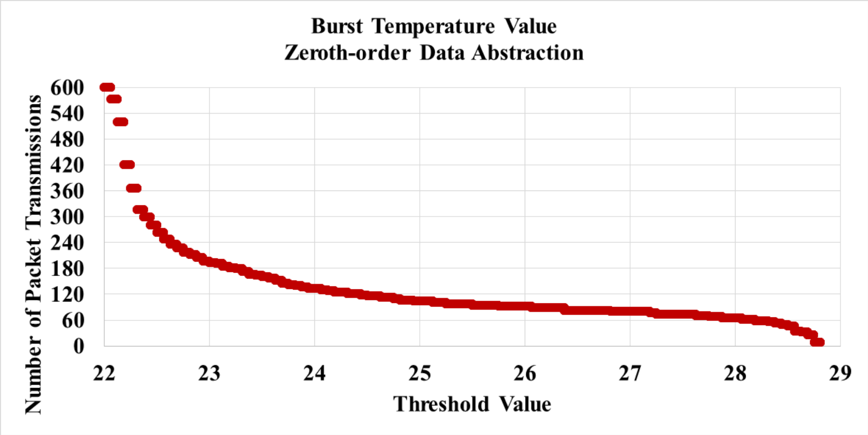

(a) Number of packet transmissions of burst temperature data in zeroth-order data abstraction

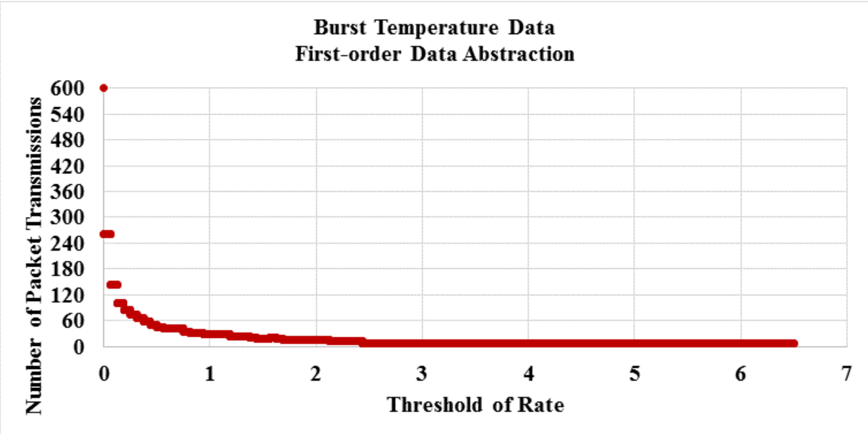

(b) Number of packet transmissions of burst temperature data in first-order data abstraction

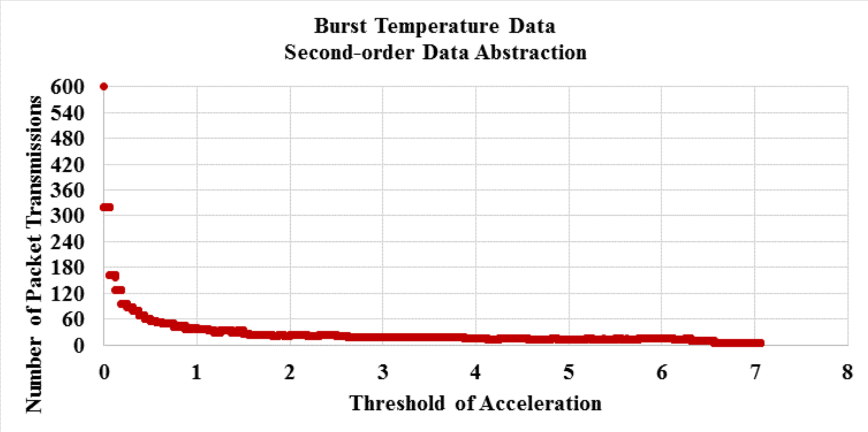

(c) Number of packet transmissions of burst temperature data in second-order data abstraction

Figure 5.1: Number of packet transmissions of burst temperature data

From the Figure 5.1, it is shown that the increment of threshold value, threshold of rate and threshold of acceleration will always reduce the number of packet transmissions.

2. Number of Data Transmitted

Number of data transmitted of burst temperature data in different orders of data abstraction are shown in Figure 5.2.

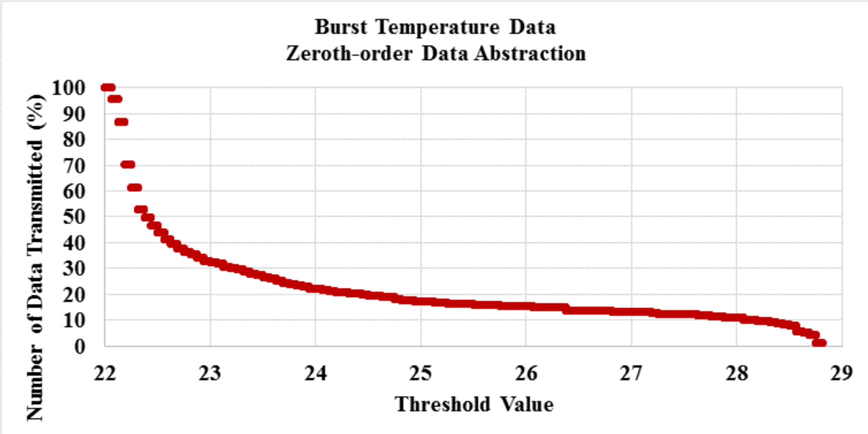

(a) Number of data transmitted of burst temperature data in zeroth-order data abstraction

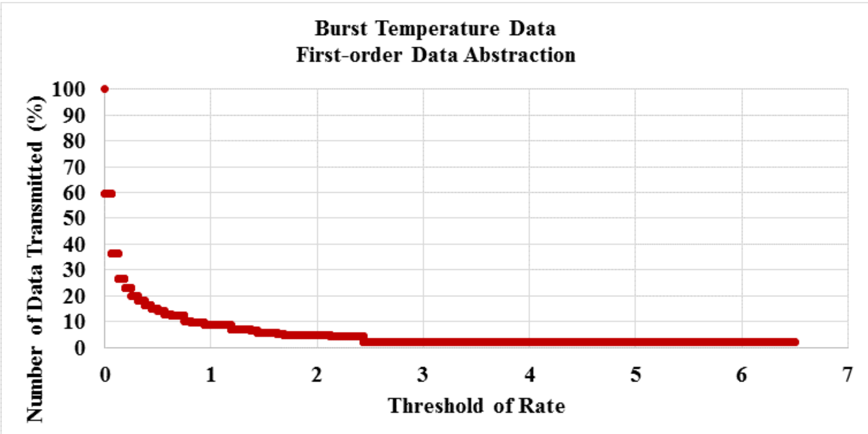

(b) Number of data transmitted of burst temperature data in first-order data abstraction

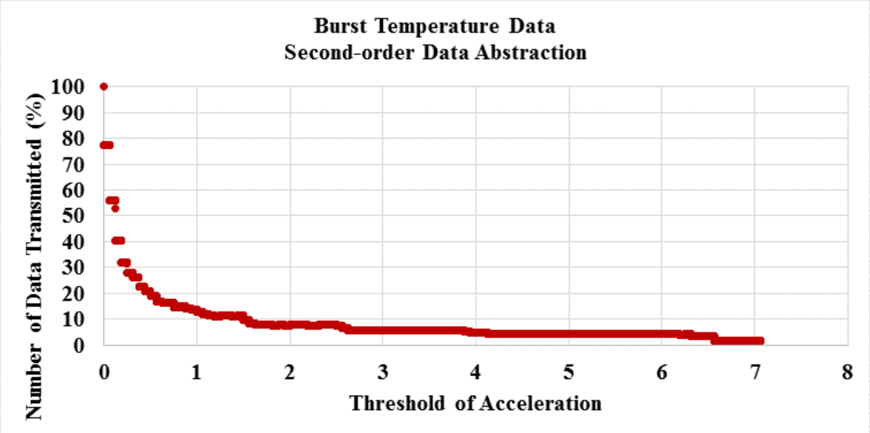

(c) Number of data transmitted of burst temperature data in second-order data abstraction

Figure 5.2: Number of data transmitted of burst temperature data

From the Figure 5.2, it is shown that the increment of threshold value will reduce the number of data transmitted. However, the increment of threshold of rate and threshold of acceleration will not necessarily reduce the number of data transmitted.

3. Root Mean Square Error

Root mean square error of burst temperature data in different orders of data abstraction and reformation are shown from Figure 5.3.

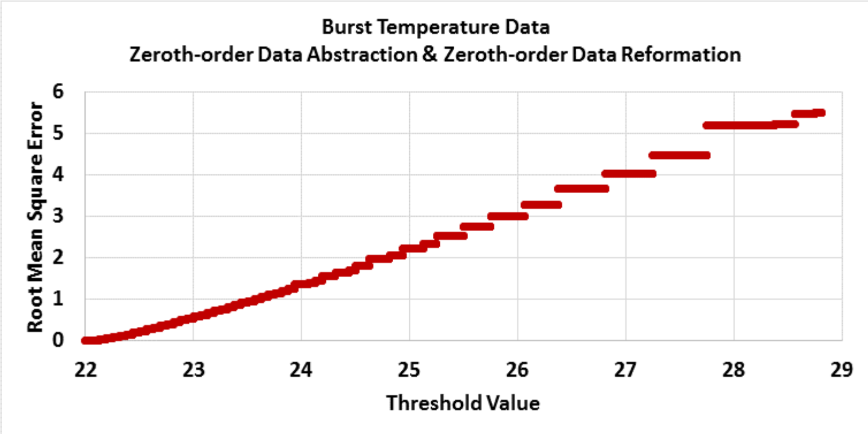

(a) Root mean square error of burst temperature data in zeroth-order data abstraction & zeroth-order data reformation

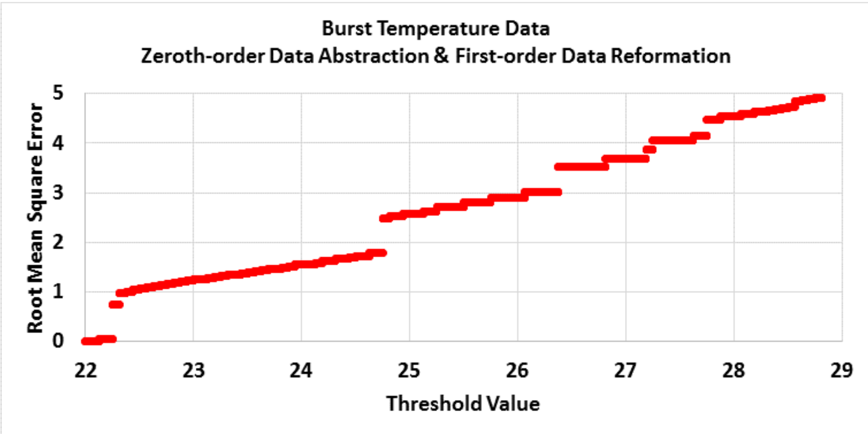

(b) Root mean square error of burst temperature data in zeroth-order data abstraction & first-order data reformation

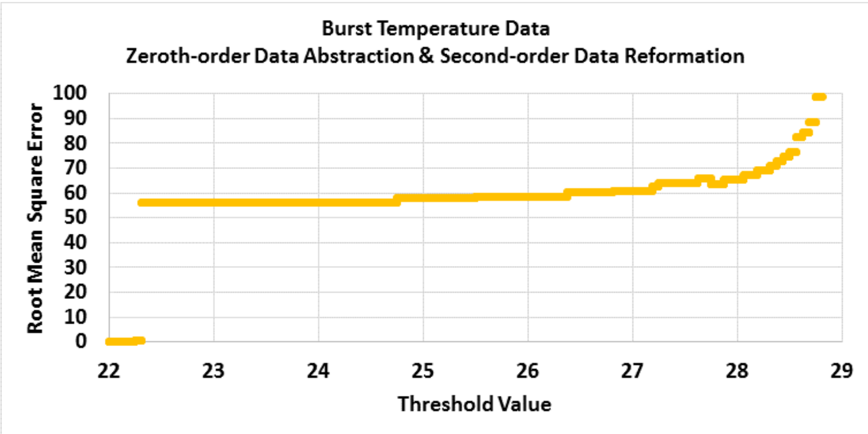

(c) Root mean square error of burst temperature data in zeroth-order data abstraction & second-order data reformation

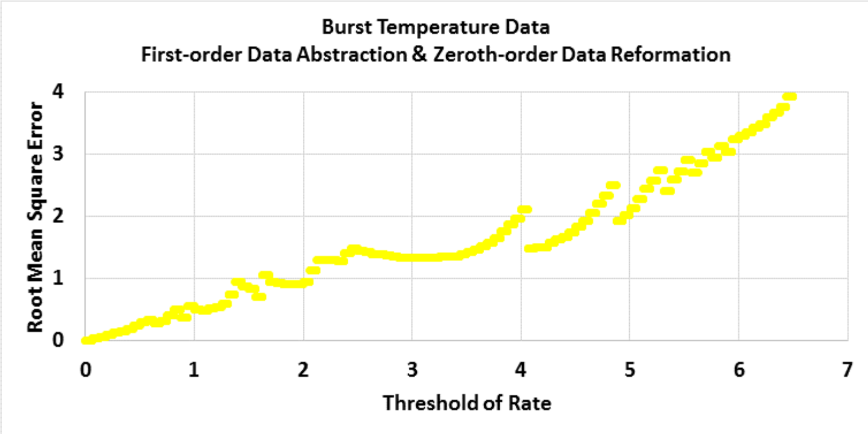

(d) Root mean square error of burst temperature data in first-order data abstraction & zeroth-order data reformation

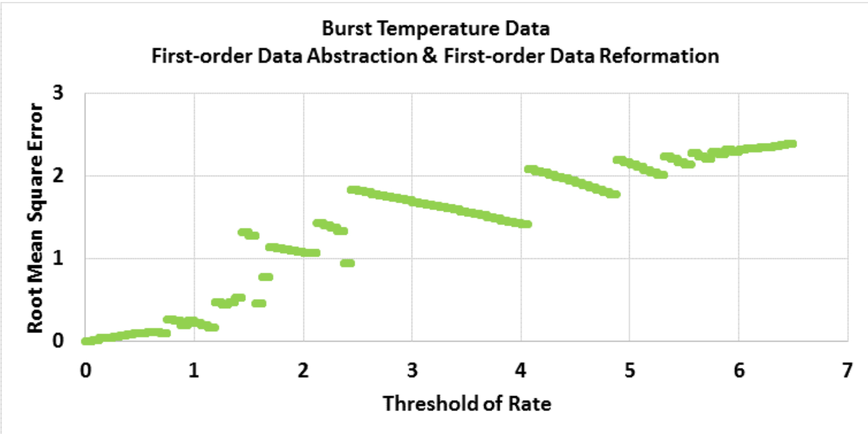

(e) Root mean square error of burst temperature data in first-order data abstraction & first-order data reformation

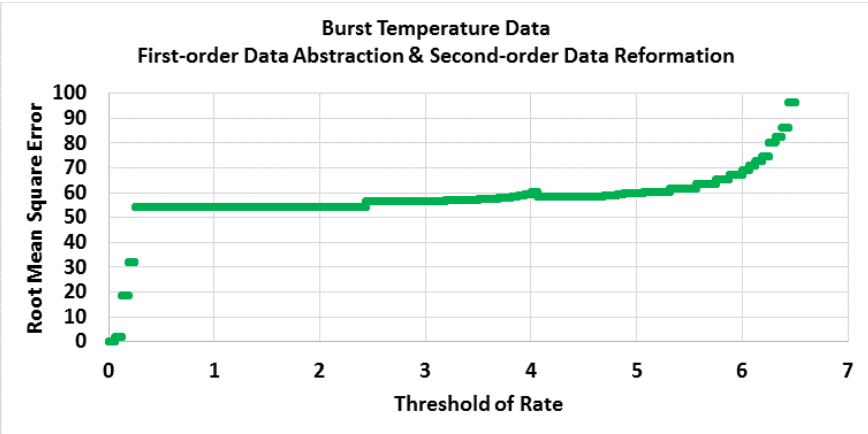

(f) Root mean square error of burst temperature data in first-order data abstraction & second-order data reformation

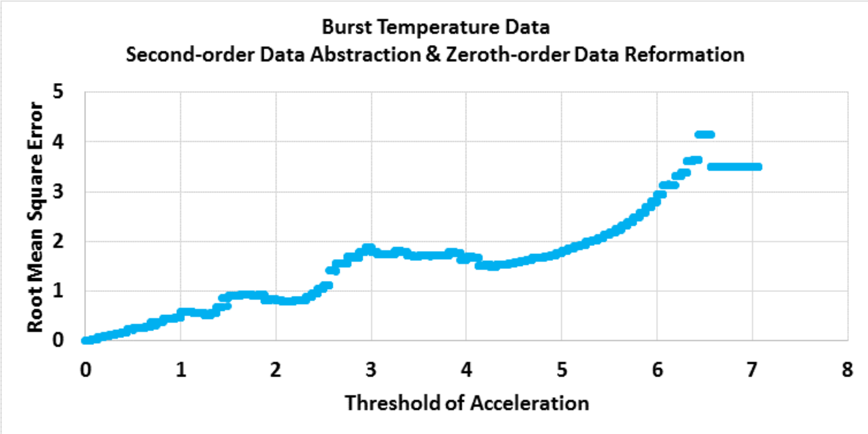

(g) Root mean square error of burst temperature data in second-order data abstraction & zeroth-order data reformation

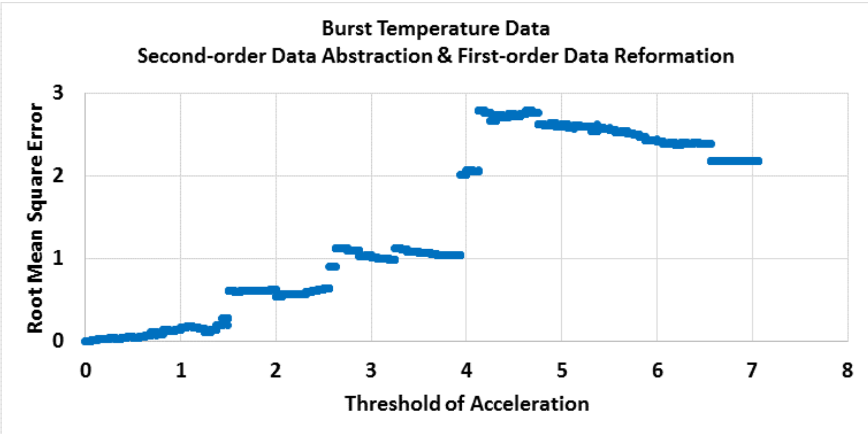

(h) Root mean square error of burst temperature data in second-order data abstraction & first-order data reformation

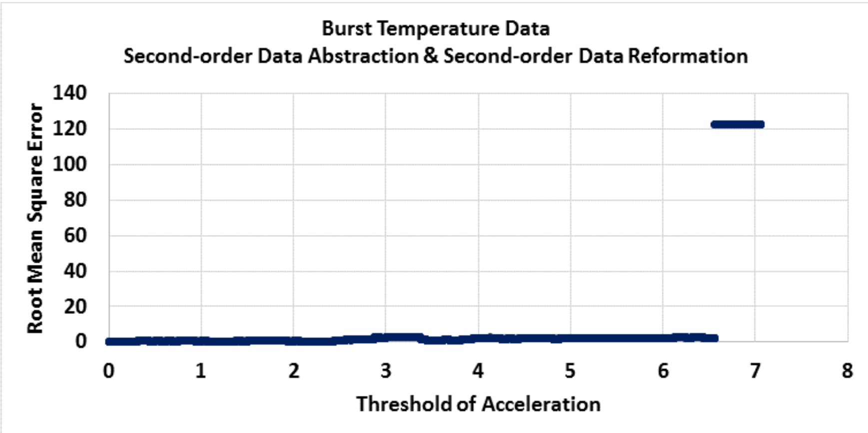

(i) Root mean square error of burst temperature data in second-order data abstraction & second-order data reformation

Figure 5.3: Root mean square error of burst temperature data

From the Figure 5.3, it is shown that the increment of threshold value, threshold of rate and threshold of acceleration will not necessarily increase the root mean square error.

4. Mean Absolute Percentage Error

Mean absolute percentage error of burst temperature data in different orders of data abstraction are shown from Figure 5.4.

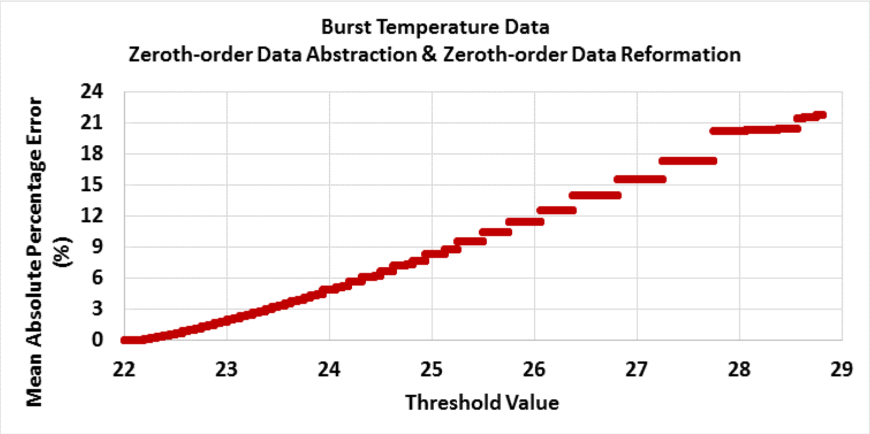

(a) Mean absolute percentage error of burst temperature data in zeroth-order data abstraction & zeroth-order data reformation

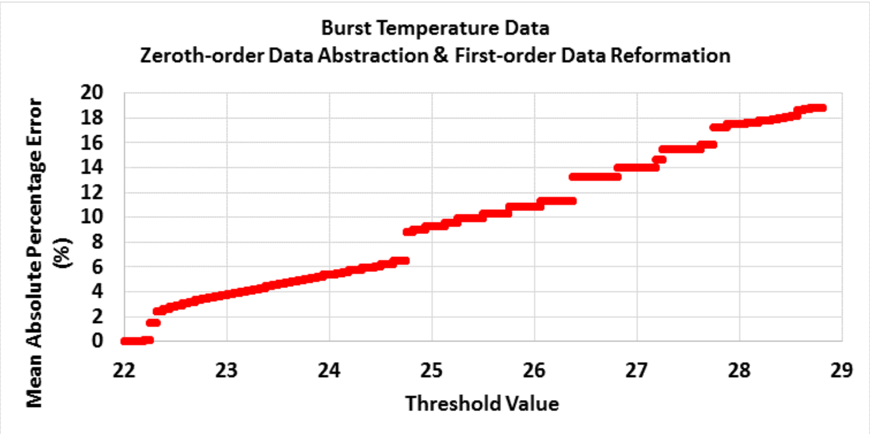

(b) Mean absolute percentage error of burst temperature data in zeroth-order data abstraction & first-order data reformation

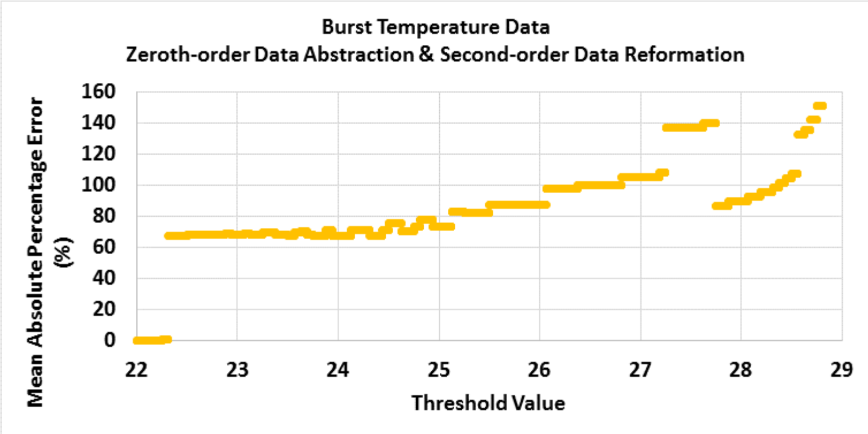

(c) Mean absolute percentage error of burst temperature data in zeroth-order data abstraction & second-order data reformation

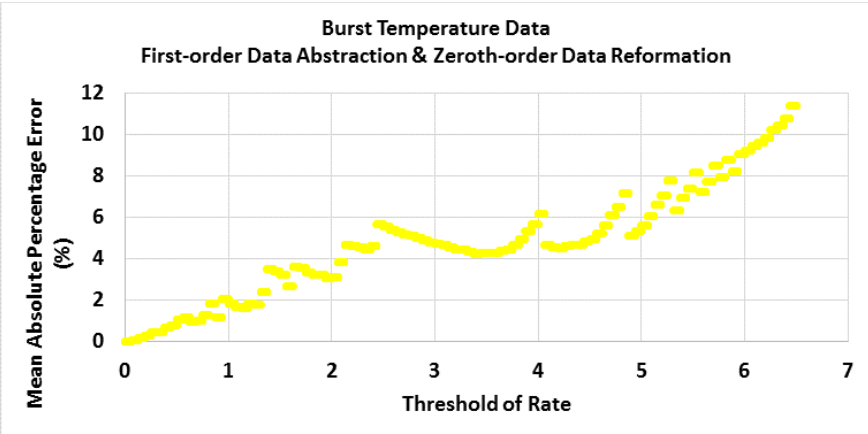

(d) Mean absolute percentage error of burst temperature data in first-order data abstraction & zeroth-order data reformation

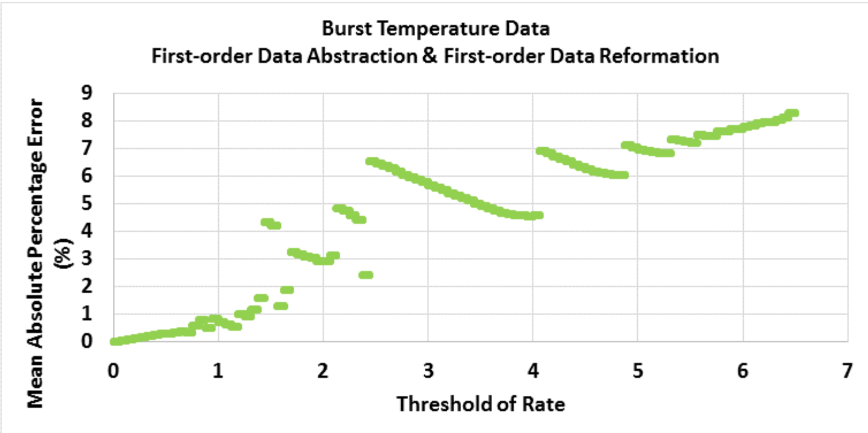

(e) Mean absolute percentage error of burst temperature data in first-order data abstraction & first-order data reformation

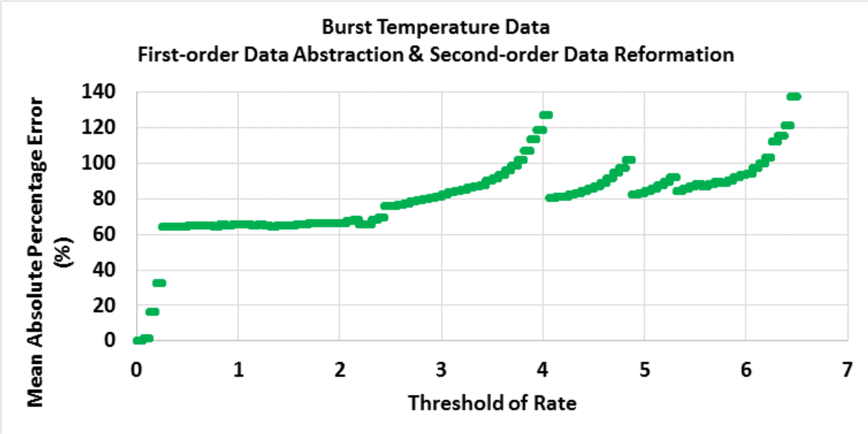

(f) Mean absolute percentage error of burst temperature data in first-order data abstraction & second-order data reformation

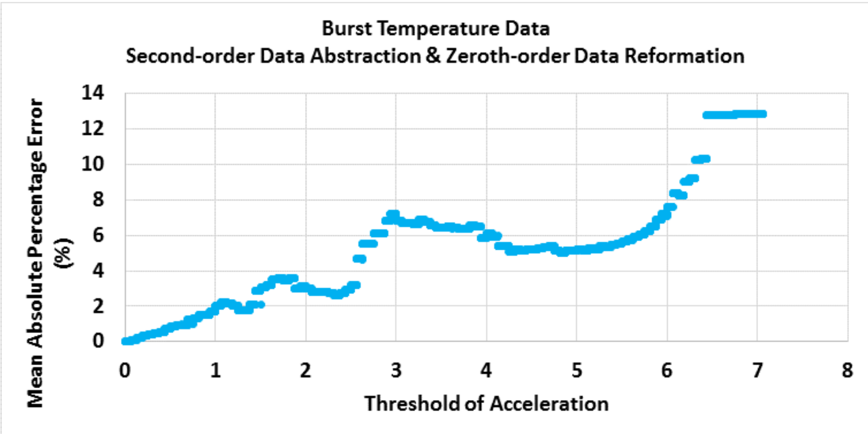

(g) Mean absolute percentage error of burst temperature data in second-order data abstraction & zeroth-order data reformation

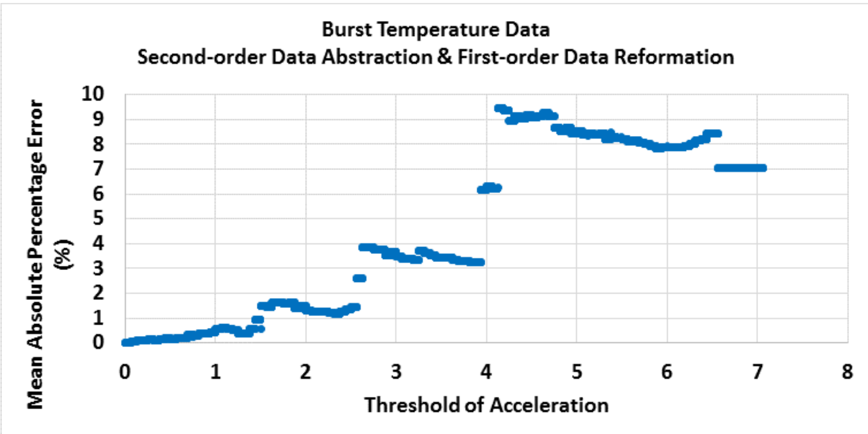

(h) Mean absolute percentage error of burst temperature data in second-order data abstraction & first-order data reformation

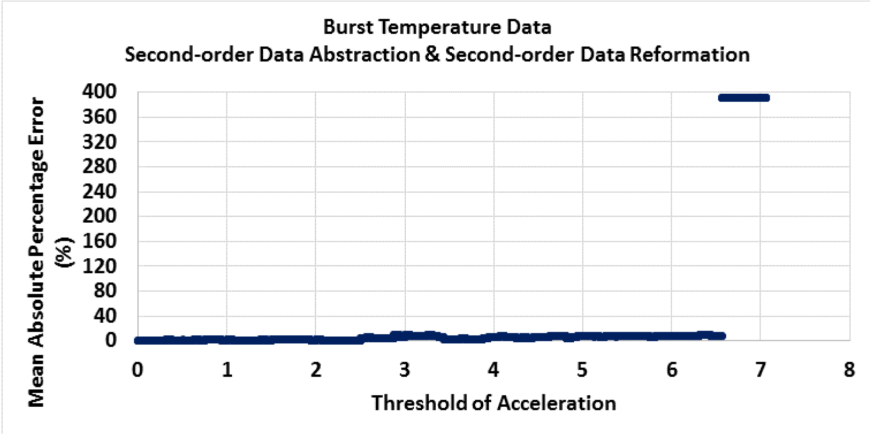

(i) Mean absolute percentage error of burst temperature data in second-order data abstraction & second-order data reformation

Figure 5.4: Mean absolute percentage error of burst temperature data

From the Figure 5.4, it is shown that the increment of threshold value, threshold of rate and threshold of acceleration will not necessarily increase the mean absolute percentage error.

5.1.2 Incremental & Decremental Temperature Data

In this experiment, the number of the packets of data is 600. The results of implementation of the DAR schemes in the terms of data abstraction (number of packet transmissions and number of data transmitted) and data reformation ($RMSE$ and $MAPE$) are as follows.

1. Number of Packet Transmissions

   Number of packet transmissions of incremental & decremental temperature data in different orders of data abstraction are shown in Figure 5.5.

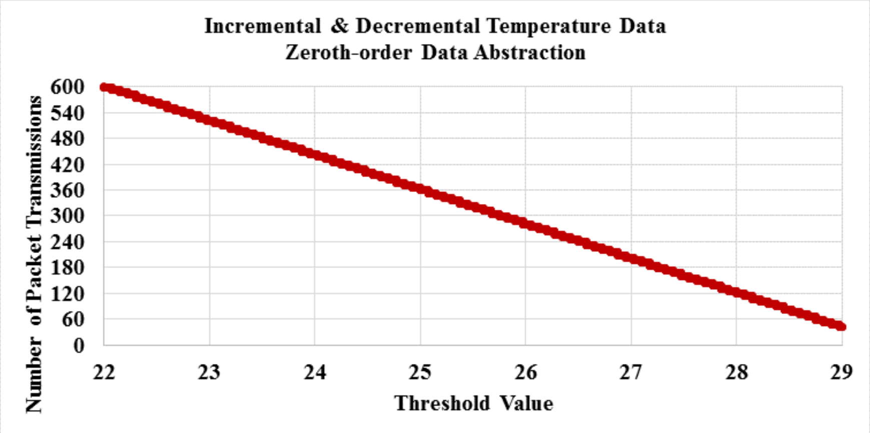

(a) Number of packet transmissions of incremental & decremental temperature data in zeroth-order data abstraction

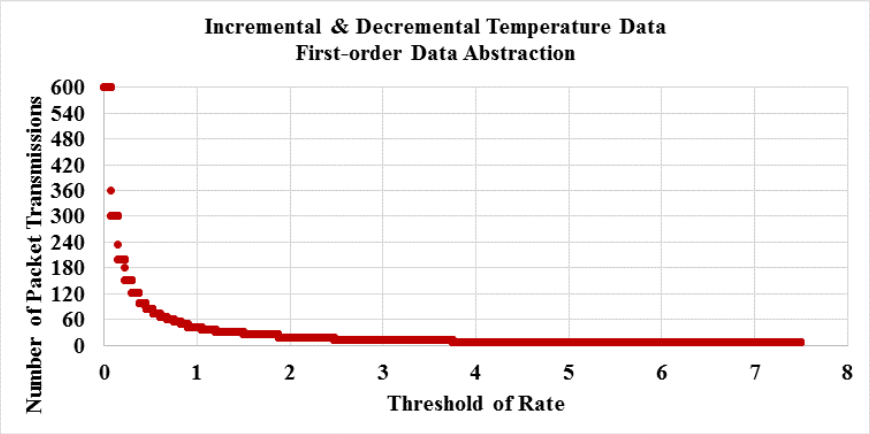

(b) Number of packet transmissions of incremental & decremental temperature data in first-order data abstraction

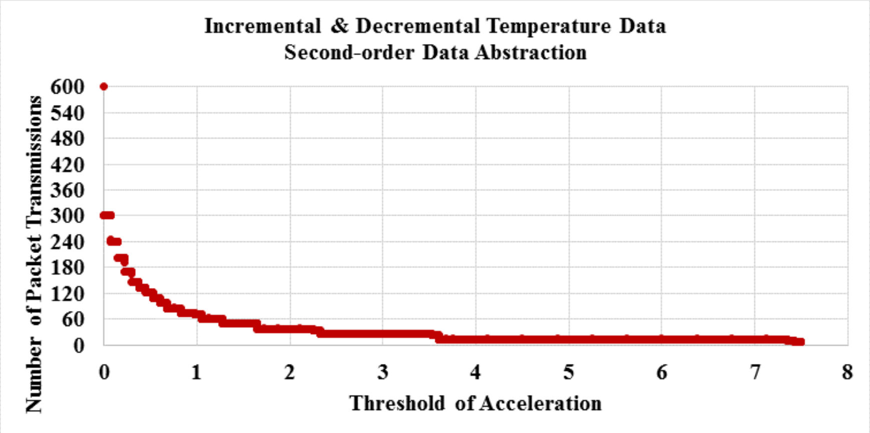

(c) Number of packet transmissions of incremental & decremental temperature data in second-order data abstraction

Figure 5.5: Number of packet transmissions of incremental & decremental temperature data

From the Figure 5.5, it is shown that the increment of threshold value will reduce the number of packet transmissions. However, the increment of threshold of rate and threshold of acceleration will not necessarily reduce the number of packet transmissions.

2. Number of Data Transmitted

Number of data transmitted of incremental & decremental temperature data in different orders of data abstraction are shown in Figure 5.6.

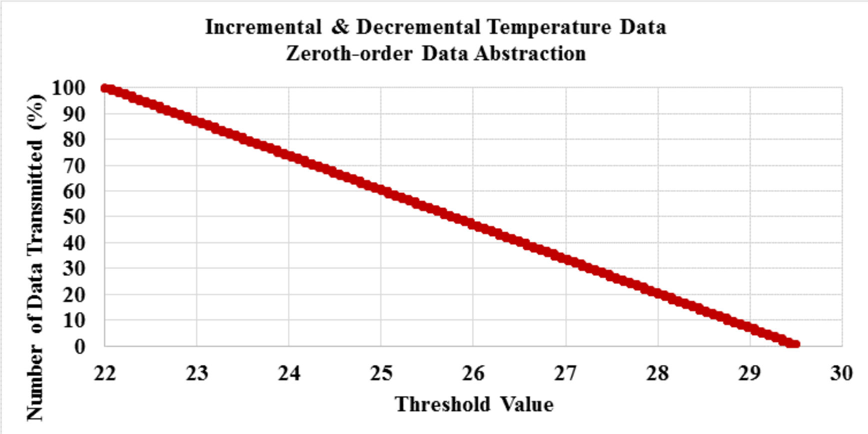

(a) Number of data transmitted of incremental & decremental temperature data in zeroth-order data abstraction

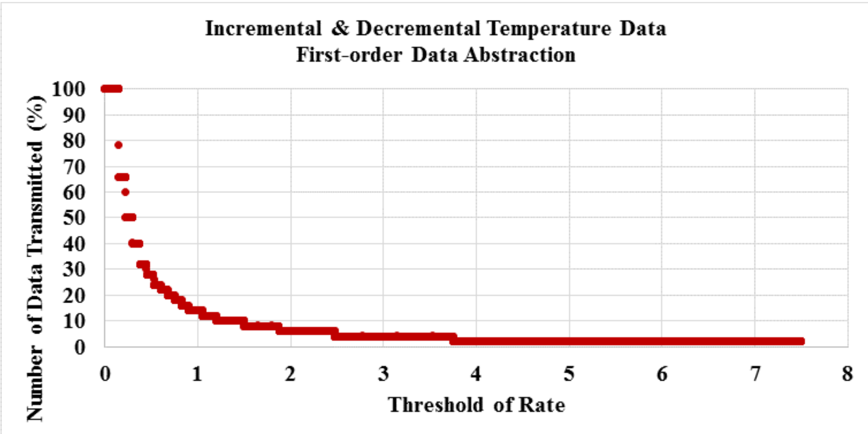

(b) Number of data transmitted of incremental & decremental temperature data in first-order data abstraction

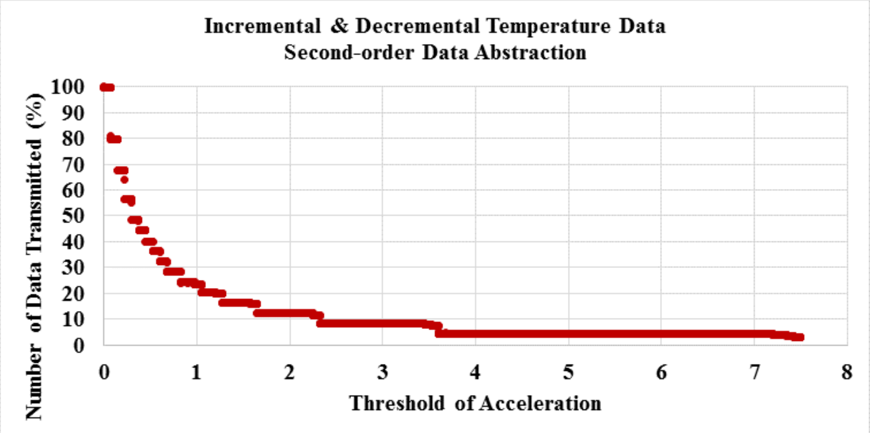

(c) Number of data transmitted of incremental & decremental temperature data in second-order data abstraction

Figure 5.6: Number of data transmitted in incremental & decremental temperature data

From the Figure 5.6, it is shown that the increment of threshold value will reduce the number of data transmitted. However, the increment of threshold of rate and threshold of acceleration will not necessarily reduce the number of data transmitted.

3. Root Mean Square Error

Root mean square error of incremental & decremental temperature data in different orders of data abstraction and reformation are shown from Figure 5.7.

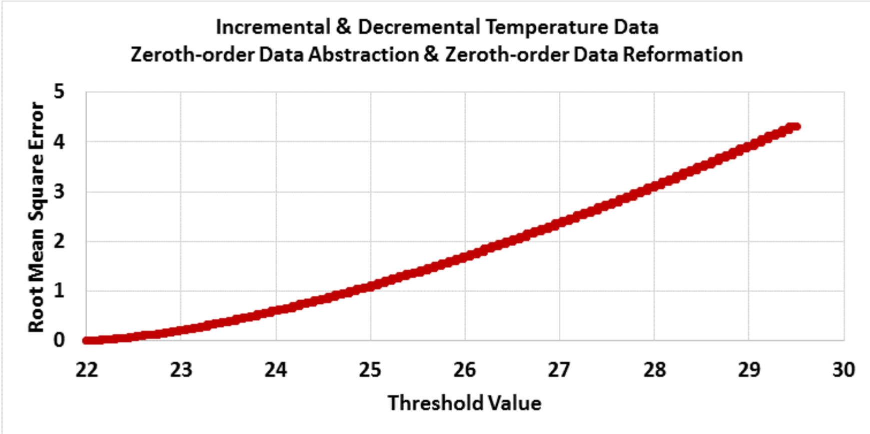

(a) Root mean square error of incremental & decremental temperature data in zeroth-order data abstraction & zeroth-order data reformation

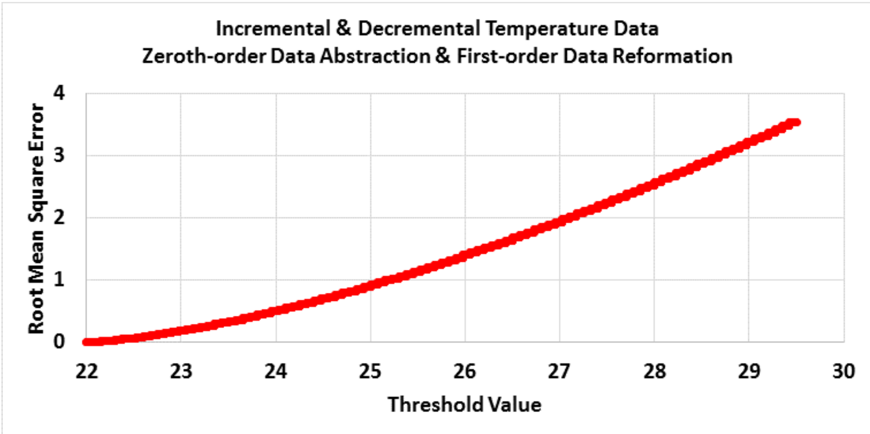

(b) Root mean square error of incremental & decremental temperature data in zeroth-order data abstraction & first-order data reformation

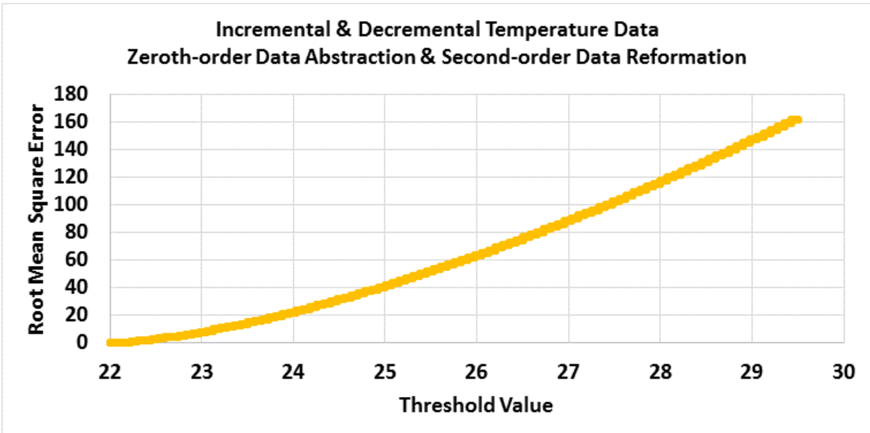

(c) Root mean square error of incremental & decremental temperature data in zeroth-order data abstraction & second-order data reformation

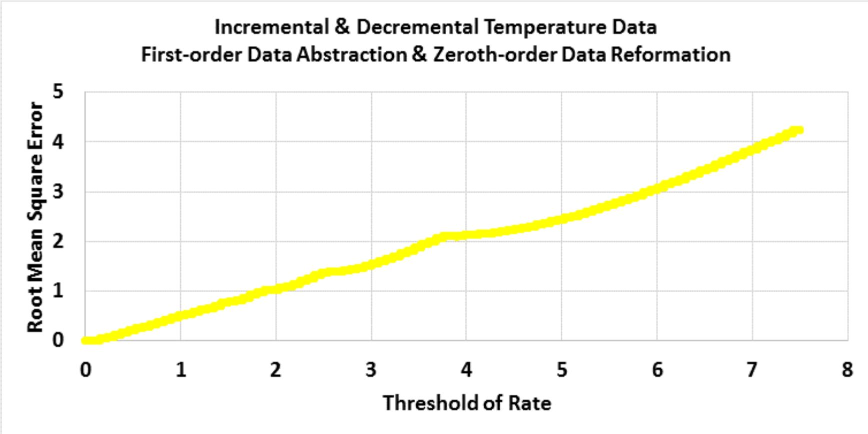

(d) Root mean square error of incremental & decremental temperature data in first-order data abstraction & zeroth-order data reformation

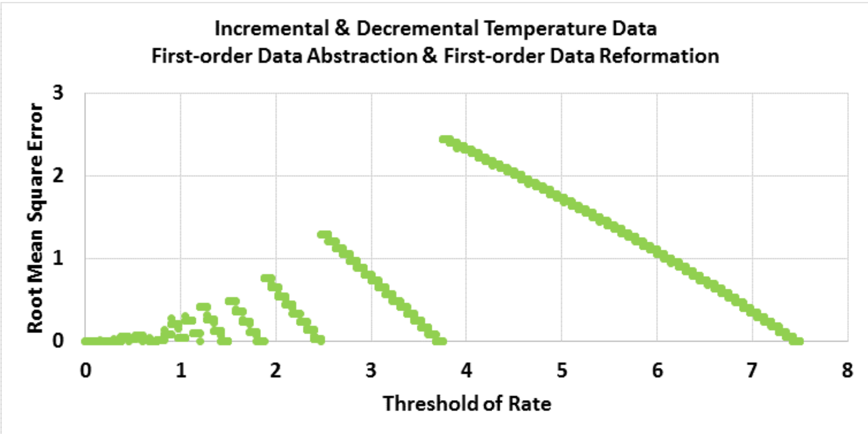

(e) Root mean square error of incremental & decremental temperature data in first-order data abstraction & first-order data reformation

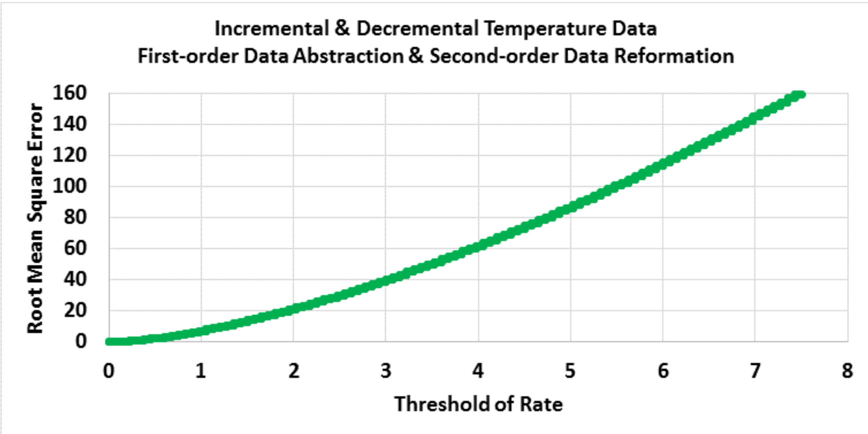

(f) Root mean square error of incremental & decremental temperature data in first-order data abstraction & second-order data reformation

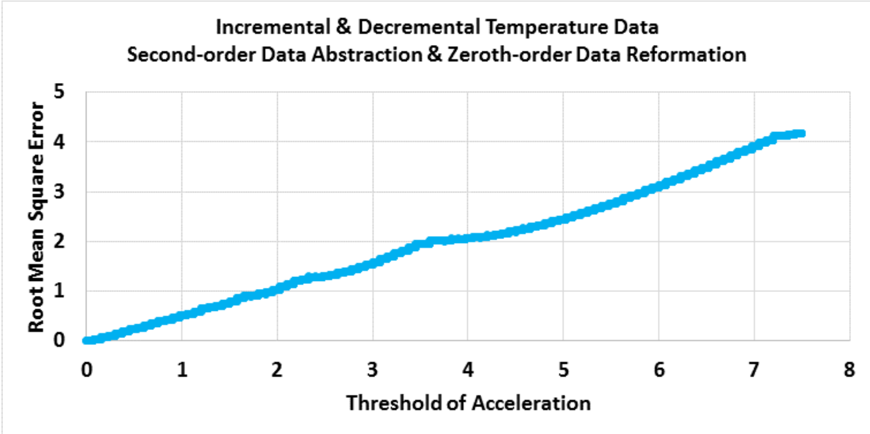

(g) Root mean square error of incremental & decremental temperature data in second-order data abstraction & zeroth-order data reformation

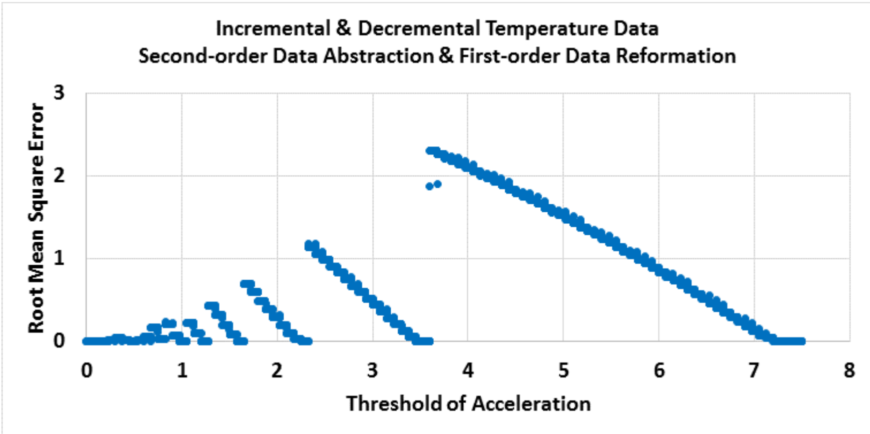

(h) Root mean square error of incremental & decremental temperature data in second-order data abstraction & first-order data reformation

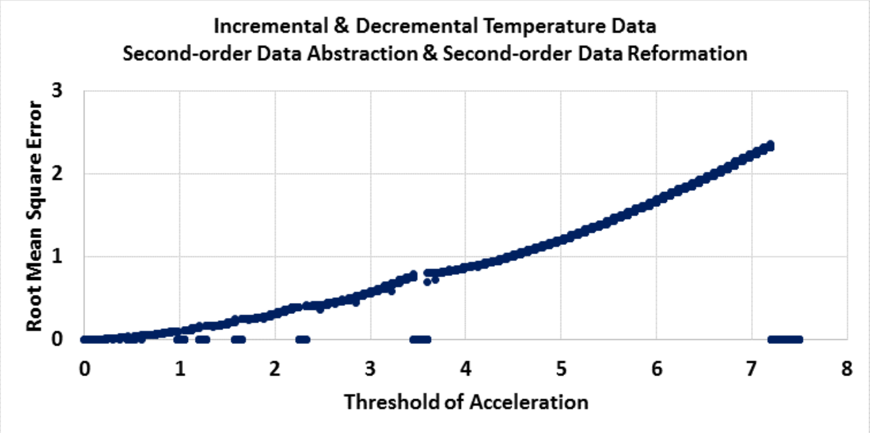

(i) Root mean square error of incremental & decremental temperature data in second-order data abstraction & second-order data reformation

Figure 5.7: Root mean square error of incremental & decremental temperature data

From the Figure 5.7, it is shown that the increment of threshold value will increase the root mean square error. However, the increment of threshold of rate and threshold of acceleration will not necessarily increase the root mean square error.

4. Mean Absolute Percentage Error

Mean absolute percentage error of incremental & decremental temperature data in different orders of data abstraction are shown from Figure 5.8.

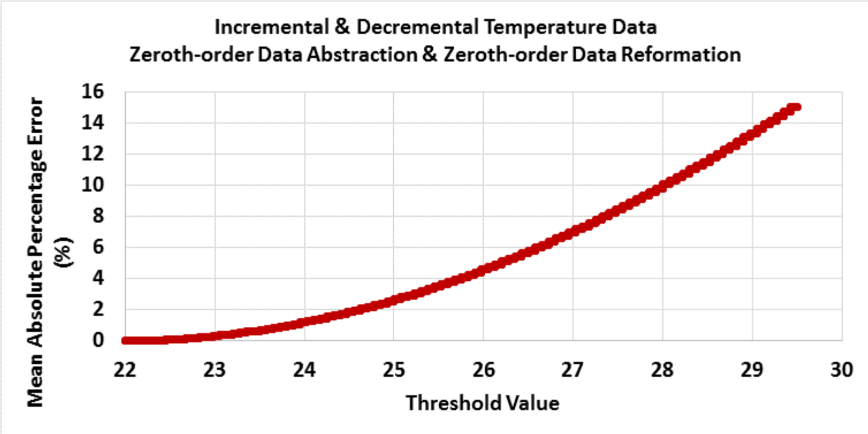

(a) Mean absolute percentage error of incremental & decremental temperature data in zeroth-order data abstraction & zeroth-order data reformation

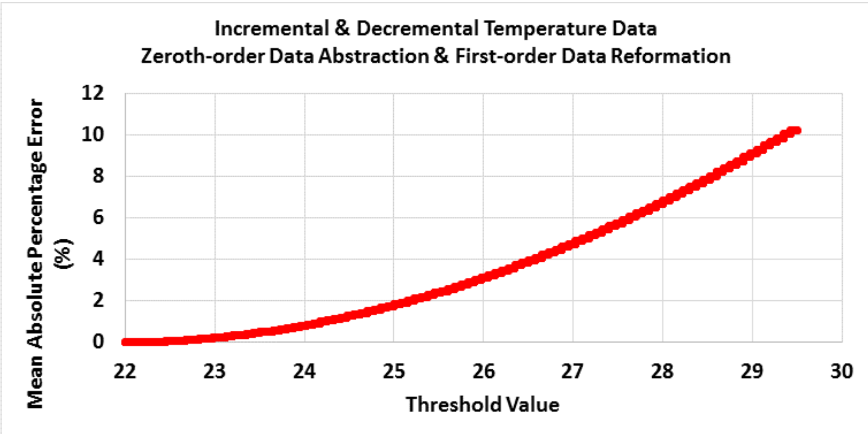

(b) Mean absolute percentage error of incremental & decremental temperature data in zeroth-order data abstraction & first-order data reformation

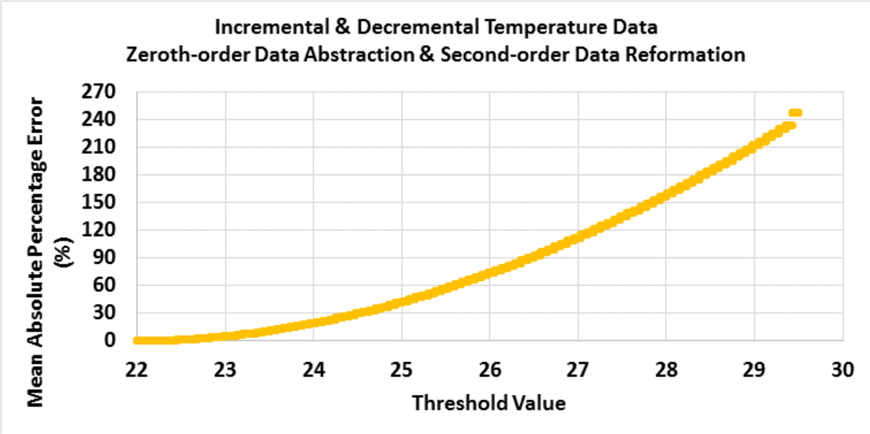

(c) Mean absolute percentage error of incremental & decremental temperature data in zeroth-order data abstraction & second-order data reformation

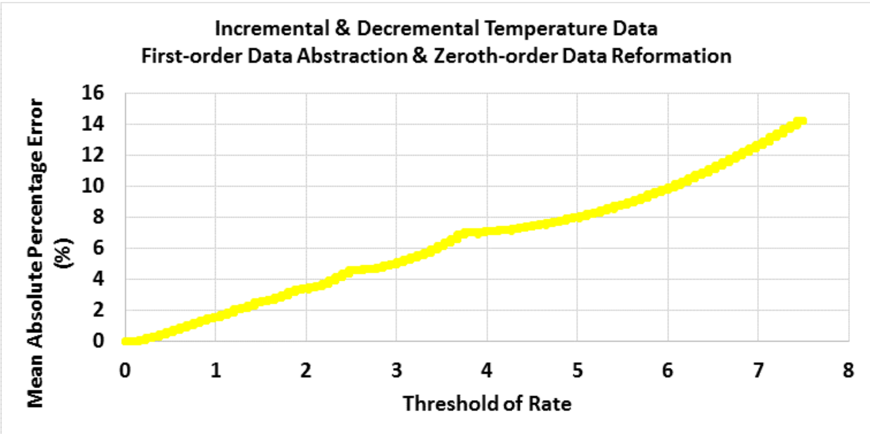

(d) Mean absolute percentage error of incremental & decremental temperature data in first-order data abstraction & zeroth-order data reformation

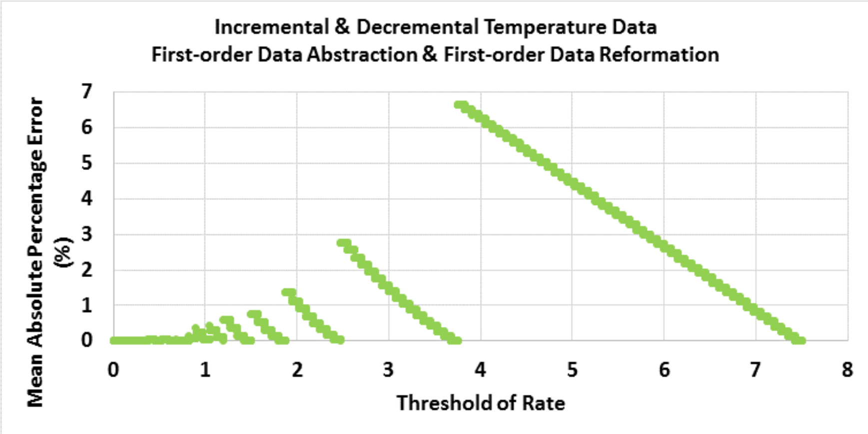

(e) Mean absolute percentage error of incremental & decremental temperature data in first-order data abstraction & first-order data reformation

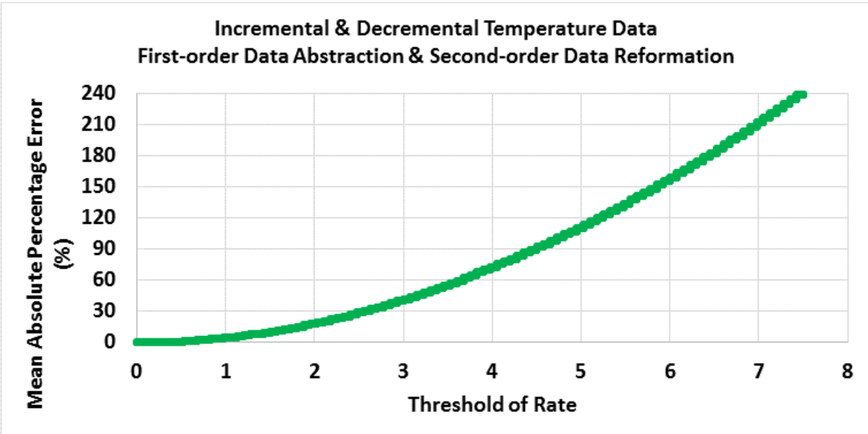

(f) Mean absolute percentage error of incremental & decremental temperature data in first-order data abstraction & second-order data reformation

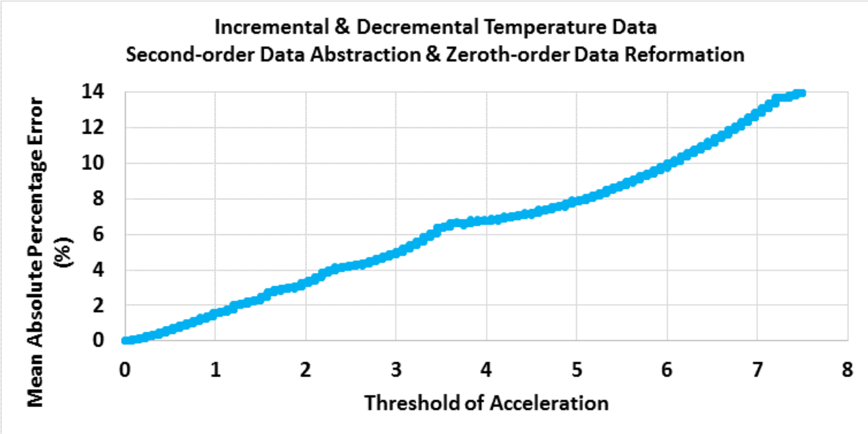

(g) Mean absolute percentage error of incremental & decremental temperature data in second-order data abstraction & zeroth-order data reformation

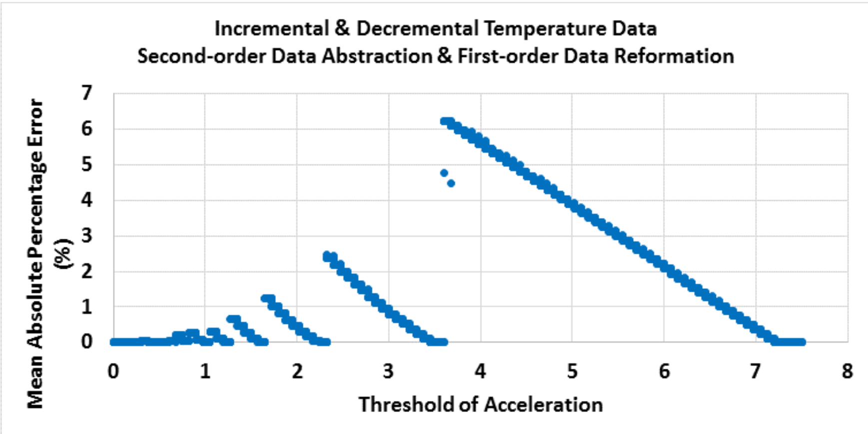

(h) Mean absolute percentage error of incremental & decremental temperature data in second-order data abstraction & first-order data reformation

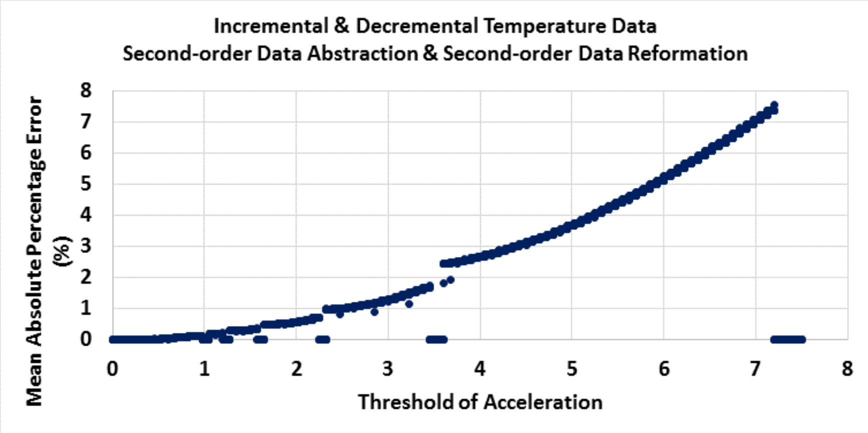

(i) Mean absolute percentage error of incremental & decremental temperature data in second-order data abstraction & second-order data reformation

Figure 5.8: Mean absolute percentage error of incremental & decremental temperature data

From the Figure 5.8, it is shown that the increment of threshold value will increase the mean absolute percentage error. However, the increment of threshold of rate and threshold of acceleration will not necessarily increase the mean absolute percentage error.

5.1.3 Random Temperature Data

In this experiment, the number of the packets of data is 600. The results of implementation of the DAR schemes in the terms of data abstraction (number of packet transmissions and number of data transmitted) and data reformation ($RMSE$ and $MAPE$) are as follows.

1. Number of Packet Transmissions

Number of packet transmissions of random temperature data in different orders of data abstraction are shown in Figure 5.9.

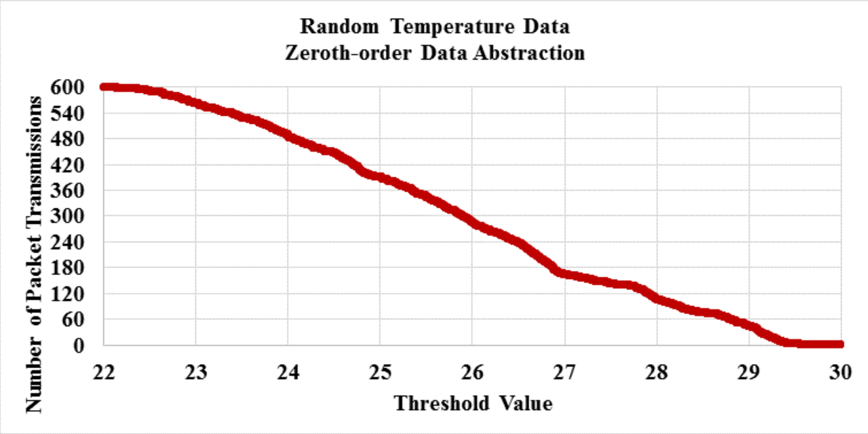

(a) Number of packet transmissions of random temperature data in zeroth-order data abstraction

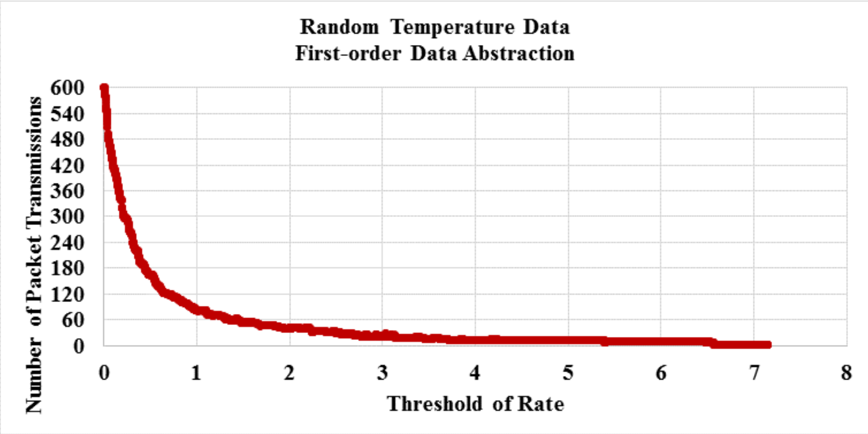

(b) Number of packet transmissions of random temperature data in first-order data abstraction

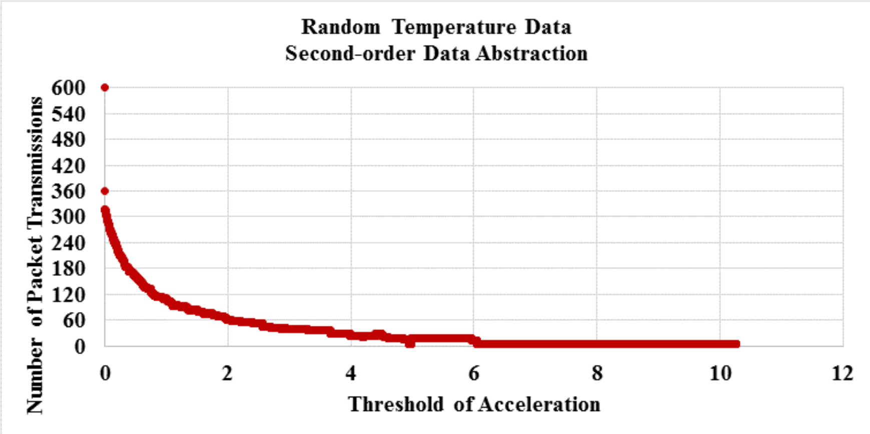

(c) Number of packet transmissions of random temperature data in second-order data abstraction

Figure 5.9: Number of packet transmissions of random temperature data

From the Figure 5.9, it is shown that the increment of threshold value will reduce the number of packet transmissions. However, the increment of threshold of rate and threshold of acceleration will not necessarily reduce the number of packet transmissions.

2. Number of Data Transmitted

Number of data transmitted of random temperature data in different orders of data abstraction are shown in Figure 5.10.

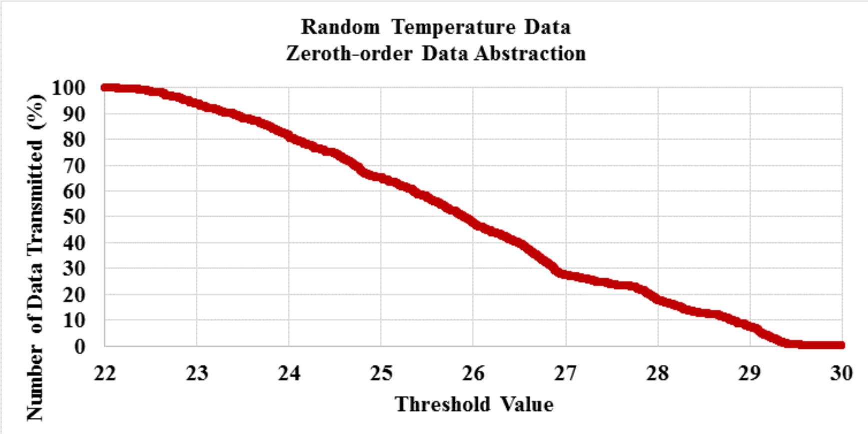

(a) Number of data transmitted of random temperature data in zeroth-order data abstraction

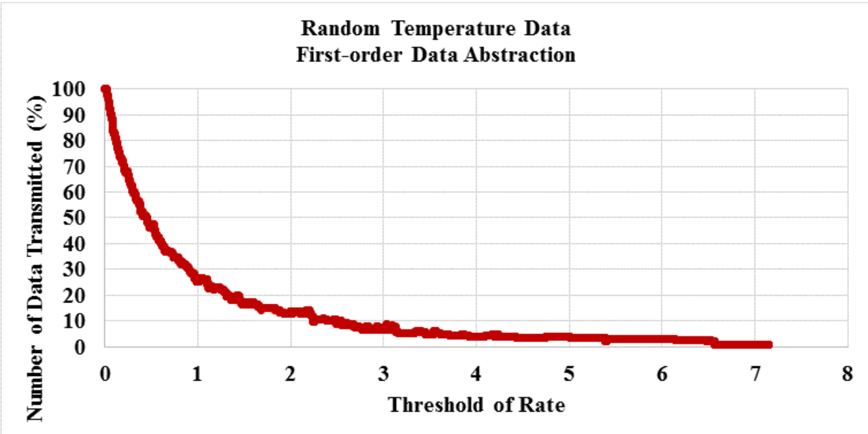

(b) Number of data transmitted of random temperature data in first-order data abstraction

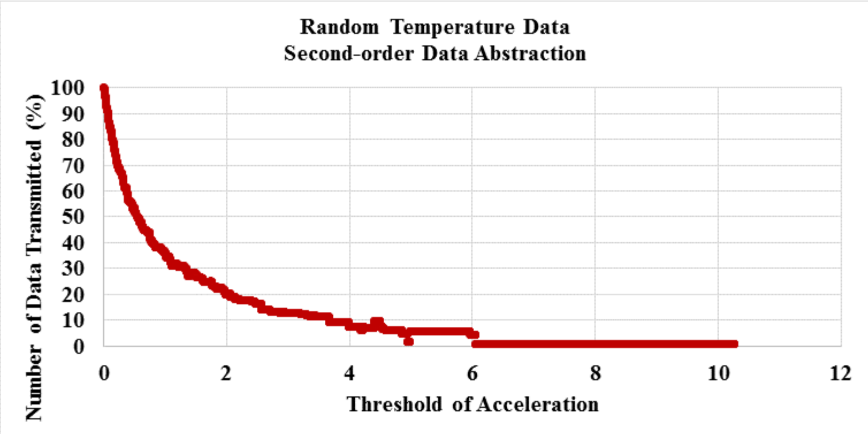

(c) Number of data transmitted of random temperature data in second-order data abstraction

Figure 5.10: Number of data transmitted of random temperature data

From the Figure 5.10, it is shown that the increment of threshold value will reduce the number of data transmitted. However, the increment of threshold of rate and threshold of acceleration will not necessarily reduce the number of data transmitted.

3. Root Mean Square Error

Root mean square error of random temperature data in different orders of data abstraction and reformation are shown from Figure 5.11.

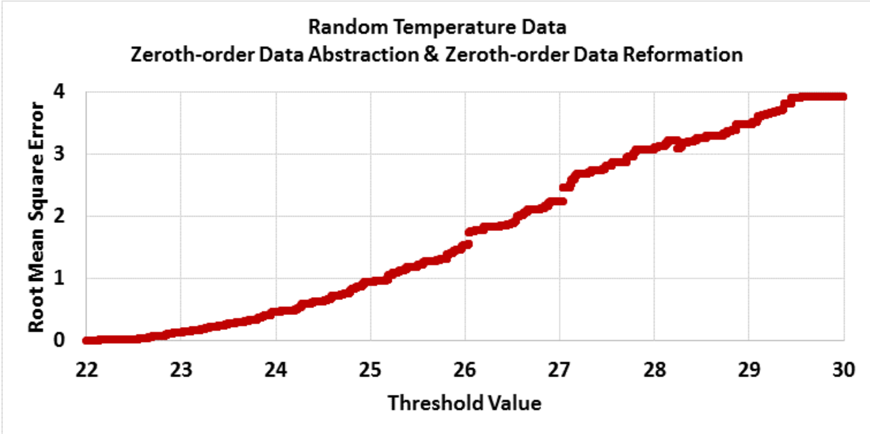

(a) Root mean square error of random temperature data in zeroth-order data abstraction & zeroth-order data reformation

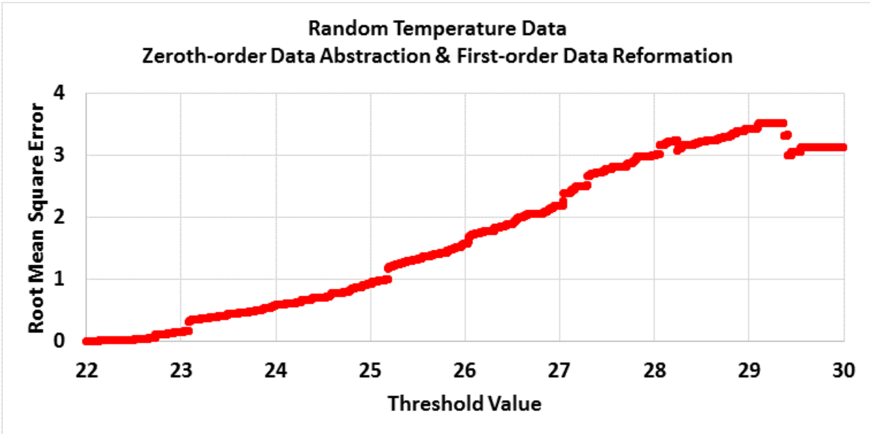

(b) Root mean square error of random temperature data in zeroth-order data abstraction & first-order data reformation

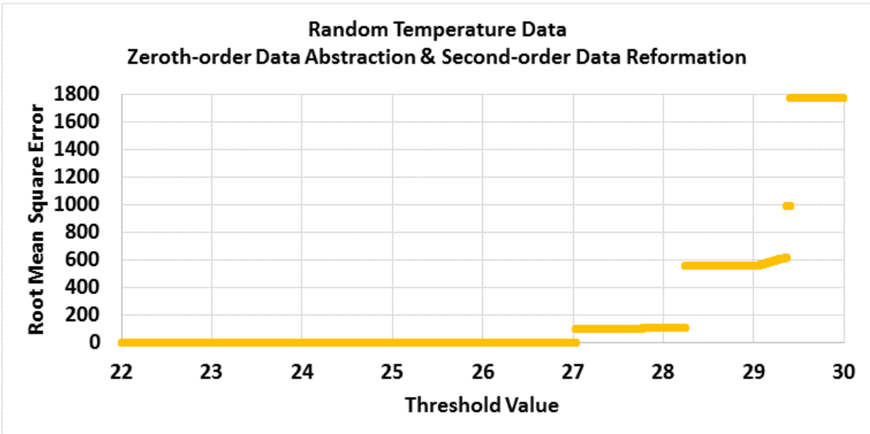

(c) Root mean square error of random temperature data in zeroth-order data abstraction & second-order data reformation

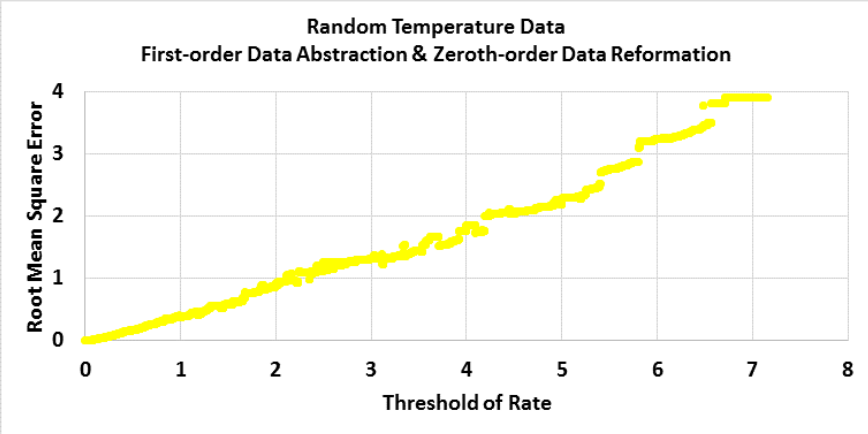

(d) Root mean square error of random temperature data in first-order data abstraction & zeroth-order data reformation

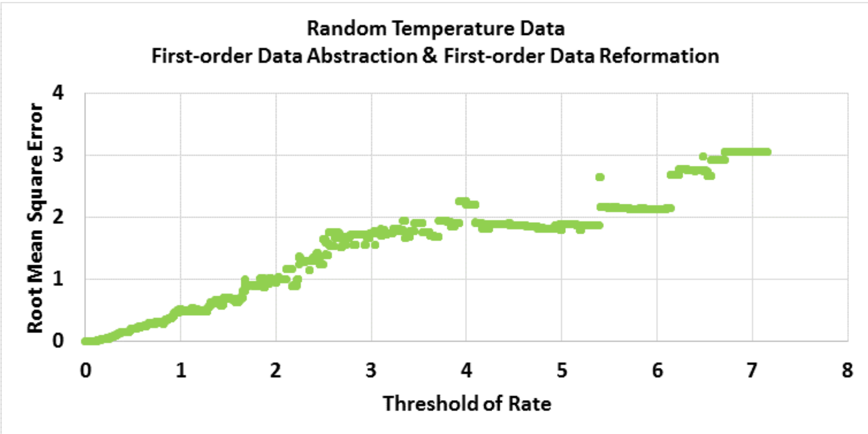

(e) Root mean square error of random temperature data in first-order data abstraction & first-order data reformation

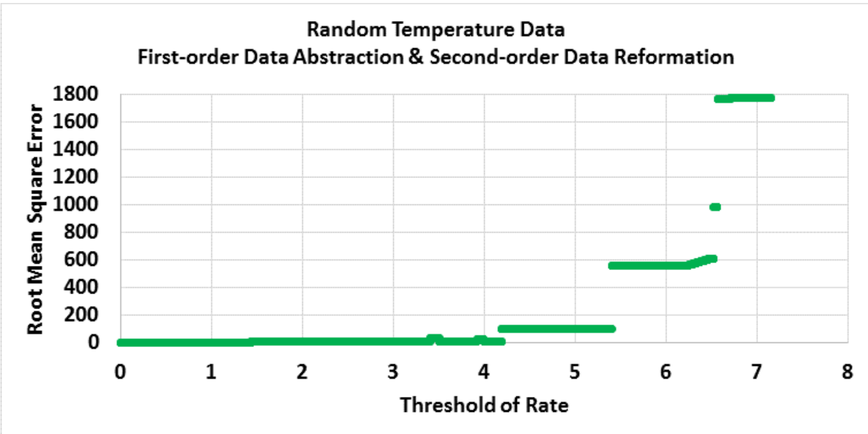

(f) Root mean square error of random temperature data in first-order data abstraction & second-order data reformation

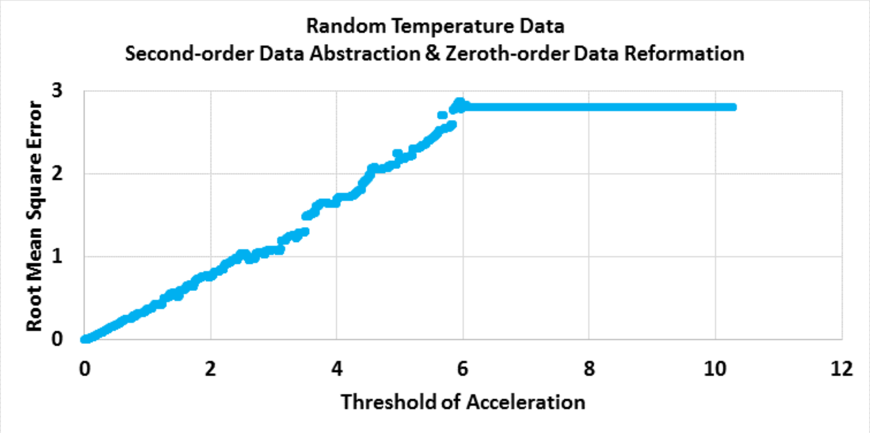

(g) Root mean square error of random temperature data in second-order data abstraction & zeroth-order data reformation

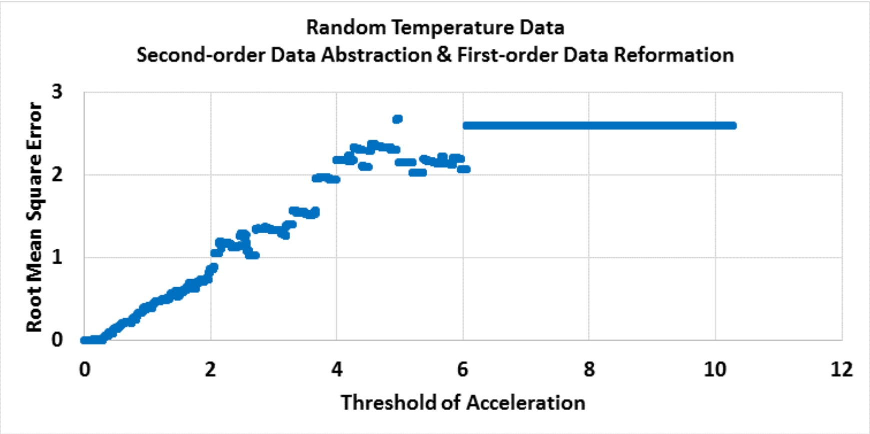

(h) Root mean square error of random temperature data in second-order data abstraction & first-order data reformation

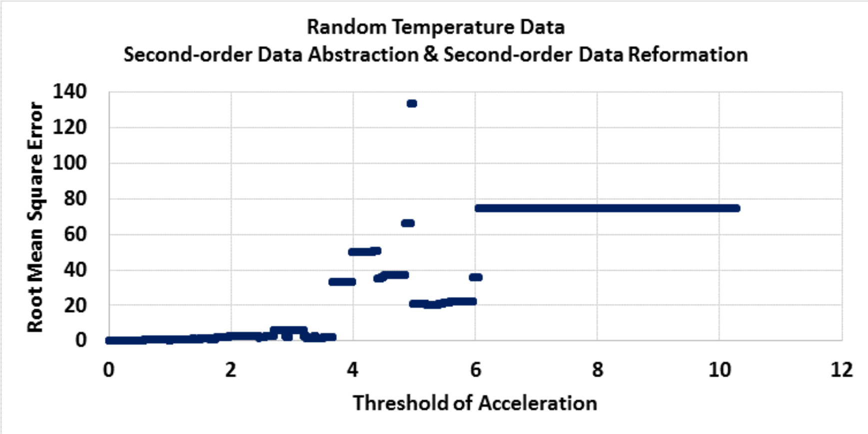

(i) Root mean square error of random temperature data in second-order data abstraction & second-order data reformation

Figure 5.11: Root mean square error of random temperature data

From the Figure 5.11, it is shown that the increment of threshold value, threshold of rate and threshold of acceleration will not necessarily increase the root mean square error.

4. Mean Absolute Percentage Error

Mean absolute percentage error of random temperature data in different orders of data abstraction are shown from Figure 5.12.

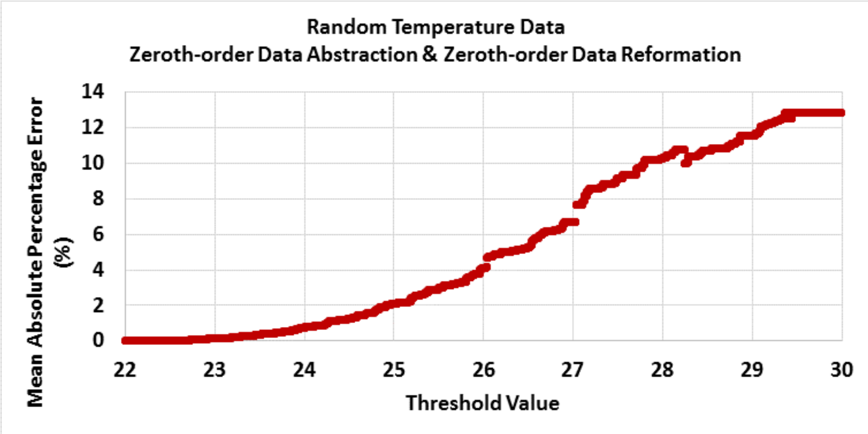

(a) Mean absolute percentage error of random temperature data in zeroth-order data abstraction & zeroth-order data reformation

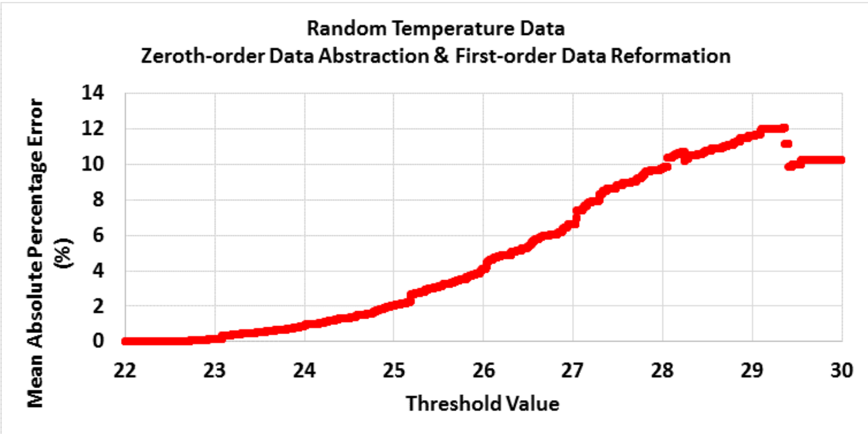

(b) Mean absolute percentage error of random temperature data in zeroth-order data abstraction & first-order data reformation

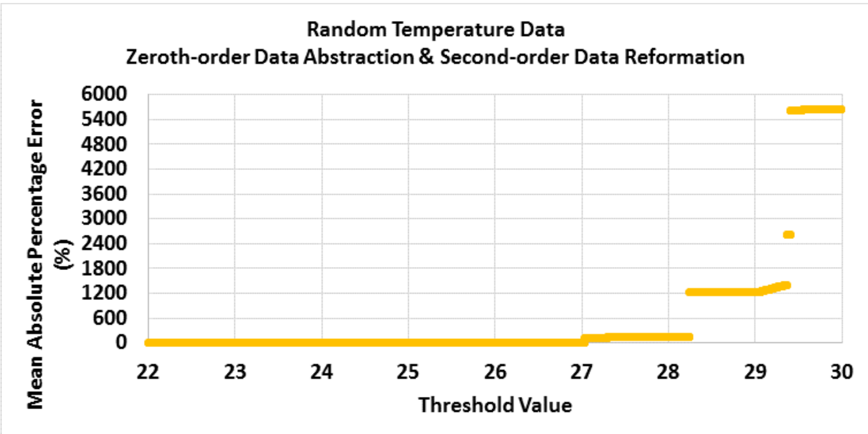

(c) Mean absolute percentage error of random temperature data in zeroth-order data abstraction & second-order data reformation

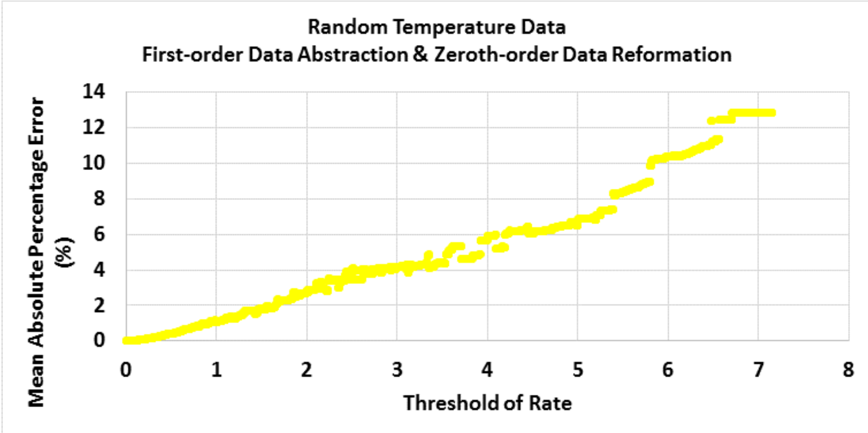

(d) Mean absolute percentage error of random temperature data in first-order data abstraction & zeroth-order data reformation

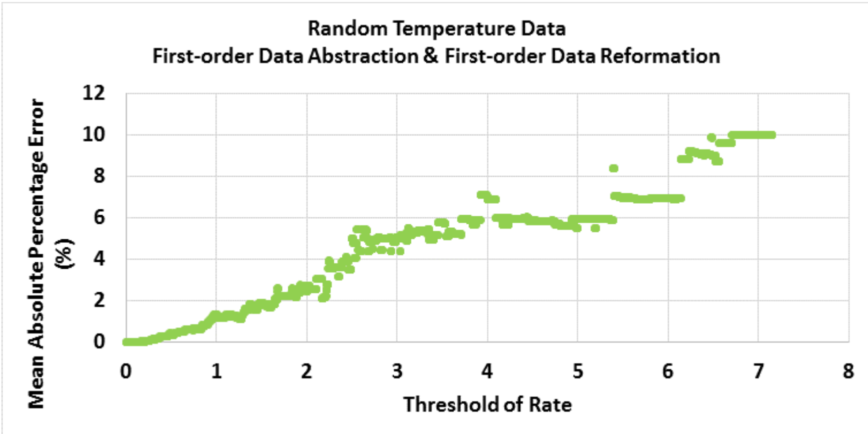

(e) Mean absolute percentage error of random temperature data in first-order data abstraction & first-order data reformation

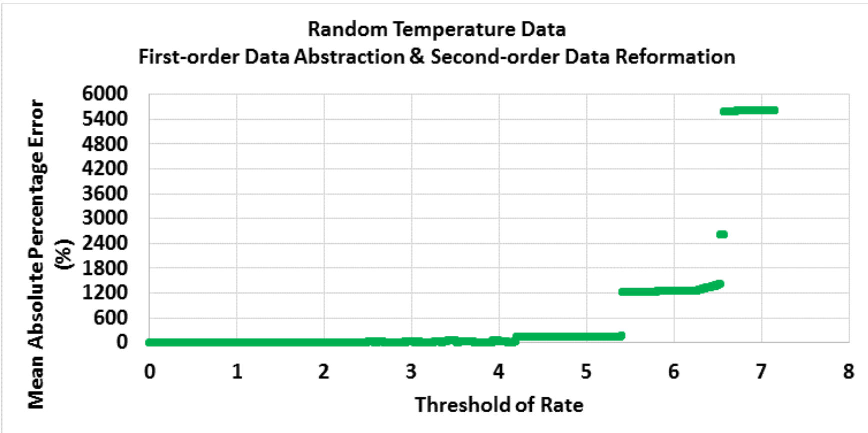

(f) Mean absolute percentage error of random temperature data in first-order data abstraction & second-order data reformation

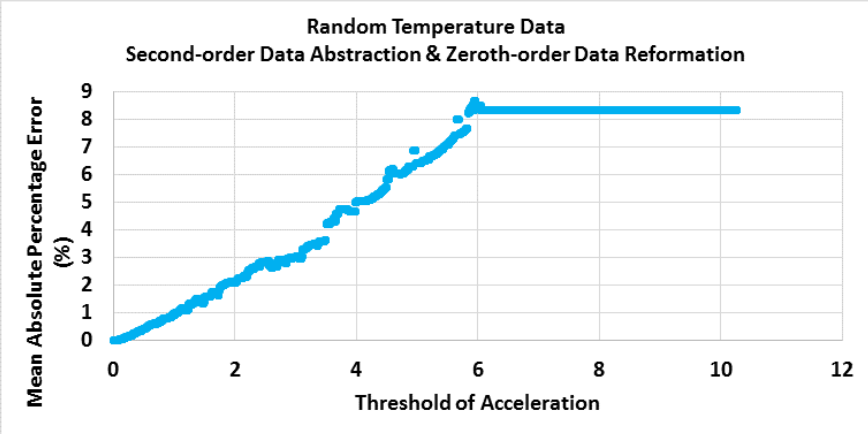

(g) Mean absolute percentage error of random temperature data in second-order data abstraction & zeroth-order data reformation

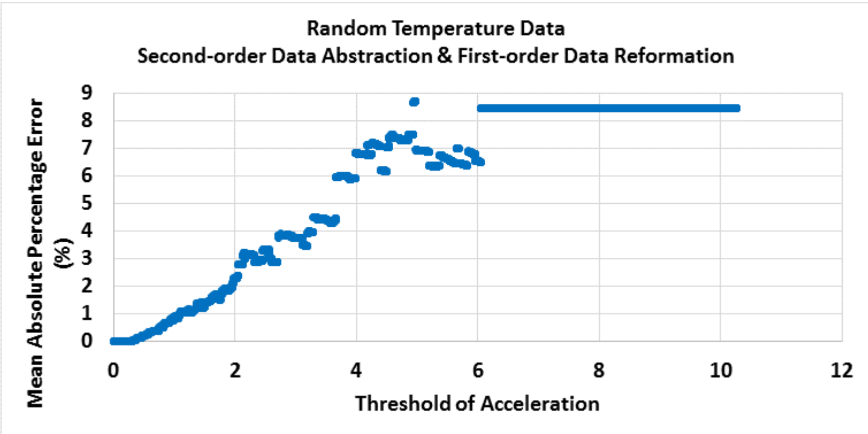

(h) Mean absolute percentage error of random temperature data in second-order data abstraction & first-order data reformation

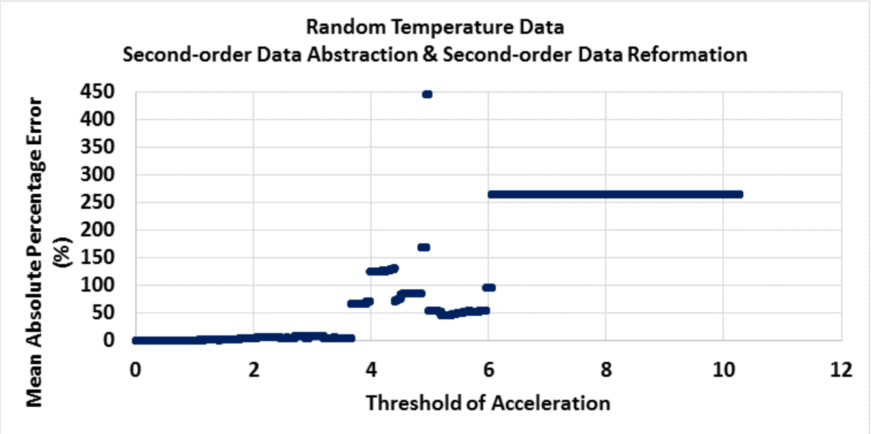

(i) Mean absolute percentage error of random temperature data in second-order data abstraction & second-order data reformation

Figure 5.12: Mean absolute percentage error of random temperature data

From the Figure 5.12, it is shown that the increment of threshold value, threshold of rate and threshold of acceleration will not necessarily increase the mean absolute percentage error.

5.2 Application/Attribute with Abrupt Sampling Rate

In accelerometer-sensed values, there are three values, which are x-, y-, and z- axis. Therefore, in order to determine the transmission of values, the magnitude of sensed movement vector, as shown in Table 5.1, will be compared with a threshold value.

Table 5.1: Magnitude of Sensed Movement Vector for Accelerometer Data

Order of Data Abstraction	Scheme
Zeroth	$\lvert v_i \rvert = \sqrt{x_i^2 + y_i^2 + z_i^2} \geq th_{value}$
First	$\lvert \Delta v_i \rvert = \sqrt{\left(x_i - x_{t_j}\right)^2 + \left(y_i - y_{t_j}\right)^2 + \left(z_i - z_{t_j}\right)^2} \geq th_{rate}$
Second	$\lvert \Delta^2 v_i \rvert = \sqrt{\left(x_i - 2x_{i-1} + x_{t_j}\right)^2 + \left(y_i - 2y_{i-1} + y_{t_j}\right)^2 + \left(z_i - 2z_{i-1} + z_{t_j}\right)^2 +} \geq th_{accel}$

$\lvert v_i \rvert$= zeroth-order magnitude of sensed movement vector
$\lvert \Delta v_i \rvert$ = first-order magnitude of sensed movement vector
$\lvert \Delta^2 v_i \rvert$ = second-order magnitude of sensed movement vector
x_i= current sensed x-axis accelerometer data
y_i= current sensed y-axis accelerometer data
z_i= current sensed z-axis accelerometer data
x_{i-1}= previous sensed x-axis accelerometer data
y_{i-1}= previous sensed y-axis accelerometer data
z_{i-1}= previous sensed z-axis accelerometer data
x_{t_j}= last reported x-axis accelerometer data
y_{t_j}= last reported y-axis accelerometer data
z_{t_j}= last reported z-axis accelerometer data

In the following section, the performance of DAR schemes in accelerometer data in different activities will be discussed.

5.2.1 Sitting Accelerometer Data

In this experiment, the number of the packets of data is 3000. The results of implementation of the DAR schemes in the terms of data abstraction (number of packet transmissions and number of data transmitted (%)) and data reformation (RMSE and MAPE) are as follows.

1. Number of Packet Transmissions

Number of packet transmissions of sitting accelerometer data in different orders of data abstraction are shown in Figure 5.13.

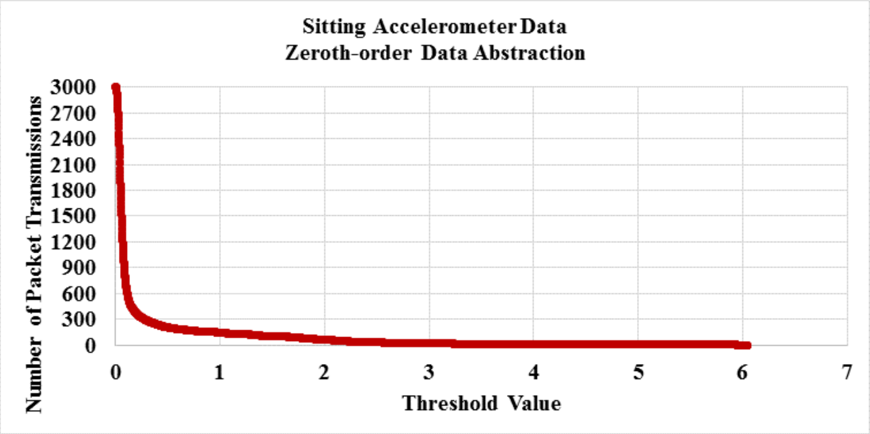

(a) Number of packet transmissions of sitting accelerometer data in zeroth-order data abstraction

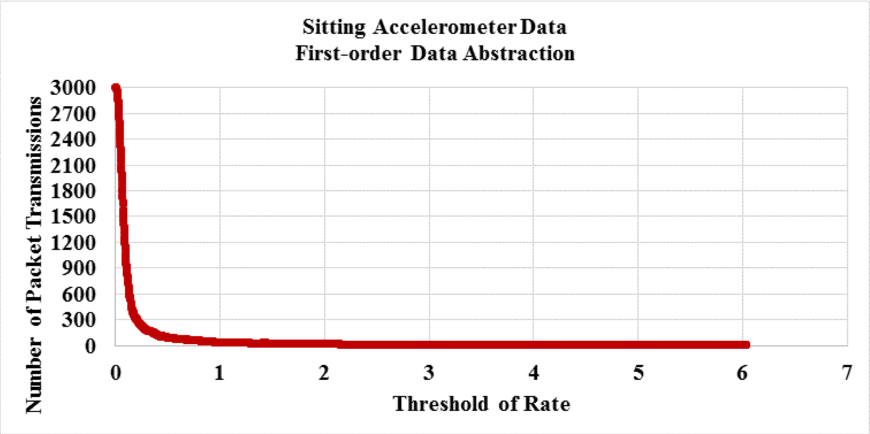

(b) Number of packet transmissions of sitting accelerometer data in first-order data abstraction

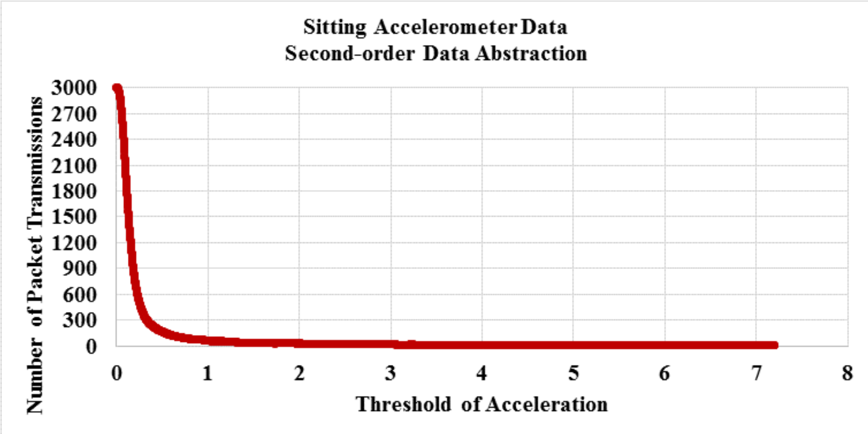

(c) Number of packet transmissions of sitting accelerometer data in second-order data abstraction

Figure 5.13: Number of packet transmissions of sitting accelerometer data

From the Figure 5.13, it is shown that the increment of threshold value will reduce the number of packet transmissions. However, the increment of threshold of rate and threshold of acceleration will not necessarily reduce the number.

2. Number of Data Transmitted

Number of data transmitted of sitting accelerometer data in different orders of data abstraction are shown in Figure 5.14.

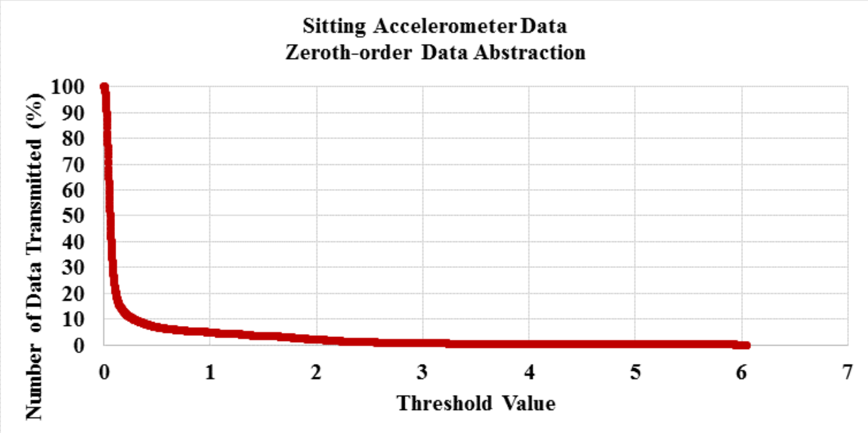

(a) Number of data transmitted of sitting accelerometer data in zeroth-order data abstraction

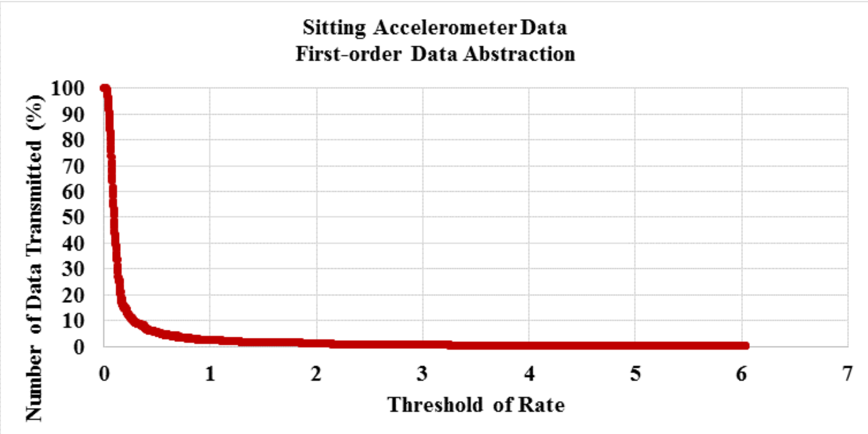

(b) Number of data transmitted of sitting accelerometer data in first-order data abstraction

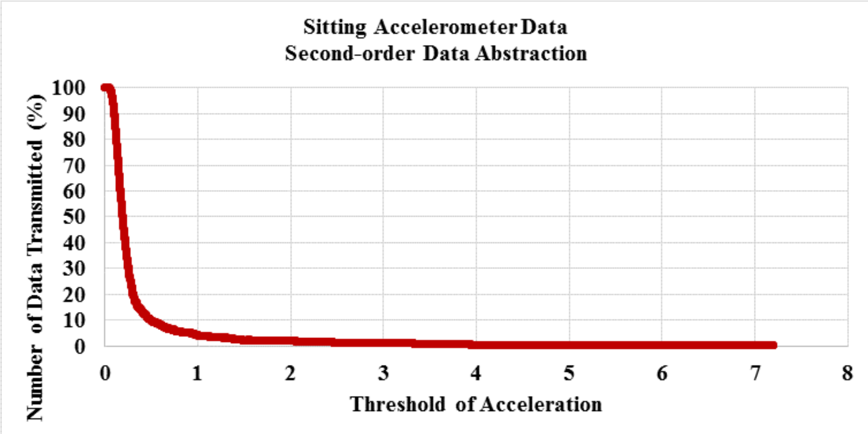

(c) Number of data transmitted of sitting accelerometer data in second-order data abstraction

Figure 5.14: Number of data transmitted of sitting accelerometer data

From the Figure 5.14, it is shown that the increment of threshold value will always reduce the number of data transmitted. However, the increment of threshold of rate and threshold of acceleration will not necessarily reduce the number of data transmitted.

3. Root Mean Square Error

Root mean square error of sitting accelerometer data in different orders of data abstraction and reformation are shown from Figure 5.15.

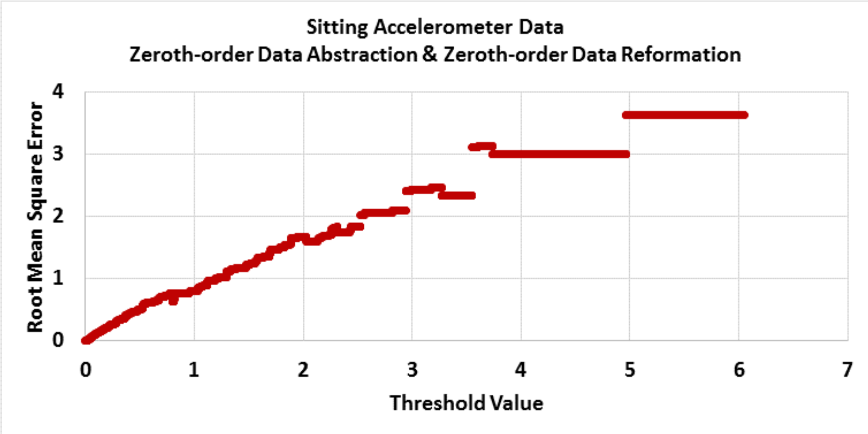

(a) Root mean square error of sitting accelerometer data in zeroth-order data abstraction & zeroth-order data reformation

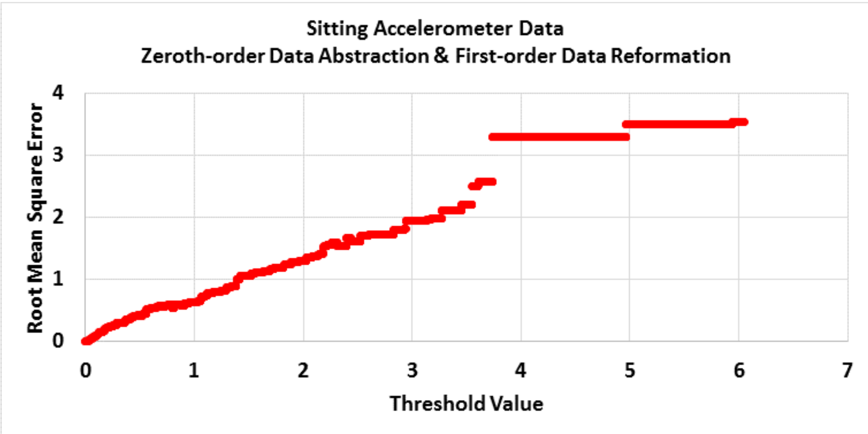

(b) Root mean square error of sitting accelerometer data in zeroth-order data abstraction & first-order data reformation

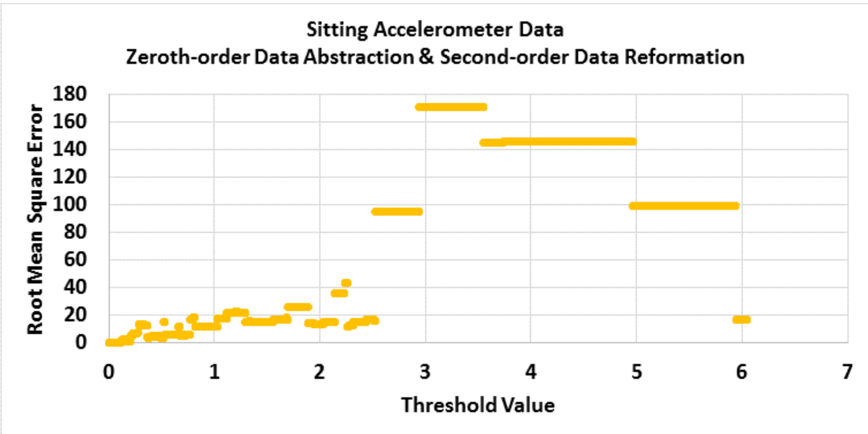

(c) Root mean square error of sitting accelerometer data in zeroth-order data abstraction & second-order data reformation

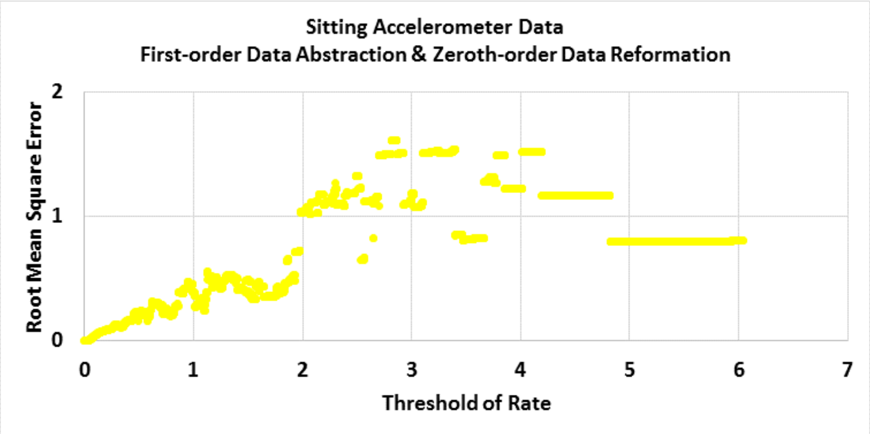

(d) Root mean square error of sitting accelerometer data in first-order data abstraction & zeroth-order data reformation

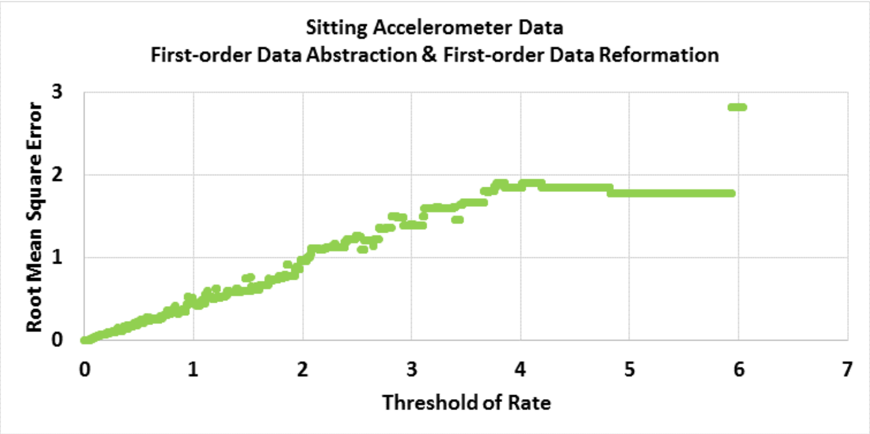

(e) Root mean square error of sitting accelerometer data in first-order data abstraction & first-order data reformation

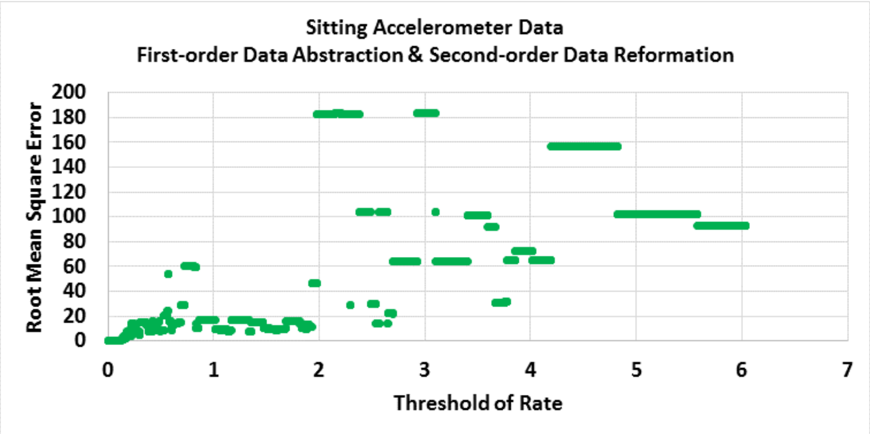

(f) Root mean square error of sitting accelerometer data in first-order data abstraction & second-order data reformation

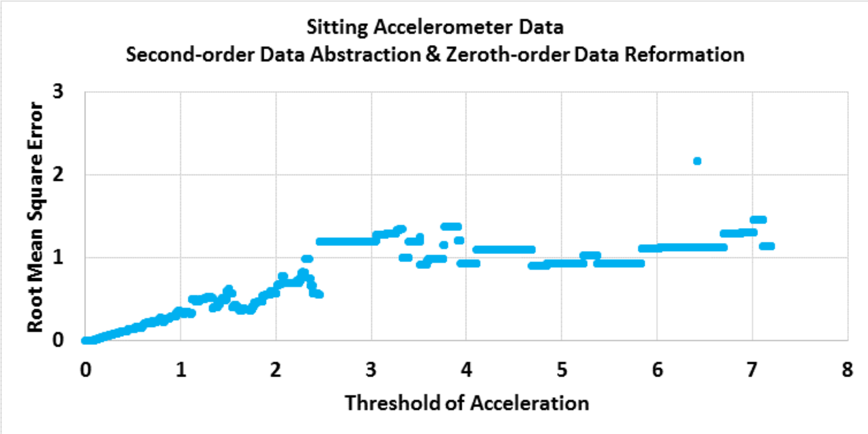

(g) Root mean square error of sitting accelerometer data in second-order data abstraction & zeroth-order data reformation

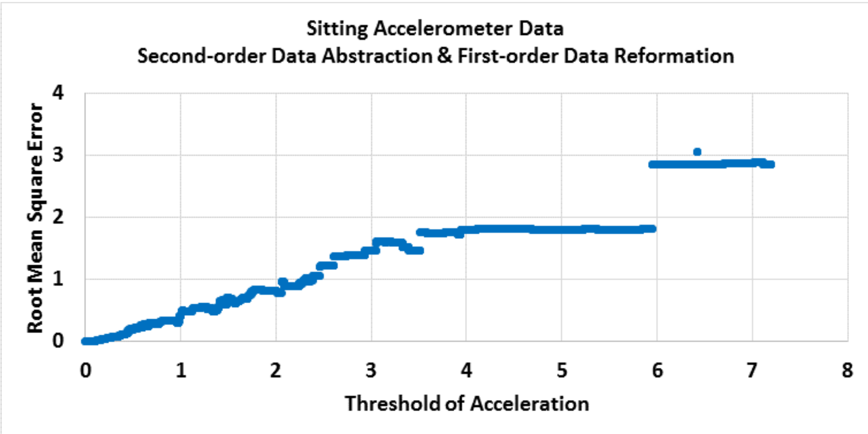

(h) Root mean square error of sitting accelerometer data in second-order data abstraction & first-order data reformation

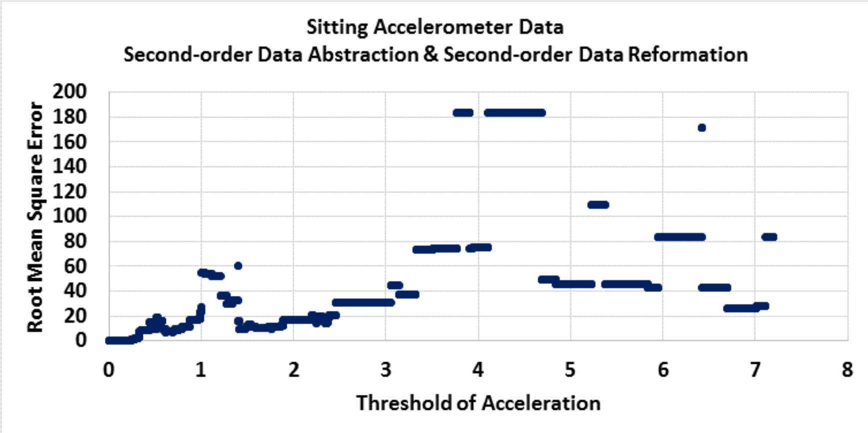

(i) Root mean square error of sitting accelerometer data in second-order data abstraction & second-order data reformation

Figure 5.15: Root mean square error of sitting accelerometer data

From the Figure 5.15, it is shown that the increment of threshold value, threshold of rate and threshold of acceleration will not necessarily increase the root mean square error.

4. Mean Absolute Percentage Error

Mean absolute percentage error of sitting accelerometer data in different orders of data abstraction are shown from Figure 5.16.

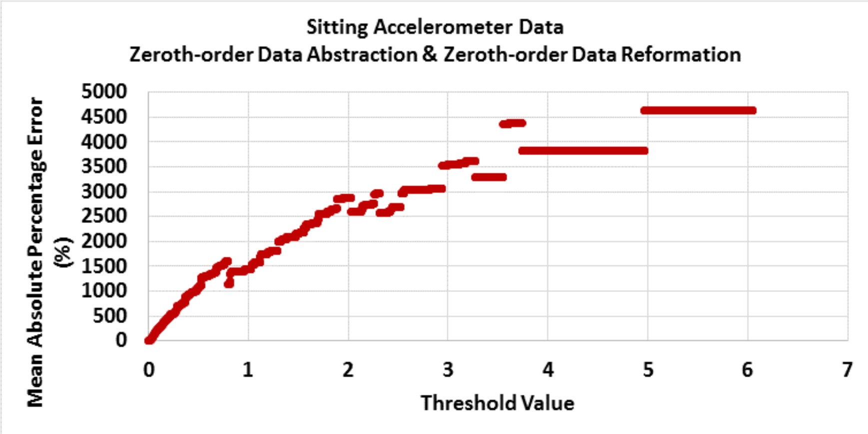

(a) Mean absolute percentage error of sitting accelerometer data in zeroth-order data abstraction & zeroth-order data reformation

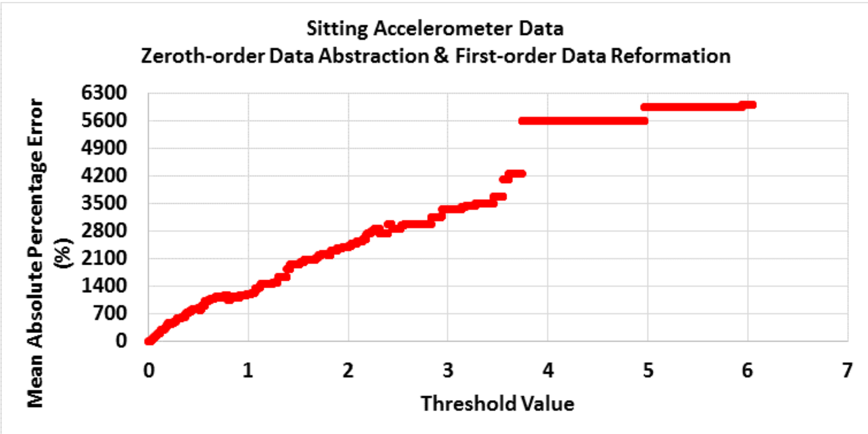

(b) Mean absolute percentage error of sitting accelerometer data in zeroth-order data abstraction & first-order data reformation

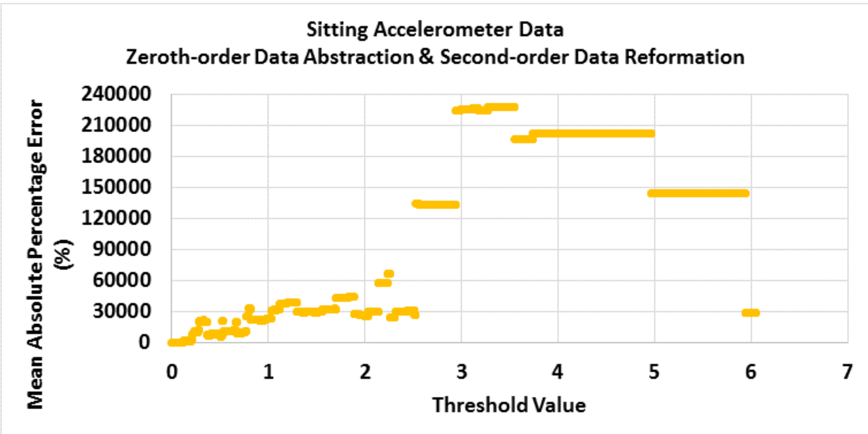

(c) Mean absolute percentage error of sitting accelerometer data in zeroth-order data abstraction & second-order data reformation

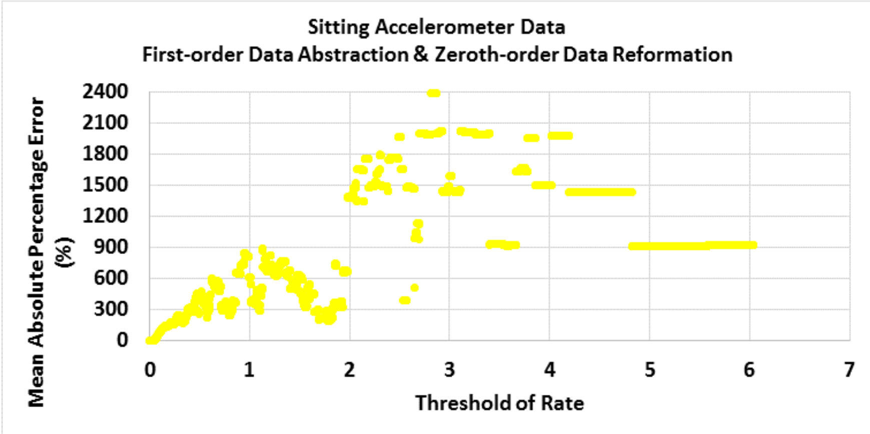

(d) Mean absolute percentage error of sitting accelerometer data in first-order data abstraction & zeroth-order data reformation

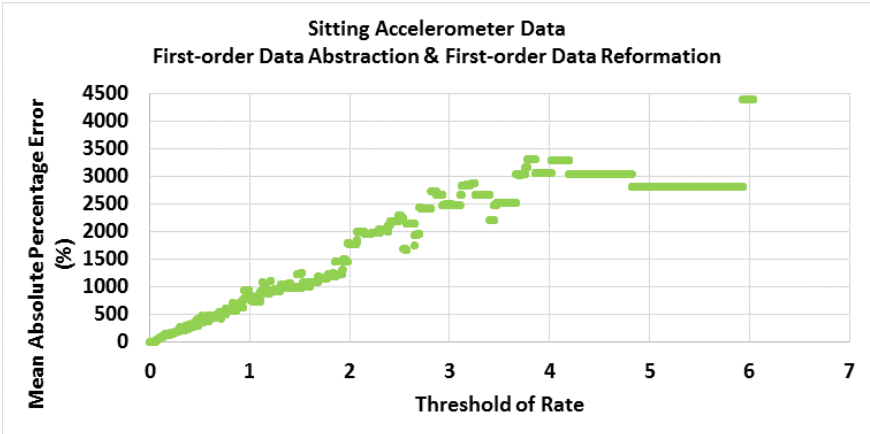

(e) Mean absolute percentage error of sitting accelerometer data in first-order data abstraction & first-order data reformation

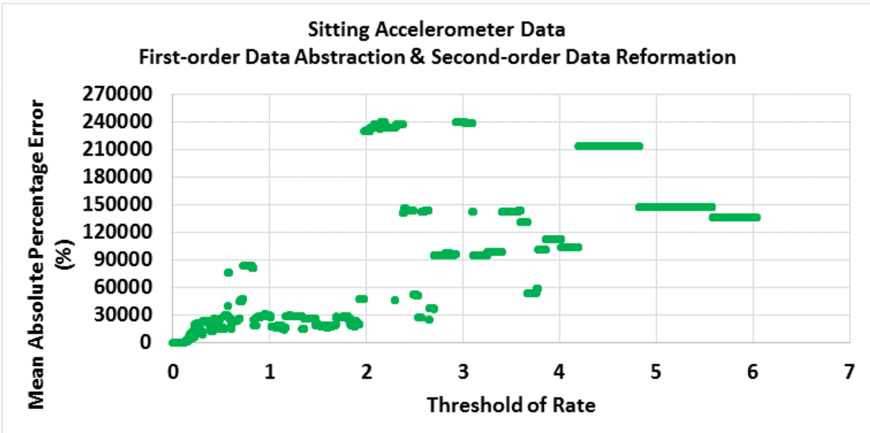

(f) Mean absolute percentage error of sitting accelerometer data in first-order data abstraction & second-order data reformation

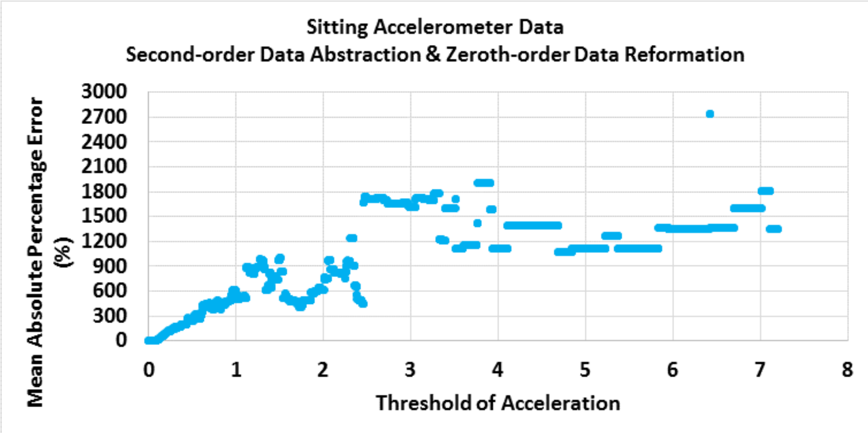

(g) Mean absolute percentage error of sitting accelerometer data in second-order data abstraction & zeroth-order data reformation

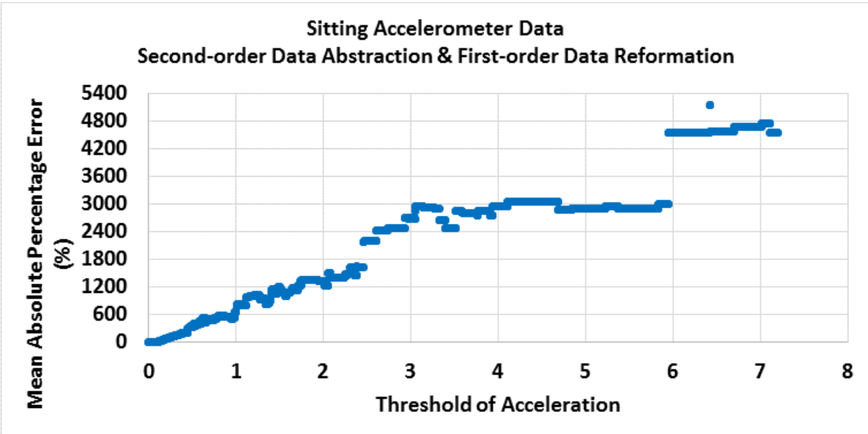

(h) Mean absolute percentage error of sitting accelerometer data in second-order data abstraction & first-order data reformation

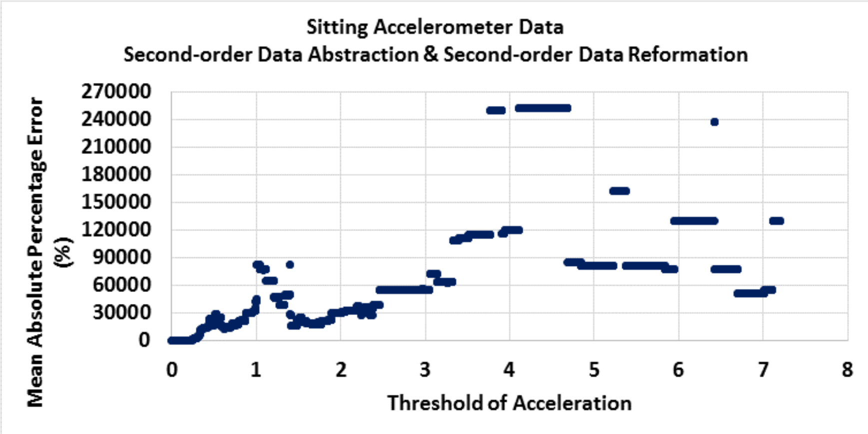

(i) Mean absolute percentage error of sitting accelerometer data in second-order data abstraction & second-order data reformation

Figure 5.16: Mean absolute percentage error of sitting accelerometer data

From the Figure 5.16, it is shown that the increment of threshold value, threshold of rate and threshold of acceleration will not necessarily increase the mean absolute percentage error.

5.2.2 Standing Accelerometer Data

In this experiment, the number of the packets of data is 3000. The results of implementation of the DAR schemes in the terms of data abstraction (number of packet transmissions and number of data transmitted (%)) and data reformation (RMSE and MAPE) are as follows.

1. Number of Packet Transmissions

   Number of packet transmissions of standing accelerometer data in different orders of data abstraction are shown in Figure 5.17.

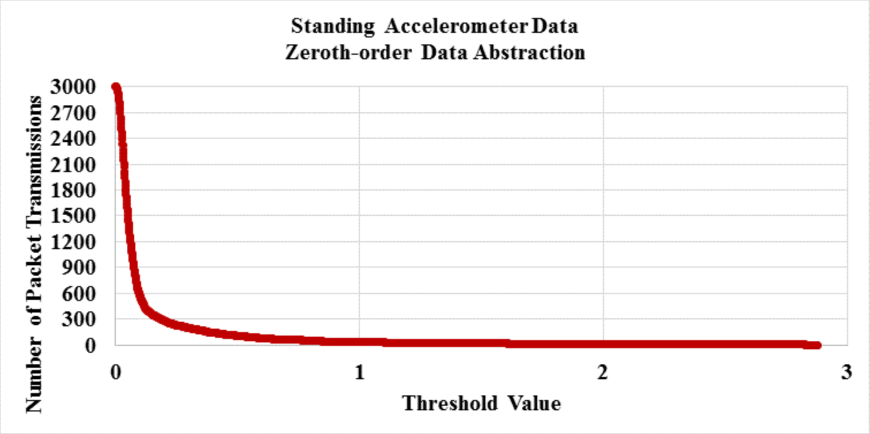

(a) Number of packet transmissions of standing accelerometer data in zeroth-order data abstraction

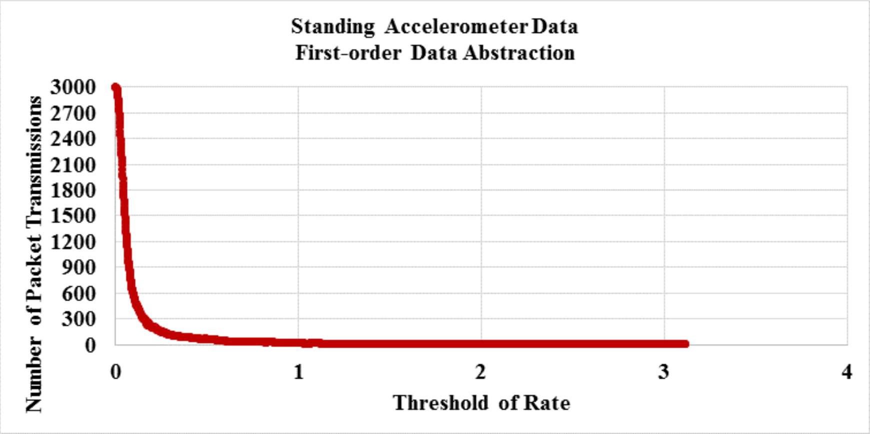

(b) Number of packet transmissions of standing accelerometer data in first-order data abstraction

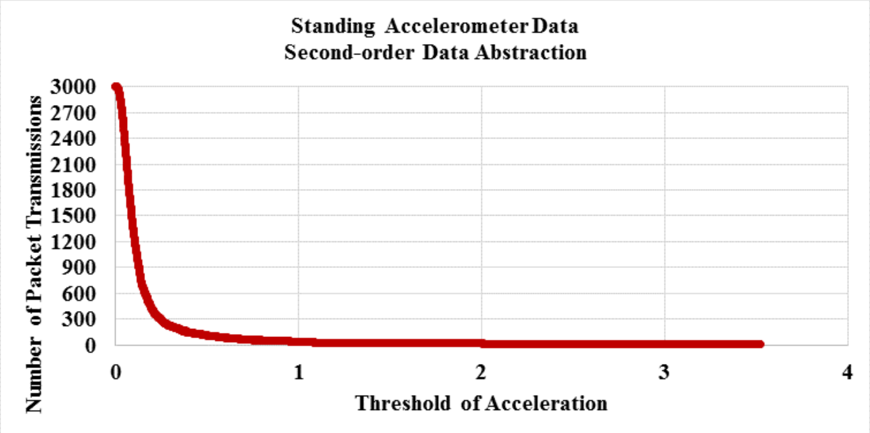

(c) Number of packet transmissions of standing accelerometer data in second-order data abstraction

Figure 5.17: Number of packet transmissions of standing accelerometer data

From the Figure 5.17, it is shown that the increment of threshold value will reduce the number of packet transmissions. However, the increment of threshold of rate and threshold of acceleration will not necessarily reduce the number.

2. Number of Data Transmitted

Number of data transmitted of standing accelerometer data in different orders of data abstraction are shown in Figure 5.18.

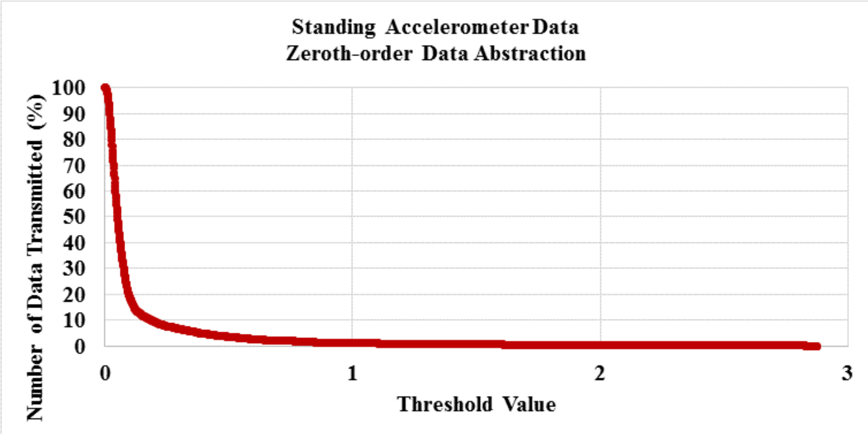

(a) Number of data transmitted of standing accelerometer data in zeroth-order data abstraction

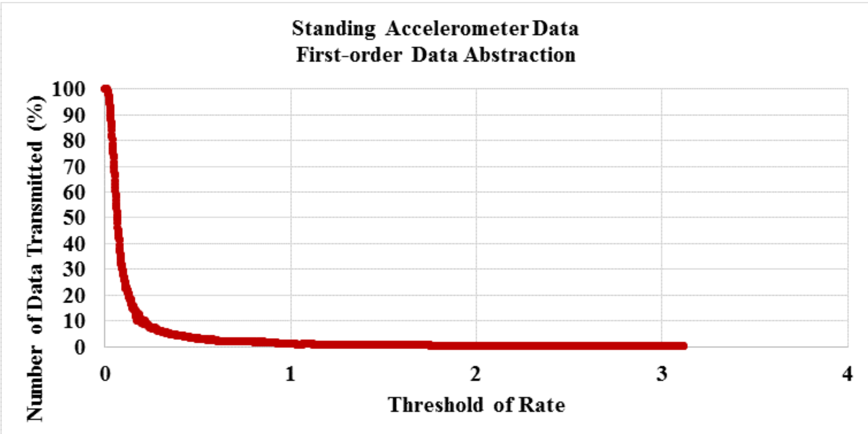

(b) Number of data transmitted of standing accelerometer data in first-order data abstraction

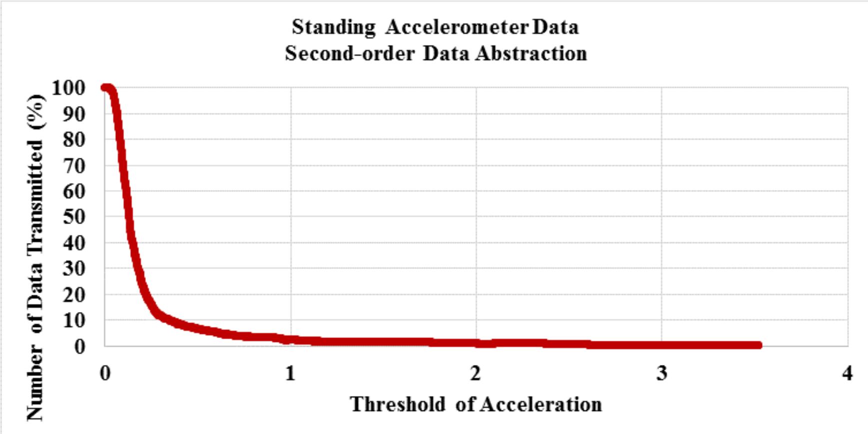

(c) Number of data transmitted of standing accelerometer data in second-order data abstraction

Figure 5.18: Number of data transmitted of standing accelerometer data

From the Figure 5.18, it is shown that the increment of threshold value will always reduce the number of data transmitted. However, the increment of threshold of rate and threshold of acceleration will not necessarily reduce the number of data transmitted.

3. Root Mean Square Error

Root mean square error of standing accelerometer data in different orders of data abstraction and reformation are shown from Figure 5.19.

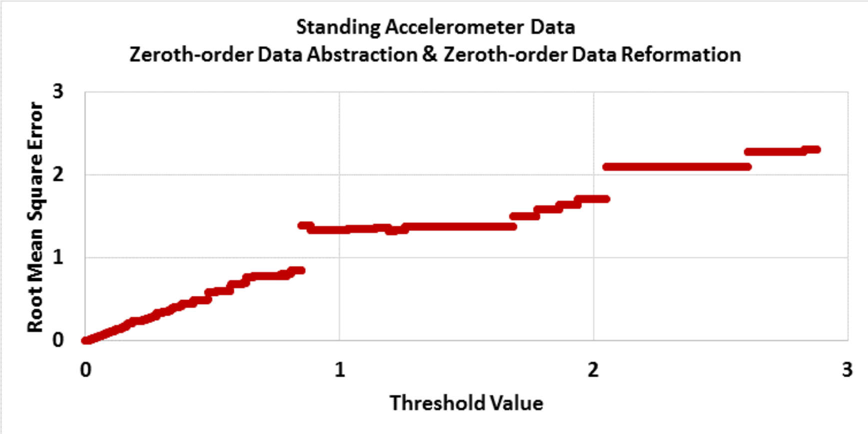

(a) Root mean square error of standing accelerometer data in zeroth-order data abstraction & zeroth-order data reformation

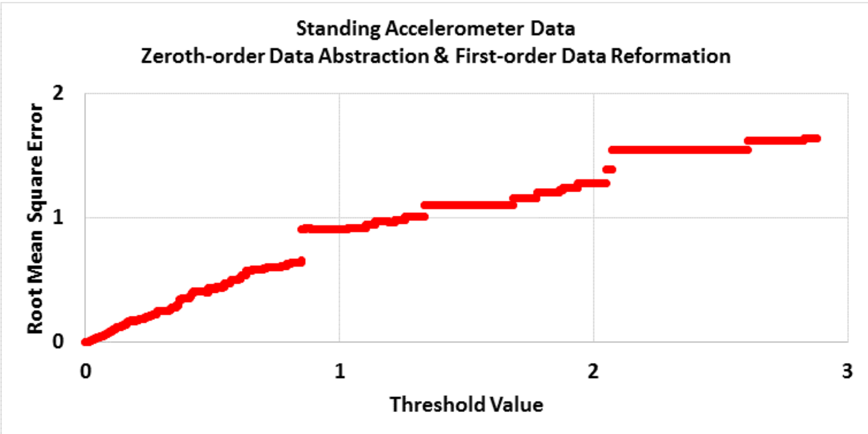

(b) Root mean square error of standing accelerometer data in zeroth-order data abstraction & first-order data reformation

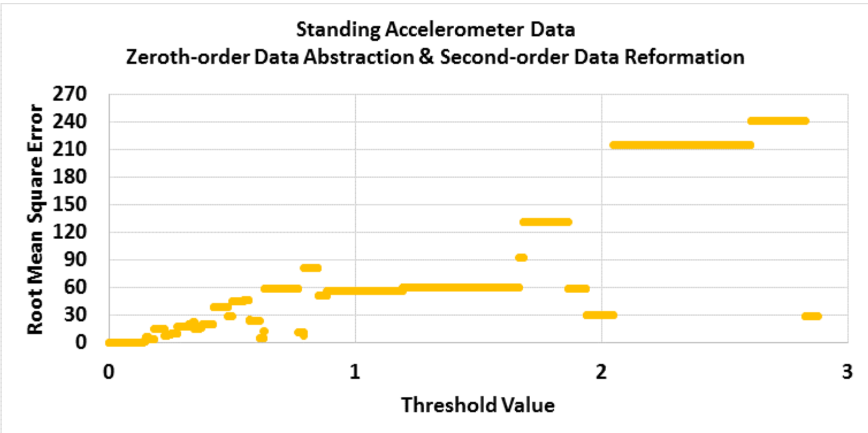

(c) Root mean square error of standing accelerometer data in zeroth-order data abstraction & second-order data reformation

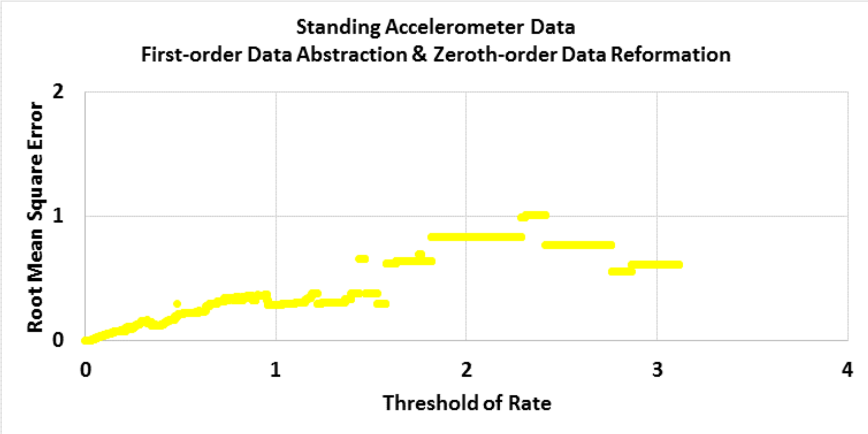

(d) Root mean square error of standing accelerometer data in first-order data abstraction & zeroth-order data reformation

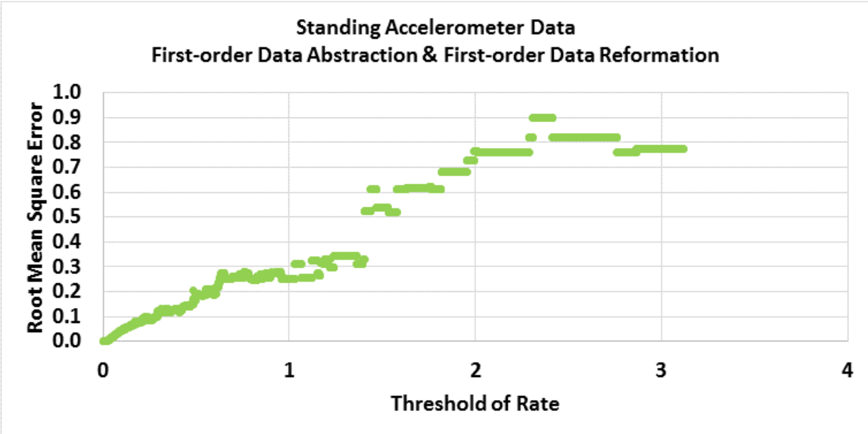

(e) Root mean square error of standing accelerometer data in first-order data abstraction & first-order data reformation

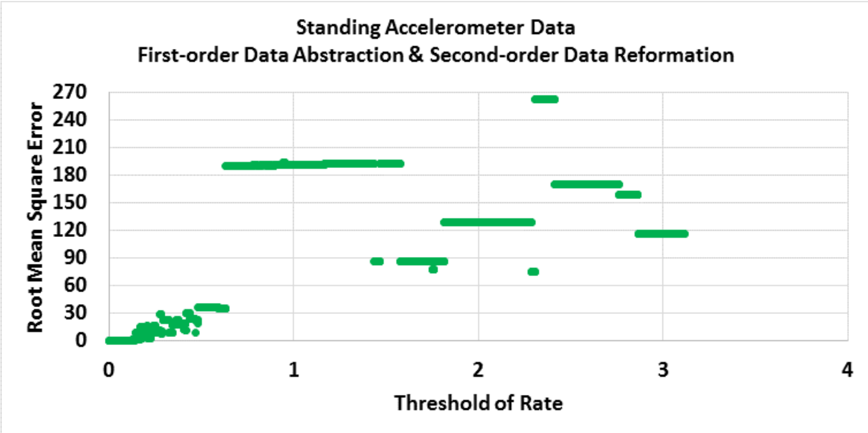

(f) Root mean square error of standing accelerometer data in first-order data abstraction & second-order data reformation

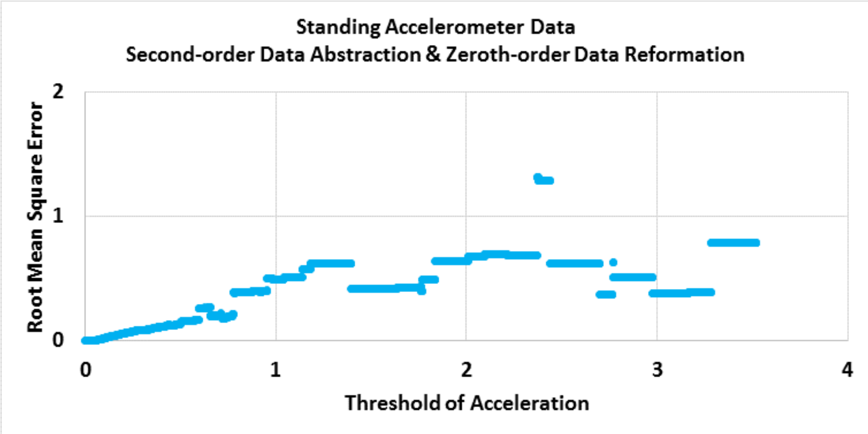

(g) Root mean square error of standing accelerometer data in second-order data abstraction & zeroth-order data reformation

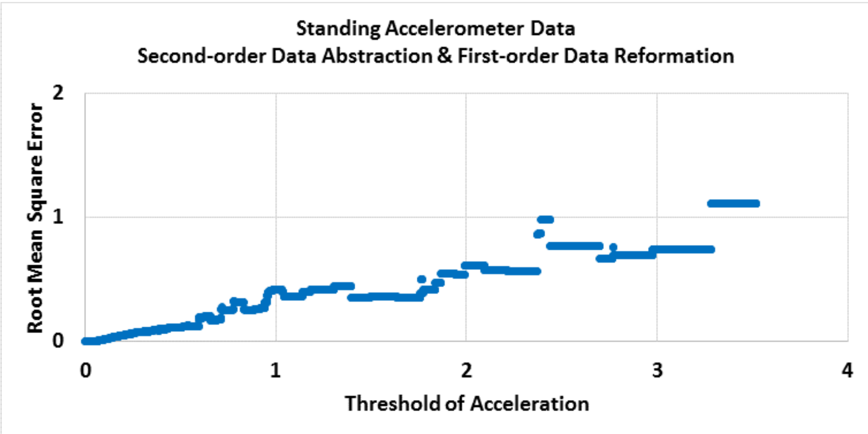

(h) Root mean square error of standing accelerometer data in second-order data abstraction & first-order data reformation

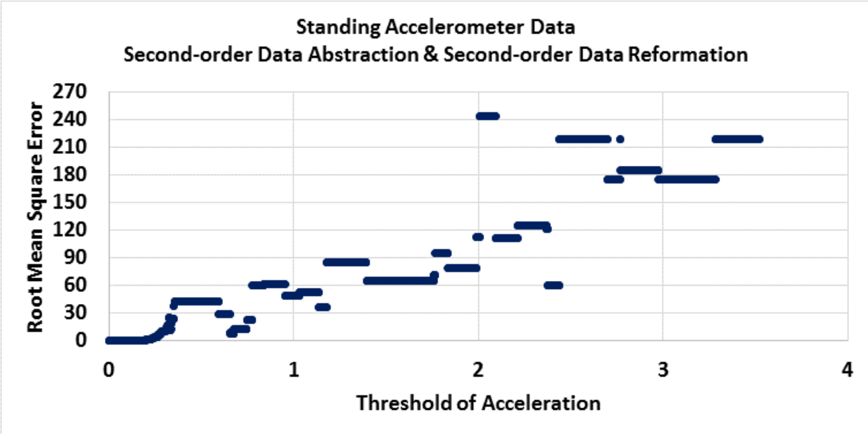

(i) Root mean square error of standing accelerometer data in second-order data abstraction & second-order data reformation

Figure 5.19: Root mean square error of standing accelerometer data

From the Figure 5.19, it is shown that the increment of threshold value, threshold of rate and threshold of acceleration will not necessarily increase the root mean square error.

4. Mean Absolute Percentage Error

Mean absolute percentage error of standing accelerometer data in different orders of data abstraction are shown from Figure 5.20.

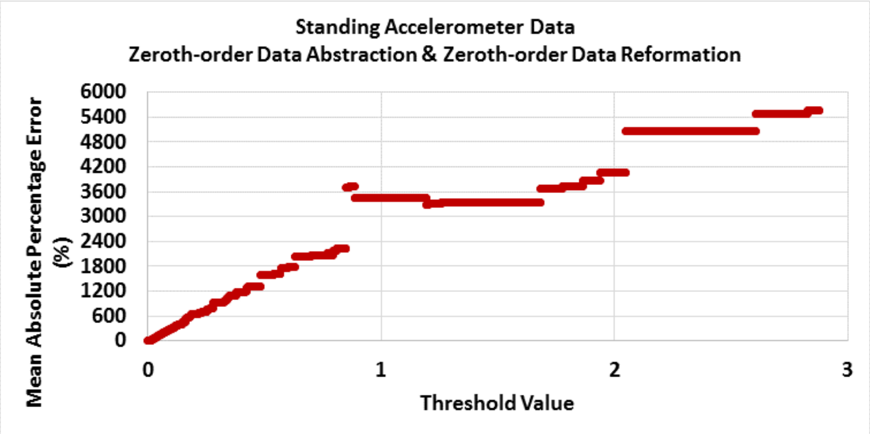

(a) Mean absolute percentage error of standing accelerometer data in zeroth-order data abstraction & zeroth-order data reformation

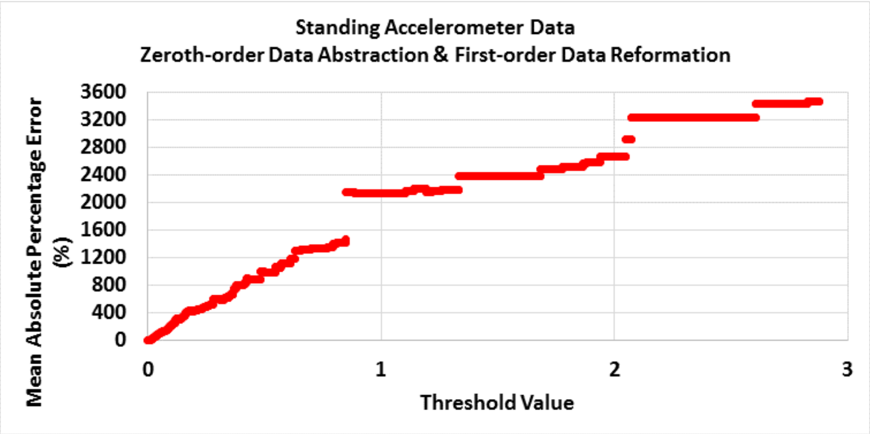

(b) Mean absolute percentage error of standing accelerometer data in zeroth-order data abstraction & first-order data reformation

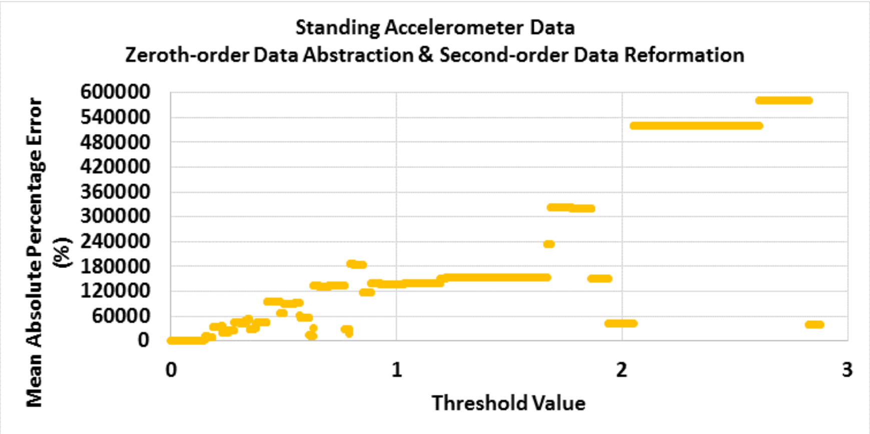

(c) Mean absolute percentage error of standing accelerometer data in zeroth-order data abstraction & second-order data reformation

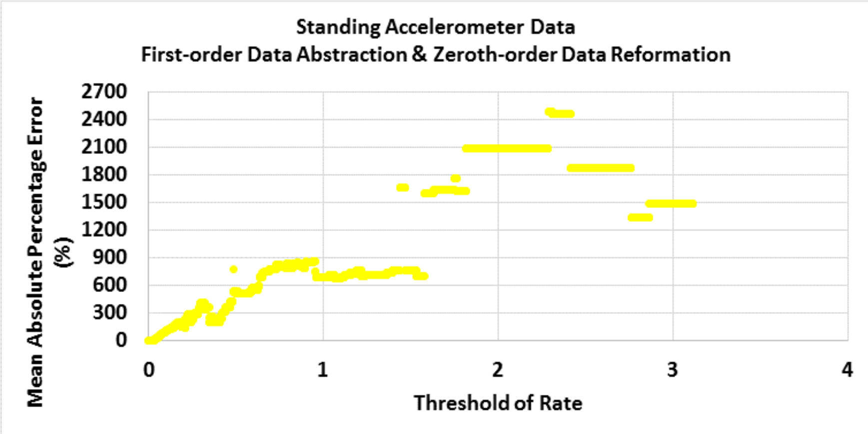

(d) Mean absolute percentage error of standing accelerometer data in first-order data abstraction & zeroth-order data reformation

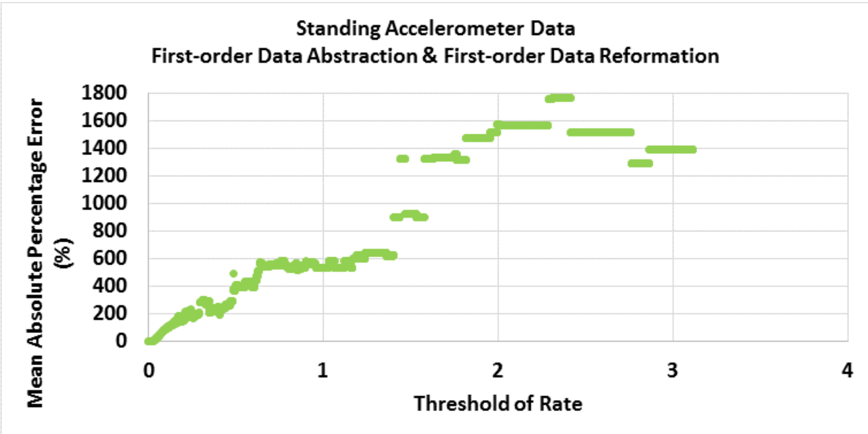

(e) Mean absolute percentage error of standing accelerometer data in first-order data abstraction & first-order data reformation

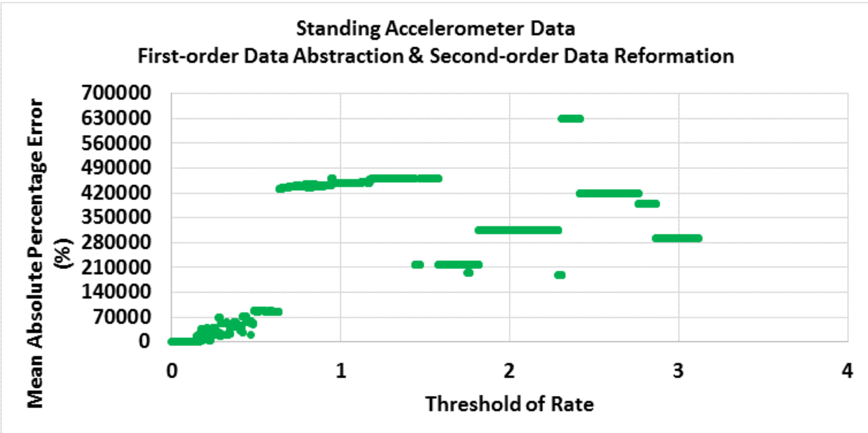

(f) Mean absolute percentage error of standing accelerometer data in first-order data abstraction & second-order data reformation

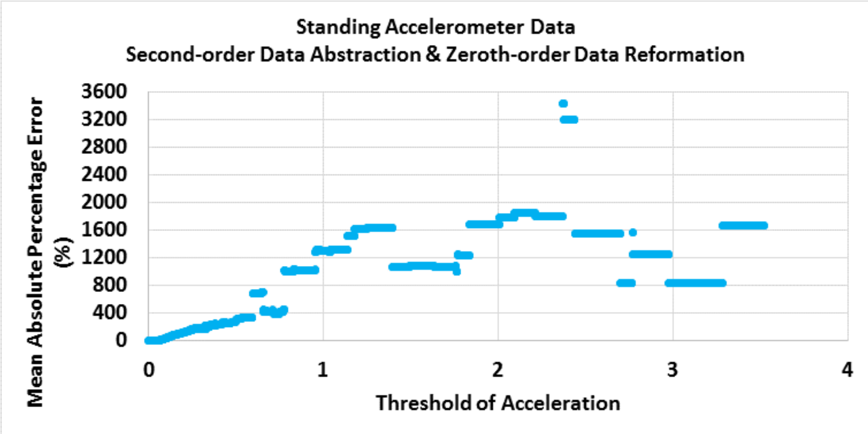

(g) Mean absolute percentage error of standing accelerometer data in second-order data abstraction & zeroth-order data reformation

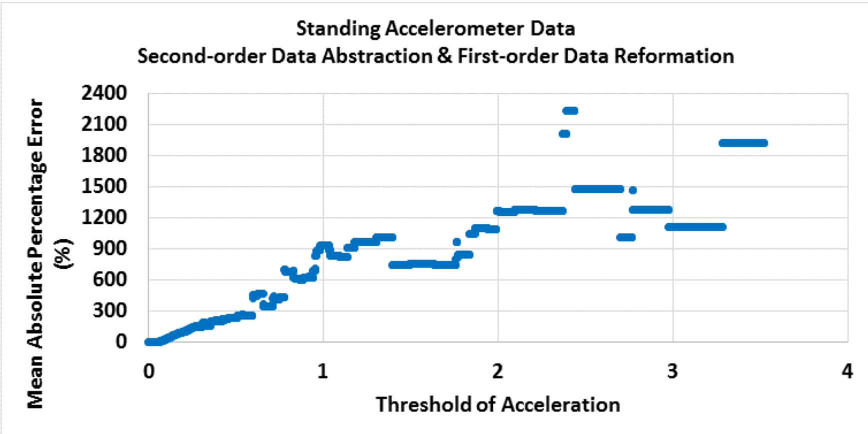

(h) Mean absolute percentage error of standing accelerometer data in second-order data abstraction & first-order data reformation

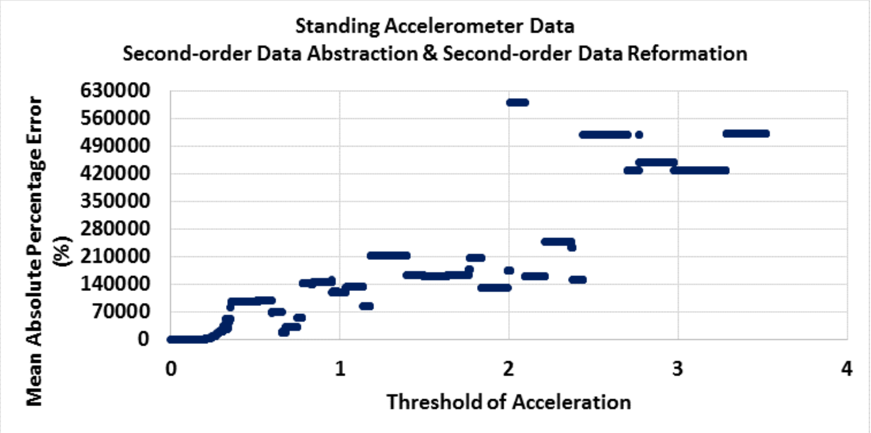

(i) Mean absolute percentage error of standing accelerometer data in second-order data abstraction & second-order data reformation

Figure 5.20: Mean absolute percentage error of standing accelerometer data

From the Figure 5.20, it is shown that the increment of threshold value, threshold of rate and threshold of acceleration will not necessarily increase the mean absolute percentage error.

5.2.3 Walking Accelerometer Data

In this experiment, the number of the packets of data is 3000. The results of implementation of the DAR schemes in the terms of data abstraction (number of packet transmissions and number of data transmitted) and data reformation (RMSE and MAPE) are as follows.

1. Number of Packet Transmissions

Number of packet transmissions of walking accelerometer data in different orders of data abstraction are shown in Figure 5.21.

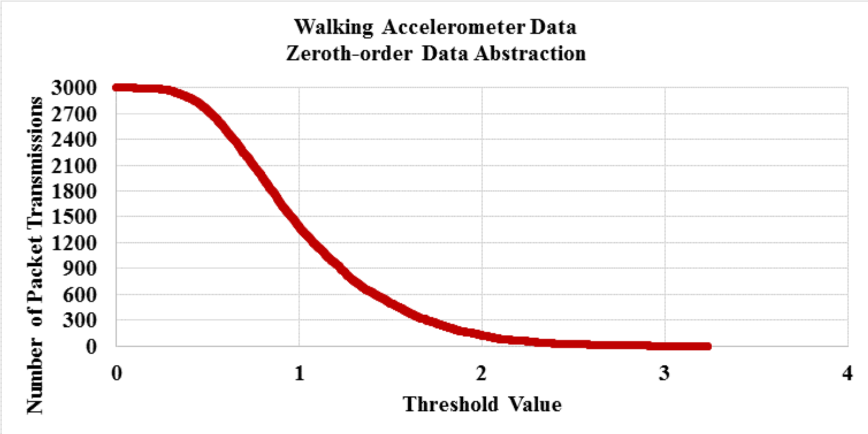

(a) Number of packet transmissions of walking accelerometer data in zeroth-order data abstraction

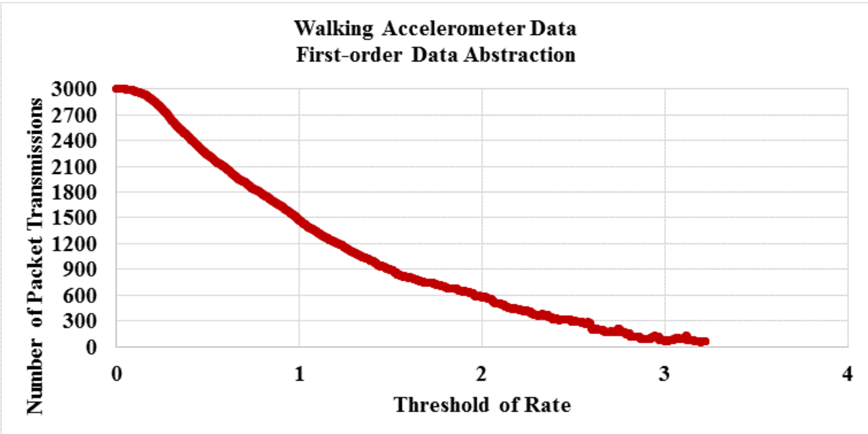

(b) Number of packet transmissions of walking accelerometer data in first-order data abstraction

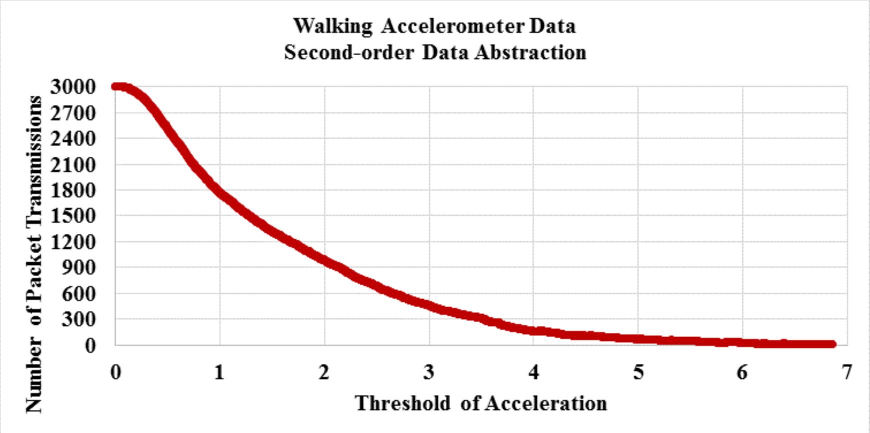

(c) Number of packet transmissions of walking accelerometer data in second-order data abstraction

Figure 5.21: Number of packet transmissions of walking accelerometer data

From the Figure 5.21, it is shown that the increment of threshold value will reduce the number of packet transmissions. However, the increment of threshold of rate and threshold of acceleration will not necessarily reduce the number.

2. Number of Data Transmitted

Number of data transmitted of walking accelerometer data in different orders of data abstraction are shown in Figure 5.22.

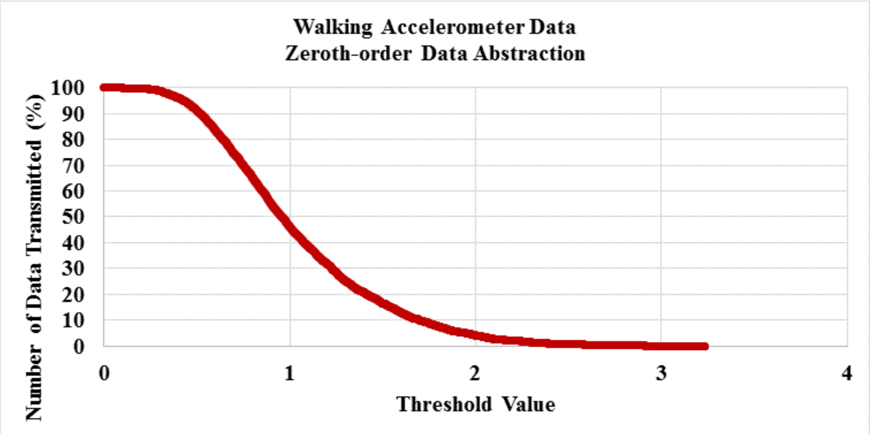

(a) Number of data transmitted of walking accelerometer data in zeroth-order data abstraction

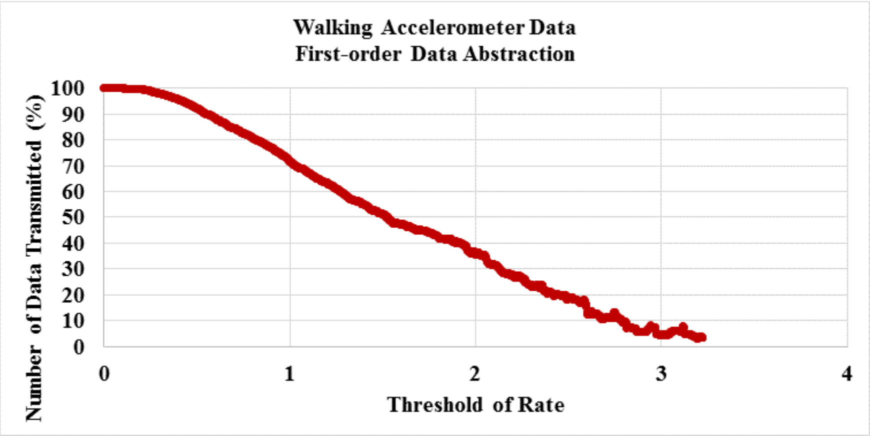

(b) Number of data transmitted of walking accelerometer data in first-order data abstraction

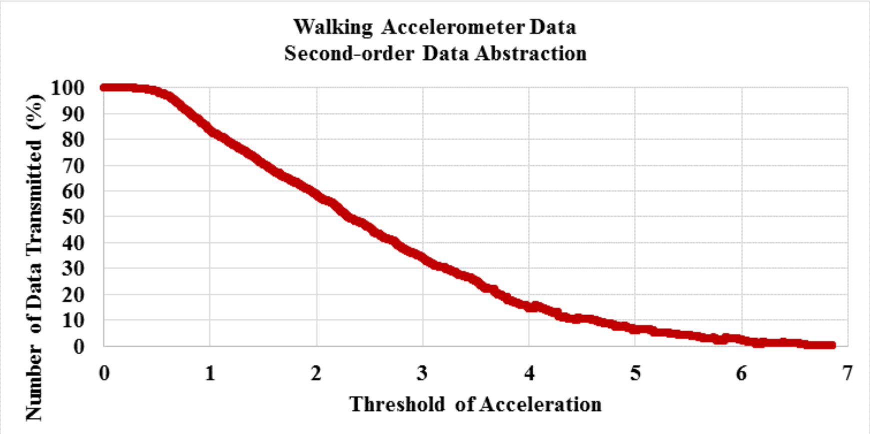

(c) Number of data transmitted of walking accelerometer data in second-order data abstraction

Figure 5.22: Number of data transmitted of walking accelerometer data

From the Figure 5.22, it is shown that the increment of threshold value will always reduce the number of data transmitted. However, the increment of threshold of rate and threshold of acceleration will not necessarily reduce the number of data transmitted.

3. Root Mean Square Error

Root mean square error of walking accelerometer data in different orders of data abstraction and reformation are shown from Figure 5.23.

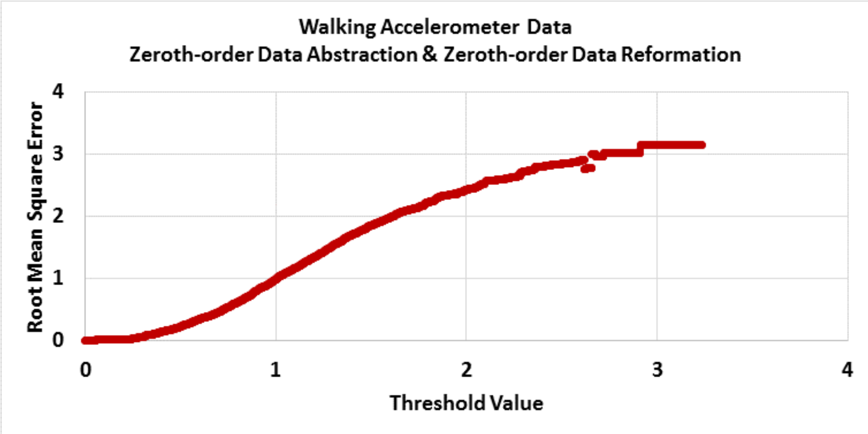

(a) Root mean square error of walking accelerometer data in zeroth-order data abstraction & zeroth-order data reformation

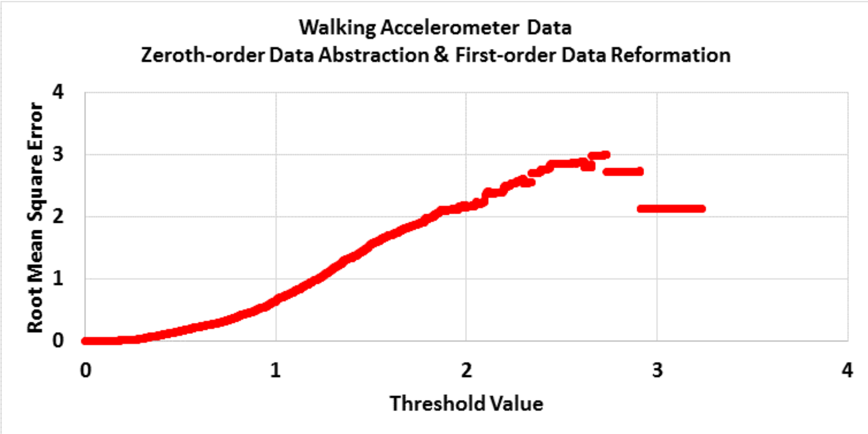

(b) Root mean square error of walking accelerometer data in zeroth-order data abstraction & first-order data reformation

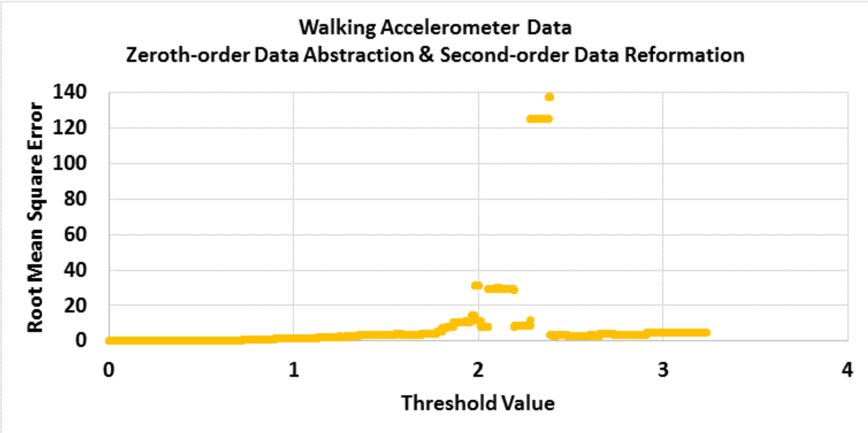

(c) Root mean square error of walking accelerometer data in zeroth-order data abstraction & second-order data reformation

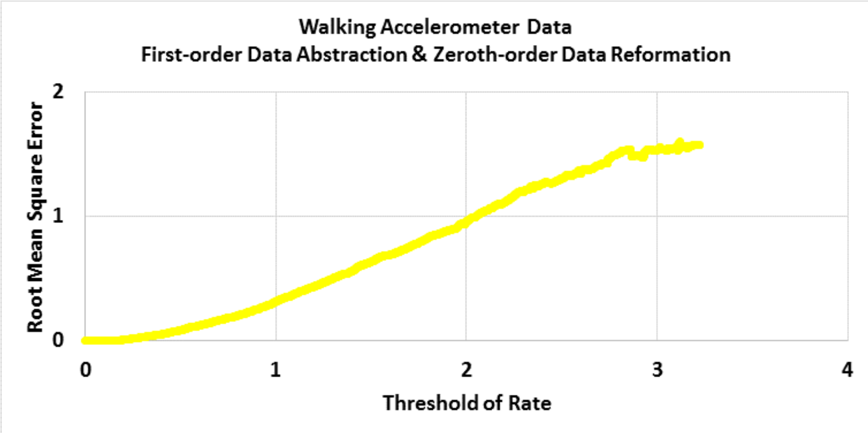

(d) Root mean square error of walking accelerometer data in first-order data abstraction & zeroth-order data reformation

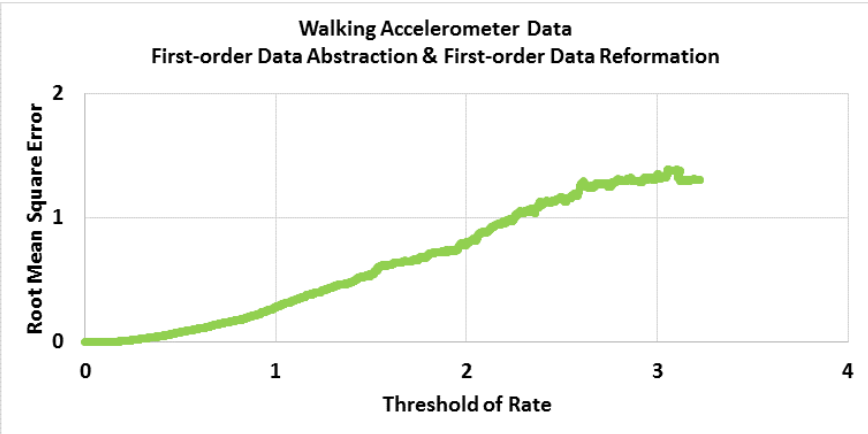

(e) Root mean square error of walking accelerometer data in first-order data abstraction & first-order data reformation

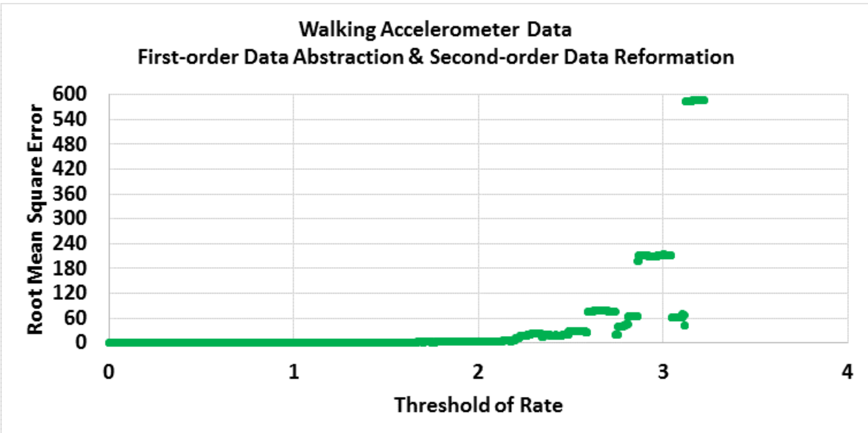

(f) Root mean square error of walking accelerometer data in first-order data abstraction & second-order data reformation

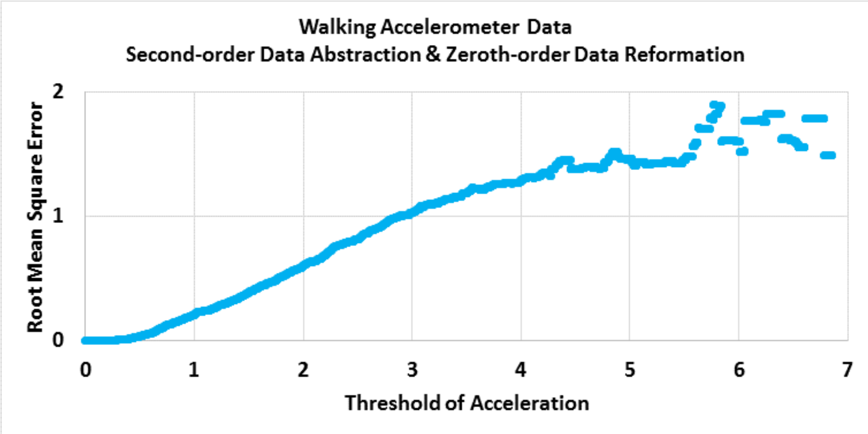

(g) Root mean square error of walking accelerometer data in second-order data abstraction & zeroth-order data reformation

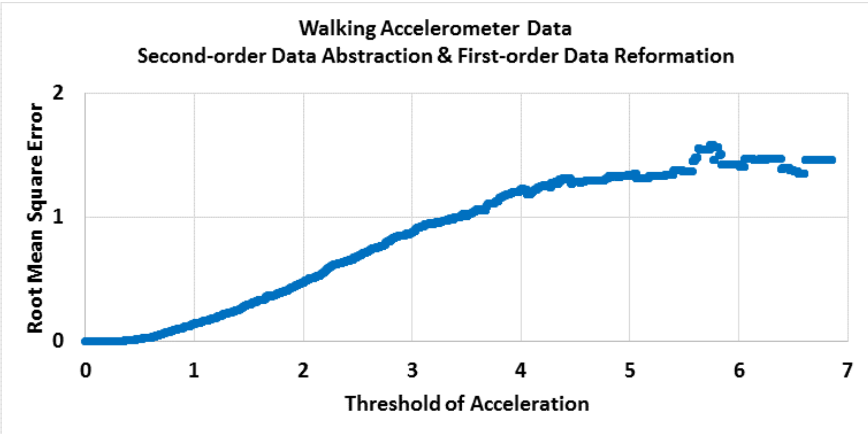

(h) Root mean square error of walking accelerometer data in second-order data abstraction & first-order data reformation

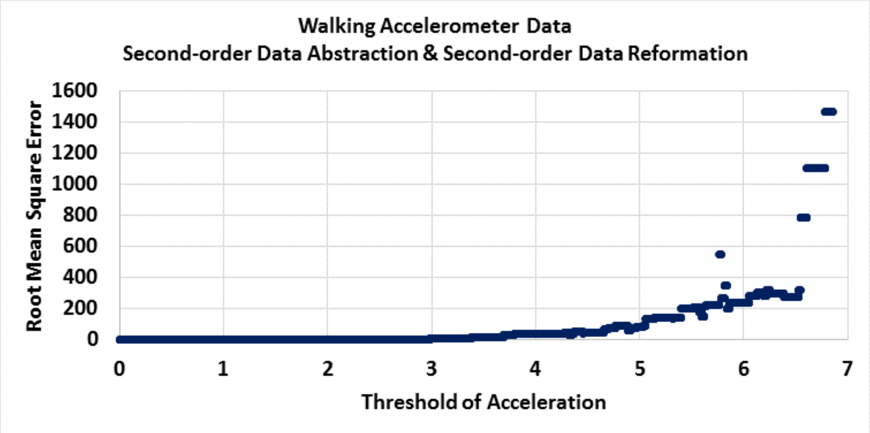

(i) Root mean square error of walking accelerometer data in second-order data abstraction & second-order data reformation

Figure 5.23: Root mean square error of walking accelerometer data

From the Figure 5.23, it is shown that the increment of threshold value, threshold of rate and threshold of acceleration will not necessarily increase the root mean square error.

4. Mean Absolute Percentage Error

Mean absolute percentage error of walking accelerometer data in different orders of data abstraction are shown from Figure 5.24.

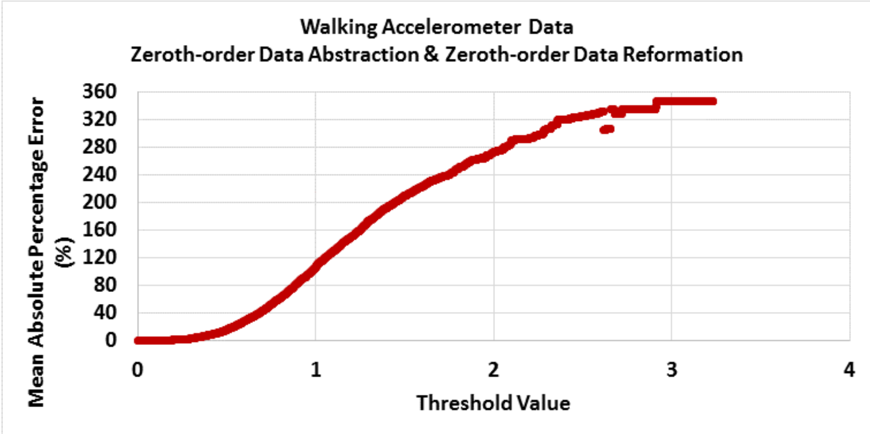

(a) Mean absolute percentage error of walking accelerometer data in zeroth-order data abstraction & zeroth-order data reformation

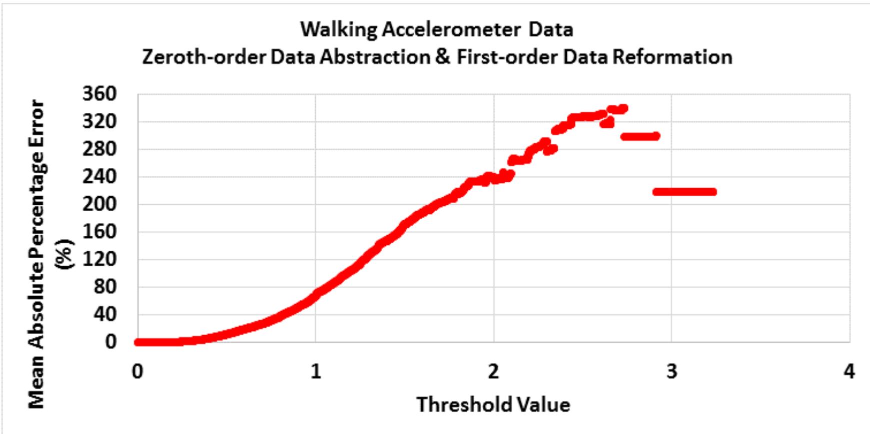

(b) Mean absolute percentage error of walking accelerometer data in zeroth-order data abstraction & first-order data reformation

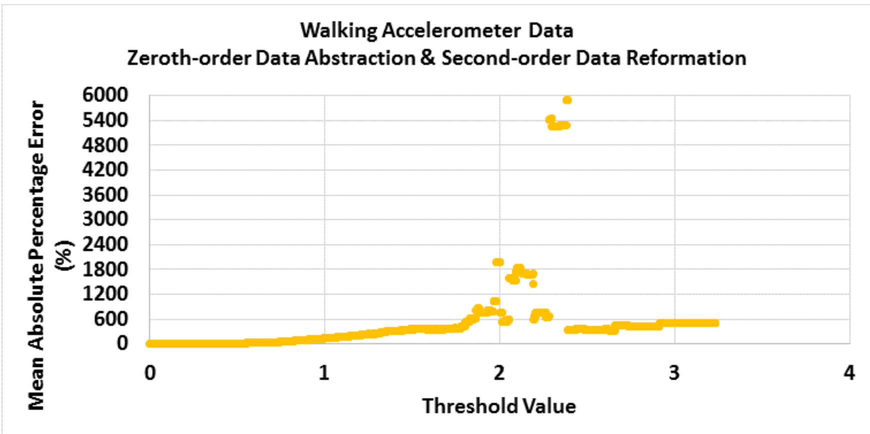

(c) Mean absolute percentage error of walking accelerometer data in zeroth-order data abstraction & second-order data reformation

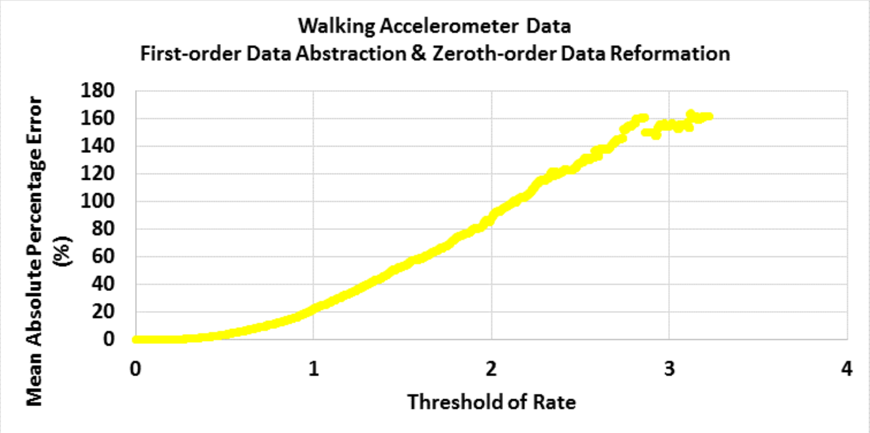

(d) Mean absolute percentage error of walking accelerometer data in first-order data abstraction & zeroth-order data reformation

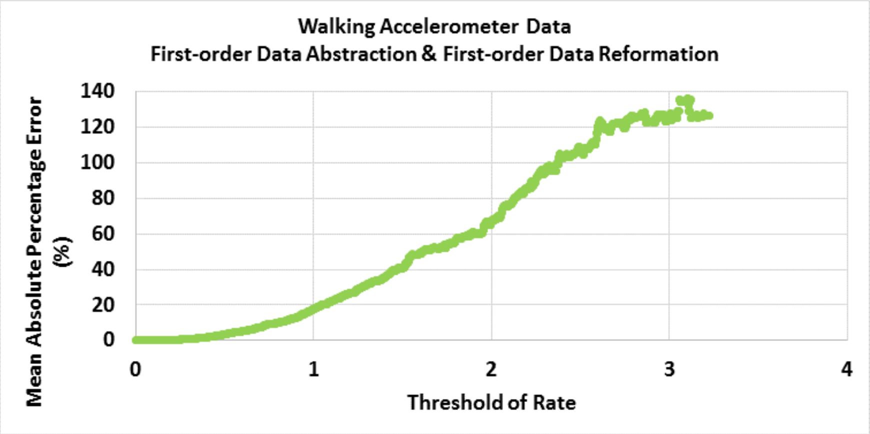

(e) Mean absolute percentage error of walking accelerometer data in first-order data abstraction & first-order data reformation

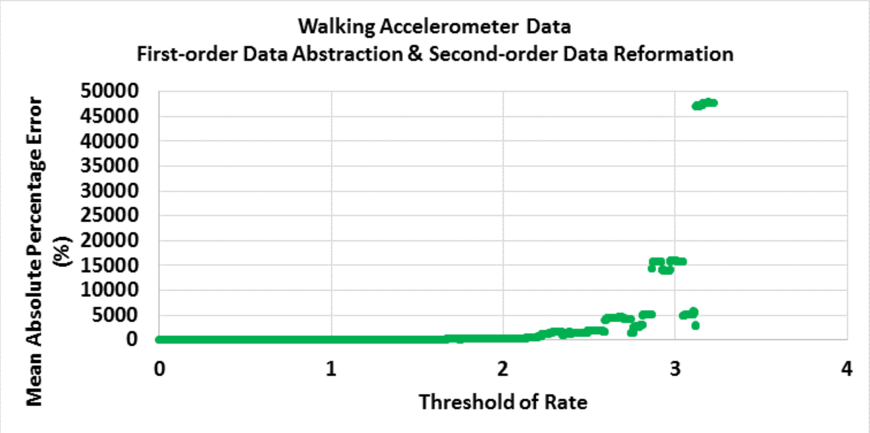

(f) Mean absolute percentage error of walking accelerometer data in first-order data abstraction & second-order data reformation

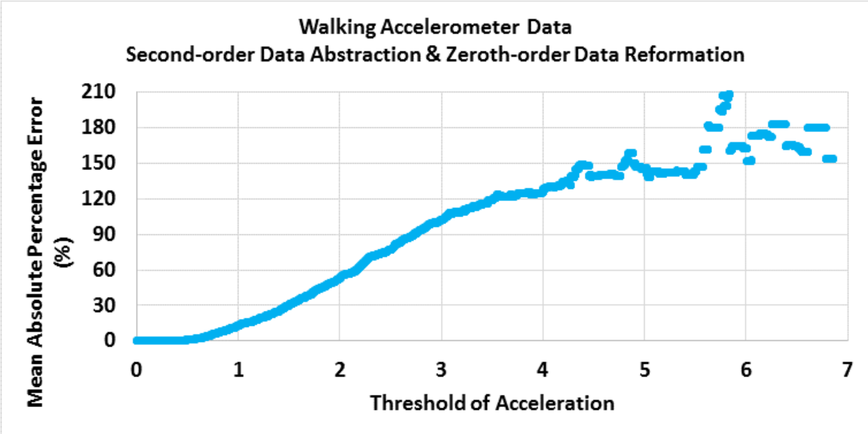

(g) Mean absolute percentage error of walking accelerometer data in second-order data abstraction & zeroth-order data reformation

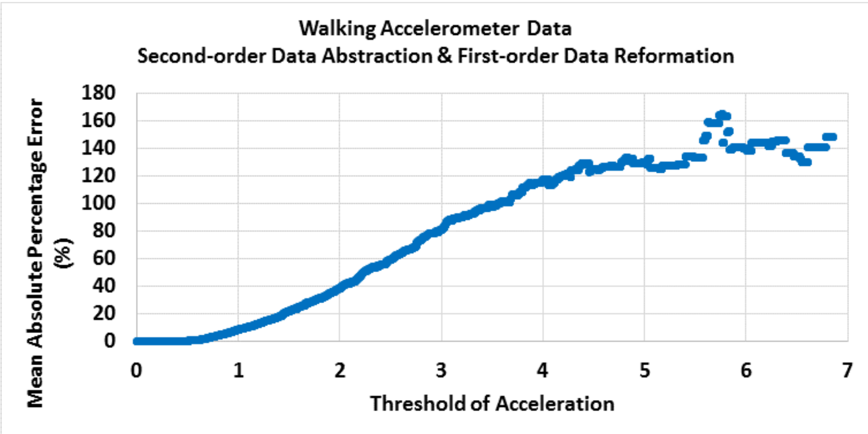

(h) Mean absolute percentage error of walking accelerometer data in second-order data abstraction & first-order data reformation

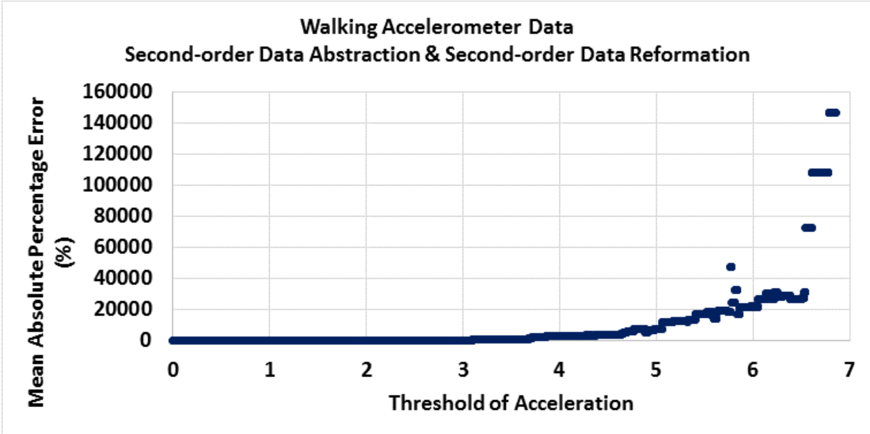

(i) Mean absolute percentage error of walking accelerometer data in second-order data abstraction & second-order data reformation

Figure 5.24: Mean absolute percentage error of walking accelerometer data

From the Figure 5.24, it is shown that the increment of threshold value, threshold of rate and threshold of acceleration will not necessarily increase the mean absolute percentage error.

5.2.4 Running Accelerometer Data

In this experiment, the number of the packets of data is 3000. The results of implementation of the DAR schemes in the terms of data abstraction (number of packet transmissions and number of data transmitted) and data reformation (RMSE and MAPE) are as follows.

1. Number of Packet Transmissions

   Number of packet transmissions of running accelerometer data in different orders of data abstraction are shown in Figure 5.25.

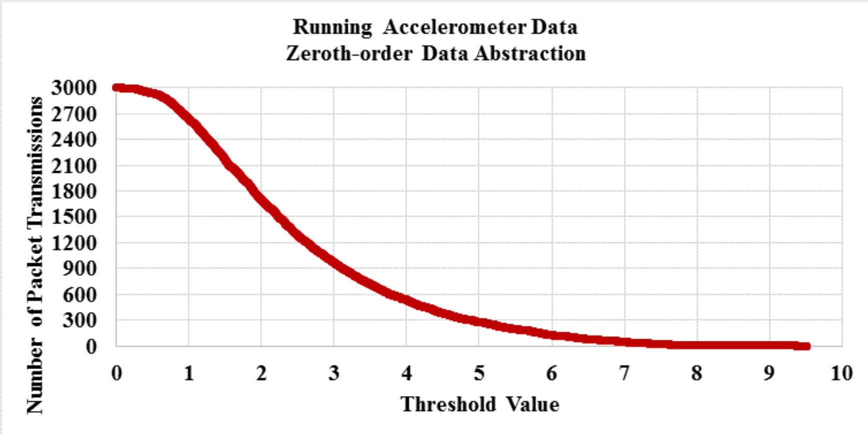

(a) Number of packet transmissions of running accelerometer data in zeroth-order data abstraction

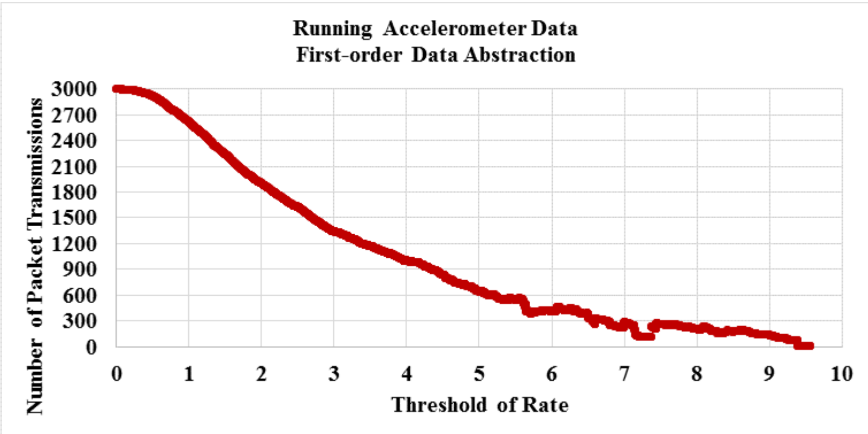

(b) Number of packet transmissions of running accelerometer data in first-order data abstraction

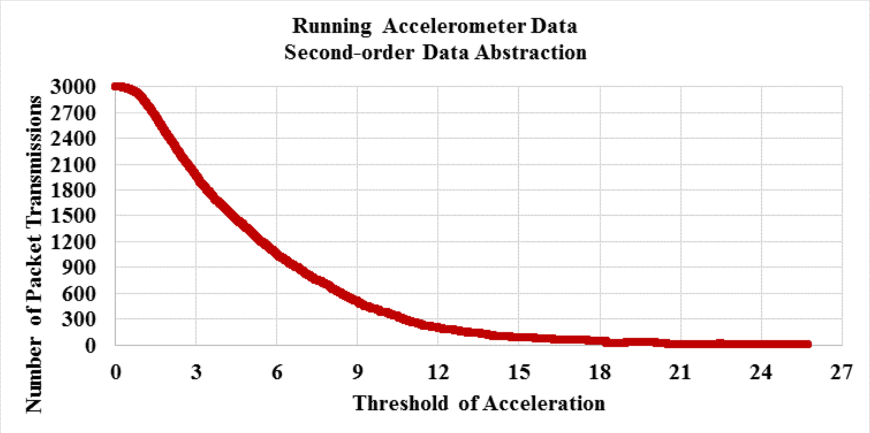

(c) Number of packet transmissions of running accelerometer data in second-order data abstraction

Figure 5.25: Number of packet transmissions of running accelerometer data

From the Figure 5.25, it is shown that the increment of threshold value will reduce the number of packet transmissions. However, the increment of threshold of rate and threshold of acceleration will not necessarily reduce the number.

2. Number of Data Transmitted

Number of data transmitted of running accelerometer data in different orders of data abstraction are shown in Figure 5.26.

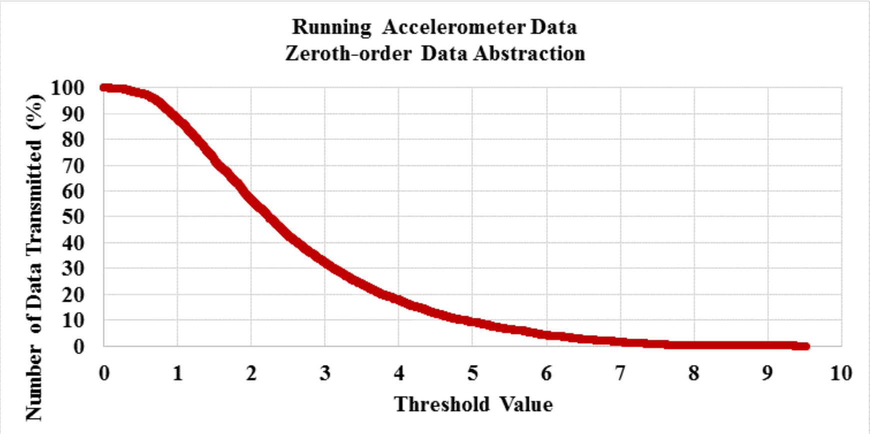

(a) Number of data transmitted of running accelerometer data in zeroth-order data abstraction

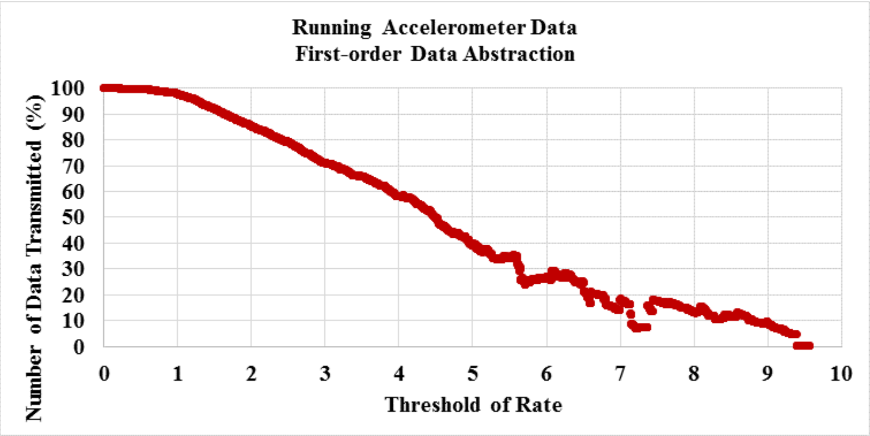

(b) Number of data transmitted of running accelerometer data in first-order data abstraction

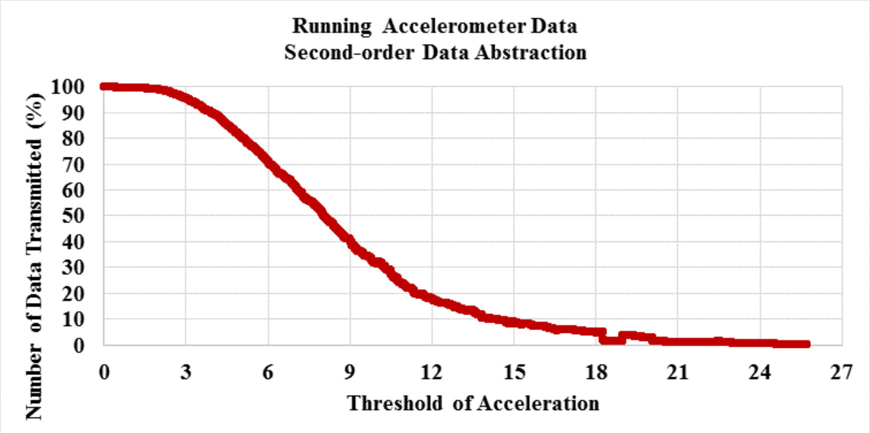

(c) Number of data transmitted of running accelerometer data in second-order data abstraction

Figure 5.26: Number of data transmitted of running accelerometer data

From the Figure 5.26, it is shown that the increment of threshold value will always reduce the number of data transmitted. However, the increment of threshold of rate and threshold of acceleration will not necessarily reduce the number of data transmitted.

3. Root Mean Square Error

Root mean square error of running accelerometer data in different orders of data abstraction and reformation are shown from Figure 5.27.

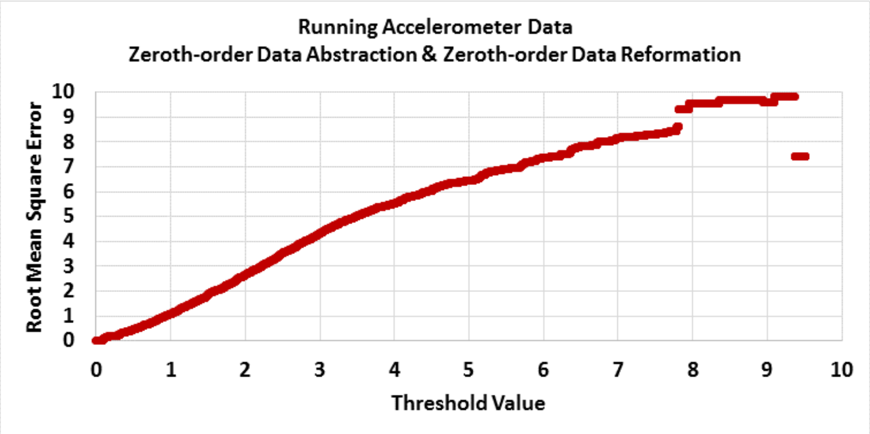

(a) Root mean square error of running accelerometer data in zeroth-order data abstraction & zeroth-order data reformation

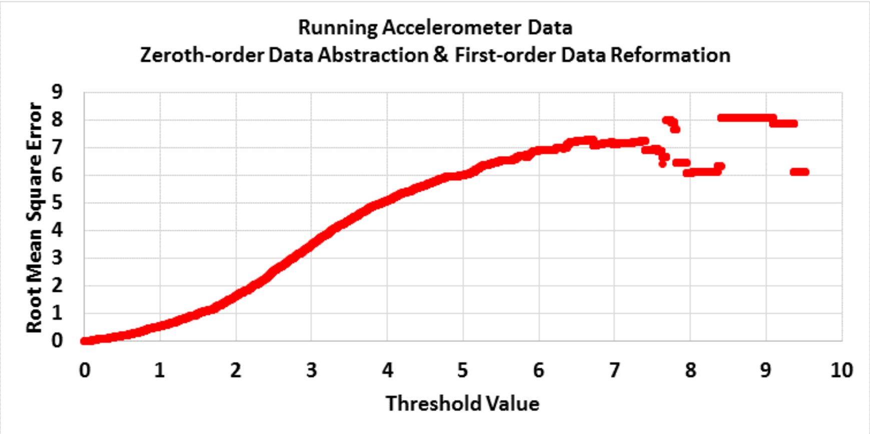

(b) Root mean square error of running accelerometer data in zeroth-order data abstraction & first-order data reformation

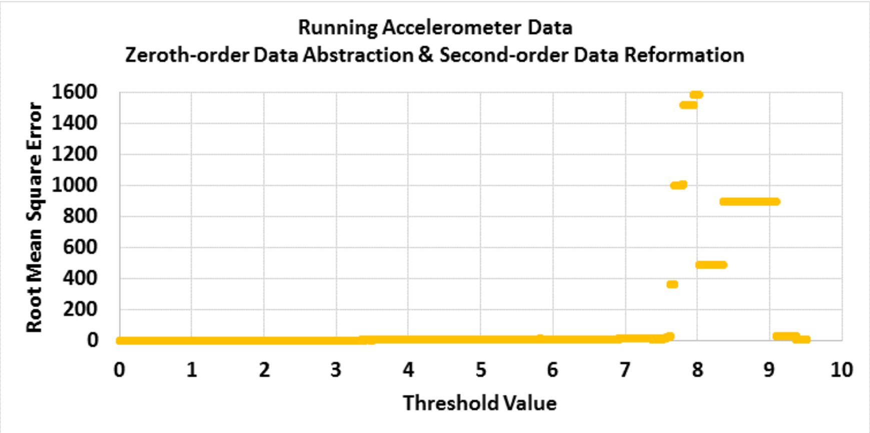

(c) Root mean square error of running accelerometer data in zeroth-order data abstraction & second-order data reformation

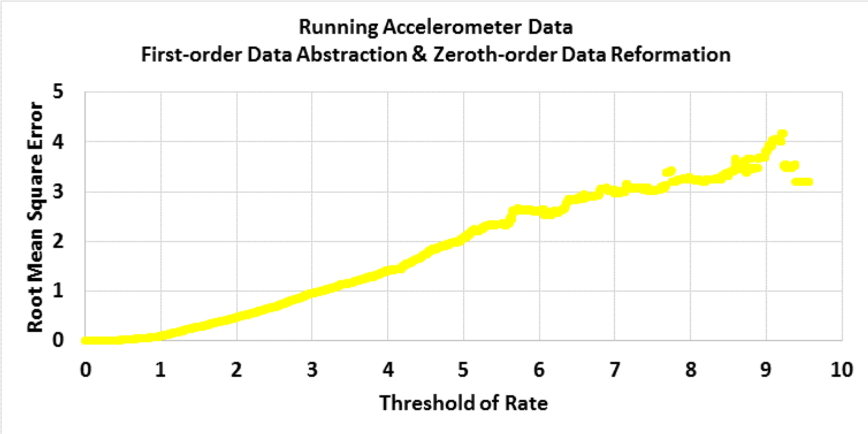

(d) Root mean square error of running accelerometer data in first-order data abstraction & zeroth-order data reformation

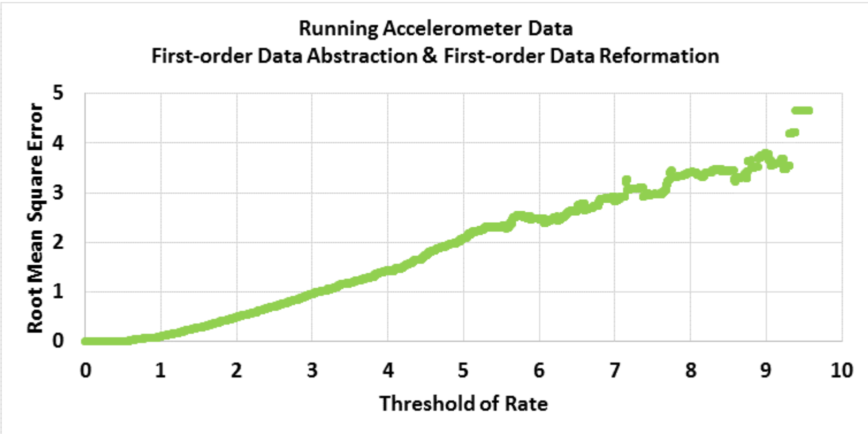

(e) Root mean square error of running accelerometer data in first-order data abstraction & first-order data reformation

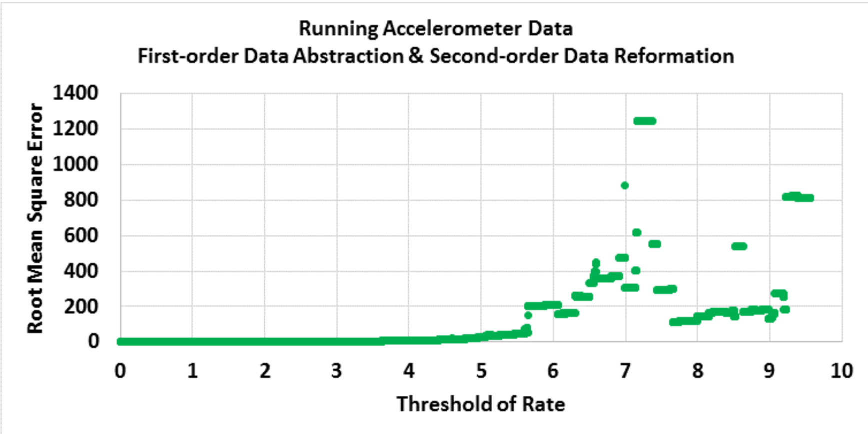

(f) Root mean square error of running accelerometer data in first-order data abstraction & second-order data reformation

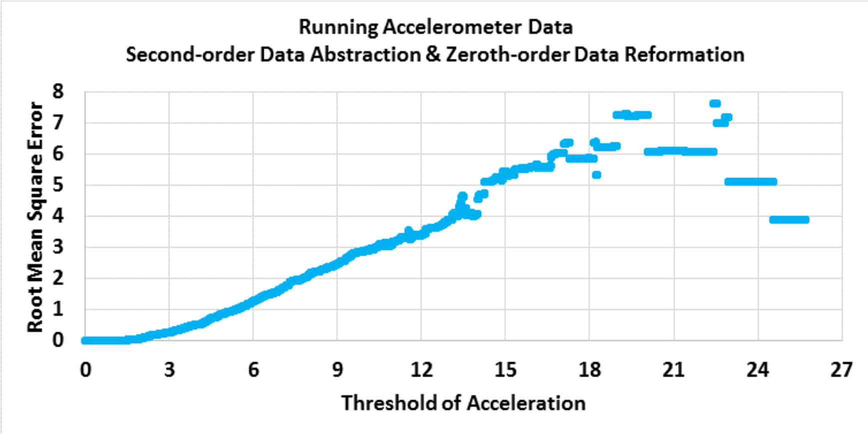

(g) Root mean square error of running accelerometer data in second-order data abstraction & zeroth-order data reformation

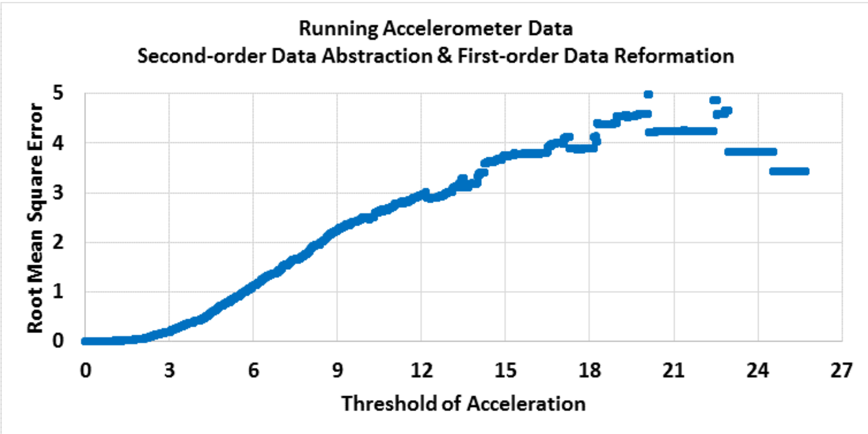

(h) Root mean square error of running accelerometer data in second-order data abstraction & first-order data reformation

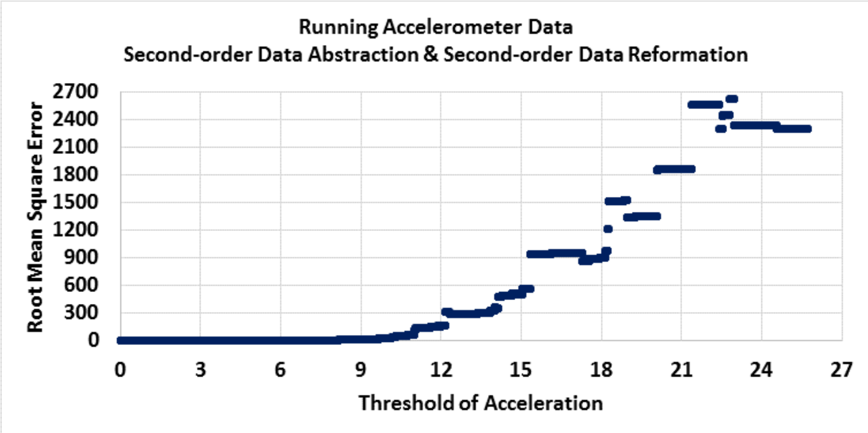

(i) Root mean square error of running accelerometer data in second-order data abstraction & second-order data reformation

Figure 5.27: Root mean square error of running accelerometer data

From the Figure 5.27, it is shown that the increment of threshold value, threshold of rate and threshold of acceleration will not necessarily increase the root mean square error.

4. Mean Absolute Percentage Error

Mean absolute percentage error of running accelerometer data in different orders of data abstraction are shown from Figure 5.28.

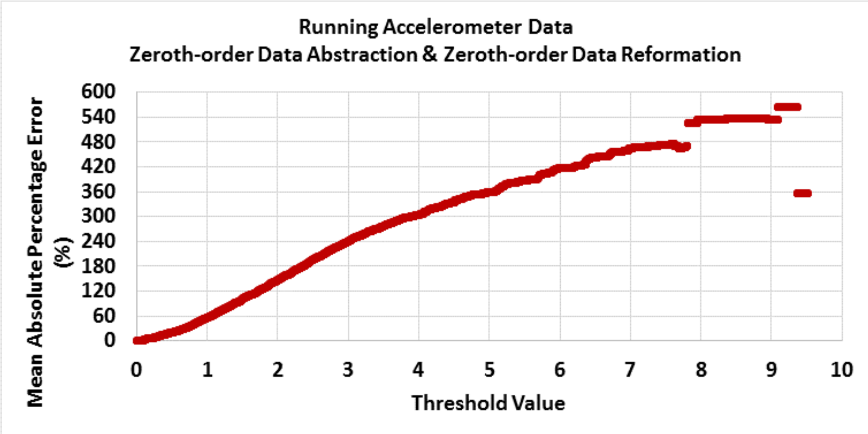

(a) Mean absolute percentage error of running accelerometer data in zeroth-order data abstraction & zeroth-order data reformation

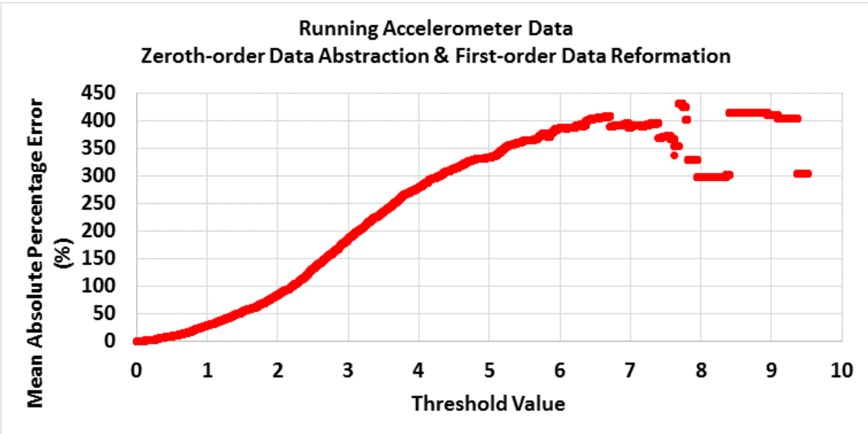

(b) Mean absolute percentage error of running accelerometer data in zeroth-order data abstraction & first-order data reformation

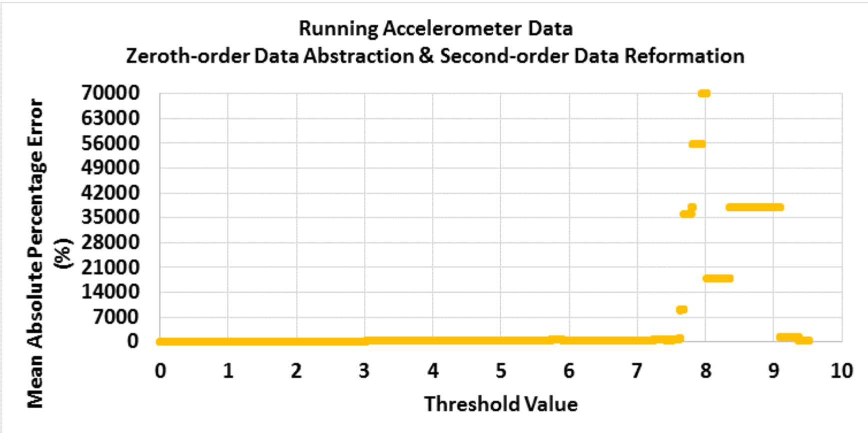

(c) Mean absolute percentage error of running accelerometer data in zeroth-order data abstraction & second-order data reformation

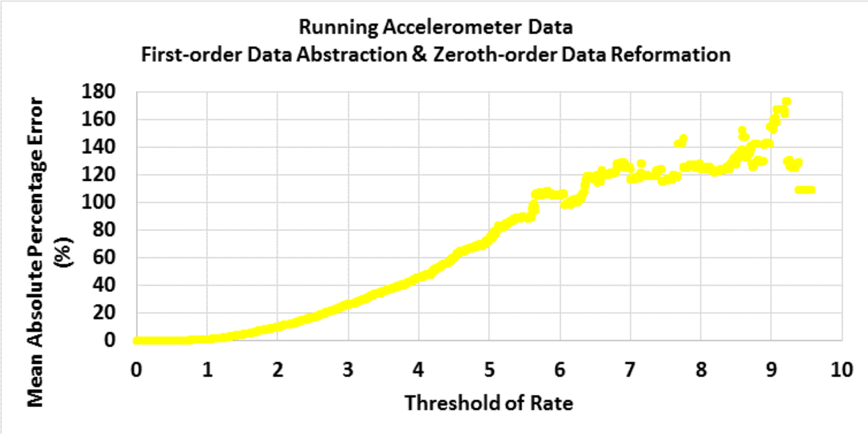

(d) Mean absolute percentage error of running accelerometer data in first-order data abstraction & zeroth-order data reformation

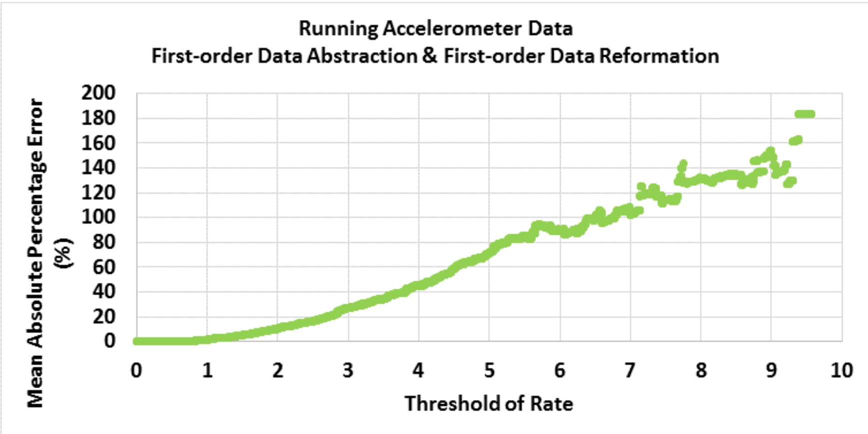

(e) Mean absolute percentage error of running accelerometer data in first-order data abstraction & first-order data reformation

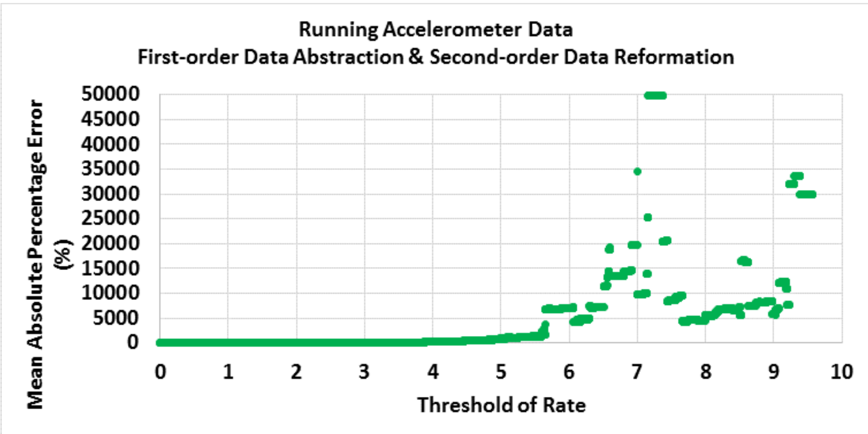

(f) Mean absolute percentage error of running accelerometer data in first-order data abstraction & second-order data reformation

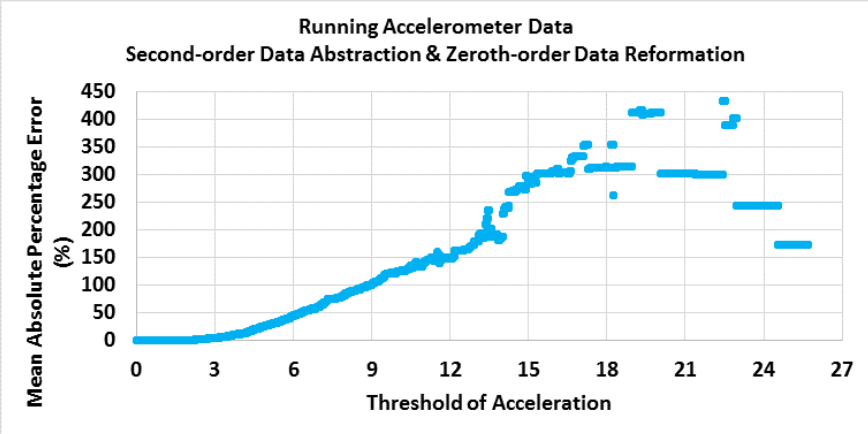

(g) Mean absolute percentage error of running accelerometer data in second-order data abstraction & zeroth-order data reformation

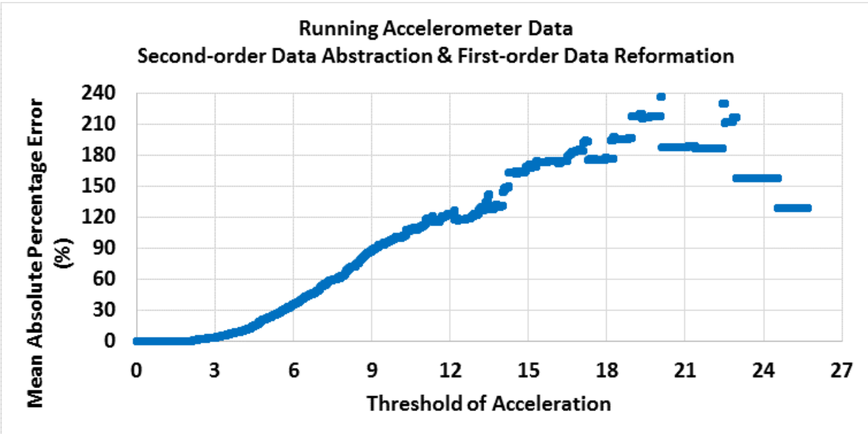

(h) Mean absolute percentage error of running accelerometer data in second-order data abstraction & first-order data reformation

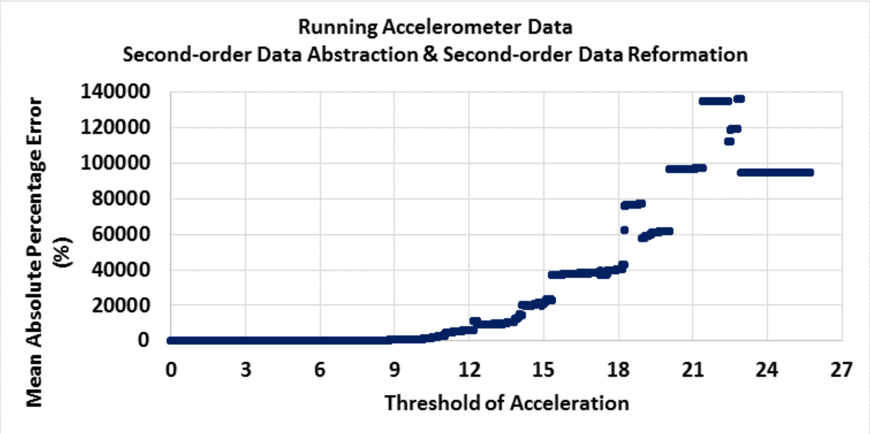

(i) Mean absolute percentage error of running accelerometer data in second-order data abstraction & second-order data reformation

Figure 5.28: Mean absolute percentage error of running accelerometer data

From the Figure 5.28, it is shown that the increment of threshold value, threshold of rate and threshold of acceleration will not necessarily increase the mean absolute percentage error.

5.3 Comparisons among Number of Packet Transmissions, Number of Data Transmitted, Root Mean Square Error, and Mean Absolute Percentage Error

This section will discuss the comparisons of parameters that are used to quantify the performance of the proposed scheme.

5.3.1 Burst Temperature Data

The comparisons among parameters (number of packet transmissions, number of data transmitted, root mean square error, and mean absolute percentage error) are as follows.

1. Number of Packet Transmissions vs. Root Mean Square Error

The comparisons of number of packet transmissions against root mean square error are shown in Figure 5.29.

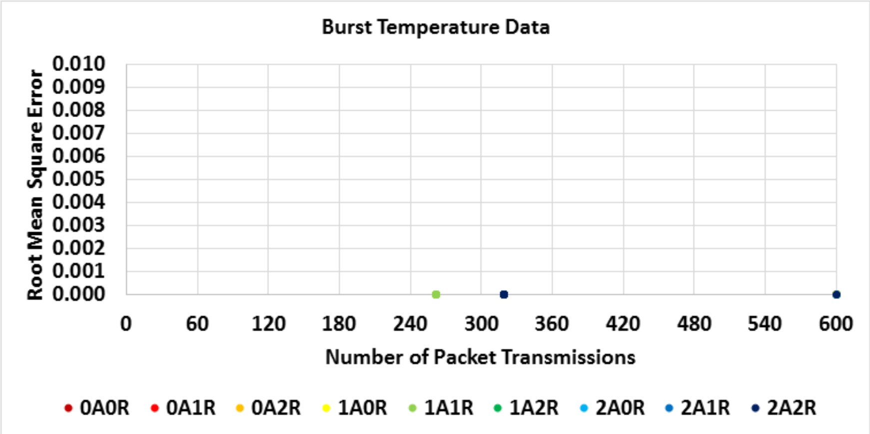

(a) Number of packet transmissions vs. root mean square error where

$$\boldsymbol{RMSE_{max} = 0.01}$$

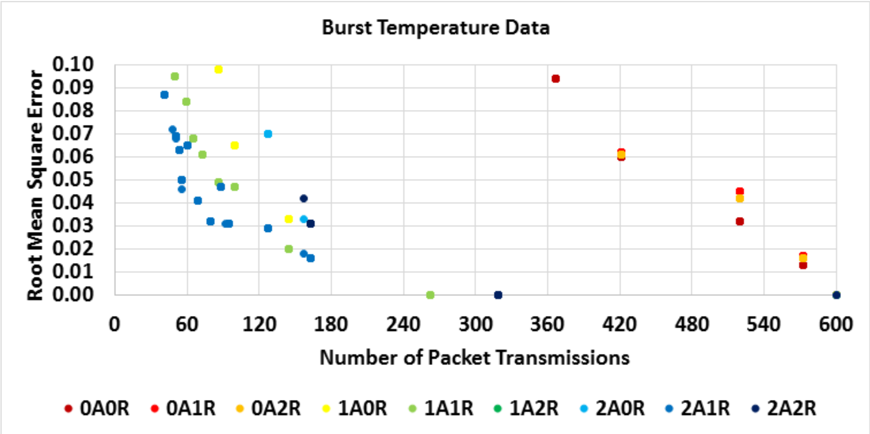

(b) Number of packet transmissions vs. root mean square error where

$$\boldsymbol{RMSE_{max} = 0.1}$$

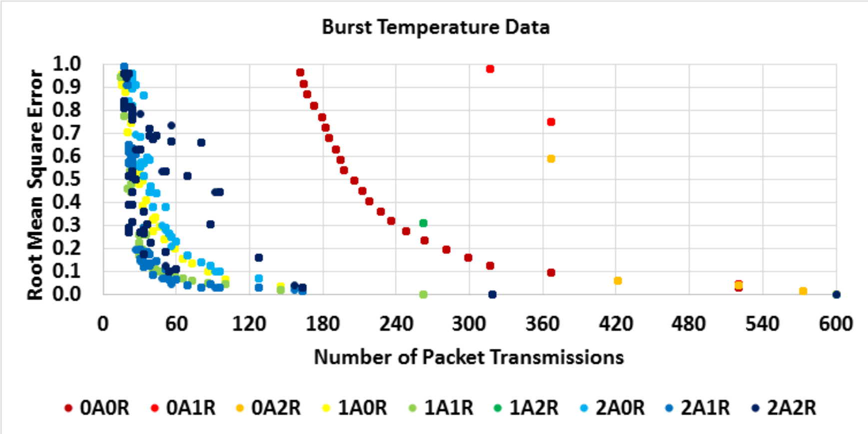

(c) Number of packet transmissions vs. root mean square error where

$$RMSE_{max} = 1$$

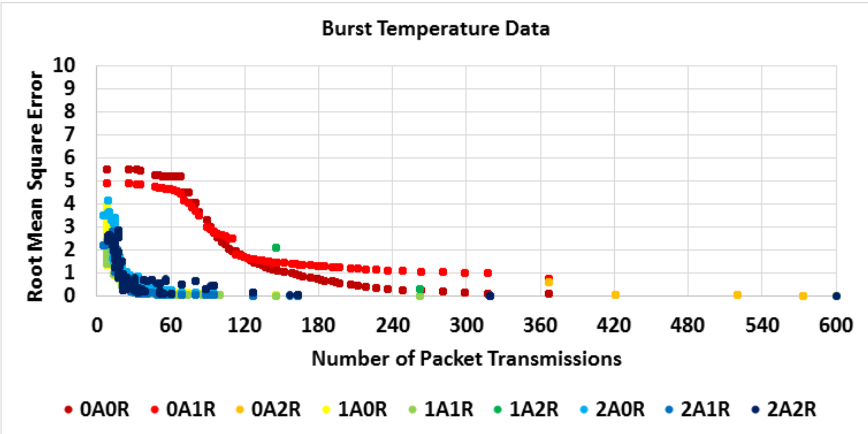

(d) Number of packet transmissions vs. root mean square error where

$$RMSE_{max} = 10$$

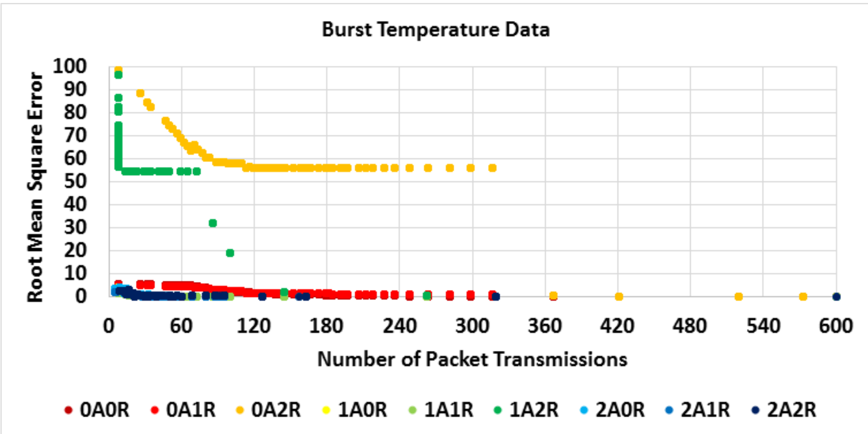

(e) Number of packet transmissions vs. root mean square error where

$$RMSE_{max} = 100$$

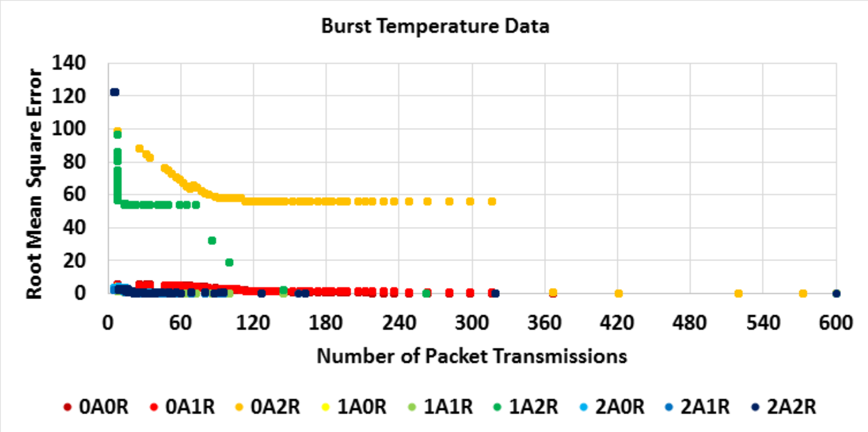

(f) Number of packet transmissions vs. root mean square error where $RMSE_{max} = 140$

Figure 5.29: Number of packet transmissions vs. root mean square error in burst temperature data

The results of DAR schemes in burst temperature data are shown more details in Table 5.2.

Table 5.2: Number of Packet Transmissions vs. Root Mean Square Error in Burst Temperature Data

RMSE	DAR	$NoPT_{min}$
= 0	0A0R	600
	0A1R	600
	0A2R	600
	1A0R	262
	1A1R	262
	1A2R	600
	2A0R	319
	2A1R	319
	2A2R	319

RMSE = root mean square error
DAR = data abstraction and reformation
0A0R = zeroth-order data abstraction & zeroth-order data reformation
0A1R = zeroth-order data abstraction & first-order data reformation
0A2R = zeroth-order data abstraction & second-order data reformation
1A0R = first-order data abstraction & zeroth-order data reformation
1A1R = first-order data abstraction & first-order data reformation
1A2R = first-order data abstraction & second-order data reformation
2A0R = second-order data abstraction & zeroth-order data reformation
2A1R = second-order data abstraction & first-order data reformation
2A2R = second-order data abstraction & second-order data reformation
$NoPT_{min}$ = minimum number of packet transmissions

From Table 5.2, it is shown that the best DAR schemes in burst temperature data where $RMSE = 0$ in the terms of number of packet transmissions are 1A0R and 1A1R.

2. Number of Packet Transmissions vs. Mean Absolute Percentage Error

The comparisons of number of packet transmissions against mean absolute percentage error are shown in Figure 5.30.

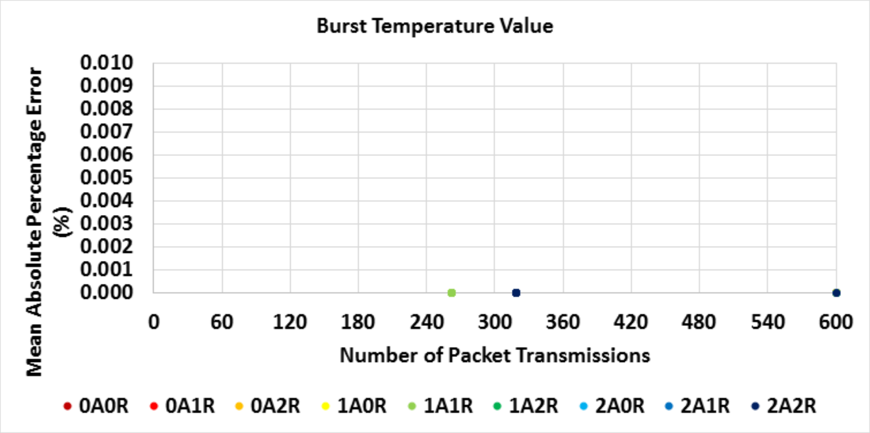

(a) Number of packet transmissions vs. mean absolute percentage error where $MAPE_{max} = 0.01\%$

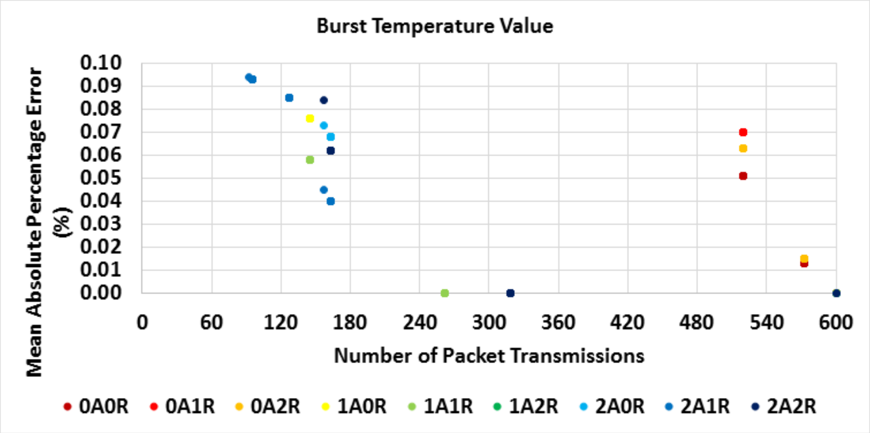

(b) Number of packet transmissions vs. mean absolute percentage error where $MAPE_{max} = 0.1\%$

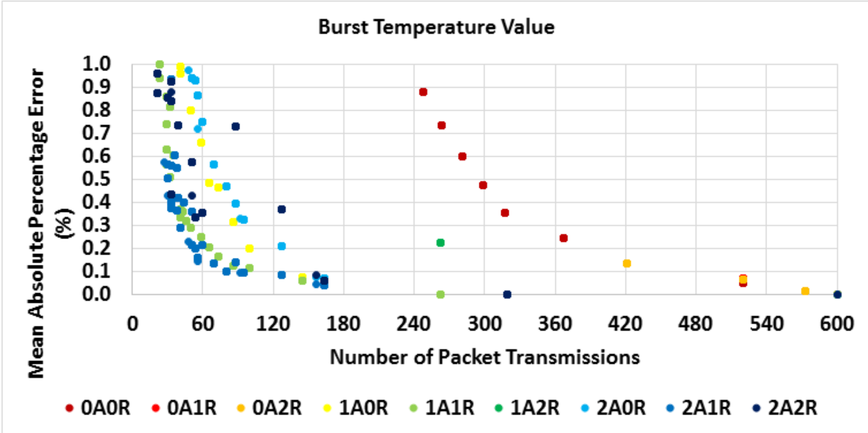

(c) Number of packet transmissions vs. mean absolute percentage error where $MAPE_{max} = 1\%$

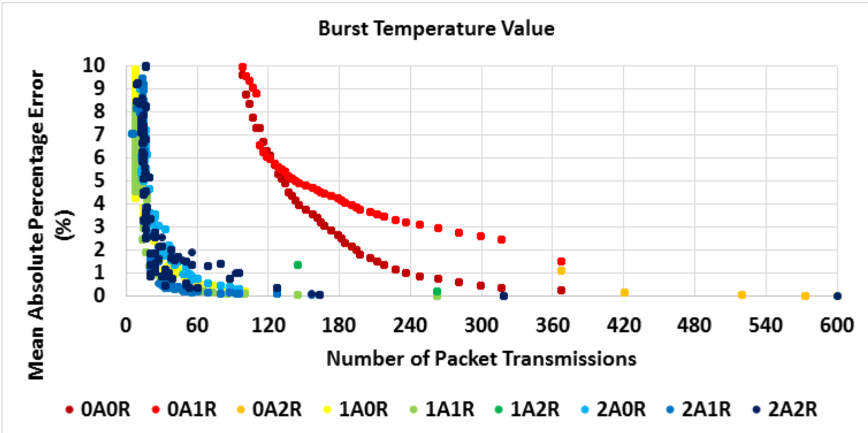

(d) Number of packet transmissions vs. mean absolute percentage error where $MAPE_{max} = 10\%$

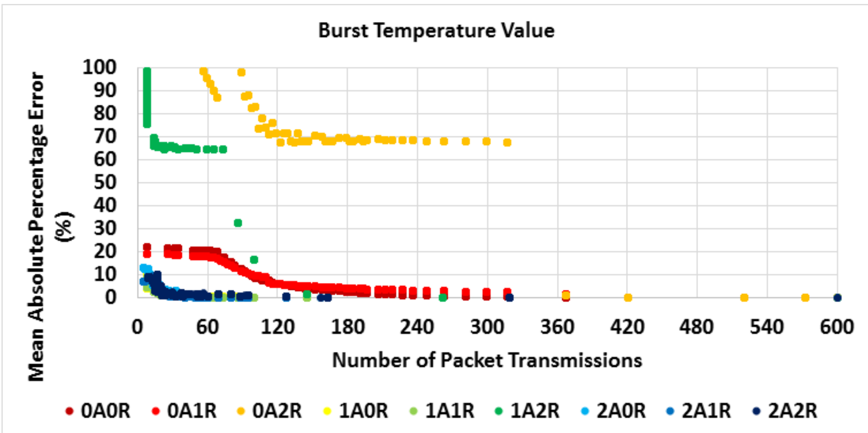

(e) Number of packet transmissions vs. mean absolute percentage error where $MAPE_{max} = 100\%$

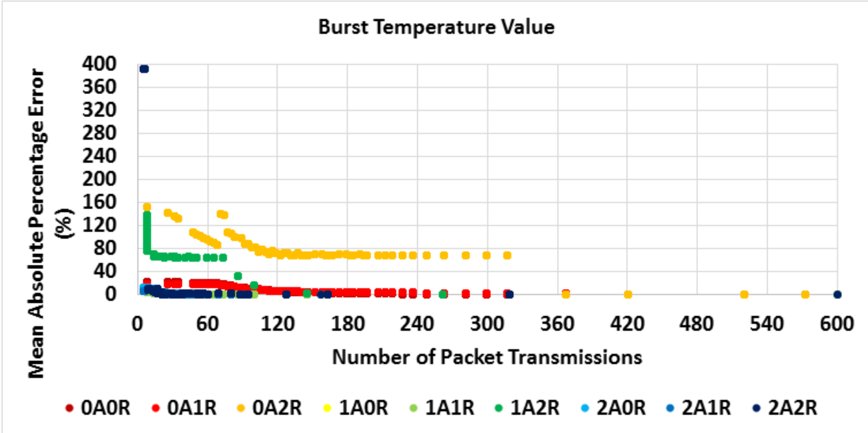

(f) Number of packet transmissions vs. mean absolute percentage error where $MAPE_{max} = 140\%$

Figure 5.30: Number of packet transmissions vs. mean absolute percentage error in burst temperature data

The results of DAR schemes in burst temperature data are shown more details in Table 5.3.

Table 5.3: Number of Packet Transmissions vs. Mean Absolute Percentage Error in Burst Temperature Data

MAPE	DAR	$NoPT_{min}$
= 0%	0A0R	600
	0A1R	600
	0A2R	600
	1A0R	262
	1A1R	262
	1A2R	600
	2A0R	319
	2A1R	319
	2A2R	319

MAPE = mean absolute percentage error
DAR = data Abstraction and Reformation
0A0R = zeroth-order data abstraction & zeroth-order data reformation
0A1R = zeroth-order data abstraction & first-order data reformation
0A2R = zeroth-order data abstraction & second-order data reformation
1A0R = first-order data abstraction & zeroth-order data reformation
1A1R = first-order data abstraction & first-order data reformation
1A2R = first-order data abstraction & second-order data reformation
2A0R = second-order data abstraction & zeroth-order data reformation
2A1R = second-order data abstraction & first-order data reformation
2A2R = second-order data abstraction & second-order data reformation
$NoPT_{min}$ = minimum number of packet transmissions

From Table 5.3, it is shown that the best DAR schemes in burst temperature data where $MAPE = 0\%$ in the terms of number of packet transmissions are 1A0R and 1A1R.

3. Number of Data Transmitted vs. Root Mean Square Error

The comparisons of number of data transmitted against root mean square error are shown in Figure 5.31.

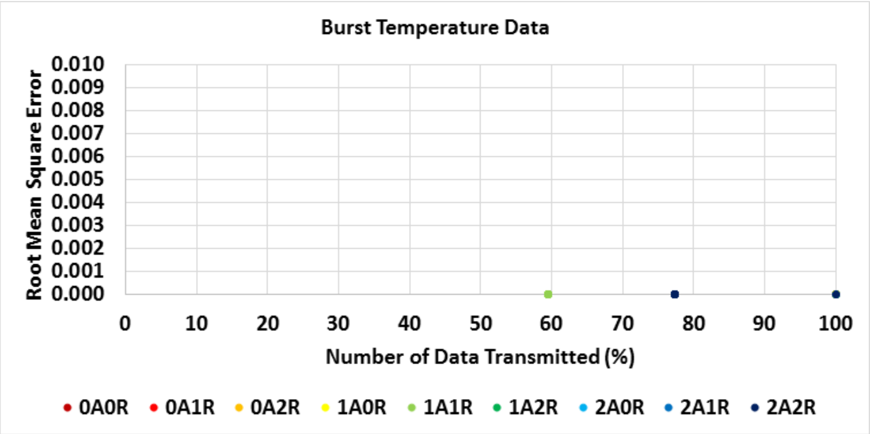

(a) Number of data transmitted vs. root mean square error where

$$\boldsymbol{RMSE_{max} = 0.01}$$

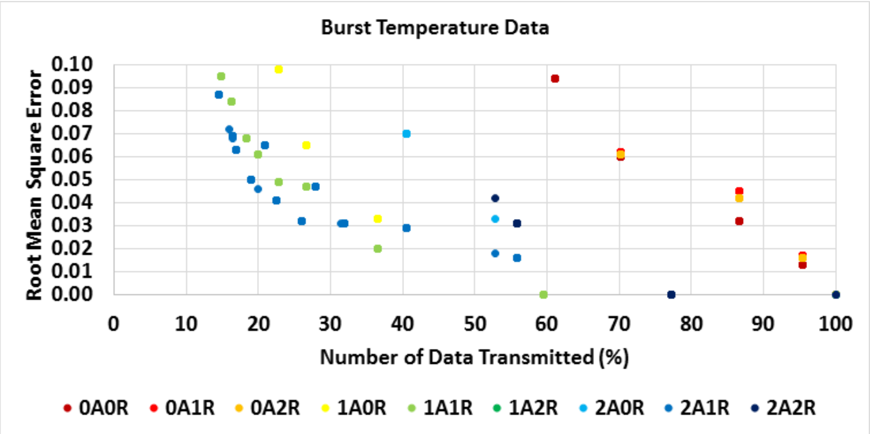

(b) Number of data transmitted vs. root mean square error where

$$\boldsymbol{RMSE_{max} = 0.1}$$

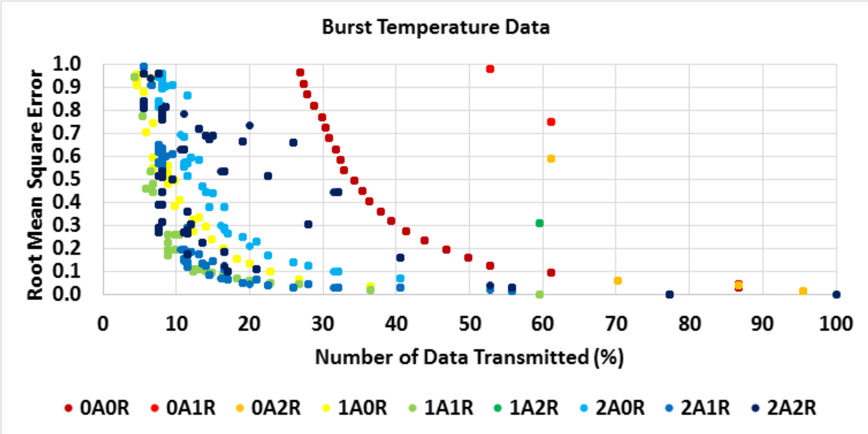

(c) Number of data transmitted vs. root mean square error where

$$RMSE_{max} = 1$$

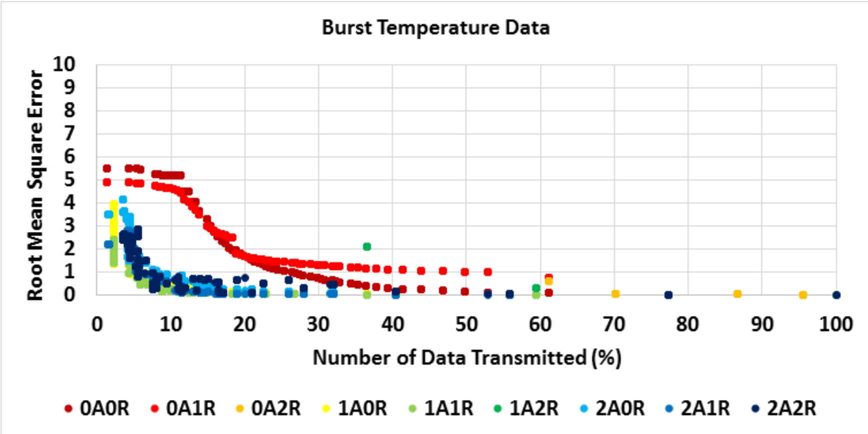

(d) Number of data transmitted vs. root mean square error where

$$RMSE_{max} = 10$$

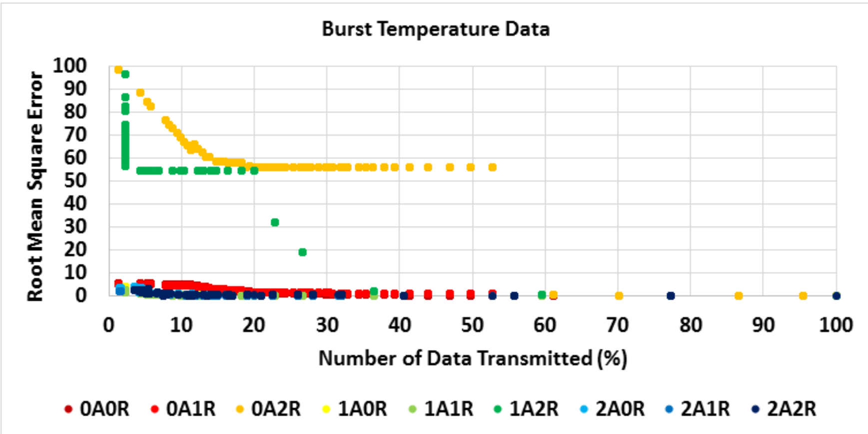

(e) Number of data transmitted vs. root mean square error where

$$RMSE_{max} = 100$$

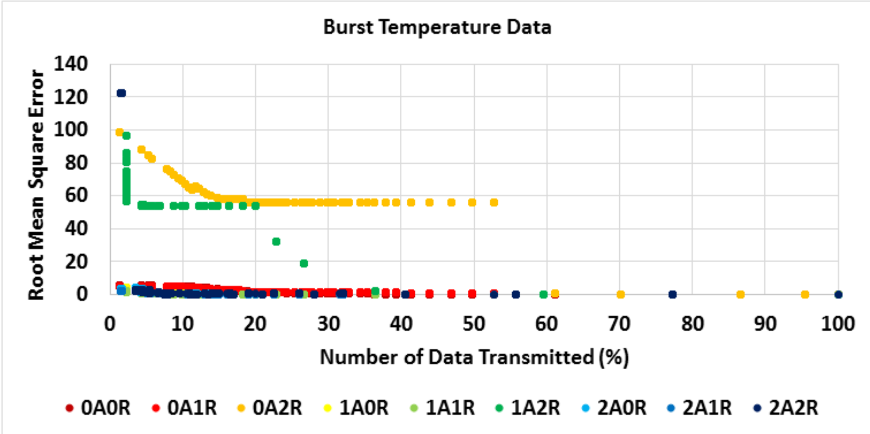

(f) Number of data transmitted vs. root mean square error where

$$RMSE_{max} = 140$$

Figure 5.31: Number of data transmitted vs. root mean square error in burst temperature data

The results of DAR schemes in burst temperature data are shown more details in Table 5.4.

Table 5.4: Number of Data Transmitted vs. Root Mean Square Error in Burst Temperature Data

RMSE	DAR	$NoDT_{min}$ (%)
= 0	0A0R	100.000
	0A1R	100.000
	0A2R	100.000
	1A0R	59.500
	1A1R	59.500
	1A2R	100.000
	2A0R	77.333
	2A1R	77.333
	2A2R	77.333

RMSE = root mean square error
DAR = data Abstraction and Reformation
0A0R = zeroth-order data abstraction & zeroth-order data reformation
0A1R = zeroth-order data abstraction & first-order data reformation
0A2R = zeroth-order data abstraction & second-order data reformation
1A0R = first-order data abstraction & zeroth-order data reformation
1A1R = first-order data abstraction & first-order data reformation
1A2R = first-order data abstraction & second-order data reformation
2A0R = second-order data abstraction & zeroth-order data reformation
2A1R = second-order data abstraction & first-order data reformation
2A2R = second-order data abstraction & second-order data reformation
$NoDT_{min}$ = minimum number of data transmitted

From Table 5.4, it is shown that the best DAR schemes in burst temperature data where $RMSE = 0$ in the terms of number of data transmitted are 1A0R and 1A1R.

4. Number of Data Transmitted vs. Mean Absolute Percentage Error

The comparisons of number of data transmitted against mean absolute percentage error are shown in Figure 5.32.

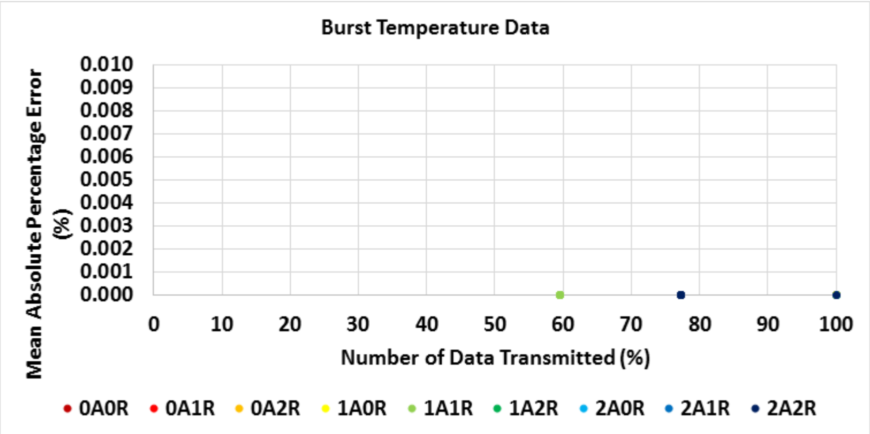

(a) Number of data transmitted vs. mean absolute percentage error where $MAPE_{max} = 0.01\%$

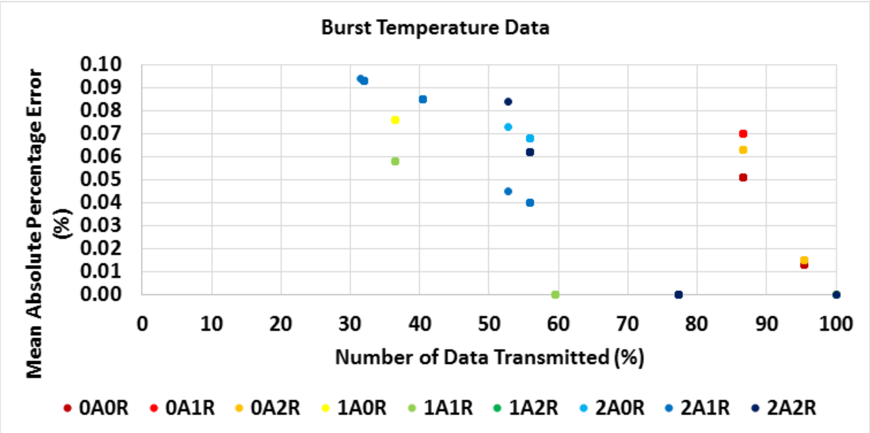

(b) Number of data transmitted vs. mean absolute percentage error where $MAPE_{max} = 0.1\%$

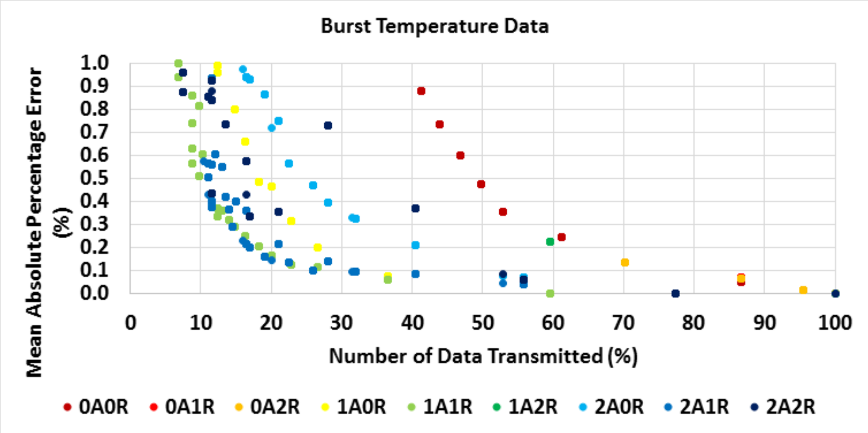

(c) Number of data transmitted vs. mean absolute percentage error where $MAPE_{max} = 1\%$

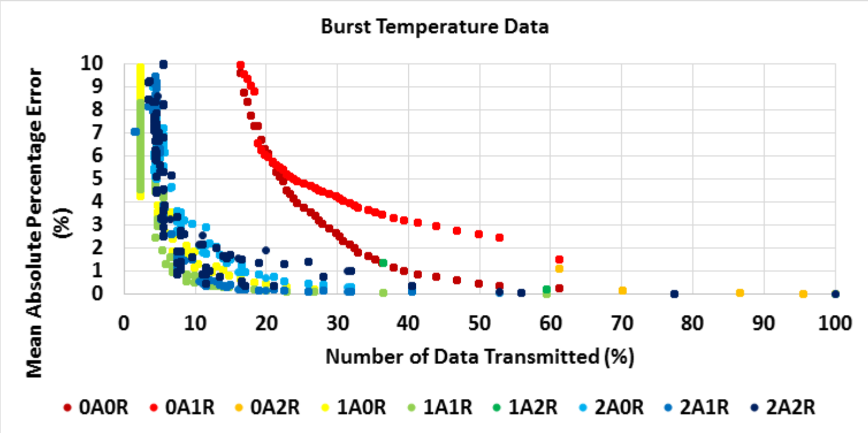

(d) Number of data transmitted vs. mean absolute percentage error where $MAPE_{max} = 10\%$

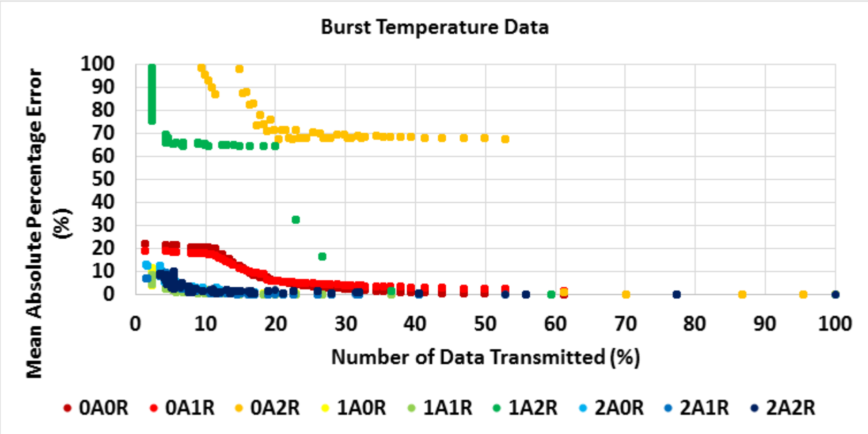

(e) Number of data transmitted vs. mean absolute percentage error where $MAPE_{max} = 100\%$

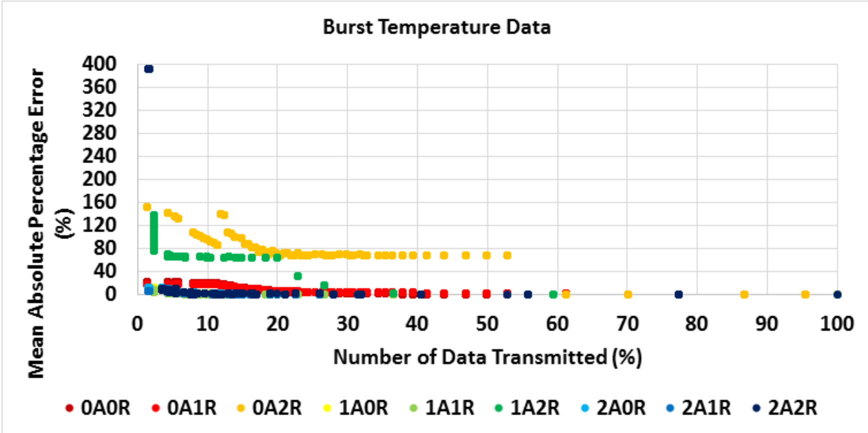

(f) Number of data transmitted vs. mean absolute percentage error where

$$MAPE_{max} = 400\%$$

Figure 5.32: Number of data transmitted vs. mean absolute percentage error in burst temperature data

The results of DAR schemes in burst temperature data are shown more details in Table 5.5.

Table 5.5: Number of Data Transmitted vs. Mean Absolute Percentage Error in Burst Temperature Data

MAPE	DAR	$NoDT_{min}$ (%)
= 0%	0A0R	100.000
	0A1R	100.000
	0A2R	100.000
	1A0R	59.500
	1A1R	59.500
	1A2R	100.000
	2A0R	77.333
	2A1R	77.333
	2A2R	77.333

MAPE = mean absolute percentage error
DAR = data Abstraction and Reformation
0A0R = zeroth-order data abstraction & zeroth-order data reformation
0A1R = zeroth-order data abstraction & first-order data reformation
0A2R = zeroth-order data abstraction & second-order data reformation
1A0R = first-order data abstraction & zeroth-order data reformation
1A1R = first-order data abstraction & first-order data reformation
1A2R = first-order data abstraction & second-order data reformation
2A0R = second-order data abstraction & zeroth-order data reformation
2A1R = second-order data abstraction & first-order data reformation
2A2R = second-order data abstraction & second-order data reformation
$NoDT_{min}$ = minimum number of data transmitted

From Table 5.5, it is shown that the best DAR schemes in burst temperature data where $MAPE = 0\%$ in the terms of number of data transmitted are 1A0R and 1A1R.

5. Root Mean Square Error vs. Number of Packet Transmissions

The comparisons of root mean square error against number of packet transmissions are shown in Figure 5.33.

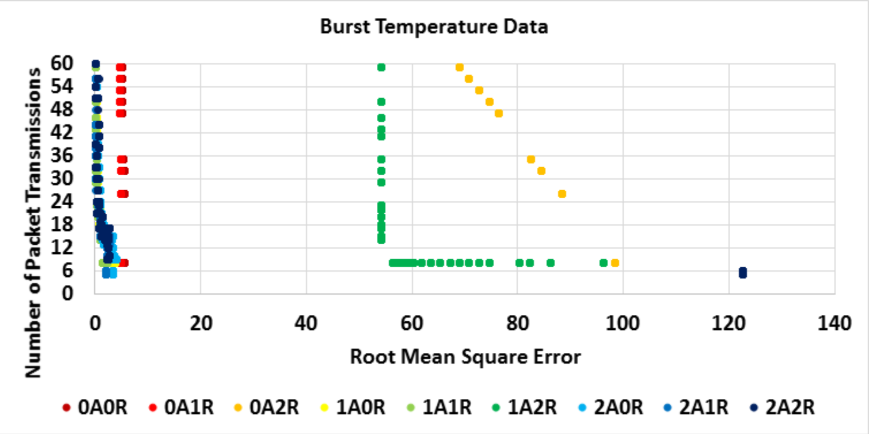

(a) Root mean square error vs. number of packet transmissions where $NoPT_{max} = 60$

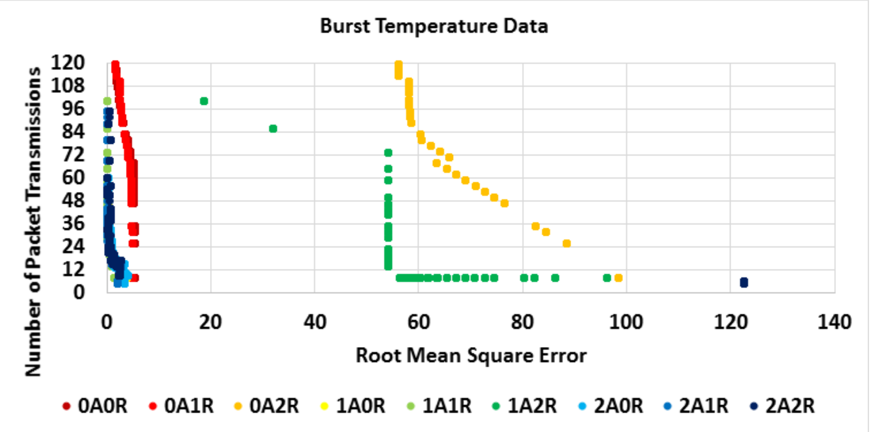

(b) Root mean square error vs. number of packet transmissions where $NoPT_{max} = 120$

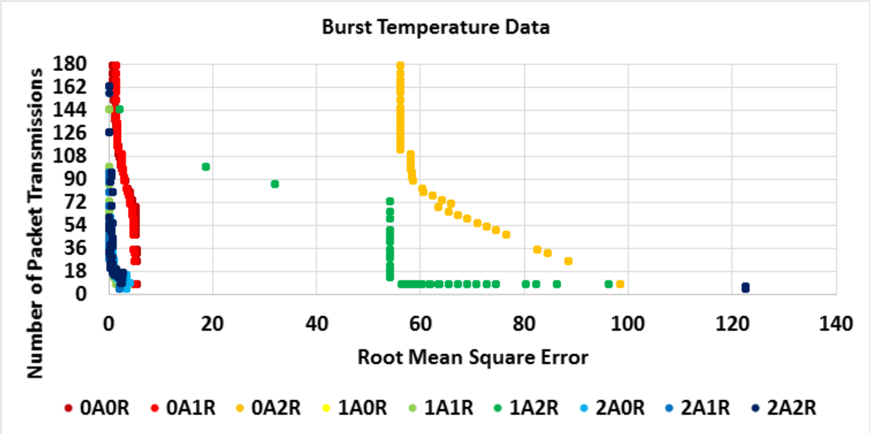

(c) Root mean square error vs. number of packet transmissions where

$$NoPT_{max} = 180$$

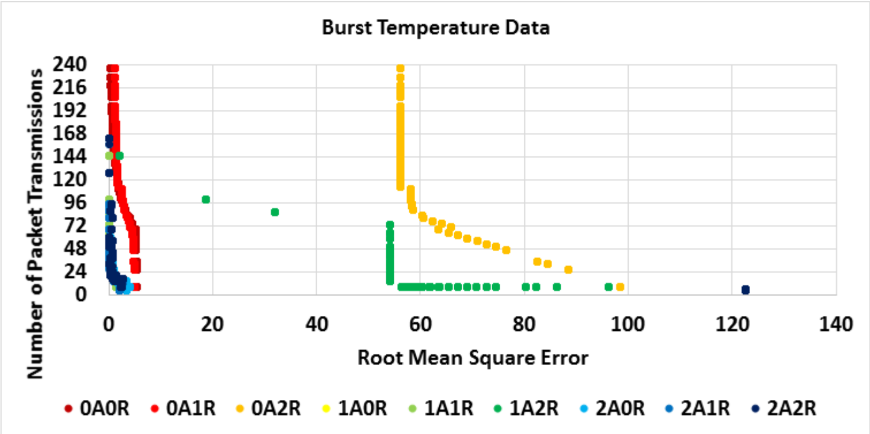

(d) Root mean square error vs. number of packet transmissions where

$$NoPT_{max} = 240$$

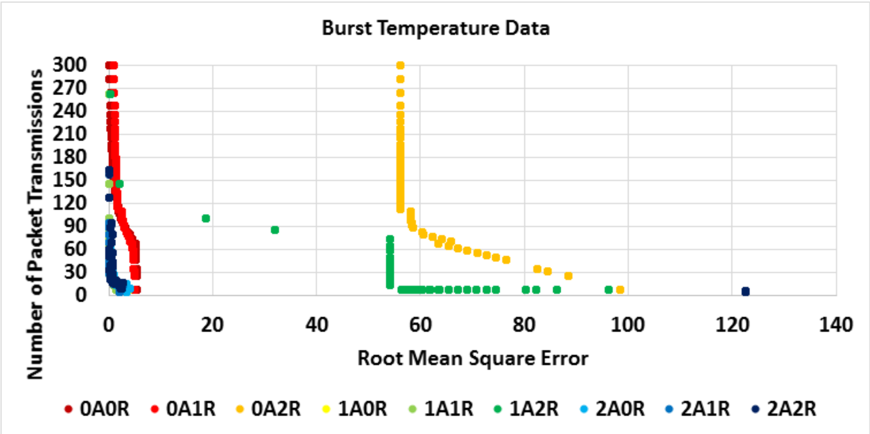

(e) Root mean square error vs. number of packet transmissions where

$$NoPT_{max} = 300$$

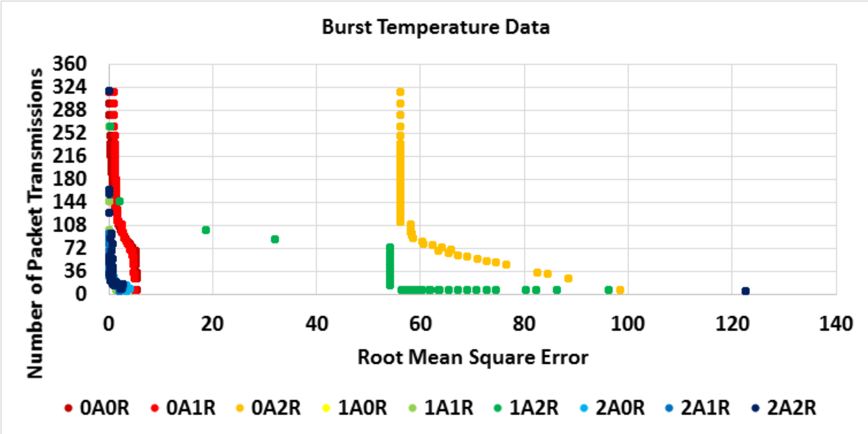

(f) Root mean square error vs. number of packet transmissions where

$$NoPT_{max} = 360$$

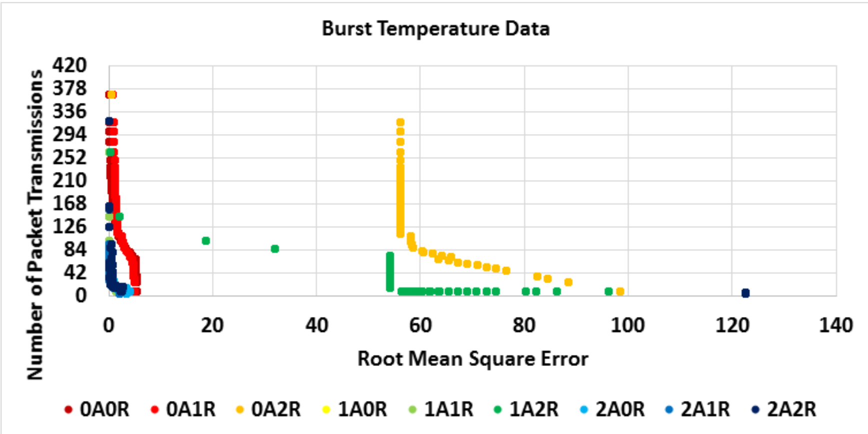

(g) Root mean square error vs. number of packet transmissions where

$$NoPT_{max} = 420$$

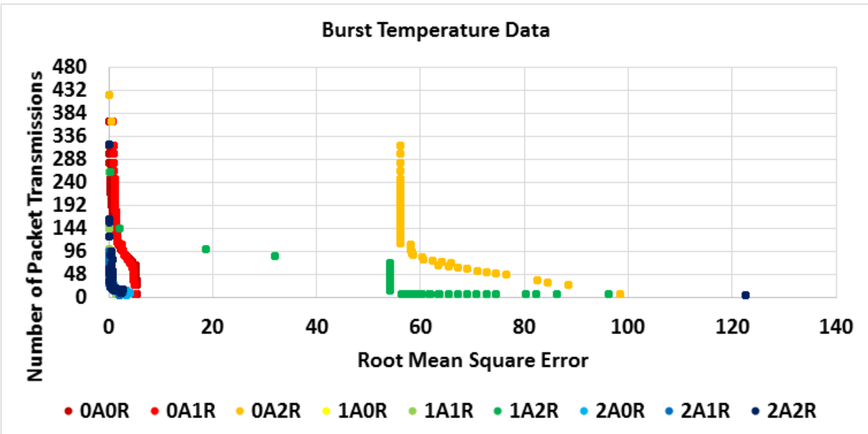

(h) Root mean square error vs. number of packet transmissions where

$$NoPT_{max} = 480$$

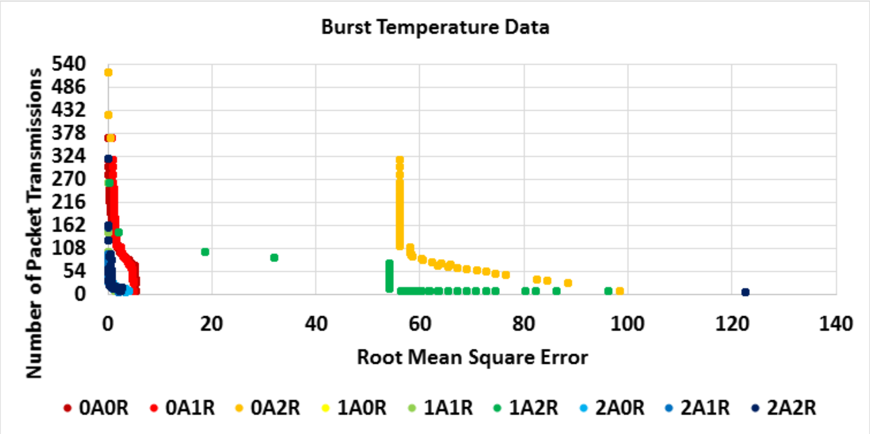

(i) Root mean square error vs. number of packet transmissions where

$$NoPT_{max} = 540$$

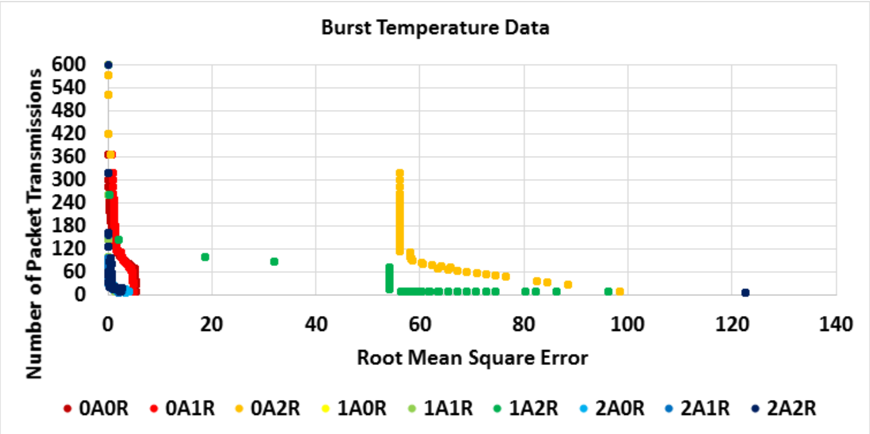

(j) Root mean square error vs. number of packet transmissions where

$$NoPT_{max} = 600$$

Figure 5.33: Root mean square error vs. number of packet transmissions in burst temperature data

The results of DAR schemes in burst temperature data are shown more details in Table 5.6.

Table 5.6: Root Mean Square Error vs. Number of Packet Transmissions in Burst Temperature Data

NoPT	DAR	$RMSE_{min}$
≤ 300	0A0R	0.160
	0A1R	1.008
	0A2R	56.143
	1A0R	0.000
	1A1R	0.000
	1A2R	0.312
	2A0R	0.031
	2A1R	0.016
	2A2R	0.031

NoPT = number of packet transmissions
DAR = data abstraction and reformation
0A0R = zeroth-order data abstraction & zeroth-order data reformation
0A1R = zeroth-order data abstraction & first-order data reformation
0A2R = zeroth-order data abstraction & second-order data reformation
1A0R = first-order data abstraction & zeroth-order data reformation
1A1R = first-order data abstraction & first-order data reformation
1A2R = first-order data abstraction & second-order data reformation
2A0R = second-order data abstraction & zeroth-order data reformation
2A1R = second-order data abstraction & first-order data reformation
2A2R = second-order data abstraction & second-order data reformation
$RMSE_{min}$ = minimum root mean square error

From Table 5.6, it is shown that the best DAR schemes in burst temperature data where $NoPT \leq 300$ in the terms of root mean square error are 1A0R and 1A1R.

6. Root Mean Square Error vs. Number of Data Transmitted

The comparisons of root mean square error against number of data transmitted are shown in Figure 5.34.

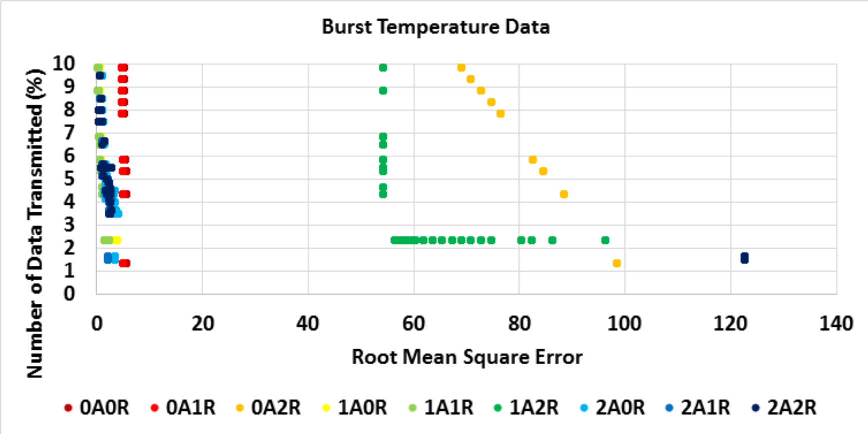

(a) Root mean square error vs. number of data transmitted where

$$NoDT_{max} = 10\%$$

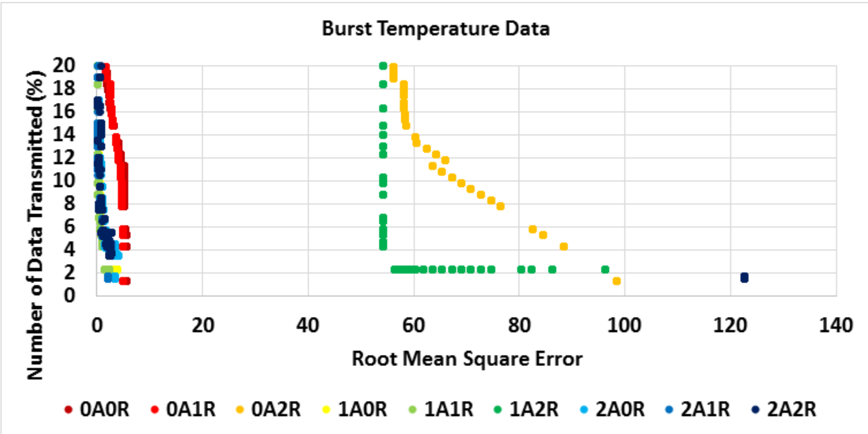

(b) Root mean square error vs. number of data transmitted where

$$NoDT_{max} = 20\%$$

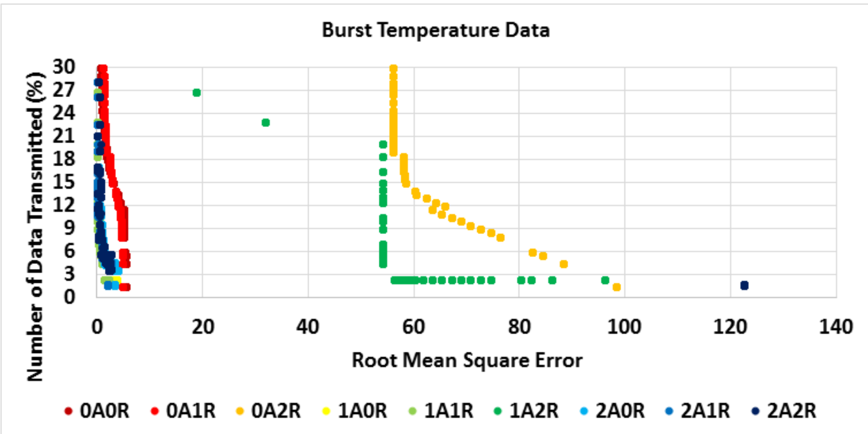

(c) Root mean square error vs. number of data transmitted (%) where

$$NoDT_{max} = 30\%$$

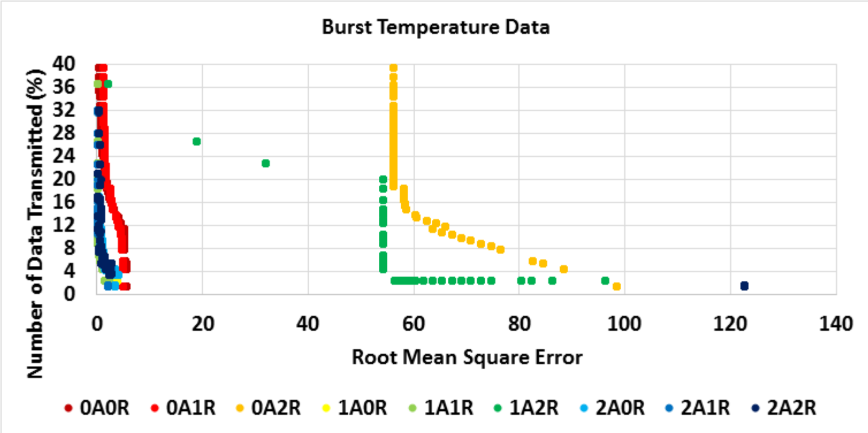

(d) Root mean square error vs. number of data transmitted where

$NoDT_{max} = 40\%$

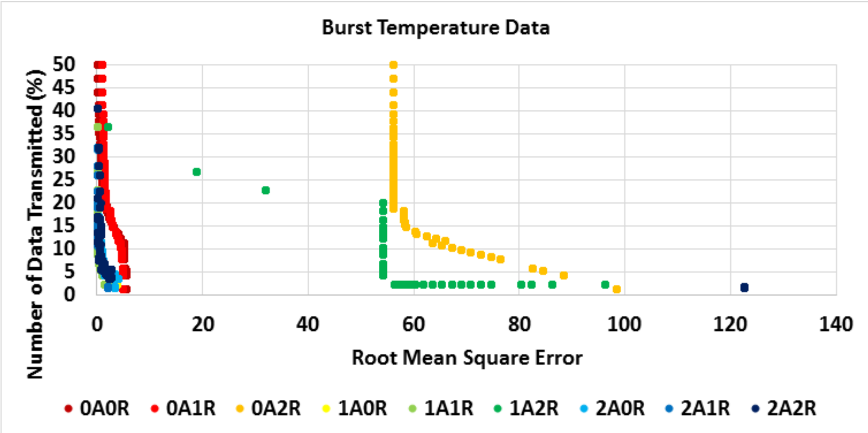

(e) Root mean square error vs. number of data transmitted where

$NoDT_{max} = 50\%$

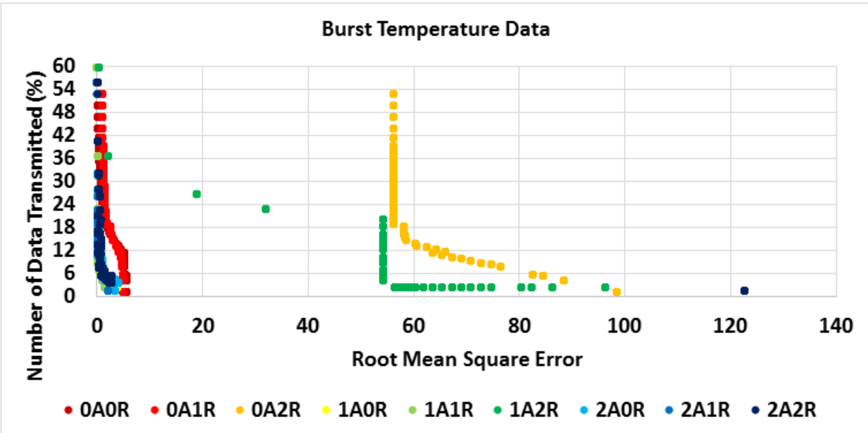

(f) Root mean square error vs. number of data transmitted where

$NoDT_{max} = 60\%$

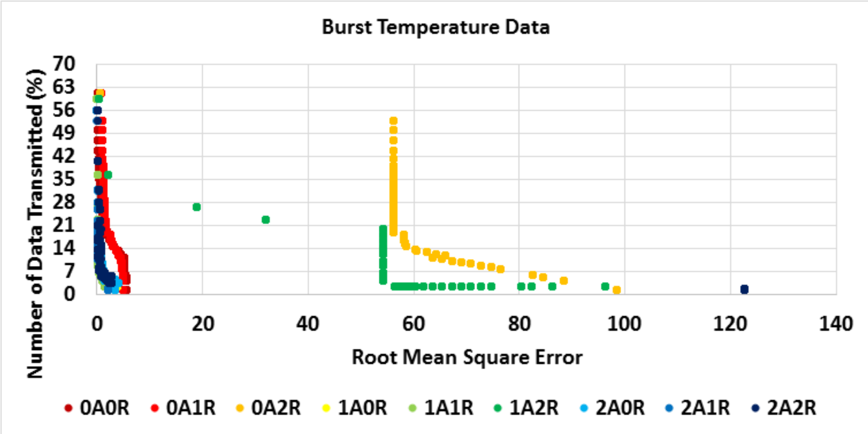

(g) Root mean square error vs. number of data transmitted where

$$NoDT_{max} = 70\%$$

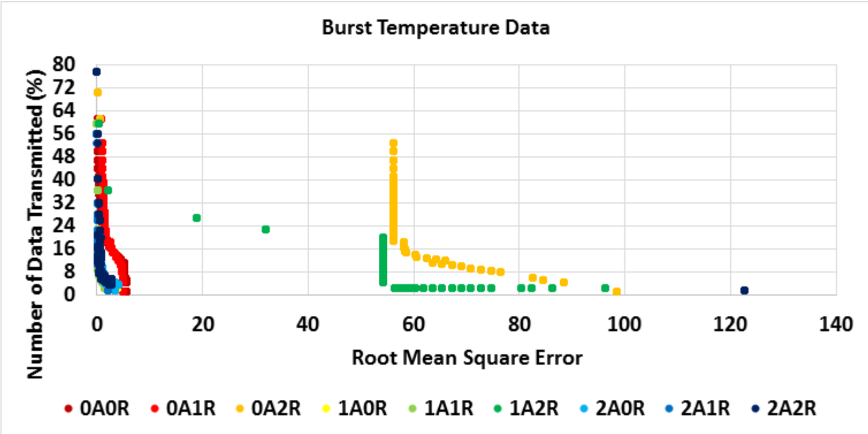

(h) Root mean square error vs. number of data transmitted where

$$NoDT_{max} = 80\%$$

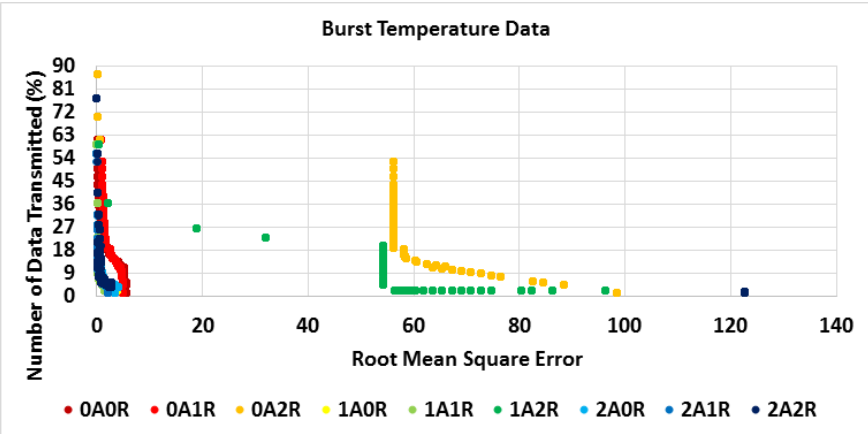

(i) Root mean square error vs. number of data transmitted where

$$NoDT_{max} = 90\%$$

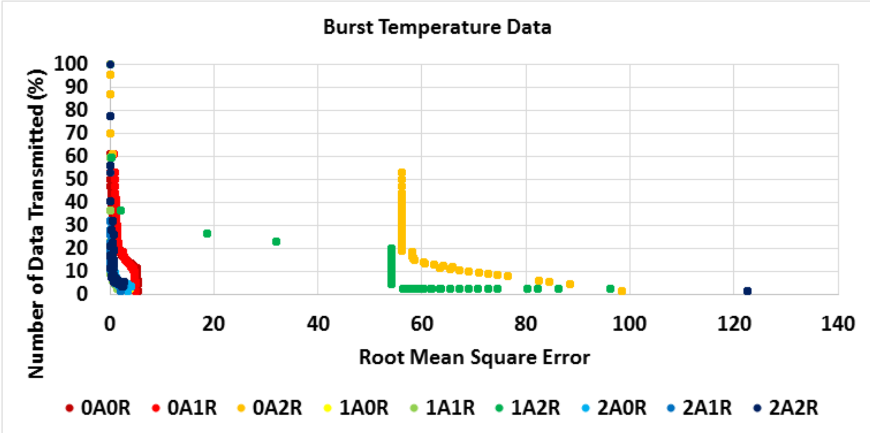

(j) Root mean square error vs. number of data transmitted where

$$NoDT_{max} = 100\%$$

Figure 5.34: Root mean square error vs. number of data transmitted in burst temperature data

The results of DAR schemes in burst temperature data are shown more details in Table 5.7.

Table 5.7: Root Mean Square Error vs. Number of Data Transmitted in Burst Temperature Data

NoDT	DAR	$RMSE_{min}$
≤ 50%	0A0R	0.160
	0A1R	1.008
	0A2R	56.143
	1A0R	0.033
	1A1R	0.020
	1A2R	2.103
	2A0R	0.070
	2A1R	0.029
	2A2R	0.102

NoDT = number of data transmitted
DAR = data abstraction and reformation
0A0R = zeroth-order data abstraction & zeroth-order data reformation
0A1R = zeroth-order data abstraction & first-order data reformation
0A2R = zeroth-order data abstraction & second-order data reformation
1A0R = first-order data abstraction & zeroth-order data reformation
1A1R = first-order data abstraction & first-order data reformation
1A2R = first-order data abstraction & second-order data reformation
2A0R = second-order data abstraction & zeroth-order data reformation
2A1R = second-order data abstraction & first-order data reformation
2A2R = second-order data abstraction & second-order data reformation
$RMSE_{min}$ = minimum root mean square error

From Table 5.7, it is shown that the best DAR schemes in burst temperature data where $NoDT \leq 50\%$ in the terms of root mean square error is 1A1R.

7. Mean Absolute Percentage Error vs. Number of Packet Transmissions

The comparisons of mean absolute percentage error against number of packet transmissions are shown in Figure 5.35.

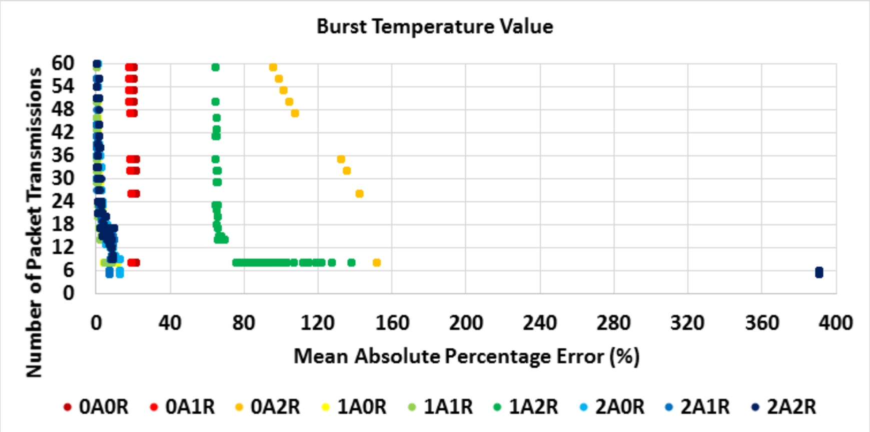

(a) Mean absolute percentage error vs. number of packet transmission where $NoPT_{max} = 60$

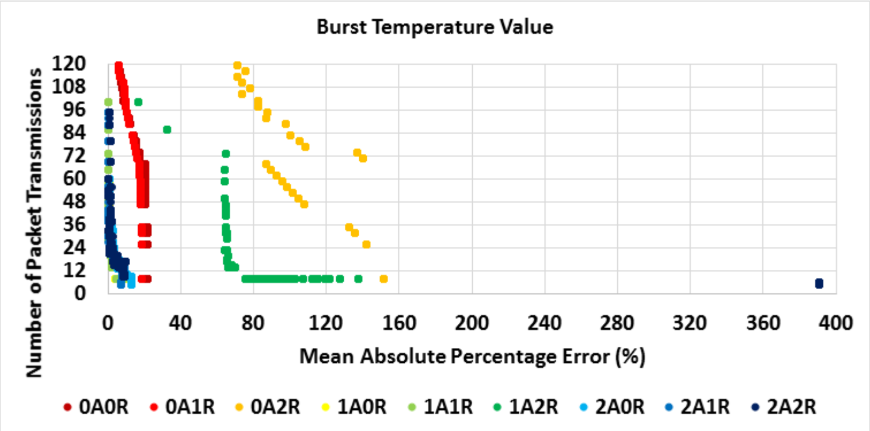

(b) Mean absolute percentage error vs. number of packet transmission where $NoPT_{max} = 120$

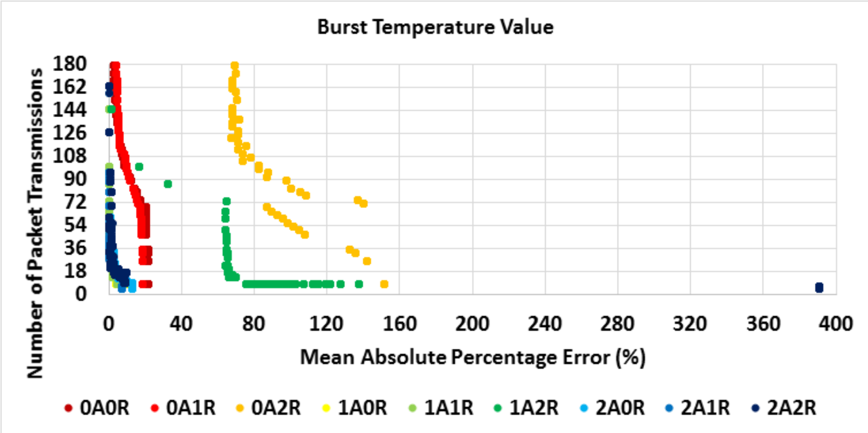

(c) Mean absolute percentage error vs. number of packet transmission

where $NoPT_{max} = 180$

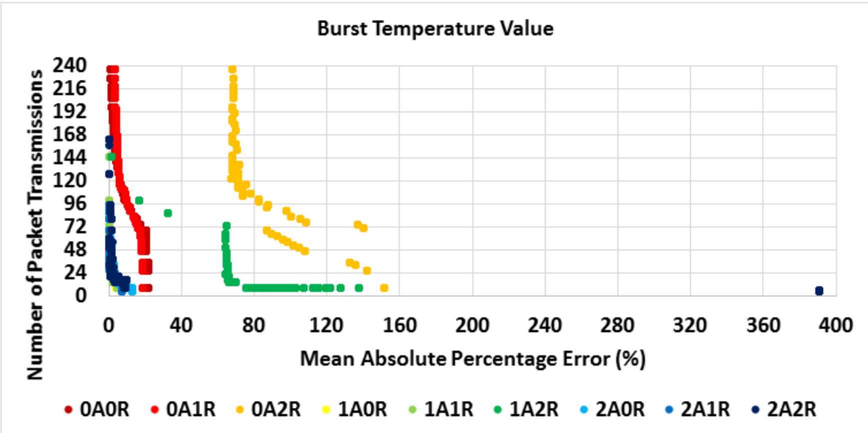

(d) Mean absolute percentage error vs. number of packet transmission

where $NoPT_{max} = 240$

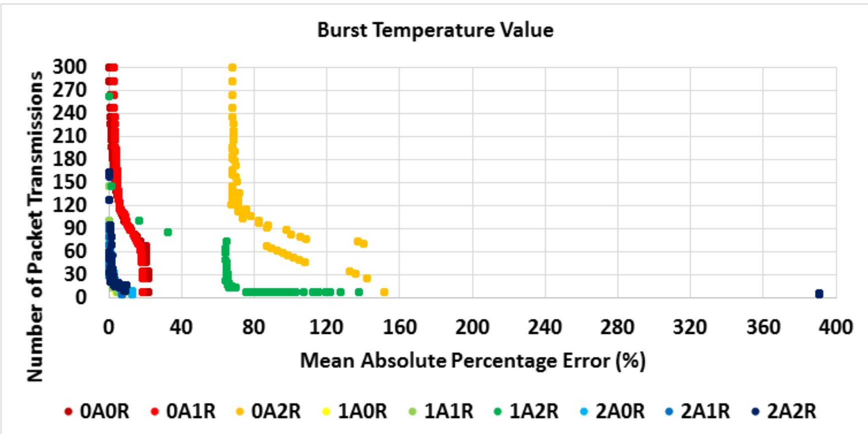

(e) Mean absolute percentage error vs. number of packet transmission

where $NoPT_{max} = 300$

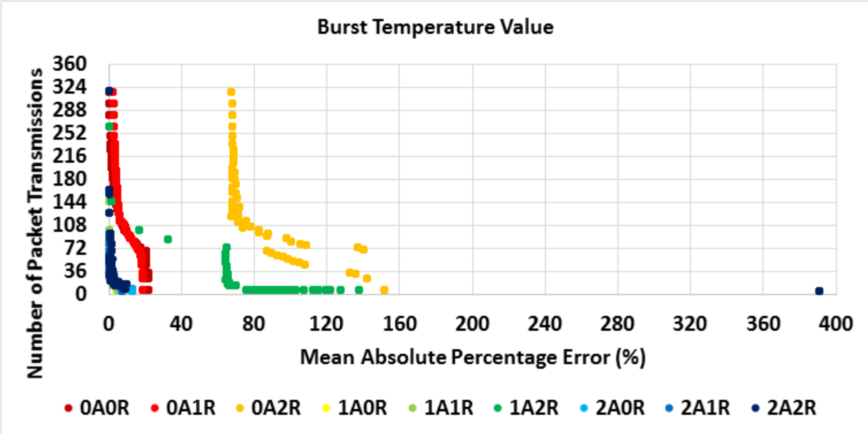

(f) Mean absolute percentage error vs. number of packet transmission where $NoPT_{max} = 360$

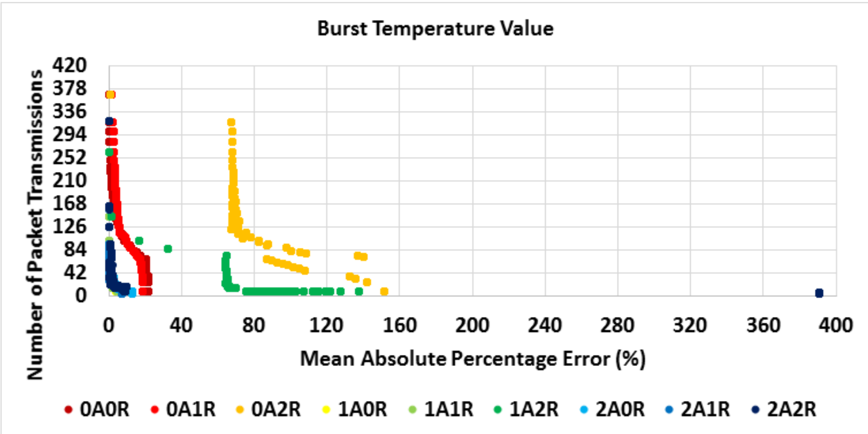

(g) Mean absolute percentage error vs. number of packet transmission where $NoPT_{max} = 420$

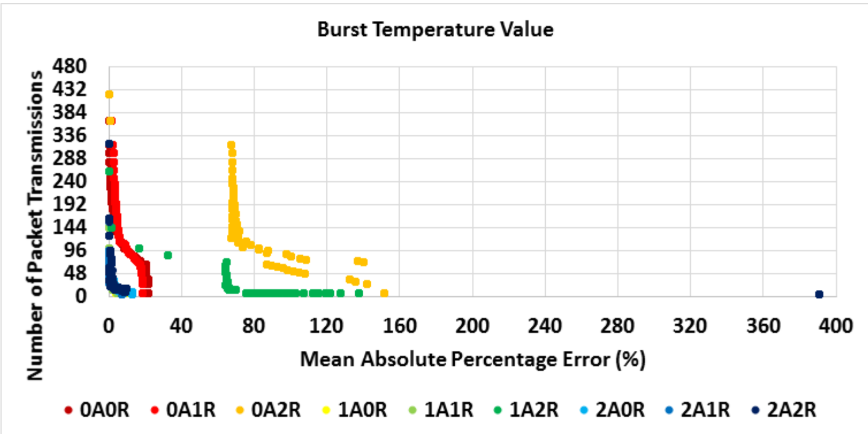

(h) Mean absolute percentage error vs. number of packet transmission where $NoPT_{max} = 480$

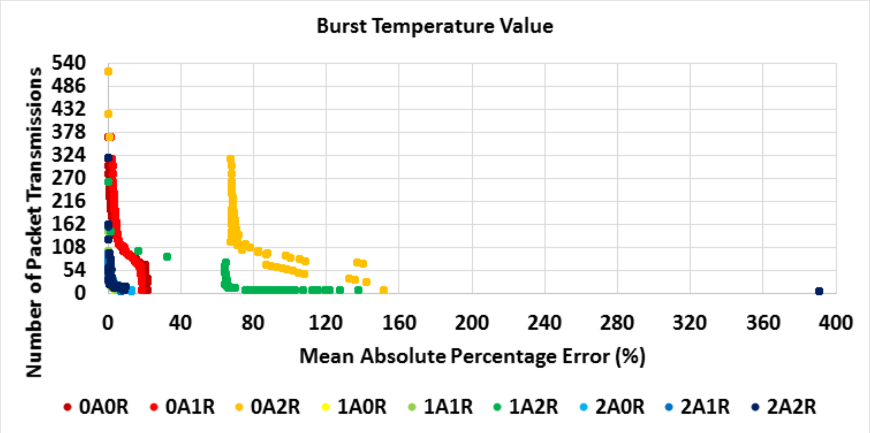

(i) Mean absolute percentage error vs. number of packet transmission where $NoPT_{max} = 540$

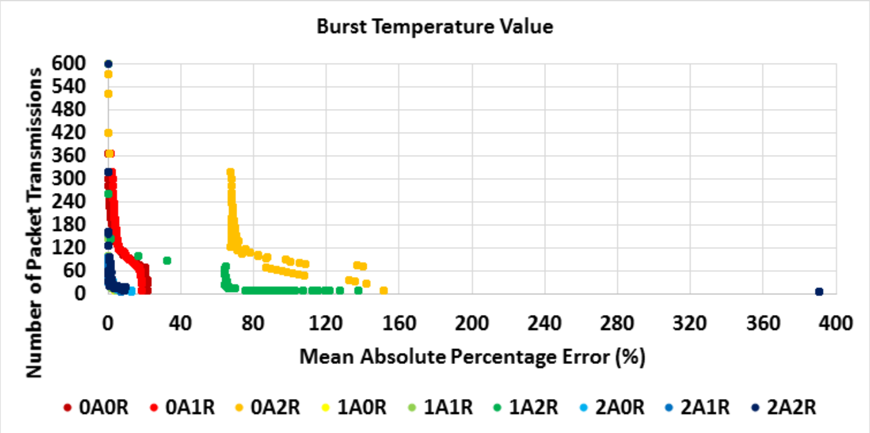

(j) Mean absolute percentage error vs. number of packet transmission where $NoPT_{max} = 600$

Figure 5.35: Mean absolute percentage error vs. number of packet transmissions in burst temperature data

The results of DAR schemes in burst temperature data are shown more details in Table 5.8.

Table 5.8: Mean Absolute Percentage Error vs. Number of Packet Transmissions in Burst Temperature Data

NoPT	DAR	$MAPE_{min}$ (%)
≤ 300	0A0R	0.473
	0A1R	2.597
	0A2R	67.546
	1A0R	0.000
	1A1R	0.000
	1A2R	0.227
	2A0R	0.068
	2A1R	0.040
	2A2R	0.062

NoPT = number of packet transmissions
DAR = data abstraction and reformation
0A0R = zeroth-order data abstraction & zeroth-order data reformation
0A1R = zeroth-order data abstraction & first-order data reformation
0A2R = zeroth-order data abstraction & second-order data reformation
1A0R = first-order data abstraction & zeroth-order data reformation
1A1R = first-order data abstraction & first-order data reformation
1A2R = first-order data abstraction & second-order data reformation
2A0R = second-order data abstraction & zeroth-order data reformation
2A1R = second-order data abstraction & first-order data reformation
2A2R = second-order data abstraction & second-order data reformation
$MAPE_{min}$ = minimum mean absolute percentage error

From Table 5.8, it is shown that the best DAR schemes in burst temperature data where $NoPT \leq 300$ in the terms of mean absolute percentage error are 1A0R and 1A1R.

8. Mean Absolute Percentage Error vs. Number of Data Transmitted

The comparisons of mean absolute percentage error against number of data transmitted are shown in Figure 5.36.

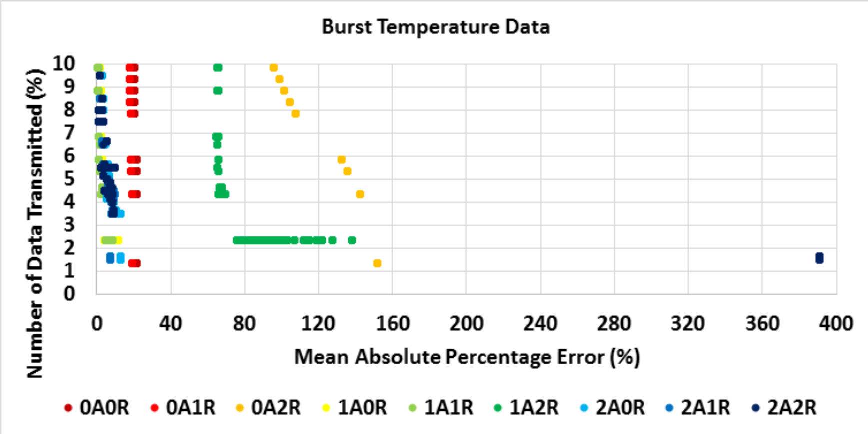

(a) Mean absolute percentage error vs. number of data transmitted where

$NoDT_{max} = 10\%$

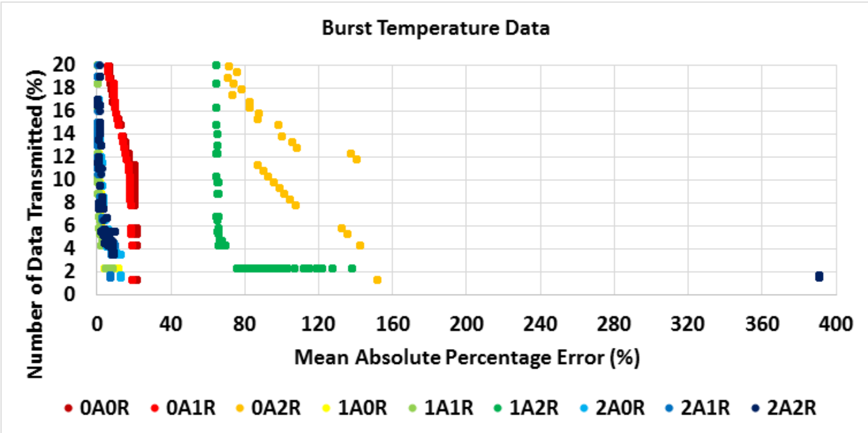

(b) Mean absolute percentage error vs. number of data transmitted where

$NoDT_{max} = 20\%$

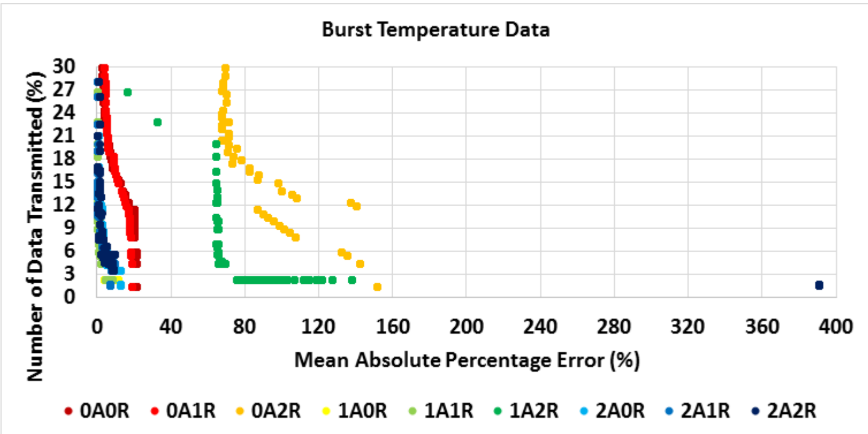

(c) Mean absolute percentage error vs. number of data transmitted where

$NoDT_{max} = 30\%$

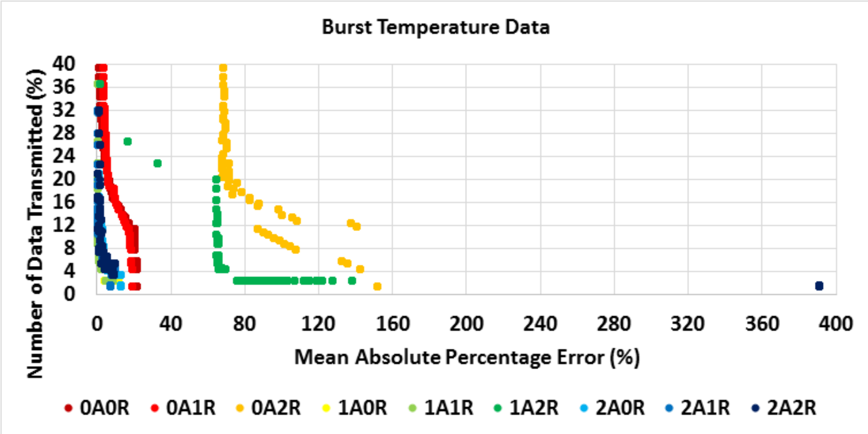

(d) Mean absolute percentage error vs. number of data transmitted where $NoDT_{max} = 40\%$

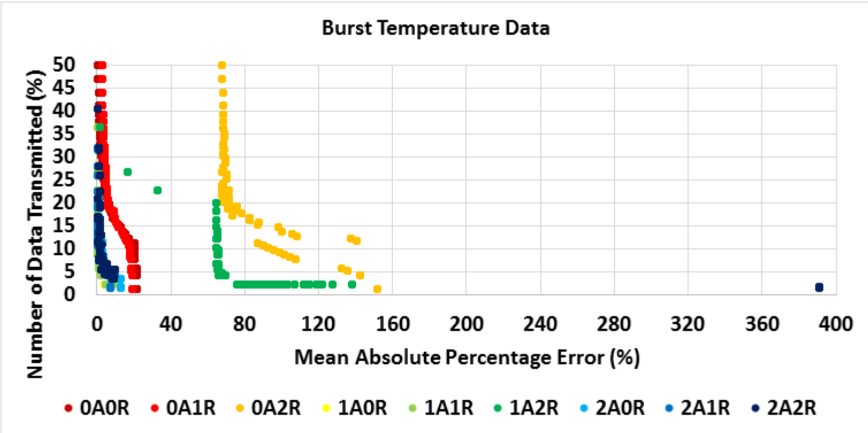

(e) Mean absolute percentage error vs. number of data transmitted where $NoDT_{max} = 50\%$

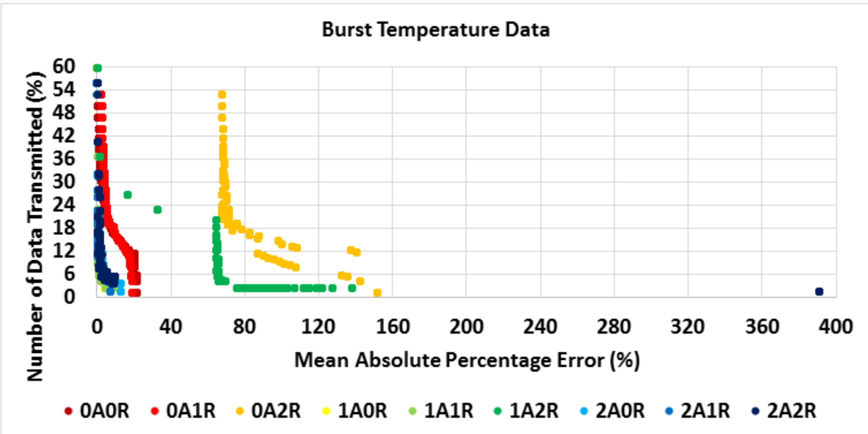

(f) Mean absolute percentage error vs. number of data transmitted where $NoDT_{max} = 60\%$

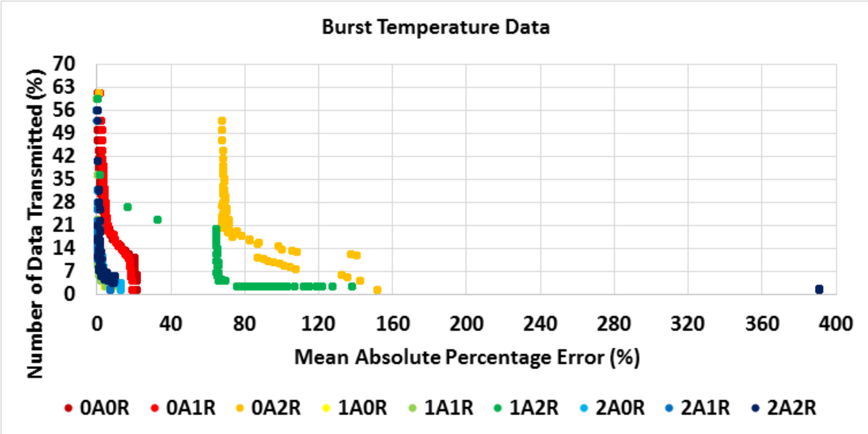

(g) Mean absolute percentage error vs. number of data transmitted where $NoDT_{max} = 70\%$

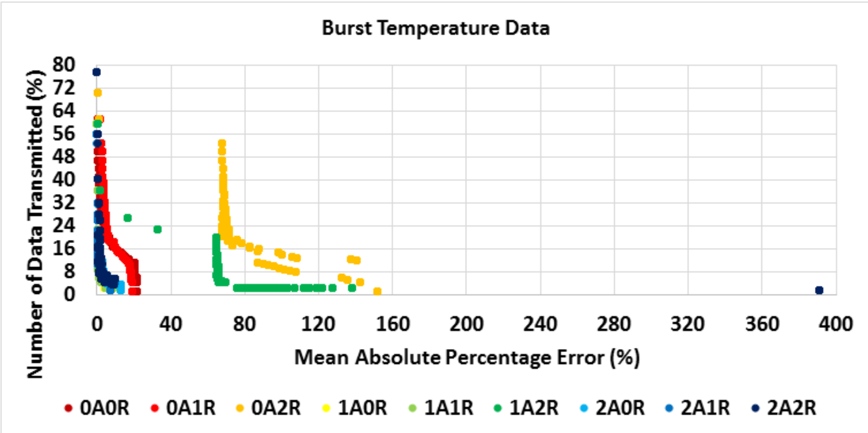

(h) Mean absolute percentage error vs. number of data transmitted where $NoDT_{max} = 80\%$

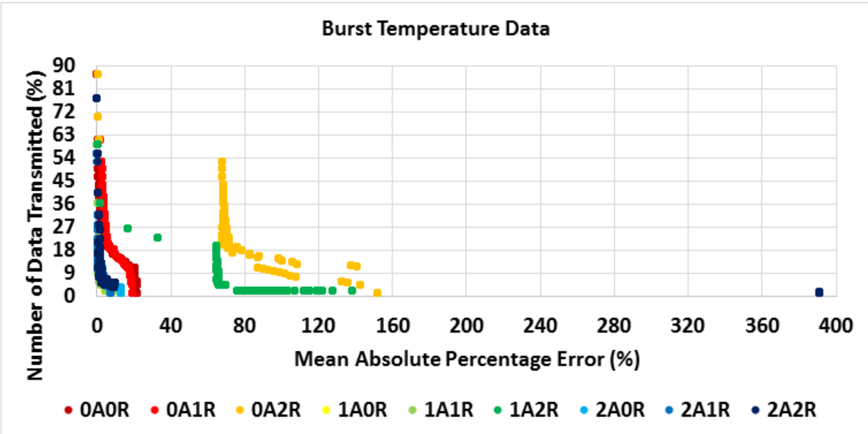

(i) Mean absolute percentage error vs. number of data transmitted where $NoDT_{max} = 90\%$

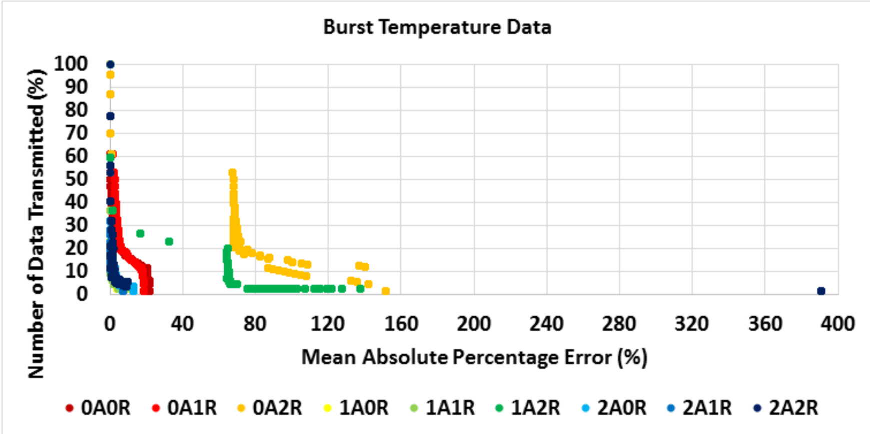

(j) Mean absolute percentage error vs. number of data transmitted (%)

where $NoDT_{max}$ = 100%

Figure 5.36: Mean absolute percentage error vs. number of data transmitted in burst temperature data

The results of DAR schemes in burst temperature data are shown more details in Table 5.9.

Table 5.9: Mean Absolute Percentage Error vs. Number of Data Transmitted in Burst Temperature Data

NoDT	DAR	$MAPE_{min}$ (%)
≤ 50%	0A0R	0.473
	0A1R	2.597
	0A2R	67.546
	1A0R	0.076
	1A1R	0.058
	1A2R	1.330
	2A0R	0.208
	2A1R	0.085
	2A2R	0.337

NoDT = number of data transmitted
DAR = data abstraction and reformation
0A0R = zeroth-order data abstraction & zeroth-order data reformation
0A1R = zeroth-order data abstraction & first-order data reformation
0A2R = zeroth-order data abstraction & second-order data reformation
1A0R = first-order data abstraction & zeroth-order data reformation
1A1R = first-order data abstraction & first-order data reformation
1A2R = first-order data abstraction & second-order data reformation
2A0R = second-order data abstraction & zeroth-order data reformation
2A1R = second-order data abstraction & first-order data reformation
2A2R = second-order data abstraction & second-order data reformation
$MAPE_{min}$ = minimum mean absolute percentage error

From Table 5.9, it is shown that the best DAR schemes in burst temperature data where $NoDT \leq 50\%$ in the terms of mean absolute percentage error is 1A1R.

9. Conclusion

From Table 5.2 – 5.9, it is concluded in Table 5.10, that the best DAR schemes in burst temperature data is 1A1R.

Table 5.10: Results of DAR Schemes in Burst Temperature Data

(a) Best DAR Schemes in Burst Temperature Data where the $NoPT \leq 300$ and $NoDT \leq 50\%$

DAR	Th	NoPT	NoDT(%)	RMSE	MAPE(%)
0A0R	22.376	299	49.833	0.160	0.473
0A1R	22.376	299	49.833	1.008	2.597
0A2R	24.314	122	20.333	56.143	67.546
1A0R	0.063	145	36.500	0.033	0.076
1A1R	0.063	145	36.500	0.020	0.058
1A2R	0.063	145	36.500	2.103	1.330
2A0R	0.126	127	40.500	0.070	0.208
2A1R	0.126	127	40.500	0.029	0.085
2A2R	0.563	54	17.000	0.102	0.337

(b) Best DAR Schemes in Burst Temperature Data where the $RMSE = 0$ and $MAPE = 0\%$

DAR	Th	NoPT	NoDT(%)	RMSE	MAPE(%)
0A0R	22.000	600	100.000	0.000	0.000
0A1R	22.000	600	100.000	0.000	0.000
0A2R	22.000	600	100.000	0.000	0.000
1A0R	0.001	262	59.500	0.000	0.000
1A1R	0.001	262	59.500	0.000	0.000
1A2R	0.000	600	100.000	0.000	0.000
2A0R	0.001	319	77.333	0.000	0.000
2A1R	0.001	319	77.333	0.000	0.000
2A2R	0.001	319	77.333	0.000	0.000

DAR = data abstraction and reformation
Th = threshold
NoPT = number of packet transmissions
NoDT = number of packet transmitted
RMSE = root mean square error
MAPE = mean absolute percentage error

5.3.2 Incremental & Decremental Temperature Data

The comparisons among parameters (number of packet transmissions, number of data transmitted, root mean square error, and mean absolute percentage error) are as follows.

1. Number of Packet Transmissions vs. Root Mean Square Error

   The comparisons of number of packet transmissions against root mean square error are shown in Figure 5.37.

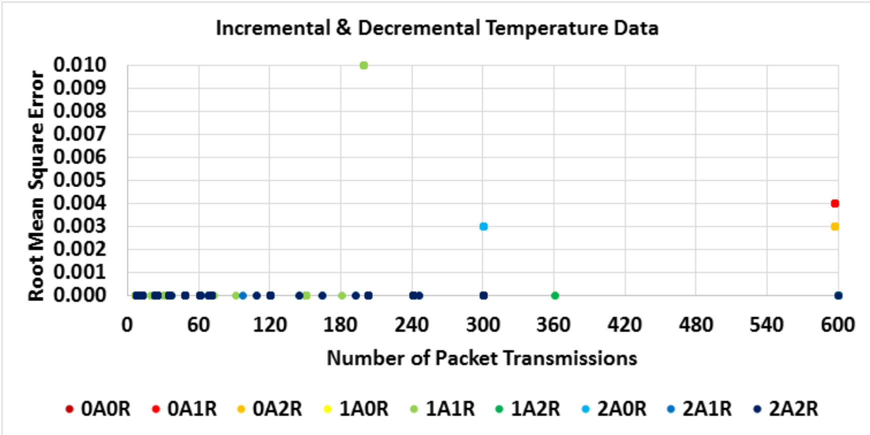

(a) Number of packet transmissions vs. root mean square error where

$$RMSE_{max} = 0.01$$

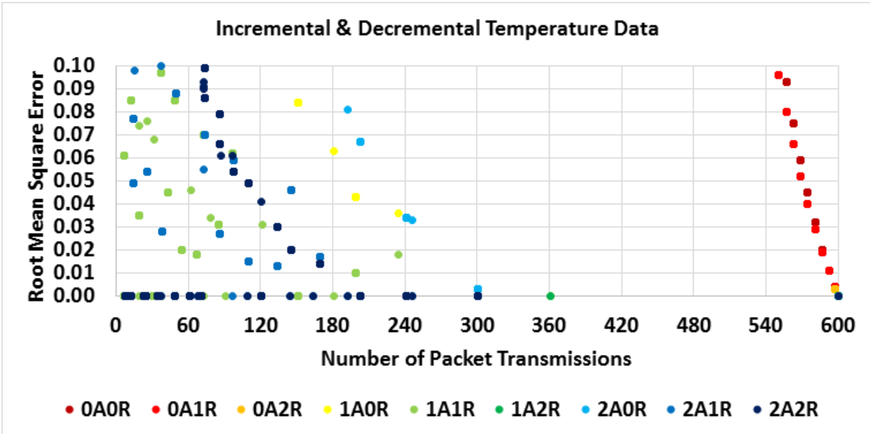

(b) Number of packet transmissions vs. root mean square error where

$$RMSE_{max} = 0.1$$

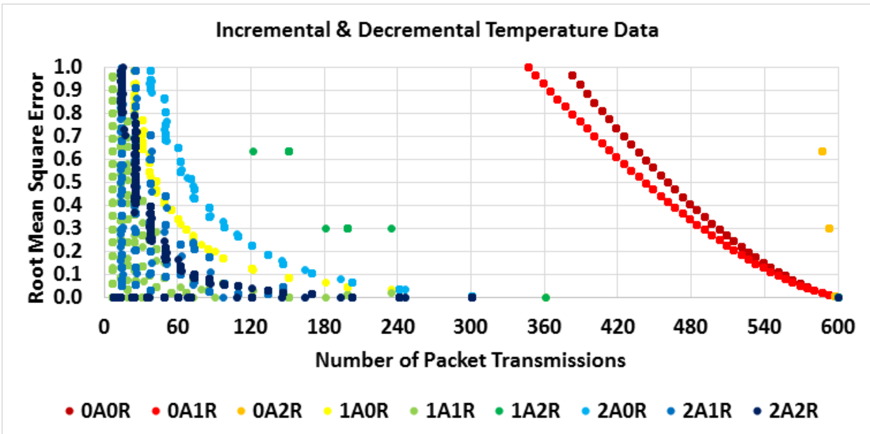

(c) Number of packet transmissions vs. root mean square error where

$$RMSE_{max} = 1$$

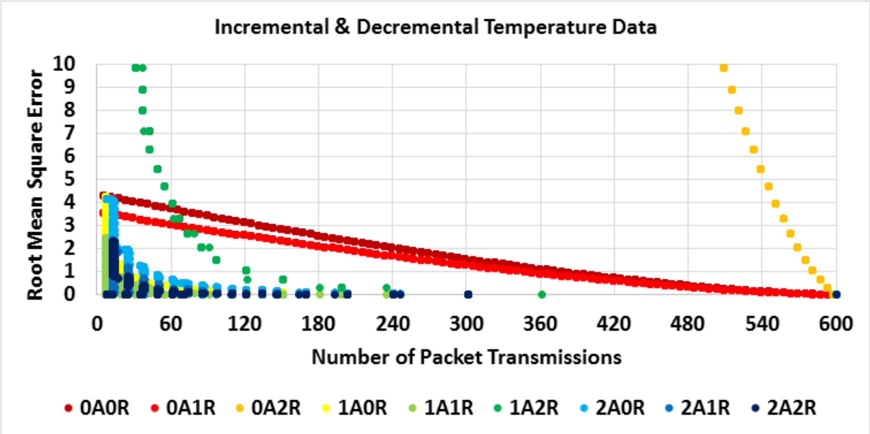

(d) Number of packet transmissions vs. root mean square error where

$$RMSE_{max} = 10$$

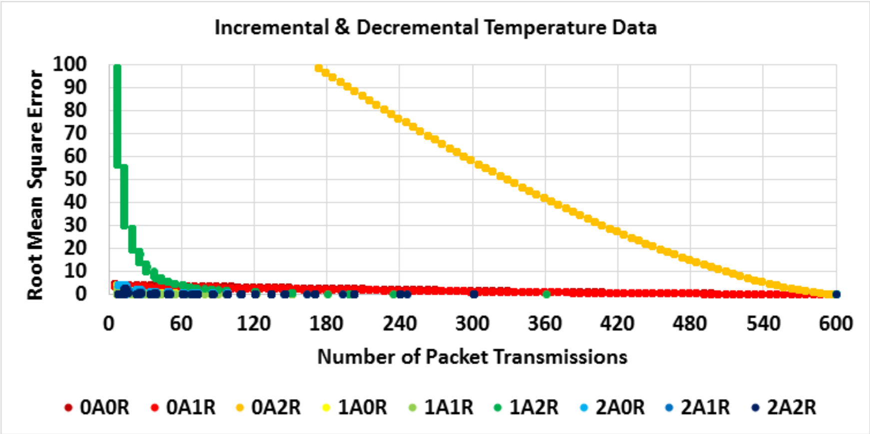

(e) Number of packet transmissions vs. root mean square error where

$$RMSE_{max} = 100$$

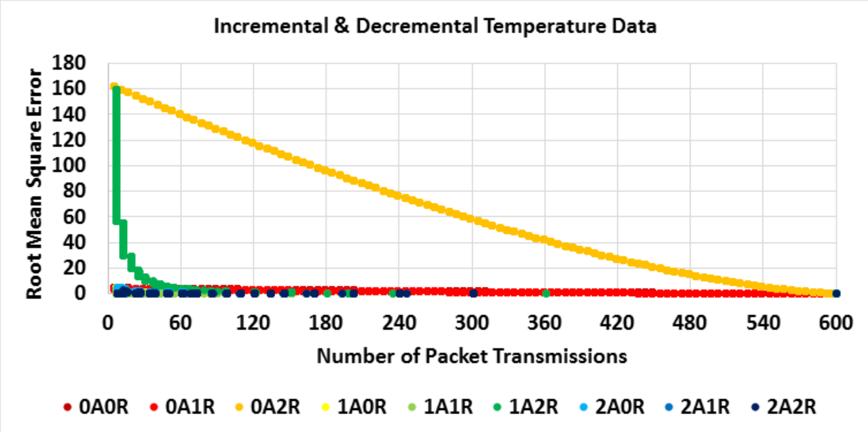

(f) Number of packet transmissions vs. root mean square error where

$$\boldsymbol{RMSE_{max} = 180}$$

Figure 5.37: Number of packet transmissions vs. root mean square error in incremental & decremental temperature data

The results of DAR schemes in incremental & decremental temperature data are shown more details in Table 5.11.

Table 5.11: Number of Packet Transmissions vs. Root Mean Square Error in Incremental & Decremental Temperature Data

RMSE	DAR	$NoPT_{min}$
= 0	0A0R	600
	0A1R	600
	0A2R	600
	1A0R	301
	1A1R	7
	1A2R	301
	2A0R	600
	2A1R	8
	2A2R	8

RMSE = root mean square error
DAR = data abstraction and reformation
0A0R = zeroth-order data abstraction & zeroth-order data reformation
0A1R = zeroth-order data abstraction & first-order data reformation
0A2R = zeroth-order data abstraction & second-order data reformation
1A0R = first-order data abstraction & zeroth-order data reformation
1A1R = first-order data abstraction & first-order data reformation
1A2R = first-order data abstraction & second-order data reformation
2A0R = second-order data abstraction & zeroth-order data reformation
2A1R = second-order data abstraction & first-order data reformation
2A2R = second-order data abstraction & second-order data reformation
$NoPT_{min}$ = minimum number of packet transmissions

From Table 5.11, it is shown that the best DAR schemes in incremental & decremental temperature data where $RMSE = 0$ in the terms of number of packet transmissions is 1A1R.

2. Number of Packet Transmissions vs. Mean Absolute Percentage Error

The comparisons of number of packet transmissions against mean absolute percentage error are shown in Figure 5.38.

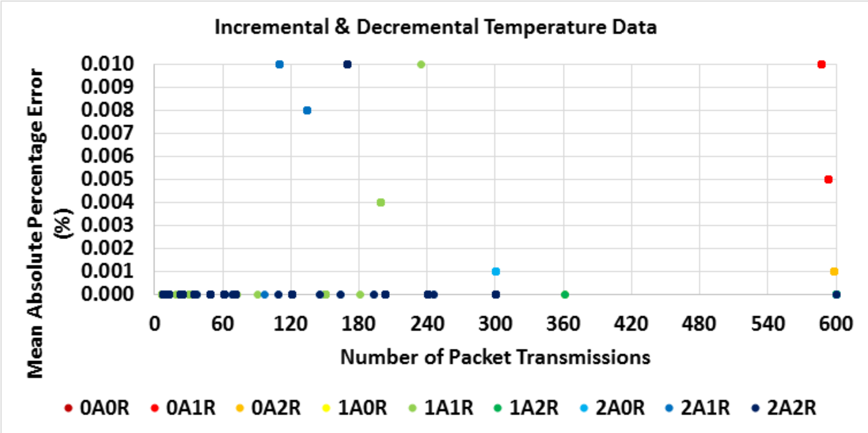

(a) Number of packet transmissions vs. mean absolute percentage error where $MAPE_{max} = 0.01\%$

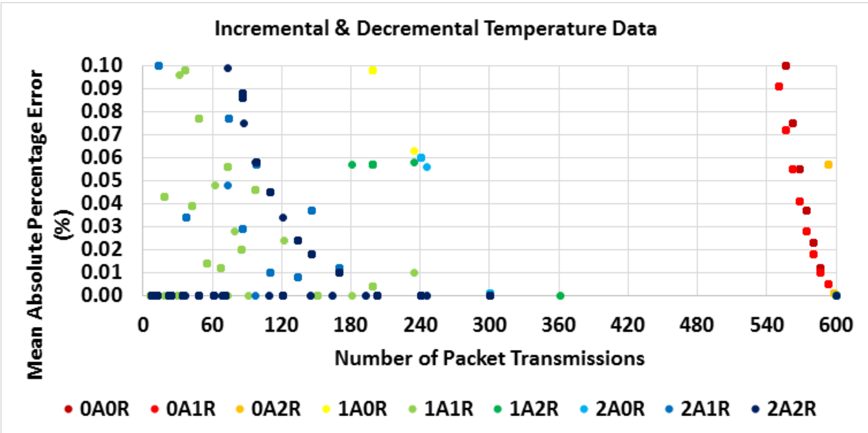

(b) Number of packet transmissions vs. mean absolute percentage error where $MAPE_{max} = 0.1\%$

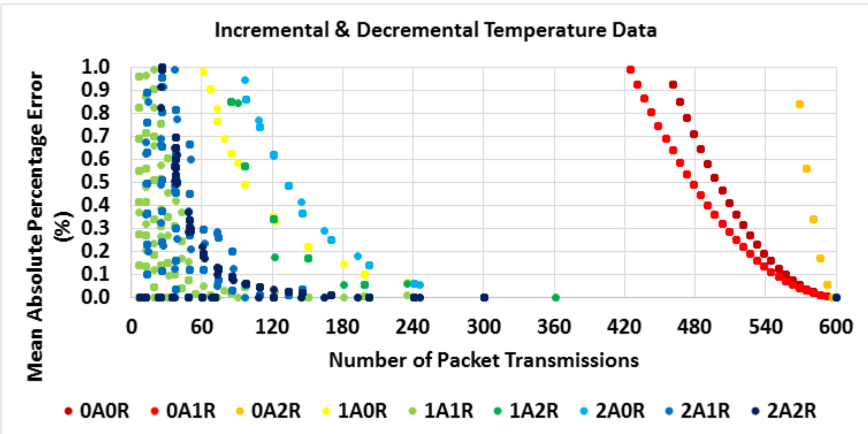

(c) Number of packet transmissions vs. mean absolute percentage error where $MAPE_{max} = 1\%$

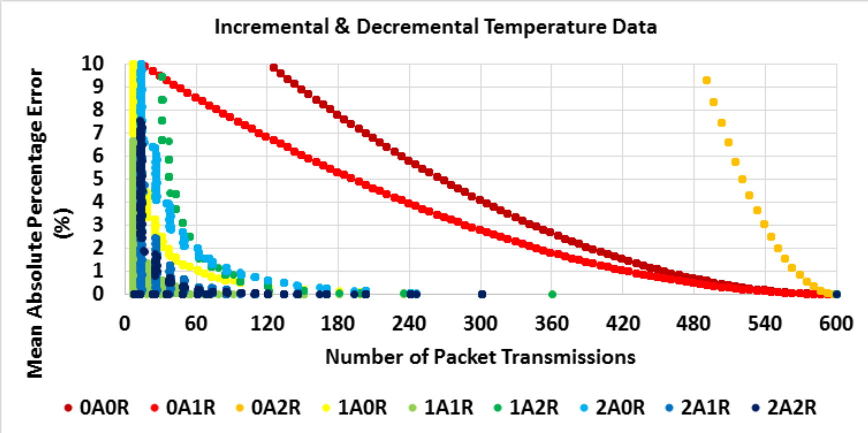

(d) Number of packet transmissions vs. mean absolute percentage error where $MAPE_{max} = 10\%$

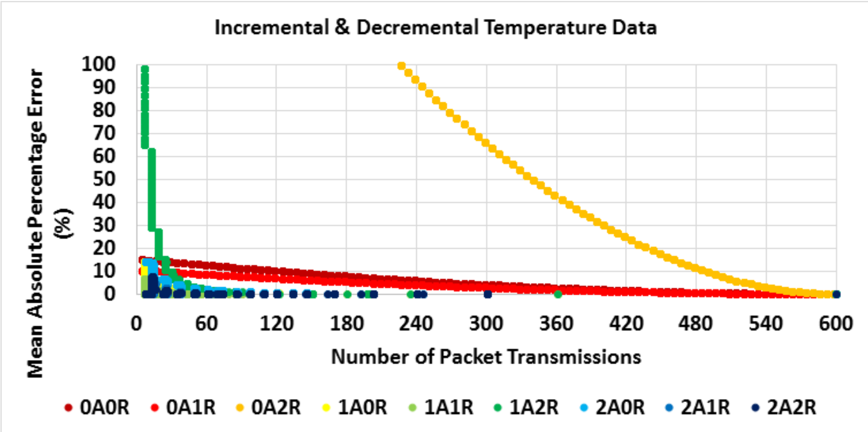

(e) Number of packet transmissions vs. mean absolute percentage error where $MAPE_{max} = 100\%$

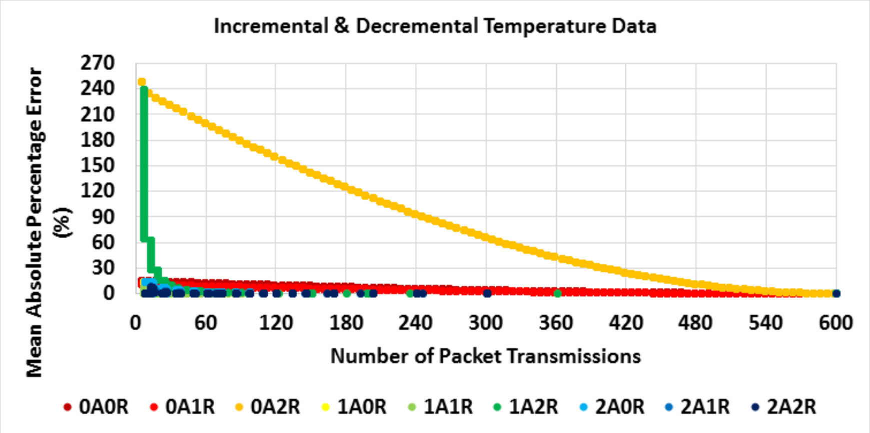

(f) Number of packet transmissions vs. mean absolute percentage error where $MAPE_{max} = 270\%$

Figure 5.38: Number of packet transmissions vs. mean absolute percentage error in incremental & decremental temperature data

The results of DAR schemes in incremental & decremental temperature data are shown more details in Table 5.12.

Table 5.12: Number of Packet Transmissions vs. Mean Absolute Percentage Error in Incremental & Decremental Temperature Data

MAPE	DAR	$NoPT_{min}$
	0A0R	600
	0A1R	600
	0A2R	600
	1A0R	301
= 0%	1A1R	7
	1A2R	301
	2A0R	600
	2A1R	8
	2A2R	8

MAPE = mean absolute percentage error
DAR = data Abstraction and Reformation
0A0R = zeroth-order data abstraction & zeroth-order data reformation
0A1R = zeroth-order data abstraction & first-order data reformation
0A2R = zeroth-order data abstraction & second-order data reformation
1A0R = first-order data abstraction & zeroth-order data reformation
1A1R = first-order data abstraction & first-order data reformation
1A2R = first-order data abstraction & second-order data reformation
2A0R = second-order data abstraction & zeroth-order data reformation
2A1R = second-order data abstraction & first-order data reformation
2A2R = second-order data abstraction & second-order data reformation
$NoPT_{min}$ = minimum number of packet transmissions

From Table 5.12, it is shown that the best DAR schemes in incremental & decremental temperature data where $MAPE = 0\%$ in the terms of number of packet transmissions is 1A1R.

3. Number of Data Transmitted vs. Root Mean Square Error

The comparisons of number of data transmitted against root mean square error are shown in Figure 5.39.

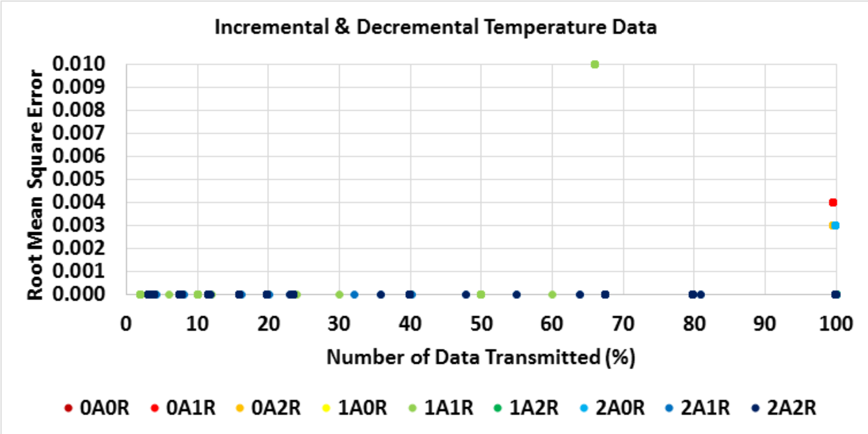

(a) Number of data transmitted vs. root mean square error where

$$RMSE_{max} = 0.01$$

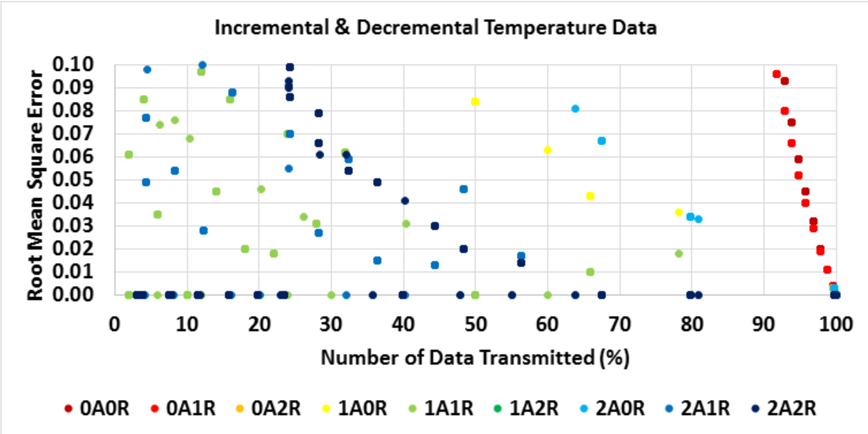

(b) Number of data transmitted vs. root mean square error where

$$RMSE_{max} = 0.1$$

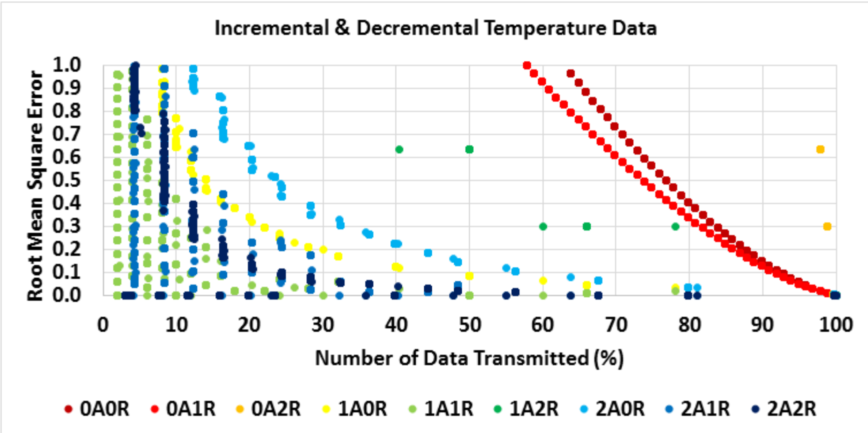

(c) Number of data transmitted vs. root mean square error where

$$RMSE_{max} = 1$$

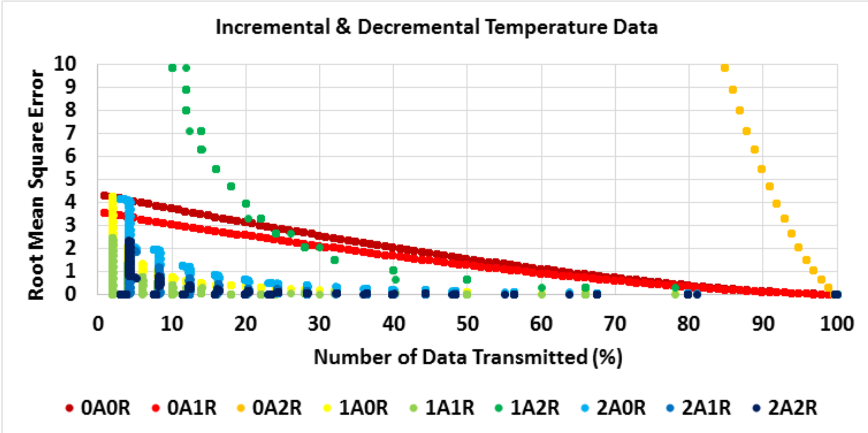

(d) Number of data transmitted vs. root mean square error where

$$RMSE_{max} = 10$$

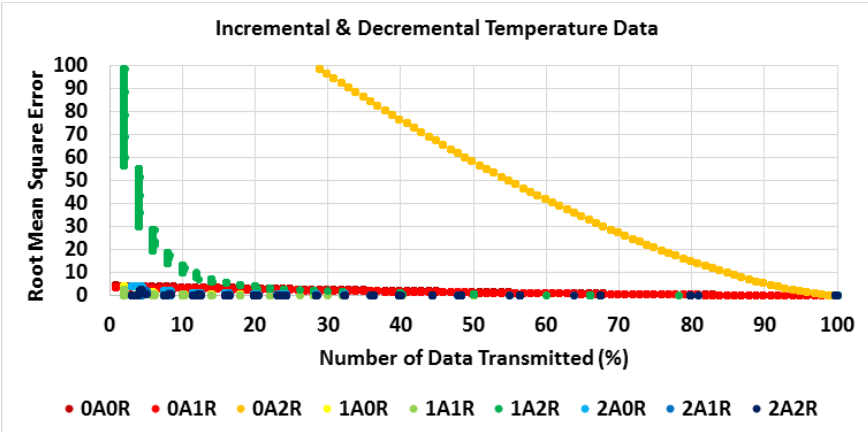

(e) Number of data transmitted vs. root mean square error where

$$RMSE_{max} = 100$$

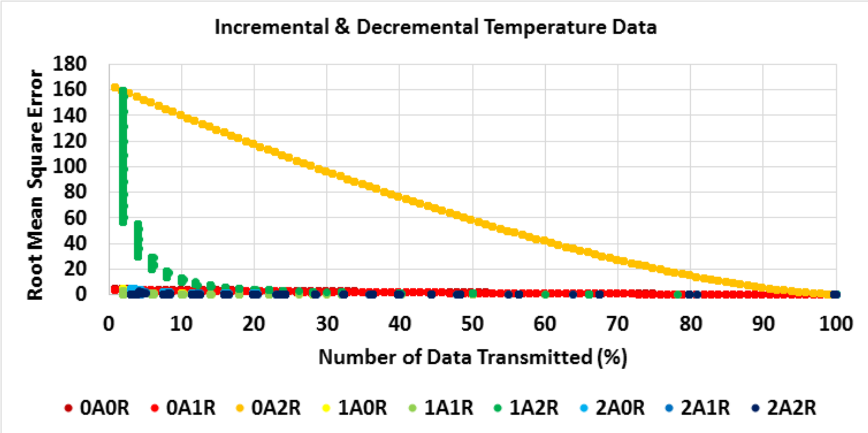

(f) Number of data transmitted vs. root mean square error where

$$RMSE_{max} = 180$$

Figure 5.39: Number of data transmitted vs. root mean square error in incremental & decremental temperature data

The results of DAR schemes in incremental & decremental temperature data are shown more details in Table 5.13.

Table 5.13: Number of Data Transmitted vs. Root Mean Square Error in Incremental & Decremental Temperature Data

RMSE	DAR	$NoDT_{min}$ (%)
= 0	0A0R	100.000
	0A1R	100.000
	0A2R	100.000
	1A0R	100.000
	1A1R	2.000
	1A2R	100.000
	2A0R	100.000
	2A1R	3.000
	2A2R	3.000

RMSE = root mean square error
DAR = data Abstraction and Reformation
0A0R = zeroth-order data abstraction & zeroth-order data reformation
0A1R = zeroth-order data abstraction & first-order data reformation
0A2R = zeroth-order data abstraction & second-order data reformation
1A0R = first-order data abstraction & zeroth-order data reformation
1A1R = first-order data abstraction & first-order data reformation
1A2R = first-order data abstraction & second-order data reformation
2A0R = second-order data abstraction & zeroth-order data reformation
2A1R = second-order data abstraction & first-order data reformation
2A2R = second-order data abstraction & second-order data reformation
$NoDT_{min}$ = minimum number of data transmitted

From Table 5.13, it is shown that the best DAR schemes in incremental & decremental temperature data where $RMSE = 0$ in the terms of number of data transmitted is 1A1R.

4. Number of Data Transmitted vs. Mean Absolute Percentage Error

The comparisons of number of data transmitted against mean absolute percentage error are shown in Figure 5.40.

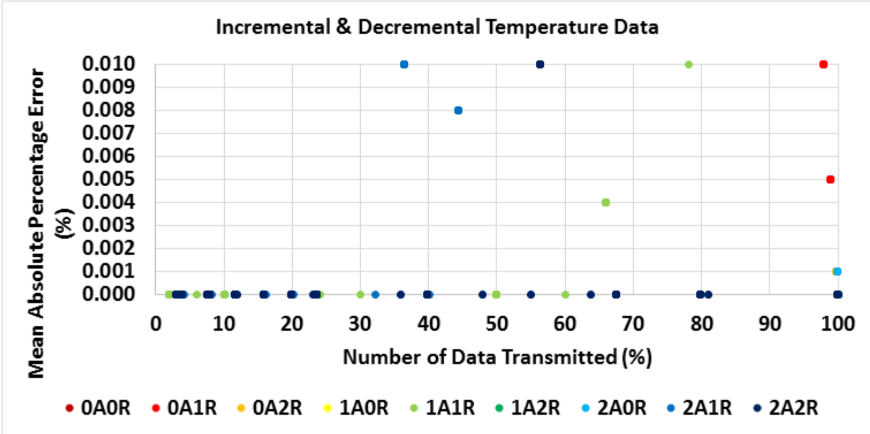

(a) Number of data transmitted vs. mean absolute percentage error where

$$MAPE_{max} = 0.01\%$$

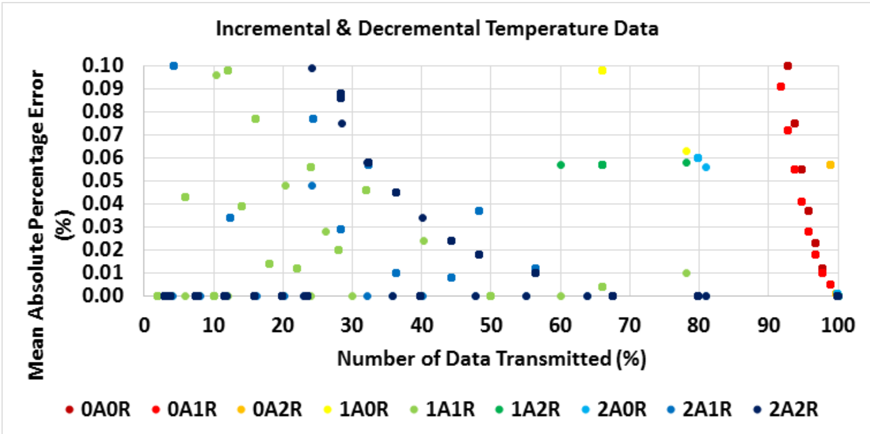

(b) Number of data transmitted vs. mean absolute percentage error where

$$MAPE_{max} = 0.1\%$$

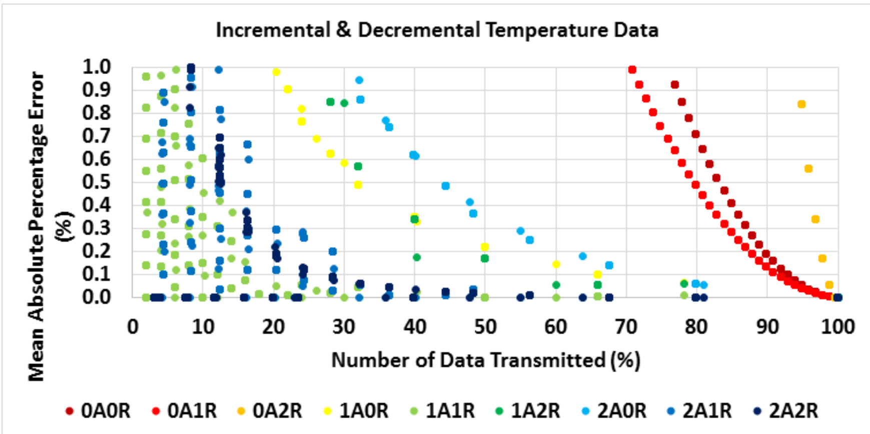

(c) Number of data transmitted vs. mean absolute percentage error where

$$MAPE_{max} = 1\%$$

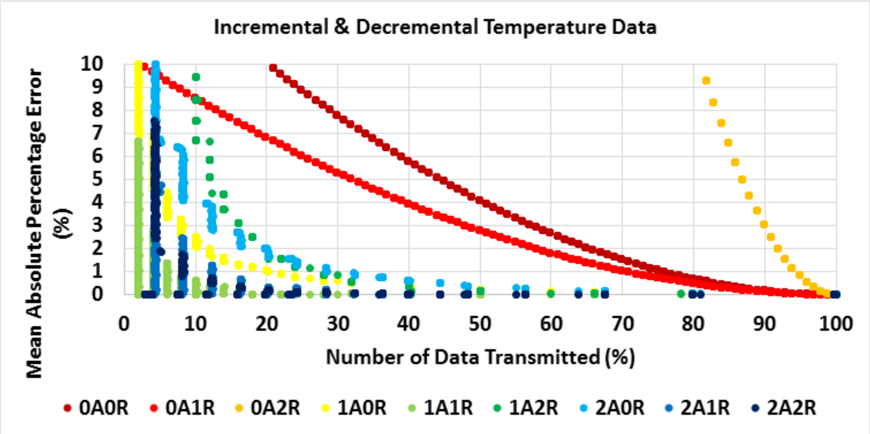

(d) Number of data transmitted vs. mean absolute percentage error where

$$MAPE_{max} = 10\%$$

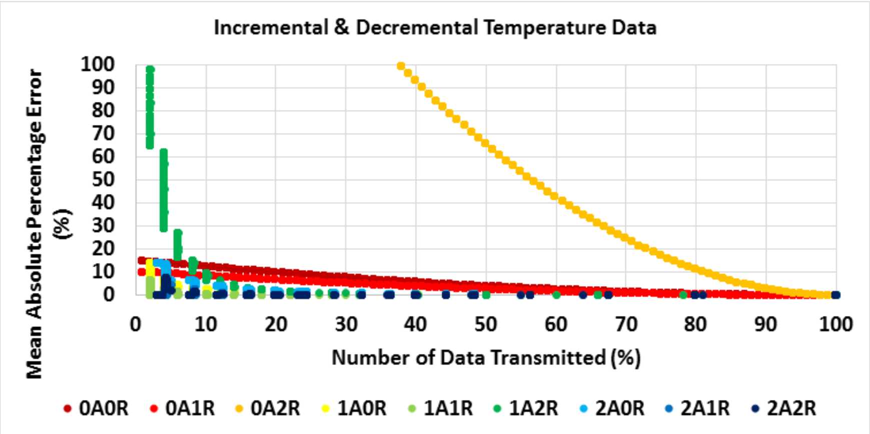

(e) Number of data transmitted vs. mean absolute percentage error where

$$MAPE_{max} = 100\%$$

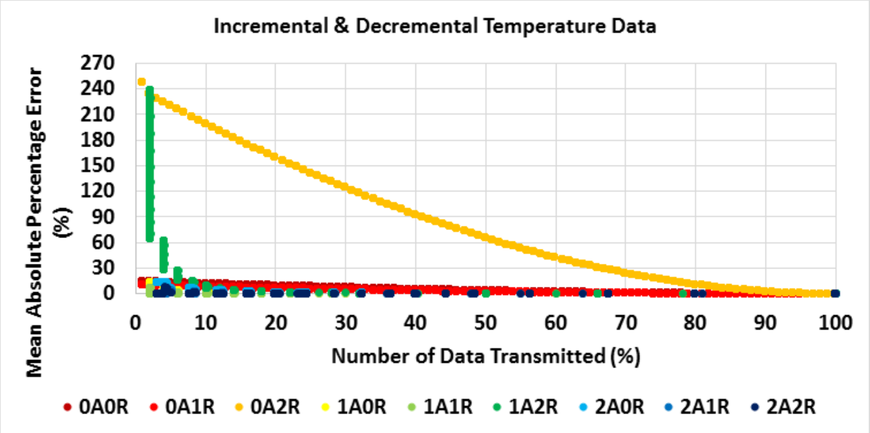

(f) Number of data transmitted vs. mean absolute percentage error where

$$\boldsymbol{MAPE_{max} = 270\%}$$

Figure 5.40: Number of data transmitted vs. mean absolute percentage error in incremental & decremental temperature data

The results of DAR schemes in incremental & decremental temperature data are shown more details in Table 5.14.

Table 5.14: Number of Data Transmitted vs. Mean Absolute Percentage Error in Incremental & Decremental Temperature Data

MAPE	DAR	$NoDT_{min}$ (%)
	0A0R	100.000
	0A1R	100.000
	0A2R	100.000
	1A0R	100.000
= 0%	1A1R	2.000
	1A2R	100.000
	2A0R	100.000
	2A1R	3.000
	2A2R	3.000

MAPE = mean absolute percentage error
DAR = data Abstraction and Reformation
0A0R = zeroth-order data abstraction & zeroth-order data reformation
0A1R = zeroth-order data abstraction & first-order data reformation
0A2R = zeroth-order data abstraction & second-order data reformation
1A0R = first-order data abstraction & zeroth-order data reformation
1A1R = first-order data abstraction & first-order data reformation
1A2R = first-order data abstraction & second-order data reformation
2A0R = second-order data abstraction & zeroth-order data reformation
2A1R = second-order data abstraction & first-order data reformation
2A2R = second-order data abstraction & second-order data reformation
$NoDT_{min}$ = minimum number of data transmitted

From Table 5.14 it is shown that the best DAR schemes in incremental & decremental temperature data where $MAPE = 0\%$ in the terms of number of data transmitted is 1A1R.

5. Root Mean Square Error vs. Number of Packet Transmissions

The comparisons of root mean square error against number of packet transmissions are shown in Figure 5.41.

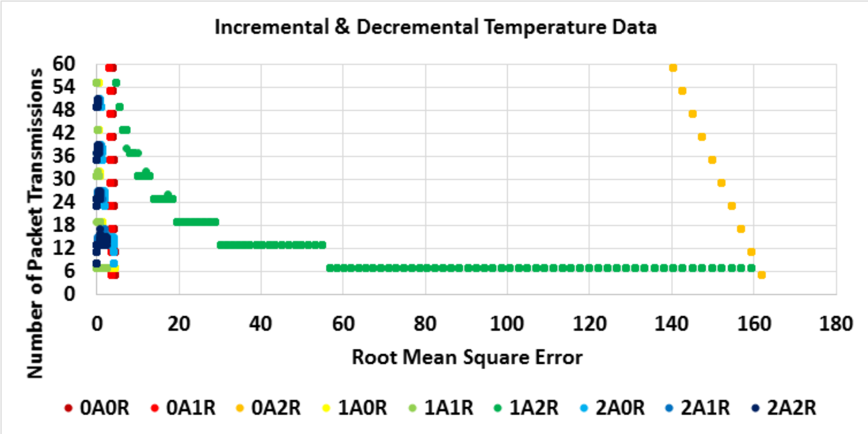

(a) Root mean square error vs. number of packet transmissions where

$$NoPT_{max} = 60$$

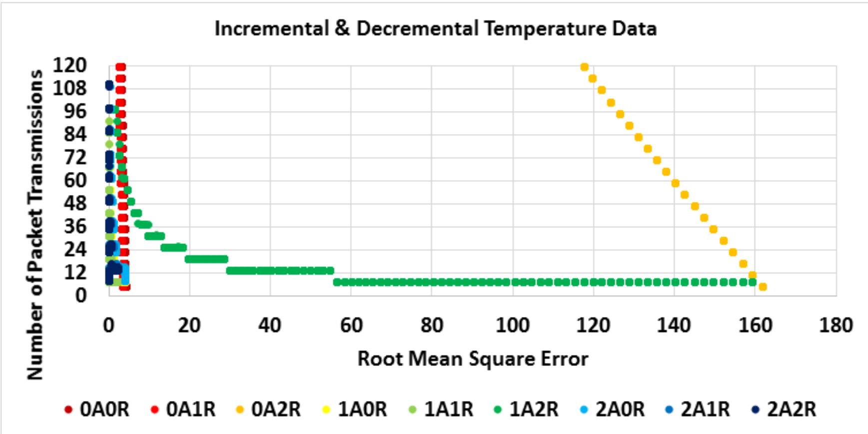

(b) Root mean square error vs. number of packet transmissions where

$$NoPT_{max} = 120$$

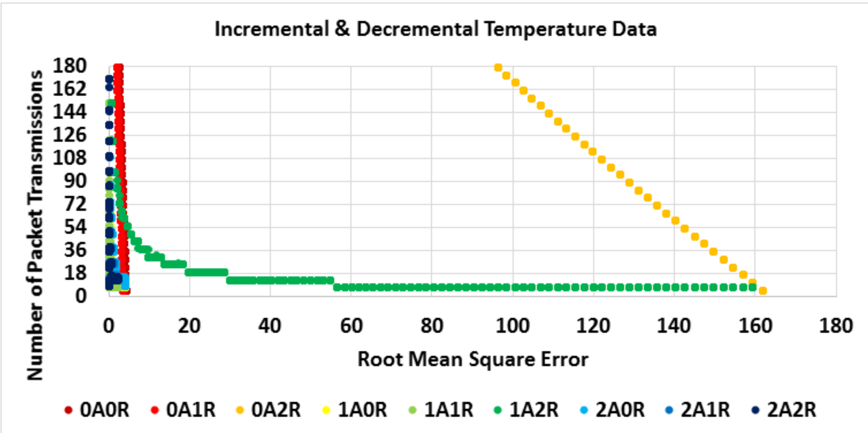

(c) Root mean square error vs. number of packet transmissions where

$$NoPT_{max} = 180$$

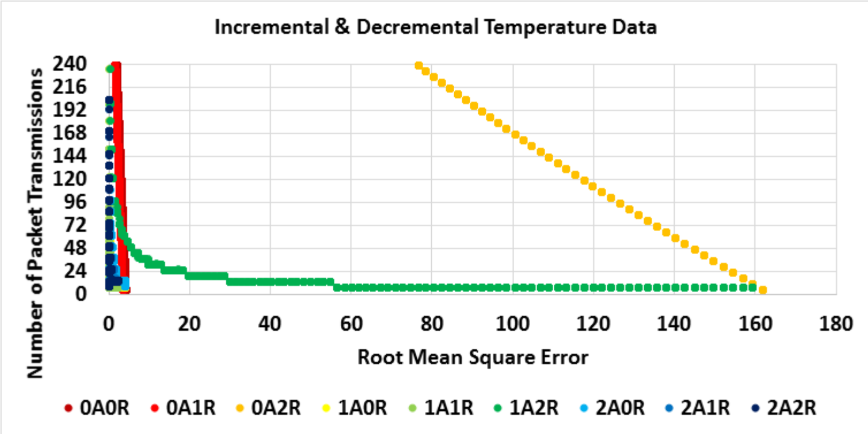

(d) Root mean square error vs. number of packet transmissions where

$$NoPT_{max} = 240$$

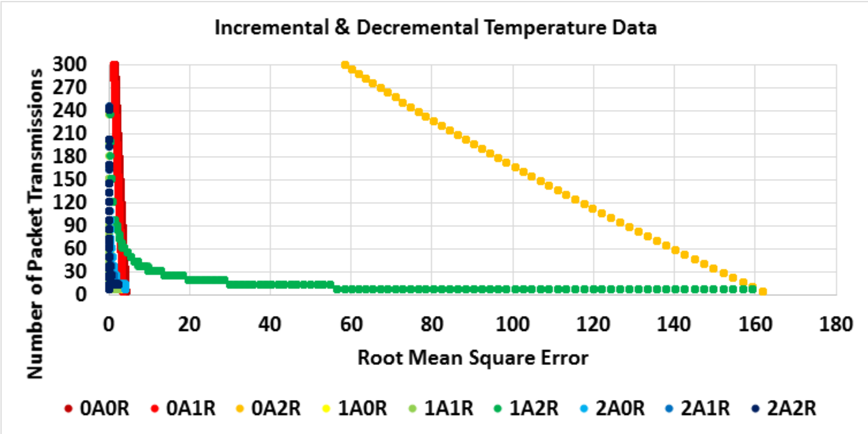

(e) Root mean square error vs. number of packet transmissions where

$$NoPT_{max} = 300$$

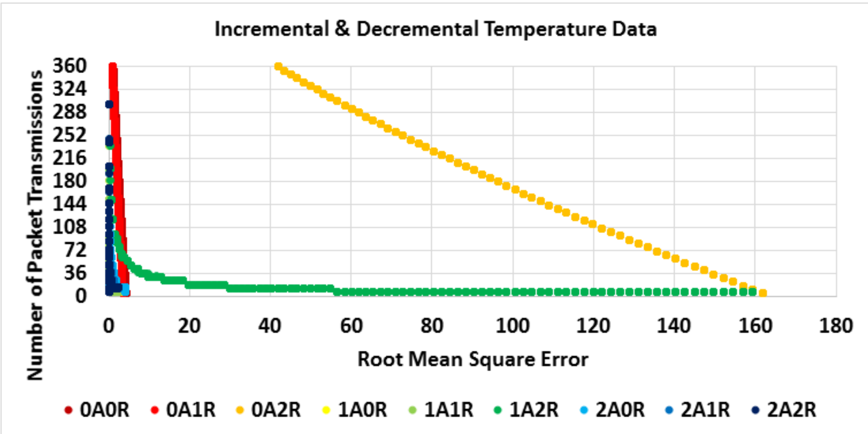

(f) Root mean square error vs. number of packet transmissions where

$$NoPT_{max} = 360$$

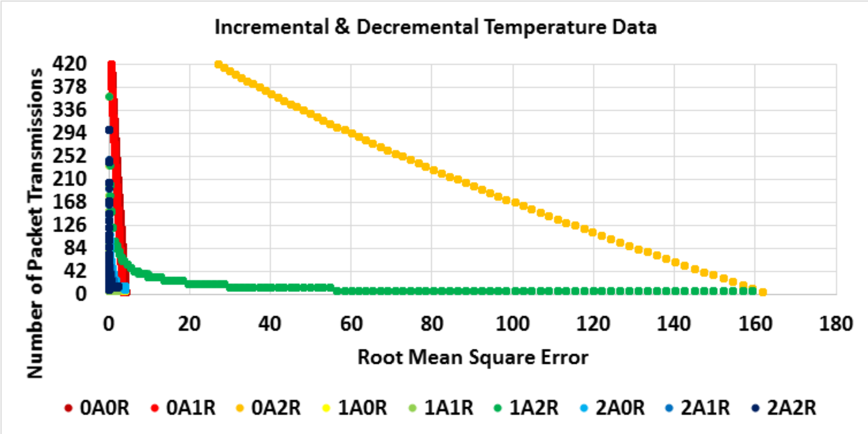

(g) Root mean square error vs. number of packet transmissions where

$$NoPT_{max} = 420$$

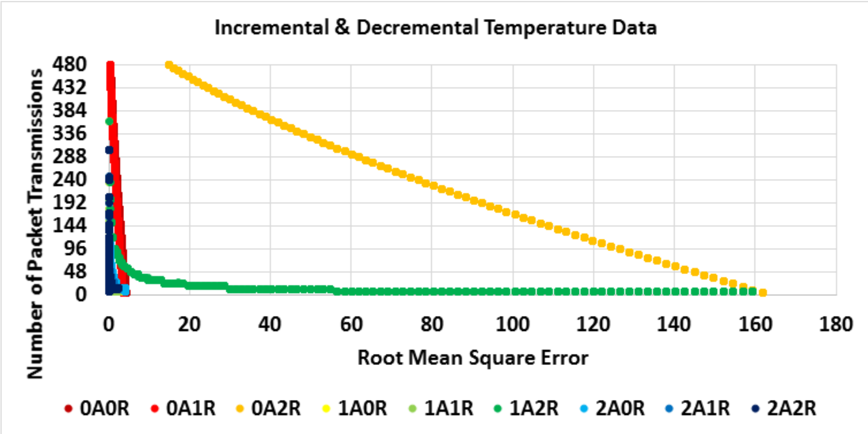

(h) Root mean square error vs. number of packet transmissions where

$$NoPT_{max} = 480$$

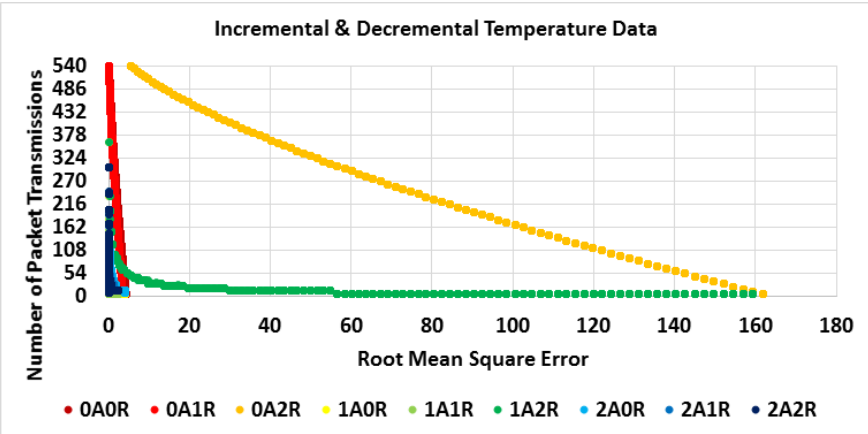

(i) Root mean square error vs. number of packet transmissions where

$$NoPT_{max} = 540$$

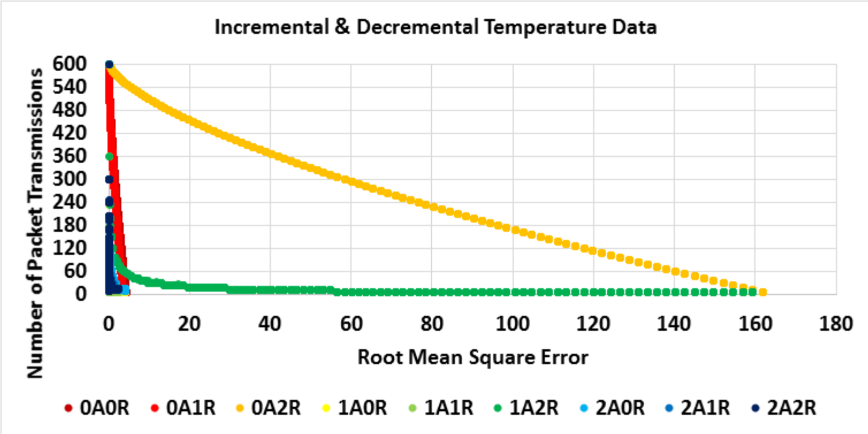

(j) Root mean square error vs. number of packet transmissions where

$$NoPT_{max} = 600$$

Figure 5.41: Root mean square error vs. number of packet transmissions in incremental & decremental temperature data

The results of DAR schemes in incremental & decremental temperature data are shown more details in Table 5.15.

Table 5.15: Root Mean Square Error vs. Number of Packet Transmissions in Incremental & Decremental Temperature Data

NoPT	DAR	$RMSE_{min}$
≤ 300	0A0R	1.562
	0A1R	1.288
	0A2R	58.377
	1A0R	0.036
	1A1R	0.000
	1A2R	0.298
	2A0R	0.033
	2A1R	0.000
	2A2R	0.000

NoPT = number of packet transmissions
DAR = data abstraction and reformation
0A0R = zeroth-order data abstraction & zeroth-order data reformation
0A1R = zeroth-order data abstraction & first-order data reformation
0A2R = zeroth-order data abstraction & second-order data reformation
1A0R = first-order data abstraction & zeroth-order data reformation
1A1R = first-order data abstraction & first-order data reformation
1A2R = first-order data abstraction & second-order data reformation
2A0R = second-order data abstraction & zeroth-order data reformation
2A1R = second-order data abstraction & first-order data reformation
2A2R = second-order data abstraction & second-order data reformation
$RMSE_{min}$ = minimum root mean square error

From Table 5.15, it is shown that the best DAR schemes in incremental & decremental temperature data where $NoPT \leq 300$ in the terms of root mean square error are 1A1R, 2A1R, and 2A2R.

6. Root Mean Square Error vs. Number of Data Transmitted

The comparisons of root mean square error against number of data transmitted are shown in Figure 5.42.

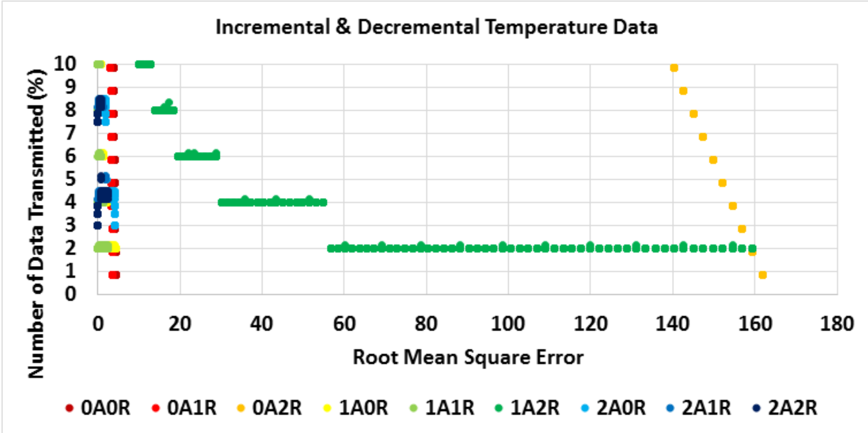

a) Root mean square error vs. number of data transmitted where

$$NoDT_{max} = 10\%$$

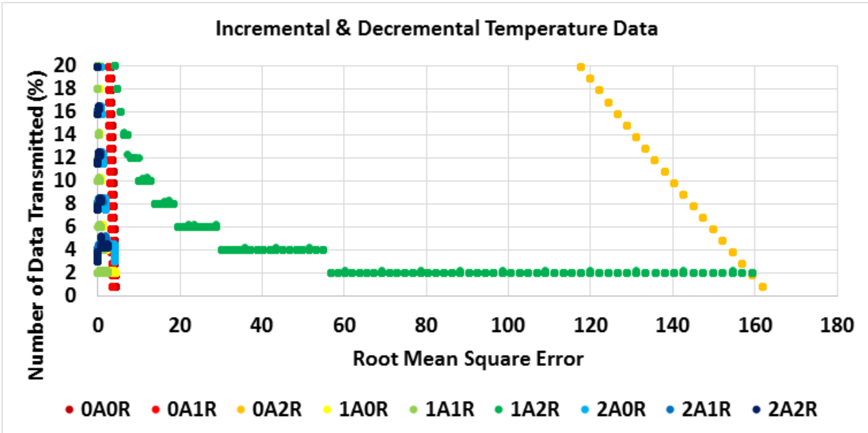

(b) Root mean square error vs. number of data transmitted where

$$NoDT_{max} = 20\%$$

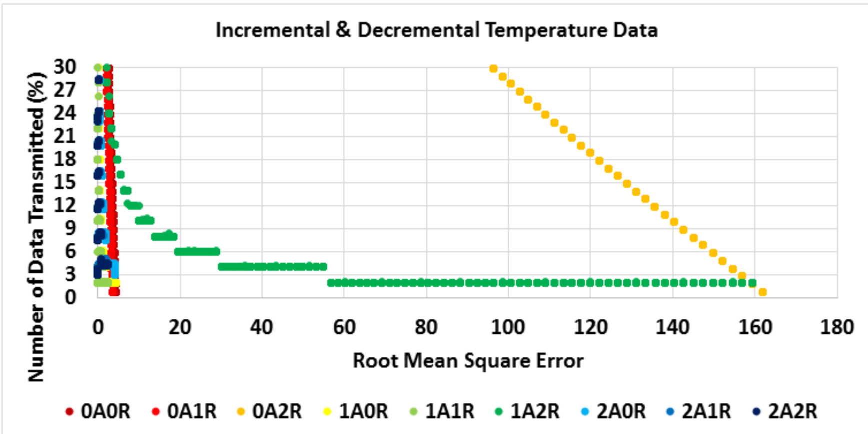

(c) Root mean square error vs. number of data transmitted (%) where

$$NoDT_{max} = 30\%$$

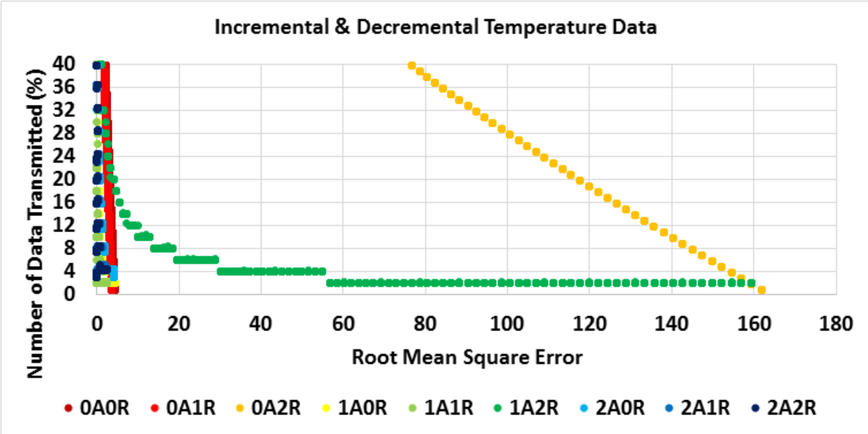

(d) Root mean square error vs. number of data transmitted where

$$NoDT_{max} = 40\%$$

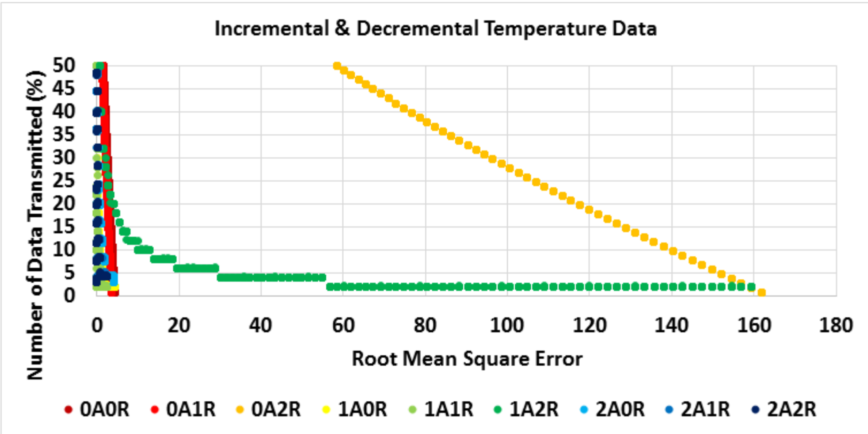

(e) Root mean square error vs. number of data transmitted where

$$NoDT_{max} = 50\%$$

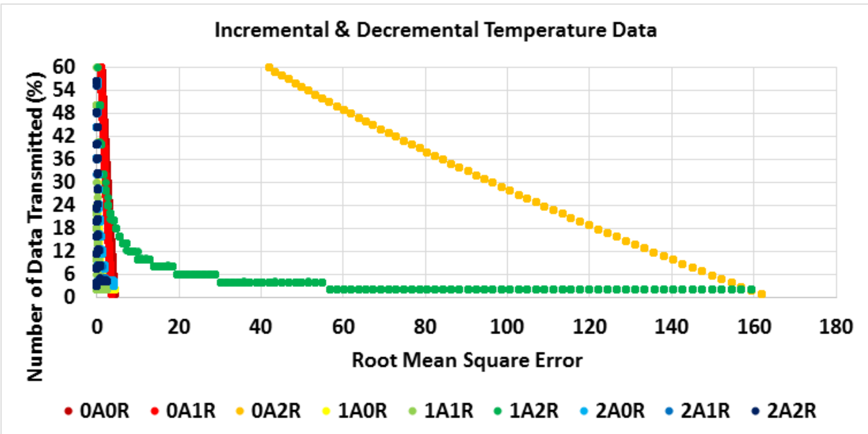

(f) Root mean square error vs. number of data transmitted where

$$NoDT_{max} = 60\%$$

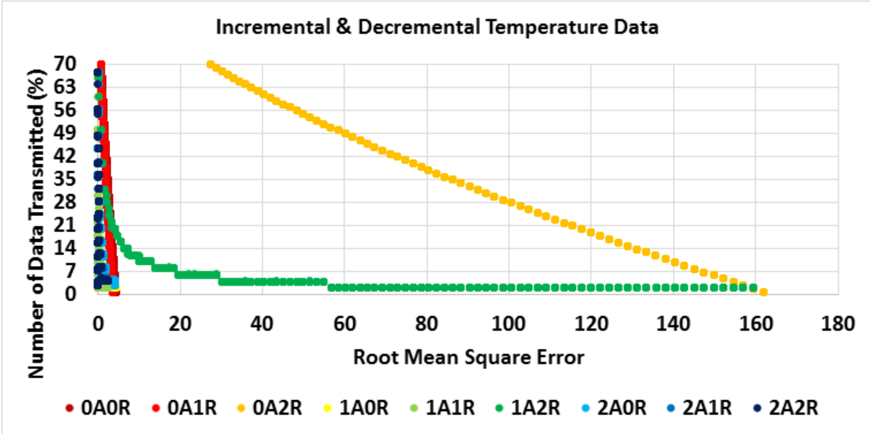

(g) Root mean square error vs. number of data transmitted where

$\boldsymbol{NoDT_{max}} = \mathbf{70\%}$

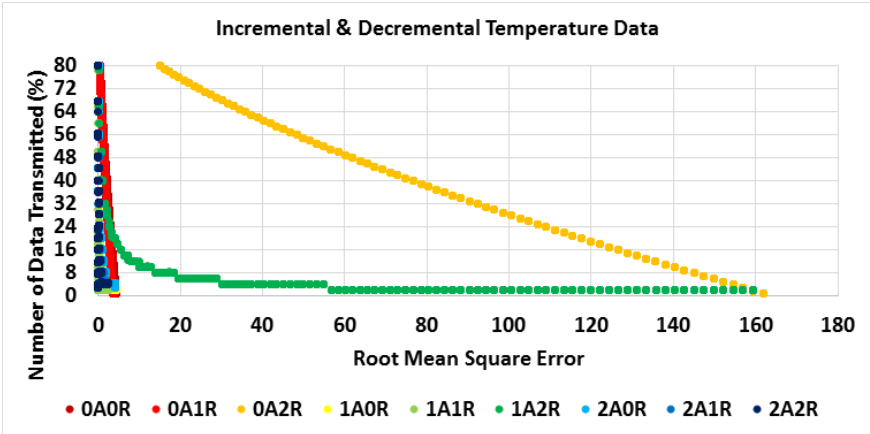

(h) Root mean square error vs. number of data transmitted where

$\boldsymbol{NoDT_{max}} = \mathbf{80\%}$

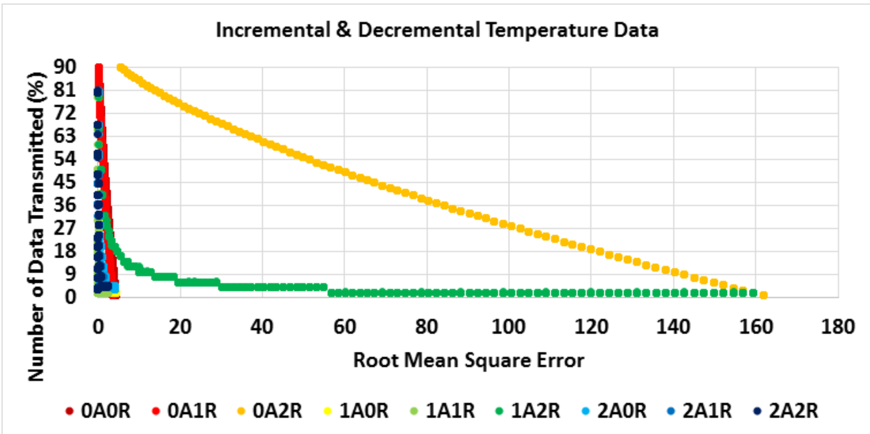

(i) Root mean square error vs. number of data transmitted where

$\boldsymbol{NoDT_{max}} = \mathbf{90\%}$

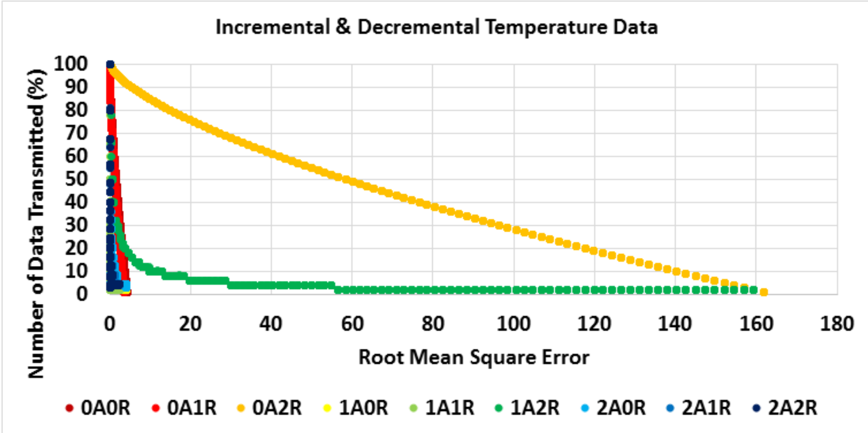

(j) Root mean square error vs. number of data transmitted where

$$NoDT_{max} = 100\%$$

Figure 5.42: Root mean square error vs. number of data transmitted in incremental & decremental temperature data

The results of DAR schemes in incremental & decremental temperature data are shown more details in Table 5.16.

Table 5.16: Root Mean Square Error vs. Number of Data Transmitted in Incremental & Decremental Temperature Data

NoDT	DAR	$RMSE_{min}$
≤ 50%	0A0R	1.562
	0A1R	1.288
	0A2R	58.377
	1A0R	0.084
	1A1R	0.000
	1A2R	0.633
	2A0R	0.144
	2A1R	0.000
	2A2R	0.000

NoDT = number of data transmitted
DAR = data abstraction and reformation
0A0R = zeroth-order data abstraction & zeroth-order data reformation
0A1R = zeroth-order data abstraction & first-order data reformation
0A2R = zeroth-order data abstraction & second-order data reformation
1A0R = first-order data abstraction & zeroth-order data reformation
1A1R = first-order data abstraction & first-order data reformation
1A2R = first-order data abstraction & second-order data reformation
2A0R = second-order data abstraction & zeroth-order data reformation
2A1R = second-order data abstraction & first-order data reformation
2A2R = second-order data abstraction & second-order data reformation
$RMSE_{min}$ = minimum root mean square error

From Table 5.16, it is shown that the best DAR schemes in incremental & decremental temperature data where $NoDT \leq 50\%$ in the terms of root mean square error are 1A1R, 2A1R, and 2A2R.

7. Mean Absolute Percentage Error vs. Number of Packet Transmissions

The comparisons of mean absolute percentage error against number of packet transmissions are shown in Figure 5.43.

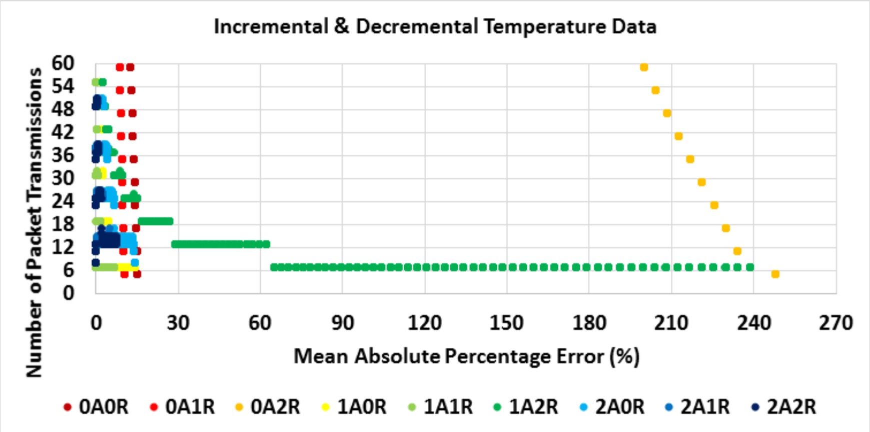

(a) Mean absolute percentage error vs. number of packet transmission where $NoPT_{max} = 60$

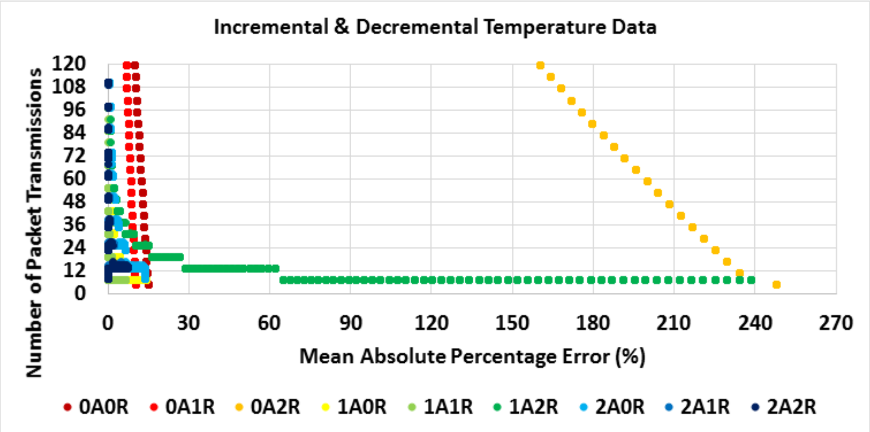

(b) Mean absolute percentage error vs. number of packet transmission where $NoPT_{max} = 120$

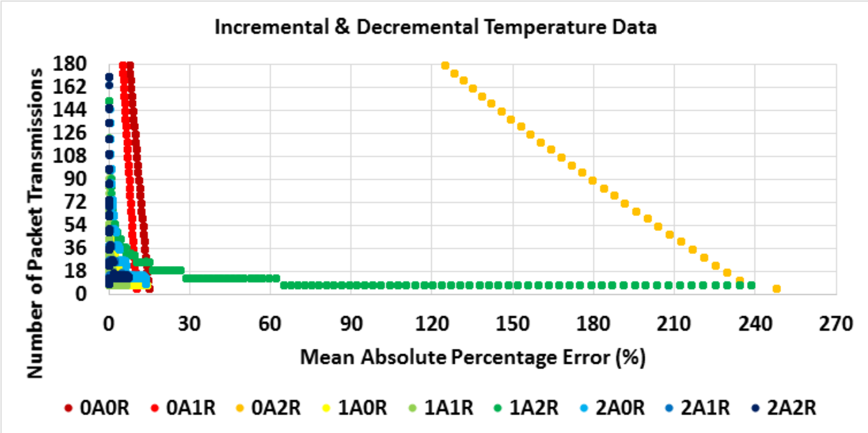

(c) Mean absolute percentage error vs. number of packet transmission

where $NoPT_{max} = 180$

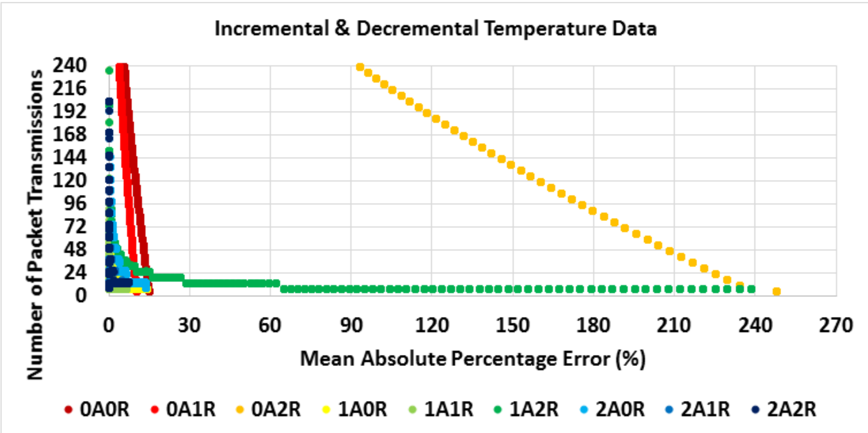

(d) Mean absolute percentage error vs. number of packet transmission

where $NoPT_{max} = 240$

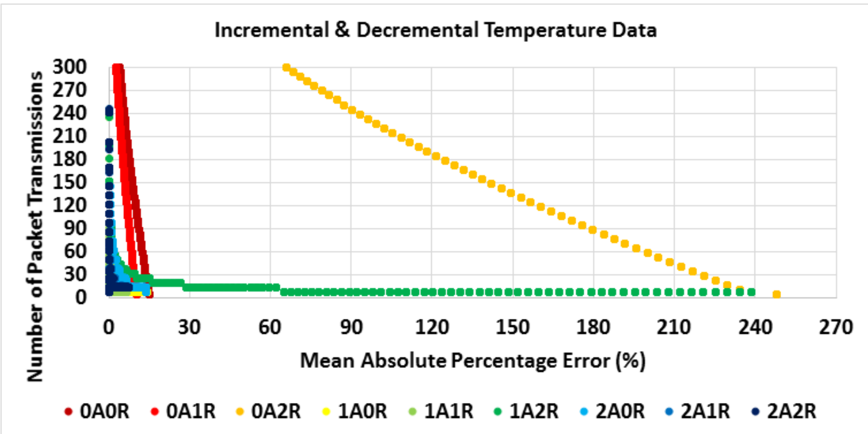

(e) Mean absolute percentage error vs. number of packet transmission

where $NoPT_{max} = 300$

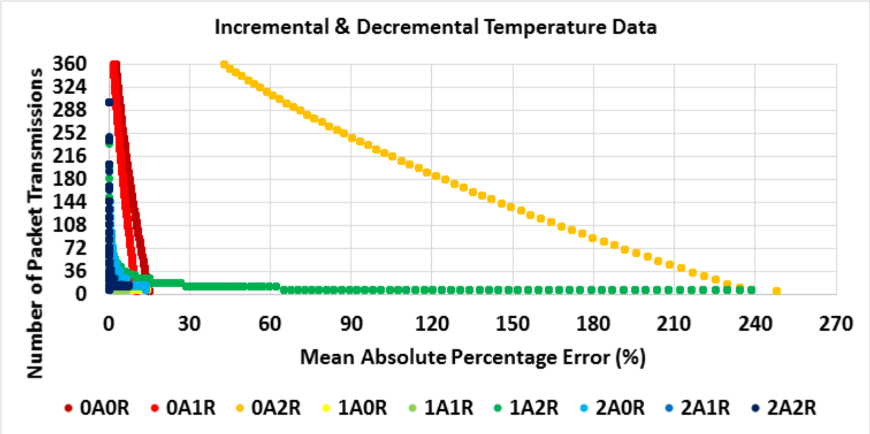

(f) Mean absolute percentage error vs. number of packet transmission where $NoPT_{max} = 360$

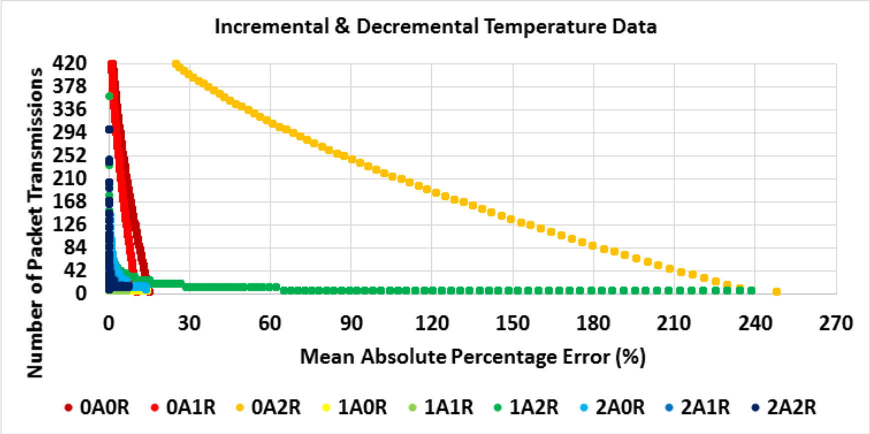

(g) Mean absolute percentage error vs. number of packet transmission where $NoPT_{max} = 420$

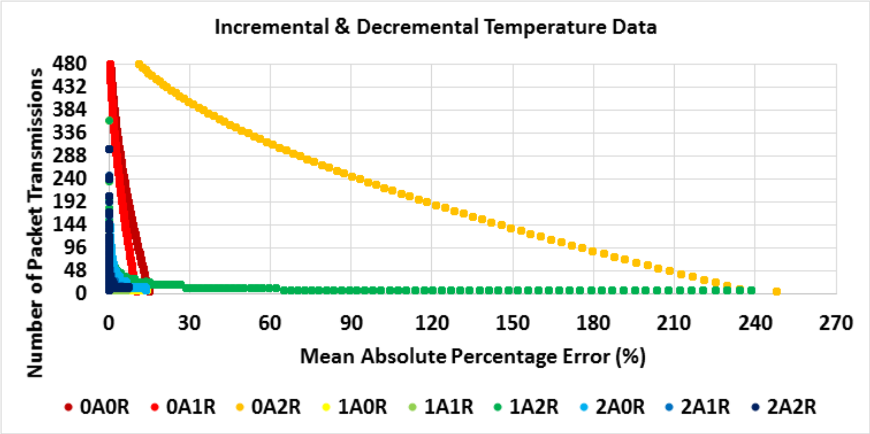

(h) Mean absolute percentage error vs. number of packet transmission where $NoPT_{max} = 480$

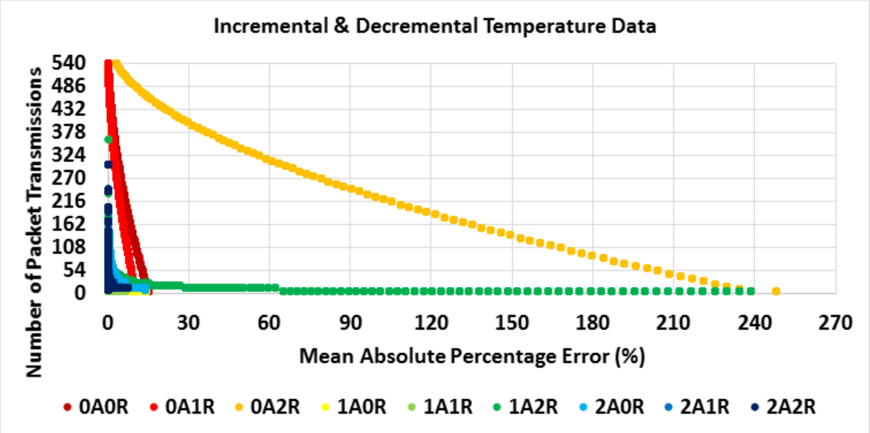

(i) Mean absolute percentage error vs. number of packet transmission where $NoPT_{max} = 540$

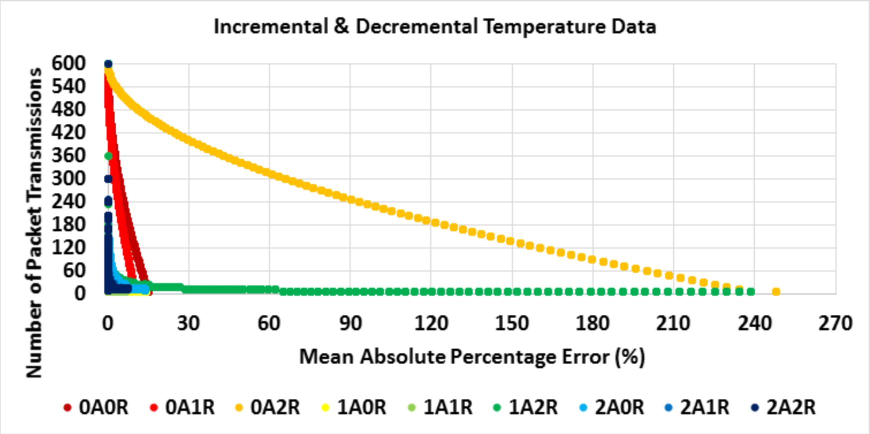

(j) Mean absolute percentage error vs. number of packet transmission where $NoPT_{max} = 600$

Figure 5.43: Mean absolute percentage error vs. number of packet transmissions in incremental & decremental temperature data

The results of DAR schemes in incremental & decremental temperature data are shown more details in Table 5.17.

Table 5.17: Mean Absolute Percentage Error vs. Number of Packet Transmissions in Incremental & Decremental Temperature Data

NoPT	DAR	$MAPE_{min}$ (%)
≤ 300	0A0R	4.105
	0A1R	2.798
	0A2R	65.993
	1A0R	0.063
	1A1R	0.000
	1A2R	0.057
	2A0R	0.056
	2A1R	0.000
	2A2R	0.000

NoPT = number of packet transmissions
DAR = data abstraction and reformation
0A0R = zeroth-order data abstraction & zeroth-order data reformation
0A1R = zeroth-order data abstraction & first-order data reformation
0A2R = zeroth-order data abstraction & second-order data reformation
1A0R = first-order data abstraction & zeroth-order data reformation
1A1R = first-order data abstraction & first-order data reformation
1A2R = first-order data abstraction & second-order data reformation
2A0R = second-order data abstraction & zeroth-order data reformation
2A1R = second-order data abstraction & first-order data reformation
2A2R = second-order data abstraction & second-order data reformation
$MAPE_{min}$ = minimum mean absolute percentage error

From Table 5.17, it is shown that the best DAR schemes in incremental & decremental temperature data where $NoPT \leq 300$ in the terms of mean absolute percentage error are 1A1R, 2A1R, and 2A2R.

8. Mean Absolute Percentage Error vs. Number of Data Transmitted

The comparisons of mean absolute percentage error against number of data transmitted are shown in Figure 5.44.

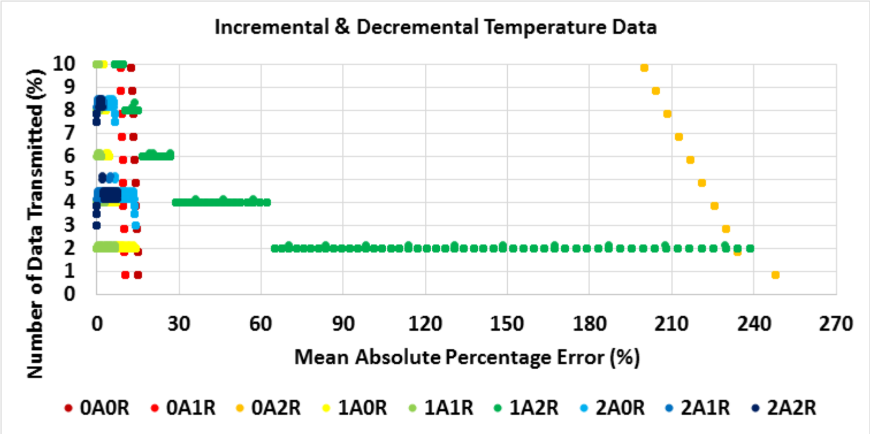

(a) Mean absolute percentage error vs. number of data transmitted where $NoDT_{max} = 10\%$

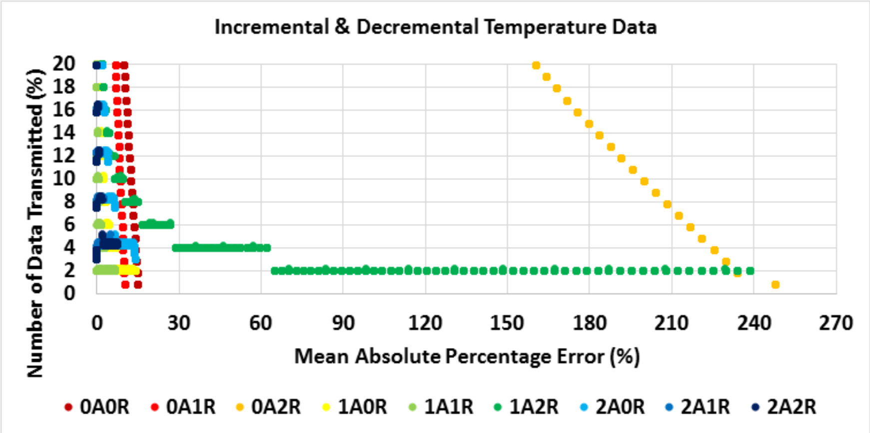

(b) Mean absolute percentage error vs. number of data transmitted where $NoDT_{max} = 20\%$

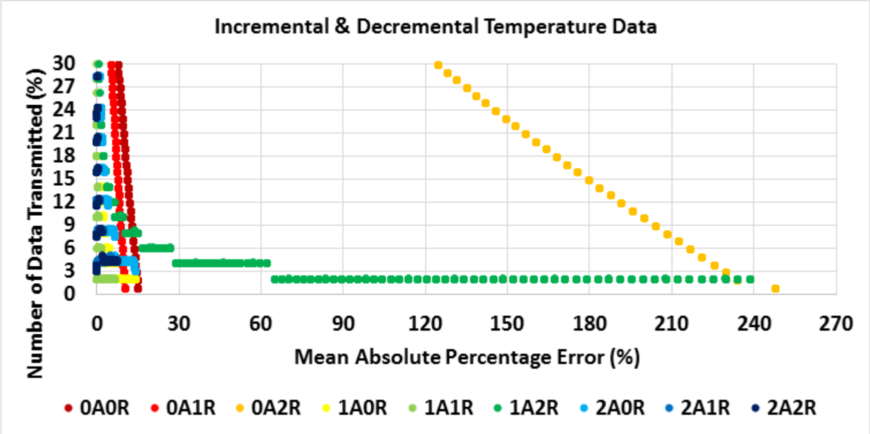

(c) Mean absolute percentage error vs. number of data transmitted where $NoDT_{max} = 30\%$

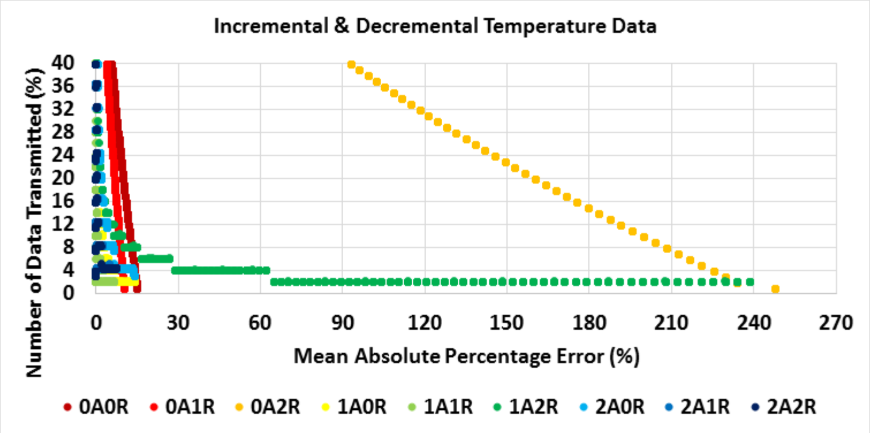

(d) Mean absolute percentage error vs. number of data transmitted where $NoDT_{max} = 40\%$

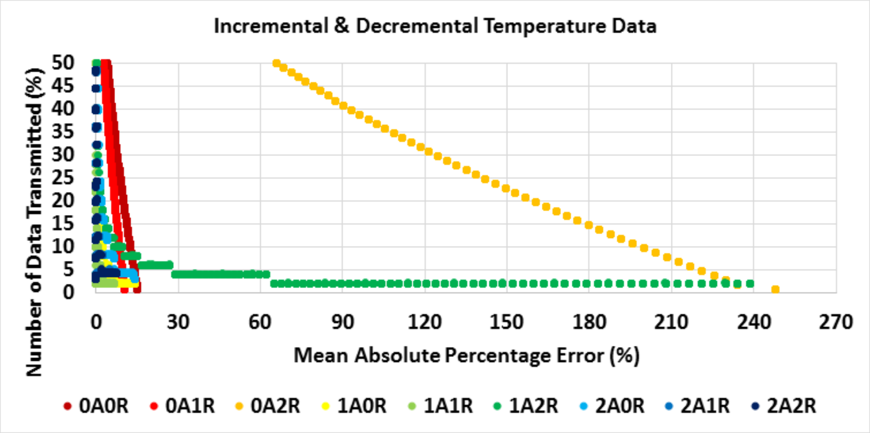

(e) Mean absolute percentage error vs. number of data transmitted where $NoDT_{max} = 50\%$

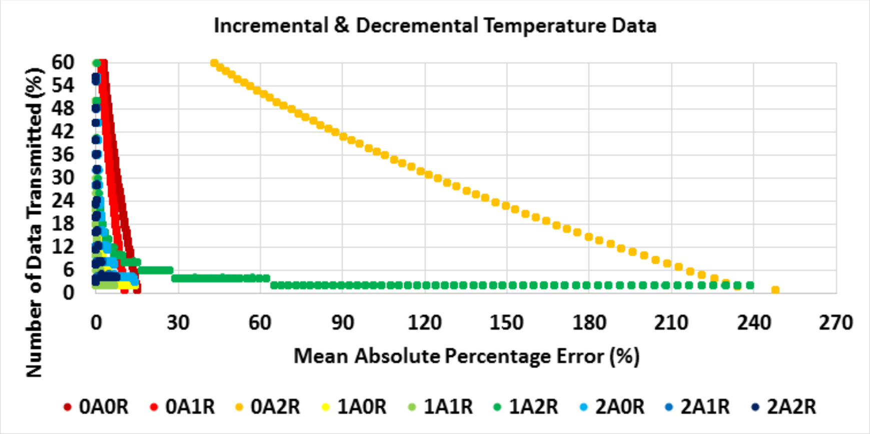

(f) Mean absolute percentage error vs. number of data transmitted where $NoDT_{max} = 60\%$

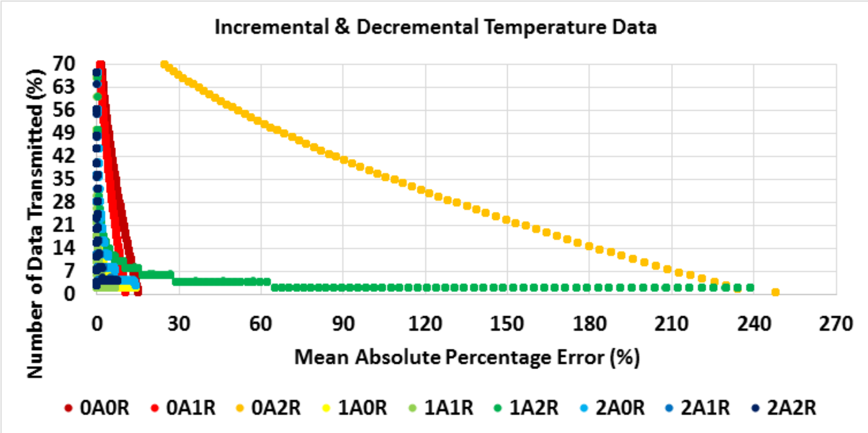

(g) Mean absolute percentage error vs. number of data transmitted where

$NoDT_{max} = 70\%$

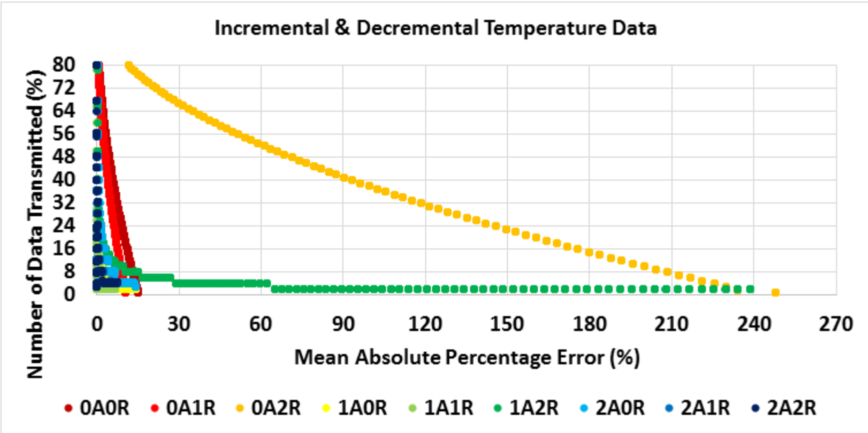

(h) Mean absolute percentage error vs. number of data transmitted where

$NoDT_{max} = 80\%$

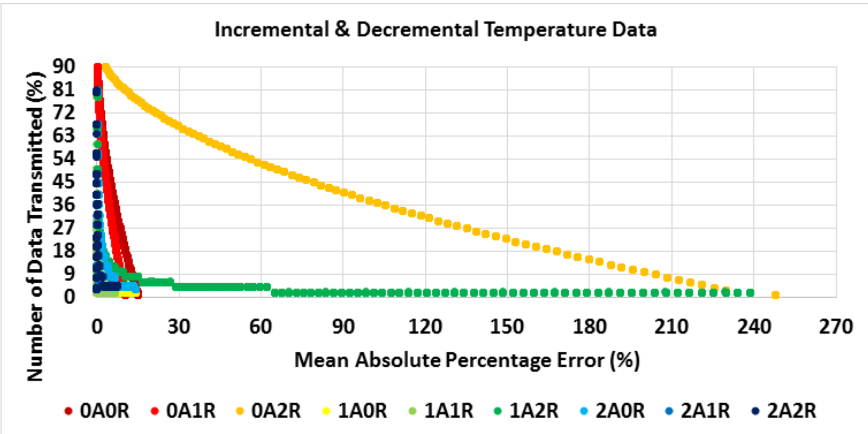

(i) Mean absolute percentage error vs. number of data transmitted where

$NoDT_{max} = 90\%$

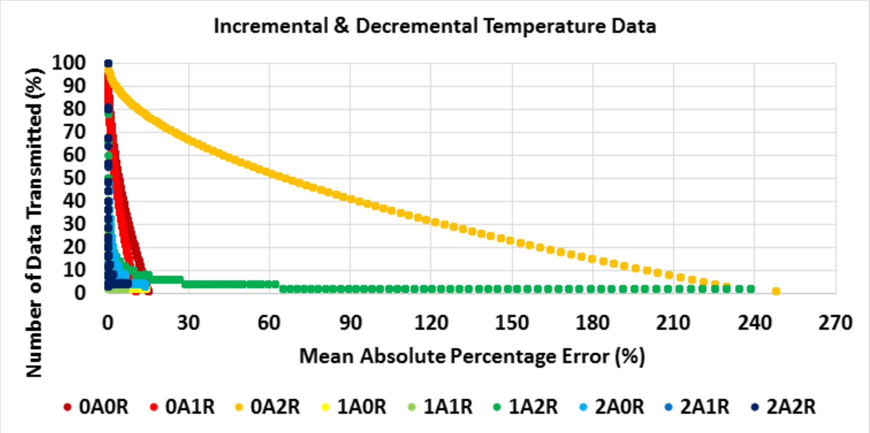

(j) Mean absolute percentage error vs. number of data transmitted (%)

where $NoDT_{max}$ = 100%

Figure 5.44: Mean absolute percentage error vs. number of data transmitted in incremental & decremental temperature data

The results of DAR schemes in incremental & decremental temperature data are shown more details in Table 5.18.

Table 5.18: Mean Absolute Percentage Error vs. Number of Data Transmitted in Incremental & Decremental Temperature Data

NoDT	DAR	$MAPE_{min}$ (%)
$\leq 50\%$	0A0R	4.105
	0A1R	2.798
	0A2R	65.993
	1A0R	0.220
	1A1R	0.000
	1A2R	0.170
	2A0R	0.365
	2A1R	0.000
	2A2R	0.000

NoDT = number of data transmitted
DAR = data abstraction and reformation
0A0R = zeroth-order data abstraction & zeroth-order data reformation
0A1R = zeroth-order data abstraction & first-order data reformation
0A2R = zeroth-order data abstraction & second-order data reformation
1A0R = first-order data abstraction & zeroth-order data reformation
1A1R = first-order data abstraction & first-order data reformation
1A2R = first-order data abstraction & second-order data reformation
2A0R = second-order data abstraction & zeroth-order data reformation
2A1R = second-order data abstraction & first-order data reformation
2A2R = second-order data abstraction & second-order data reformation
$MAPE_{min}$ = minimum mean absolute percentage error

From Table 5.18, it is shown that the best DAR schemes in incremental & decremental temperature data where $NoDT \leq 50\%$ in the terms of mean absolute percentage error are 1A1R, 2A1R, and 2A2R.

9. Conclusion

From Table 5.11 – 5.18, it is concluded in Table 5.19, that the best DAR schemes in incremental & decremental temperature data is 1A1R.

Table 5.19: Results of DAR Schemes in Incremental & Decremental Temperature Data

(a) Best DAR Schemes in Incremental & Decremental Temperature Data where the $NoPT \leq 300$ and $NoDT \leq 50\%$

DAR	Th	NoPT	NoDT(%)	RMSE	MAPE(%)
0A0R	25.751	299	49.833	1.562	4.105
0A1R	25.751	299	49.833	1.288	2.798
0A2R	25.751	299	49.833	58.377	65.993
1A0R	0.150	235	39.167	0.036	0.063
1A1R	7.426	7	1.167	0.000	0.000
1A2R	0.225	181	30.167	0.298	0.057
2A0R	0.075	246	41.000	0.033	0.056
2A1R	7.426	8	1.333	0.000	0.000
2A2R	7.426	8	1.333	0.000	0.000

(b) Best DAR Schemes in Incremental & Decremental Temperature Data where the $RMSE = 0$ and $MAPE = 0\%$

DAR	Th	NoPT	NoDT(%)	RMSE	MAPE(%)
0A0R	22.000	600	100.000	0.000	0.000
0A1R	22.000	600	100.000	0.000	0.000
0A2R	22.000	600	100.000	0.000	0.000
1A0R	0.076	301	50.167	0.000	0.000
1A1R	7.426	7	1.167	0.000	0.000
1A2R	0.076	301	50.167	0.000	0.000
2A0R	0.000	600	100.000	0.000	0.000
2A1R	7.426	8	1.333	0.000	0.000
2A2R	7.426	8	1.333	0.000	0.000

DAR = data abstraction and reformation
Th = threshold
NoPT = number of packet transmissions
NoDT = number of packet transmitted
RMSE = root mean square error
MAPE = mean absolute percentage error

5.3.3 Random Temperature Data

The comparisons among parameters (number of packet transmissions, number of data transmitted, root mean square error, and mean absolute percentage error) are as follows.

1. Number of Packet Transmissions vs. Root Mean Square Error

   The comparisons of number of packet transmissions against root mean square error are shown in Figure 5.45.

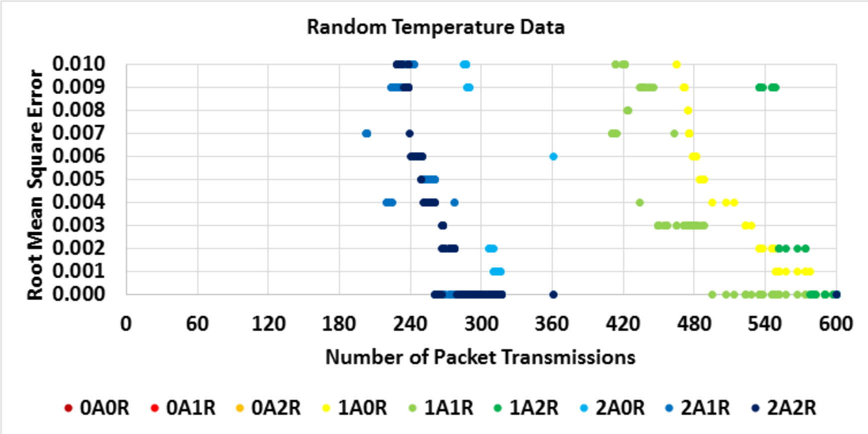

(a) Number of packet transmissions vs. root mean square error where $RMSE_{max} = 0.01$

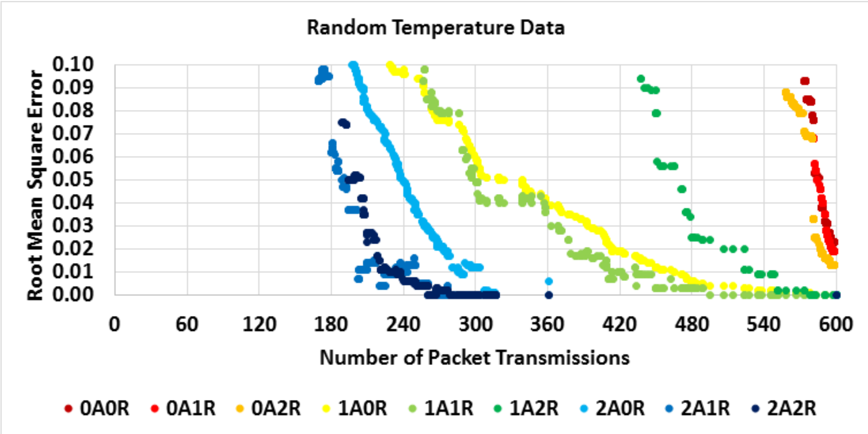

(b) Number of packet transmissions vs. root mean square error where $RMSE_{max} = 0.1$

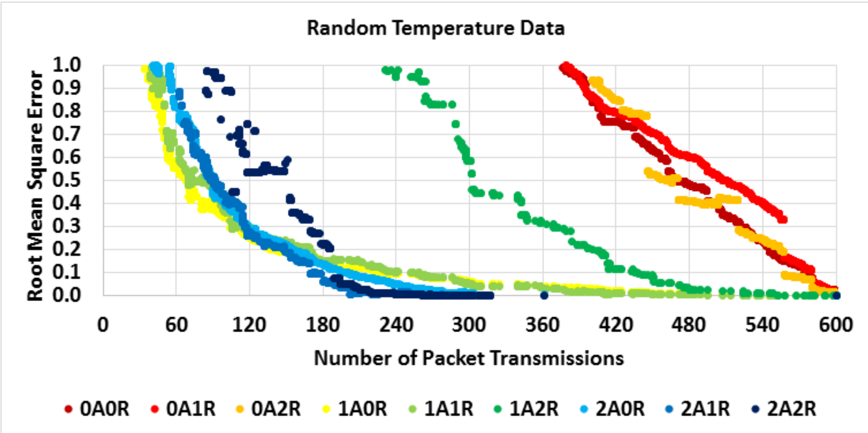

(c) Number of packet transmissions vs. root mean square error where $RMSE_{max} = 1$

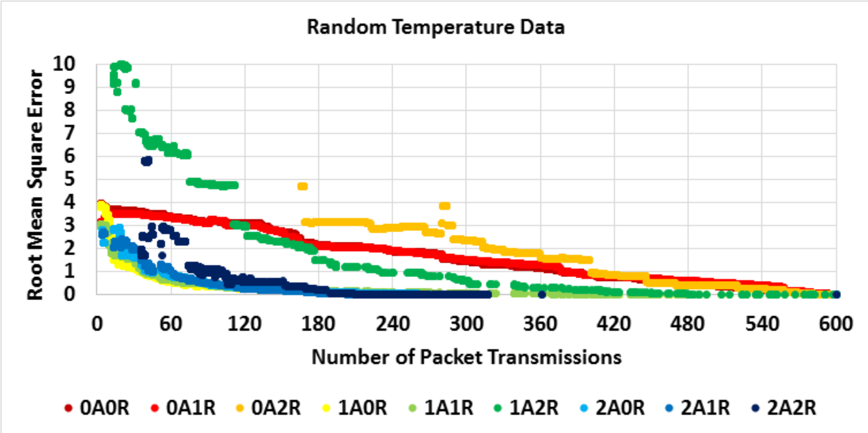

(d) Number of packet transmissions vs. root mean square error where

$$RMSE_{max} = 10$$

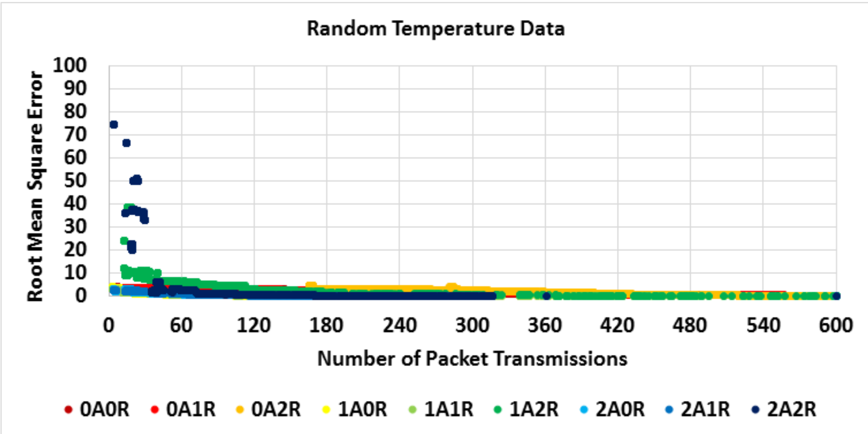

(e) Number of packet transmissions vs. root mean square error where

$$RMSE_{max} = 100$$

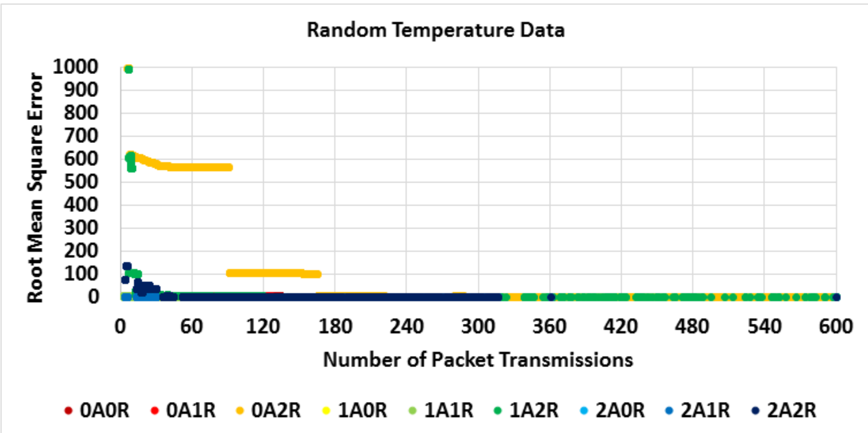

(f) Number of packet transmissions vs. root mean square error where

$$RMSE_{max} = 1000$$

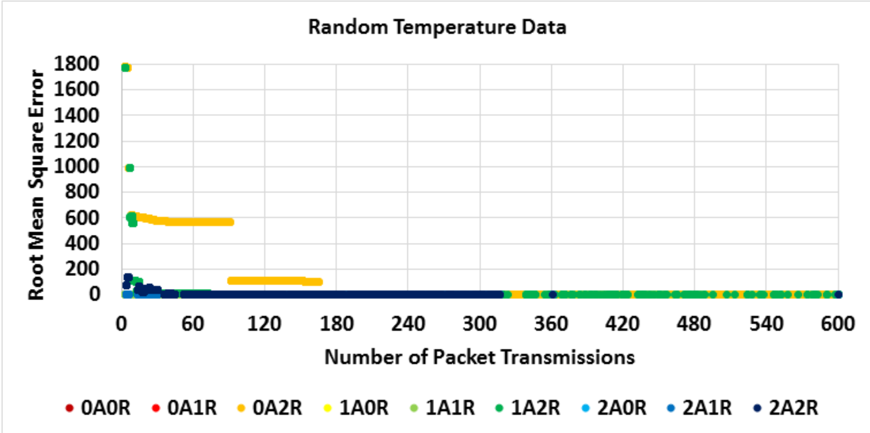

(g) Number of packet transmissions vs. root mean square error where

$$\boldsymbol{RMSE_{max}} = \mathbf{1800}$$

Figure 5.45: Number of packet transmissions vs. root mean square error in random temperature data

The results of DAR schemes in random temperature data are shown more details in Table 5.20.

Table 5.20: Number of Packet Transmissions vs. Root Mean Square Error in Random Temperature Data

RMSE	DAR	$NoPT_{min}$
= 0	0A0R	600
	0A1R	600
	0A2R	600
	1A0R	580
	1A1R	495
	1A2R	578
	2A0R	317
	2A1R	261
	2A2R	261

RMSE = root mean square error
DAR = data abstraction and reformation
0A0R = zeroth-order data abstraction & zeroth-order data reformation
0A1R = zeroth-order data abstraction & first-order data reformation
0A2R = zeroth-order data abstraction & second-order data reformation
1A0R = first-order data abstraction & zeroth-order data reformation
1A1R = first-order data abstraction & first-order data reformation
1A2R = first-order data abstraction & second-order data reformation
2A0R = second-order data abstraction & zeroth-order data reformation
2A1R = second-order data abstraction & first-order data reformation
2A2R = second-order data abstraction & second-order data reformation
$NoPT_{min}$ = minimum number of packet transmissions

From Table 5.20, it is shown that the best DAR schemes in random temperature data where $RMSE = 0$ in the terms of number of packet transmissions are 2A1R and 2A2R.

2. Number of Packet Transmissions vs. Mean Absolute Percentage Error

The comparisons of number of packet transmissions against mean absolute percentage error are shown in Figure 5.46.

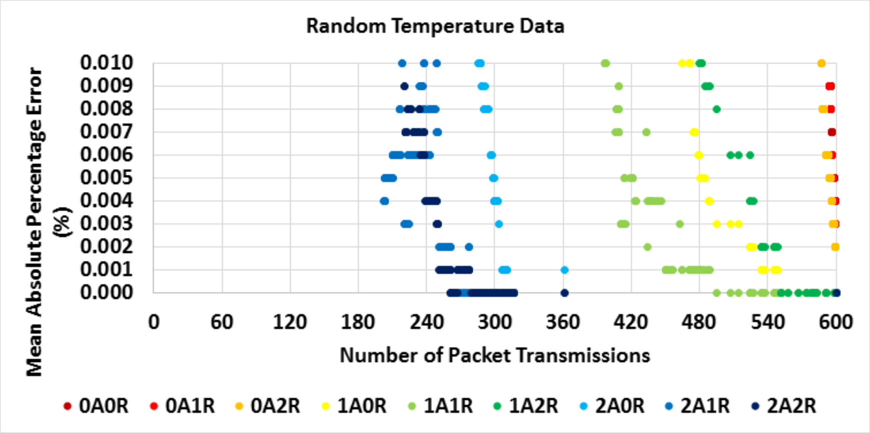

(a) Number of packet transmissions vs. mean absolute percentage error where $MAPE_{max} = 0.01\%$

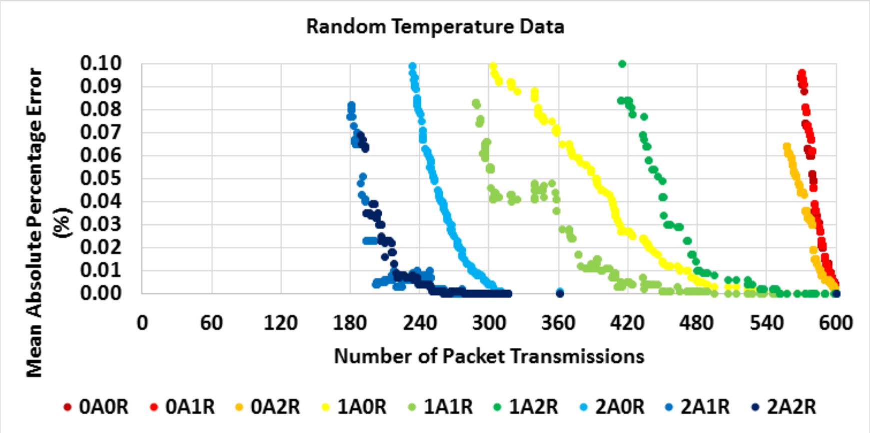

(b) Number of packet transmissions vs. mean absolute percentage error where $MAPE_{max} = 0.1\%$

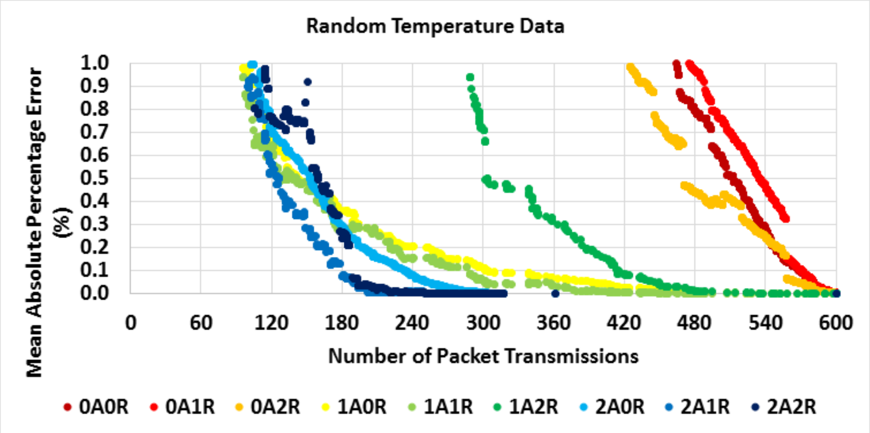

(c) Number of packet transmissions vs. mean absolute percentage error where $MAPE_{max} = 1\%$

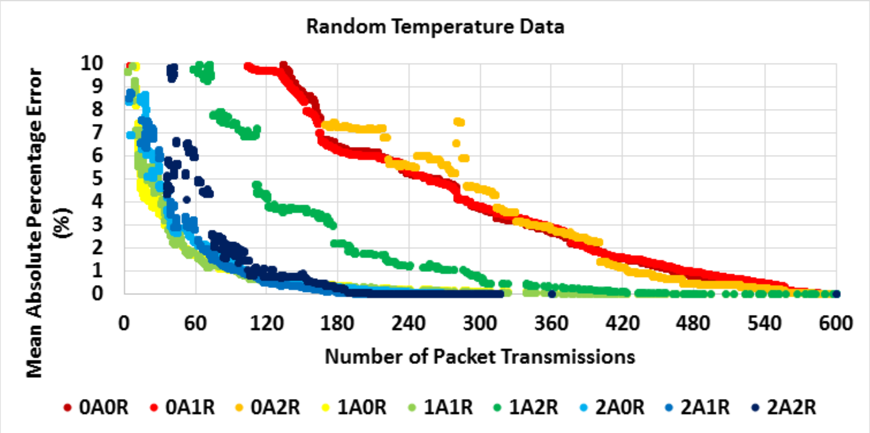

(d) Number of packet transmissions vs. mean absolute percentage error where $MAPE_{max} = 10\%$

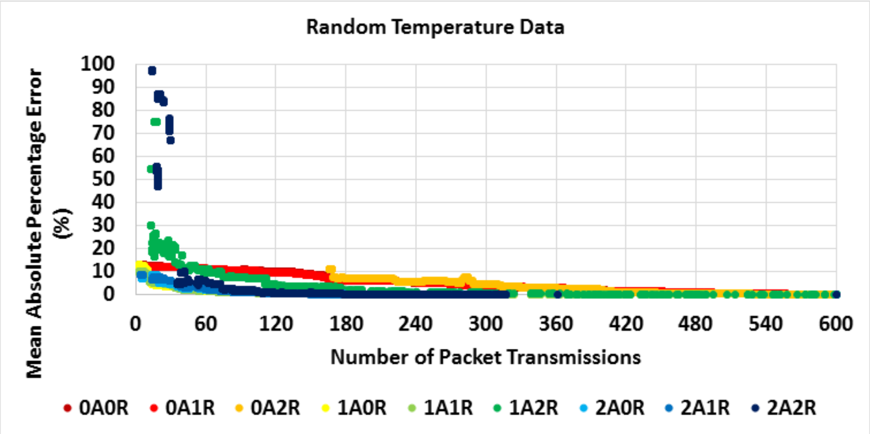

(e) Number of packet transmissions vs. mean absolute percentage error where $MAPE_{max} = 100\%$

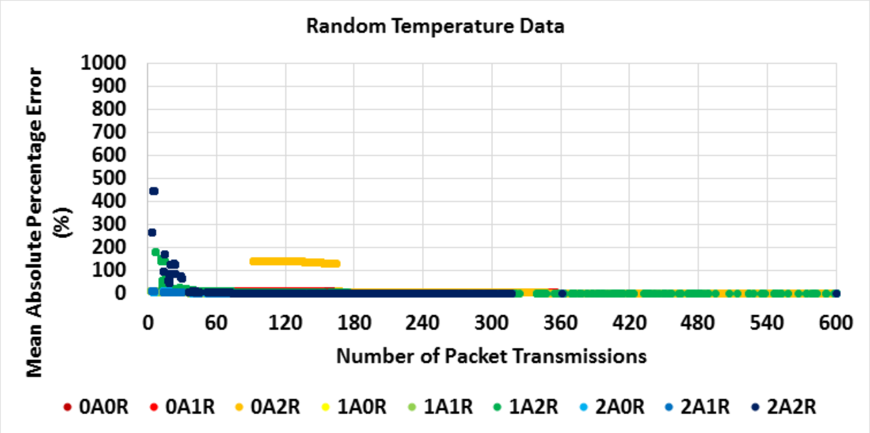

(f) Number of packet transmissions vs. mean absolute percentage error where $MAPE_{max} = 1000\%$

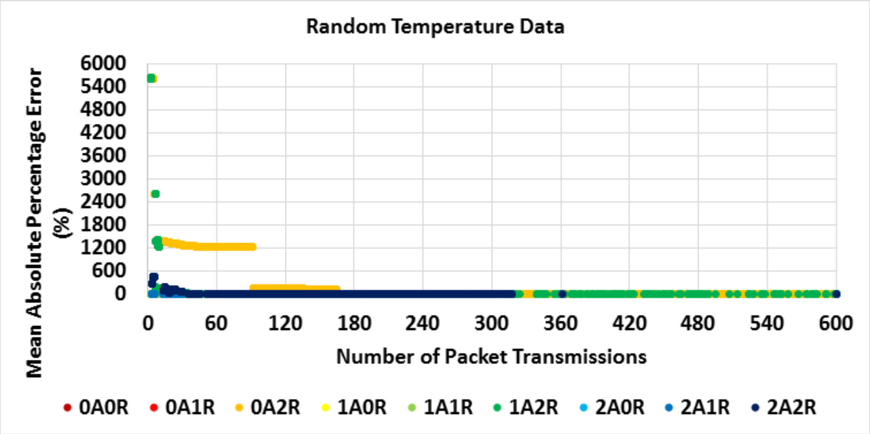

(f) Number of packet transmissions vs. mean absolute percentage error where $MAPE_{max} = 6000\%$

Figure 5.46: Number of packet transmissions vs. mean absolute percentage error in random temperature data

The results of DAR schemes in random temperature data are shown more details in Table 5.21.

Table 5.21: Number of Packet Transmissions vs. Mean Absolute Percentage Error in Random Temperature Data

MAPE	DAR	$NoPT_{min}$
= 0%	0A0R	600
	0A1R	600
	0A2R	600
	1A0R	552
	1A1R	495
	1A2R	552
	2A0R	313
	2A1R	261
	2A2R	261

MAPE = mean absolute percentage error
DAR = data Abstraction and Reformation
0A0R = zeroth-order data abstraction & zeroth-order data reformation
0A1R = zeroth-order data abstraction & first-order data reformation
0A2R = zeroth-order data abstraction & second-order data reformation
1A0R = first-order data abstraction & zeroth-order data reformation
1A1R = first-order data abstraction & first-order data reformation
1A2R = first-order data abstraction & second-order data reformation
2A0R = second-order data abstraction & zeroth-order data reformation
2A1R = second-order data abstraction & first-order data reformation
2A2R = second-order data abstraction & second-order data reformation
$NoPT_{min}$ = minimum number of packet transmissions

From Table 5.21, it is shown that the best DAR schemes in random temperature data where $MAPE = 0\%$ in the terms of number of packet transmissions are 2A1R and 2A2R.

3. Number of Data Transmitted vs. Root Mean Square Error

The comparisons of number of data transmitted against root mean square error are shown in Figure 5.47.

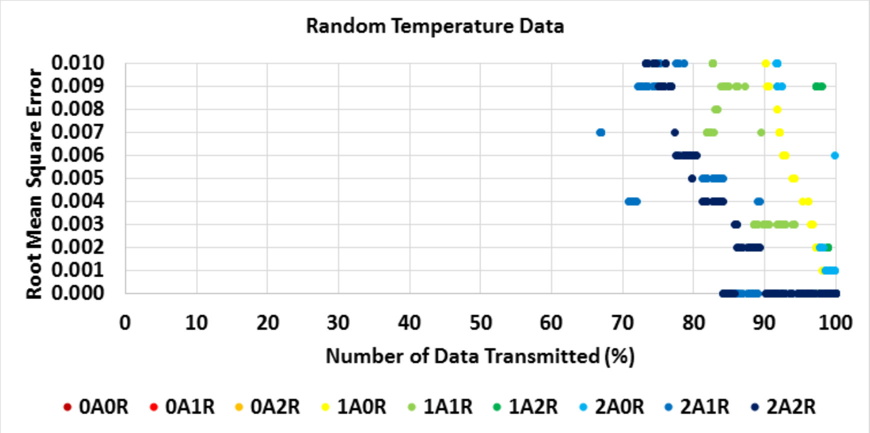

(a) Number of data transmitted vs. root mean square error where

$$RMSE_{max} = 0.01$$

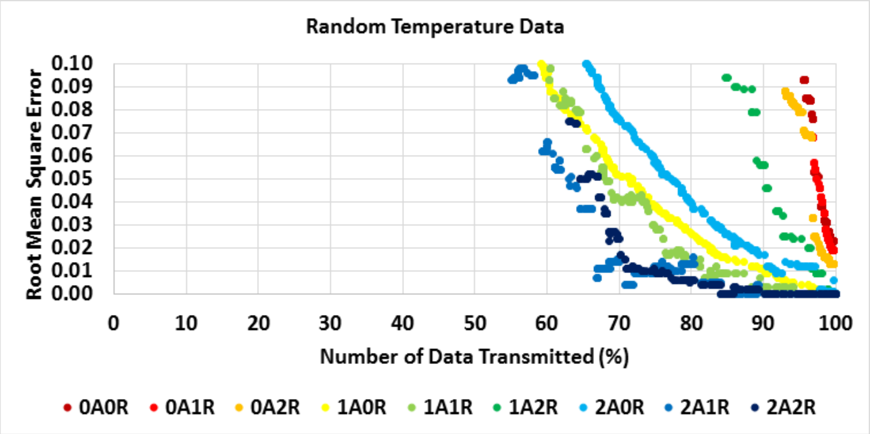

(b) Number of data transmitted vs. root mean square error where

$$RMSE_{max} = 0.1$$

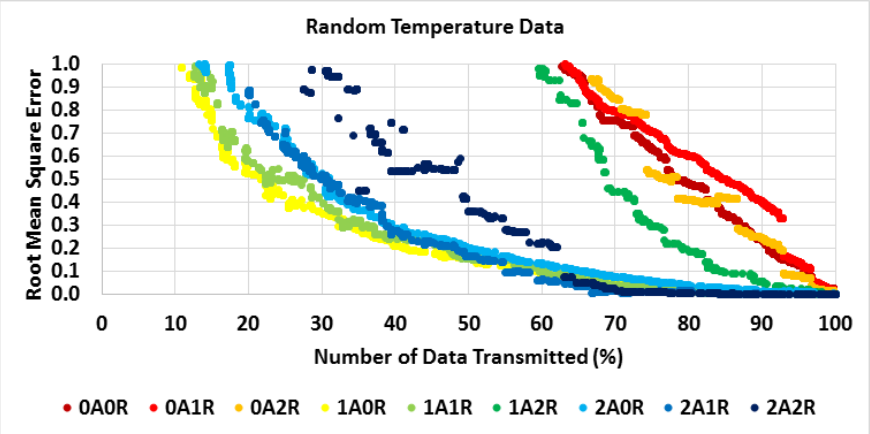

(c) Number of data transmitted vs. root mean square error where

$$RMSE_{max} = 1$$

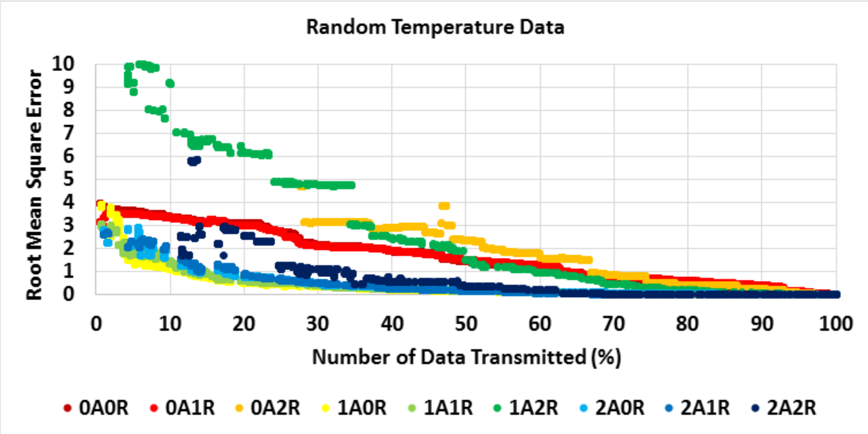

(d) Number of data transmitted vs. root mean square error where

$$RMSE_{max} = 10$$

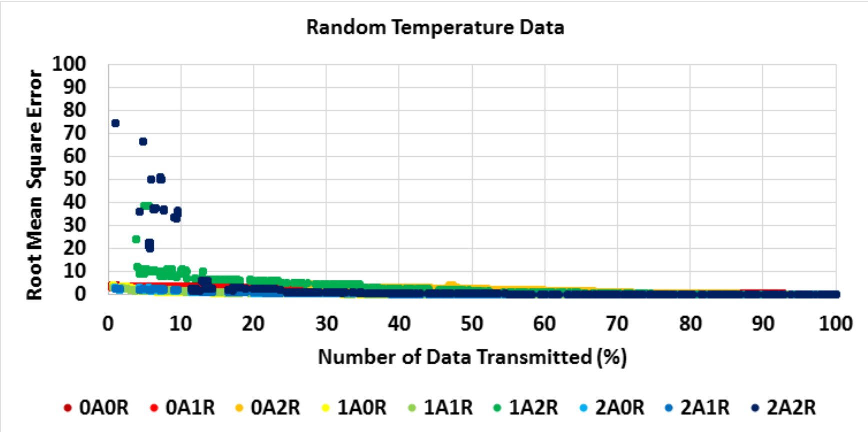

(e) Number of data transmitted vs. root mean square error where

$$RMSE_{max} = 100$$

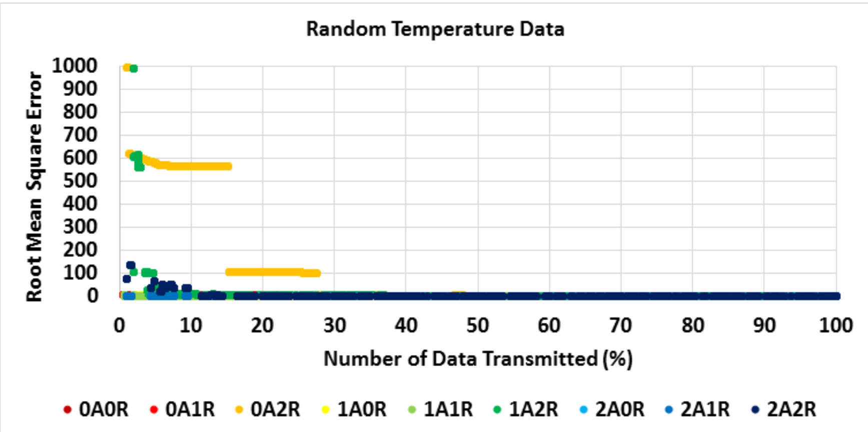

(f) Number of data transmitted vs. root mean square error where

$$RMSE_{max} = 1000$$

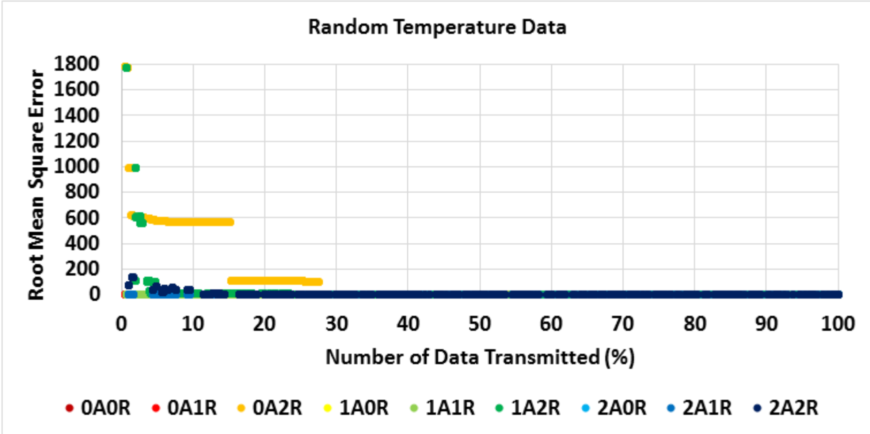

(g) Number of data transmitted vs. root mean square error where

$$RMSE_{max} = 1800$$

Figure 5.47: Number of data transmitted vs. root mean square error in random temperature data

The results of DAR schemes in random temperature data are shown more details in Table 5.22.

Table 5.22: Number of Data Transmitted vs. Root Mean Square Error in Random Temperature Data

RMSE	DAR	$NoDT_{min}$ (%)
= 0	0A0R	100.000
	0A1R	100.000
	0A2R	100.000
	1A0R	100.000
	1A1R	95.333
	1A2R	99.667
	2A0R	100.000
	2A1R	84.167
	2A2R	84.167

RMSE = root mean square error
DAR = data Abstraction and Reformation
0A0R = zeroth-order data abstraction & zeroth-order data reformation
0A1R = zeroth-order data abstraction & first-order data reformation
0A2R = zeroth-order data abstraction & second-order data reformation
1A0R = first-order data abstraction & zeroth-order data reformation
1A1R = first-order data abstraction & first-order data reformation
1A2R = first-order data abstraction & second-order data reformation
2A0R = second-order data abstraction & zeroth-order data reformation
2A1R = second-order data abstraction & first-order data reformation
2A2R = second-order data abstraction & second-order data reformation
$NoDT_{min}$ = minimum number of data transmitted

From Table 5.22, it is shown that the best DAR schemes in random temperature data where $RMSE = 0$ in the terms of number of data transmitted are 2A1R and 2A2R.

4. Number of Data Transmitted vs. Mean Absolute Percentage Error

The comparisons of number of data transmitted against mean absolute percentage error are shown in Figure 5.48.

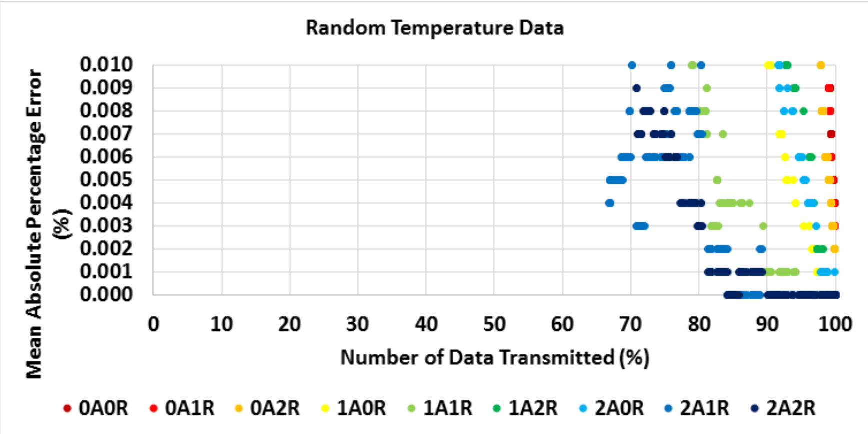

(a) Number of data transmitted vs. mean absolute percentage error where $MAPE_{max} = 0.01\%$

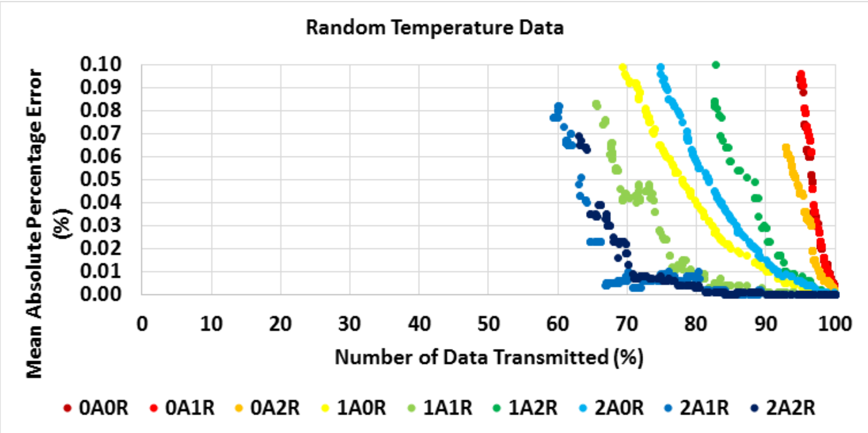

(b) Number of data transmitted vs. mean absolute percentage error where $MAPE_{max} = 0.1\%$

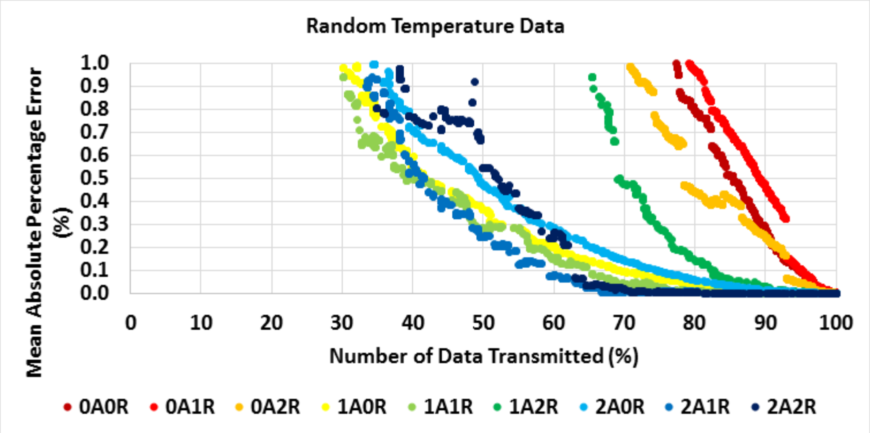

(c) Number of data transmitted vs. mean absolute percentage error where

$$MAPE_{max} = 1\%$$

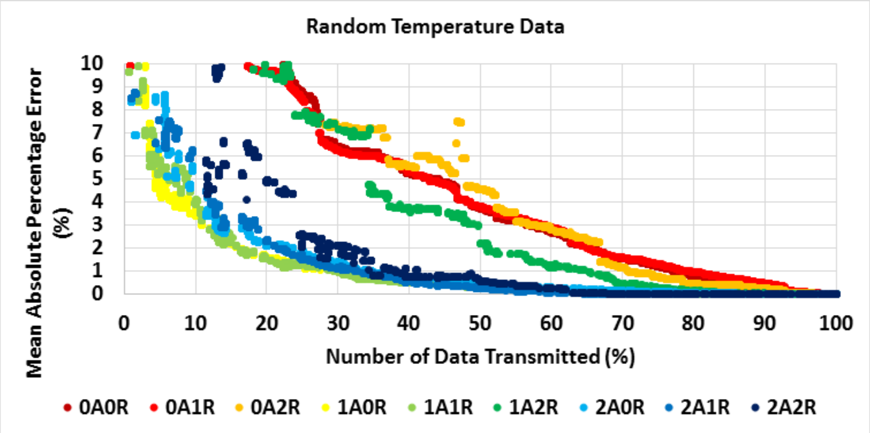

(d) Number of data transmitted vs. mean absolute percentage error where

$$MAPE_{max} = 10\%$$

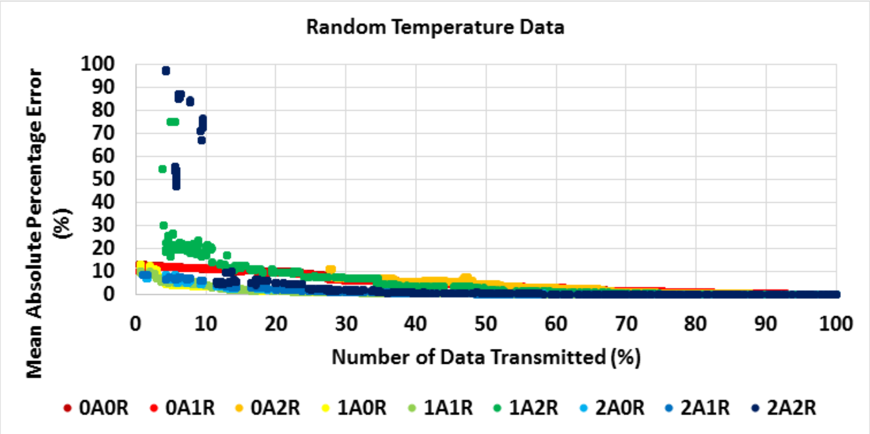

(e) Number of data transmitted vs. mean absolute percentage error where

$$MAPE_{max} = 100\%$$

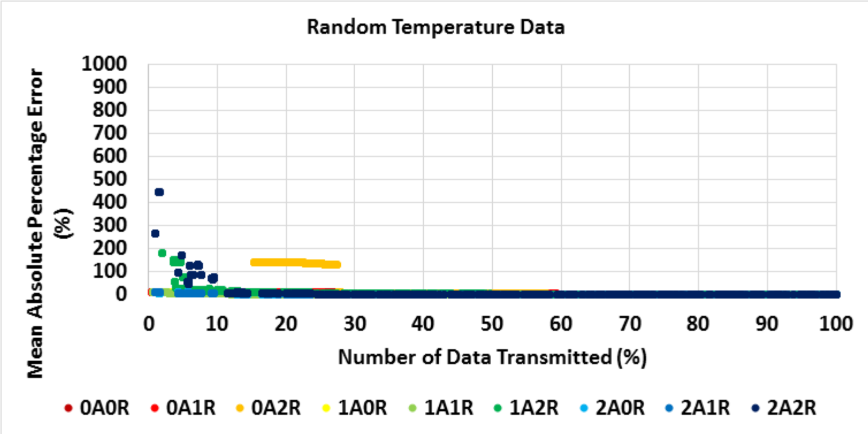

(f) Number of data transmitted vs. mean absolute percentage error where

$$MAPE_{max} = 1000\%$$

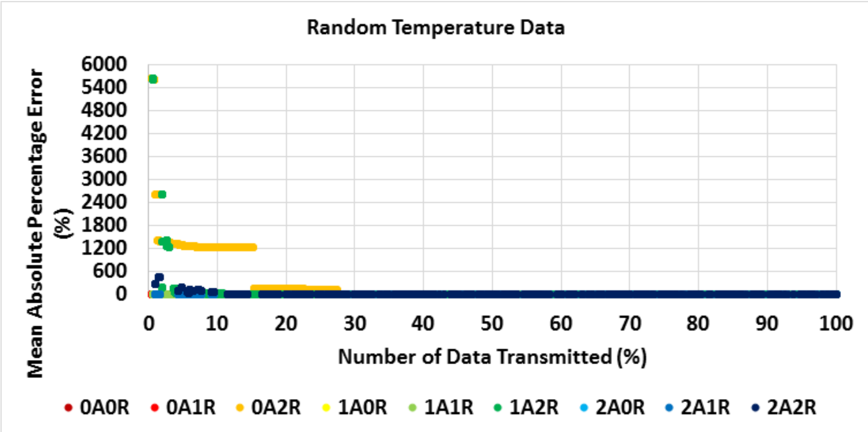

(g) Number of data transmitted vs. mean absolute percentage error where

$$MAPE_{max} = 6000\%$$

Figure 5.48: Number of data transmitted vs. mean absolute percentage error in random temperature data

The results of DAR schemes in random temperature data are shown more details in Table 5.23.

Table 5.23: Number of Data Transmitted vs. Mean Absolute Percentage Error in Random Temperature Data

MAPE	DAR	$NoDT_{min}$ (%)
= 0%	0A0R	100.000
	0A1R	100.000
	0A2R	100.000
	1A0R	99.000
	1A1R	95.333
	1A2R	99.000
	2A0R	99.333
	2A1R	84.167
	2A2R	84.167

MAPE = mean absolute percentage error
DAR = data Abstraction and Reformation
0A0R = zeroth-order data abstraction & zeroth-order data reformation
0A1R = zeroth-order data abstraction & first-order data reformation
0A2R = zeroth-order data abstraction & second-order data reformation
1A0R = first-order data abstraction & zeroth-order data reformation
1A1R = first-order data abstraction & first-order data reformation
1A2R = first-order data abstraction & second-order data reformation
2A0R = second-order data abstraction & zeroth-order data reformation
2A1R = second-order data abstraction & first-order data reformation
2A2R = second-order data abstraction & second-order data reformation
$NoDT_{min}$ = minimum number of data transmitted

From Table 5.23, it is shown that the best DAR schemes in random temperature data where $MAPE = 0\%$ in the terms of number of data transmitted are 2A1R and 2A2R.

5. Root Mean Square Error vs. Number of Packet Transmissions

The comparisons of root mean square error against number of packet transmissions are shown in Figure 5.49.

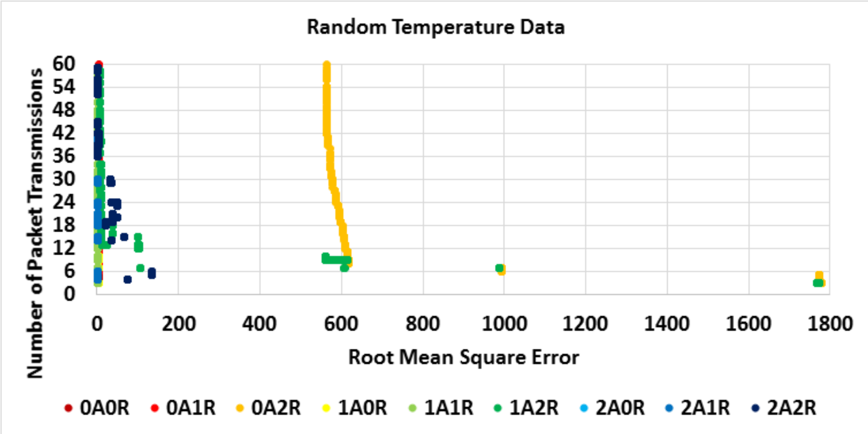

(a) Root mean square error vs. number of packet transmissions where

$NoPT_{max} = 60$

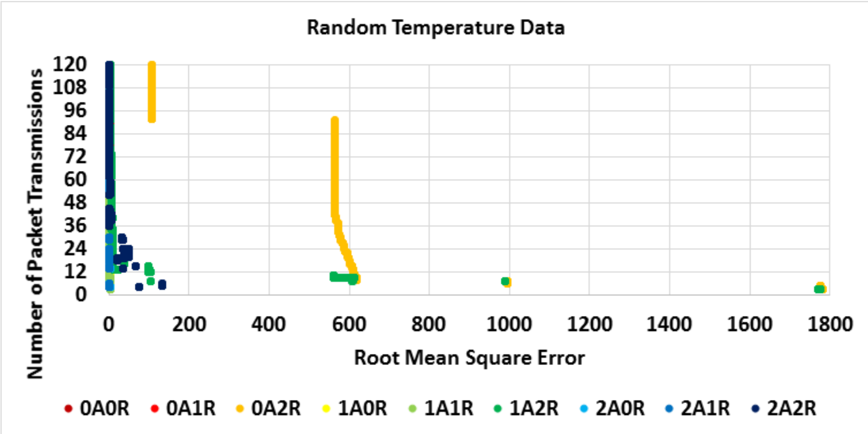

(b) Root mean square error vs. number of packet transmissions where

$NoPT_{max} = 120$

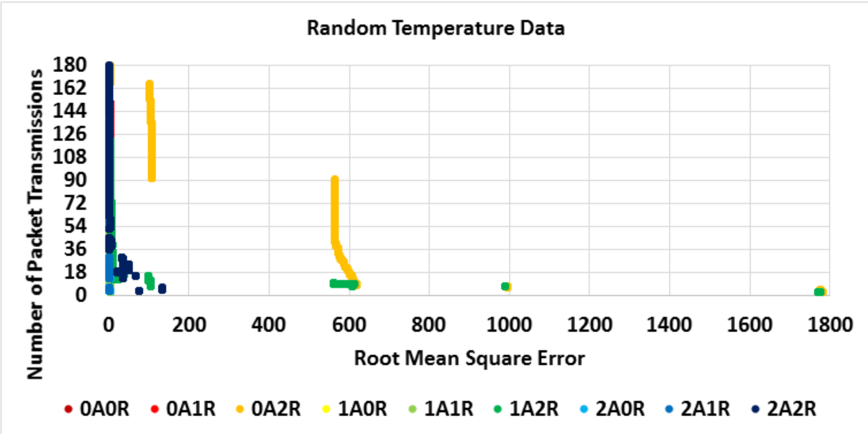

(c) Root mean square error vs. number of packet transmissions where

$NoPT_{max} = 180$

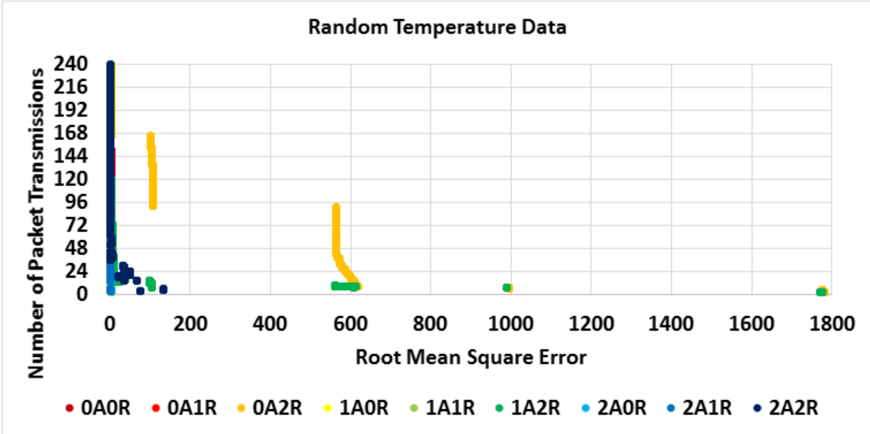

(d) Root mean square error vs. number of packet transmissions where

$$NoPT_{max} = 240$$

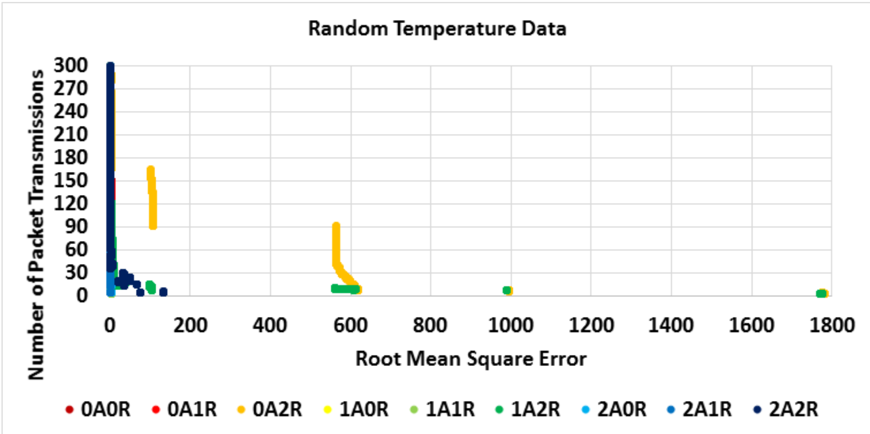

(e) Root mean square error vs. number of packet transmissions where

$$NoPT_{max} = 300$$

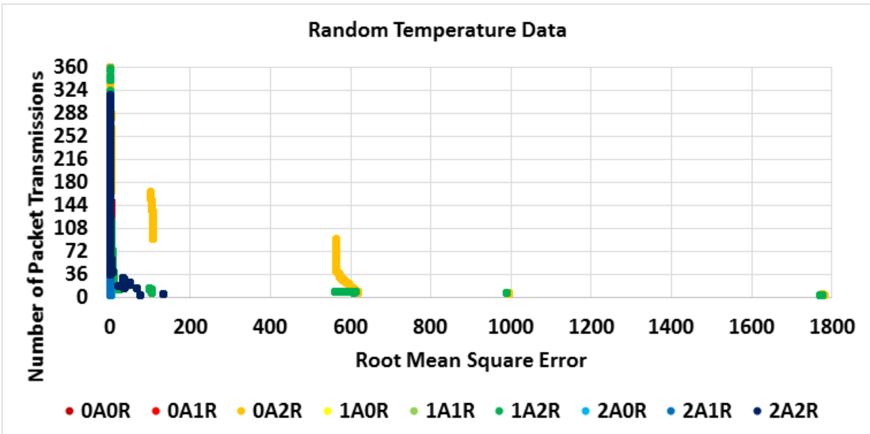

(f) Root mean square error vs. number of packet transmissions where

$$NoPT_{max} = 360$$

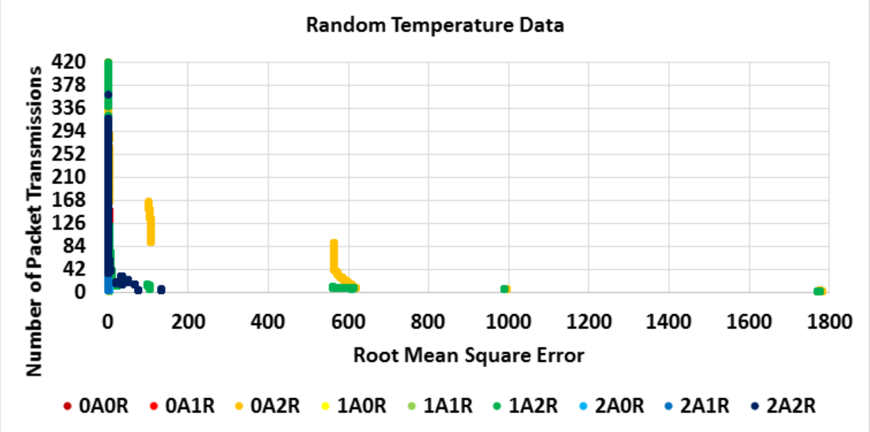

(g) Root mean square error vs. number of packet transmissions where

$NoPT_{max} = 420$

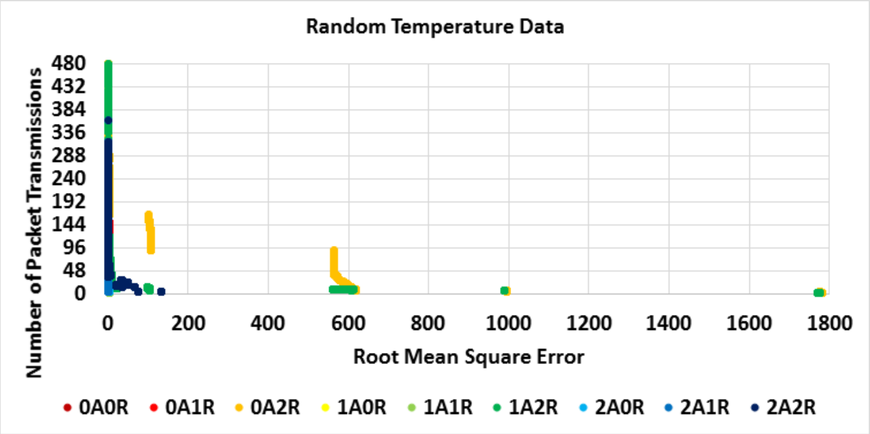

(h) Root mean square error vs. number of packet transmissions where

$NoPT_{max} = 480$

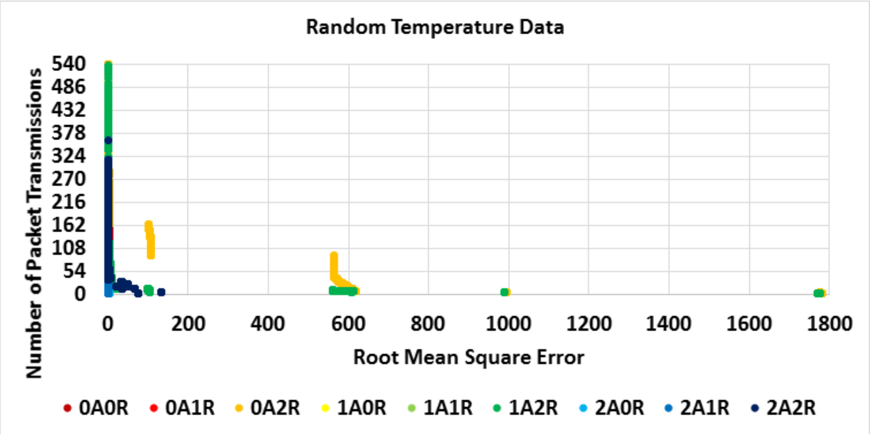

(i) Root mean square error vs. number of packet transmissions where

$NoPT_{max} = 540$

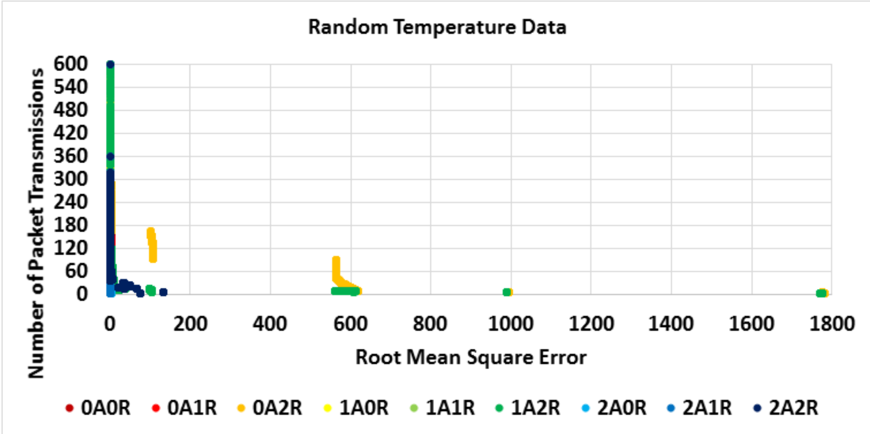

(j) Root mean square error vs. number of packet transmissions where $NoPT_{max} = 600$

Figure 5.49: Root mean square error vs. number of packet transmissions in random temperature data

The results of DAR schemes in random temperature data are shown more details in Table 5.24.

Table 5.24: Root Mean Square Error vs. Number of Packet Transmissions in Random Temperature Data

NoPT	DAR	$RMSE_{min}$
≤ 300	0A0R	1.450
	0A1R	1.511
	0A2R	2.346
	1A0R	0.061
	1A1R	0.051
	1A2R	0.587
	2A0R	0.009
	2A1R	0.000
	2A2R	0.000

NoPT = number of packet transmissions
DAR = data abstraction and reformation
0A0R = zeroth-order data abstraction & zeroth-order data reformation
0A1R = zeroth-order data abstraction & first-order data reformation
0A2R = zeroth-order data abstraction & second-order data reformation
1A0R = first-order data abstraction & zeroth-order data reformation
1A1R = first-order data abstraction & first-order data reformation
1A2R = first-order data abstraction & second-order data reformation
2A0R = second-order data abstraction & zeroth-order data reformation
2A1R = second-order data abstraction & first-order data reformation
2A2R = second-order data abstraction & second-order data reformation
$RMSE_{min}$ = minimum root mean square error

From Table 5.24, it is shown that the best DAR schemes in random temperature data where $NoPT \leq 300$ in the terms of root mean square error are 2A1R and 2A2R.

6. Root Mean Square Error vs. Number of Data Transmitted

The comparisons of root mean square error against number of data transmitted are shown in Figure 5.50.

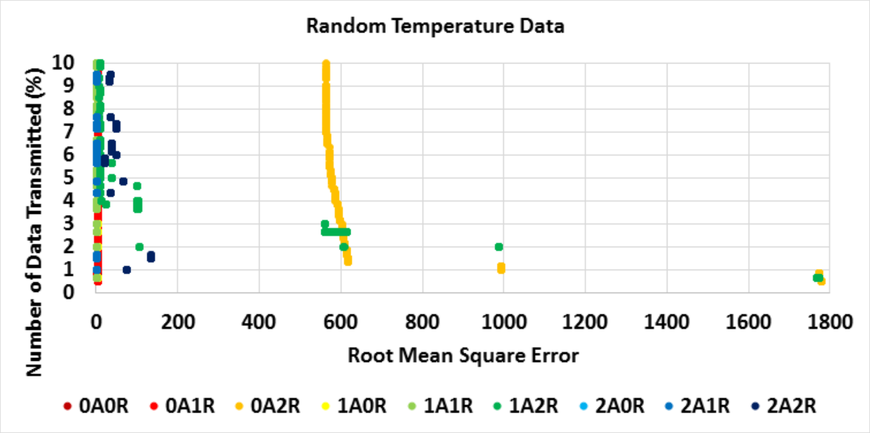

(a) Root mean square error vs. number of data transmitted where $NoDT_{max} = 10\%$

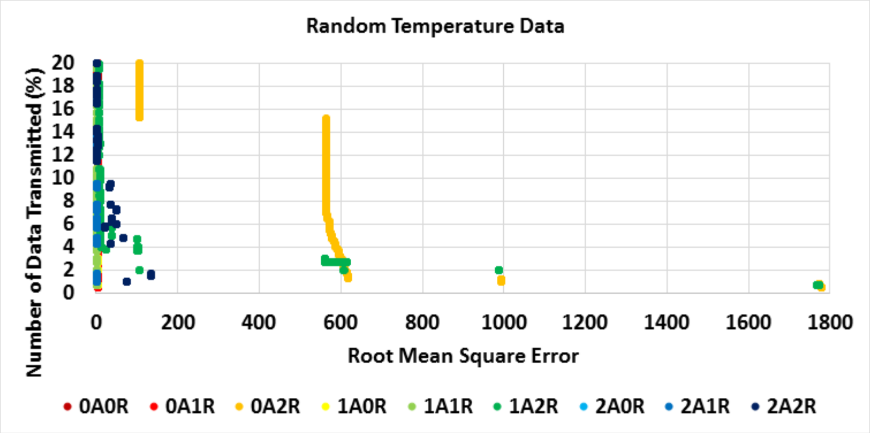

(b) Root mean square error vs. number of data transmitted where $NoDT_{max} = 20\%$

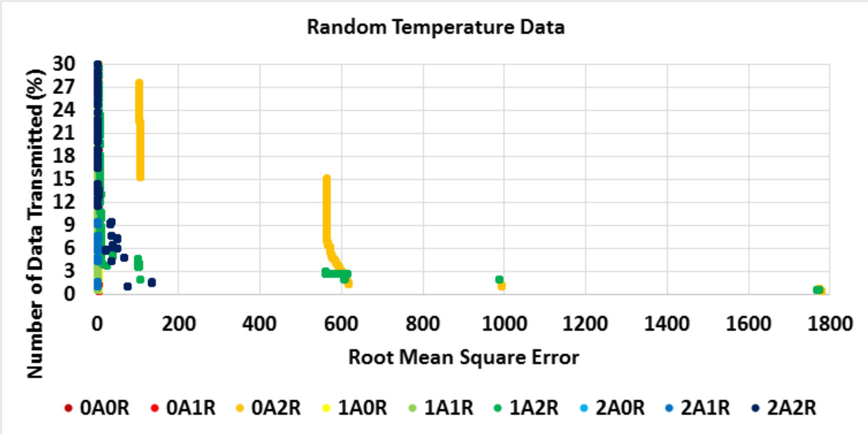

(c) Root mean square error vs. number of data transmitted (%) where

$$NoDT_{max} = 30\%$$

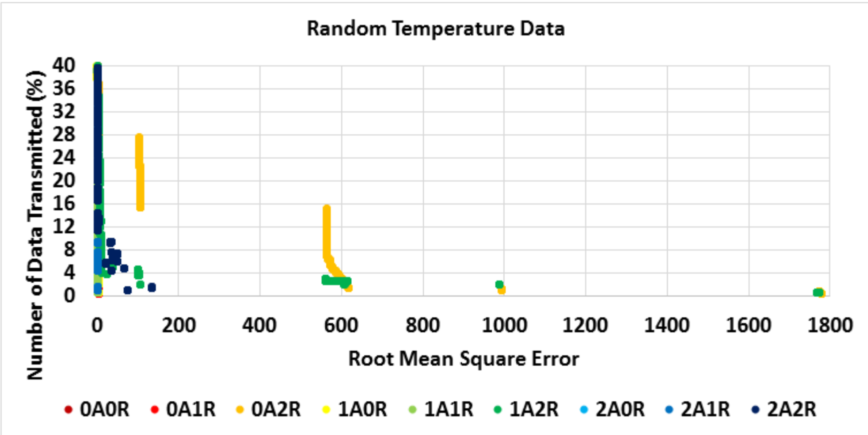

(d) Root mean square error vs. number of data transmitted where

$$NoDT_{max} = 40\%$$

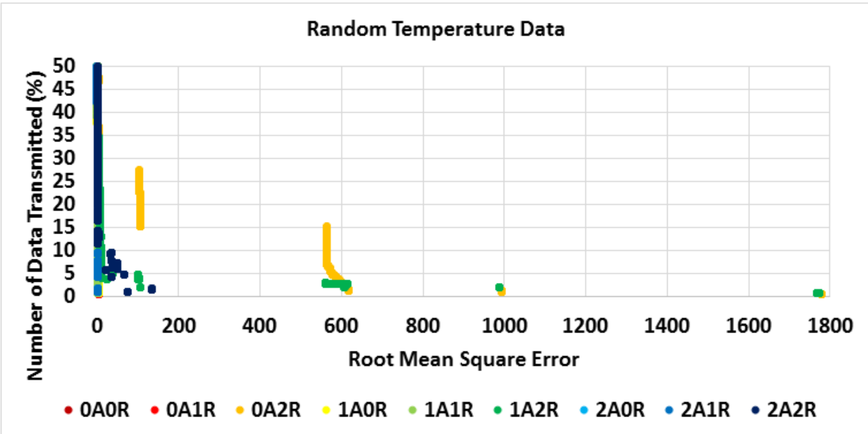

(e) Root mean square error vs. number of data transmitted where

$$NoDT_{max} = 50\%$$

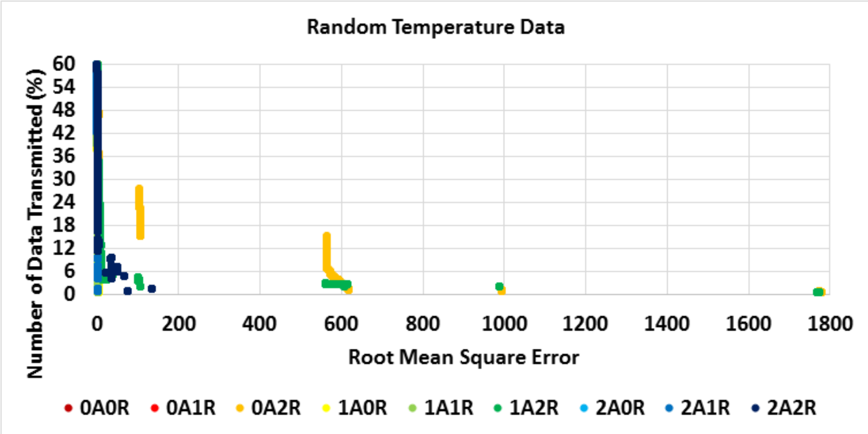

(f) Root mean square error vs. number of data transmitted where

$\boldsymbol{NoDT_{max}} = \mathbf{60\%}$

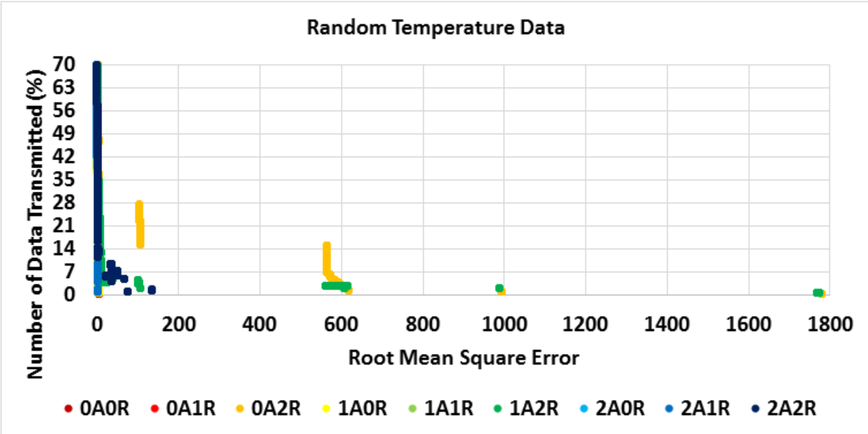

(g) Root mean square error vs. number of data transmitted where

$\boldsymbol{NoDT_{max}} = \mathbf{70\%}$

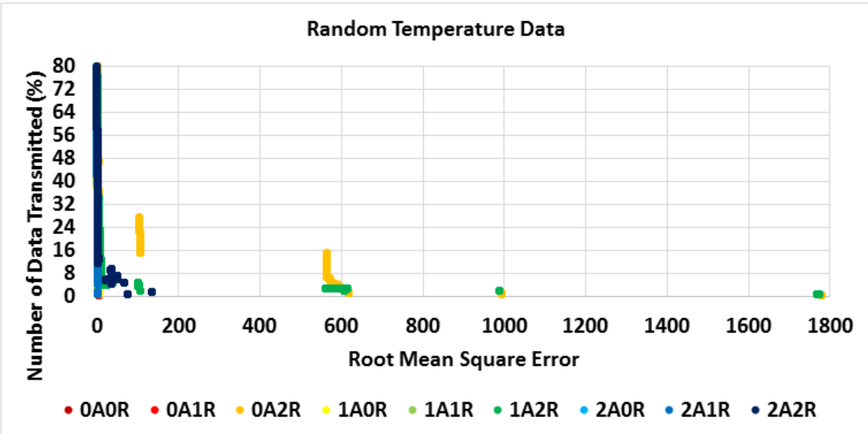

(h) Root mean square error vs. number of data transmitted where

$\boldsymbol{NoDT_{max}} = \mathbf{80\%}$

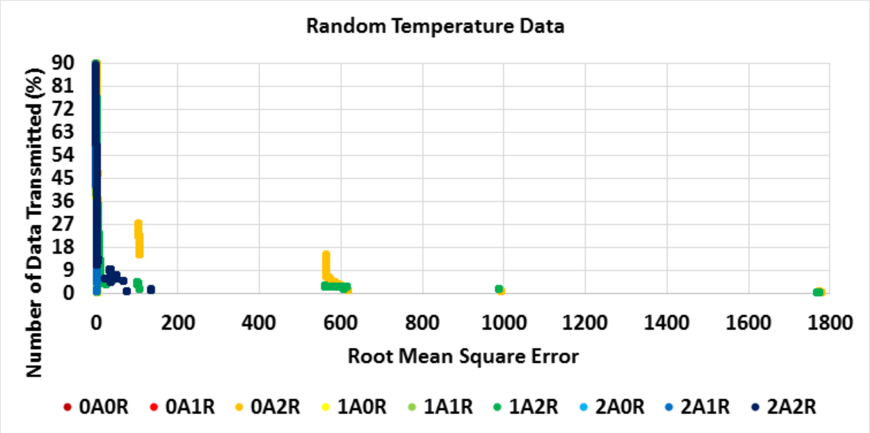

(i) Root mean square error vs. number of data transmitted where

$\boldsymbol{NoDT_{max}} = \mathbf{90\%}$

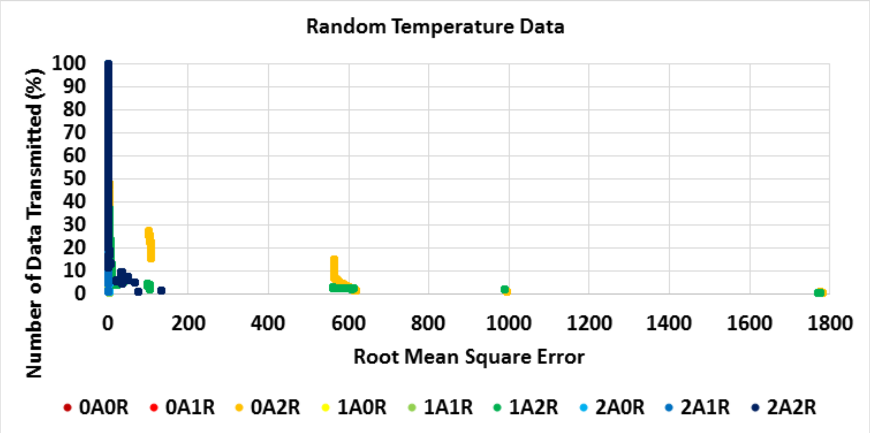

(j) Root mean square error vs. number of data transmitted where

$\boldsymbol{NoDT_{max}} = \mathbf{100\%}$

Figure 5.50: Root mean square error vs. number of data transmitted in random temperature data

The results of DAR schemes in random temperature data are shown more details in Table 5.25.

Table 5.25: Root Mean Square Error vs. Number of Data Transmitted in Random Temperature Data

NoDT	DAR	$RMSE_{min}$
	0A0R	1.450
	0A1R	1.511
	0A2R	2.346
	1A0R	0.153
$\leq 50\%$	1A1R	0.154
	1A2R	1.508
	2A0R	0.201
	2A1R	0.164
	2A2R	0.361

NoDT = number of data transmitted
DAR = data abstraction and reformation
0A0R = zeroth-order data abstraction & zeroth-order data reformation
0A1R = zeroth-order data abstraction & first-order data reformation
0A2R = zeroth-order data abstraction & second-order data reformation
1A0R = first-order data abstraction & zeroth-order data reformation
1A1R = first-order data abstraction & first-order data reformation
1A2R = first-order data abstraction & second-order data reformation
2A0R = second-order data abstraction & zeroth-order data reformation
2A1R = second-order data abstraction & first-order data reformation
2A2R = second-order data abstraction & second-order data reformation
$RMSE_{min}$ = minimum root mean square error

From Table 5.25, it is shown that the best DAR schemes in random temperature data where $NoDT \leq 50\%$ in the terms of root mean square error is 1A0R.

7. Mean Absolute Percentage Error vs. Number of Packet Transmissions

The comparisons of mean absolute percentage error against number of packet transmissions are shown in Figure 5.51.

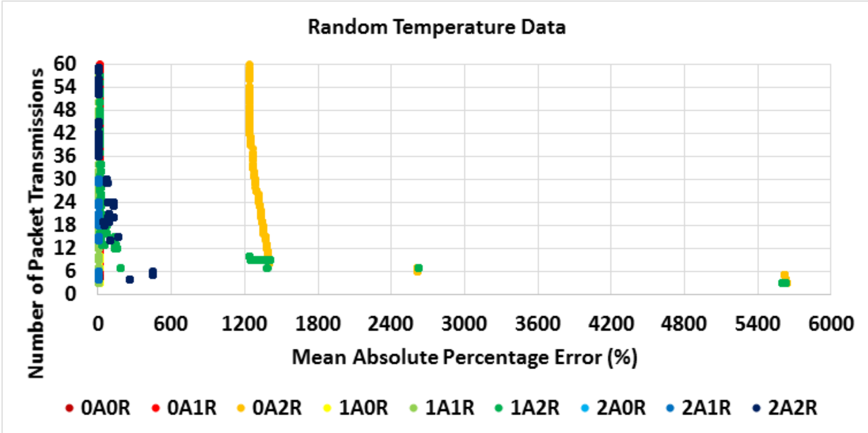

(a) Mean absolute percentage error vs. number of packet transmission where $NoPT_{max} = 60$

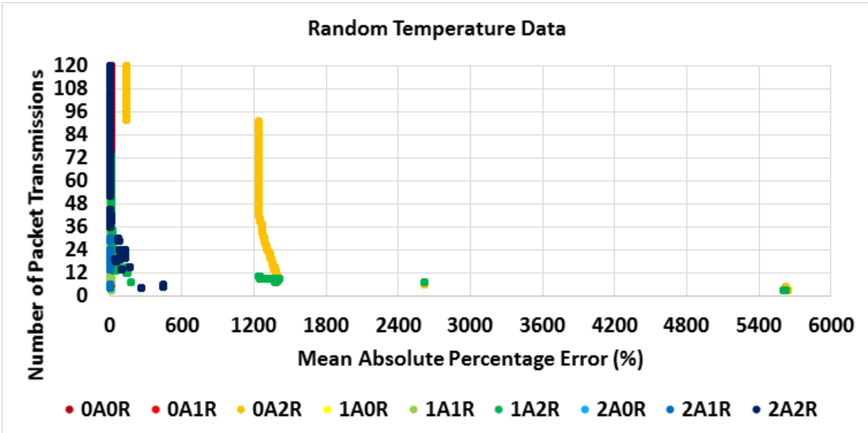

(b) Mean absolute percentage error vs. number of packet transmission where $NoPT_{max} = 120$

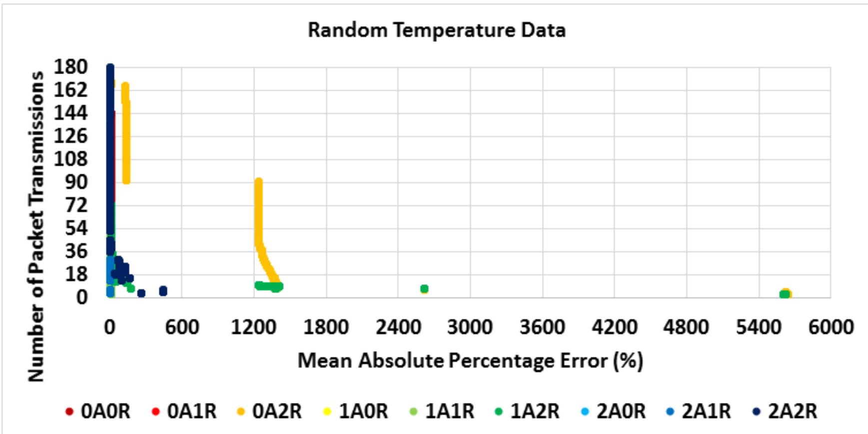

(c) Mean absolute percentage error vs. number of packet transmission where $NoPT_{max} = 180$

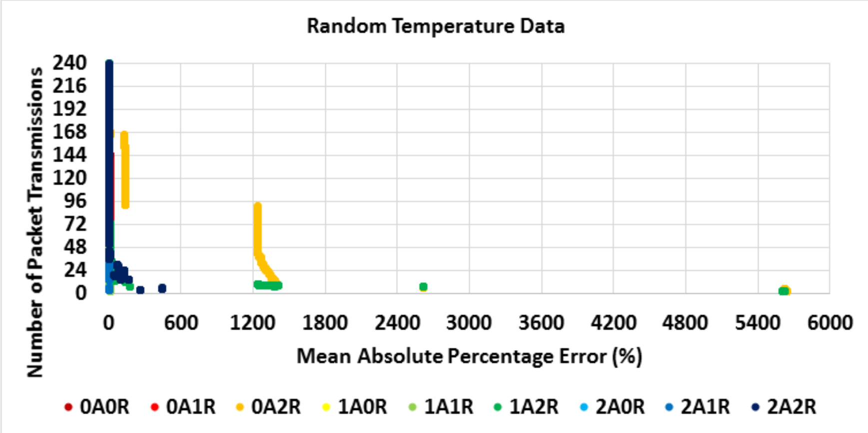

(d) Mean absolute percentage error vs. number of packet transmission where $NoPT_{max} = 240$

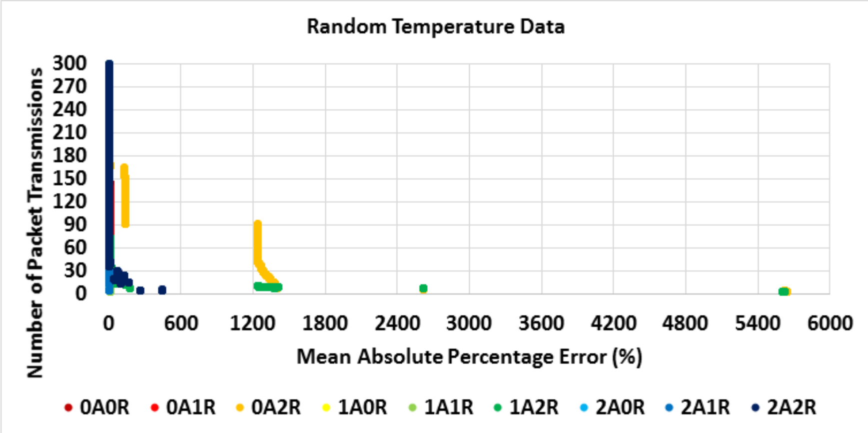

(e) Mean absolute percentage error vs. number of packet transmission where $NoPT_{max} = 300$

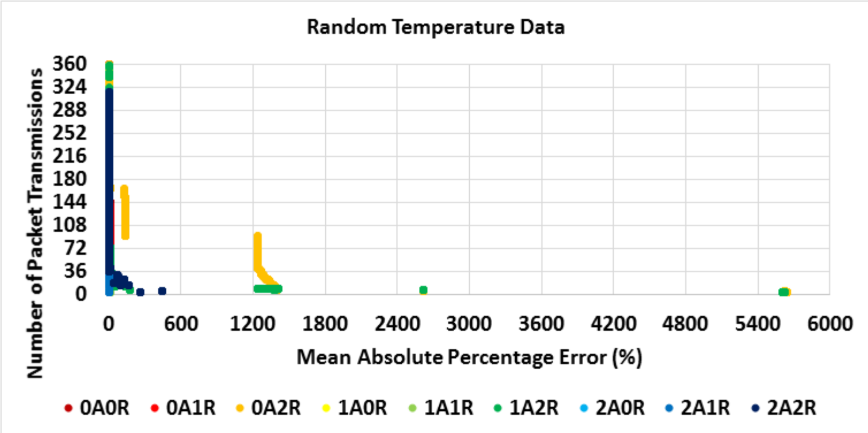

(f) Mean absolute percentage error vs. number of packet transmission where $NoPT_{max} = 360$

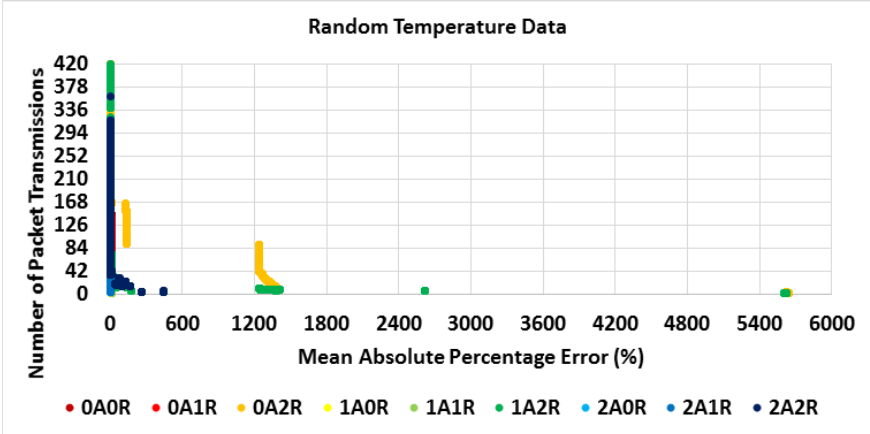

(g) Mean absolute percentage error vs. number of packet transmission where $NoPT_{max} = 420$

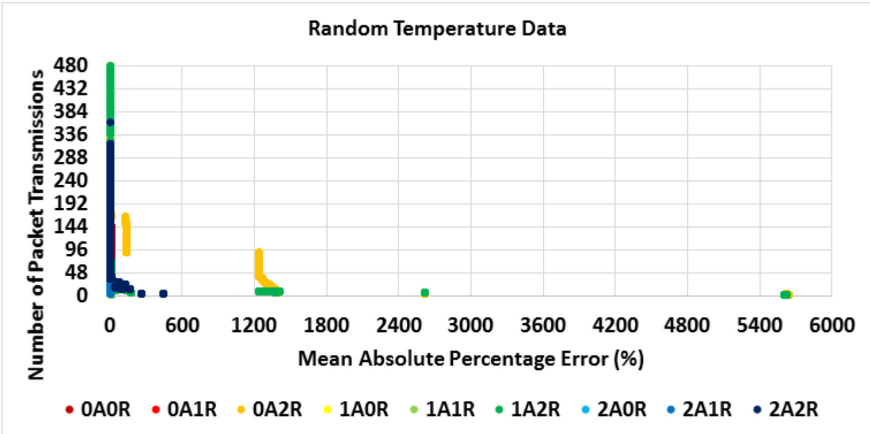

(h) Mean absolute percentage error vs. number of packet transmission where $NoPT_{max} = 480$

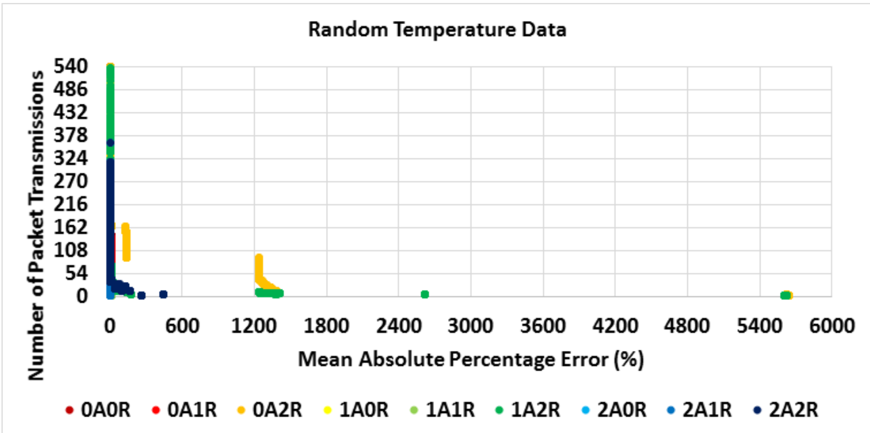

(i) Mean absolute percentage error vs. number of packet transmission where $NoPT_{max} = 540$

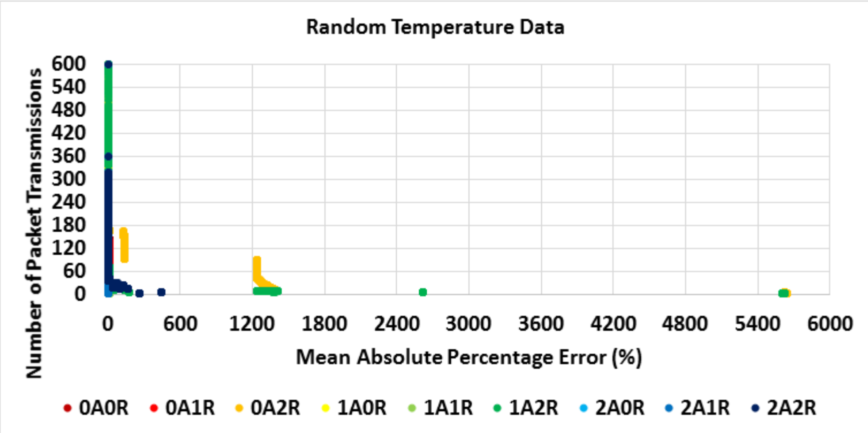

(j) Mean absolute percentage error vs. number of packet transmission where $NoPT_{max} = 600$

Figure 5.51: Mean absolute percentage error vs. number of packet transmissions in random temperature data

The results of DAR schemes in random temperature data are shown more details in Table 5.26.

Table 5.26: Mean Absolute Percentage Error vs. Number of Packet Transmissions in Random Temperature Data

NoPT	DAR	$MAPE_{min}$ (%)
≤ 300	0A0R	3.721
	0A1R	3.782
	0A2R	4.541
	1A0R	0.114
	1A1R	0.059
	1A2R	0.719
	2A0R	0.004
	2A1R	0.000
	2A2R	0.000

NoPT = number of packet transmissions
DAR = data abstraction and reformation
0A0R = zeroth-order data abstraction & zeroth-order data reformation
0A1R = zeroth-order data abstraction & first-order data reformation
0A2R = zeroth-order data abstraction & second-order data reformation
1A0R = first-order data abstraction & zeroth-order data reformation
1A1R = first-order data abstraction & first-order data reformation
1A2R = first-order data abstraction & second-order data reformation
2A0R = second-order data abstraction & zeroth-order data reformation
2A1R = second-order data abstraction & first-order data reformation
2A2R = second-order data abstraction & second-order data reformation
$MAPE_{min}$ = minimum mean absolute percentage error

From Table 5.26, it is shown that the best DAR schemes in random temperature data where $NoPT \leq 300$ in the terms of mean absolute percentage error are 2A1R and 2A2R.

8. Mean Absolute Percentage Error vs. Number of Data Transmitted

The comparisons of mean absolute percentage error against number of data transmitted are shown in Figure 5.52.

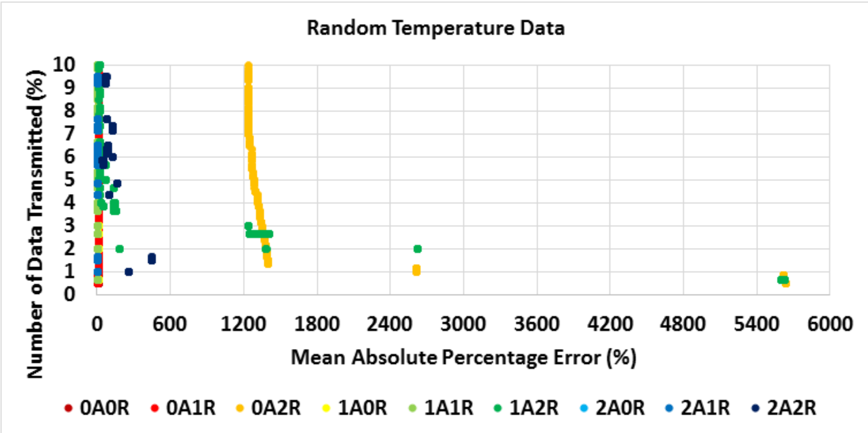

(a) Mean absolute percentage error vs. number of data transmitted where $NoDT_{max} = 10\%$

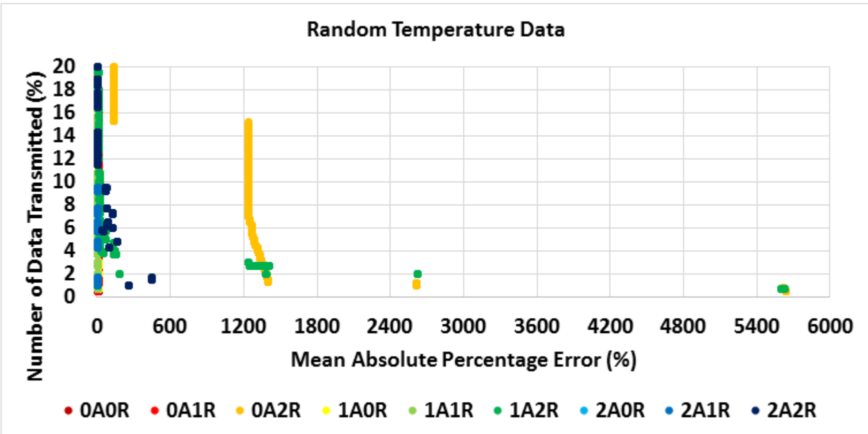

(b) Mean absolute percentage error vs. number of data transmitted where $NoDT_{max} = 20\%$

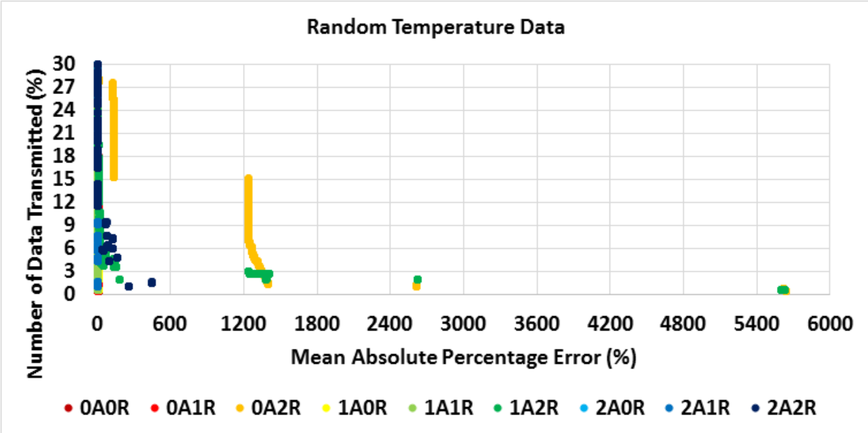

(c) Mean absolute percentage error vs. number of data transmitted where

$\boldsymbol{NoDT_{max}} = \mathbf{30\%}$

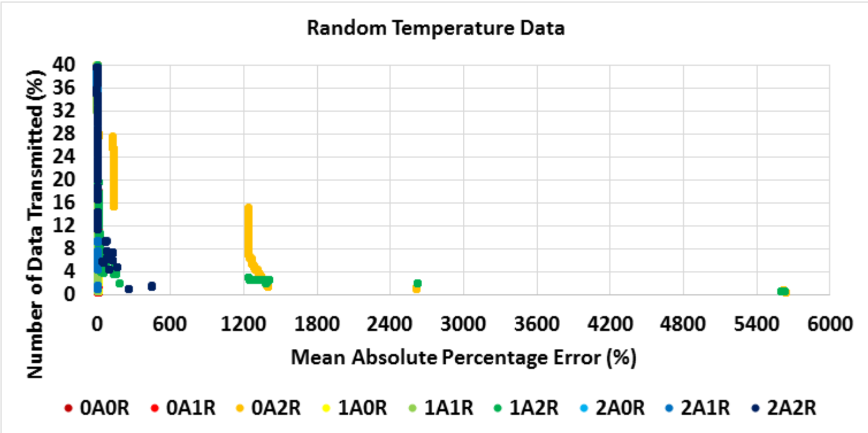

(d) Mean absolute percentage error vs. number of data transmitted where

$\boldsymbol{NoDT_{max}} = \mathbf{40\%}$

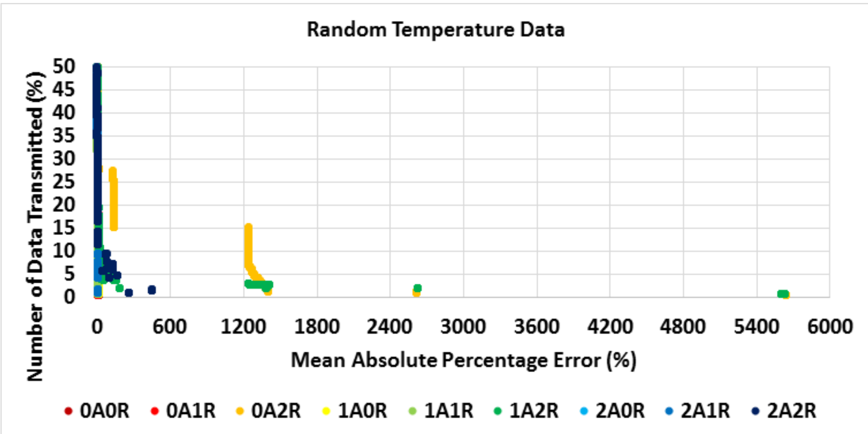

(e) Mean absolute percentage error vs. number of data transmitted where

$\boldsymbol{NoDT_{max}} = \mathbf{50\%}$

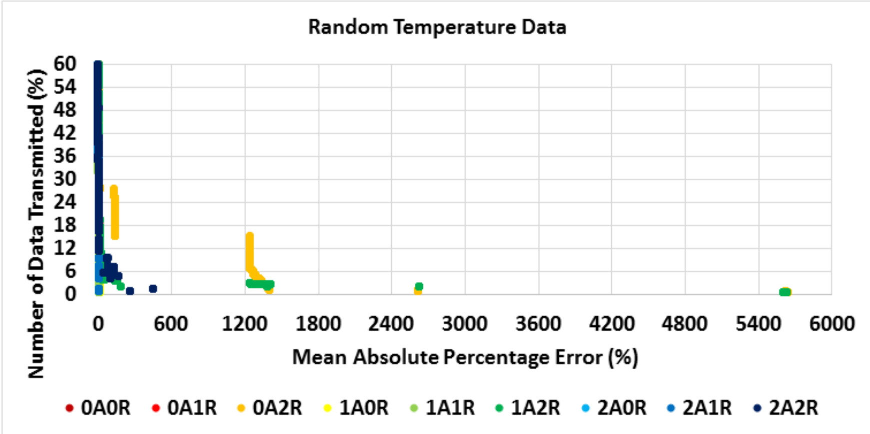

(f) Mean absolute percentage error vs. number of data transmitted where

$NoDT_{max} = 60\%$

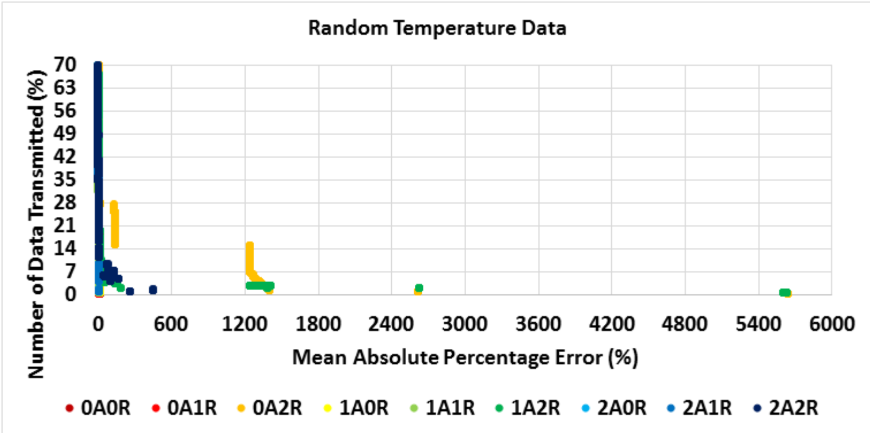

(g) Mean absolute percentage error vs. number of data transmitted where

$NoDT_{max} = 70\%$

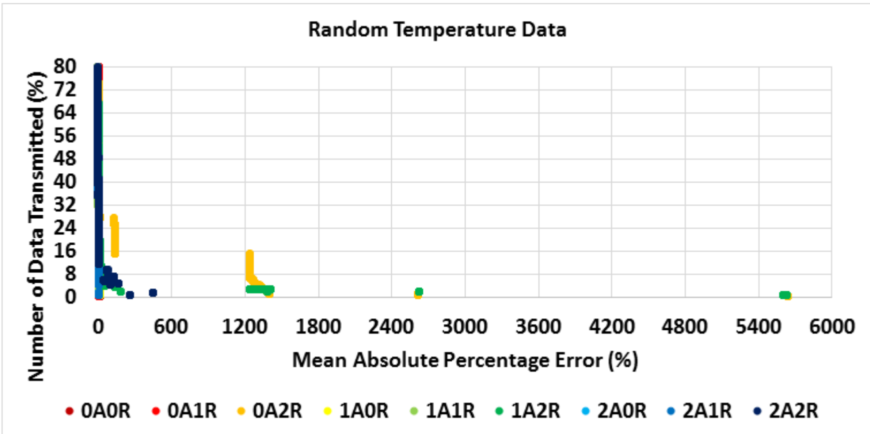

(h) Mean absolute percentage error vs. number of data transmitted where

$NoDT_{max} = 80\%$

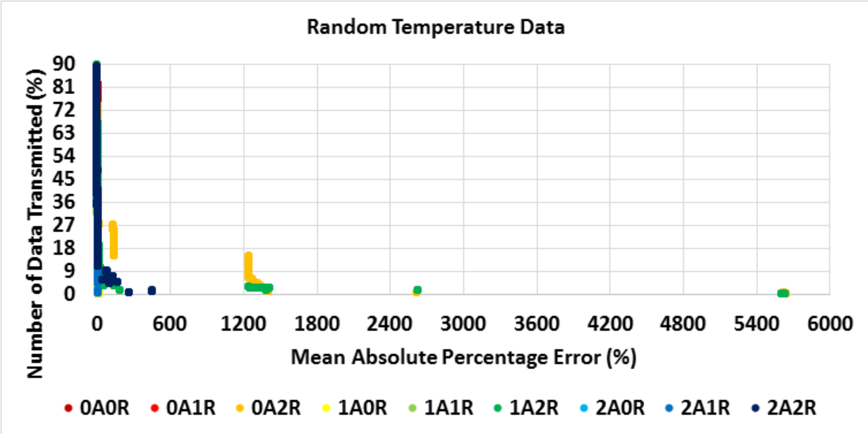

(i) Mean absolute percentage error vs. number of data transmitted where

$NoDT_{max}$ = 90%

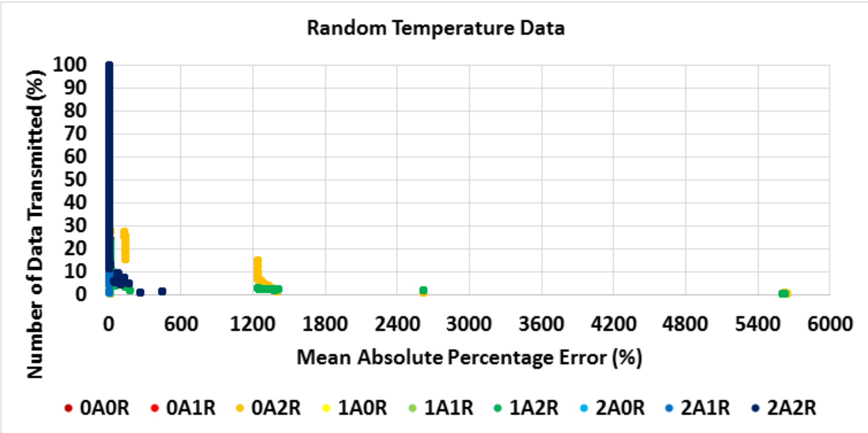

(j) Mean absolute percentage error vs. number of data transmitted (%)

where $NoDT_{max}$ = 100%

Figure 5.52: Mean absolute percentage error vs. number of data transmitted in random temperature data

The results of DAR schemes in random temperature data are shown more details in Table 5.27.

Table 5.27: Mean Absolute Percentage Error vs. Number of Data Transmitted in Random Temperature Data

NoDT	DAR	$MAPE_{min}$ (%)
$\leq 50\%$	0A0R	3.721
	0A1R	3.782
	0A2R	4.541
	1A0R	0.365
	1A1R	0.279
	1A2R	2.200
	2A0R	0.475
	2A1R	0.246
	2A2R	0.545

NoDT = number of data transmitted
DAR = data abstraction and reformation
0A0R = zeroth-order data abstraction & zeroth-order data reformation
0A1R = zeroth-order data abstraction & first-order data reformation
0A2R = zeroth-order data abstraction & second-order data reformation
1A0R = first-order data abstraction & zeroth-order data reformation
1A1R = first-order data abstraction & first-order data reformation
1A2R = first-order data abstraction & second-order data reformation
2A0R = second-order data abstraction & zeroth-order data reformation
2A1R = second-order data abstraction & first-order data reformation
2A2R = second-order data abstraction & second-order data reformation
$MAPE_{min}$ = minimum mean absolute percentage error

From Table 5.27, it is shown that the best DAR schemes in random temperature data where $NoDT \leq 50\%$ in the terms of mean absolute percentage error is 2A1R.

9. Conclusion

From Table 5.20 – 5.27, it is concluded in Table 5.28, that the best DAR schemes in burst temperature data is 2A1R.

Table 5.28: Results of DAR Schemes in Random Temperature Data

(a) Best DAR Schemes in Random Temperature Data where the $NoPT \leq 300$ and the $NoDT \leq 50\%$

DAR	Th	NoPT	NoDT(%)	RMSE	MAPE(%)
0A0R	25.895	300	50.000	1.450	3.721
0A1R	25.895	300	50.000	1.511	3.782
0A2R	25.895	300	50.000	2.346	4.541
1A0R	0.447	177	50.000	0.153	0.365
1A1R	0.454	176	49.667	0.154	0.279
1A2R	0.447	177	50.000	1.508	2.200
2A0R	0.545	155	50.000	0.201	0.475
2A1R	0.553	154	49.667	0.164	0.246
2A2R	0.545	155	50.000	0.361	0.545

(b) Best DAR Schemes in Random Temperature Data where the $RMSE = 0$ and $MAPE = 0\%$

DAR	Th	NoPT	NoDT(%)	RMSE	MAPE(%)
0A0R	22.000	600	100.000	0.000	0.000
0A1R	22.000	600	100.000	0.000	0.000
0A2R	22.000	600	100.000	0.000	0.000
1A0R	0.017	580	100.000	0.000	0.000
1A1R	0.042	495	95.333	0.000	0.000
1A2R	0.018	578	99.667	0.000	0.000
2A0R	0.002	317	100.000	0.000	0.000
2A1R	0.104	261	84.167	0.000	0.000
2A2R	0.104	261	84.167	0.000	0.000

DAR = data abstraction and reformation
Th = threshold
NoPT = number of packet transmissions
NoDT = number of packet transmitted
RMSE = root mean square error
MAPE = mean absolute percentage error

5.3.4 Sitting Accelerometer Data

The comparisons among parameters (number of packet transmissions, number of data transmitted, root mean square error, and mean absolute percentage error) are as follows.

1. Number of Packet Transmissions vs. Root Mean Square Error

The comparisons of number of packet transmissions against root mean square error are shown in Figure 5.53.

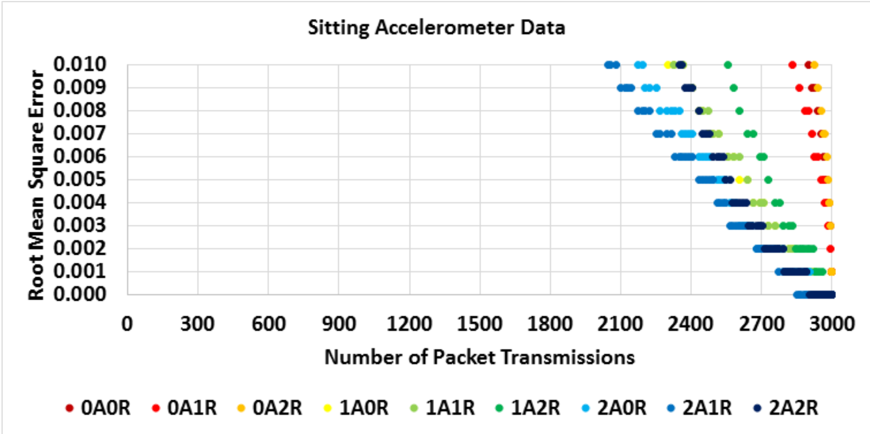

(a) Number of packet transmissions vs. root mean square error where

$$RMSE_{max} = 0.01$$

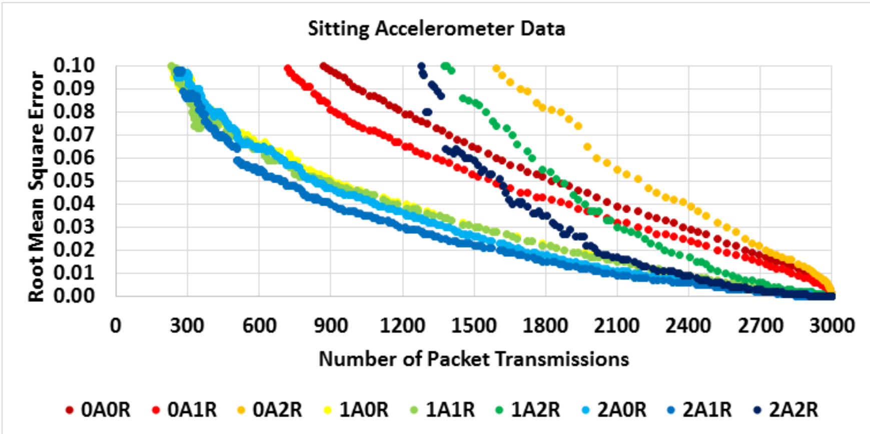

(b) Number of packet transmissions vs. root mean square error where

$$RMSE_{max} = 0.1$$

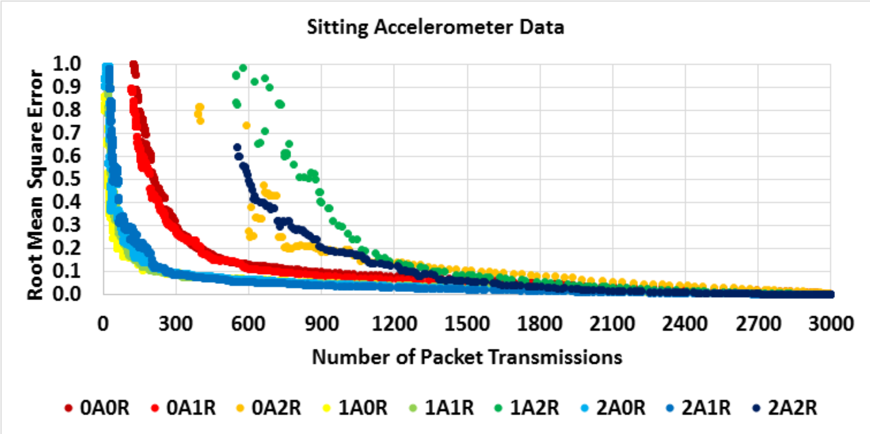

(c) Number of packet transmissions vs. root mean square error where

$$RMSE_{max} = 1$$

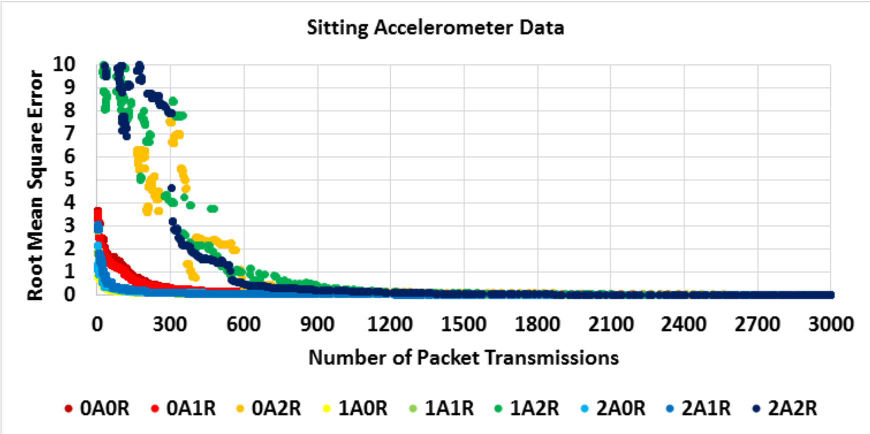

(d) Number of packet transmissions vs. root mean square error where

$$RMSE_{max} = 10$$

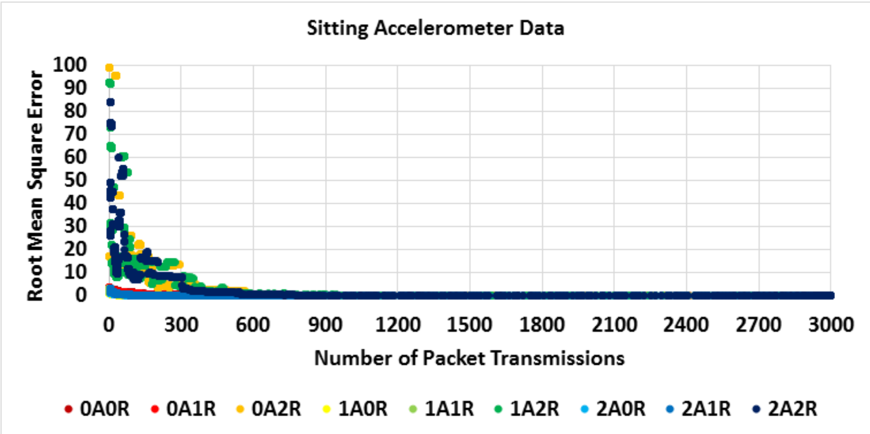

(e) Number of packet transmissions vs. root mean square error where

$$RMSE_{max} = 100$$

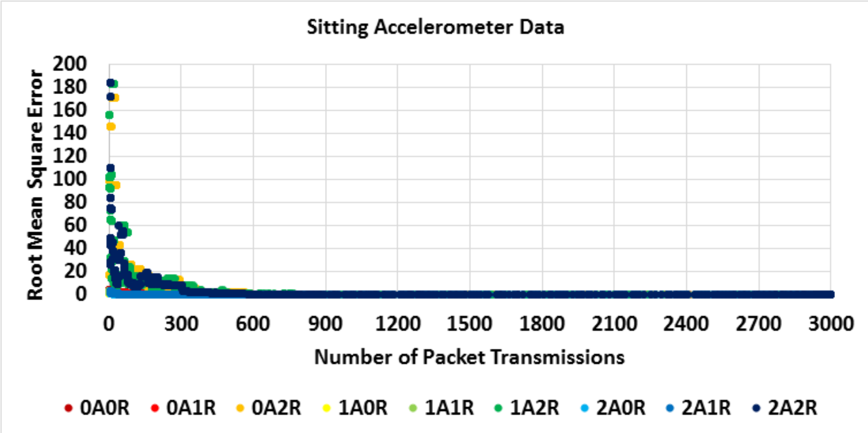

(f) Number of packet transmissions vs. root mean square error where

$$\boldsymbol{RMSE_{max} = 200}$$

Figure 5.53: Number of packet transmissions vs. root mean square error in sitting accelerometer data

The results of DAR schemes in sitting accelerometer data are shown more details in Table 5.29.

Table 5.29: Number of Packet Transmissions vs. Root Mean Square Error in Sitting Accelerometer Data

RMSE	DAR	$NoPT_{min}$
≤ 0.25	0A0R	340
	0A1R	321
	0A2R	605
	1A0R	39
	1A1R	80
	1A2R	1025
	2A0R	80
	2A1R	110
	2A2R	865

RMSE = root mean square error
DAR = data abstraction and reformation
0A0R = zeroth-order data abstraction & zeroth-order data reformation
0A1R = zeroth-order data abstraction & first-order data reformation
0A2R = zeroth-order data abstraction & second-order data reformation
1A0R = first-order data abstraction & zeroth-order data reformation
1A1R = first-order data abstraction & first-order data reformation
1A2R = first-order data abstraction & second-order data reformation
2A0R = second-order data abstraction & zeroth-order data reformation
2A1R = second-order data abstraction & first-order data reformation
2A2R = second-order data abstraction & second-order data reformation
$NoPT_{min}$ = minimum number of packet transmissions

From Table 5.29, it is shown that the best DAR schemes in sitting accelerometer data where $RMSE\ \leq 0.25$ in the terms of number of packet transmissions is 1A0R.

2. Number of Packet Transmissions vs. Mean Absolute Percentage Error

The comparisons of number of packet transmissions against mean absolute percentage error are shown in Figure 5.54.

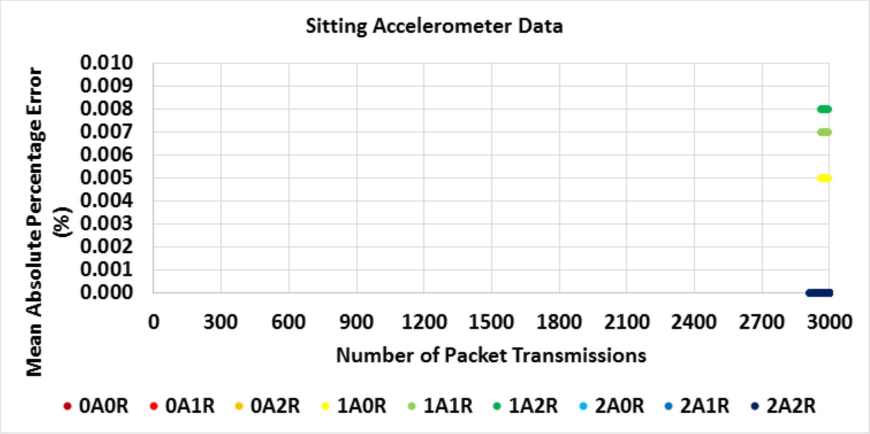

(a) Number of packet transmissions vs. mean absolute percentage error where $MAPE_{max} = 0.01\%$

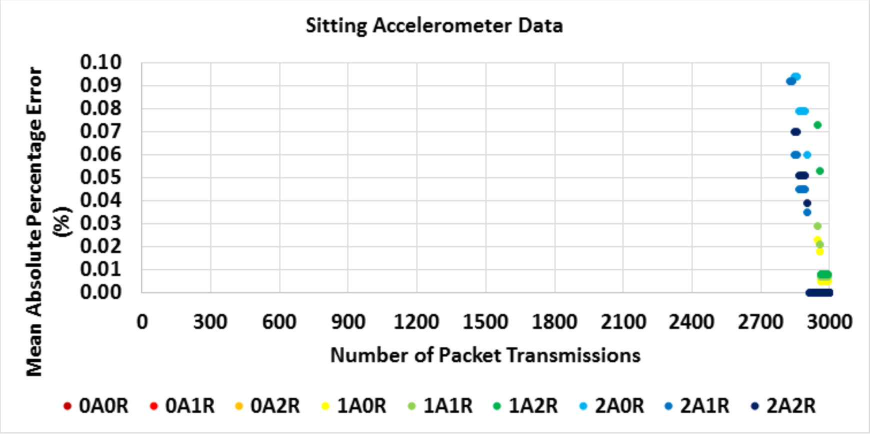

(b) Number of packet transmissions vs. mean absolute percentage error where $MAPE_{max} = 0.1\%$

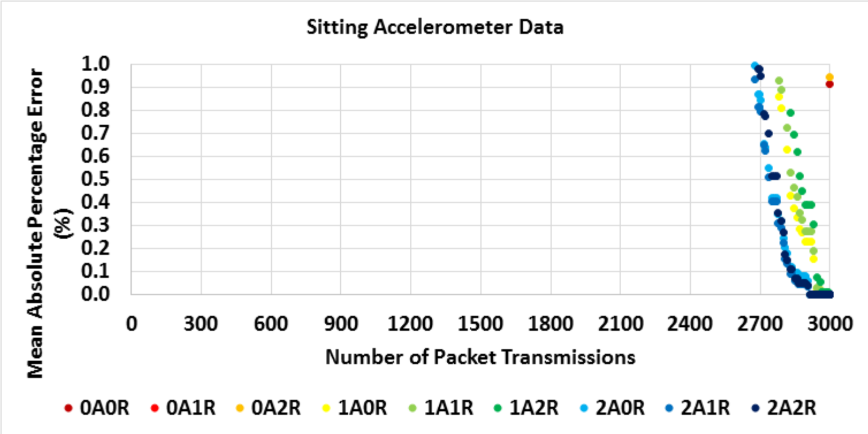

(c) Number of packet transmissions vs. mean absolute percentage error where $MAPE_{max} = 1\%$

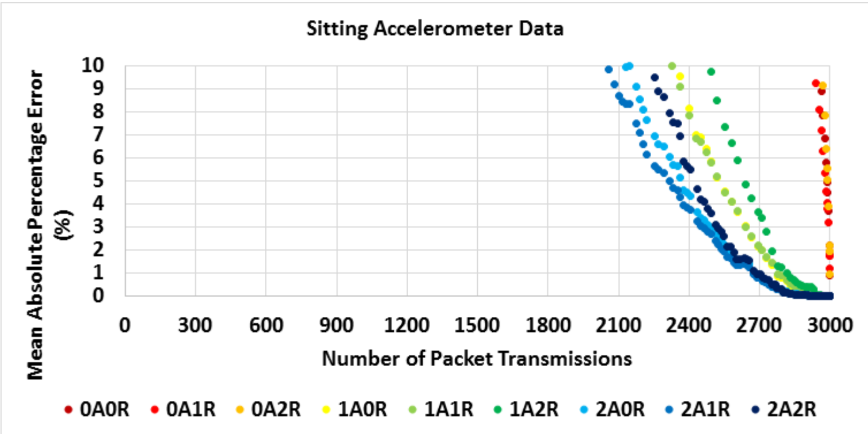

(d) Number of packet transmissions vs. mean absolute percentage error where $MAPE_{max} = 10\%$

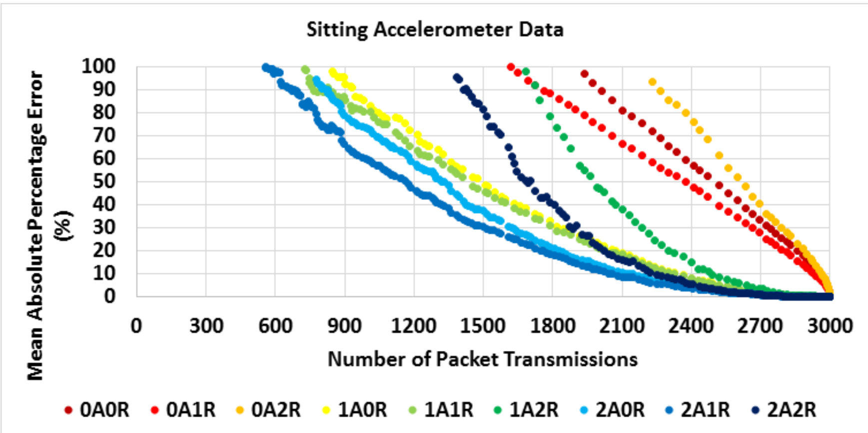

(e) Number of packet transmissions vs. mean absolute percentage error where $MAPE_{max} = 100\%$

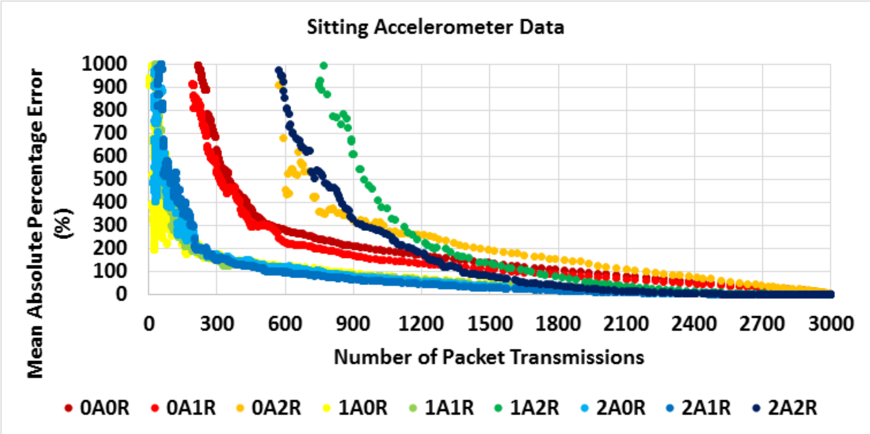

(f) Number of packet transmissions vs. mean absolute percentage error where $MAPE_{max} = 1000\%$

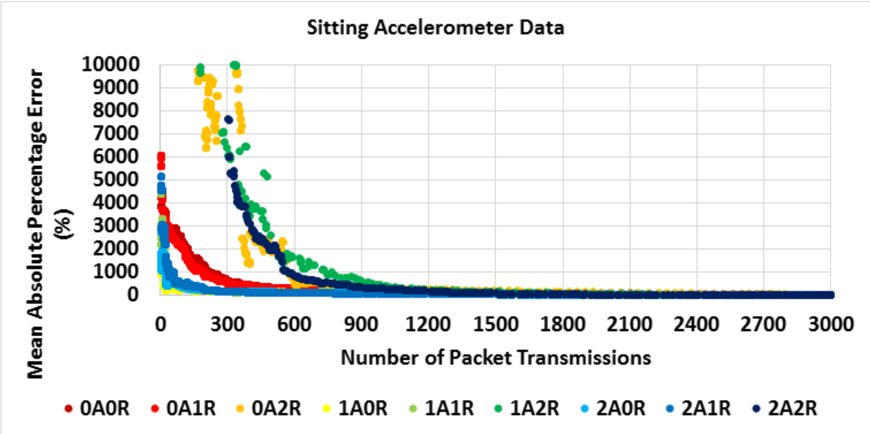

(g) Number of packet transmissions vs. mean absolute percentage error where $MAPE_{max} = 10000\%$

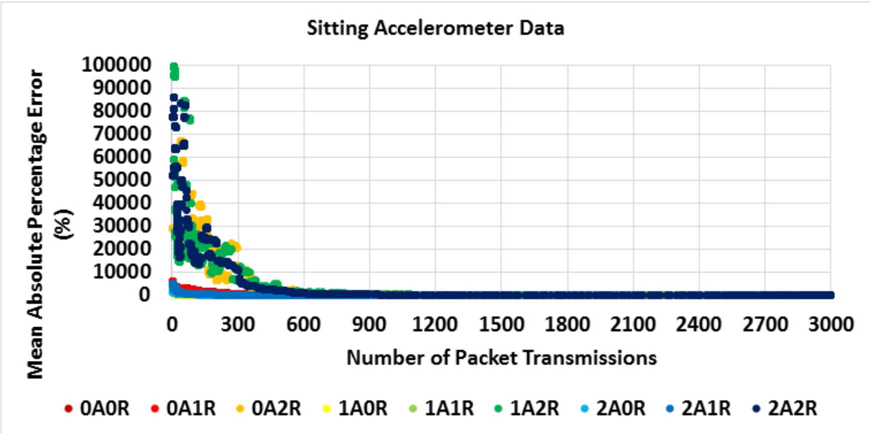

(h) Number of packet transmissions vs. mean absolute percentage error where $MAPE_{max} = 100000\%$

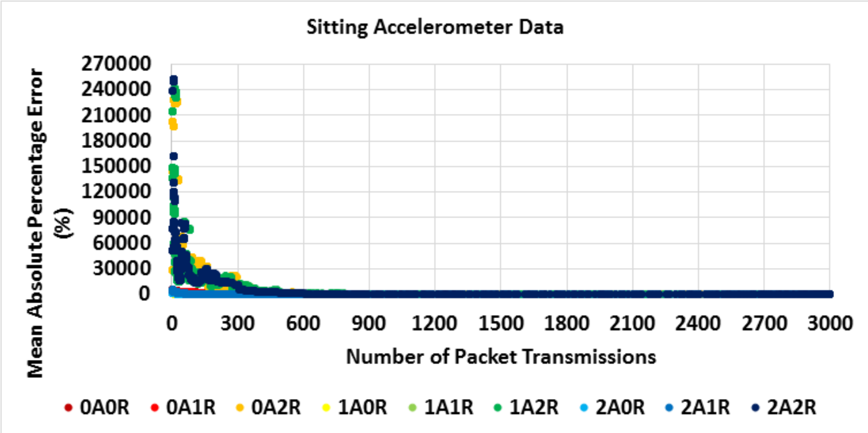

(i) Number of packet transmissions vs. mean absolute percentage error where $MAPE_{max} = 270000\%$

Figure 5.54: Number of packet transmissions vs. mean absolute percentage error in sitting accelerometer data

The results of DAR schemes in sitting accelerometer data are shown more details in Table 5.30.

Table 5.30: Number of Packet Transmissions vs. Mean Absolute Percentage Error in Sitting Accelerometer Data

MAPE	DAR	$NoPT_{min}$
≤2.5%	0A0R	2997
	0A1R	2997
	0A2R	2997
	1A0R	2692
	1A1R	2692
	1A2R	2755
	2A0R	2535
	2A1R	2512
	2A2R	2564

MAPE = mean absolute percentage error
DAR = data Abstraction and Reformation
0A0R = zeroth-order data abstraction & zeroth-order data reformation
0A1R = zeroth-order data abstraction & first-order data reformation
0A2R = zeroth-order data abstraction & second-order data reformation
1A0R = first-order data abstraction & zeroth-order data reformation
1A1R = first-order data abstraction & first-order data reformation
1A2R = first-order data abstraction & second-order data reformation
2A0R = second-order data abstraction & zeroth-order data reformation
2A1R = second-order data abstraction & first-order data reformation
2A2R = second-order data abstraction & second-order data reformation
$NoPT_{min}$ = minimum number of packet transmissions

From Table 5.30, it is shown that the best DAR schemes in sitting accelerometer data where $MAPE \leq 2.5\%$ in the terms of number of packet transmissions is 2A1R.

3. Number of Data Transmitted vs. Root Mean Square Error

The comparisons of number of data transmitted against root mean square error are shown in Figure 5.55.

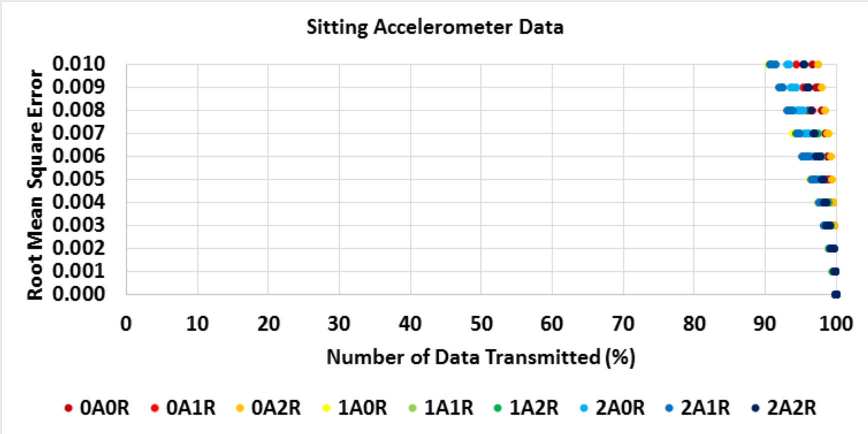

(a) Number of data transmitted vs. root mean square error where

$$RMSE_{max} = 0.01$$

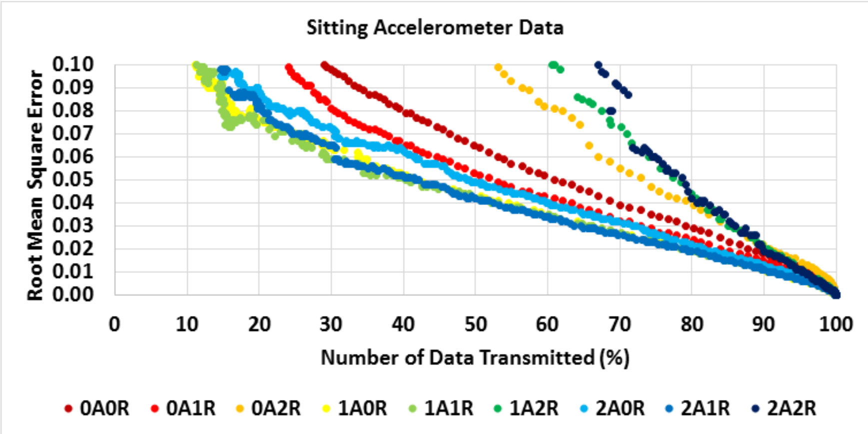

(b) Number of data transmitted vs. root mean square error where

$$RMSE_{max} = 0.1$$

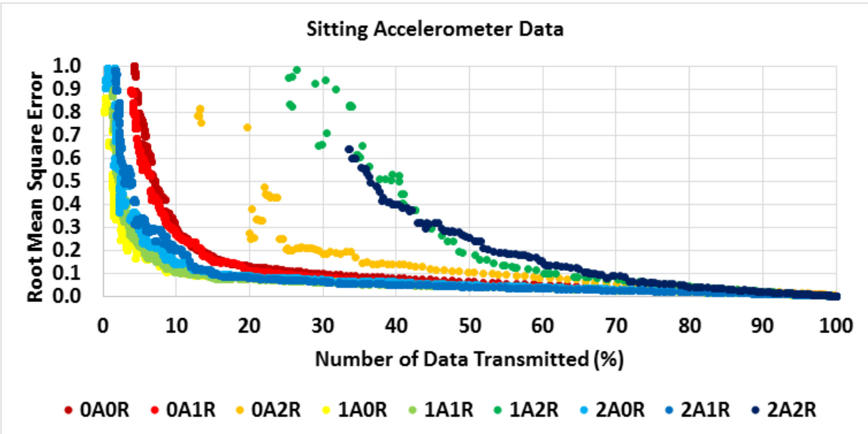

(c) Number of data transmitted vs. root mean square error where

$$RMSE_{max} = 1$$

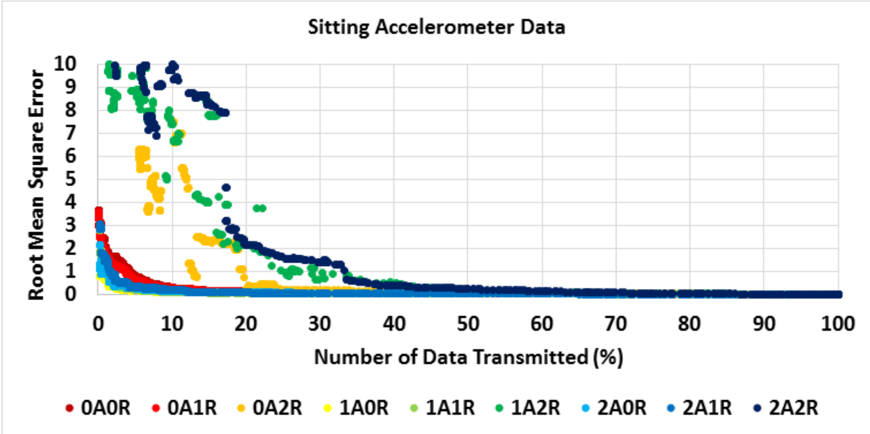

(d) Number of data transmitted vs. root mean square error where

$$RMSE_{max} = 10$$

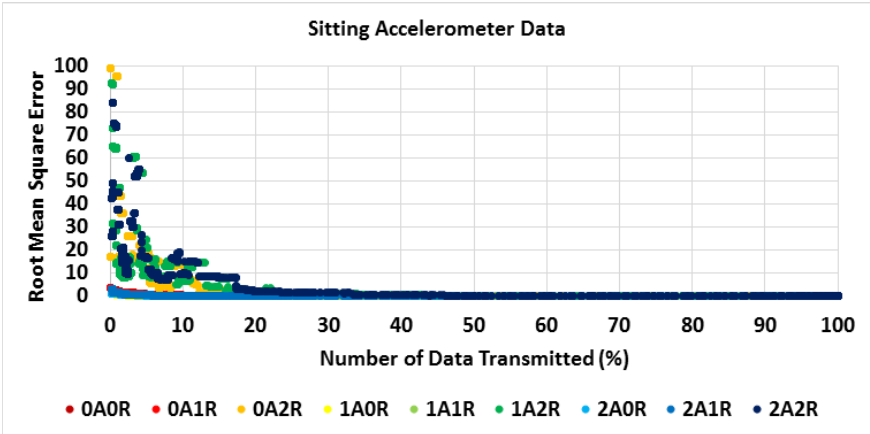

(e) Number of data transmitted vs. root mean square error where

$$RMSE_{max} = 100$$

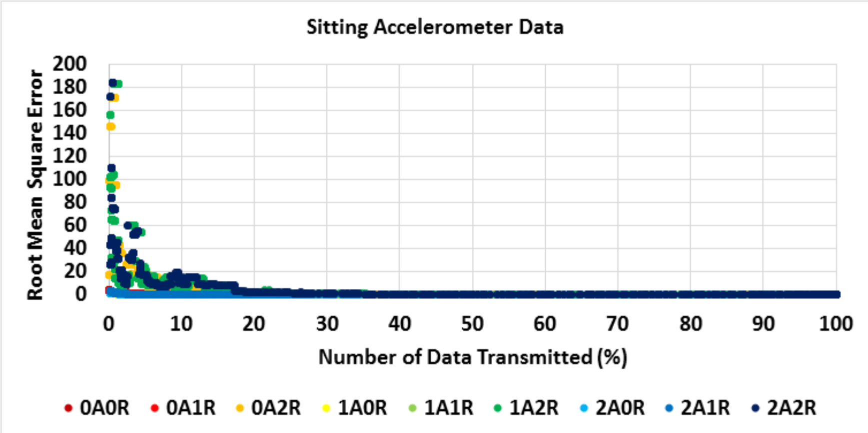

(f) Number of data transmitted vs. root mean square error where

$$RMSE_{max} = 200$$

Figure 5.55: Number of data transmitted vs. root mean square error in sitting accelerometer data

The results of DAR schemes in sitting accelerometer data are shown more details in Table 5.31.

Table 5.31: Number of Data Transmitted vs. Root Mean Square Error in Sitting Accelerometer Data

RMSE	DAR	$NoDT_{min}$ (%)
≤ 0.25	0A0R	11.333
	0A1R	10.700
	0A2R	20.167
	1A0R	2.433
	1A1R	4.633
	1A2R	46.967
	2A0R	5.400
	2A1R	7.033
	2A2R	50.733

RMSE = root mean square error
DAR = data Abstraction and Reformation
0A0R = zeroth-order data abstraction & zeroth-order data reformation
0A1R = zeroth-order data abstraction & first-order data reformation
0A2R = zeroth-order data abstraction & second-order data reformation
1A0R = first-order data abstraction & zeroth-order data reformation
1A1R = first-order data abstraction & first-order data reformation
1A2R = first-order data abstraction & second-order data reformation
2A0R = second-order data abstraction & zeroth-order data reformation
2A1R = second-order data abstraction & first-order data reformation
2A2R = second-order data abstraction & second-order data reformation
$NoDT_{min}$ = minimum number of data transmitted

From Table 5.31, it is shown that the best DAR schemes in sitting accelerometer data where $RMSE \leq 0.25$ in the terms of number of data transmitted is 1A0R.

4. Number of Data Transmitted vs. Mean Absolute Percentage Error

The comparisons of number of data transmitted against mean absolute percentage error are shown in Figure 5.56.

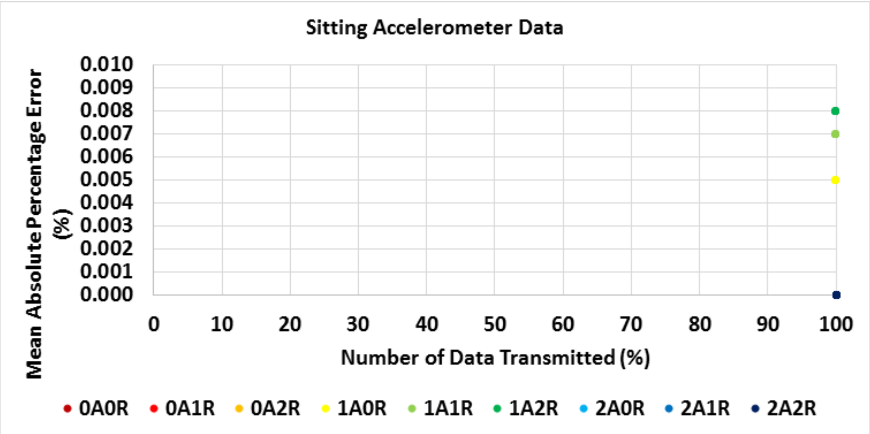

(a) Number of data transmitted vs. mean absolute percentage error where $MAPE_{max} = 0.01\%$

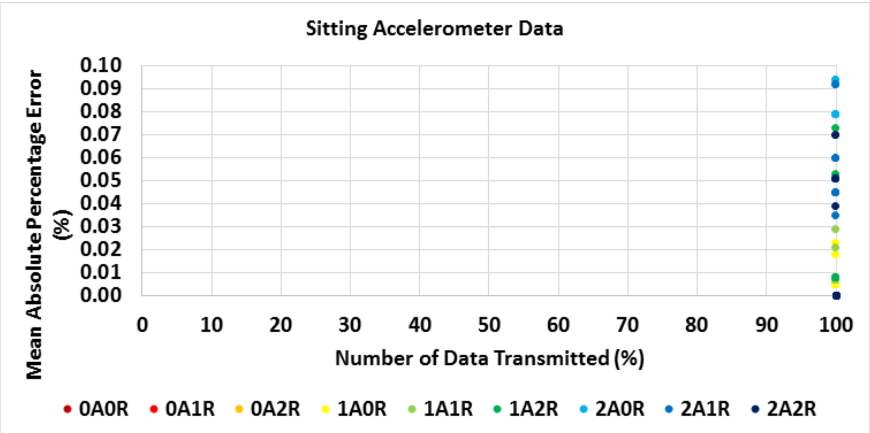

(b) Number of data transmitted vs. mean absolute percentage error where $MAPE_{max} = 0.1\%$

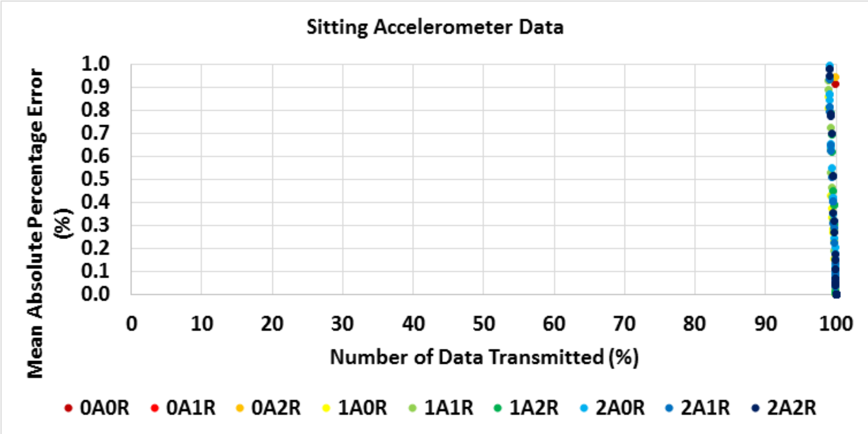

(c) Number of data transmitted vs. mean absolute percentage error where

$$MAPE_{max} = 1\%$$

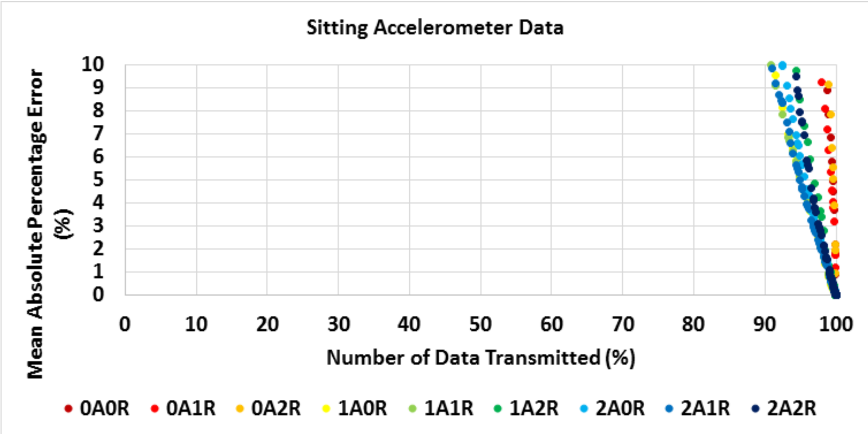

(d) Number of data transmitted vs. mean absolute percentage error where

$$MAPE_{max} = 10\%$$

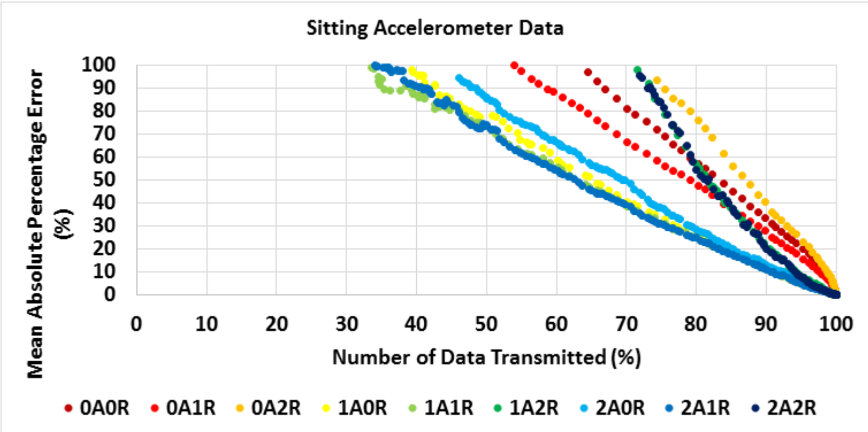

(e) Number of data transmitted vs. mean absolute percentage error where

$$MAPE_{max} = 100\%$$

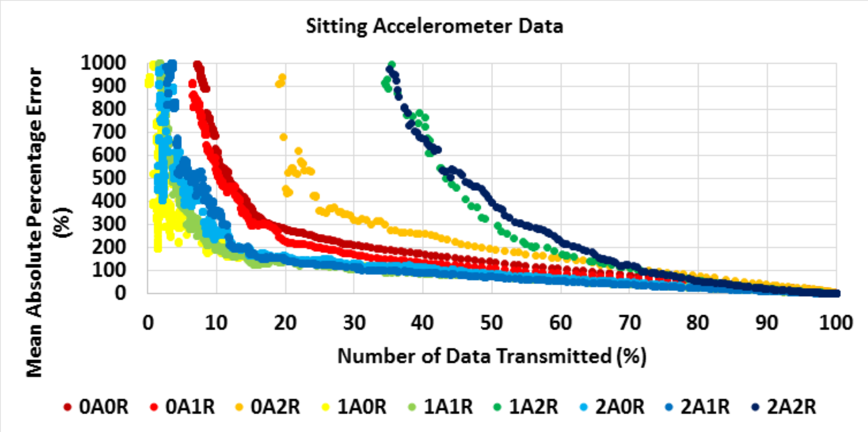

(f) Number of data transmitted vs. mean absolute percentage error where

$$MAPE_{max} = 1000\%$$

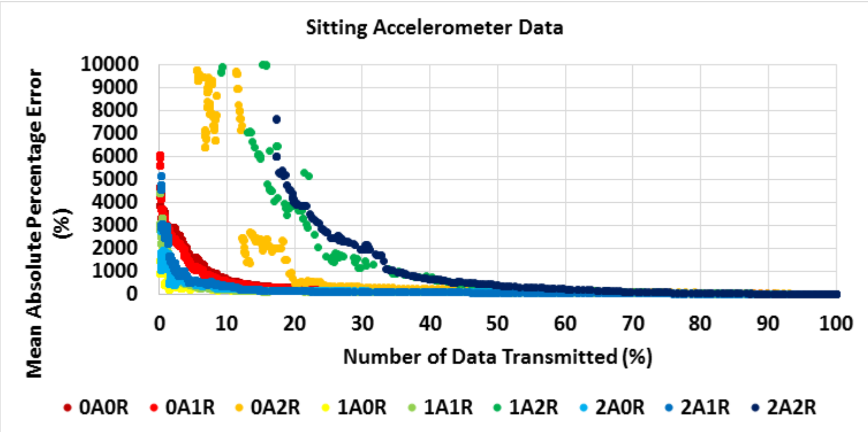

(g) Number of data transmitted vs. mean absolute percentage error where

$$MAPE_{max} = 10000\%$$

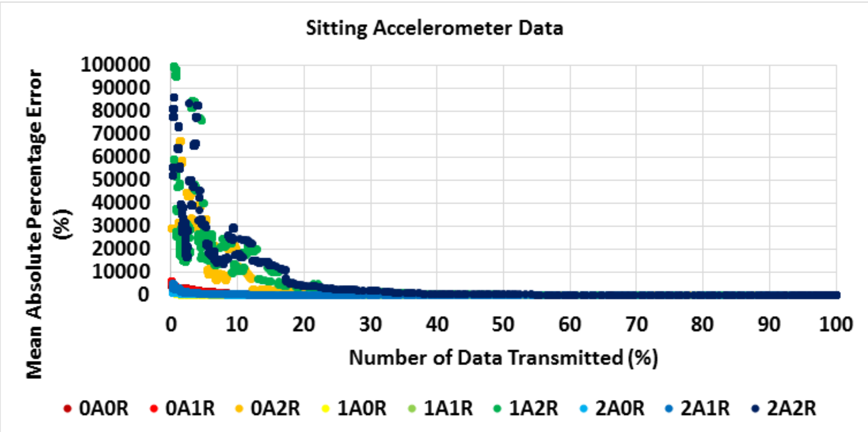

(h) Number of data transmitted vs. mean absolute percentage error where

$$MAPE_{max} = 100000\%$$

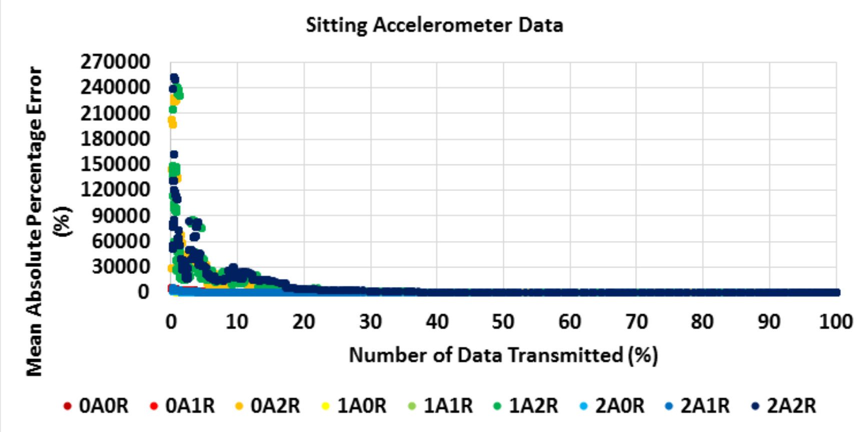

(i) Number of data transmitted vs. mean absolute percentage error where

$$MAPE_{max} = 270000\%$$

Figure 5.56: Number of data transmitted vs. mean absolute percentage error in sitting accelerometer data

The results of DAR schemes in sitting accelerometer data are shown more details in Table 5.32.

Table 5.32: Number of Data Transmitted vs. Mean Absolute Percentage Error in Sitting Accelerometer Data

MAPE	DAR	$NoDT_{min}$ (%)
≤ 2.5%	0A0R	99.900
	0A1R	99.900
	0A2R	99.900
	1A0R	97.800
	1A1R	97.800
	1A2R	98.533
	2A0R	97.833
	2A1R	97.567
	2A2R	98.267

MAPE = mean absolute percentage error
DAR = data Abstraction and Reformation
0A0R = zeroth-order data abstraction & zeroth-order data reformation
0A1R = zeroth-order data abstraction & first-order data reformation
0A2R = zeroth-order data abstraction & second-order data reformation
1A0R = first-order data abstraction & zeroth-order data reformation
1A1R = first-order data abstraction & first-order data reformation
1A2R = first-order data abstraction & second-order data reformation
2A0R = second-order data abstraction & zeroth-order data reformation
2A1R = second-order data abstraction & first-order data reformation
2A2R = second-order data abstraction & second-order data reformation
$NoDT_{min}$ = minimum number of data transmitted

From Table 5.32, it is shown that the best DAR schemes in sitting accelerometer data where $MAPE \leq 2.5\%$ in the terms of number of data transmitted is 2A1R.

5. Root Mean Square Error vs. Number of Packet Transmissions

The comparisons of root mean square error against number of packet transmissions are shown in Figure 5.33.

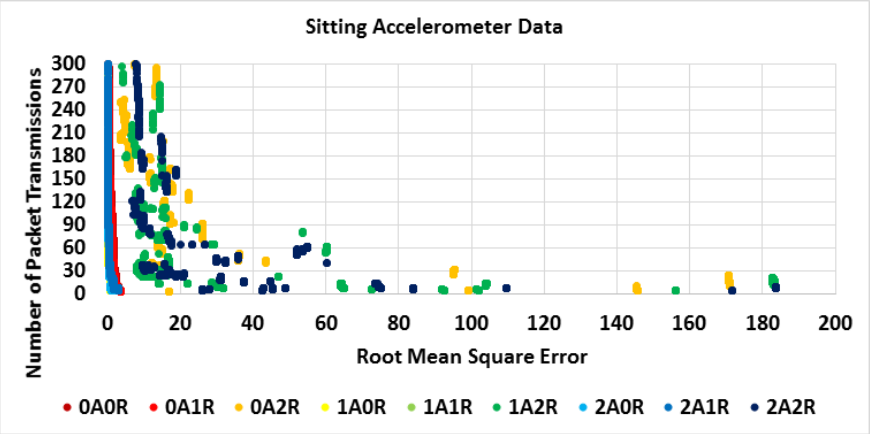

(a) Root mean square error vs. number of packet transmissions where $NoPT_{max} = 300$

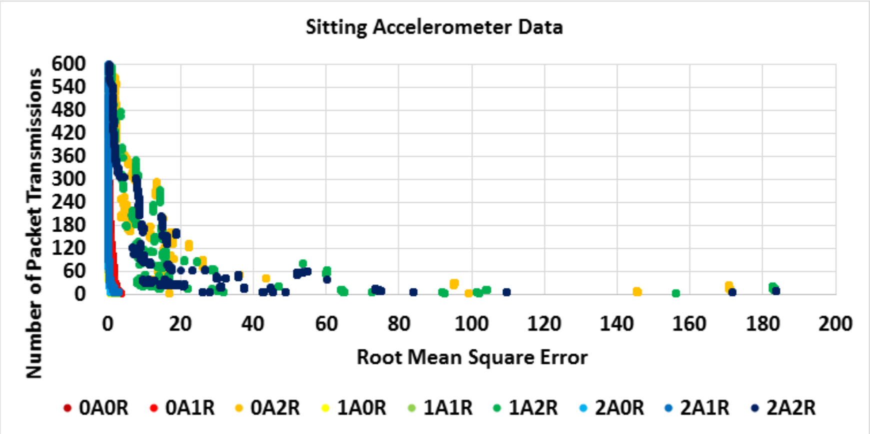

(b) Root mean square error vs. number of packet transmissions where $NoPT_{max} = 600$

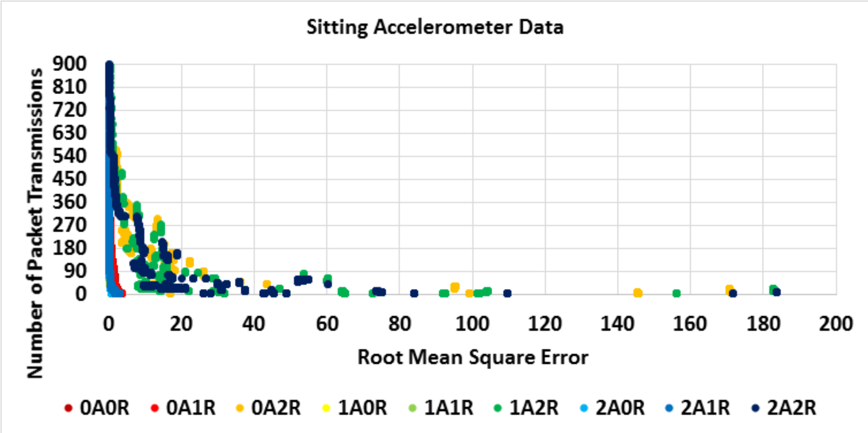

(c) Root mean square error vs. number of packet transmissions where

$$NoPT_{max} = 900$$

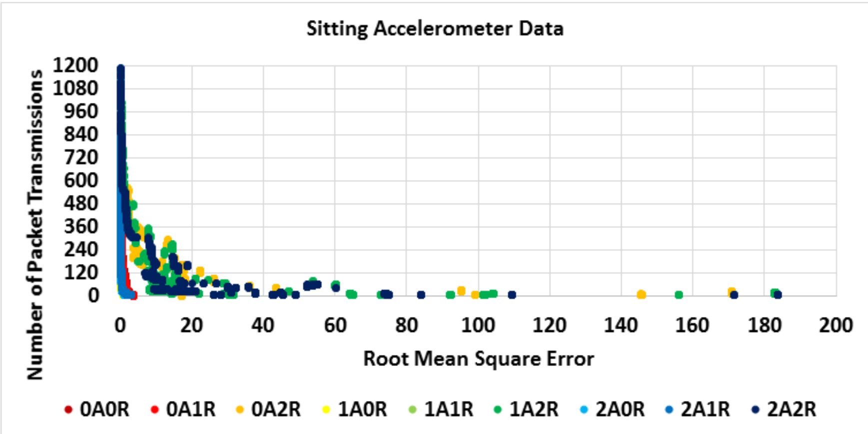

(d) Root mean square error vs. number of packet transmissions where

$$NoPT_{max} = 1200$$

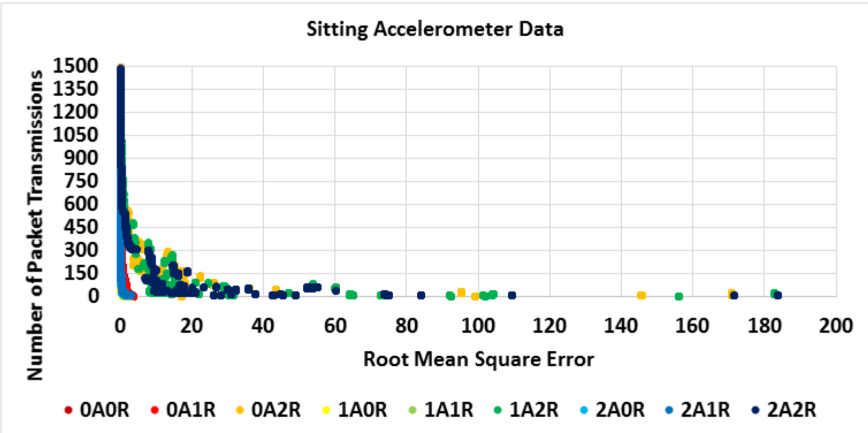

(e) Root mean square error vs. number of packet transmissions where

$$NoPT_{max} = 1500$$

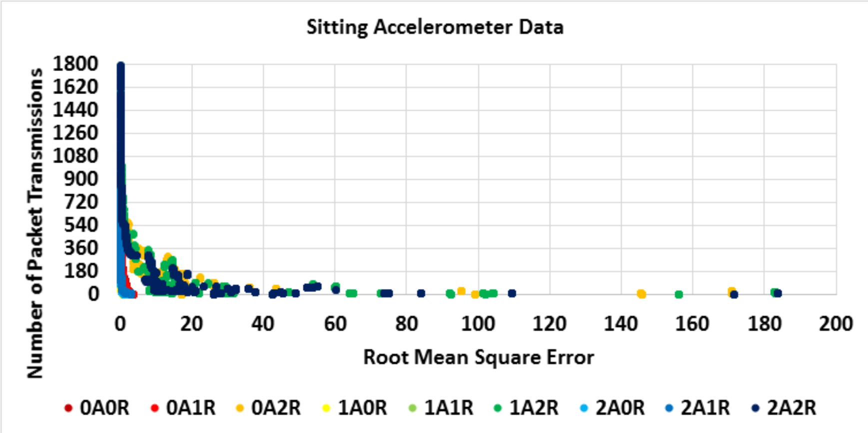

(f) Root mean square error vs. number of packet transmissions where

$$NoPT_{max} = 1800$$

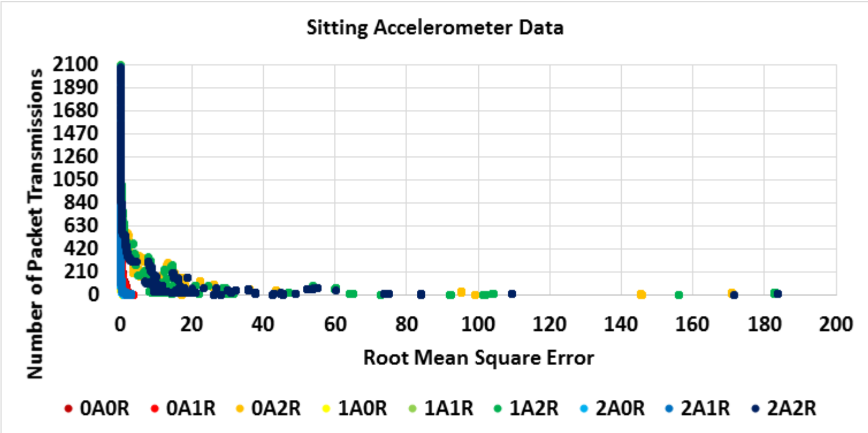

(g) Root mean square error vs. number of packet transmissions where

$$NoPT_{max} = 2100$$

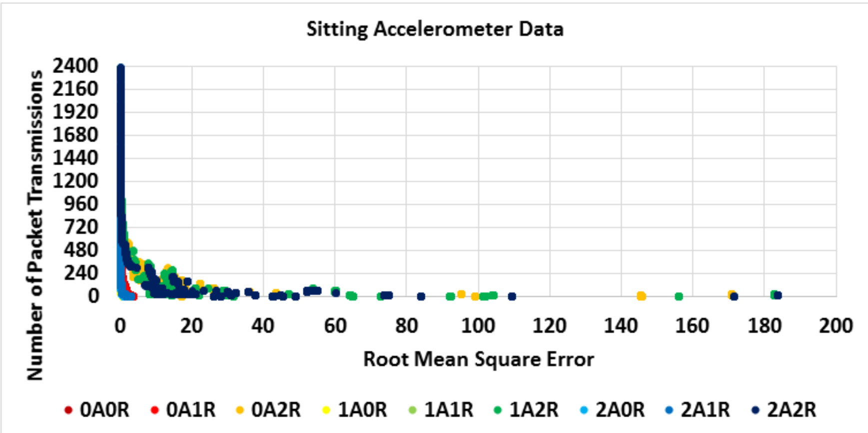

(h) Root mean square error vs. number of packet transmissions where

$$NoPT_{max} = 2400$$

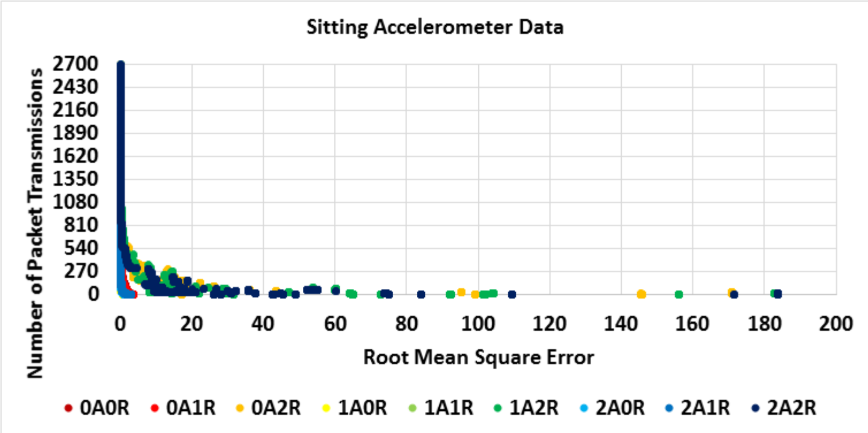

(i) Root mean square error vs. number of packet transmissions where

$$\boldsymbol{NoPT_{max} = 2700}$$

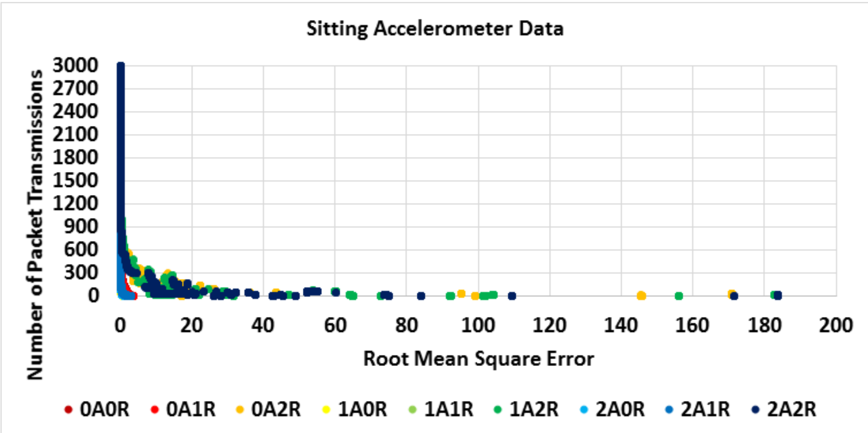

(j) Root mean square error vs. number of packet transmissions where

$$\boldsymbol{NoPT_{max} = 3000}$$

Figure 5.57: Root mean square error vs. number of packet transmissions in sitting accelerometer data

The results of DAR schemes in sitting accelerometer data are shown more details in Table 5.33.

Table 5.33: Root Mean Square Error vs. Number of Packet Transmissions in Sitting Accelerometer Data

NoPT	DAR	$RMSE_{min}$
≤ 2250	0A0R	0.035
	0A1R	0.029
	0A2R	0.047
	1A0R	0.012
	1A1R	0.012
	1A2R	0.023
	2A0R	0.009
	2A1R	0.008
	2A2R	0.013

NoPT = number of packet transmissions
DAR = data abstraction and reformation
0A0R = zeroth-order data abstraction & zeroth-order data reformation
0A1R = zeroth-order data abstraction & first-order data reformation
0A2R = zeroth-order data abstraction & second-order data reformation
1A0R = first-order data abstraction & zeroth-order data reformation
1A1R = first-order data abstraction & first-order data reformation
1A2R = first-order data abstraction & second-order data reformation
2A0R = second-order data abstraction & zeroth-order data reformation
2A1R = second-order data abstraction & first-order data reformation
2A2R = second-order data abstraction & second-order data reformation
$RMSE_{min}$ = minimum root mean square error

From Table 5.33, it is shown that the best DAR schemes in sitting accelerometer data where $NoPT \leq 2250$ in the terms of root mean square error is 2A1R.

6. Root Mean Square Error vs. Number of Data Transmitted

The comparisons of root mean square error against number of data transmitted are shown in Figure 5.58.

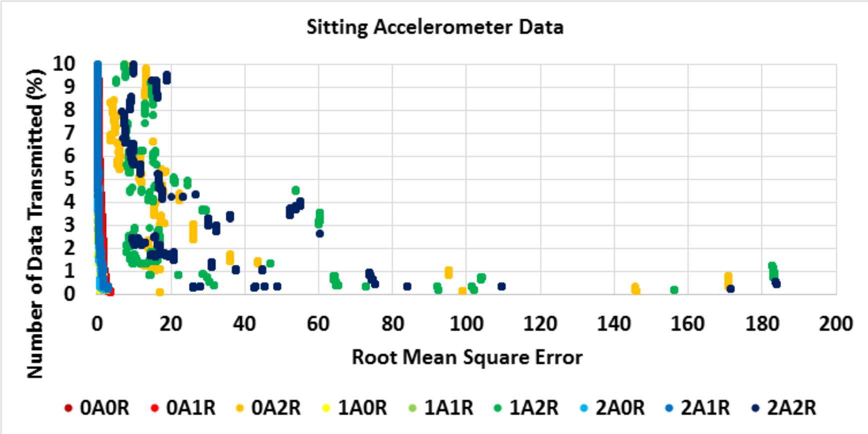

(a) Root mean square error vs. number of data transmitted where

$NoDT_{max} = 10\%$

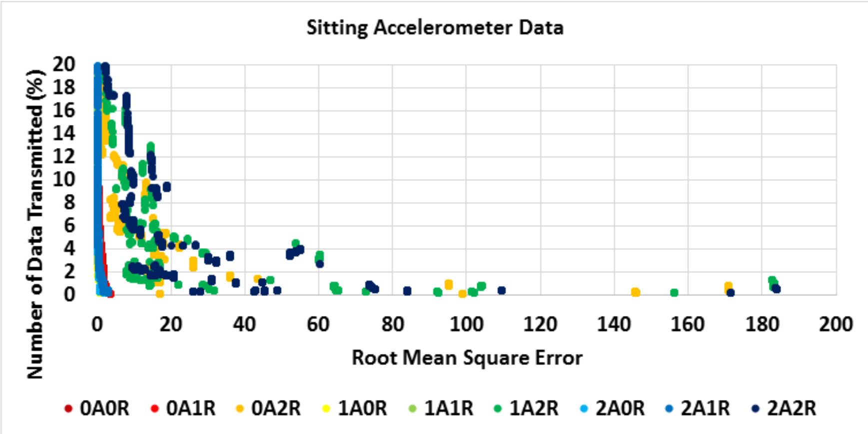

(b) Root mean square error vs. number of data transmitted where

$NoDT_{max} = 20\%$

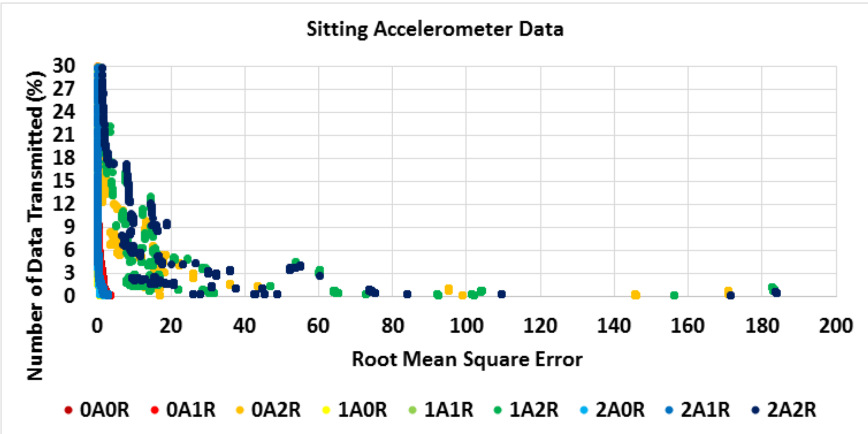

(c) Root mean square error vs. number of data transmitted (%) where

$NoDT_{max} = 30\%$

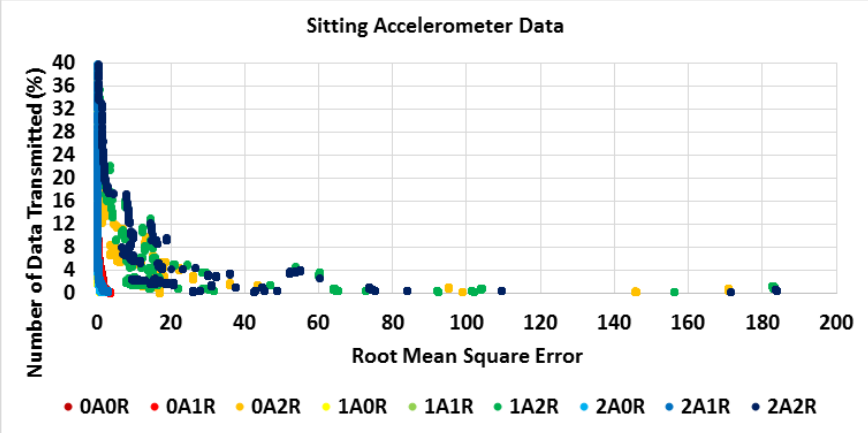

(d) Root mean square error vs. number of data transmitted where

$$NoDT_{max} = 40\%$$

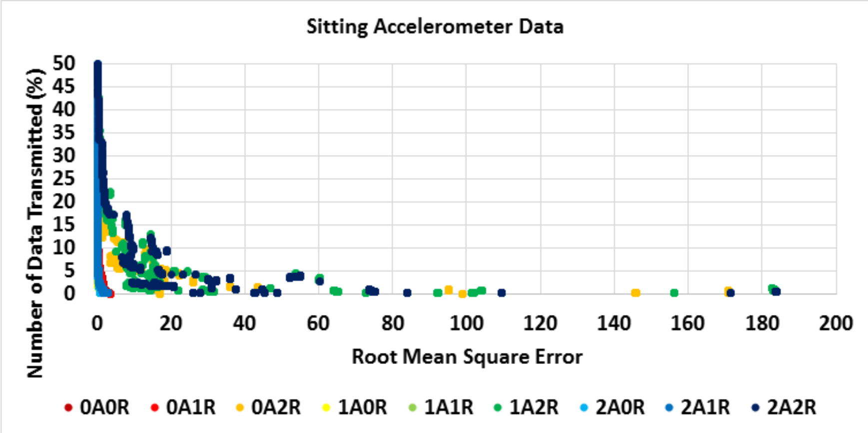

(e) Root mean square error vs. number of data transmitted where

$$NoDT_{max} = 50\%$$

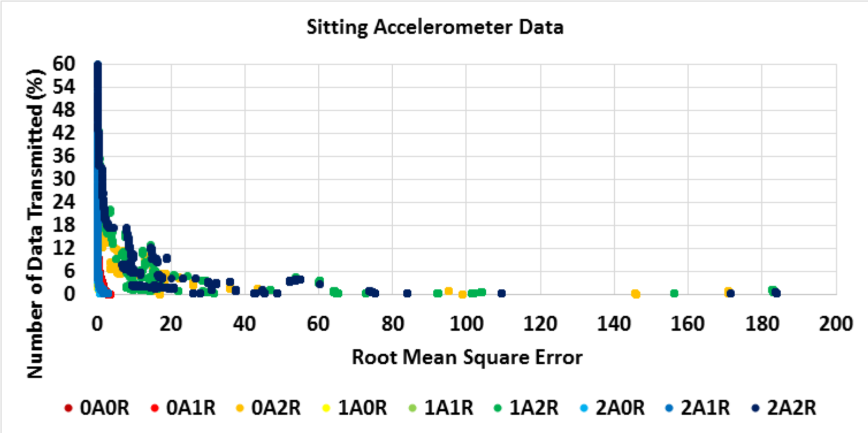

(f) Root mean square error vs. number of data transmitted where

$$NoDT_{max} = 60\%$$

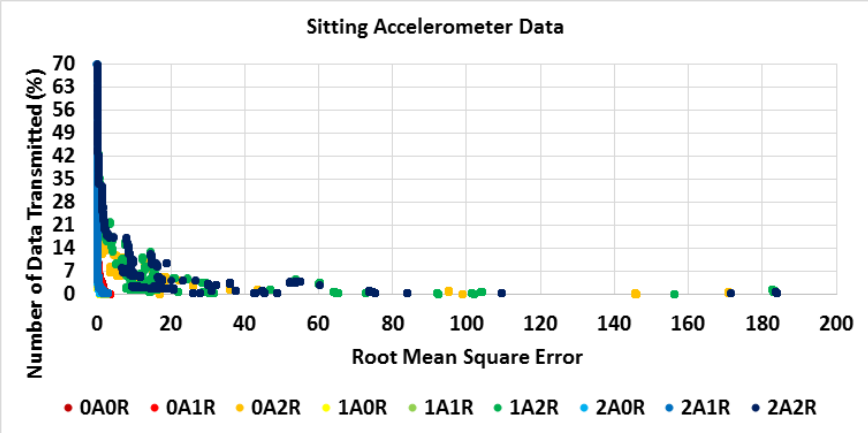

(g) Root mean square error vs. number of data transmitted where

$$NoDT_{max} = 70\%$$

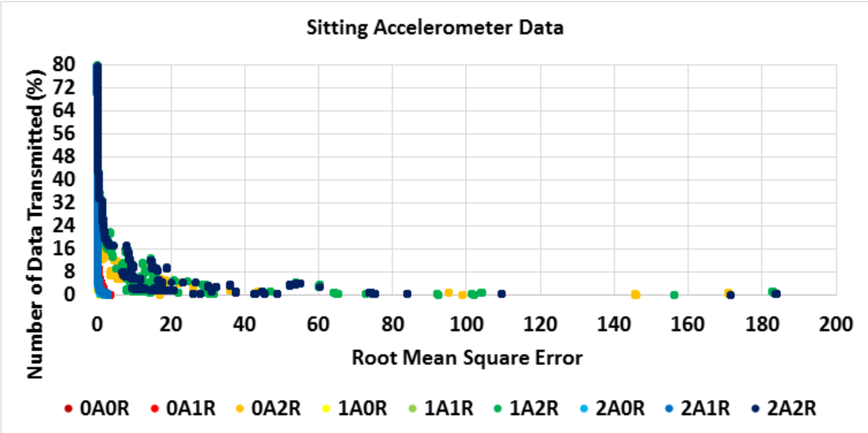

(h) Root mean square error vs. number of data transmitted where

$$NoDT_{max} = 80\%$$

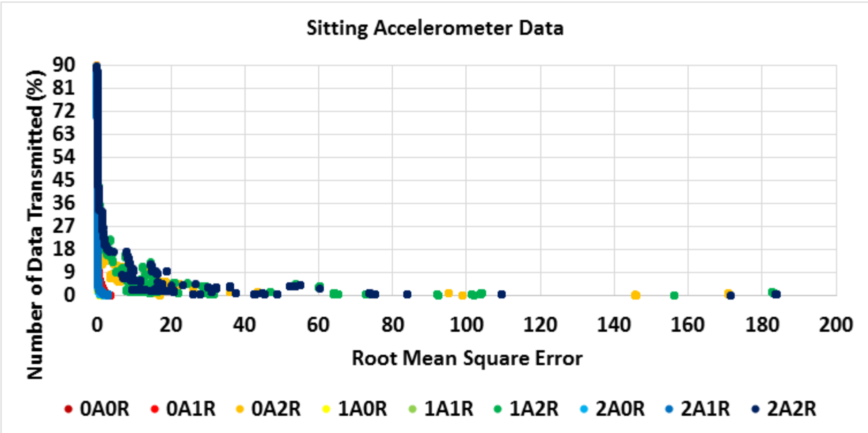

(i) Root mean square error vs. number of data transmitted where

$$NoDT_{max} = 90\%$$

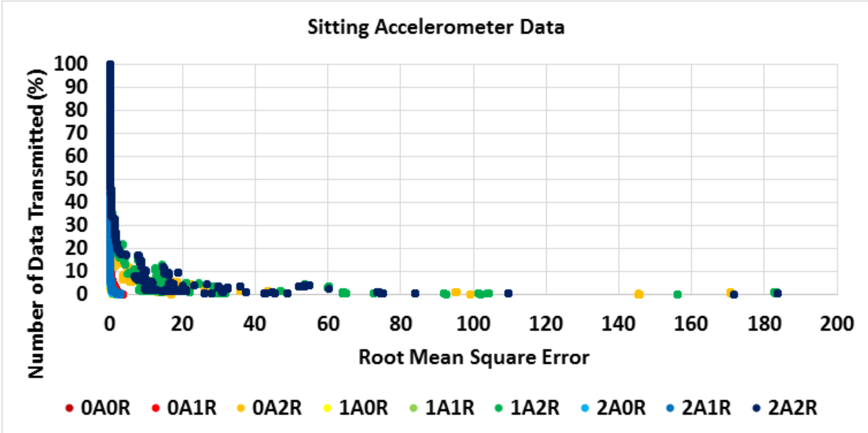

(j) Root mean square error vs. number of data transmitted where

$$\boldsymbol{NoDT_{max}} = \mathbf{100\%}$$

Figure 5.58: Root mean square error vs. number of data transmitted in sitting accelerometer data

The results of DAR schemes in sitting accelerometer data are shown more details in Table 5.34.

Table 5.34: Root Mean Square Error vs. Number of Data Transmitted in Sitting Accelerometer Data

NoDT	DAR	$RMSE_{min}$
≤ 75%	0A0R	0.035
	0A1R	0.029
	0A2R	0.047
	1A0R	0.024
	1A1R	0.024
	1A2R	0.060
	2A0R	0.026
	2A1R	**0.023**
	2A2R	0.060

NoDT = number of data transmitted
DAR = data abstraction and reformation
0A0R = zeroth-order data abstraction & zeroth-order data reformation
0A1R = zeroth-order data abstraction & first-order data reformation
0A2R = zeroth-order data abstraction & second-order data reformation
1A0R = first-order data abstraction & zeroth-order data reformation
1A1R = first-order data abstraction & first-order data reformation
1A2R = first-order data abstraction & second-order data reformation
2A0R = second-order data abstraction & zeroth-order data reformation
2A1R = second-order data abstraction & first-order data reformation
2A2R = second-order data abstraction & second-order data reformation
$RMSE_{min}$ = minimum root mean square error

From Table 5.34, it is shown that the best DAR schemes in sitting accelerometer data where $NoDT \leq 75\%$ in the terms of root mean square error is 2A1R.

7. Mean Absolute Percentage Error vs. Number of Packet Transmissions

The comparisons of mean absolute percentage error against number of packet transmissions are shown in Figure 5.59.

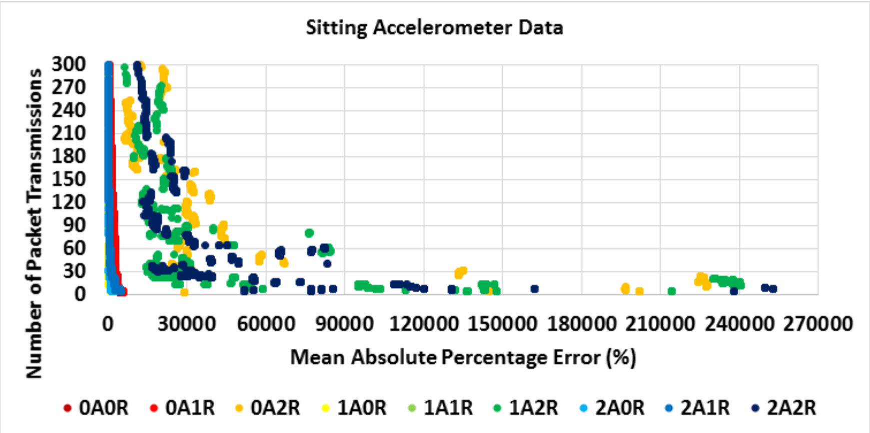

(a) Mean absolute percentage error vs. number of packet transmission where $NoPT_{max} = 300$

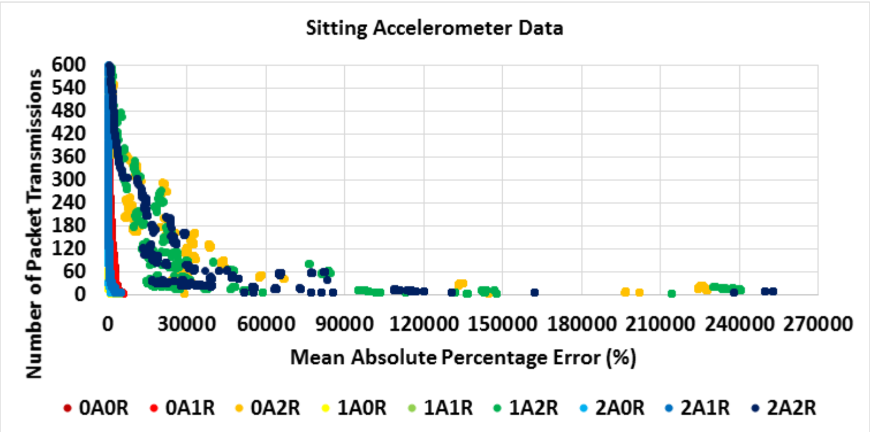

(b) Mean absolute percentage error vs. number of packet transmission where $NoPT_{max} = 600$

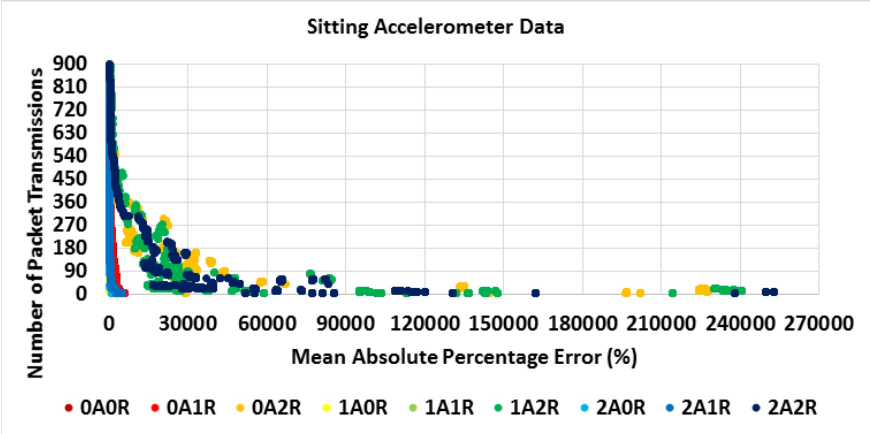

(c) Mean absolute percentage error vs. number of packet transmission where $NoPT_{max} = 900$

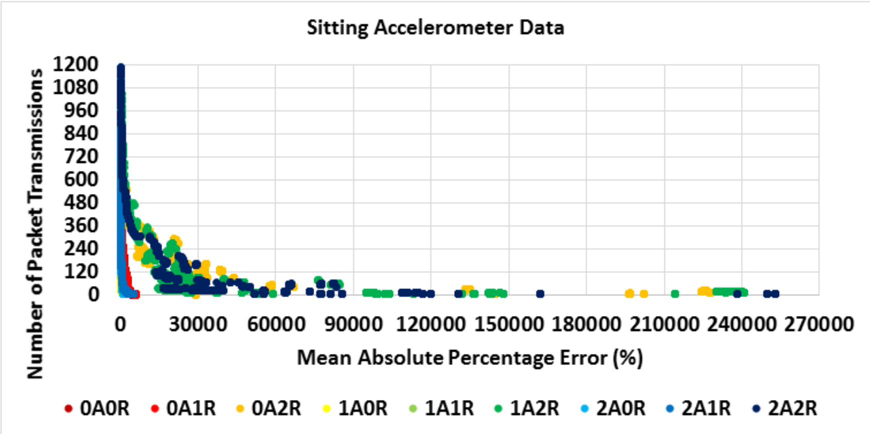

(d) Mean absolute percentage error vs. number of packet transmission where $NoPT_{max} = 1200$

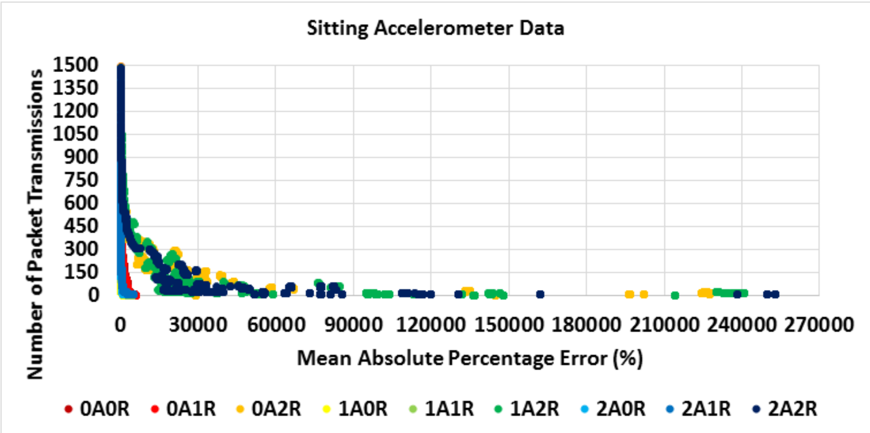

(e) Mean absolute percentage error vs. number of packet transmission where $NoPT_{max} = 1500$

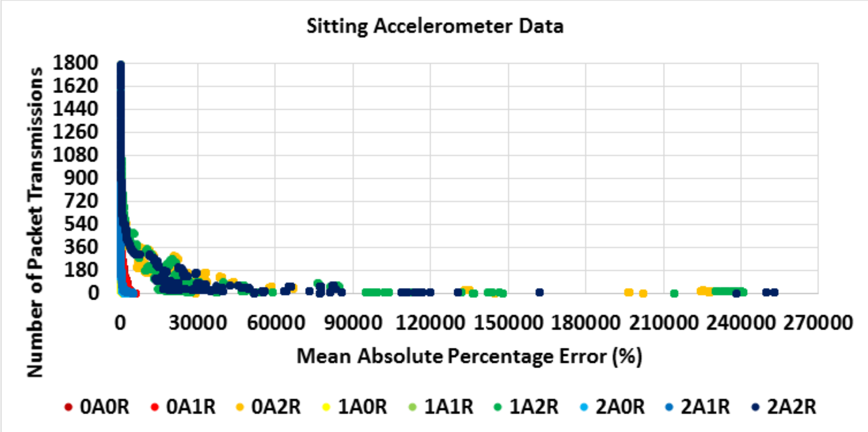

(f) Mean absolute percentage error vs. number of packet transmission

where $NoPT_{max} = 1800$

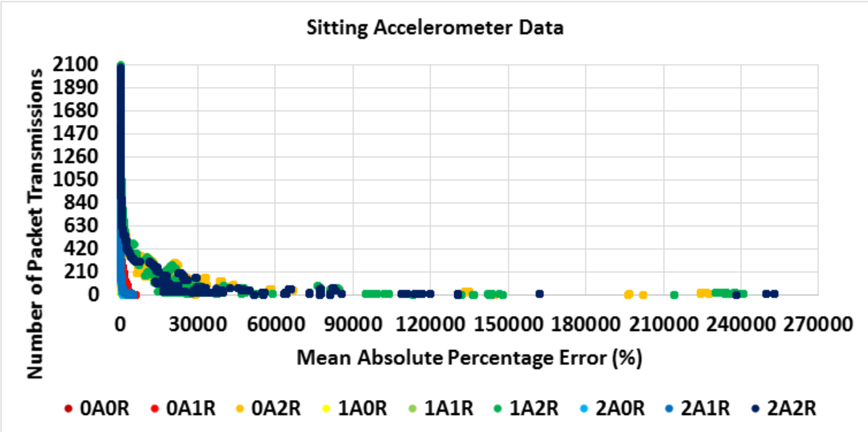

(g) Mean absolute percentage error vs. number of packet transmission

where $NoPT_{max} = 2100$

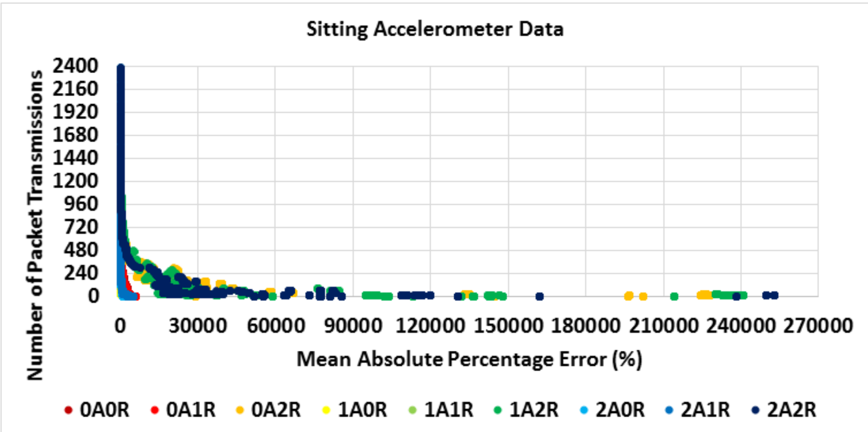

(h) Mean absolute percentage error vs. number of packet transmission

where $NoPT_{max} = 2400$

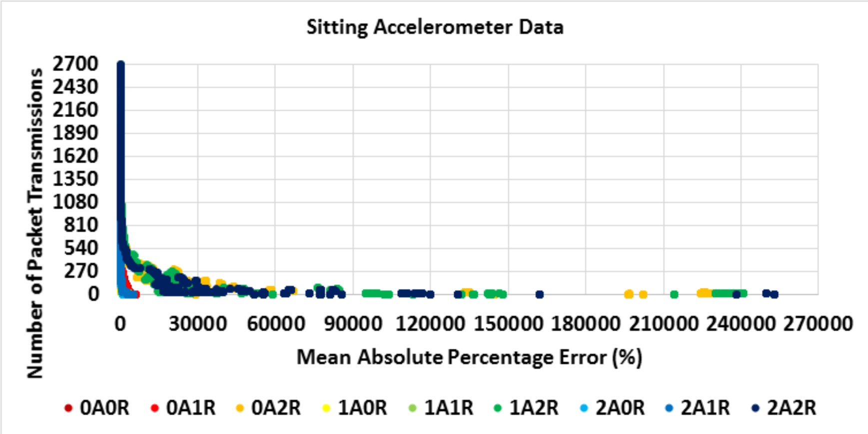

(i) Mean absolute percentage error vs. number of packet transmission

where $NoPT_{max} = 2700$

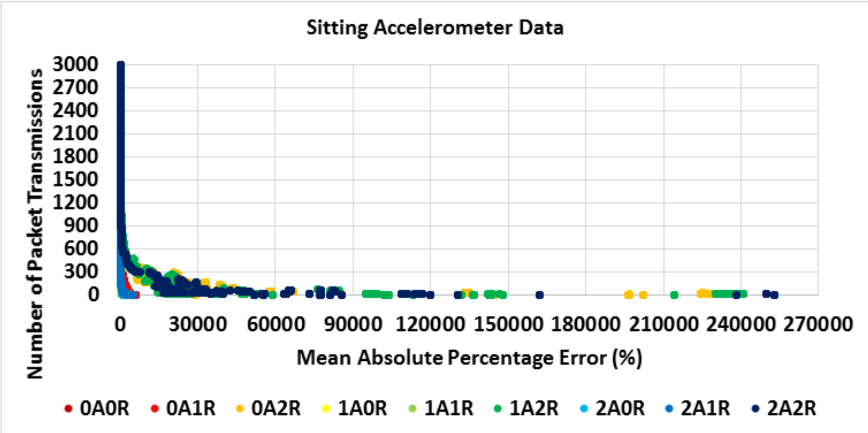

(j) Mean absolute percentage error vs. number of packet transmission

where $NoPT_{max} = 3000$

Figure 5.59: Mean absolute percentage error vs. number of packet transmissions in sitting accelerometer data

The results of DAR schemes in sitting accelerometer data are shown more details in Table 5.35.

Table 5.35: Mean Absolute Percentage Error vs. Number of Packet Transmissions in Sitting Accelerometer Data

NoPT	DAR	$MAPE_{min}$ (%)
≤ 2250	0A0R	71.764
	0A1R	58.264
	0A2R	93.515
	1A0R	12.855
	1A1R	12.422
	1A2R	24.345
	2A0R	7.622
	2A1R	6.155
	2A2R	10.673

NoPT = number of packet transmissions
DAR = data abstraction and reformation
0A0R = zeroth-order data abstraction & zeroth-order data reformation
0A1R = zeroth-order data abstraction & first-order data reformation
0A2R = zeroth-order data abstraction & second-order data reformation
1A0R = first-order data abstraction & zeroth-order data reformation
1A1R = first-order data abstraction & first-order data reformation
1A2R = first-order data abstraction & second-order data reformation
2A0R = second-order data abstraction & zeroth-order data reformation
2A1R = second-order data abstraction & first-order data reformation
2A2R = second-order data abstraction & second-order data reformation
$MAPE_{min}$ = minimum mean absolute percentage error

From Table 5.35, it is shown that the best DAR schemes in sitting accelerometer data where $NoPT \leq 2250$ in the terms of mean absolute percentage error is 2A1R.

8. Mean Absolute Percentage Error vs. Number of Data Transmitted

The comparisons of mean absolute percentage error against number of data transmitted are shown in Figure 5.60.

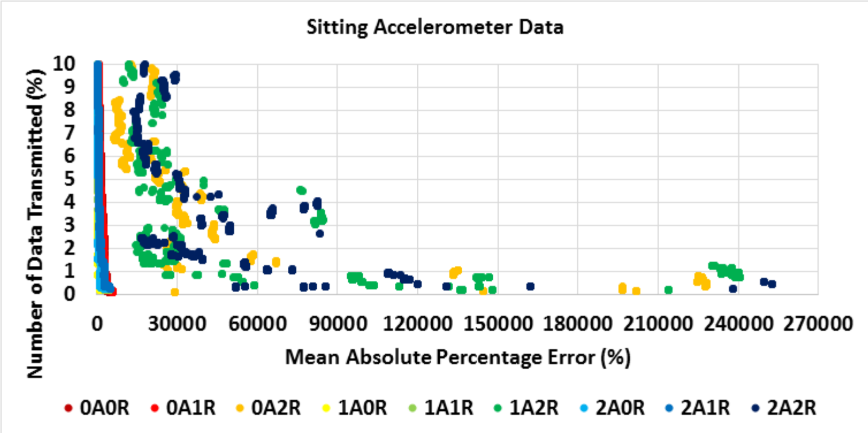

(a) Mean absolute percentage error vs. number of data transmitted where

$NoDT_{max} = 10\%$

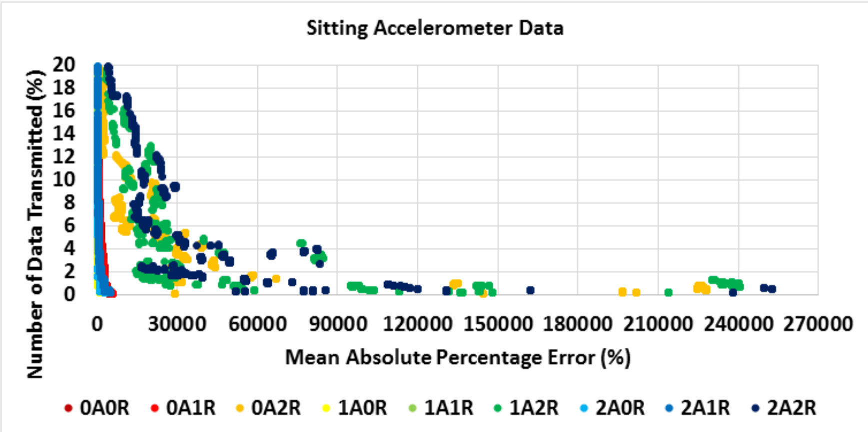

(b) Mean absolute percentage error vs. number of data transmitted where

$NoDT_{max} = 20\%$

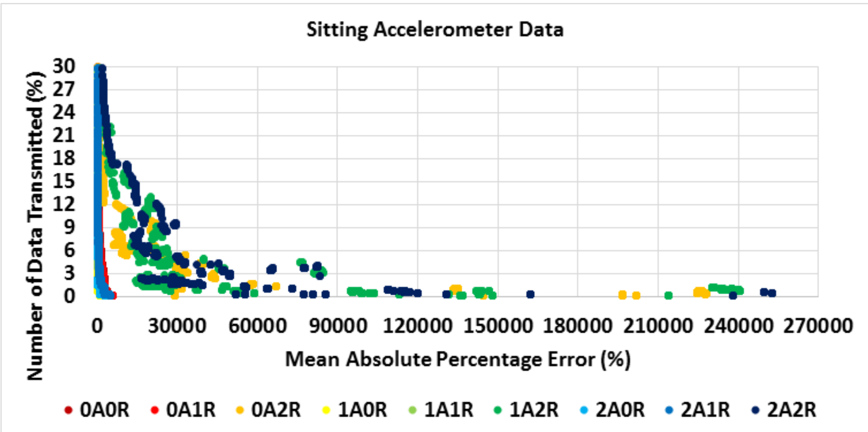

(c) Mean absolute percentage error vs. number of data transmitted where

$NoDT_{max} = 30\%$

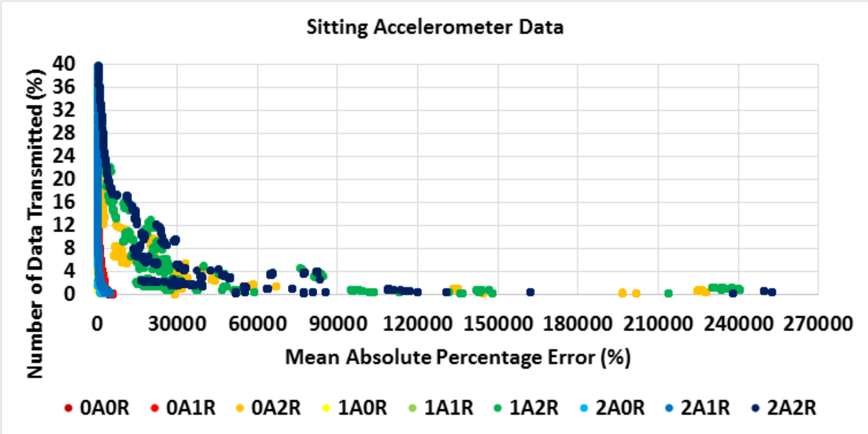

(d) Mean absolute percentage error vs. number of data transmitted where

$$NoDT_{max} = 40\%$$

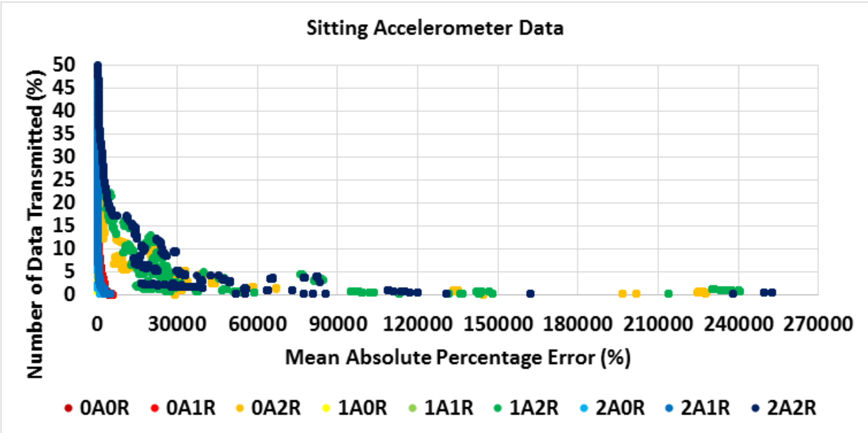

(e) Mean absolute percentage error vs. number of data transmitted where

$$NoDT_{max} = 50\%$$

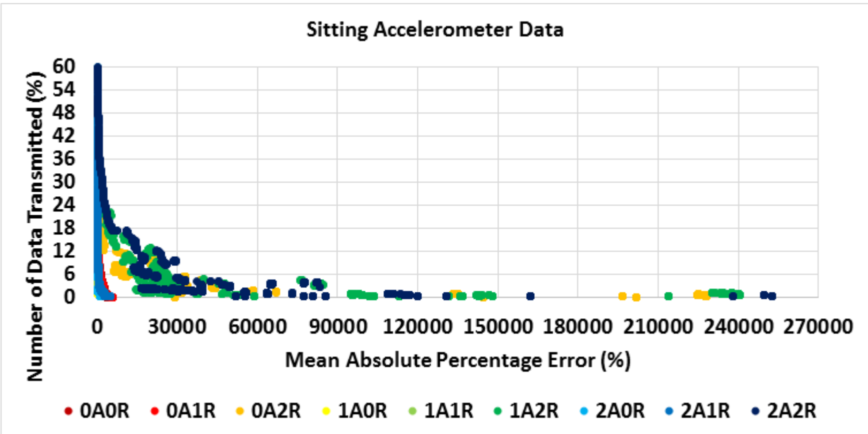

(f) Mean absolute percentage error vs. number of data transmitted where

$$NoDT_{max} = 60\%$$

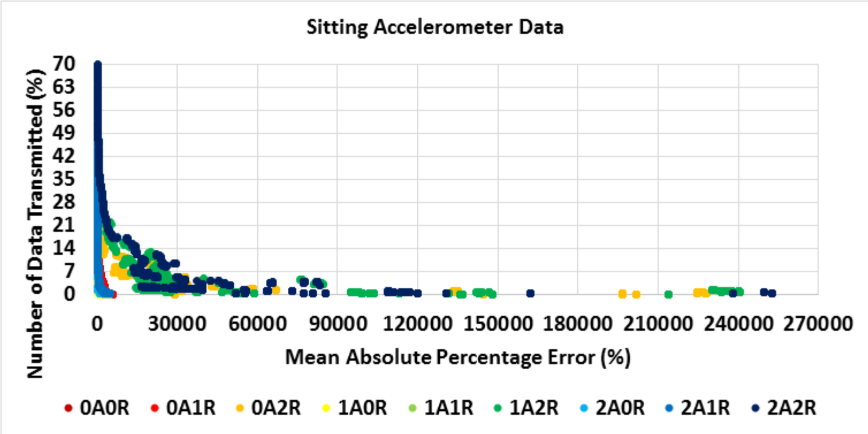

(g) Mean absolute percentage error vs. number of data transmitted where

$NoDT_{max} = 70\%$

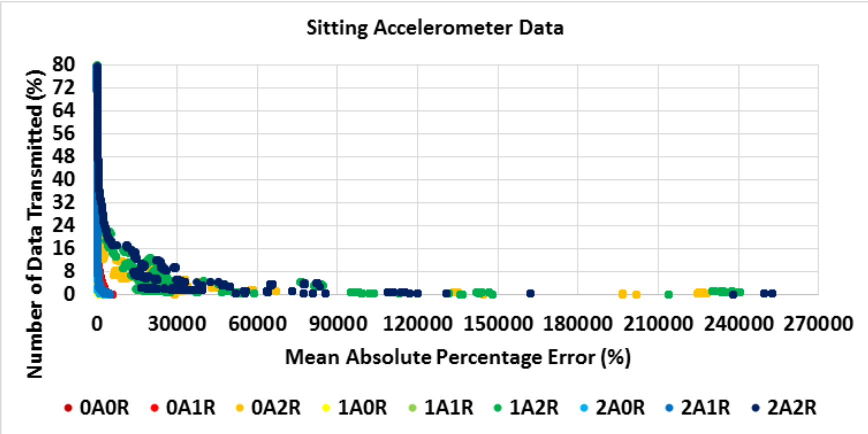

(h) Mean absolute percentage error vs. number of data transmitted where

$NoDT_{max} = 80\%$

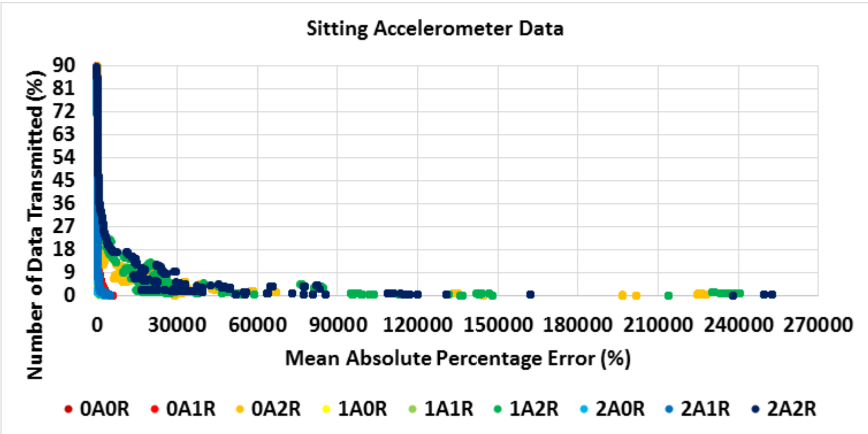

(i) Mean absolute percentage error vs. number of data transmitted where

$NoDT_{max} = 90\%$

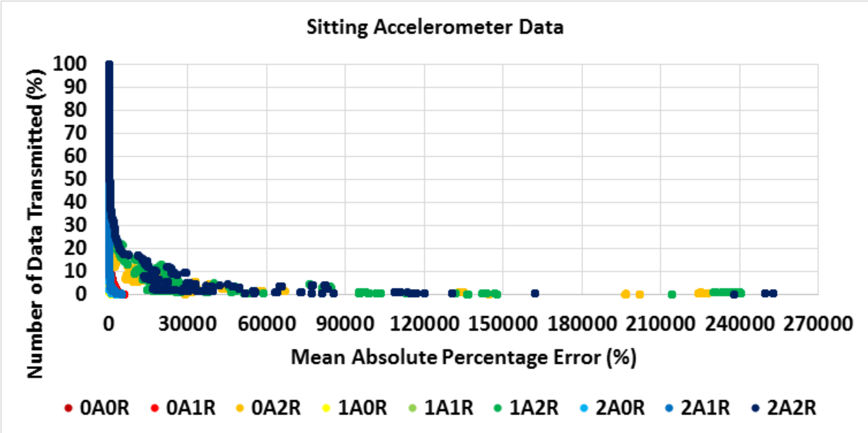

(j) Mean absolute percentage error vs. number of data transmitted (%)

where $NoDT_{max}$ = 100%

Figure 5.60: Mean absolute percentage error vs. number of data transmitted in sitting accelerometer data

The results of DAR schemes in sitting accelerometer data are shown more details in Table 5.36.

Table 5.36: Mean Absolute Percentage Error vs. Number of Data Transmitted in Sitting Accelerometer Data

NoDT	DAR	$MAPE_{min}$ (%)
≤ 75%	0A0R	71.764
	0A1R	58.264
	0A2R	93.515
	1A0R	35.055
	1A1R	33.313
	1A2R	85.629
	2A0R	37.859
	2A1R	31.043
	2A2R	83.902

NoDT = number of data transmitted
DAR = data abstraction and reformation
0A0R = zeroth-order data abstraction & zeroth-order data reformation
0A1R = zeroth-order data abstraction & first-order data reformation
0A2R = zeroth-order data abstraction & second-order data reformation
1A0R = first-order data abstraction & zeroth-order data reformation
1A1R = first-order data abstraction & first-order data reformation
1A2R = first-order data abstraction & second-order data reformation
2A0R = second-order data abstraction & zeroth-order data reformation
2A1R = second-order data abstraction & first-order data reformation
2A2R = second-order data abstraction & second-order data reformation
$MAPE_{min}$ = minimum mean absolute percentage error

From Table 5.36, it is shown that the best DAR schemes in sitting accelerometer data where $NoDT \leq 75\%$ in the terms of mean absolute percentage error is 1A1R.

9. Conclusion

From Table 5.29 – 5.36, it is concluded in Table 5.37, that the best DAR schemes in sitting accelerometer data is 2A1R.

Table 5.37: Results of DAR Schemes in Sitting Accelerometer Data

(a) Best DAR Schemes in Sitting Accelerometer Data where the $NoPT \leq 2250$ and $NoDT \leq 75\%$

DAR	Th	NoPT	NoDT(%)	RMSE	MAPE(%)
0A0R	0.039	2230	74.333	0.035	71.764
0A1R	0.039	2230	74.333	0.029	58.264
0A2R	0.039	2230	74.333	0.047	93.515
1A0R	0.068	1741	74.033	0.024	35.055
1A1R	0.068	1741	74.033	0.024	33.313
1A2R	0.068	1741	74.033	0.060	85.629
2A0R	0.135	1475	74.833	0.026	37.859
2A1R	0.135	1475	74.833	0.023	31.043
2A2R	0.135	1475	74.833	0.060	83.902

(b) Best DAR Schemes in Sitting Accelerometer Data where the and $RMSE \leq 0.25$ $MAPE \leq 2.5\%$

DAR	Th	NoPT	NoDT(%)	RMSE	MAPE(%)
0A0R	0.005	2997	99.900	0.001	2.198
0A1R	0.005	2997	99.900	0.001	1.965
0A2R	0.005	2997	99.900	0.001	2.188
1A0R	0.034	2692	97.800	0.004	2.144
1A1R	0.034	2692	97.800	0.004	2.202
1A2R	0.031	2755	98.533	0.004	1.944
2A0R	0.072	2535	97.833	0.005	2.446
2A1R	0.074	2512	97.567	0.004	2.382
2A2R	0.070	2564	98.267	0.005	2.154

DAR = data abstraction and reformation
Th = threshold
NoPT = number of packet transmissions
NoDT = number of packet transmitted
RMSE = root mean square error
MAPE = mean absolute percentage error

5.3.5 Standing Accelerometer Data

The comparisons among parameters (number of packet transmissions, number of data transmitted, root mean square error, and mean absolute percentage error) are as follows.

1. Number of Packet Transmissions vs. Root Mean Square Error

   The comparisons of number of packet transmissions against root mean square error are shown in Figure 5.61.

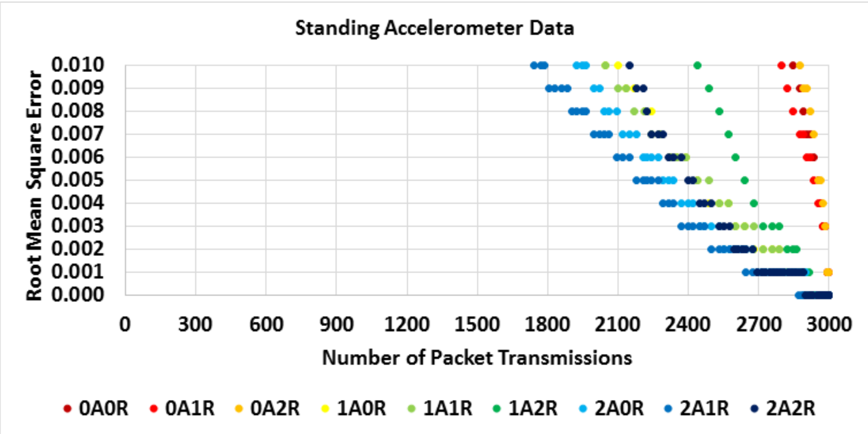

(a) Number of packet transmissions vs. root mean square error where $RMSE_{max} = 0.01$

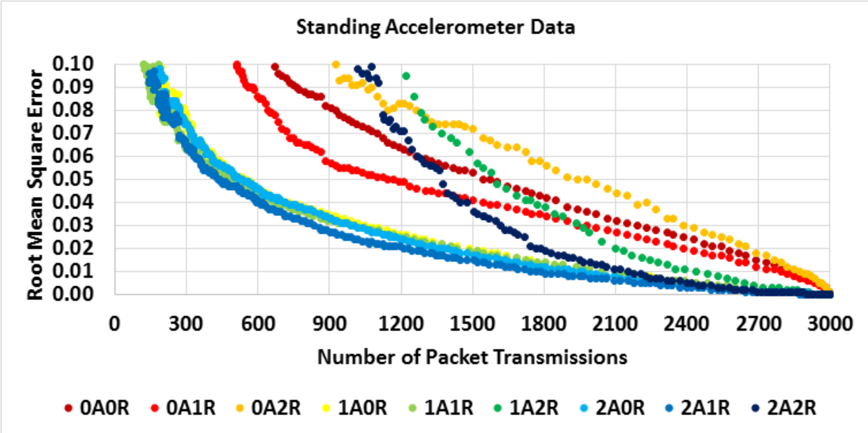

(b) Number of packet transmissions vs. root mean square error where

$$RMSE_{max} = 0.1$$

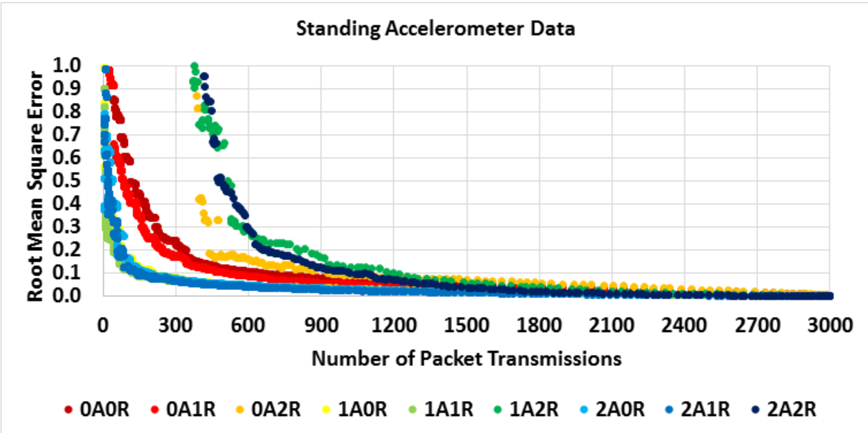

(c) Number of packet transmissions vs. root mean square error where

$$RMSE_{max} = 1$$

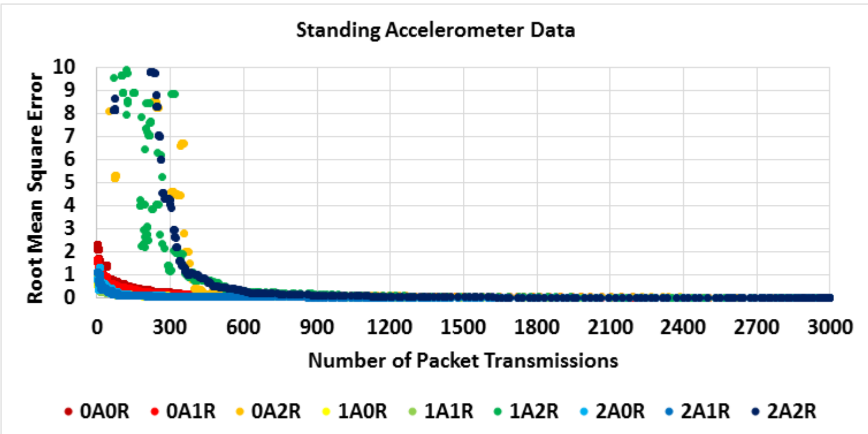

(d) Number of packet transmissions vs. root mean square error where

$$RMSE_{max} = 10$$

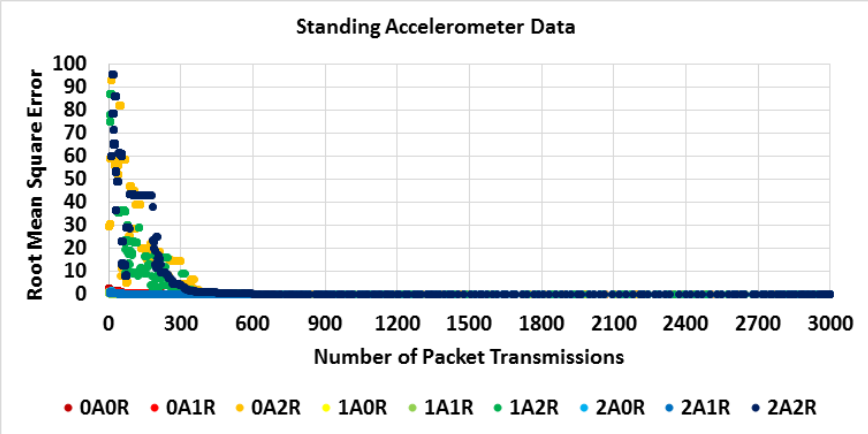

(e) Number of packet transmissions vs. root mean square error where

$$RMSE_{max} = 100$$

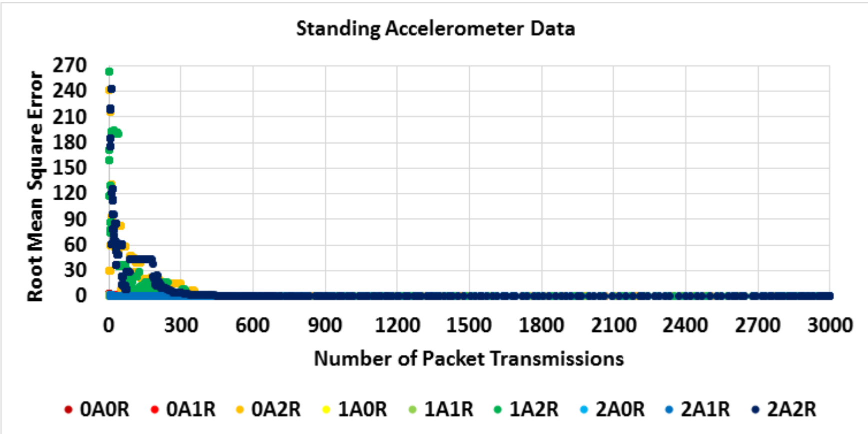

(f) Number of packet transmissions vs. root mean square error where

$$RMSE_{max} = 270$$

Figure 5.61: Number of packet transmissions vs. root mean square error in standing accelerometer data

The results of DAR schemes in standing accelerometer data are shown more details in Table 5.38.

Table 5.38: Number of Packet Transmissions vs. Root Mean Square Error in Standing Accelerometer Data

RMSE	DAR	$NoPT_{min}$
≤ 0.25	0A0R	256
	0A1R	187
	0A2R	437
	1A0R	42
	1A1R	30
	1A2R	644
	2A0R	56
	2A1R	59
	2A2R	628

RMSE = root mean square error
DAR = data abstraction and reformation
0A0R = zeroth-order data abstraction & zeroth-order data reformation
0A1R = zeroth-order data abstraction & first-order data reformation
0A2R = zeroth-order data abstraction & second-order data reformation
1A0R = first-order data abstraction & zeroth-order data reformation
1A1R = first-order data abstraction & first-order data reformation
1A2R = first-order data abstraction & second-order data reformation
2A0R = second-order data abstraction & zeroth-order data reformation
2A1R = second-order data abstraction & first-order data reformation
2A2R = second-order data abstraction & second-order data reformation
$NoPT_{min}$ = minimum number of packet transmissions

From Table 5.38, it is shown that the best DAR schemes in standing accelerometer data where $RMSE \leq 0.25$ in the terms of number of packet transmissions is 1A1R.

2. Number of Packet Transmissions vs. Mean Absolute Percentage Error

The comparisons of number of packet transmissions against mean absolute percentage error are shown in Figure 5.62.

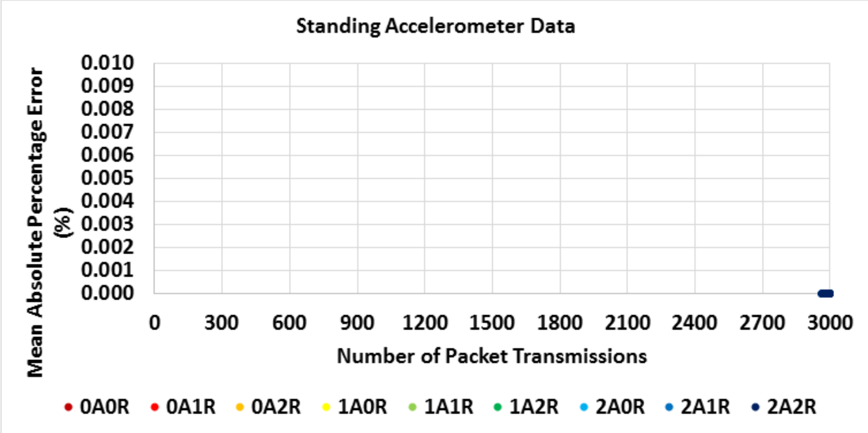

(a) Number of packet transmissions vs. mean absolute percentage error where $MAPE_{max} = 0.01\%$

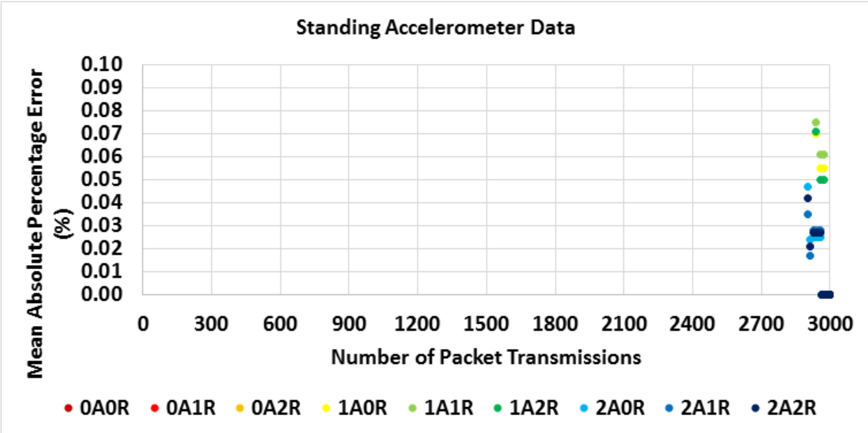

(b) Number of packet transmissions vs. mean absolute percentage error where $MAPE_{max} = 0.1\%$

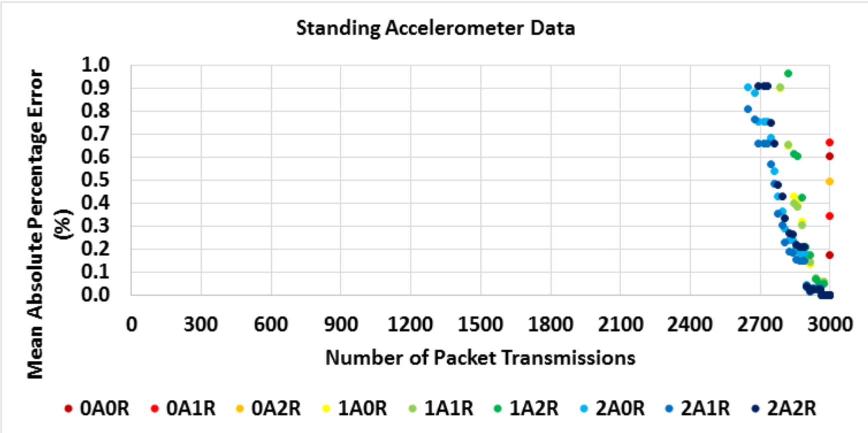

(c) Number of packet transmissions vs. mean absolute percentage error where $MAPE_{max} = 1\%$

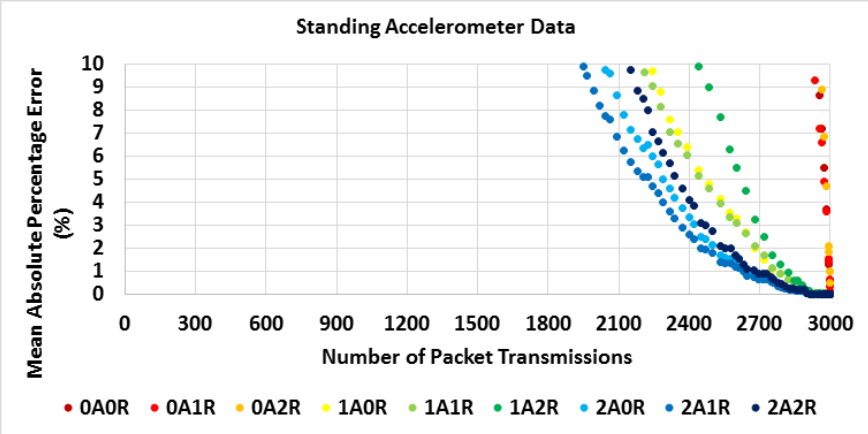

(d) Number of packet transmissions vs. mean absolute percentage error where $MAPE_{max} = 10\%$

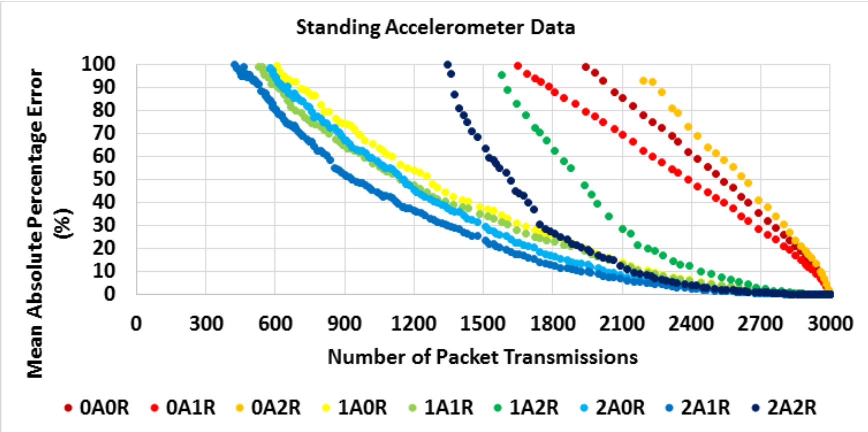

(e) Number of packet transmissions vs. mean absolute percentage error where $MAPE_{max} = 100\%$

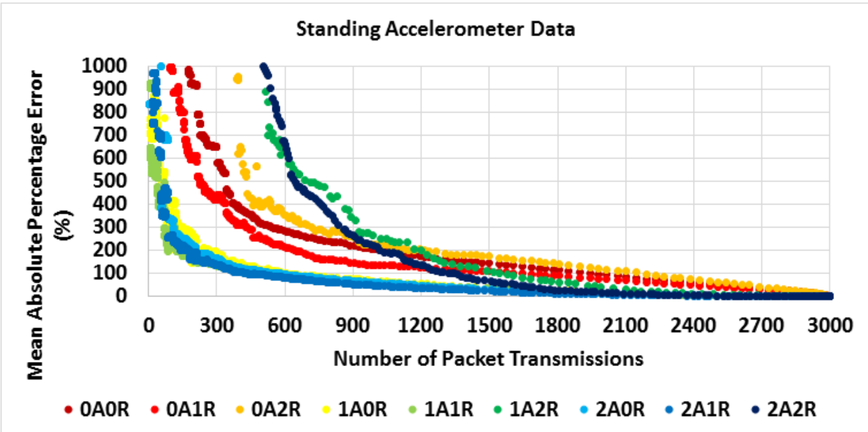

(f) Number of packet transmissions vs. mean absolute percentage error where $MAPE_{max} = 1000\%$

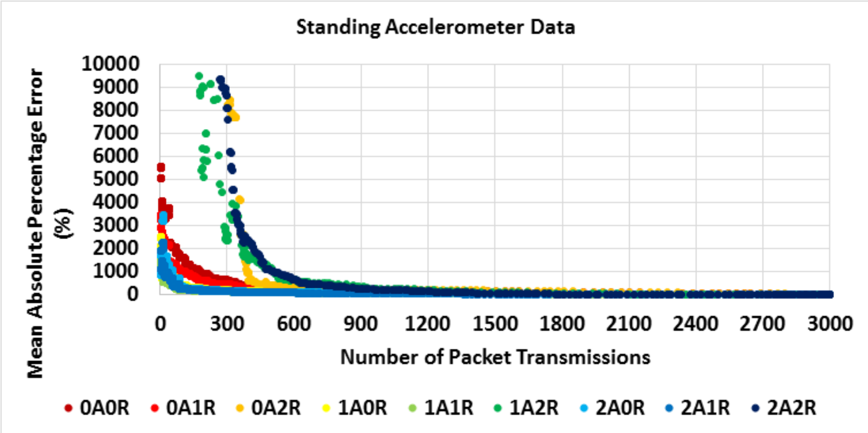

(g) Number of packet transmissions vs. mean absolute percentage error where $MAPE_{max} = 10000\%$

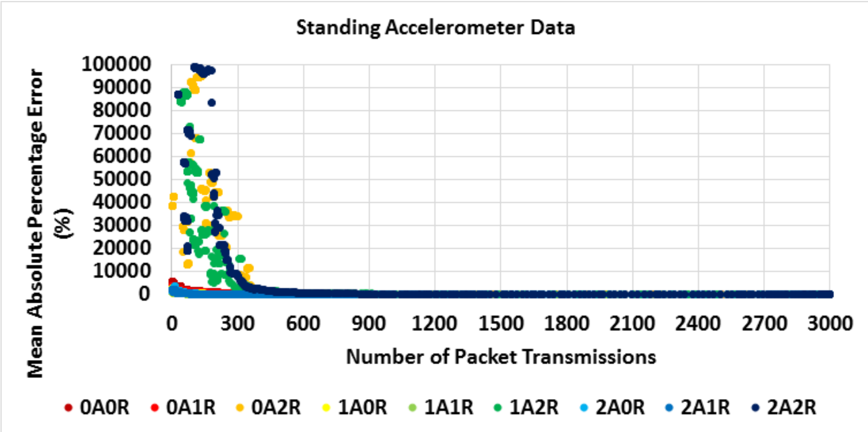

(h) Number of packet transmissions vs. mean absolute percentage error where $MAPE_{max} = 100000\%$

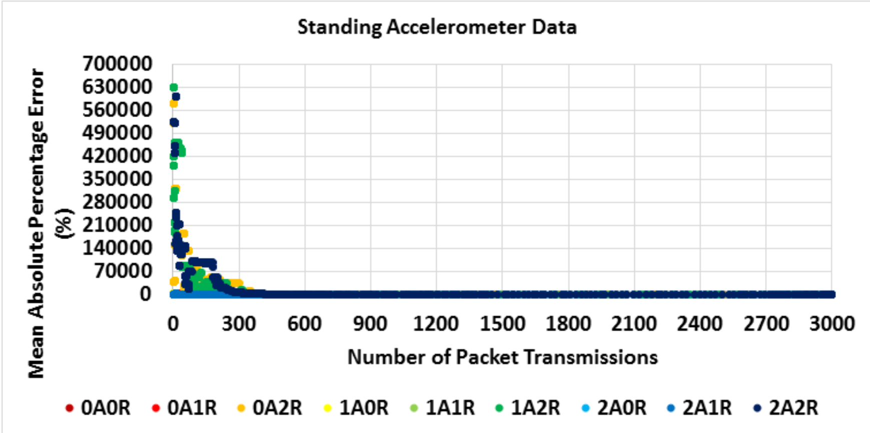

(i) Number of packet transmissions vs. mean absolute percentage error

where $MAPE_{max} = 700000\%$

Figure 5.62: Number of packet transmissions vs. mean absolute percentage error in standing accelerometer data

The results of DAR schemes in standing accelerometer data are shown more details in Table 5.39.

Table 5.39: Number of Packet Transmissions vs. Mean Absolute Percentage Error in Standing Accelerometer Data

MAPE	DAR	$NoPT_{min}$
≤2.5%	0A0R	2993
	0A1R	2993
	0A2R	2993
	1A0R	2679
	1A1R	2679
	1A2R	2718
	2A0R	2449
	2A1R	2419
	2A2R	2531

MAPE = mean absolute percentage error
DAR = data Abstraction and Reformation
0A0R = zeroth-order data abstraction & zeroth-order data reformation
0A1R = zeroth-order data abstraction & first-order data reformation
0A2R = zeroth-order data abstraction & second-order data reformation
1A0R = first-order data abstraction & zeroth-order data reformation
1A1R = first-order data abstraction & first-order data reformation
1A2R = first-order data abstraction & second-order data reformation
2A0R = second-order data abstraction & zeroth-order data reformation
2A1R = second-order data abstraction & first-order data reformation
2A2R = second-order data abstraction & second-order data reformation
$NoPT_{min}$ = minimum number of packet transmissions

From Table 5.39, it is shown that the best DAR schemes in standing accelerometer data where $MAPE = 2.5\%$ in the terms of number of packet transmissions is 2A1R.

3. Number of Data Transmitted vs. Root Mean Square Error

The comparisons of number of data transmitted against root mean square error are shown in Figure 5.63.

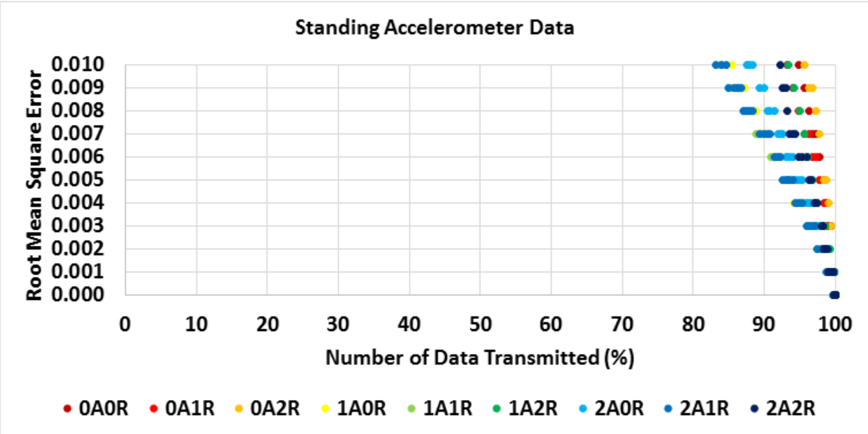

(a) Number of data transmitted vs. root mean square error where $RMSE_{max} = 0.01$

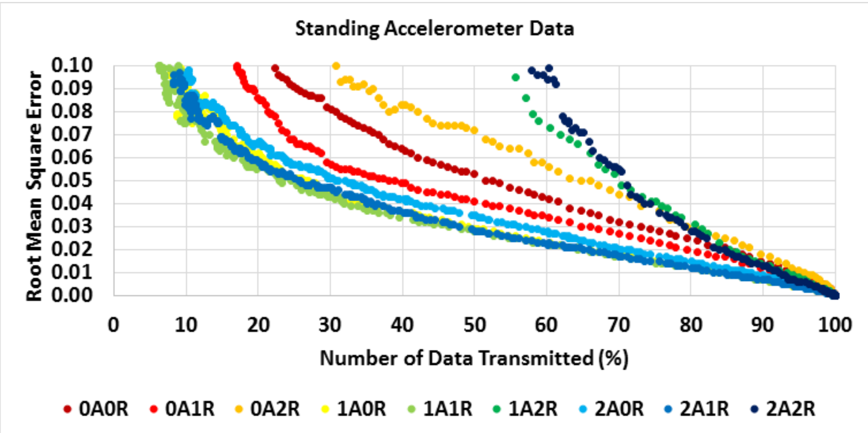

(b) Number of data transmitted vs. root mean square error where $RMSE_{max} = 0.1$

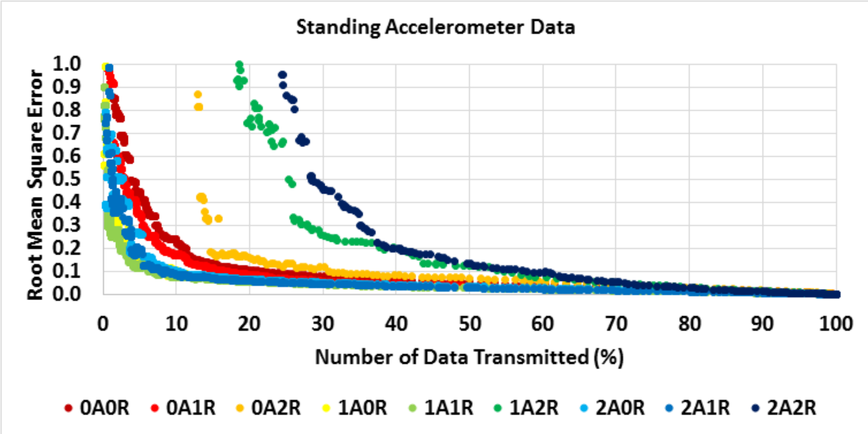

(c) Number of data transmitted vs. root mean square error where

$$RMSE_{max} = 1$$

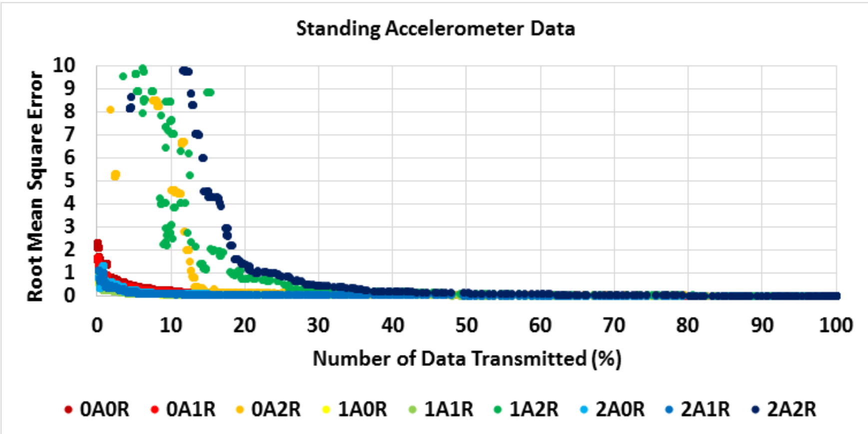

(d) Number of data transmitted vs. root mean square error where

$$RMSE_{max} = 10$$

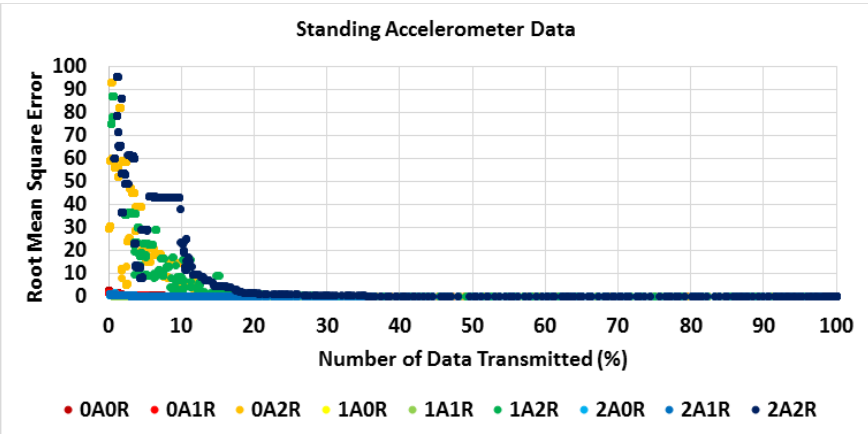

(e) Number of data transmitted vs. root mean square error where

$$RMSE_{max} = 100$$

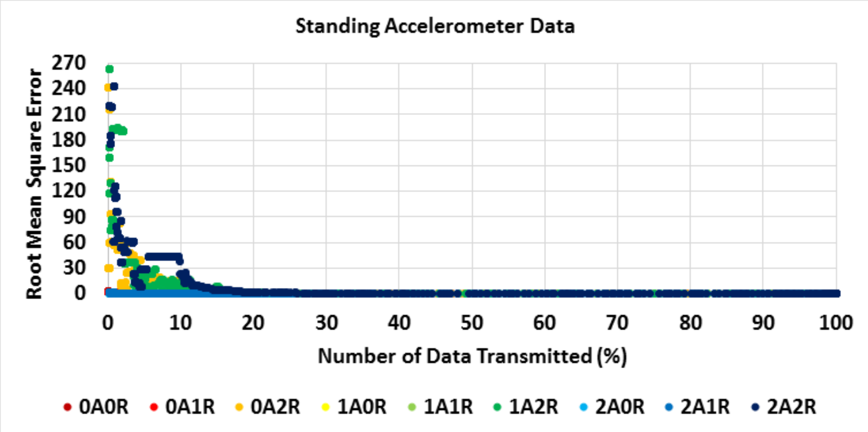

(f) Number of data transmitted vs. root mean square error where

$$\boldsymbol{RMSE_{max} = 270}$$

Figure 5.63: Number of data transmitted vs. root mean square error in standing accelerometer data

The results of DAR schemes in standing accelerometer data are shown more details in Table 5.40.

Table 5.40: Number of Data Transmitted vs. Root Mean Square Error in Standing Accelerometer Data

RMSE	DAR	$NoDT_{min}$ (%)
≤ 0.25	0A0R	8.533
	0A1R	6.233
	0A2R	14.567
	1A0R	2.233
	1A1R	1.733
	1A2R	31.200
	2A0R	3.600
	2A1R	3.833
	2A2R	37.433

RMSE = root mean square error
DAR = data Abstraction and Reformation
0A0R = zeroth-order data abstraction & zeroth-order data reformation
0A1R = zeroth-order data abstraction & first-order data reformation
0A2R = zeroth-order data abstraction & second-order data reformation
1A0R = first-order data abstraction & zeroth-order data reformation
1A1R = first-order data abstraction & first-order data reformation
1A2R = first-order data abstraction & second-order data reformation
2A0R = second-order data abstraction & zeroth-order data reformation
2A1R = second-order data abstraction & first-order data reformation
2A2R = second-order data abstraction & second-order data reformation
$NoDT_{min}$ = minimum number of data transmitted

From Table 5.40, it is shown that the best DAR schemes in standing accelerometer data where $RMSE \leq 0.25$ in the terms of number of data transmitted is 1A1R.

4. Number of Data Transmitted vs. Mean Absolute Percentage Error

The comparisons of number of data transmitted against mean absolute percentage error are shown in Figure 5.64.

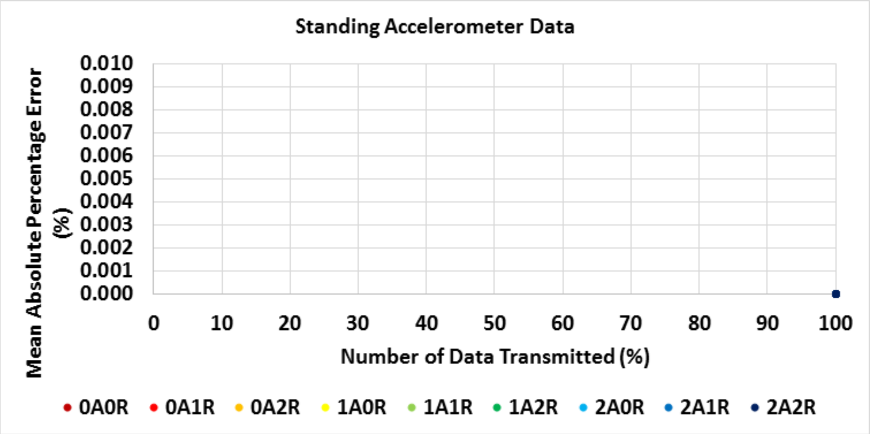

(a) Number of data transmitted vs. mean absolute percentage error where $MAPE_{max} = 0.01\%$

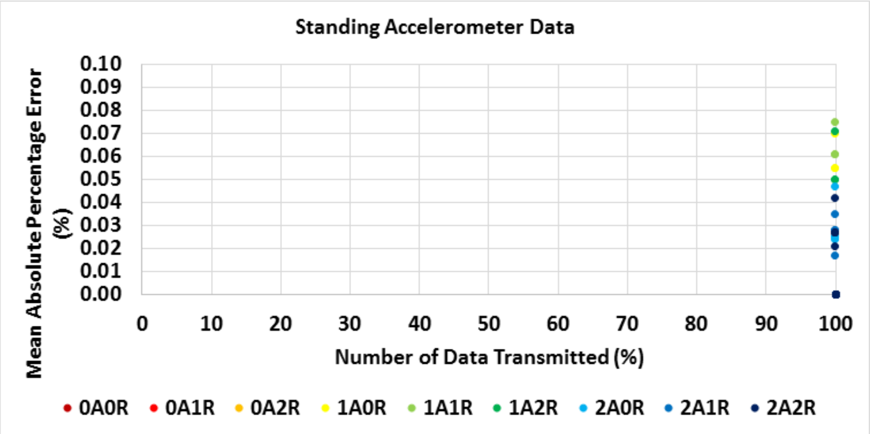

(b) Number of data transmitted vs. mean absolute percentage error where $MAPE_{max} = 0.1\%$

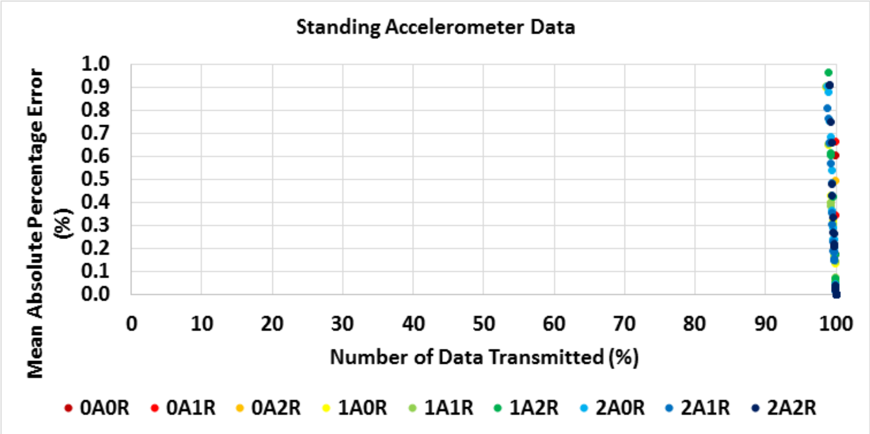

(c) Number of data transmitted vs. mean absolute percentage error where

$$MAPE_{max} = 1\%$$

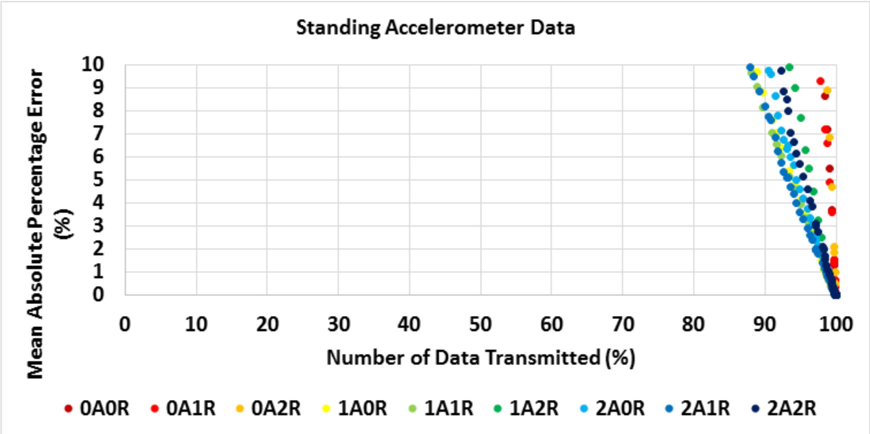

(d) Number of data transmitted vs. mean absolute percentage error where

$$MAPE_{max} = 10\%$$

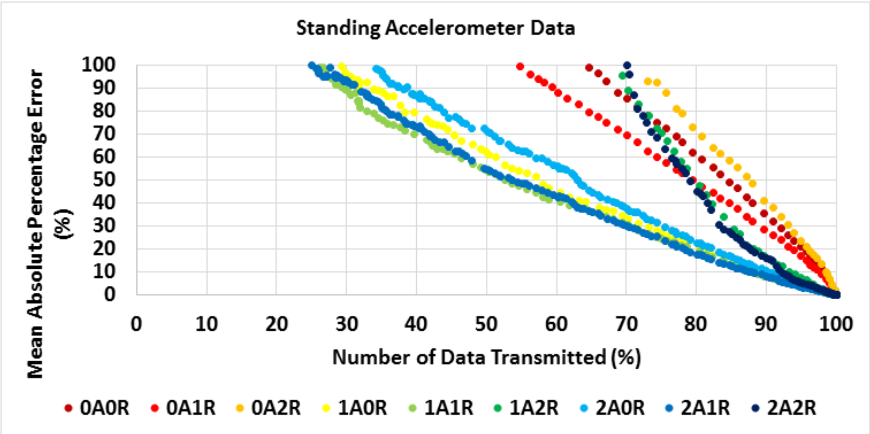

(e) Number of data transmitted vs. mean absolute percentage error where

$$MAPE_{max} = 100\%$$

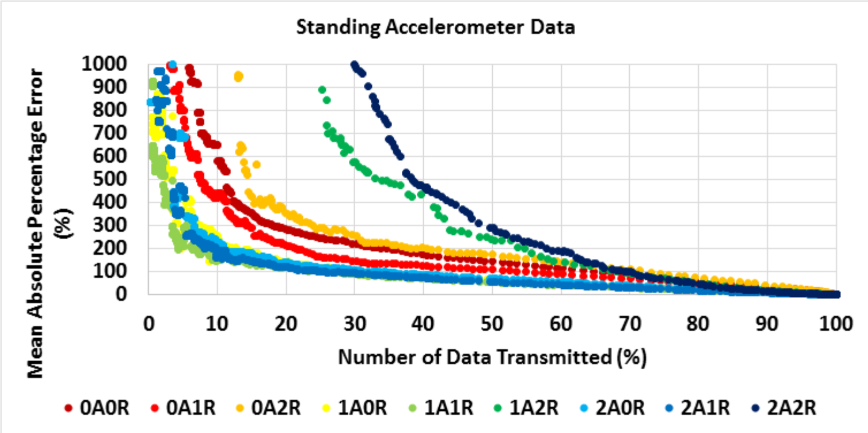

(f) Number of data transmitted vs. mean absolute percentage error where

$$MAPE_{max} = 1000\%$$

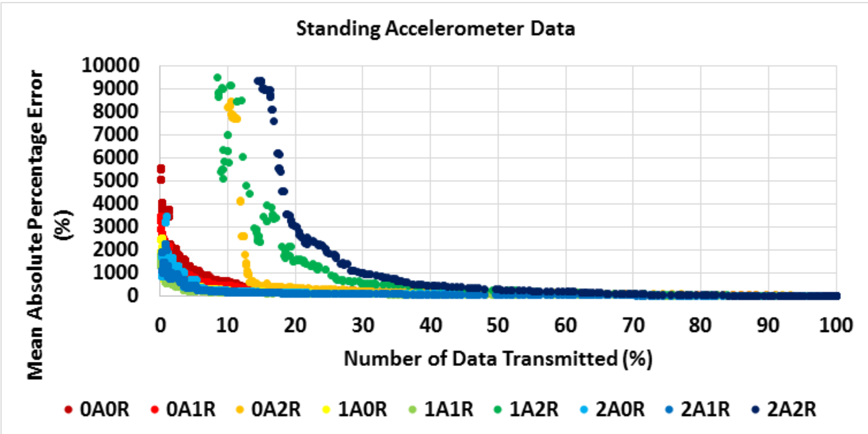

(g) Number of data transmitted vs. mean absolute percentage error where

$$MAPE_{max} = 10000\%$$

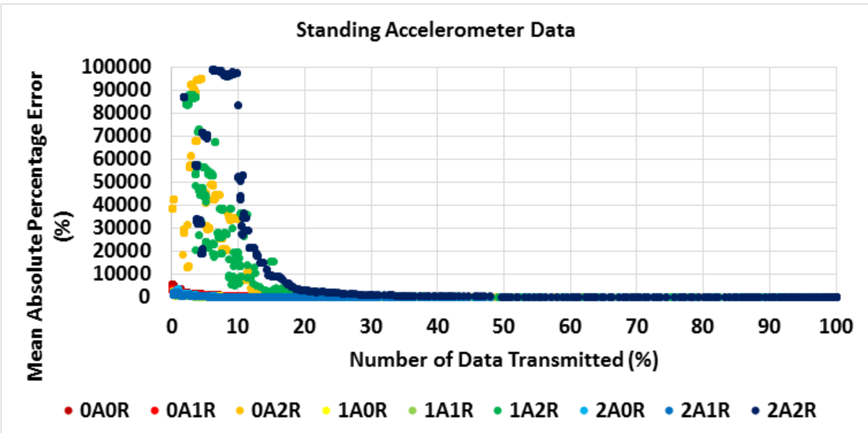

(h) Number of data transmitted vs. mean absolute percentage error where

$$MAPE_{max} = 100000\%$$

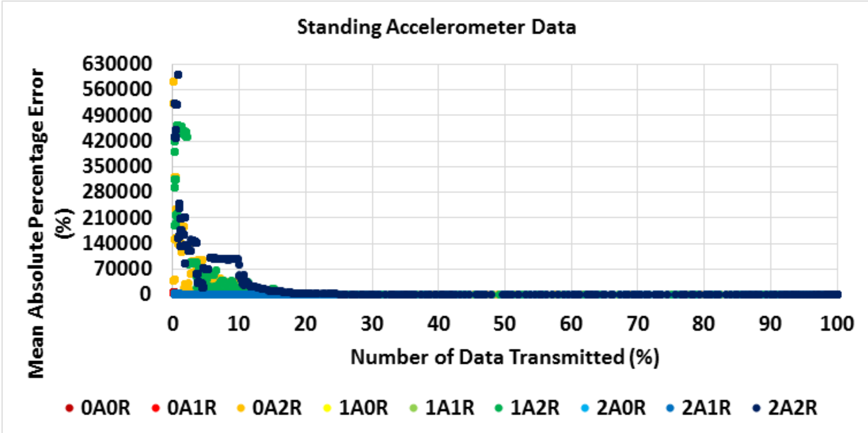

(i) Number of data transmitted vs. mean absolute percentage error where

$$\boldsymbol{MAPE_{max} = 630000\%}$$

Figure 5.64: Number of data transmitted vs. mean absolute percentage error in standing accelerometer data

The results of DAR schemes in standing accelerometer data are shown more details in Table 5.41.

Table 5.41: Number of Data Transmitted vs. Mean Absolute Percentage Error in Standing Accelerometer Data

MAPE	DAR	$NoDT_{min}$ (%)
≤ 2.5%	0A0R	99.767
	0A1R	99.767
	0A2R	99.767
	1A0R	97.500
	1A1R	97.500
	1A2R	98.033
	2A0R	97.133
	2A1R	96.633
	2A2R	98.067

MAPE = mean absolute percentage error
DAR = data Abstraction and Reformation
0A0R = zeroth-order data abstraction & zeroth-order data reformation
0A1R = zeroth-order data abstraction & first-order data reformation
0A2R = zeroth-order data abstraction & second-order data reformation
1A0R = first-order data abstraction & zeroth-order data reformation
1A1R = first-order data abstraction & first-order data reformation
1A2R = first-order data abstraction & second-order data reformation
2A0R = second-order data abstraction & zeroth-order data reformation
2A1R = second-order data abstraction & first-order data reformation
2A2R = second-order data abstraction & second-order data reformation
$NoDT_{min}$ = minimum number of data transmitted

From Table 5.41, it is shown that the best DAR schemes in standing accelerometer data where $MAPE \leq 0.25\%$ in the terms of number of data transmitted is 2A1R.

5. Root Mean Square Error vs. Number of Packet Transmissions

The comparisons of root mean square error against number of packet transmissions are shown in Figure 5.65.

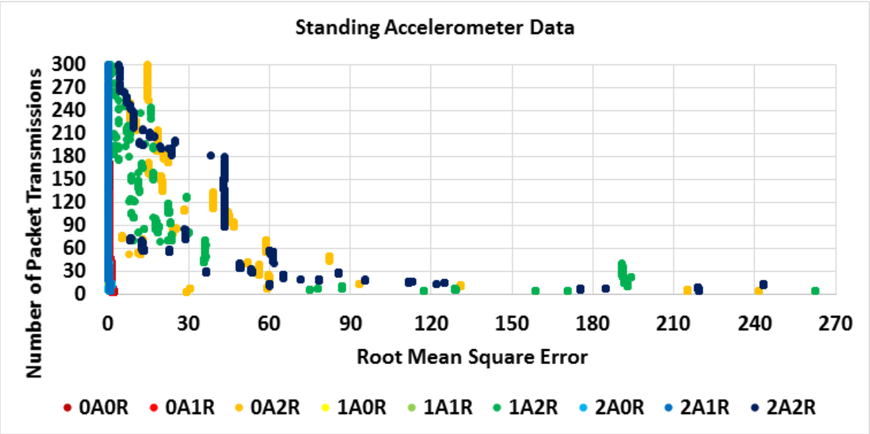

(a) Root mean square error vs. number of packet transmissions where $NoPT_{max} = 300$

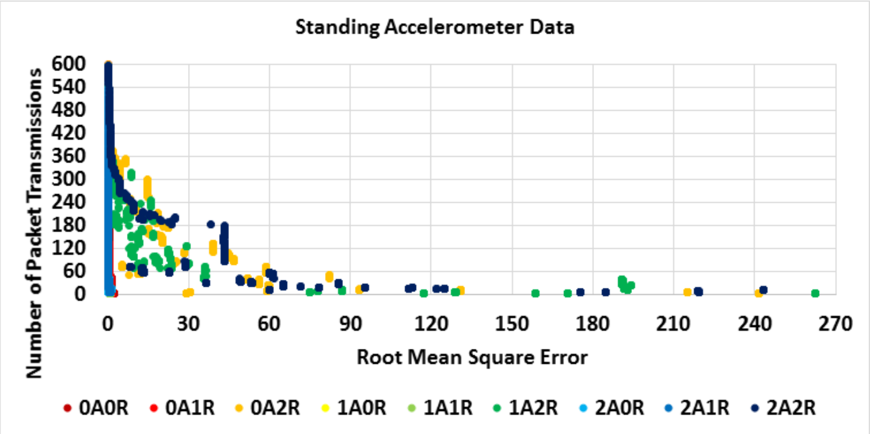

(b) Root mean square error vs. number of packet transmissions where $NoPT_{max} = 600$

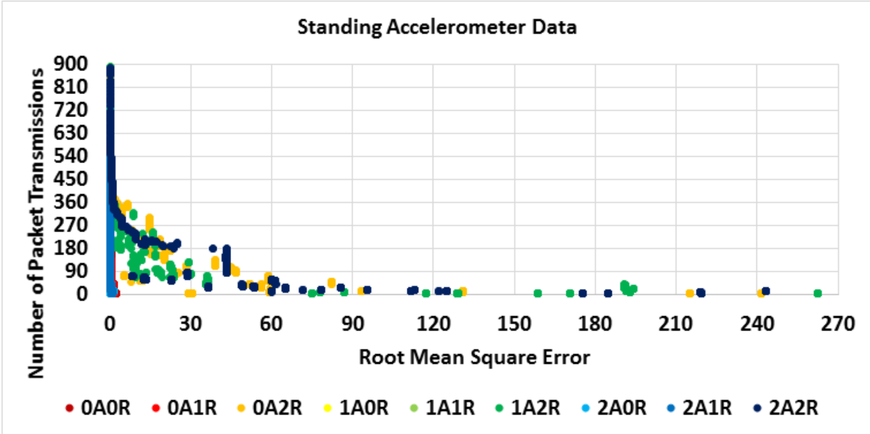

(c) Root mean square error vs. number of packet transmissions where

$$NoPT_{max} = 900$$

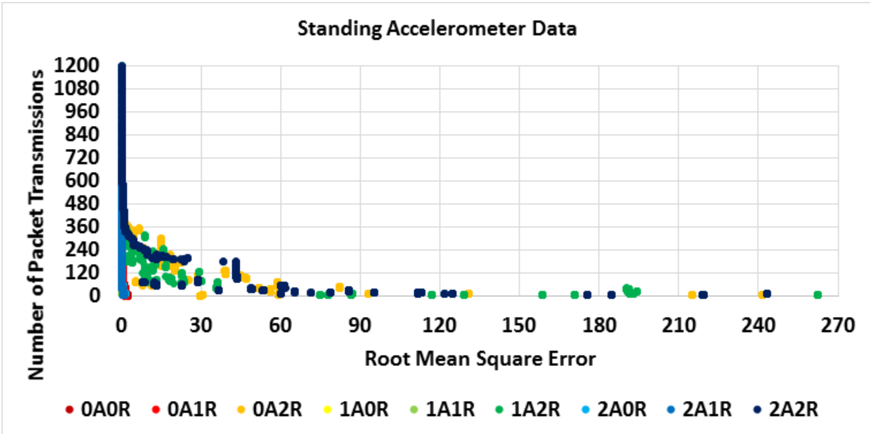

(d) Root mean square error vs. number of packet transmissions where

$$NoPT_{max} = 1200$$

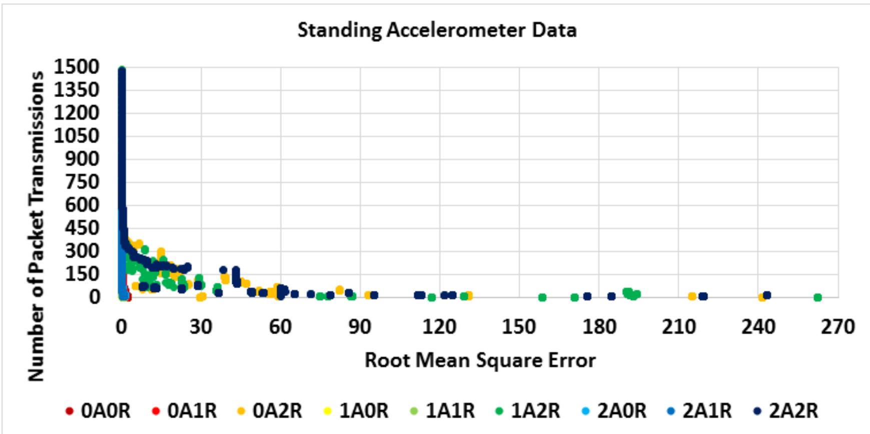

(e) Root mean square error vs. number of packet transmissions where

$$NoPT_{max} = 1500$$

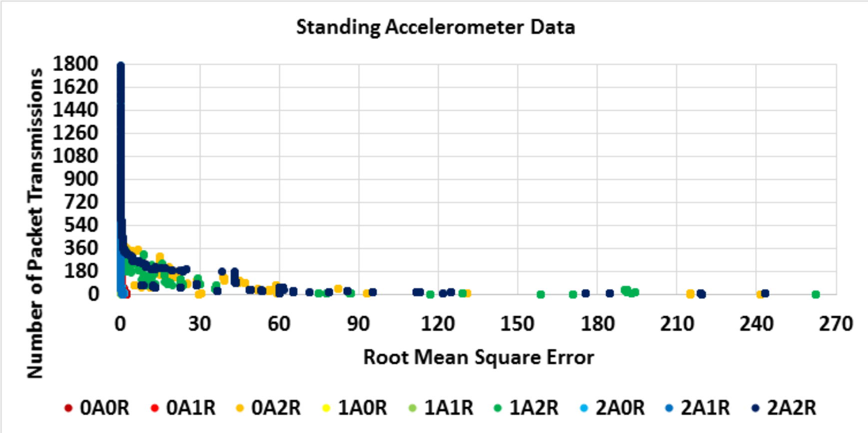

(f) Root mean square error vs. number of packet transmissions where

$$NoPT_{max} = 1800$$

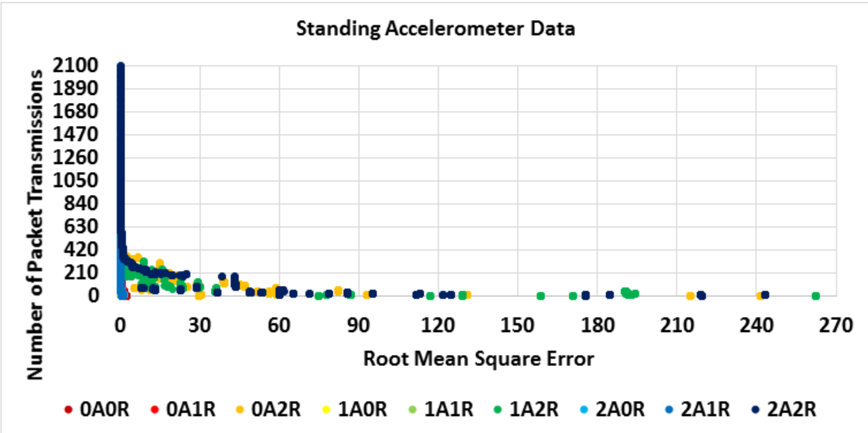

(g) Root mean square error vs. number of packet transmissions where

$$NoPT_{max} = 2100$$

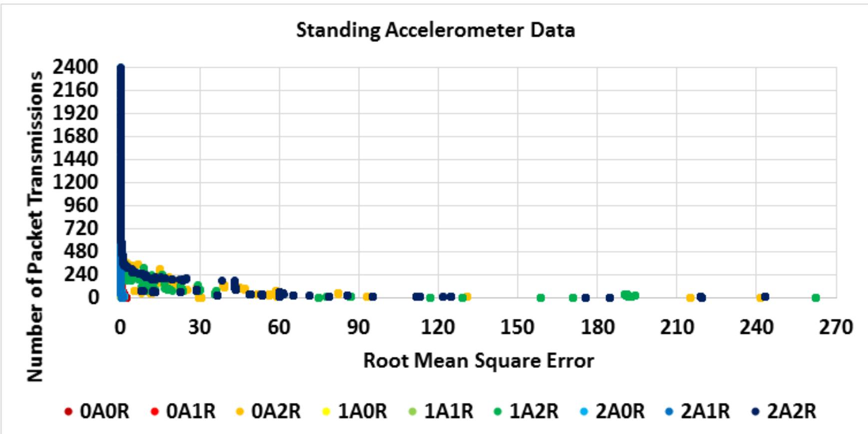

(h) Root mean square error vs. number of packet transmissions where

$$NoPT_{max} = 2400$$

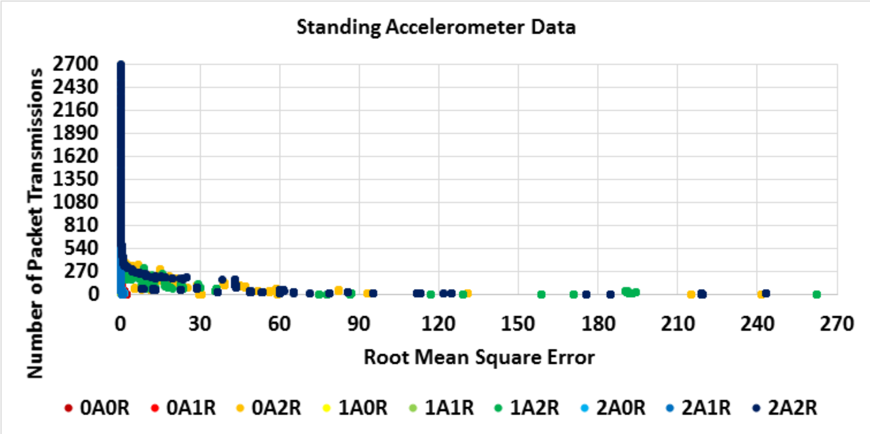

(i) Root mean square error vs. number of packet transmissions where

$$NoPT_{max} = 2700$$

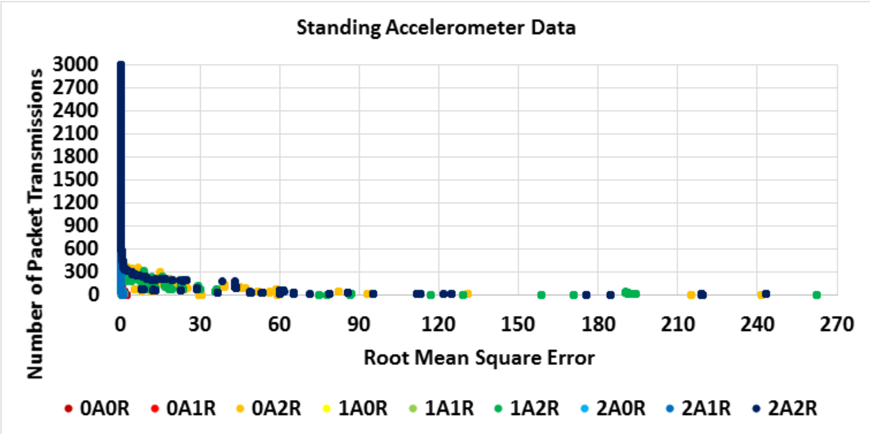

(j) Root mean square error vs. number of packet transmissions where

$$NoPT_{max} = 3000$$

Figure 5.65: Root mean square error vs. number of packet transmissions in standing accelerometer data

The results of DAR schemes in standing accelerometer data are shown more details in Table 5.42.

Table 5.42: Root Mean Square Error vs. Number of Packet Transmissions in Standing Accelerometer Data

NoPT	DAR	$RMSE_{min}$
≤ 2250	0A0R	0.029
	0A1R	0.024
	0A2R	0.039
	1A0R	0.008
	1A1R	0.007
	1A2R	0.015
	2A0R	0.006
	2A1R	0.005
	2A2R	0.007

NoPT = number of packet transmissions
DAR = data abstraction and reformation
0A0R = zeroth-order data abstraction & zeroth-order data reformation
0A1R = zeroth-order data abstraction & first-order data reformation
0A2R = zeroth-order data abstraction & second-order data reformation
1A0R = first-order data abstraction & zeroth-order data reformation
1A1R = first-order data abstraction & first-order data reformation
1A2R = first-order data abstraction & second-order data reformation
2A0R = second-order data abstraction & zeroth-order data reformation
2A1R = second-order data abstraction & first-order data reformation
2A2R = second-order data abstraction & second-order data reformation
$RMSE_{min}$ = minimum root mean square error

From Table 5.42, it is shown that the best DAR schemes in standing accelerometer data where $NoPT \leq 2250$ in the terms of root mean square error is 2A1R.

6. Root Mean Square Error vs. Number of Data Transmitted

The comparisons of root mean square error against number of data transmitted are shown in Figure 5.66.

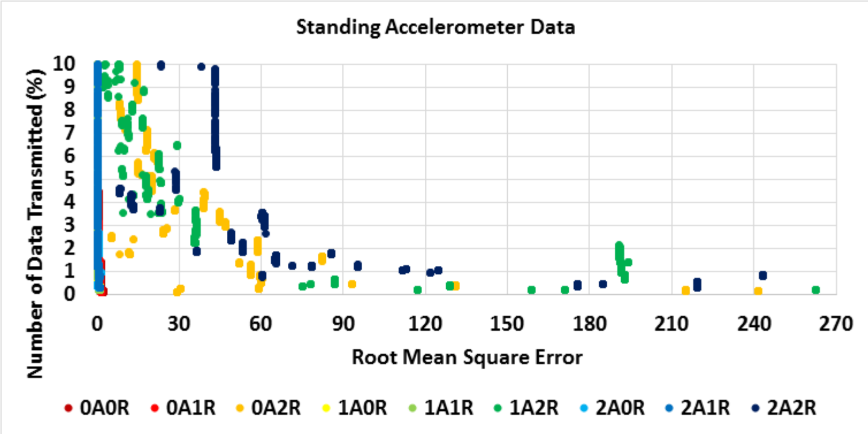

(a) Root mean square error vs. number of data transmitted where

$\boldsymbol{NoDT_{max}} = \mathbf{10\%}$

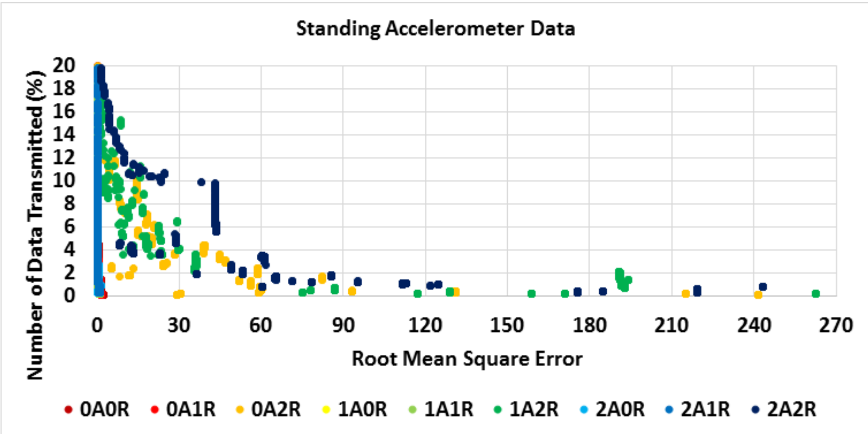

(b) Root mean square error vs. number of data transmitted where

$\boldsymbol{NoDT_{max}} = \mathbf{20\%}$

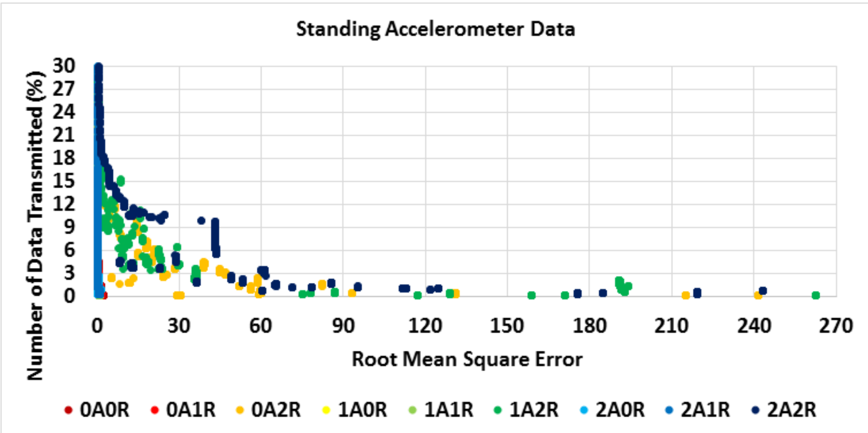

(c) Root mean square error vs. number of data transmitted (%) where

$\boldsymbol{NoDT_{max}} = \mathbf{30\%}$

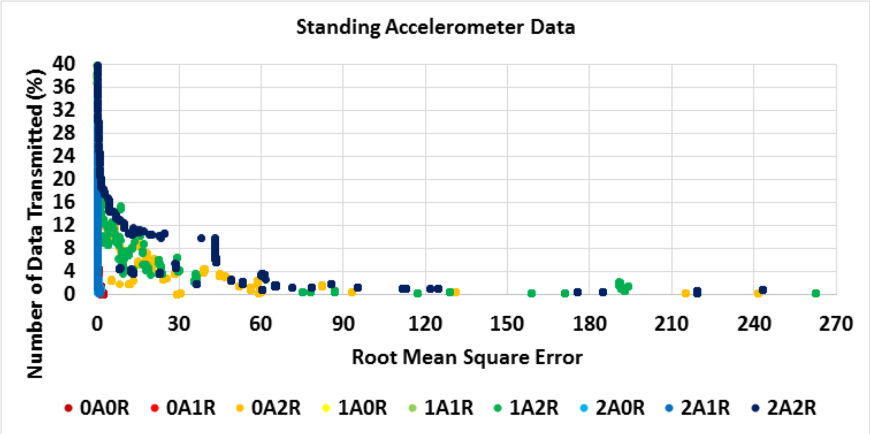

(d) Root mean square error vs. number of data transmitted where

$NoDT_{max} = 40\%$

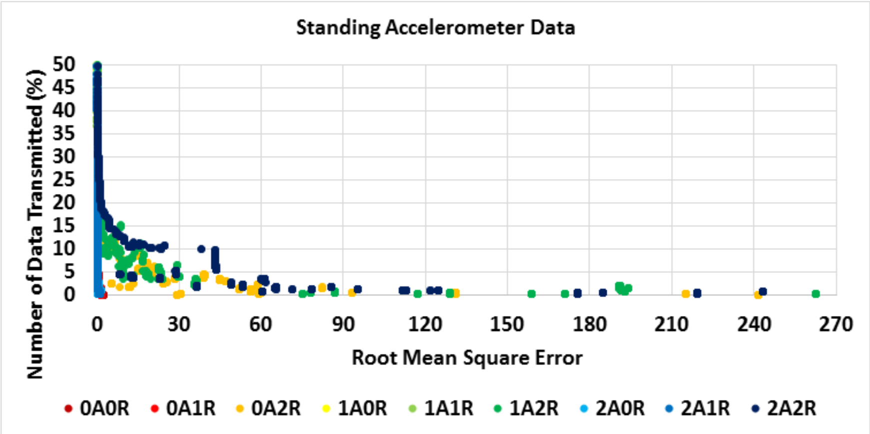

(e) Root mean square error vs. number of data transmitted where

$NoDT_{max} = 50\%$

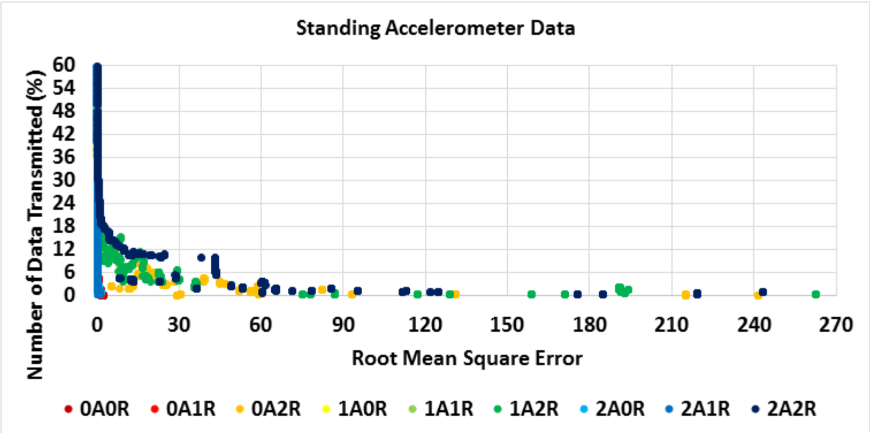

(f) Root mean square error vs. number of data transmitted where

$NoDT_{max} = 60\%$

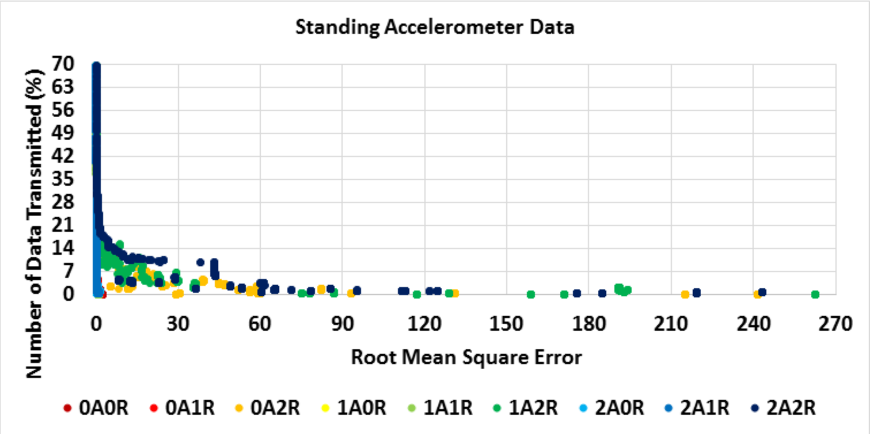

(g) Root mean square error vs. number of data transmitted where

$$NoDT_{max} = 70\%$$

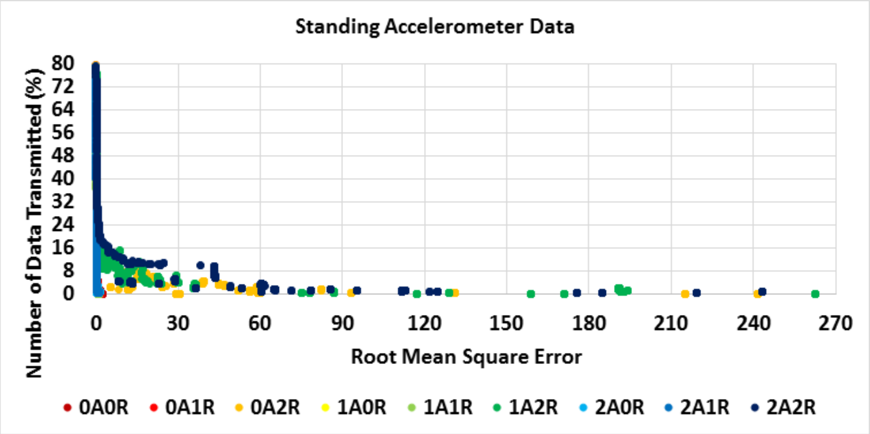

(h) Root mean square error vs. number of data transmitted where

$$NoDT_{max} = 80\%$$

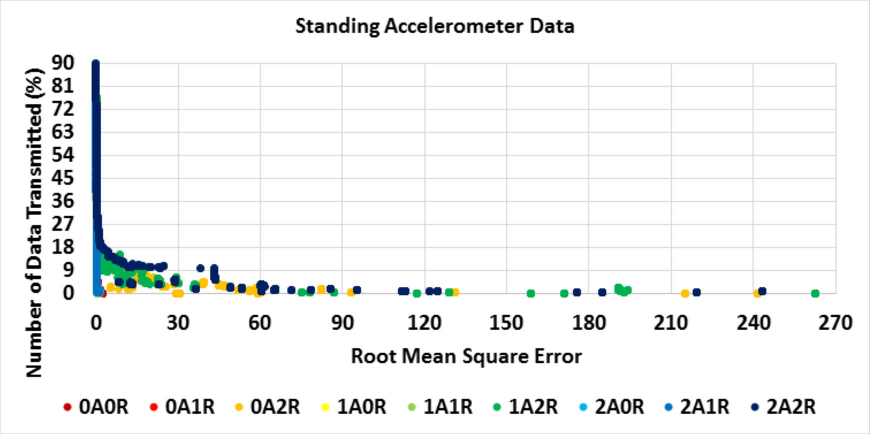

(i) Root mean square error vs. number of data transmitted where

$$NoDT_{max} = 90\%$$

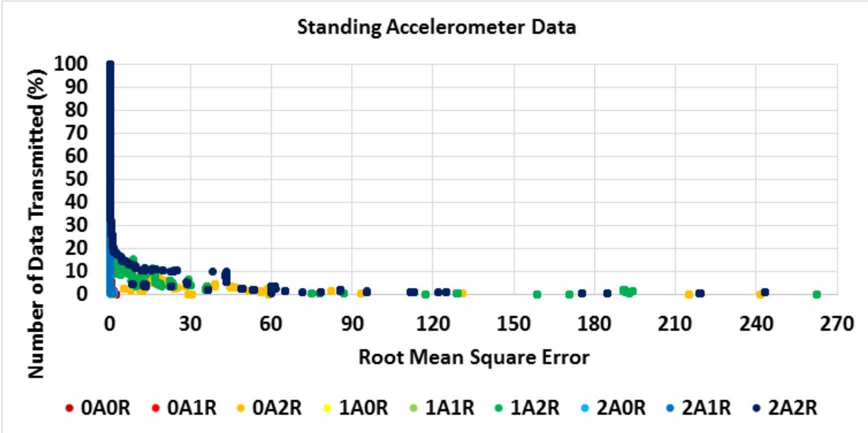

(j) Root mean square error vs. number of data transmitted where

$$NoDT_{max} = 100\%$$

Figure 5.66: Root mean square error vs. number of data transmitted in standing accelerometer data

The results of DAR schemes in standing accelerometer data are shown more details in Table 5.43.

Table 5.43: Root Mean Square Error vs. Number of Data Transmitted in Standing Accelerometer Data

NoDT	DAR	$RMSE_{min}$
≤ 75%	0A0R	0.029
	0A1R	0.024
	0A2R	0.039
	1A0R	0.015
	1A1R	0.015
	1A2R	0.041
	2A0R	0.018
	2A1R	0.015
	2A2R	0.040

NoDT = number of data transmitted
DAR = data abstraction and reformation
0A0R = zeroth-order data abstraction & zeroth-order data reformation
0A1R = zeroth-order data abstraction & first-order data reformation
0A2R = zeroth-order data abstraction & second-order data reformation
1A0R = first-order data abstraction & zeroth-order data reformation
1A1R = first-order data abstraction & first-order data reformation
1A2R = first-order data abstraction & second-order data reformation
2A0R = second-order data abstraction & zeroth-order data reformation
2A1R = second-order data abstraction & first-order data reformation
2A2R = second-order data abstraction & second-order data reformation
$RMSE_{min}$ = minimum root mean square error

From Table 5.43, it is shown that the best DAR schemes in standing accelerometer data where $NoDT \leq 75\%$ in the terms of root mean square error are 1A0R, 1A1R, and 2A1R.

7. Mean Absolute Percentage Error vs. Number of Packet Transmissions

The comparisons of mean absolute percentage error against number of packet transmissions are shown in Figure 5.67.

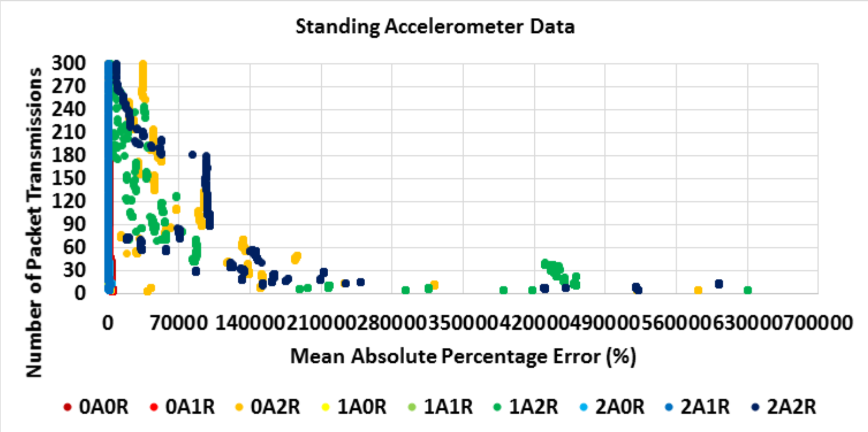

(a) Mean absolute percentage error vs. number of packet transmission where $NoPT_{max} = 300$

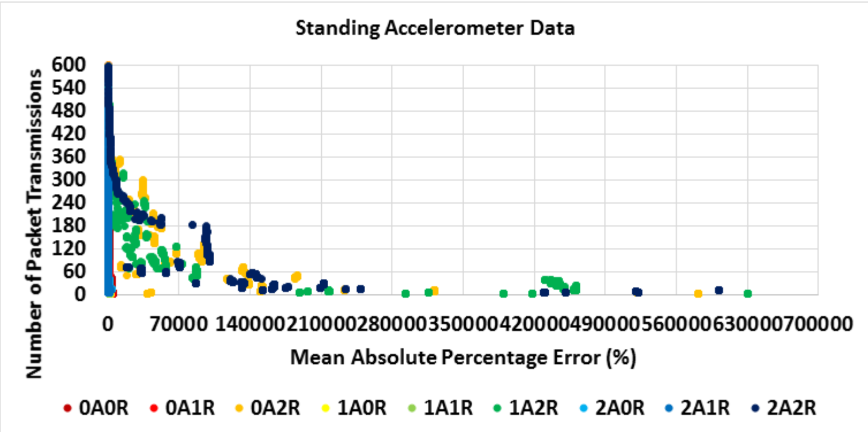

(b) Mean absolute percentage error vs. number of packet transmission where $NoPT_{max} = 600$

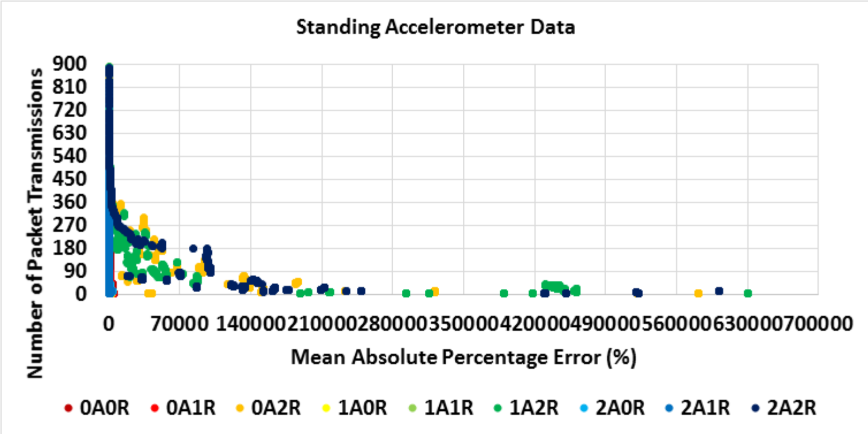

(c) Mean absolute percentage error vs. number of packet transmission

where $NoPT_{max} = 900$

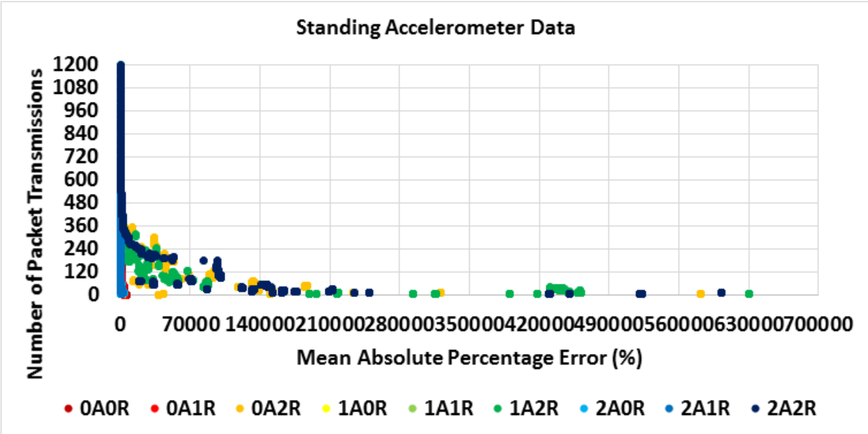

(d) Mean absolute percentage error vs. number of packet transmission

where $NoPT_{max} = 1200$

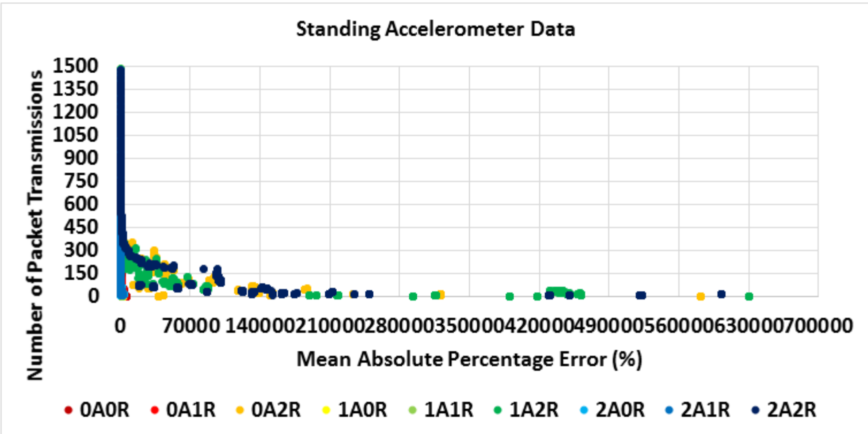

(e) Mean absolute percentage error vs. number of packet transmission

where $NoPT_{max} = 1500$

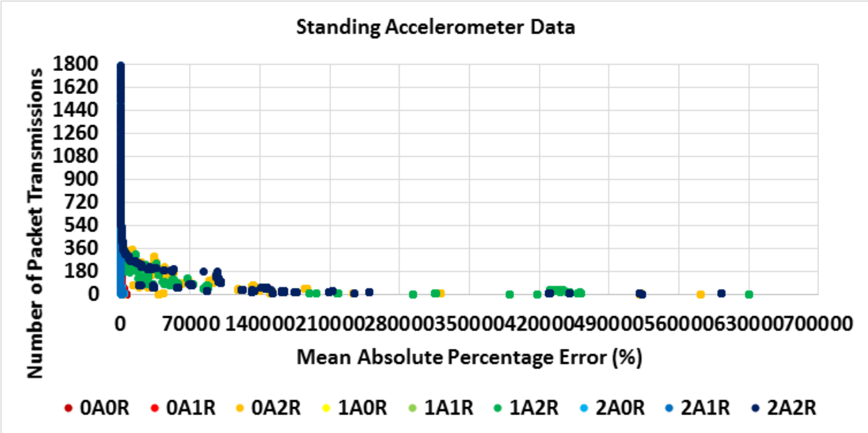

(f) Mean absolute percentage error vs. number of packet transmission where $NoPT_{max} = 1800$

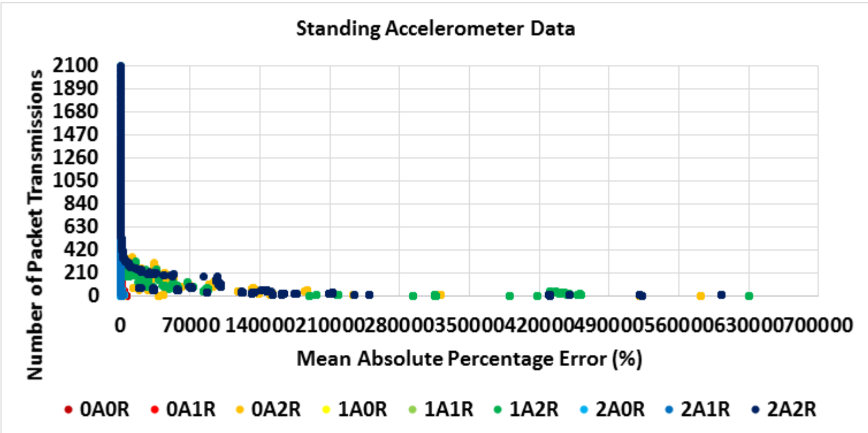

(g) Mean absolute percentage error vs. number of packet transmission where $NoPT_{max} = 2100$

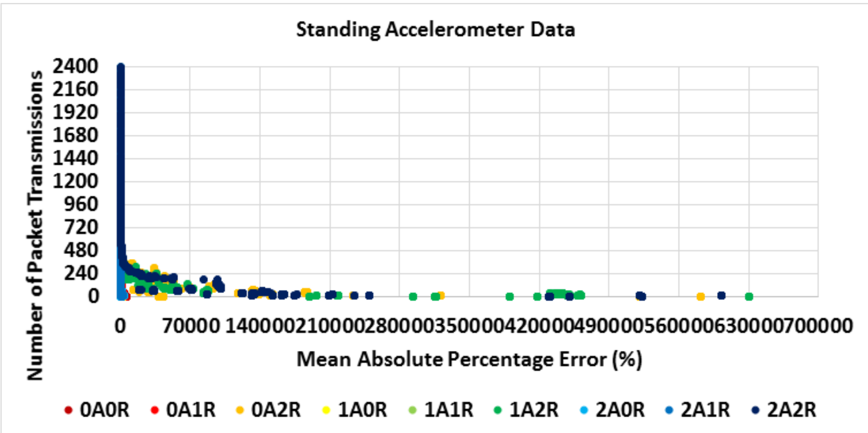

(h) Mean absolute percentage error vs. number of packet transmission where $NoPT_{max} = 2400$

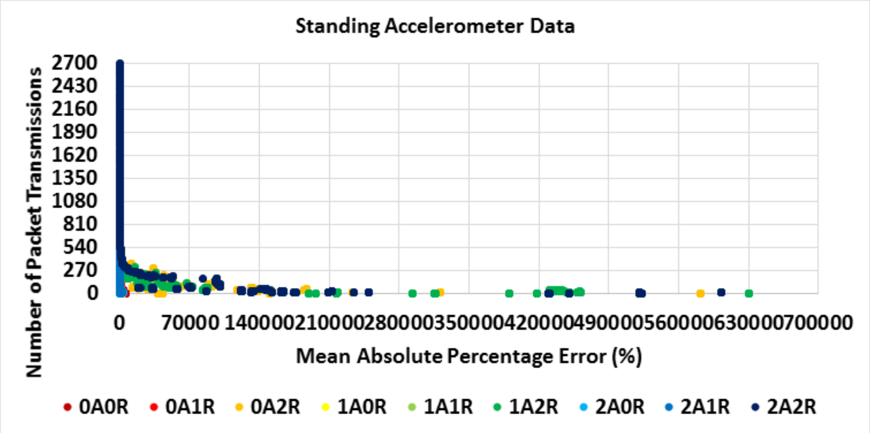

(i) Mean absolute percentage error vs. number of packet transmission where $NoPT_{max} = 2700$

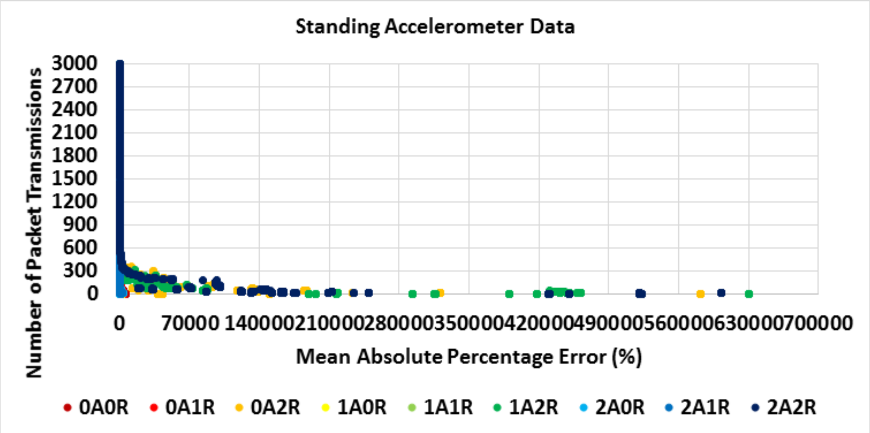

(j) Mean absolute percentage error vs. number of packet transmission where $NoPT_{max} = 3000$

Figure 5.67: Mean absolute percentage error vs. number of packet transmissions in standing accelerometer data

The results of DAR schemes in standing accelerometer data are shown more details in Table 5.44.

Table 5.44: Mean Absolute Percentage Error vs. Number of Packet Transmissions in Standing Accelerometer Data

NoPT	DAR	$MAPE_{min}$ (%)
≤ 2250	0A0R	75.065
	0A1R	60.019
	0A2R	92.369
	1A0R	9.706
	1A1R	9.019
	1A2R	18.856
	2A0R	6.006
	2A1R	4.692
	2A2R	7.056

NoPT = number of packet transmissions
DAR = data abstraction and reformation
0A0R = zeroth-order data abstraction & zeroth-order data reformation
0A1R = zeroth-order data abstraction & first-order data reformation
0A2R = zeroth-order data abstraction & second-order data reformation
1A0R = first-order data abstraction & zeroth-order data reformation
1A1R = first-order data abstraction & first-order data reformation
1A2R = first-order data abstraction & second-order data reformation
2A0R = second-order data abstraction & zeroth-order data reformation
2A1R = second-order data abstraction & first-order data reformation
2A2R = second-order data abstraction & second-order data reformation
$MAPE_{min}$ = minimum mean absolute percentage error

From Table 5.44, it is shown that the best DAR schemes in standing accelerometer data where $NoPT \leq 2250$ in the terms of mean absolute percentage error is 2A1R.

8. Mean Absolute Percentage Error vs. Number of Data Transmitted

The comparisons of mean absolute percentage error against number of data transmitted are shown in Figure 5.68.

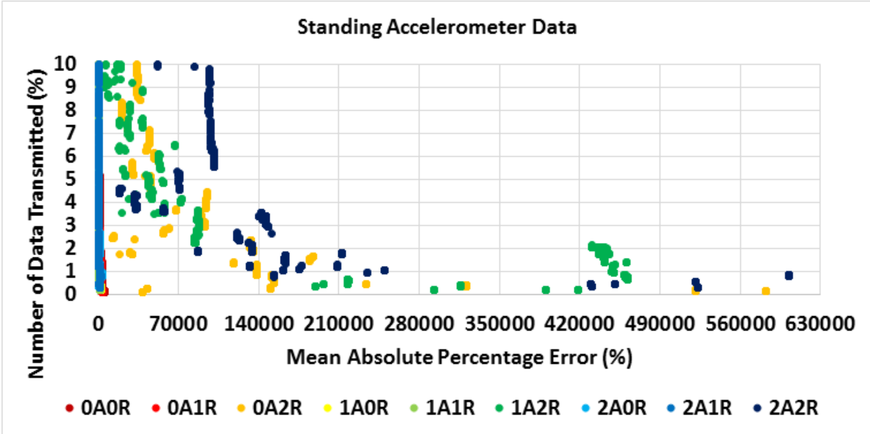

(a) Mean absolute percentage error vs. number of data transmitted where

$NoDT_{max} = 10\%$

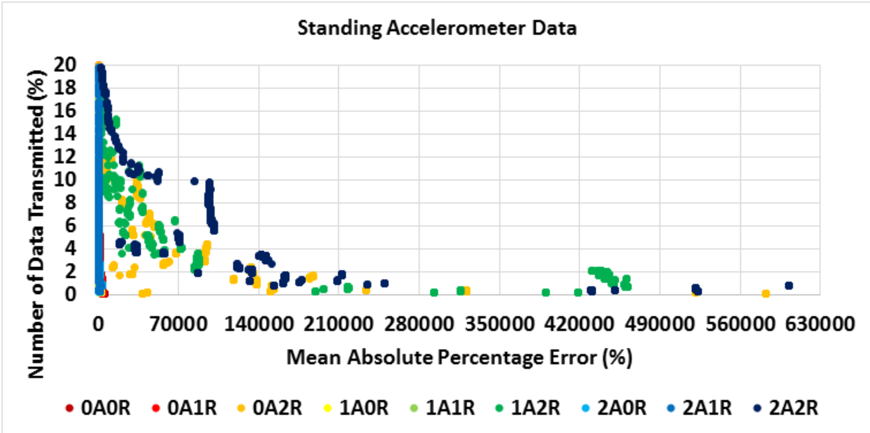

(b) Mean absolute percentage error vs. number of data transmitted where

$NoDT_{max} = 20\%$

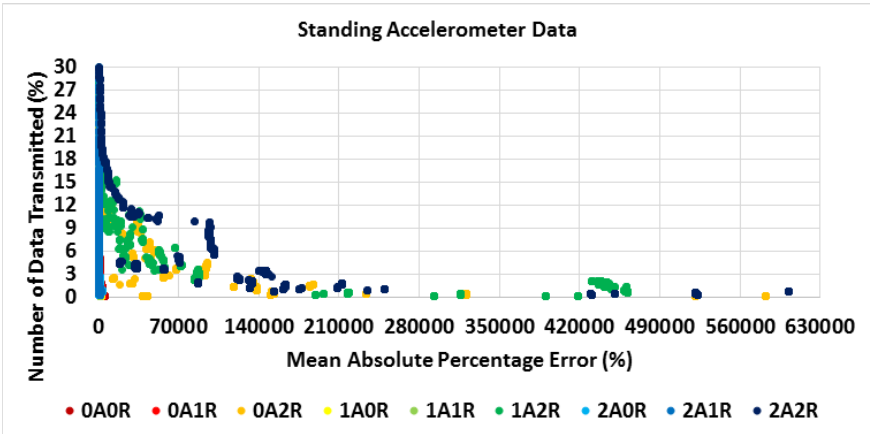

(c) Mean absolute percentage error vs. number of data transmitted where

$NoDT_{max} = 30\%$

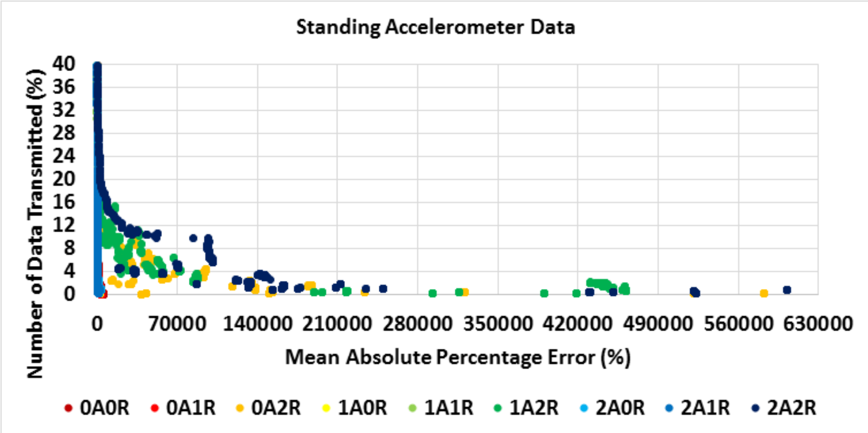

(d) Mean absolute percentage error vs. number of data transmitted where

$NoDT_{max} = 40\%$

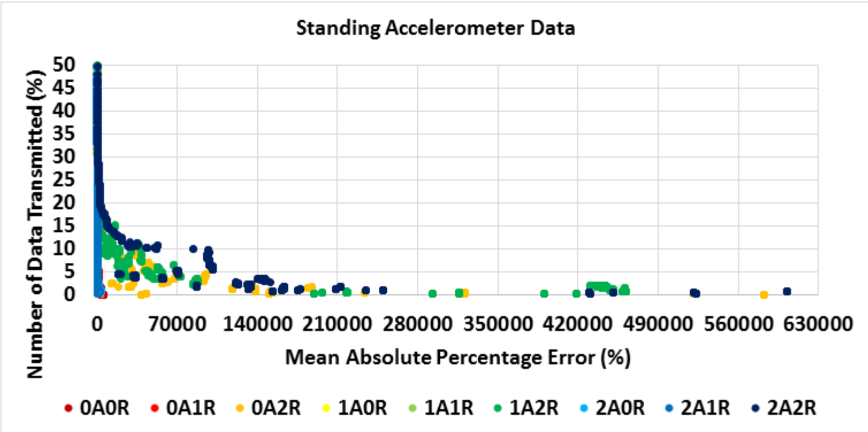

(e) Mean absolute percentage error vs. number of data transmitted where

$NoDT_{max} = 50\%$

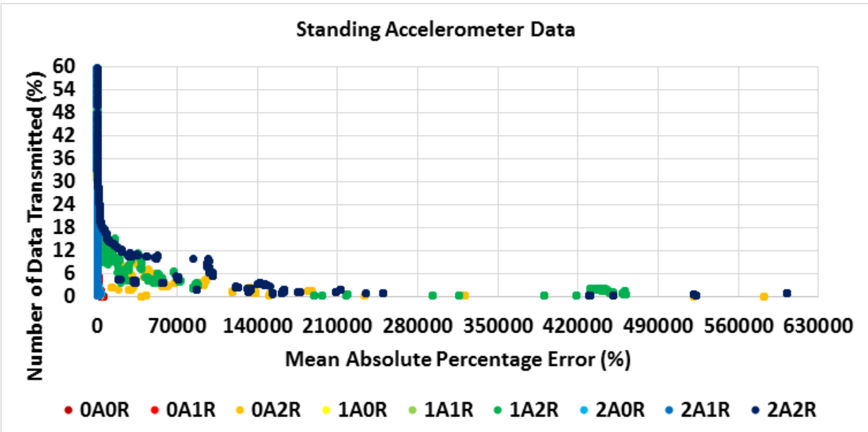

(f) Mean absolute percentage error vs. number of data transmitted where

$NoDT_{max} = 60\%$

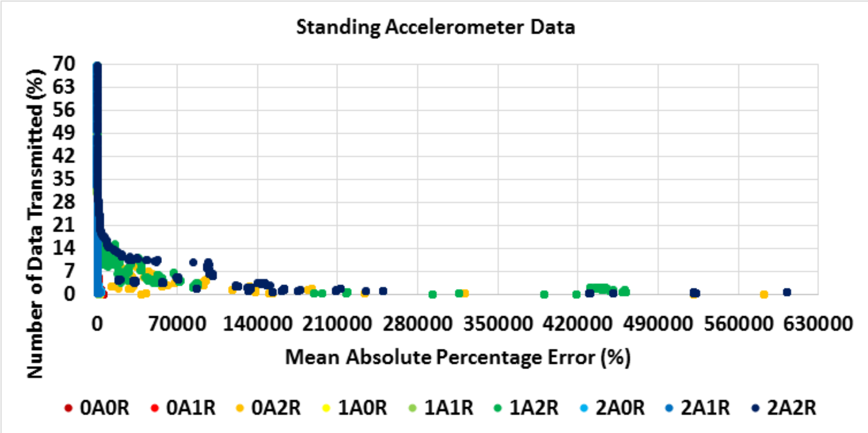

(g) Mean absolute percentage error vs. number of data transmitted where

$$NoDT_{max} = 70\%$$

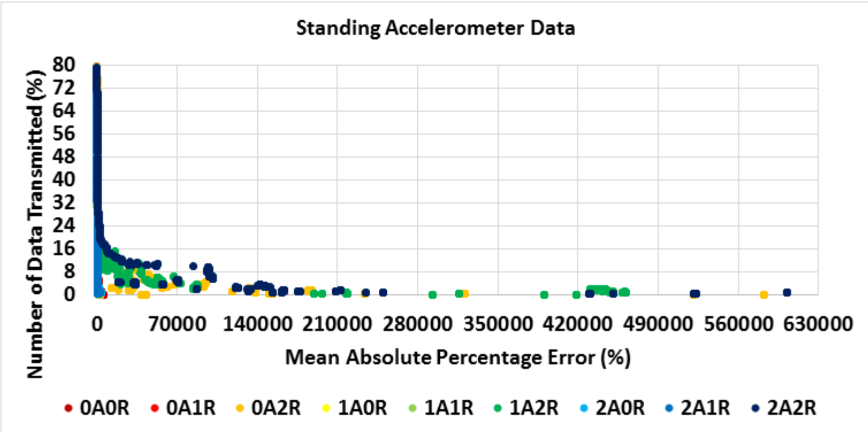

(h) Mean absolute percentage error vs. number of data transmitted where

$$NoDT_{max} = 80\%$$

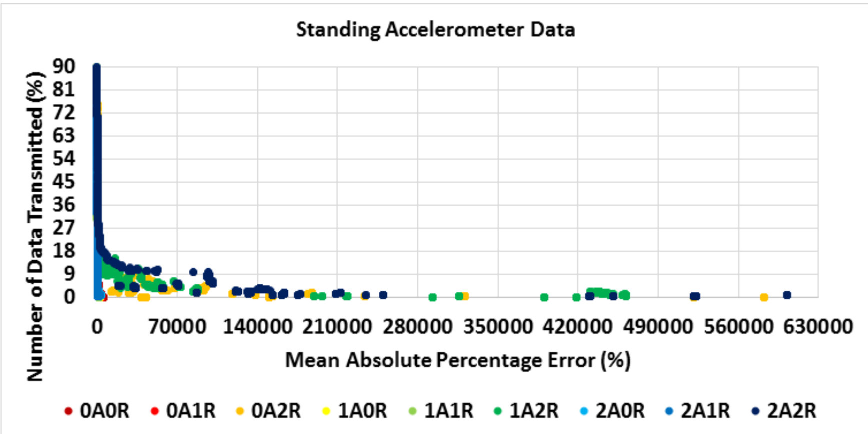

(i) Mean absolute percentage error vs. number of data transmitted where

$$NoDT_{max} = 90\%$$

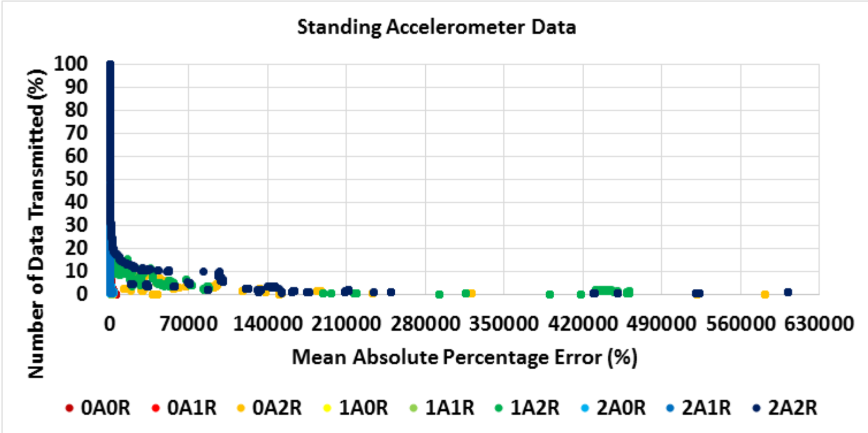

(j) Mean absolute percentage error vs. number of data transmitted where $NoDT_{max} = 100\%$

Figure 5.68: Mean absolute percentage error vs. number of data transmitted in standing accelerometer data

The results of DAR schemes in standing accelerometer data are shown more details in Table 5.45.

Table 5.45: Mean Absolute Percentage Error vs. Number of Data Transmitted in Standing Accelerometer Data

NoDT	DAR	$MAPE_{min}$ (%)
≤ 75%	0A0R	75.065
	0A1R	60.019
	0A2R	92.369
	1A0R	28.188
	1A1R	25.181
	1A2R	72.377
	2A0R	31.636
	2A1R	25.341
	2A2R	68.645

NoDT = number of data transmitted
DAR = data abstraction and reformation
0A0R = zeroth-order data abstraction & zeroth-order data reformation
0A1R = zeroth-order data abstraction & first-order data reformation
0A2R = zeroth-order data abstraction & second-order data reformation
1A0R = first-order data abstraction & zeroth-order data reformation
1A1R = first-order data abstraction & first-order data reformation
1A2R = first-order data abstraction & second-order data reformation
2A0R = second-order data abstraction & zeroth-order data reformation
2A1R = second-order data abstraction & first-order data reformation
2A2R = second-order data abstraction & second-order data reformation
$MAPE_{min}$ = minimum mean absolute percentage error

From Table 5.45, it is shown that the best DAR schemes in standing accelerometer data where $NoDT \leq 75\%$ in the terms of mean absolute percentage error is 1A1R.

9. Conclusion

From Table 5.38 – 5.45, it is concluded in Table 5.46, that the best DAR schemes in standing accelerometer data is 2A1R.

Table 5.46: Results of DAR Schemes in Standing Accelerometer Data

(a) Best DAR Schemes in Standing Accelerometer Data where the $NoPT \leq 2250$ and $NoDT \leq 75\%$

DAR	Th	NoPT	NoDT(%)	RMSE	MAPE(%)
0A0R	0.032	2232	74.400	0.029	75.065
0A1R	0.032	2232	74.400	0.024	60.019
0A2R	0.032	2232	74.400	0.040	92.369
1A0R	0.046	1724	74.467	0.015	28.188
1A1R	0.046	1724	74.467	0.015	25.181
1A2R	0.046	1724	74.467	0.041	72.377
2A0R	0.090	1476	74.400	0.018	31.636
2A1R	0.090	1476	74.400	0.015	25.341
2A2R	0.090	1476	74.400	0.040	68.645

(b) Best DAR Schemes in Standing Accelerometer Data where the $RMSE \leq 0.25$ and $MAPE \leq 2.5\%$

DAR	Th	NoPT	NoDT(%)	RMSE	MAPE(%)
0A0R	0.005	2993	99.767	0.001	1.450
0A1R	0.005	2993	99.767	0.001	1.559
0A2R	0.005	2993	99.767	0.001	2.081
1A0R	0.021	2679	97.500	0.002	1.984
1A1R	0.021	2679	97.500	0.003	2.098
1A2R	0.020	2718	98.033	0.003	2.482
2A0R	0.048	2449	97.133	0.003	2.487
2A1R	0.049	2419	96.633	0.003	2.398
2A2R	0.045	2531	98.067	0.003	2.112

DAR = data abstraction and reformation
Th = threshold
NoPT = number of packet transmissions
NoDT = number of packet transmitted
RMSE = root mean square error
MAPE = mean absolute percentage error

5.3.6 Walking Accelerometer Data

The comparisons among parameters (number of packet transmissions, number of data transmitted, root mean square error, and mean absolute percentage error) are as follows.

1. Number of Packet Transmissions vs. Root Mean Square Error

   The comparisons of number of packet transmissions against root mean square error are shown in Figure 5.69.

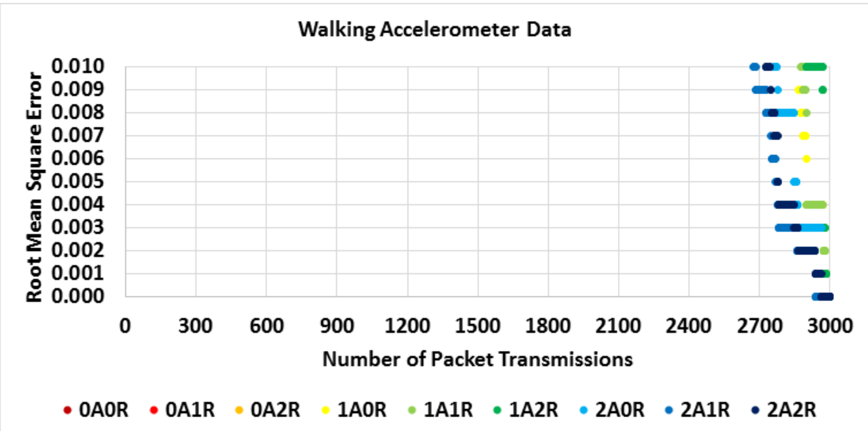

(a) Number of packet transmissions vs. root mean square error where $RMSE_{max} = 0.01$

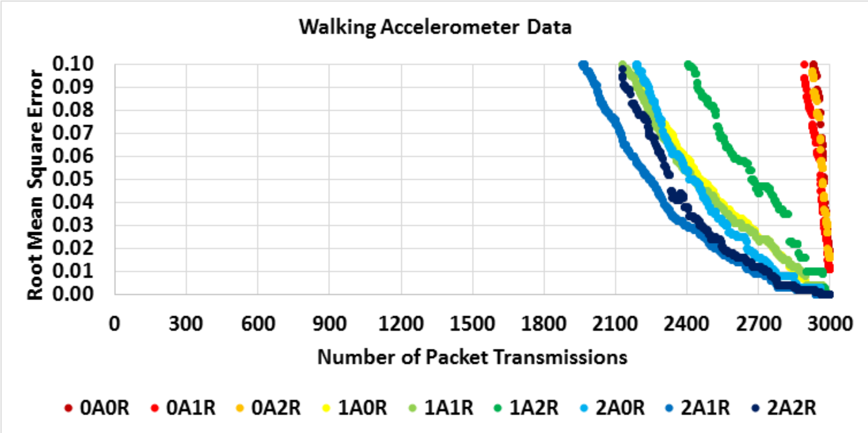

(b) Number of packet transmissions vs. root mean square error where

$$RMSE_{max} = 0.1$$

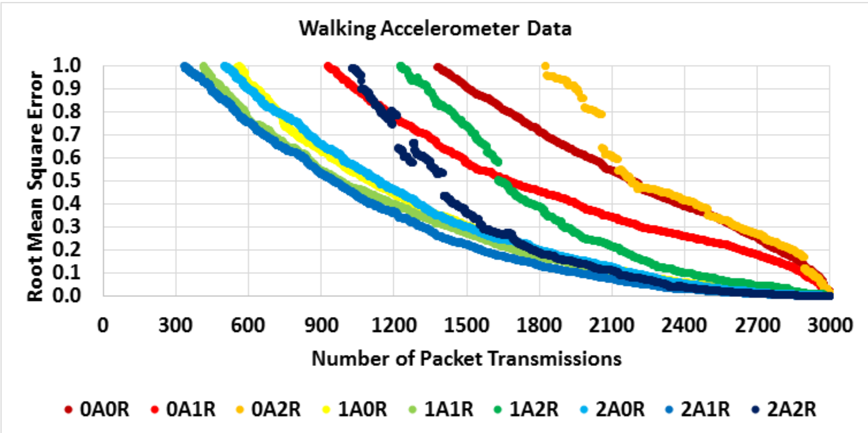

(c) Number of packet transmissions vs. root mean square error where

$$RMSE_{max} = 1$$

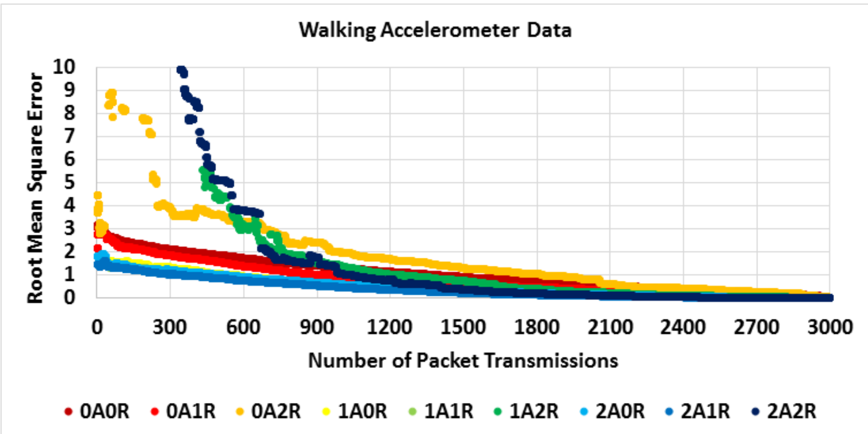

(d) Number of packet transmissions vs. root mean square error where

$$RMSE_{max} = 10$$

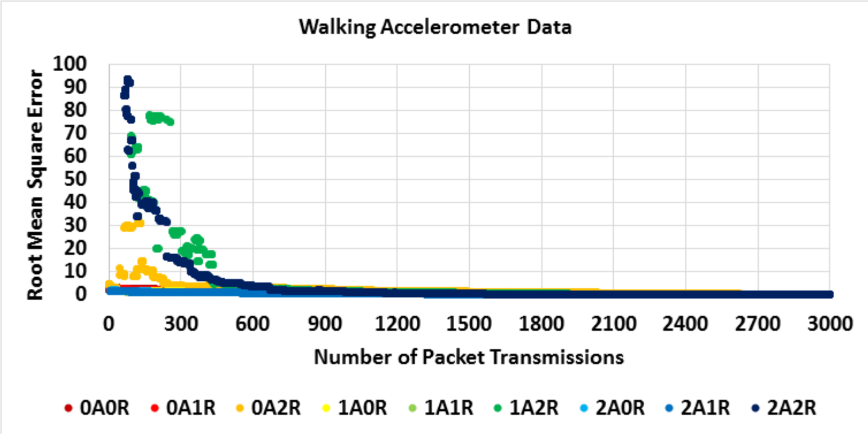

(e) Number of packet transmissions vs. root mean square error where

$$RMSE_{max} = 100$$

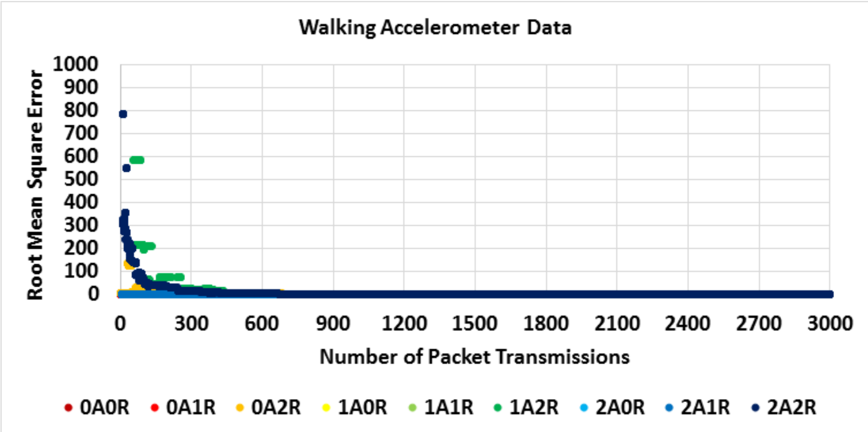

(f) Number of packet transmissions vs. root mean square error where

$$RMSE_{max} = 1000$$

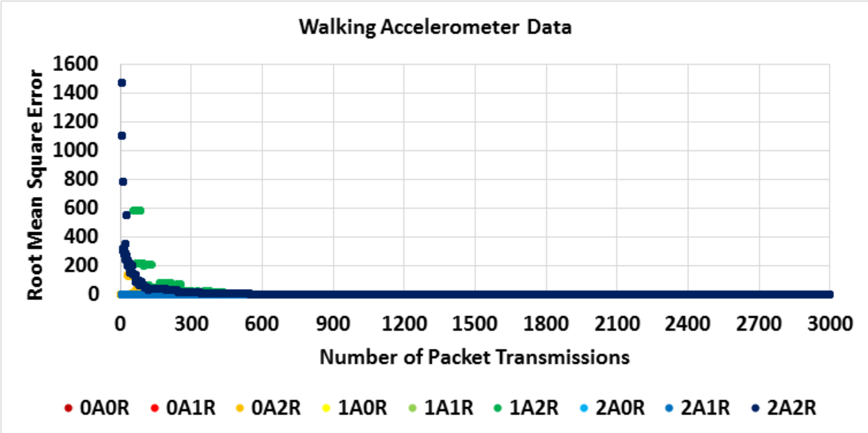

(g) Number of packet transmissions vs. root mean square error where

$$RMSE_{max} = 1600$$

Figure 5.69: Number of packet transmissions vs. root mean square error in walking accelerometer data

The results of DAR schemes in walking accelerometer data are shown more details in Table 5.47.

Table 5.47: Number of Packet Transmissions vs. Root Mean Square Error in Walking Accelerometer Data

RMSE	DAR	$NoPT_{min}$
≤ 0.25	0A0R	2706
	0A1R	2447
	0A2R	2733
	1A0R	1646
	1A1R	1566
	1A2R	1985
	2A0R	1622
	2A1R	1408
	2A2R	1692

RMSE = root mean square error
DAR = data abstraction and reformation
0A0R = zeroth-order data abstraction & zeroth-order data reformation
0A1R = zeroth-order data abstraction & first-order data reformation
0A2R = zeroth-order data abstraction & second-order data reformation
1A0R = first-order data abstraction & zeroth-order data reformation
1A1R = first-order data abstraction & first-order data reformation
1A2R = first-order data abstraction & second-order data reformation
2A0R = second-order data abstraction & zeroth-order data reformation
2A1R = second-order data abstraction & first-order data reformation
2A2R = second-order data abstraction & second-order data reformation
$NoPT_{min}$ = minimum number of packet transmissions

From Table 5.47, it is shown that the best DAR schemes in walking accelerometer data where $RMSE \leq 0.25$ in the terms of number of packet transmissions is 2A1R.

2. Number of Packet Transmissions vs. Mean Absolute Percentage Error

The comparisons of number of packet transmissions against mean absolute percentage error are shown in Figure 5.70.

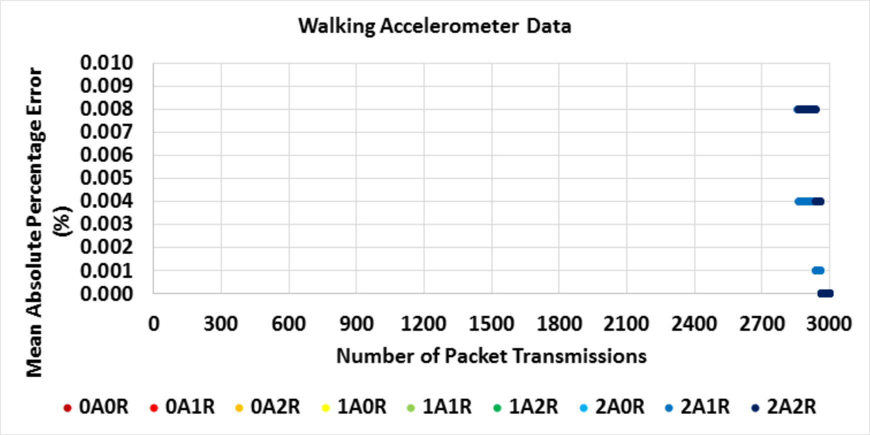

(a) Number of packet transmissions vs. mean absolute percentage error where $MAPE_{max} = 0.01\%$

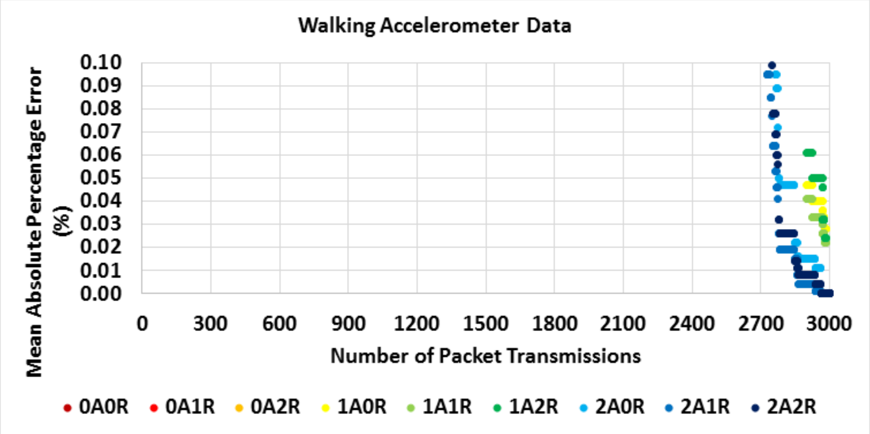

(b) Number of packet transmissions vs. mean absolute percentage error where $MAPE_{max} = 0.1\%$

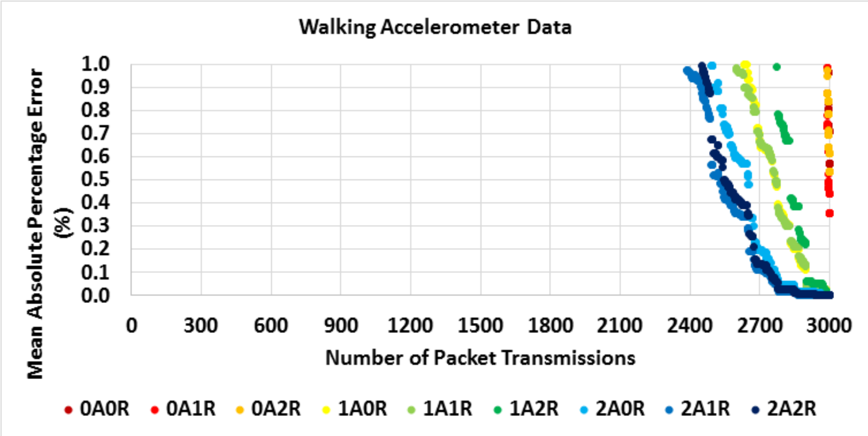

(c) Number of packet transmissions vs. mean absolute percentage error

where $MAPE_{max} = 1\%$

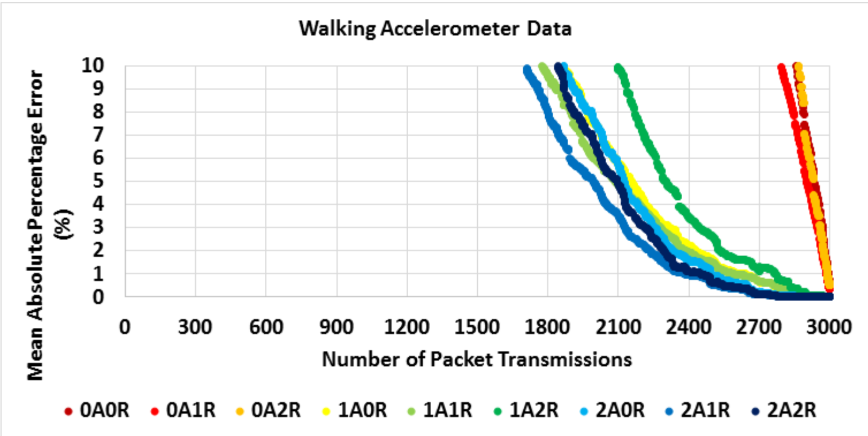

(d) Number of packet transmissions vs. mean absolute percentage error

where $MAPE_{max} = 10\%$

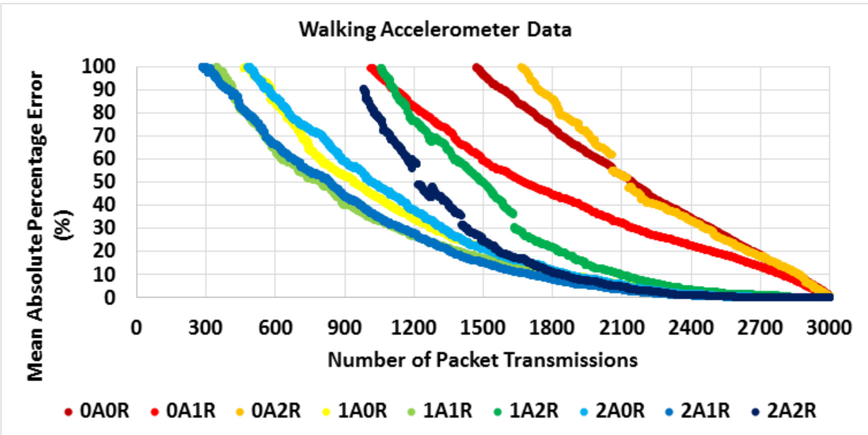

(e) Number of packet transmissions vs. mean absolute percentage error

where $MAPE_{max} = 100\%$

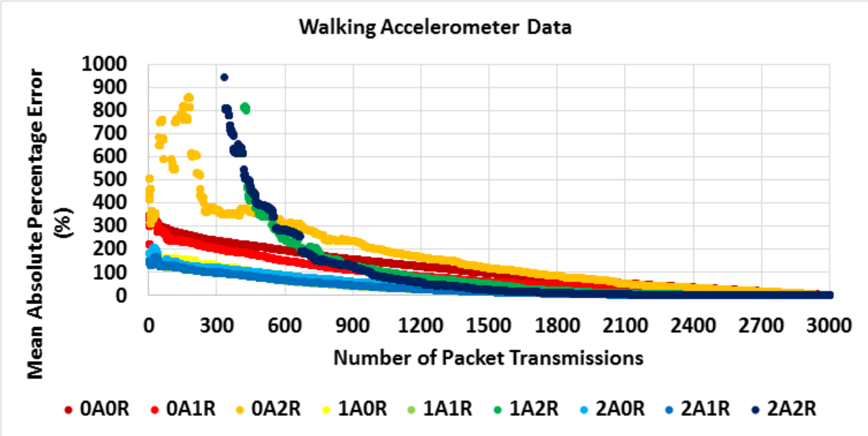

(f) Number of packet transmissions vs. mean absolute percentage error where $MAPE_{max} = 1000\%$

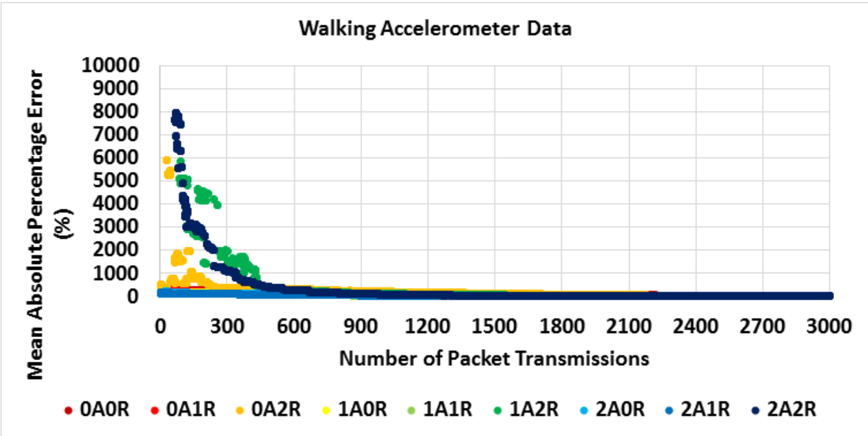

(g) Number of packet transmissions vs. mean absolute percentage error where $MAPE_{max} = 10000\%$

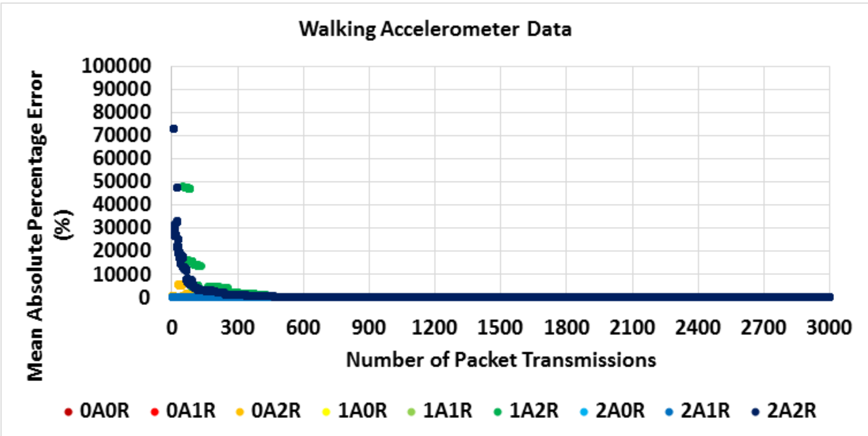

(h) Number of packet transmissions vs. mean absolute percentage error where $MAPE_{max} = 100000\%$

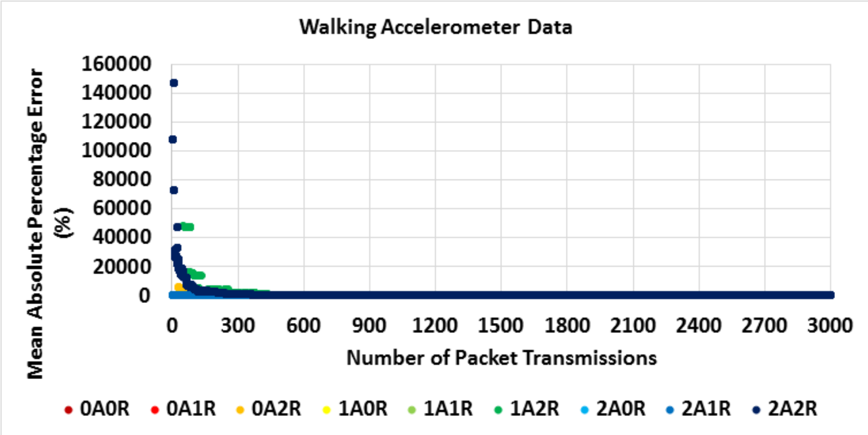

(i) Number of packet transmissions vs. mean absolute percentage error where $MAPE_{max} = 160000\%$

Figure 5.70: Number of packet transmissions vs. mean absolute percentage error in walking accelerometer data

The results of DAR schemes in walking accelerometer data are shown more details in Table 5.48.

Table 5.48: Number of Packet Transmissions vs. Mean Absolute Percentage Error in Walking Accelerometer Data

MAPE	DAR	$NoPT_{min}$
≤ 2.5%	0A0R	2973
	0A1R	2958
	0A2R	2969
	1A0R	2356
	1A1R	2343
	1A2R	2516
	2A0R	2294
	2A1R	2177
	2A2R	2256

MAPE = mean absolute percentage error
DAR = data Abstraction and Reformation
0A0R = zeroth-order data abstraction & zeroth-order data reformation
0A1R = zeroth-order data abstraction & first-order data reformation
0A2R = zeroth-order data abstraction & second-order data reformation
1A0R = first-order data abstraction & zeroth-order data reformation
1A1R = first-order data abstraction & first-order data reformation
1A2R = first-order data abstraction & second-order data reformation
2A0R = second-order data abstraction & zeroth-order data reformation
2A1R = second-order data abstraction & first-order data reformation
2A2R = second-order data abstraction & second-order data reformation
$NoPT_{min}$ = minimum number of packet transmissions

From Table 5.48, it is shown that the best DAR schemes in walking accelerometer data where $MAPE \leq 2.5\%$ in the terms of number of packet transmissions is 2A1R.

3. Number of Data Transmitted vs. Root Mean Square Error

The comparisons of number of data transmitted against root mean square error are shown in Figure 5.71.

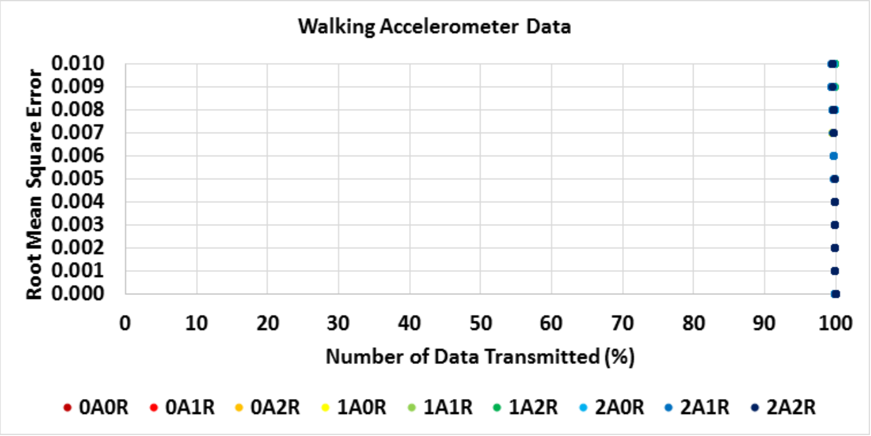

(a) Number of data transmitted vs. root mean square error where $RMSE_{max} = 0.01$

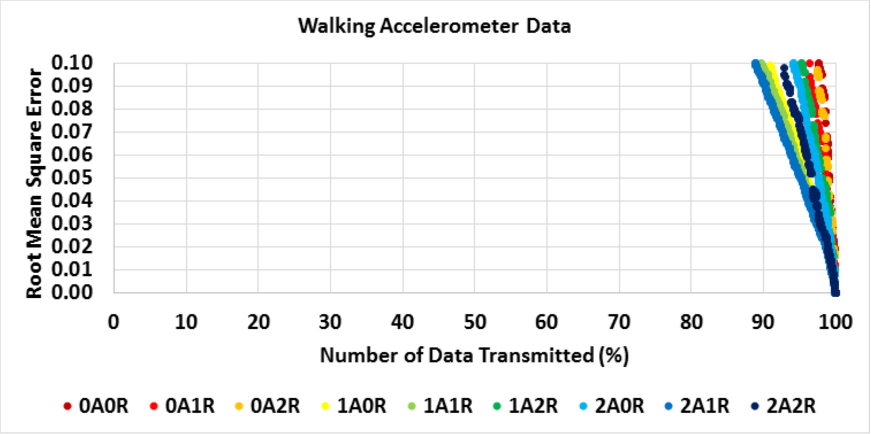

(b) Number of data transmitted vs. root mean square error where $RMSE_{max} = 0.1$

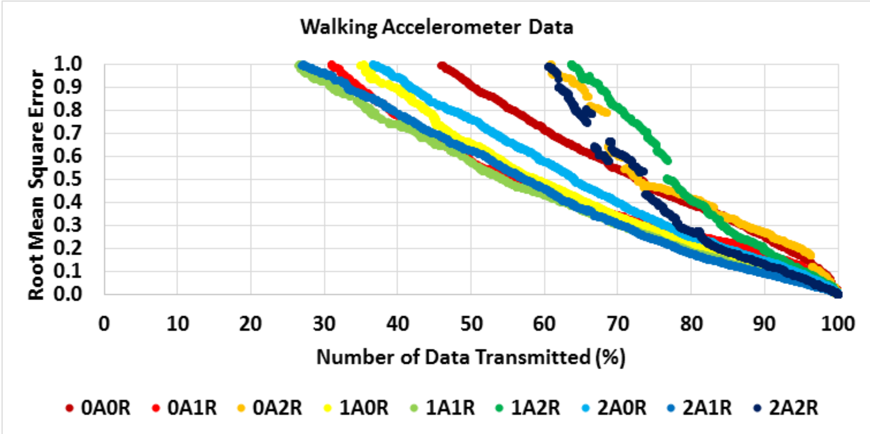

(c) Number of data transmitted vs. root mean square error where

$$\boldsymbol{RMSE_{max} = 1}$$

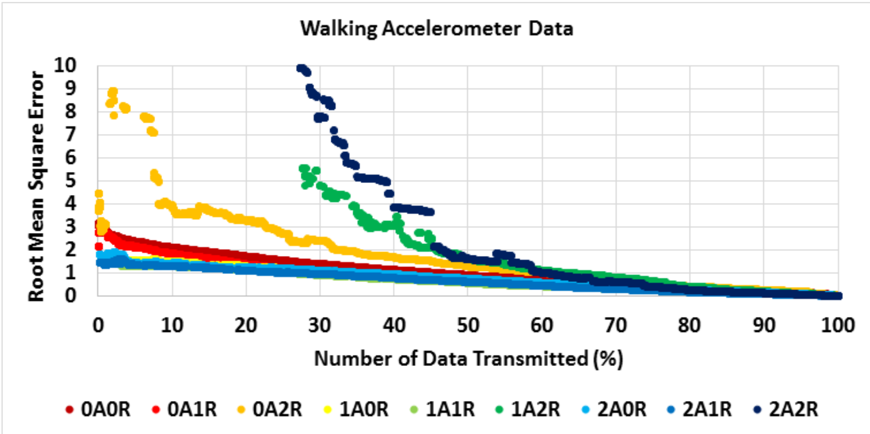

(d) Number of data transmitted vs. root mean square error where

$$\boldsymbol{RMSE_{max} = 10}$$

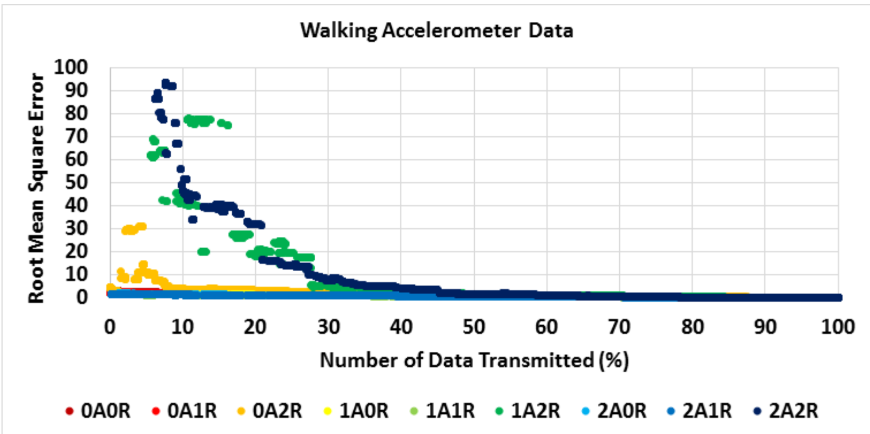

(e) Number of data transmitted vs. root mean square error where

$$\boldsymbol{RMSE_{max} = 100}$$

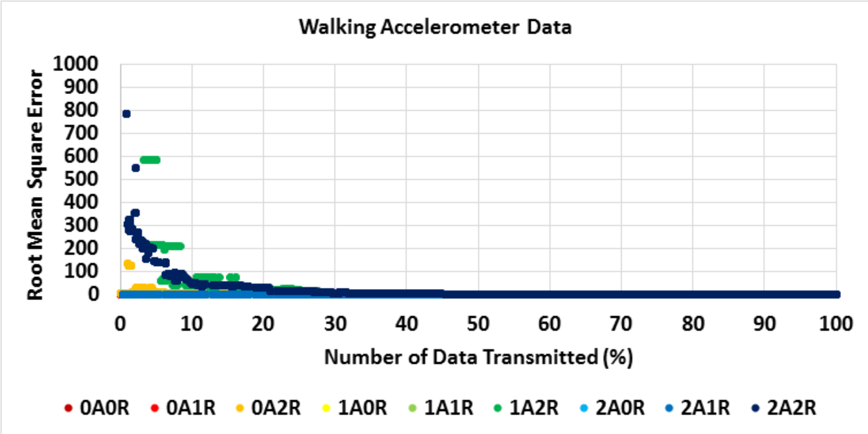

(f) Number of data transmitted vs. root mean square error where

$$RMSE_{max} = 1000$$

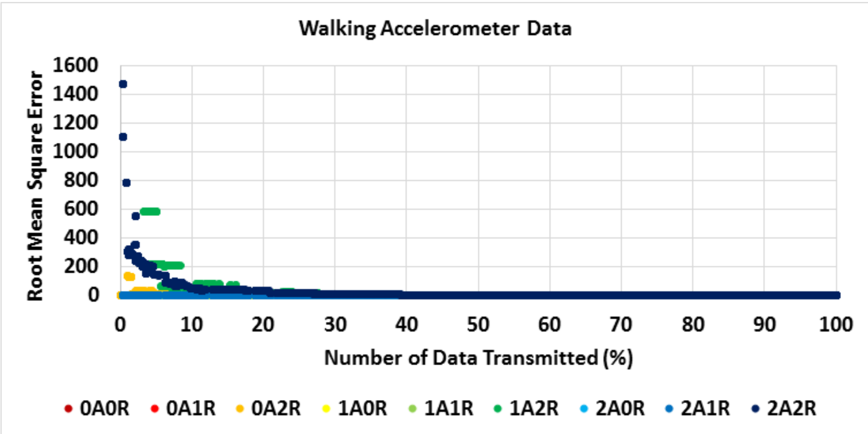

(g) Number of data transmitted vs. root mean square error where

$$RMSE_{max} = 1600$$

Figure 5.71: Number of data transmitted vs. root mean square error in walking accelerometer data

The results of DAR schemes in walking accelerometer data are shown more details in Table 5.49.

Table 5.49: Number of Data Transmitted vs. Root Mean Square Error in Walking Accelerometer Data

RMSE	DAR	$NoDT_{min}$ (%)
≤ 0.25	0A0R	90.200
	0A1R	81.567
	0A2R	91.100
	1A0R	77.333
	1A1R	74.867
	1A2R	86.433
	2A0R	79.900
	2A1R	73.800
	2A2R	81.433

RMSE = root mean square error
DAR = data Abstraction and Reformation
0A0R = zeroth-order data abstraction & zeroth-order data reformation
0A1R = zeroth-order data abstraction & first-order data reformation
0A2R = zeroth-order data abstraction & second-order data reformation
1A0R = first-order data abstraction & zeroth-order data reformation
1A1R = first-order data abstraction & first-order data reformation
1A2R = first-order data abstraction & second-order data reformation
2A0R = second-order data abstraction & zeroth-order data reformation
2A1R = second-order data abstraction & first-order data reformation
2A2R = second-order data abstraction & second-order data reformation
$NoDT_{min}$ = minimum number of data transmitted

From Table 5.49, it is shown that the best DAR schemes in walking accelerometer data where $RMSE \leq 0.25$ in the terms of number of data transmitted is 2A1R.

4. Number of Data Transmitted vs. Mean Absolute Percentage Error

The comparisons of number of data transmitted against mean absolute percentage error are shown in Figure 5.72.

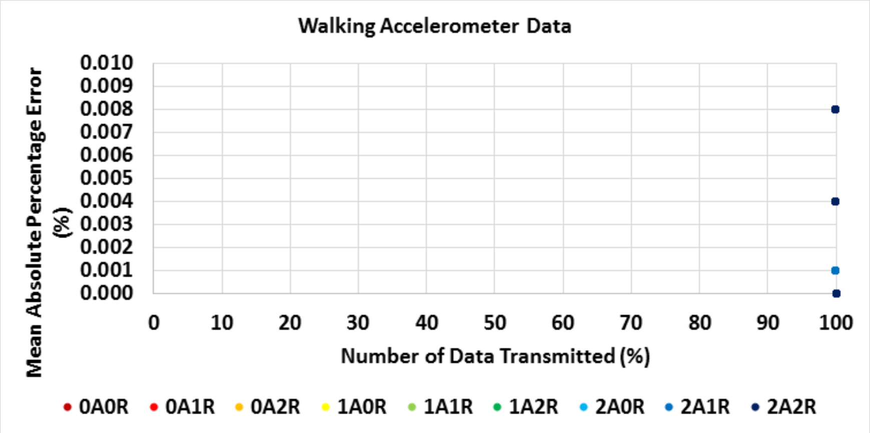

(a) Number of data transmitted vs. mean absolute percentage error where

$$MAPE_{max} = 0.01\%$$

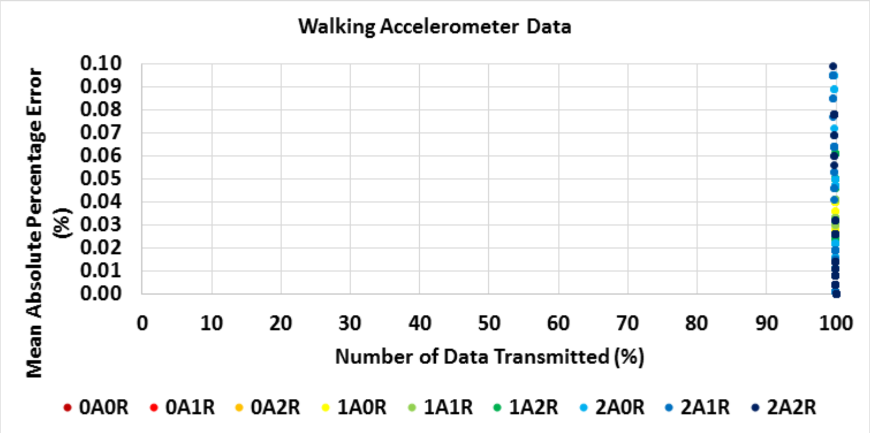

(b) Number of data transmitted vs. mean absolute percentage error where

$$MAPE_{max} = 0.1\%$$

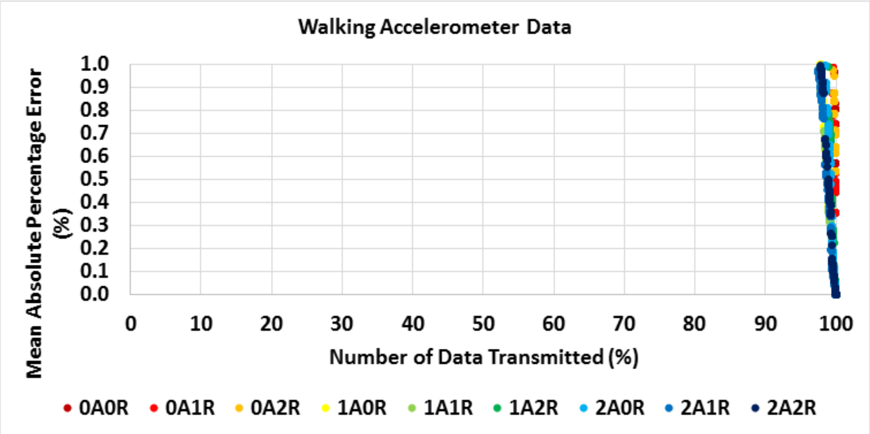

(c) Number of data transmitted vs. mean absolute percentage error where

$$MAPE_{max} = 1\%$$

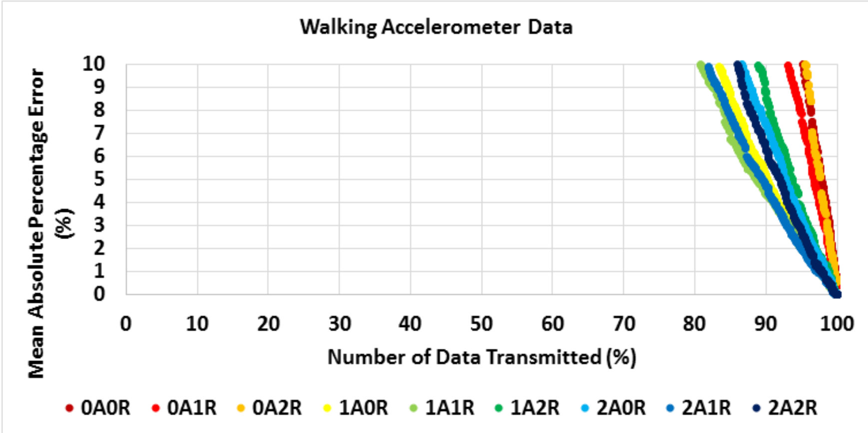

(d) Number of data transmitted vs. mean absolute percentage error where

$$MAPE_{max} = 10\%$$

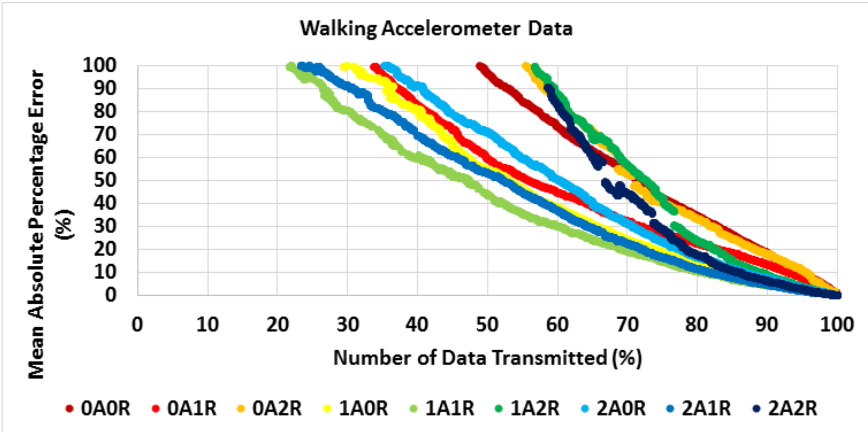

(e) Number of data transmitted vs. mean absolute percentage error where

$$MAPE_{max} = 100\%$$

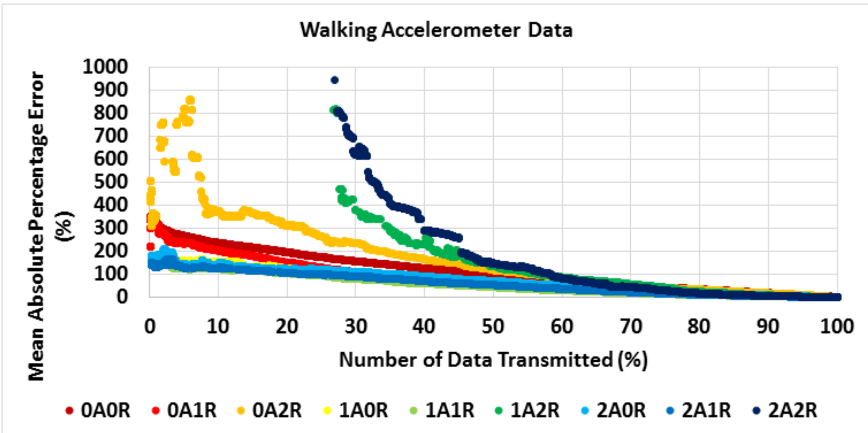

(f) Number of data transmitted vs. mean absolute percentage error where

$$MAPE_{max} = 1000\%$$

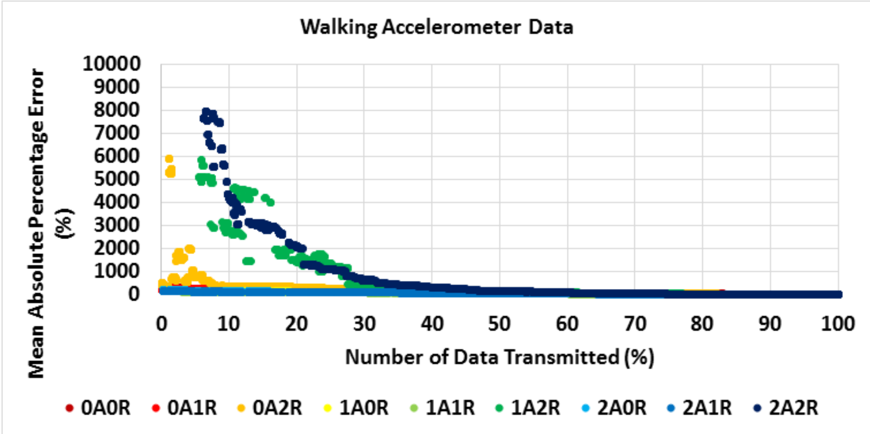

(g) Number of data transmitted vs. mean absolute percentage error where

$$MAPE_{max} = 10000\%$$

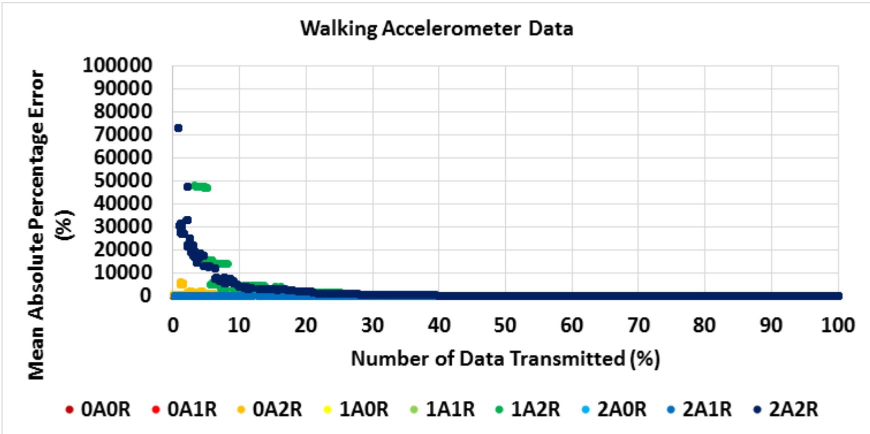

(h) Number of data transmitted vs. mean absolute percentage error where

$$MAPE_{max} = 100000\%$$

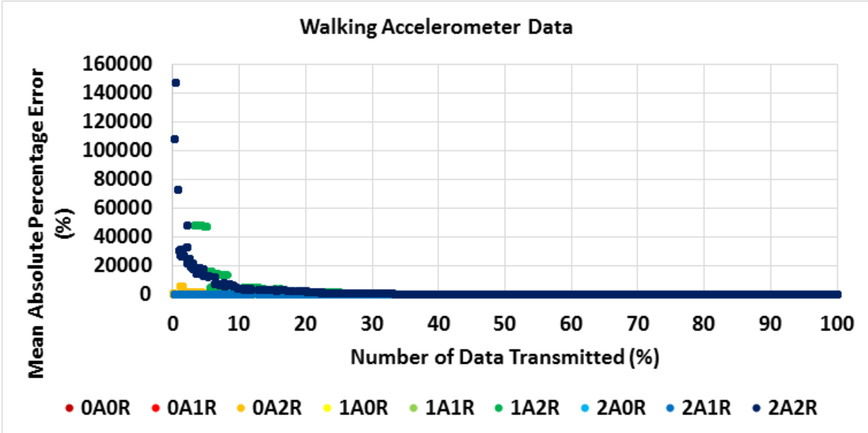

(i) Number of data transmitted vs. mean absolute percentage error where

$$MAPE_{max} = 160000\%$$

Figure 5.72: Number of data transmitted vs. mean absolute percentage error in walking accelerometer data

The results of DAR schemes in walking accelerometer data are shown more details in Table 5.50.

Table 5.50: Number of Data Transmitted vs. Mean Absolute Percentage Error in Walking Accelerometer Data

MAPE	DAR	$NoDT_{min}$ (%)
	0A0R	99.100
	0A1R	98.600
	0A2R	98.967
	1A0R	94.633
≤ 2.5%	1A1R	94.333
	1A2R	96.700
	2A0R	96.067
	2A1R	93.933
	2A2R	95.433

MAPE = mean absolute percentage error
DAR = data Abstraction and Reformation
0A0R = zeroth-order data abstraction & zeroth-order data reformation
0A1R = zeroth-order data abstraction & first-order data reformation
0A2R = zeroth-order data abstraction & second-order data reformation
1A0R = first-order data abstraction & zeroth-order data reformation
1A1R = first-order data abstraction & first-order data reformation
1A2R = first-order data abstraction & second-order data reformation
2A0R = second-order data abstraction & zeroth-order data reformation
2A1R = second-order data abstraction & first-order data reformation
2A2R = second-order data abstraction & second-order data reformation
$NoDT_{min}$ = minimum number of data transmitted

From Table 5.50, it is shown that the best DAR schemes in walking accelerometer data where $MAPE \leq 0.1\%$ in the terms of number of data transmitted is 2A1R.

5. Root Mean Square Error vs. Number of Packet Transmissions

The comparisons of root mean square error against number of packet transmissions are shown in Figure 5.73.

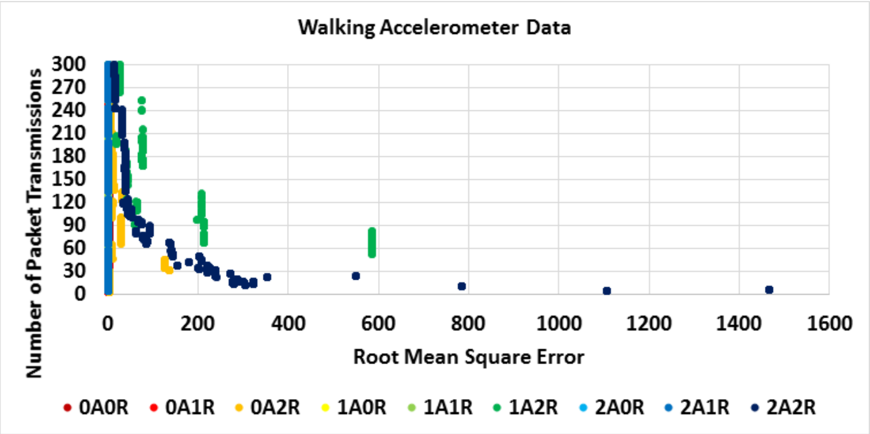

(a) Root mean square error vs. number of packet transmissions where $NoPT_{max} = 300$

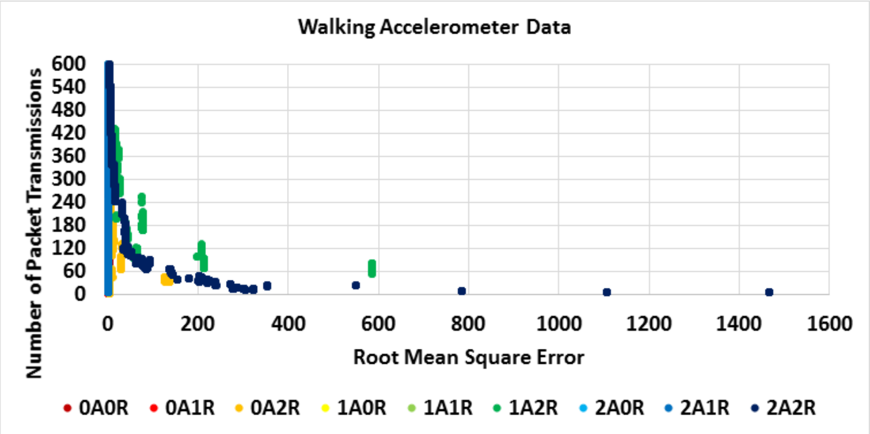

(b) Root mean square error vs. number of packet transmissions where $NoPT_{max} = 600$

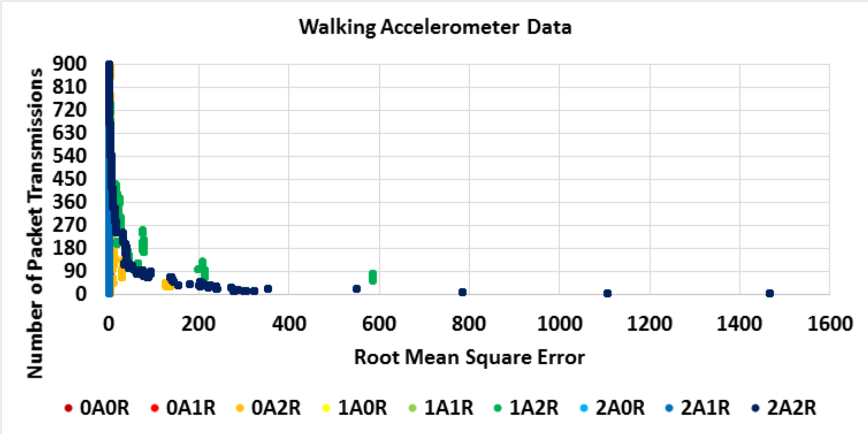

(c) Root mean square error vs. number of packet transmissions where

$$NoPT_{max} = 900$$

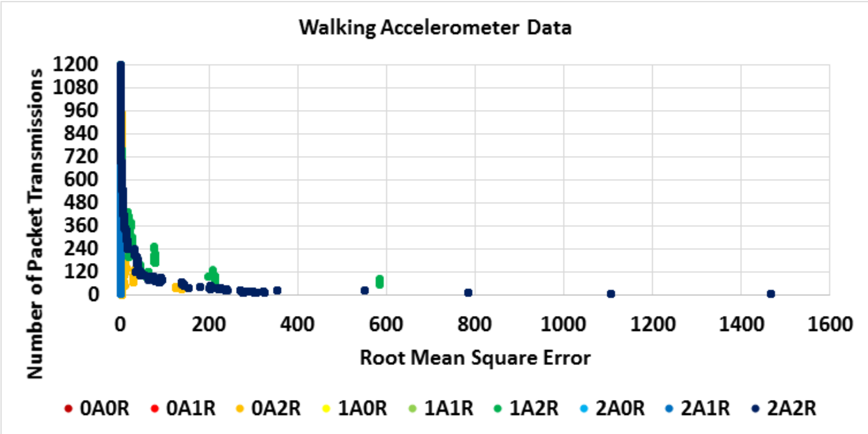

(d) Root mean square error vs. number of packet transmissions where

$$NoPT_{max} = 1200$$

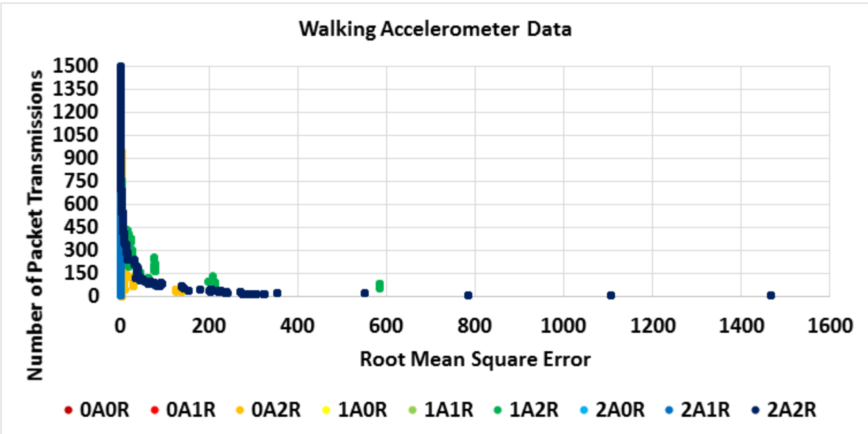

(e) Root mean square error vs. number of packet transmissions where

$$NoPT_{max} = 1500$$

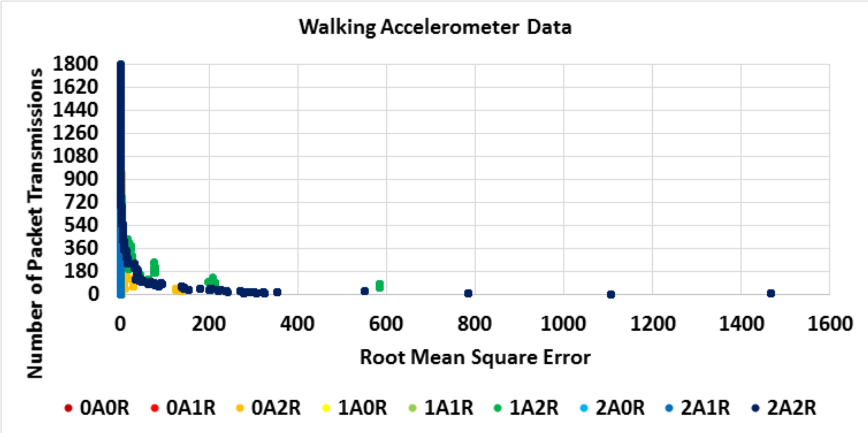

(f) Root mean square error vs. number of packet transmissions where

$$NoPT_{max} = 1800$$

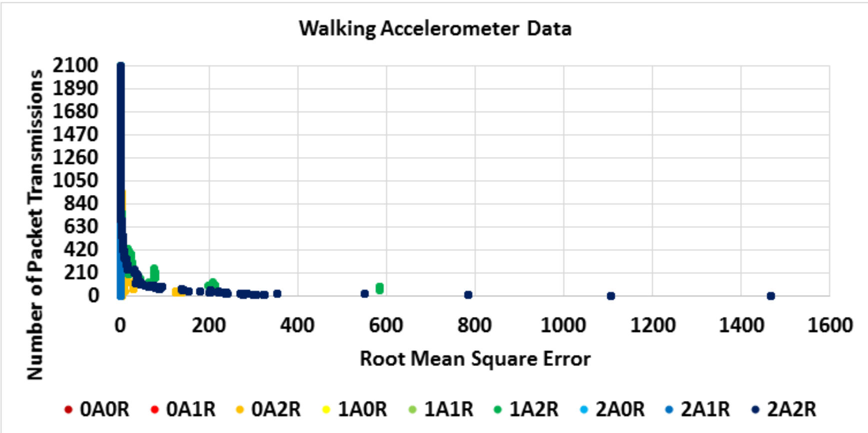

(g) Root mean square error vs. number of packet transmissions where

$$NoPT_{max} = 2100$$

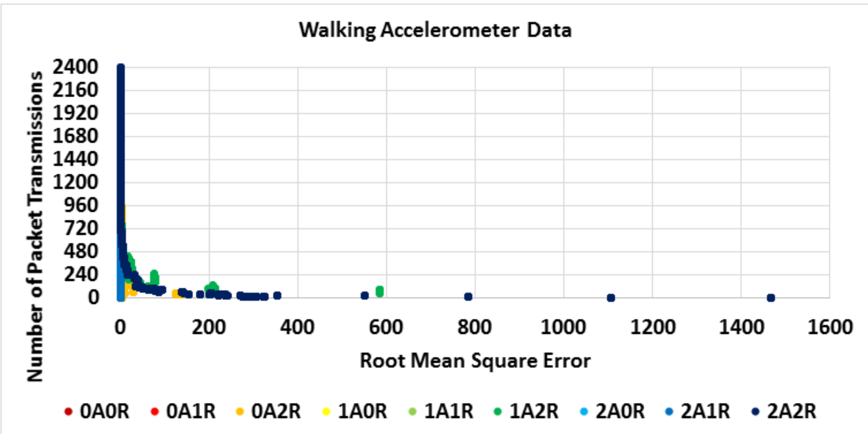

(h) Root mean square error vs. number of packet transmissions where

$$NoPT_{max} = 2400$$

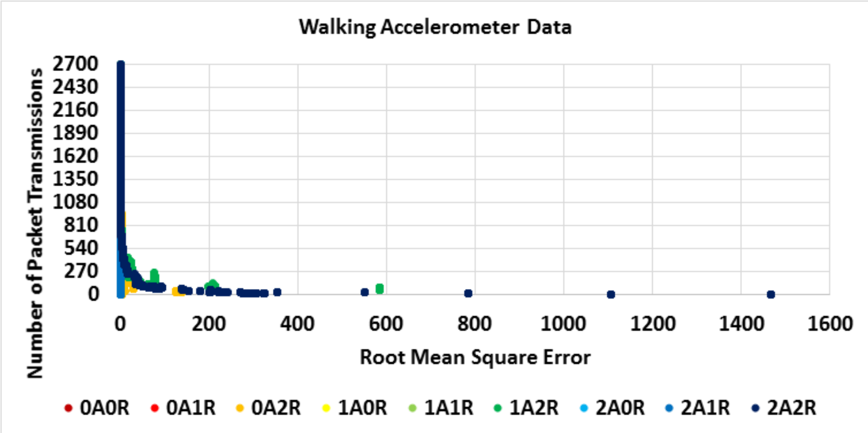

(i) Root mean square error vs. number of packet transmissions where

$$NoPT_{max} = 2700$$

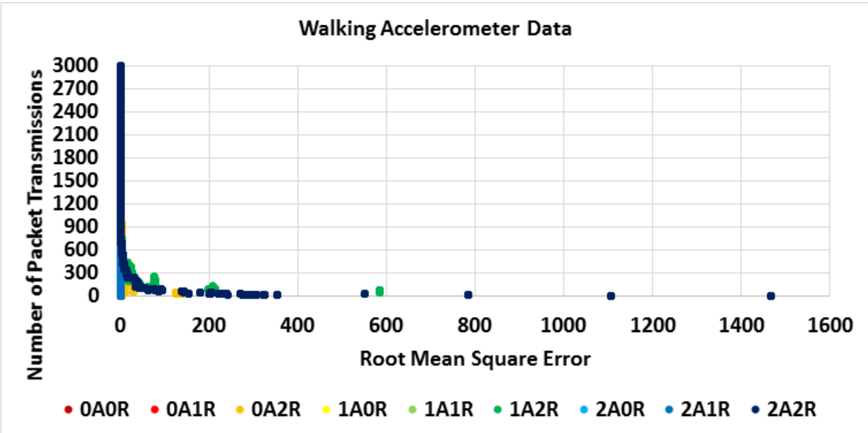

(j) Root mean square error vs. number of packet transmissions where

$$NoPT_{max} = 3000$$

Figure 5.73: Root mean square error vs. number of packet transmissions in walking accelerometer data

The results of DAR schemes in walking accelerometer data are shown more details in Table 5.51.

Table 5.51: Root Mean Square Error vs. Number of Packet Transmissions in Walking Accelerometer Data

NoPT	DAR	$RMSE_{min}$
≤ 2250	0A0R	0.455
	0A1R	0.293
	0A2R	0.463
	1A0R	0.084
	1A1R	0.079
	1A2R	0.148
	2A0R	0.086
	2A1R	0.050
	2A2R	0.069

NoPT = number of packet transmissions
DAR = data abstraction and reformation
0A0R = zeroth-order data abstraction & zeroth-order data reformation
0A1R = zeroth-order data abstraction & first-order data reformation
0A2R = zeroth-order data abstraction & second-order data reformation
1A0R = first-order data abstraction & zeroth-order data reformation
1A1R = first-order data abstraction & first-order data reformation
1A2R = first-order data abstraction & second-order data reformation
2A0R = second-order data abstraction & zeroth-order data reformation
2A1R = second-order data abstraction & first-order data reformation
2A2R = second-order data abstraction & second-order data reformation
$RMSE_{min}$ = minimum root mean square error

From Table 5.51, it is shown that the best DAR schemes in walking accelerometer data where $NoPT \leq 2250$ in the terms of root mean square error is 2A1R.

6. Root Mean Square Error vs. Number of Data Transmitted

The comparisons of root mean square error against number of data transmitted are shown in Figure 5.74.

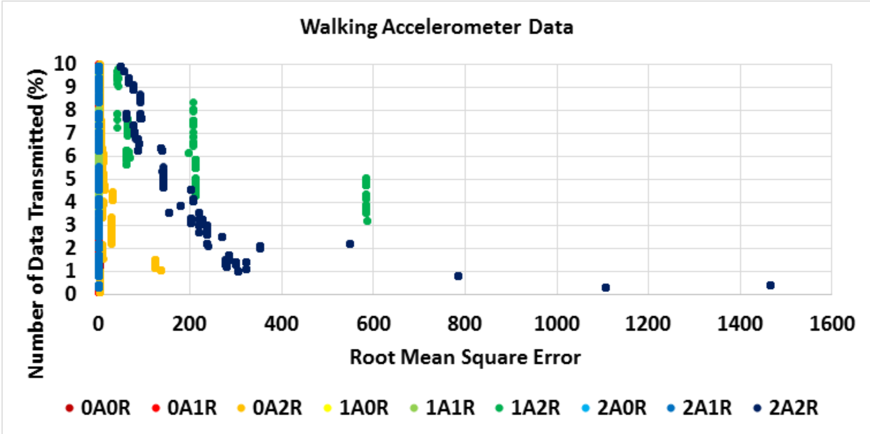

(a) Root mean square error vs. number of data transmitted where

$$NoDT_{max} = 10\%$$

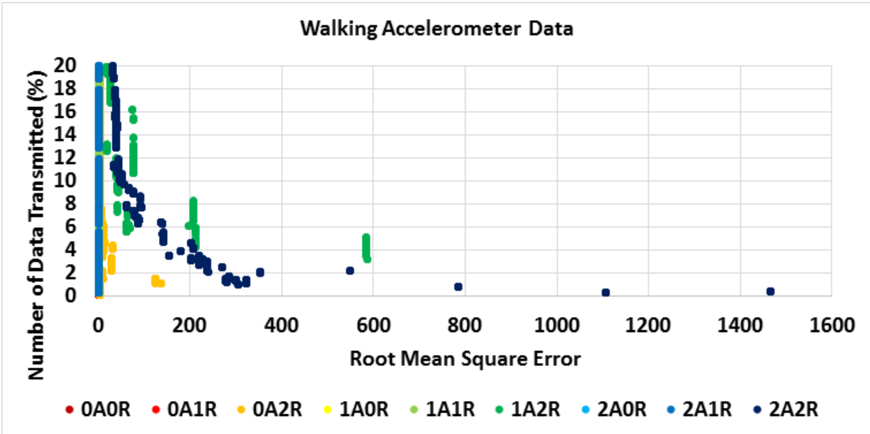

(b) Root mean square error vs. number of data transmitted where

$$NoDT_{max} = 20\%$$

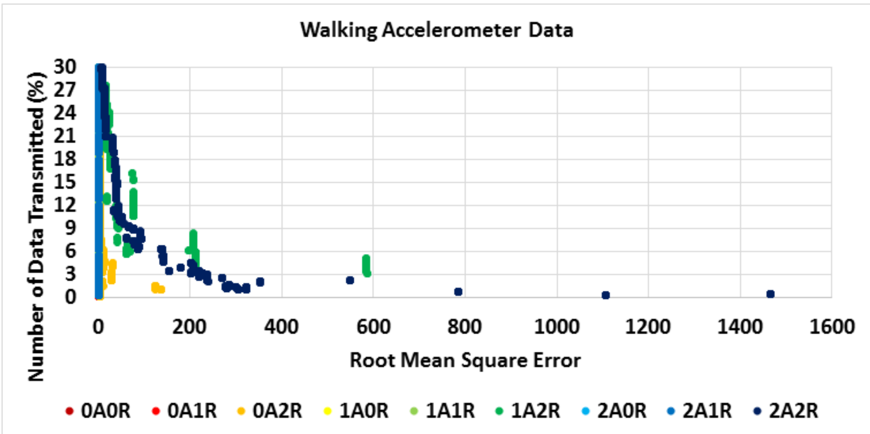

(c) Root mean square error vs. number of data transmitted (%) where

$$NoDT_{max} = 30\%$$

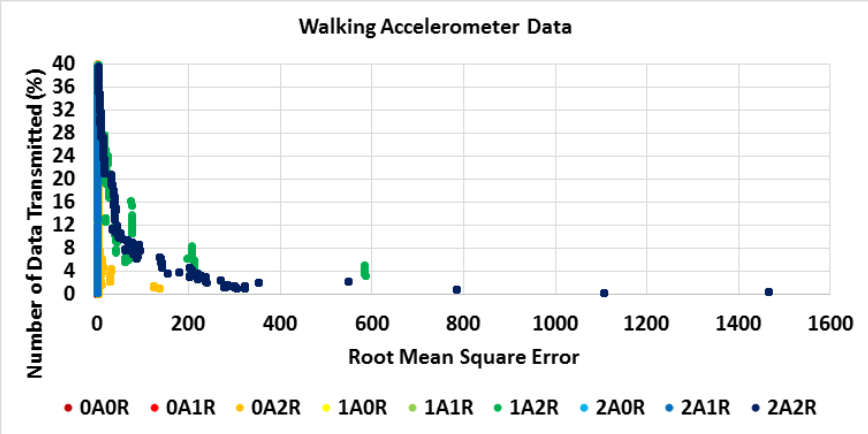

(d) Root mean square error vs. number of data transmitted where

$NoDT_{max}$ = **40%**

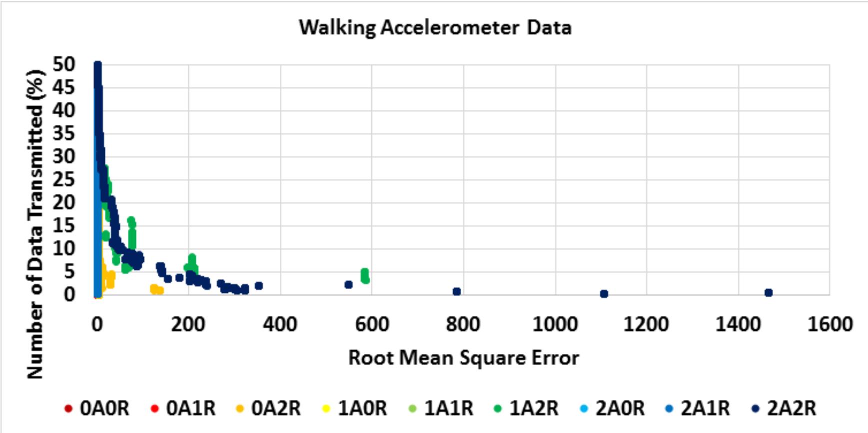

(e) Root mean square error vs. number of data transmitted where

$NoDT_{max}$ = **50%**

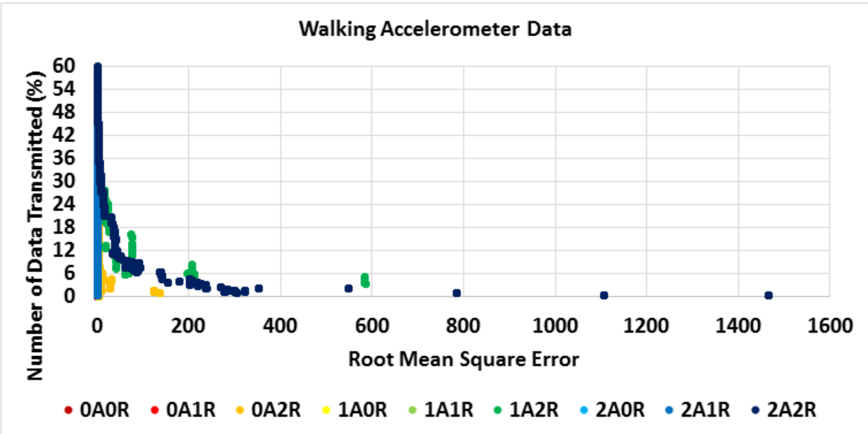

(f) Root mean square error vs. number of data transmitted where

$NoDT_{max}$ = **60%**

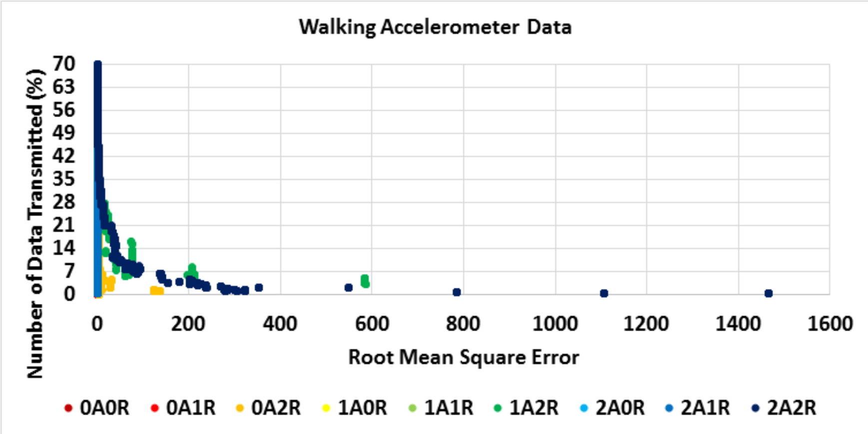

(g) Root mean square error vs. number of data transmitted where

$$NoDT_{max} = 70\%$$

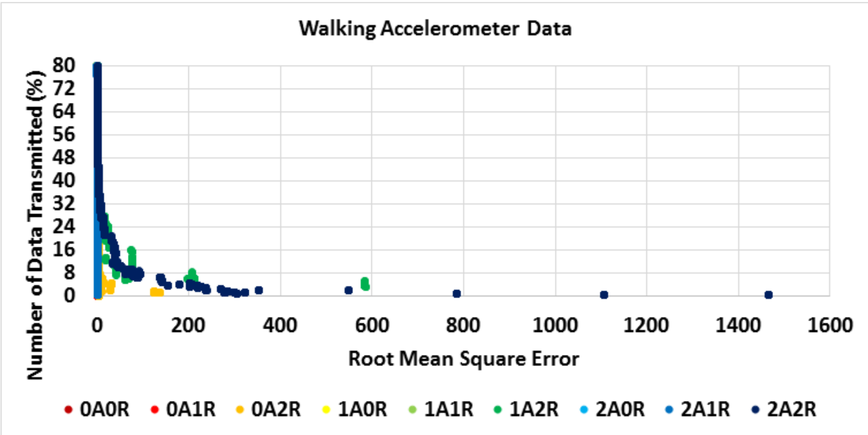

(h) Root mean square error vs. number of data transmitted where

$$NoDT_{max} = 80\%$$

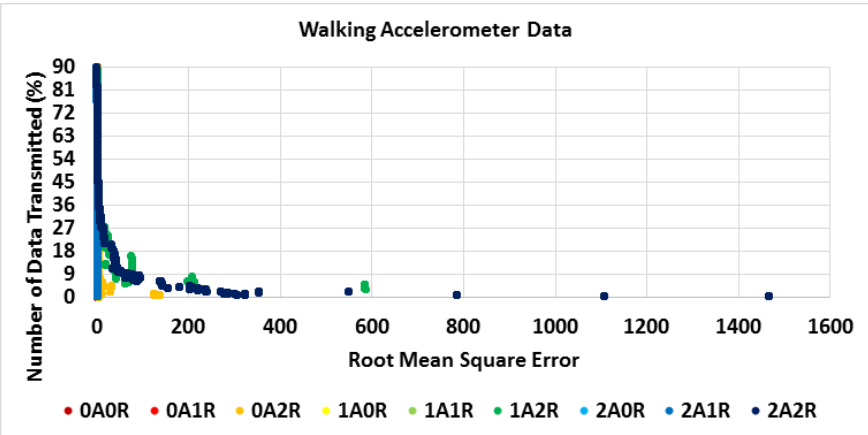

(i) Root mean square error vs. number of data transmitted where

$$NoDT_{max} = 90\%$$

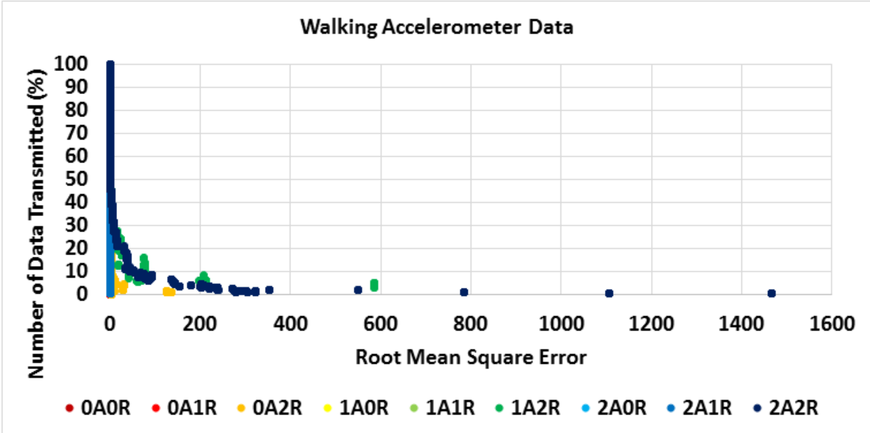

(j) Root mean square error vs. number of data transmitted where

$$\boldsymbol{NoDT_{max}} = \mathbf{100\%}$$

Figure 5.74: Root mean square error vs. number of data transmitted in walking accelerometer data

The results of DAR schemes in walking accelerometer data are shown more details in Table 5.52.

Table 5.52: Root Mean Square Error vs. Number of Data Transmitted in Walking Accelerometer Data

NoDT	DAR	$RMSE_{min}$
≤ 75%	0A0R	0.455
	0A1R	0.293
	0A2R	0.463
	1A0R	0.279
	1A1R	0.247
	1A2R	0.658
	2A0R	0.322
	2A1R	0.238
	2A2R	0.406

NoDT = number of data transmitted
DAR = data abstraction and reformation
0A0R = zeroth-order data abstraction & zeroth-order data reformation
0A1R = zeroth-order data abstraction & first-order data reformation
0A2R = zeroth-order data abstraction & second-order data reformation
1A0R = first-order data abstraction & zeroth-order data reformation
1A1R = first-order data abstraction & first-order data reformation
1A2R = first-order data abstraction & second-order data reformation
2A0R = second-order data abstraction & zeroth-order data reformation
2A1R = second-order data abstraction & first-order data reformation
2A2R = second-order data abstraction & second-order data reformation
$RMSE_{min}$ = minimum root mean square error

From Table 5.52, it is shown that the best DAR schemes in walking accelerometer data where $NoDT \leq 75\%$ in the terms of root mean square error is 2A1R.

7. Mean Absolute Percentage Error vs. Number of Packet Transmissions

The comparisons of mean absolute percentage error against number of packet transmissions are shown in Figure 5.75.

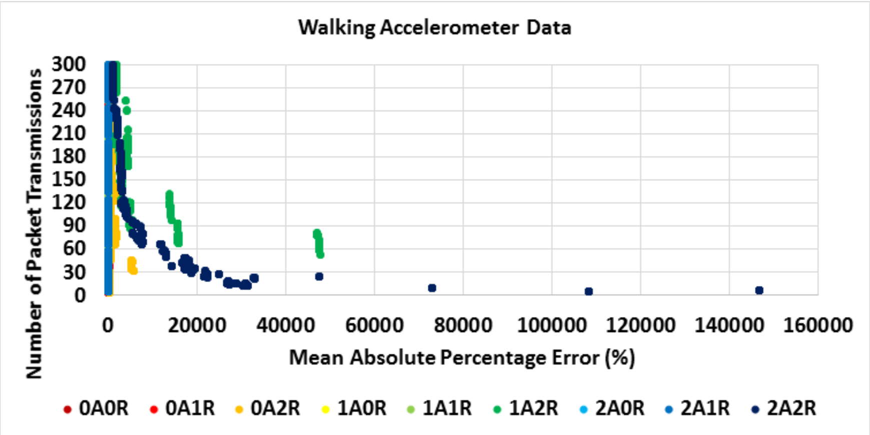

(a) Mean absolute percentage error vs. number of packet transmission where $NoPT_{max} = 300$

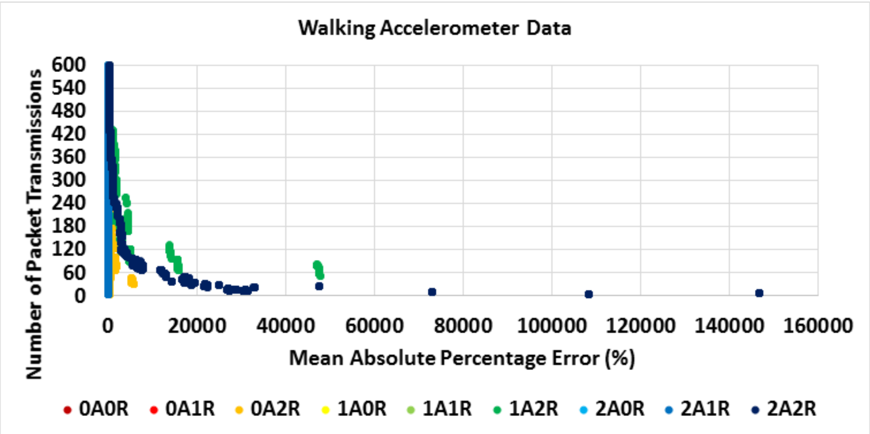

(b) Mean absolute percentage error vs. number of packet transmission where $NoPT_{max} = 600$

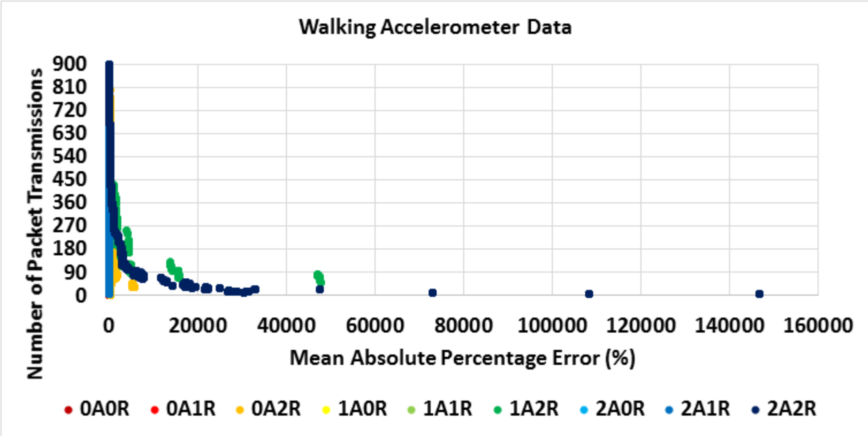

(c) Mean absolute percentage error vs. number of packet transmission where $NoPT_{max} = 900$

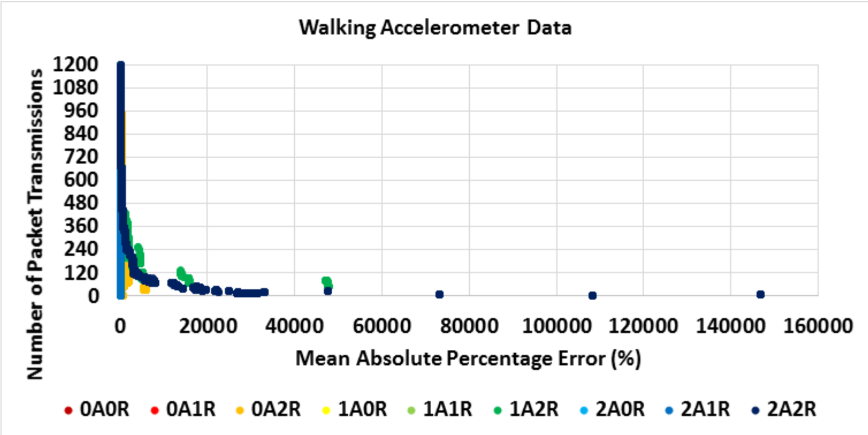

(d) Mean absolute percentage error vs. number of packet transmission where $NoPT_{max} = 1200$

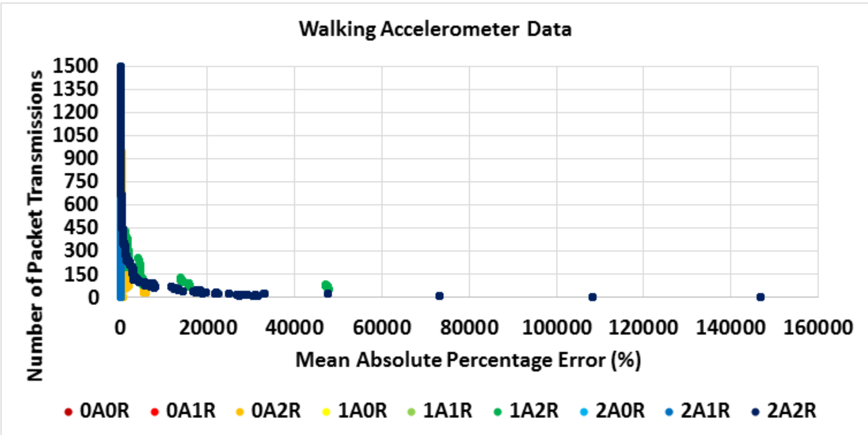

(e) Mean absolute percentage error vs. number of packet transmission where $NoPT_{max} = 1500$

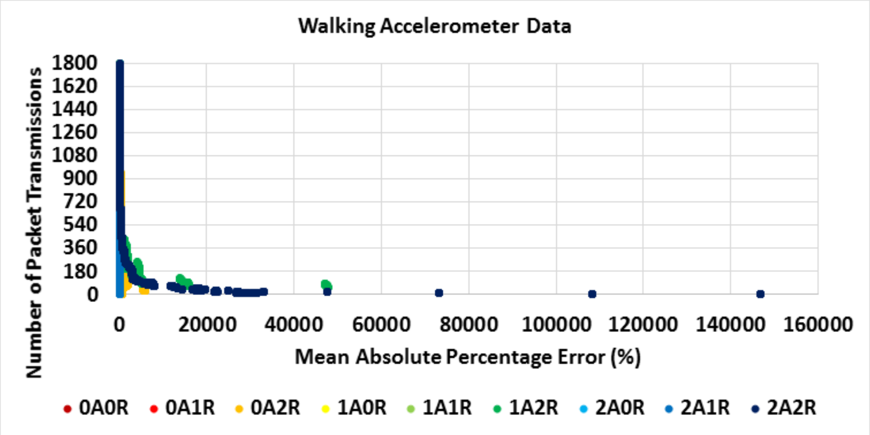

(f) Mean absolute percentage error vs. number of packet transmission

where $NoPT_{max} = 1800$

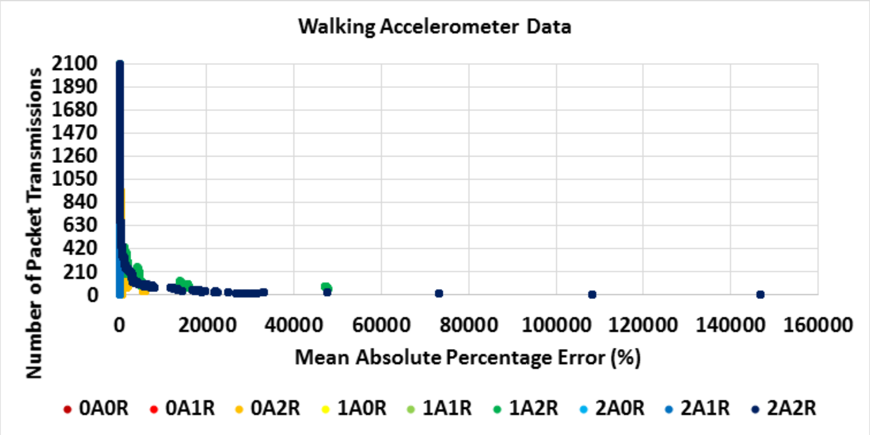

(g) Mean absolute percentage error vs. number of packet transmission

where $NoPT_{max} = 2100$

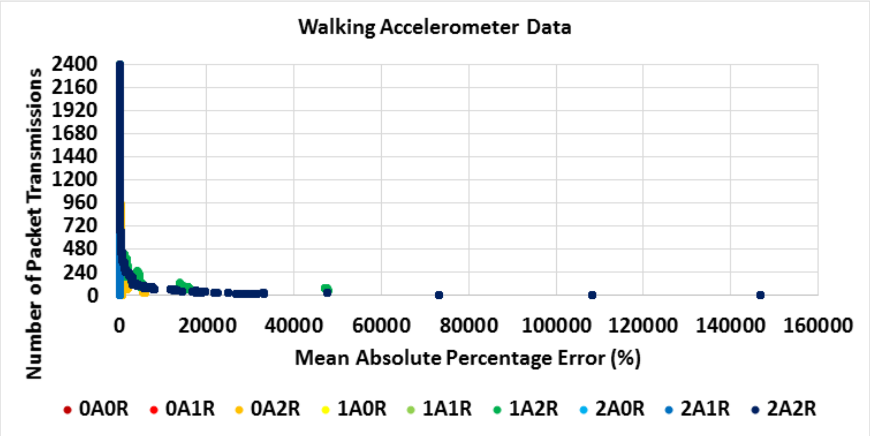

(h) Mean absolute percentage error vs. number of packet transmission

where $NoPT_{max} = 2400$

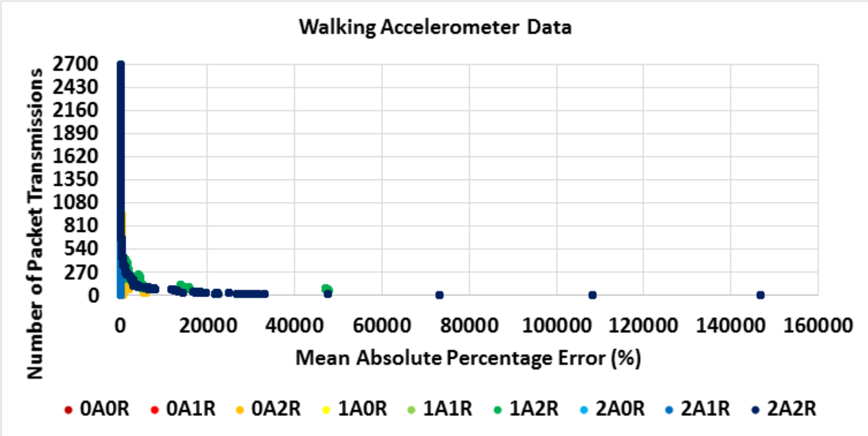

(i) Mean absolute percentage error vs. number of packet transmission where $NoPT_{max} = 2700$

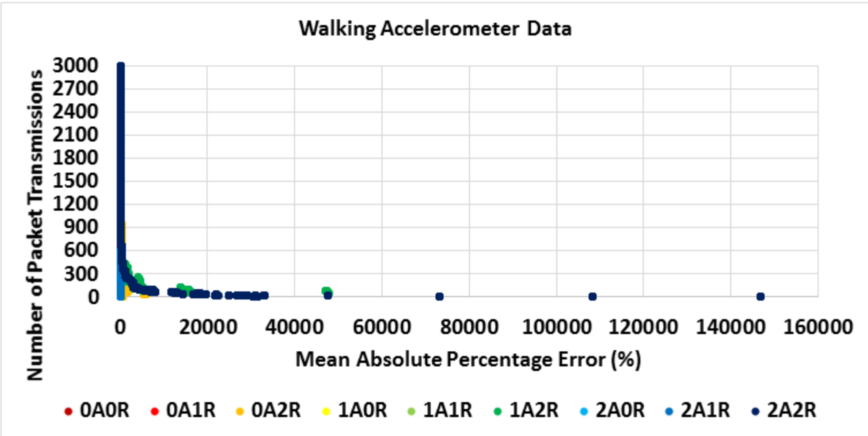

(j) Mean absolute percentage error vs. number of packet transmission where $NoPT_{max} = 3000$

Figure 5.75: Mean absolute percentage error vs. number of packet transmissions in walking accelerometer data

The results of DAR schemes in walking accelerometer data are shown more details in Table 5.53.

Table 5.53: Mean Absolute Percentage Error vs. Number of Packet Transmissions in Walking Accelerometer Data

NoPT	DAR	$MAPE_{min}$ (%)
≤ 2250	0A0R	42.551
	0A1R	26.816
	0A2R	40.426
	1A0R	3.631
	1A1R	3.361
	1A2R	6.206
	2A0R	3.063
	2A1R	1.882
	2A2R	2.541

NoPT = number of packet transmissions
DAR = data abstraction and reformation
0A0R = zeroth-order data abstraction & zeroth-order data reformation
0A1R = zeroth-order data abstraction & first-order data reformation
0A2R = zeroth-order data abstraction & second-order data reformation
1A0R = first-order data abstraction & zeroth-order data reformation
1A1R = first-order data abstraction & first-order data reformation
1A2R = first-order data abstraction & second-order data reformation
2A0R = second-order data abstraction & zeroth-order data reformation
2A1R = second-order data abstraction & first-order data reformation
2A2R = second-order data abstraction & second-order data reformation
$MAPE_{min}$ = minimum mean absolute percentage error

From Table 5.53, it is shown that the best DAR schemes in walking accelerometer data where $NoPT \leq 2250$ in the terms of mean absolute percentage error is 2A1R.

8. Mean Absolute Percentage Error vs. Number of Data Transmitted

The comparisons of mean absolute percentage error against number of data transmitted are shown in Figure 5.76.

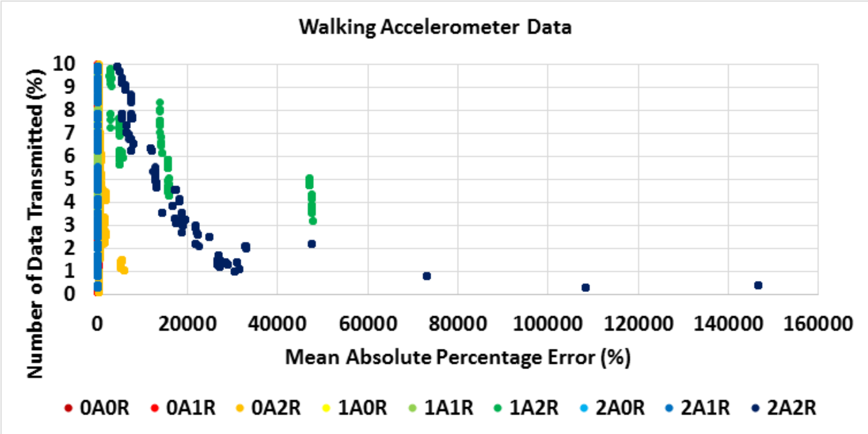

(a) Mean absolute percentage error vs. number of data transmitted where $NoDT_{max} = 10\%$

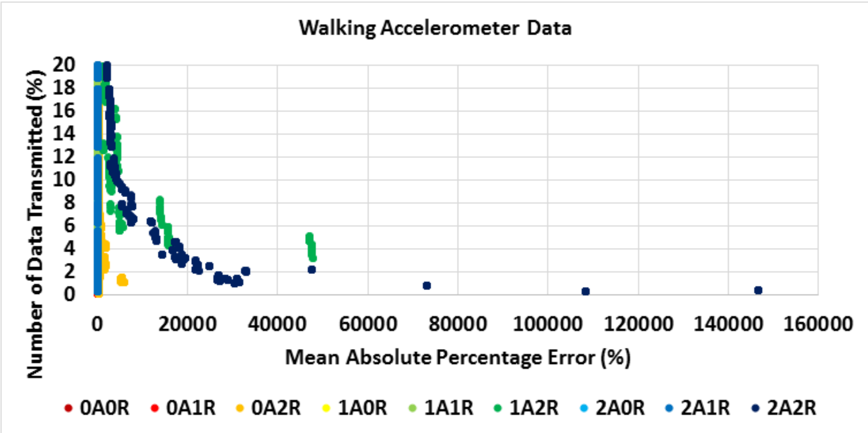

(b) Mean absolute percentage error vs. number of data transmitted where $NoDT_{max} = 20\%$

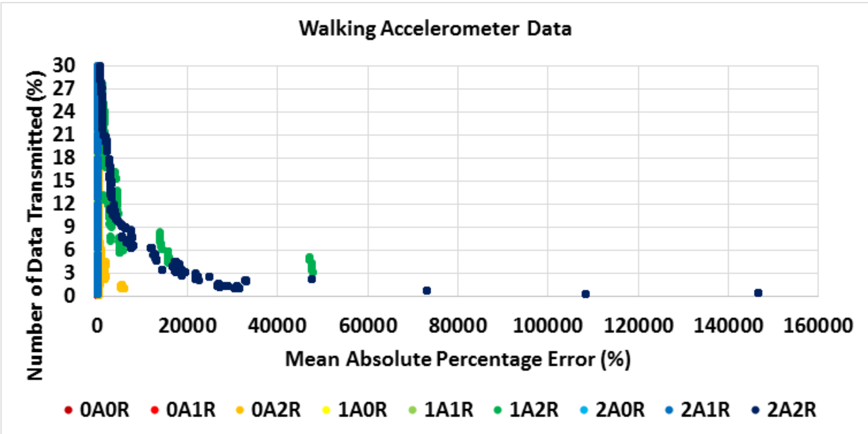

(c) Mean absolute percentage error vs. number of data transmitted where $NoDT_{max} = 30\%$

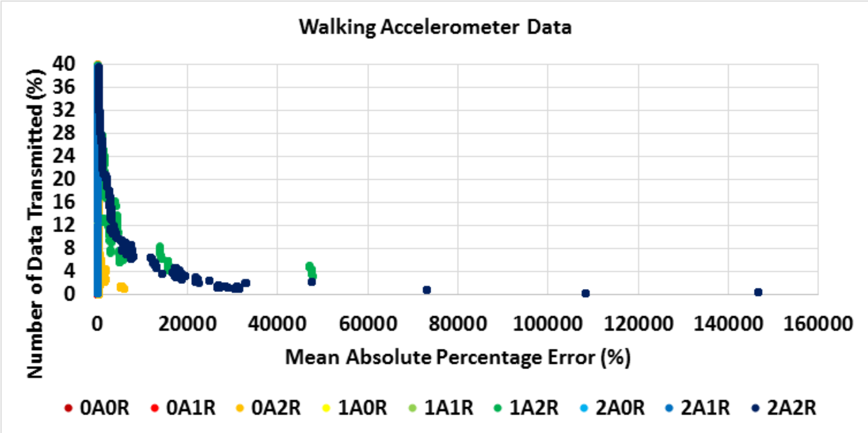

(d) Mean absolute percentage error vs. number of data transmitted where $NoDT_{max} = 40\%$

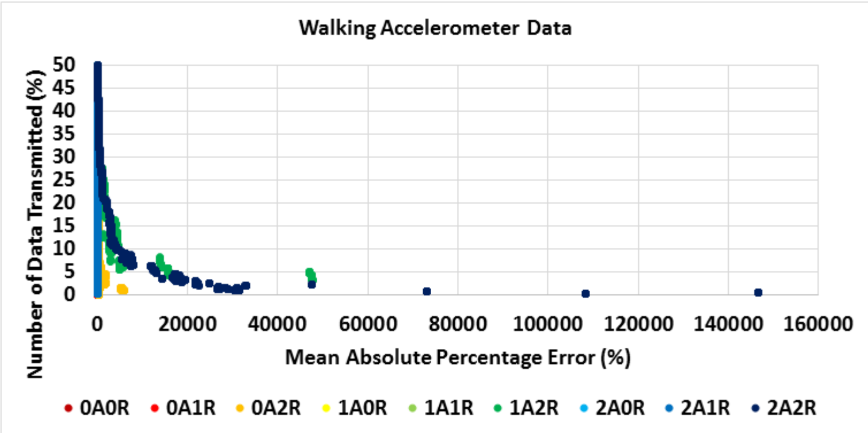

(e) Mean absolute percentage error vs. number of data transmitted where $NoDT_{max} = 50\%$

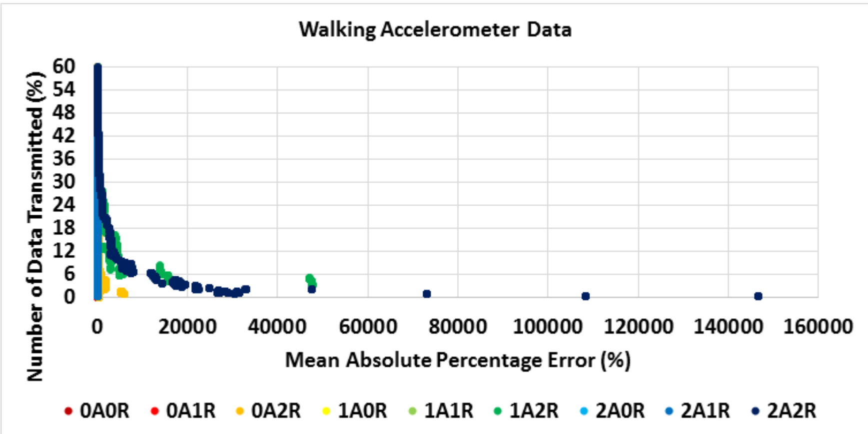

(f) Mean absolute percentage error vs. number of data transmitted where $NoDT_{max} = 60\%$

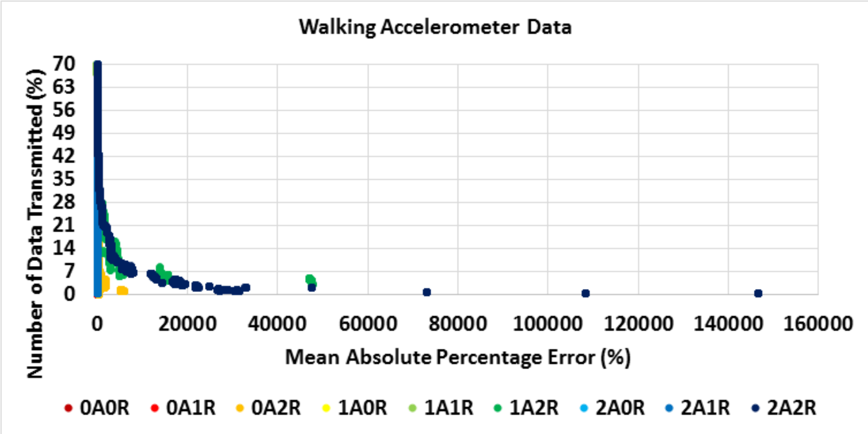

(g) Mean absolute percentage error vs. number of data transmitted where

$NoDT_{max} = 70\%$

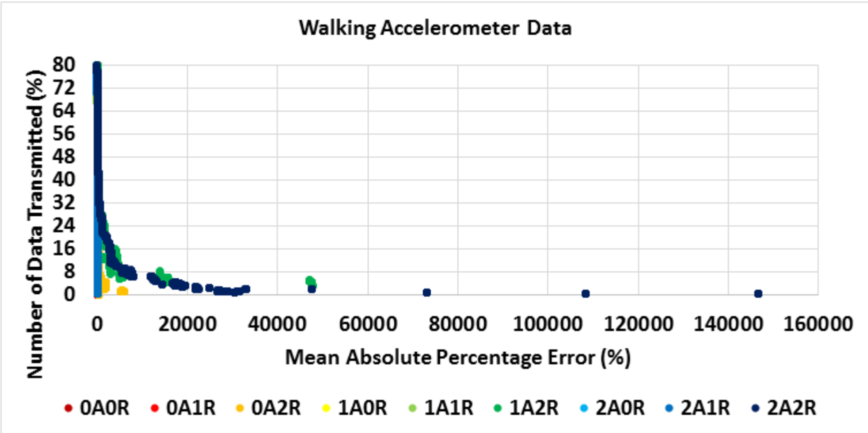

(h) Mean absolute percentage error vs. number of data transmitted where

$NoDT_{max} = 80\%$

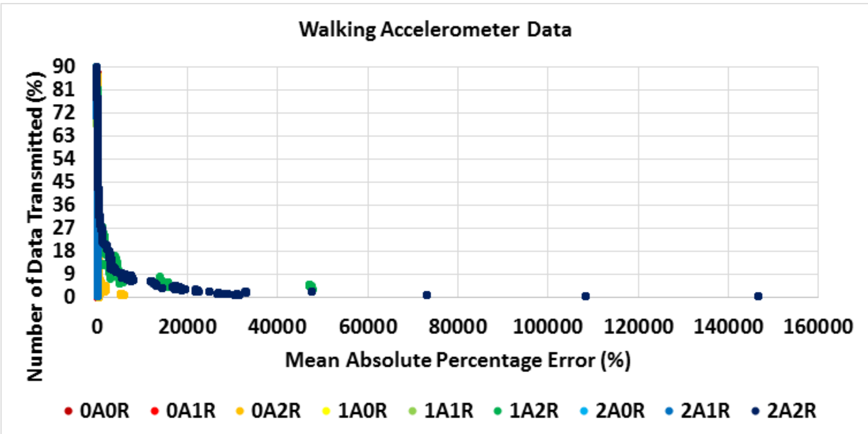

(i) Mean absolute percentage error vs. number of data transmitted where

$NoDT_{max} = 90\%$

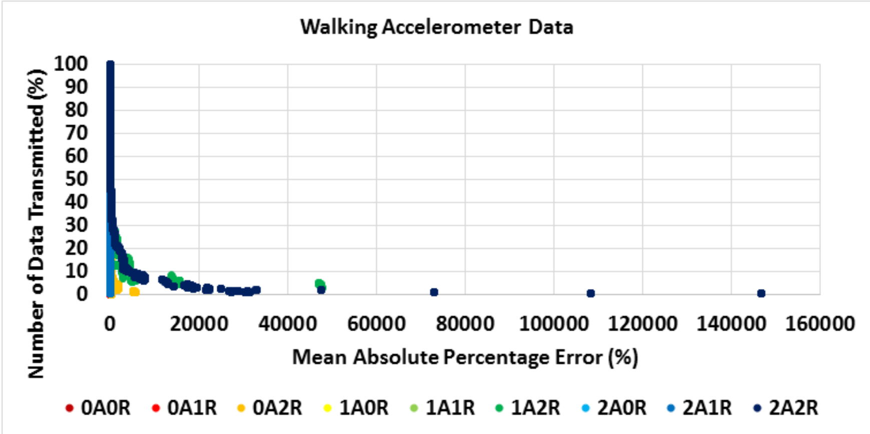

(j) Mean absolute percentage error vs. number of data transmitted (%) where $NoDT_{max} = 100\%$

Figure 5.76: Mean absolute percentage error vs. number of data transmitted in walking accelerometer data

The results of DAR schemes in walking accelerometer data are shown more details in Table 5.54.

Table 5.54: Mean Absolute Percentage Error vs. Number of Data Transmitted in Walking Accelerometer Data

NoDT	DAR	$MAPE_{min}$ (%)
≤ 75%	0A0R	42.551
	0A1R	26.816
	0A2R	40.426
	1A0R	18.878
	1A1R	14.950
	1A2R	42.631
	2A0R	23.266
	2A1R	16.513
	2A2R	28.755

NoDT = number of data transmitted
DAR = data abstraction and reformation
0A0R = zeroth-order data abstraction & zeroth-order data reformation
0A1R = zeroth-order data abstraction & first-order data reformation
0A2R = zeroth-order data abstraction & second-order data reformation
1A0R = first-order data abstraction & zeroth-order data reformation
1A1R = first-order data abstraction & first-order data reformation
1A2R = first-order data abstraction & second-order data reformation
2A0R = second-order data abstraction & zeroth-order data reformation
2A1R = second-order data abstraction & first-order data reformation
2A2R = second-order data abstraction & second-order data reformation
$MAPE_{min}$ = minimum mean absolute percentage error

From Table 5.54, it is shown that the best DAR schemes in walking accelerometer data where $NoDT \leq 75\%$ in the terms of mean absolute percentage error is 1A1R.

9. Conclusion

From Table 5.47 – 5.54, it is concluded in Table 5.55, that the best DAR schemes in walking accelerometer data is 2A1R.

Table 5.55: Results of DAR Schemes in Walking Accelerometer Data

(a) Best DAR Schemes in Walking Accelerometer Data where the $NoPT \leq 2250$ and $NoDT \leq 75\%$

DAR	Th	NoPT	NoDT(%)	RMSE	MAPE(%)
0A0R	0.693	2248	74.933	0.455	42.551
0A1R	0.693	2248	74.933	0.293	26.816
0A2R	0.693	2248	74.933	0.468	40.426
1A0R	0.944	1572	75.000	0.247	14.950
1A1R	0.944	1572	75.000	0.247	14.950
1A2R	0.945	1569	74.933	0.248	15.003
2A0R	1.346	1439	75.000	0.322	23.266
2A1R	1.346	1439	75.000	0.238	16.513
2A2R	1.346	1439	75.000	0.406	28.755

(b) Best DAR Schemes in Walking Accelerometer Data where the $RMSE \leq 0.25$ and $MAPE \leq 2.5\%$

DAR	Th	NoPT	NoDT(%)	RMSE	MAPE(%)
0A0R	0.270	2973	99.100	0.050	2.450
0A1R	0.310	2958	98.600	0.050	2.448
0A2R	0.288	2969	98.967	0.049	2.278
1A0R	0.442	2347	94.400	0.061	2.376
1A1R	0.443	2345	94.367	0.062	2.402
1A2R	0.444	2343	94.333	0.062	2.410
2A0R	0.631	2294	96.067	0.074	2.499
2A1R	0.698	2177	93.933	0.060	2.479
2A2R	0.657	2256	95.433	0.068	2.488

DAR = data abstraction and reformation
Th = threshold
NoPT = number of packet transmissions
NoDT = number of packet transmitted
RMSE = root mean square error
MAPE = mean absolute percentage error

5.3.7 Running Accelerometer Data

The comparisons among parameters (number of packet transmissions, number of data transmitted, root mean square error, and mean absolute percentage error) are as follows.

1. Number of Packet Transmissions vs. Root Mean Square Error

   The comparisons of number of packet transmissions against root mean square error are shown in Figure 5.77.

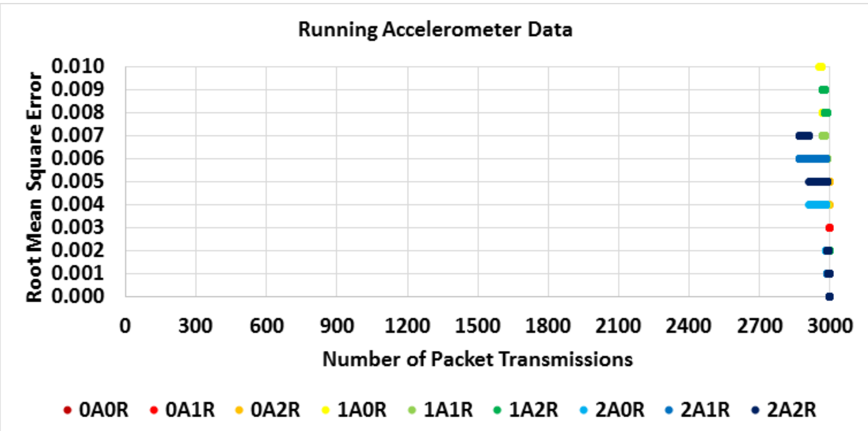

(a) Number of packet transmissions vs. root mean square error where $RMSE_{max} = 0.01$

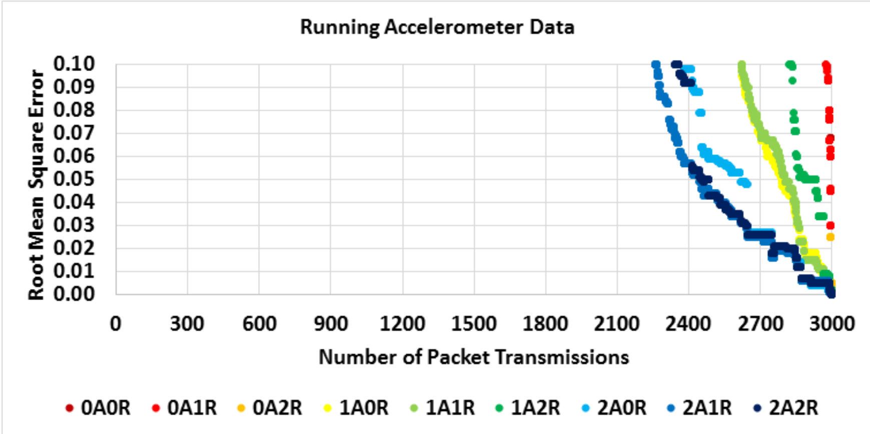

(b) Number of packet transmissions vs. root mean square error where

$$\boldsymbol{RMSE_{max} = 0.1}$$

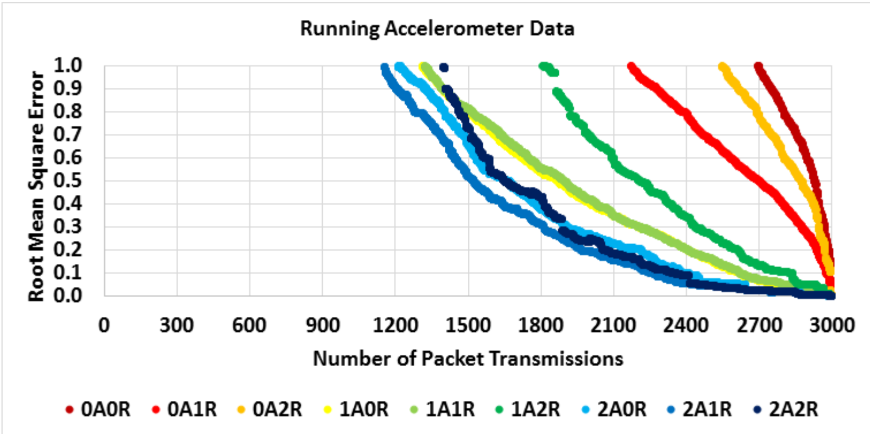

(c) Number of packet transmissions vs. root mean square error where

$$\boldsymbol{RMSE_{max} = 1}$$

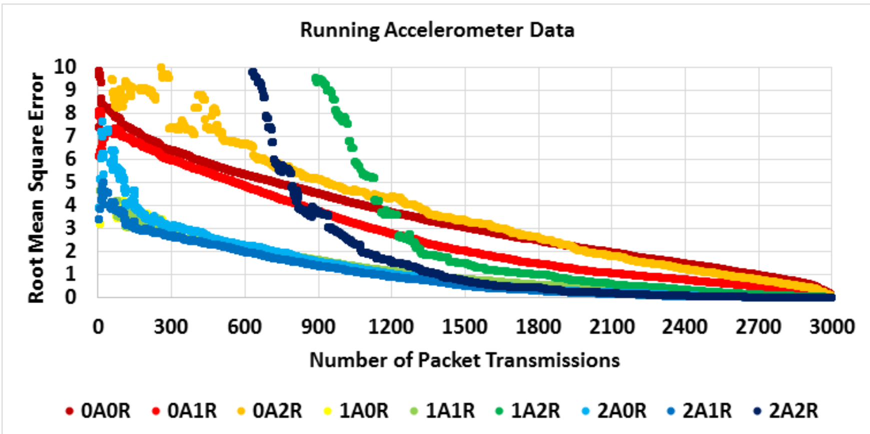

(d) Number of packet transmissions vs. root mean square error where

$$\boldsymbol{RMSE_{max} = 10}$$

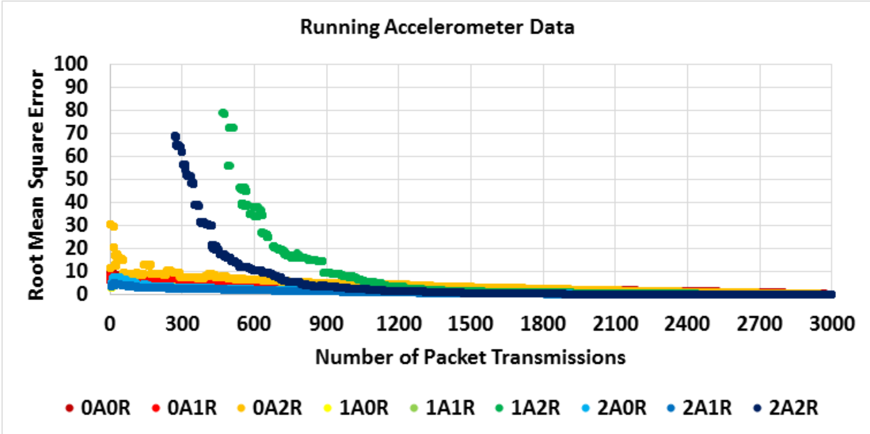

(e) Number of packet transmissions vs. root mean square error where

$$RMSE_{max} = 100$$

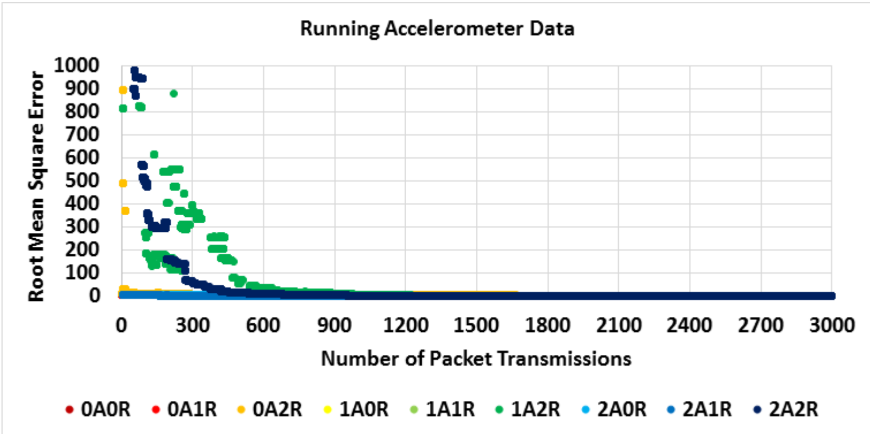

(f) Number of packet transmissions vs. root mean square error where

$$RMSE_{max} = 1000$$

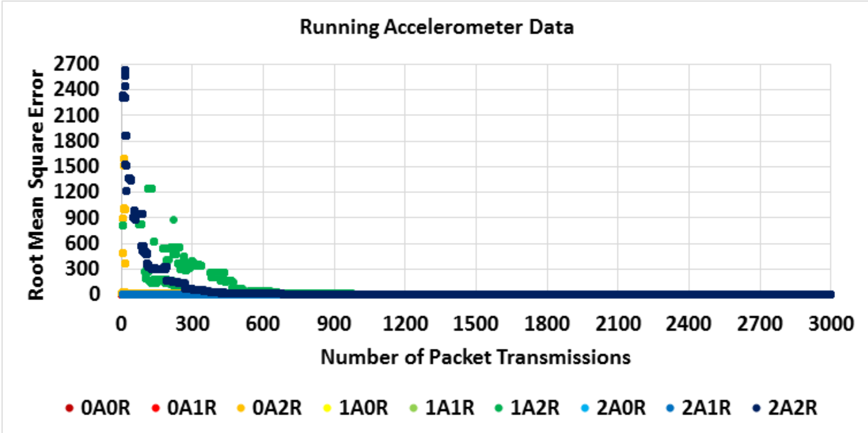

(g) Number of packet transmissions vs. root mean square error where

$$\boldsymbol{RMSE_{max} = 2700}$$

Figure 5.77: Number of packet transmissions vs. root mean square error in running accelerometer data

The results of DAR schemes in running accelerometer data are shown more details in Table 5.56.

Table 5.56: Number of Packet Transmissions vs. Root Mean Square Error in Running Accelerometer Data

RMSE	DAR	$NoPT_{min}$
≤ 0.25	0A0R	2977
	0A1R	2914
	0A2R	2956
	1A0R	2312
	1A1R	2312
	1A2R	2524
	2A0R	2040
	2A1R	1887
	2A2R	1944

RMSE = root mean square error
DAR = data abstraction and reformation
0A0R = zeroth-order data abstraction & zeroth-order data reformation
0A1R = zeroth-order data abstraction & first-order data reformation
0A2R = zeroth-order data abstraction & second-order data reformation
1A0R = first-order data abstraction & zeroth-order data reformation
1A1R = first-order data abstraction & first-order data reformation
1A2R = first-order data abstraction & second-order data reformation
2A0R = second-order data abstraction & zeroth-order data reformation
2A1R = second-order data abstraction & first-order data reformation
2A2R = second-order data abstraction & second-order data reformation
$NoPT_{min}$ = minimum number of packet transmissions

From Table 5.56, it is shown that the best DAR schemes in running accelerometer data where $RMSE \leq 0.25$ in the terms of number of packet transmissions is 2A1R.

2. Number of Packet Transmissions vs. Mean Absolute Percentage Error

The comparisons of number of packet transmissions against mean absolute percentage error are shown in Figure 5.78.

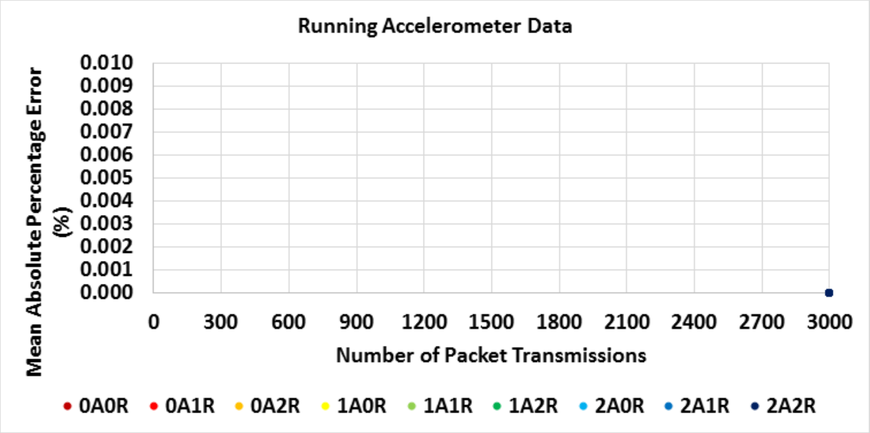

(a) Number of packet transmissions vs. mean absolute percentage error where $MAPE_{max} = 0.01\%$

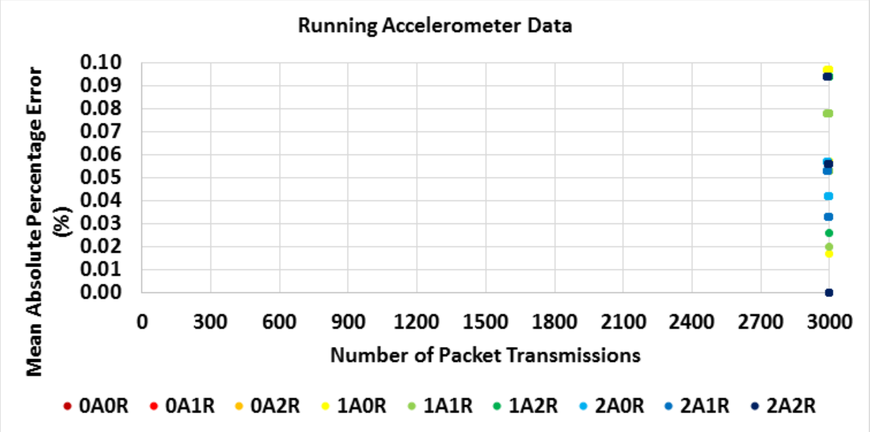

(b) Number of packet transmissions vs. mean absolute percentage error where $MAPE_{max} = 0.1\%$

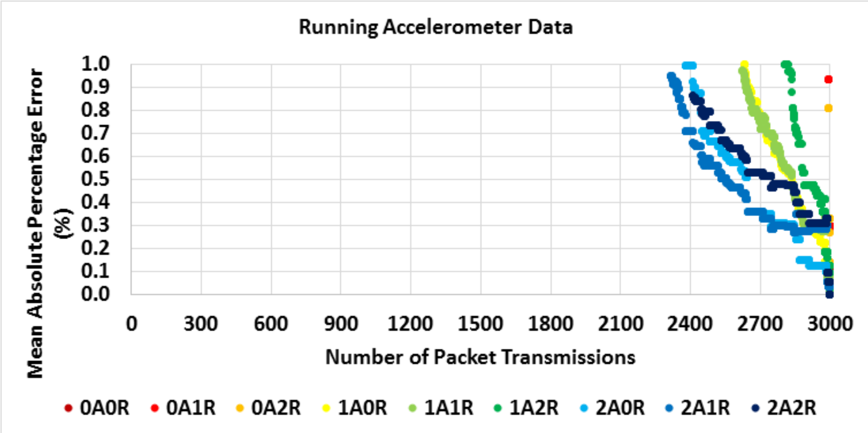

(c) Number of packet transmissions vs. mean absolute percentage error

where $MAPE_{max} = 1\%$

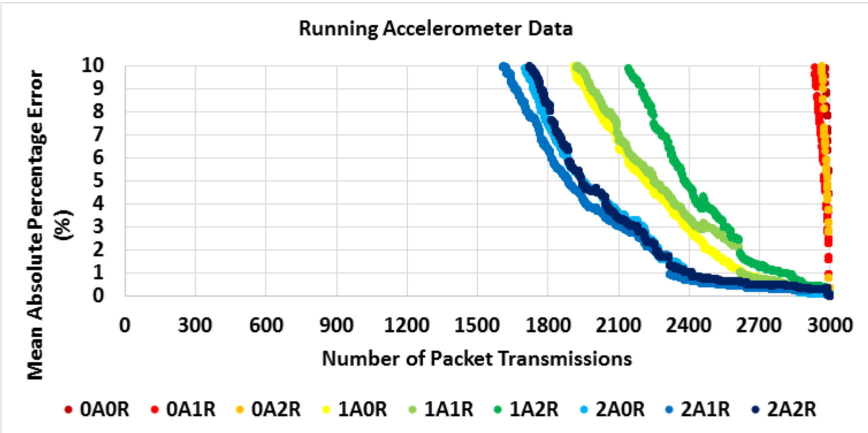

(d) Number of packet transmissions vs. mean absolute percentage error

where $MAPE_{max} = 10\%$

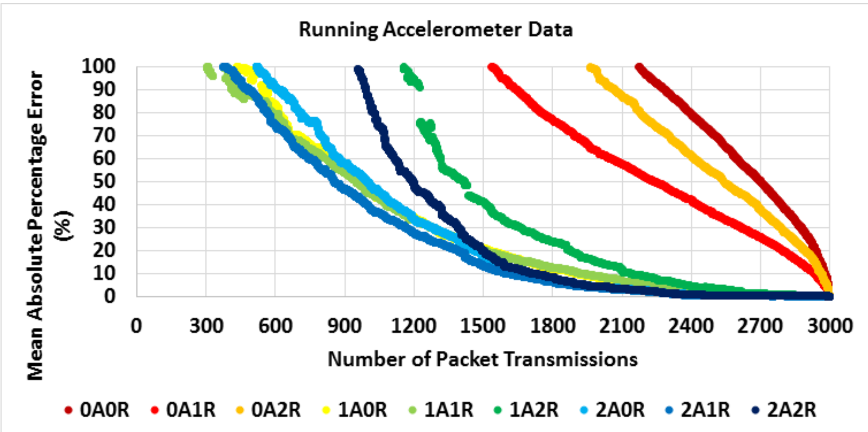

(e) Number of packet transmissions vs. mean absolute percentage error

where $MAPE_{max} = 100\%$

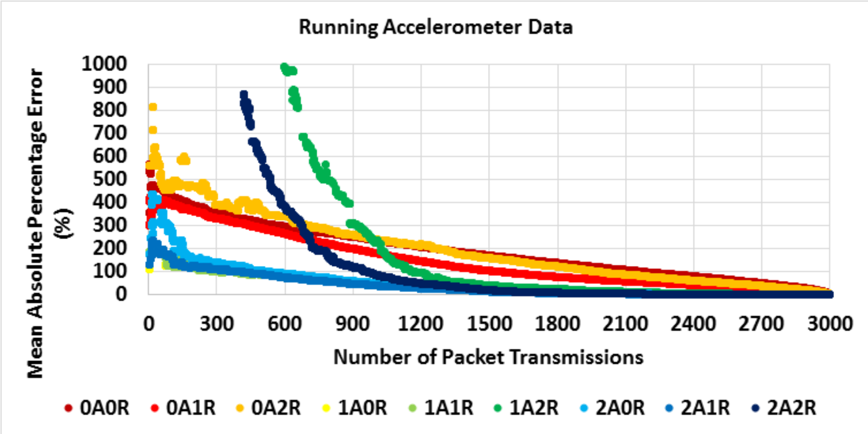

(f) Number of packet transmissions vs. mean absolute percentage error where $MAPE_{max} = 1000\%$

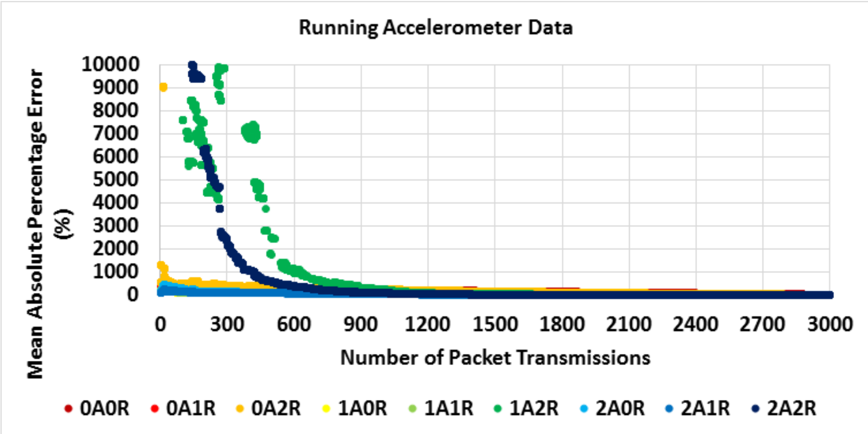

(g) Number of packet transmissions vs. mean absolute percentage error where $MAPE_{max} = 10000\%$

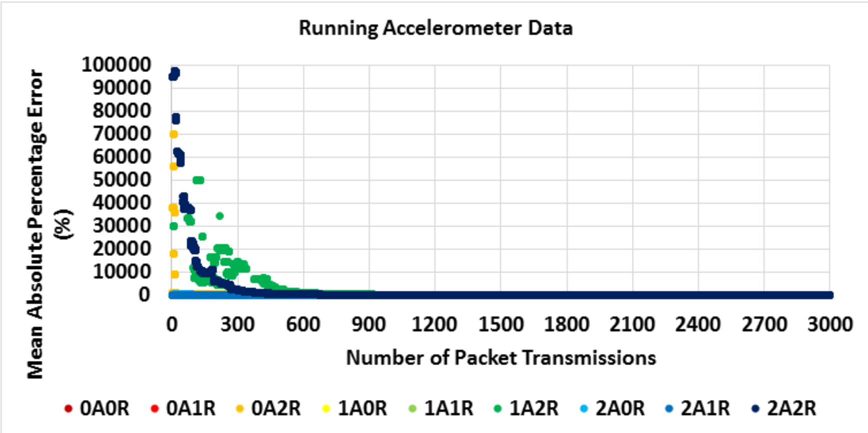

(h) Number of packet transmissions vs. mean absolute percentage error where $MAPE_{max} = 100000\%$

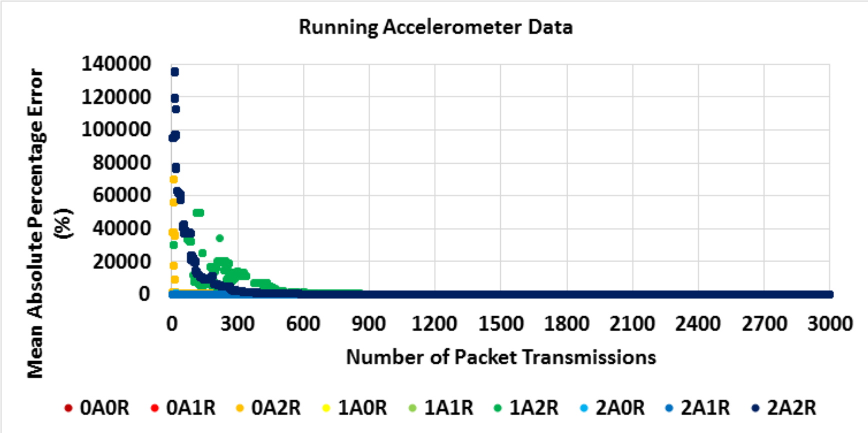

(i) Number of packet transmissions vs. mean absolute percentage error

where $MAPE_{max} = 140000\%$

Figure 5.78: Number of packet transmissions vs. mean absolute percentage error in running accelerometer data

The results of DAR schemes in running accelerometer data are shown more details in Table 5.57.

Table 5.57: Number of Packet Transmissions vs. Mean Absolute Percentage Error in Running Accelerometer Data

MAPE	DAR	$NoPT_{min}$
$\leq 2.5\%$	0A0R	2995
	0A1R	2992
	0A2R	2995
	1A0R	2438
	1A1R	2546
	1A2R	2605
	2A0R	2228
	2A1R	2206
	2A2R	2217

MAPE = mean absolute percentage error
DAR = data Abstraction and Reformation
0A0R = zeroth-order data abstraction & zeroth-order data reformation
0A1R = zeroth-order data abstraction & first-order data reformation
0A2R = zeroth-order data abstraction & second-order data reformation
1A0R = first-order data abstraction & zeroth-order data reformation
1A1R = first-order data abstraction & first-order data reformation
1A2R = first-order data abstraction & second-order data reformation
2A0R = second-order data abstraction & zeroth-order data reformation
2A1R = second-order data abstraction & first-order data reformation
2A2R = second-order data abstraction & second-order data reformation
$NoPT_{min}$ = minimum number of packet transmissions

From Table 5.57, it is shown that the best DAR schemes in running accelerometer data where $MAPE \leq 2.5\%$ in the terms of number of packet transmissions is 2A1R.

3. Number of Data Transmitted vs. Root Mean Square Error

The comparisons of number of data transmitted against root mean square error are shown in Figure 5.79.

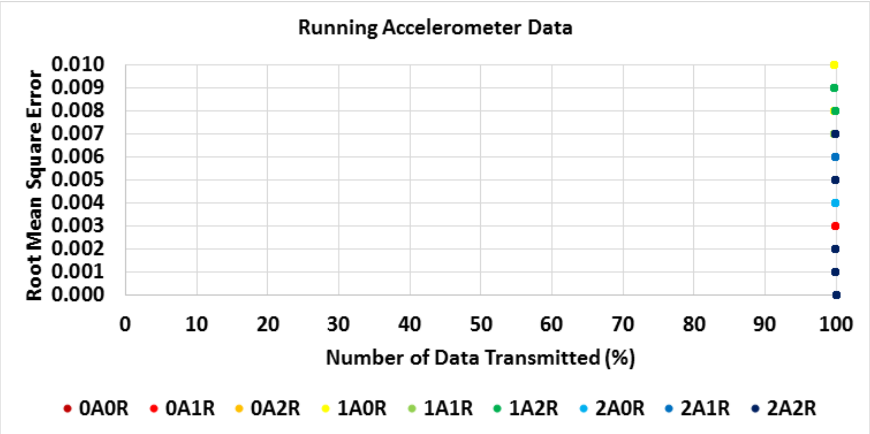

(a) Number of data transmitted vs. root mean square error where $RMSE_{max} = 0.01$

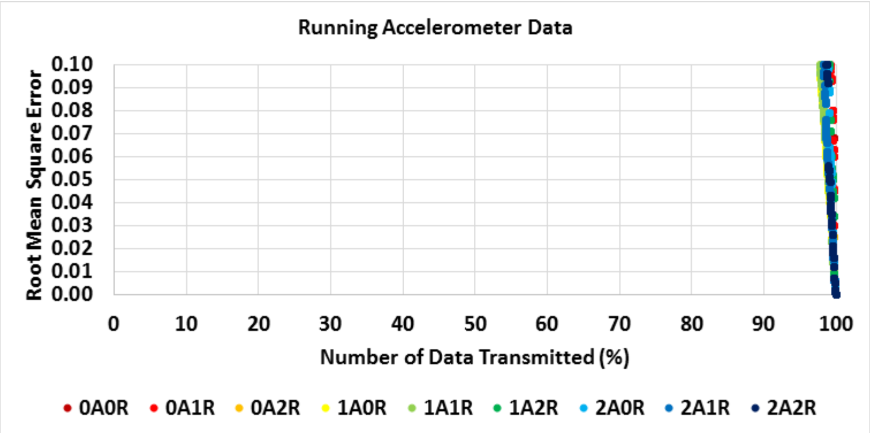

(b) Number of data transmitted vs. root mean square error where $RMSE_{max} = 0.1$

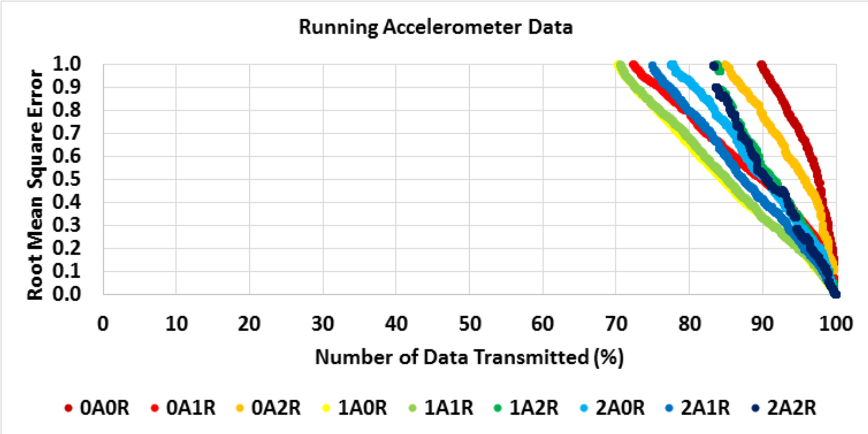

(c) Number of data transmitted vs. root mean square error where

$$RMSE_{max} = 1$$

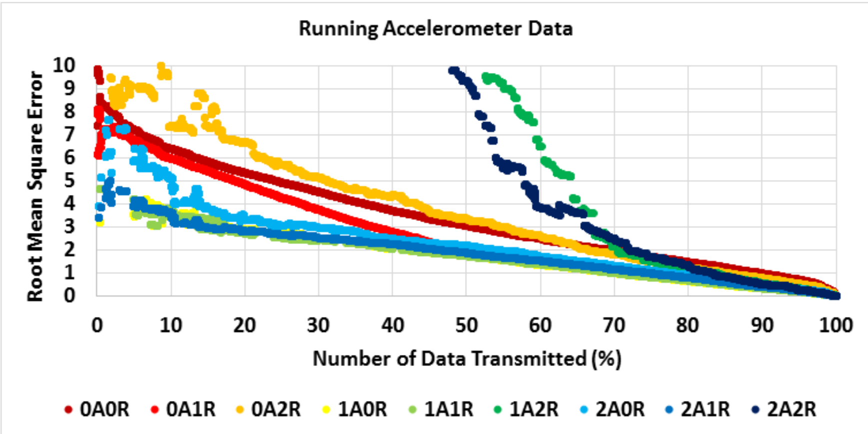

(d) Number of data transmitted vs. root mean square error where

$$RMSE_{max} = 10$$

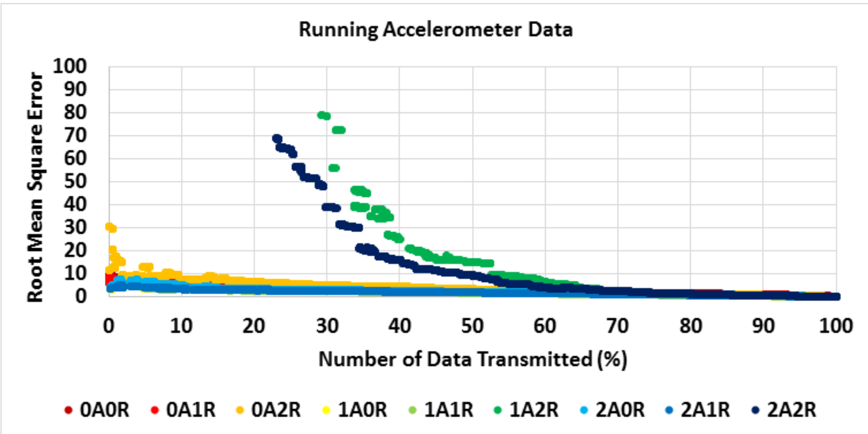

(e) Number of data transmitted vs. root mean square error where

$$RMSE_{max} = 100$$

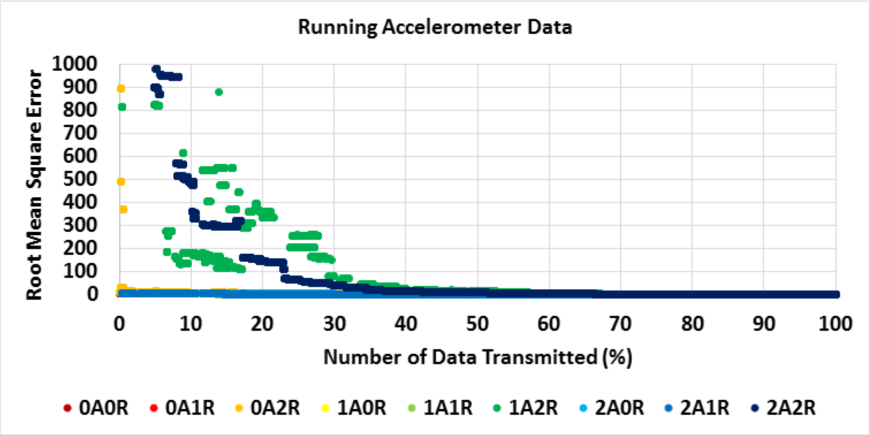

(f) Number of data transmitted vs. root mean square error where

$$\boldsymbol{RMSE_{max} = 1000}$$

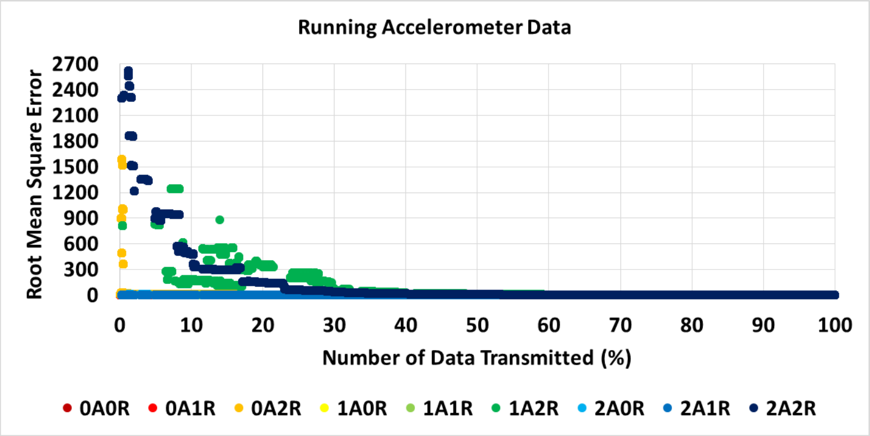

(g) Number of data transmitted vs. root mean square error where

$$\boldsymbol{RMSE_{max} = 2700}$$

Figure 5.79: Number of data transmitted vs. root mean square error in running accelerometer data

The results of DAR schemes in running accelerometer data are shown more details in Table 5.58.

Table 5.58: Number of Data Transmitted vs. Root Mean Square Error in Running Accelerometer Data

RMSE	DAR	$NoDT_{min}$ (%)
≤ 0.25	0A0R	99.233
	0A1R	97.133
	0A2R	98.533
	1A0R	93.200
	1A1R	93.200
	1A2R	96.667
	2A0R	96.300
	2A1R	94.633
	2A2R	95.333

RMSE = root mean square error
DAR = data Abstraction and Reformation
0A0R = zeroth-order data abstraction & zeroth-order data reformation
0A1R = zeroth-order data abstraction & first-order data reformation
0A2R = zeroth-order data abstraction & second-order data reformation
1A0R = first-order data abstraction & zeroth-order data reformation
1A1R = first-order data abstraction & first-order data reformation
1A2R = first-order data abstraction & second-order data reformation
2A0R = second-order data abstraction & zeroth-order data reformation
2A1R = second-order data abstraction & first-order data reformation
2A2R = second-order data abstraction & second-order data reformation
$NoDT_{min}$ = minimum number of data transmitted

From Table 5.58, it is shown that the best DAR schemes in running accelerometer data where $RMSE \leq 0.1$ in the terms of number of data transmitted are 1A0R and 1A1R.

4. Number of Data Transmitted vs. Mean Absolute Percentage Error

The comparisons of number of data transmitted against mean absolute percentage error are shown in Figure 5.80.

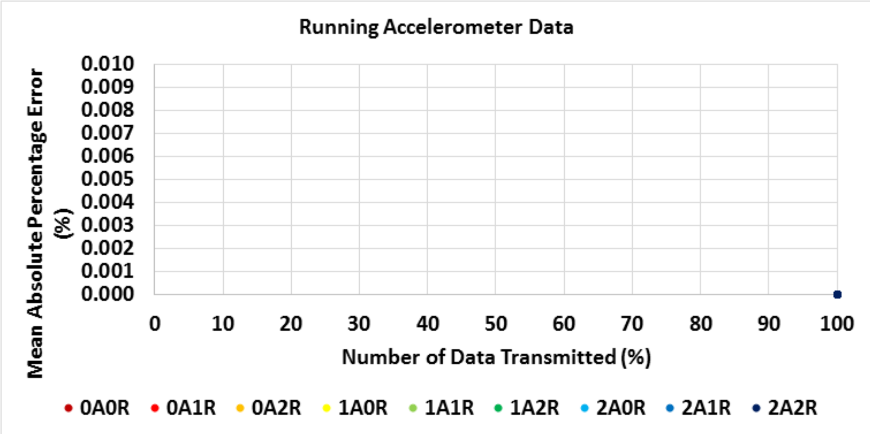

(a) Number of data transmitted vs. mean absolute percentage error where

$$MAPE_{max} = 0.01\%$$

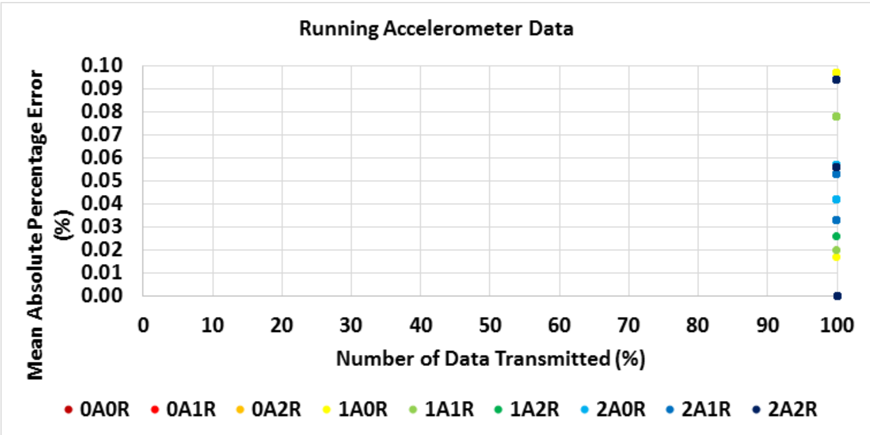

(b) Number of data transmitted vs. mean absolute percentage error where

$$MAPE_{max} = 0.1\%$$

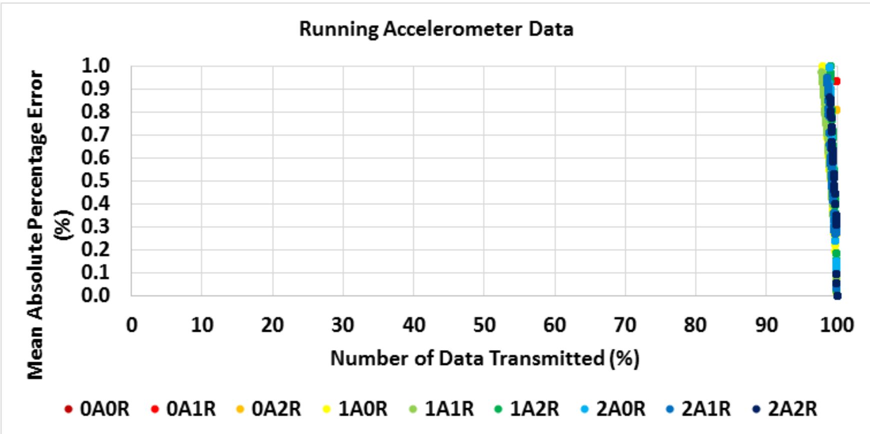

(c) Number of data transmitted vs. mean absolute percentage error where

$$MAPE_{max} = 1\%$$

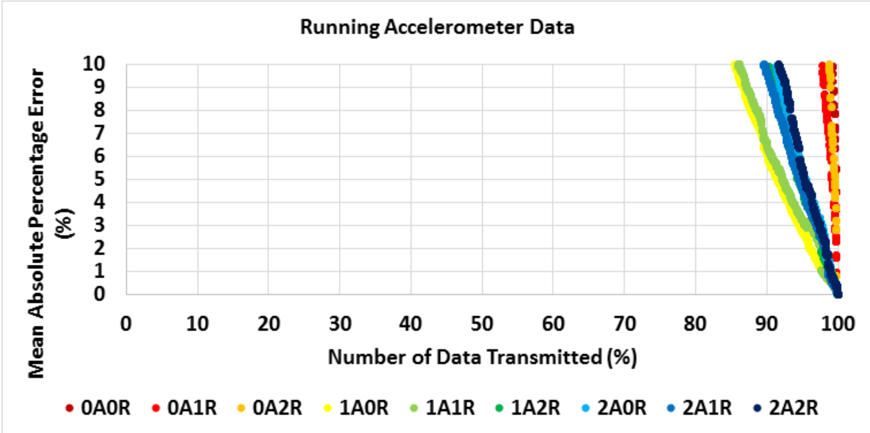

(d) Number of data transmitted vs. mean absolute percentage error where

$$MAPE_{max} = 10\%$$

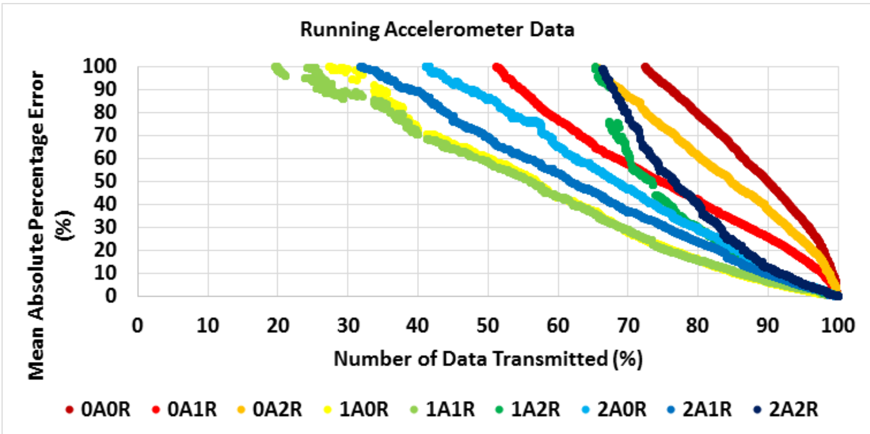

(e) Number of data transmitted vs. mean absolute percentage error where

$$MAPE_{max} = 100\%$$

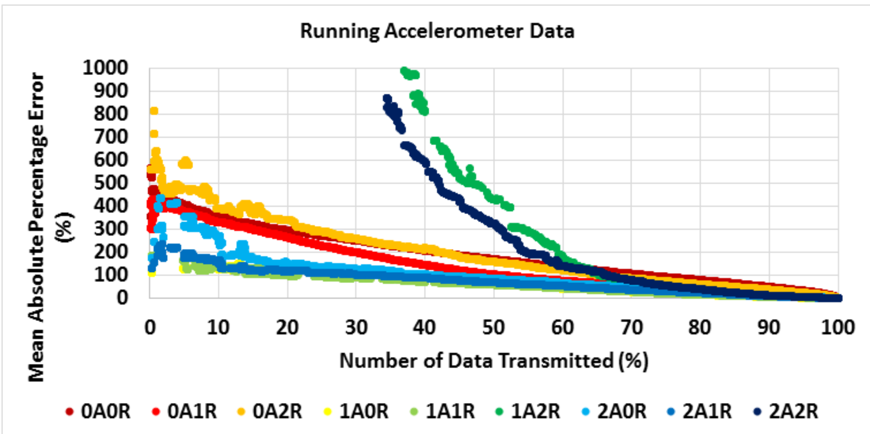

(f) Number of data transmitted vs. mean absolute percentage error where

$$MAPE_{max} = 1000\%$$

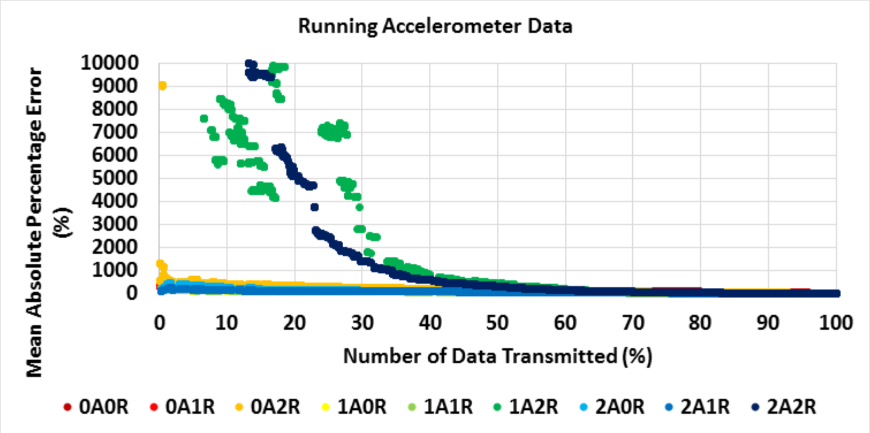

(g) Number of data transmitted vs. mean absolute percentage error where

$$MAPE_{max} = 10000\%$$

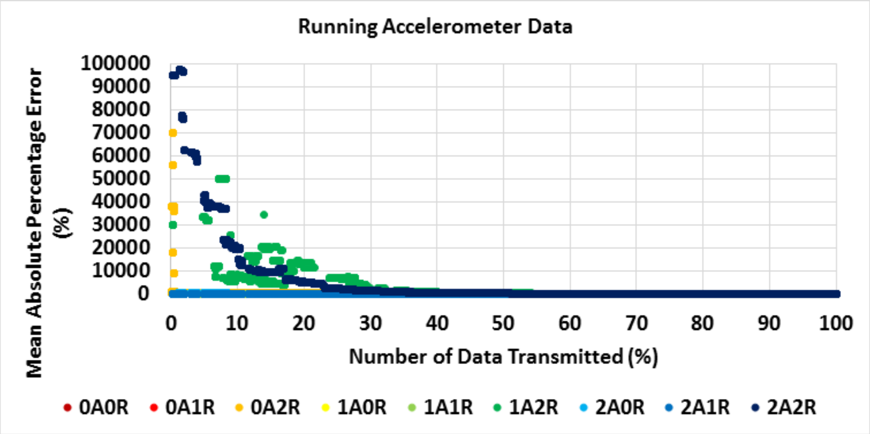

(h) Number of data transmitted vs. mean absolute percentage error where

$$MAPE_{max} = 100000\%$$

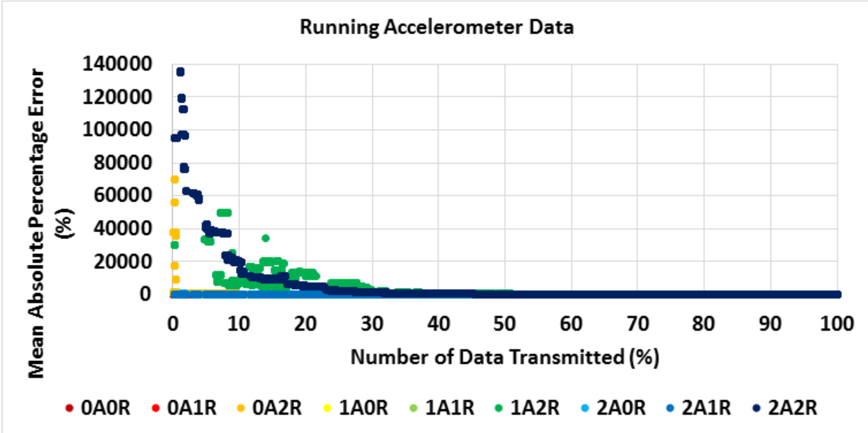

(i) Number of data transmitted vs. mean absolute percentage error where

$$MAPE_{max} = 140000\%$$

Figure 5.80: Number of data transmitted vs. mean absolute percentage error in running accelerometer data

The results of DAR schemes in running accelerometer data are shown more details in Table 5.59.

Table 5.59: Number of Data Transmitted vs. Mean Absolute Percentage Error in Running Accelerometer Data

MAPE	DAR	$NoDT_{min}$ (%)
≤ 2.5%	0A0R	99.833
	0A1R	99.733
	0A2R	99.833
	1A0R	95.500
	1A1R	96.933
	1A2R	97.533
	2A0R	98.100
	2A1R	97.733
	2A2R	97.967

MAPE = mean absolute percentage error
DAR = data Abstraction and Reformation
0A0R = zeroth-order data abstraction & zeroth-order data reformation
0A1R = zeroth-order data abstraction & first-order data reformation
0A2R = zeroth-order data abstraction & second-order data reformation
1A0R = first-order data abstraction & zeroth-order data reformation
1A1R = first-order data abstraction & first-order data reformation
1A2R = first-order data abstraction & second-order data reformation
2A0R = second-order data abstraction & zeroth-order data reformation
2A1R = second-order data abstraction & first-order data reformation
2A2R = second-order data abstraction & second-order data reformation
$NoDT_{min}$ = minimum number of data transmitted

From Table 5.59, it is shown that the best DAR schemes in running accelerometer data where $MAPE \leq 2.5\%$ in the terms of number of data transmitted is 1A0R.

5. Root Mean Square Error vs. Number of Packet Transmissions

The comparisons of root mean square error against number of packet transmissions are shown in Figure 5.81.

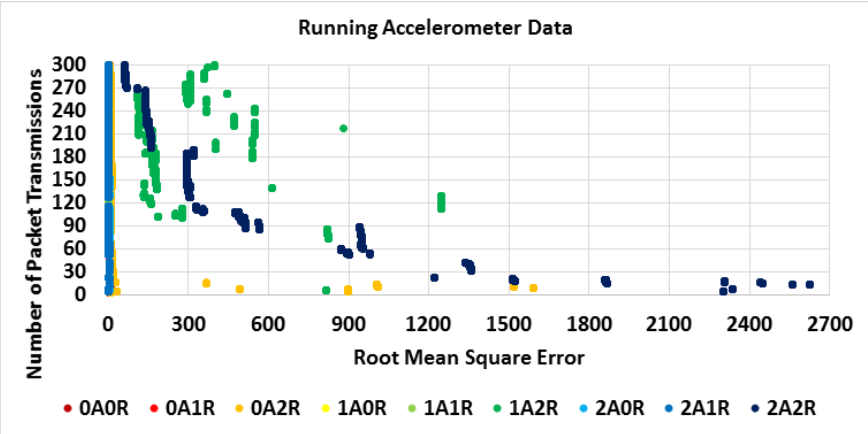

(a) Root mean square error vs. number of packet transmissions where $NoPT_{max} = 300$

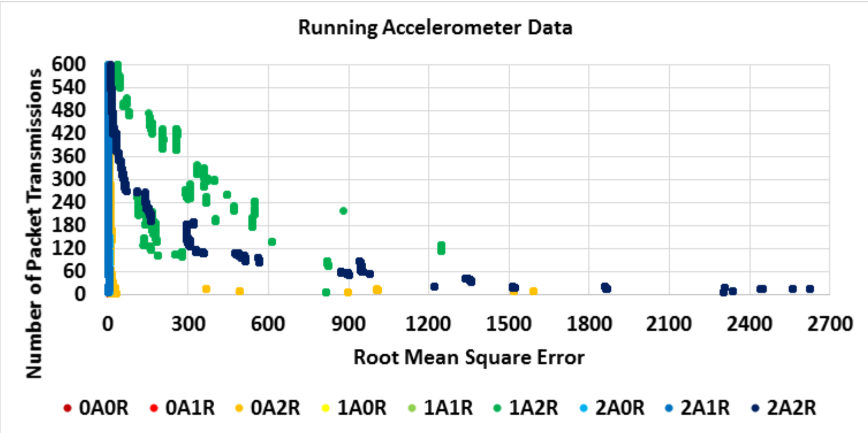

(b) Root mean square error vs. number of packet transmissions where $NoPT_{max} = 600$

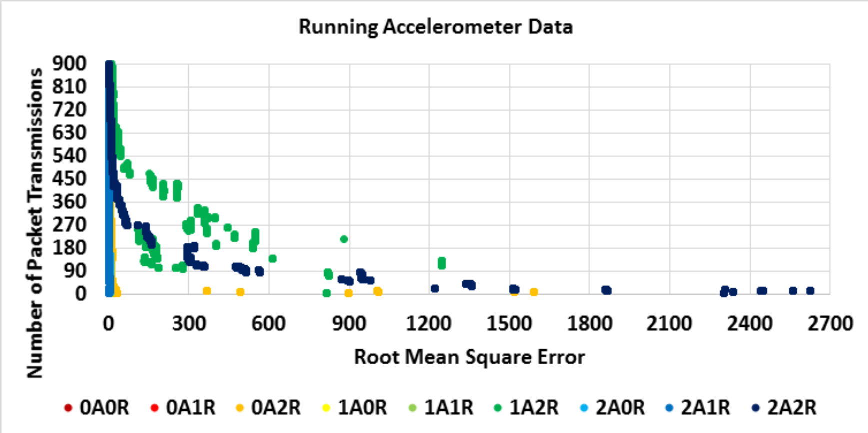

(c) Root mean square error vs. number of packet transmissions where

$$NoPT_{max} = 900$$

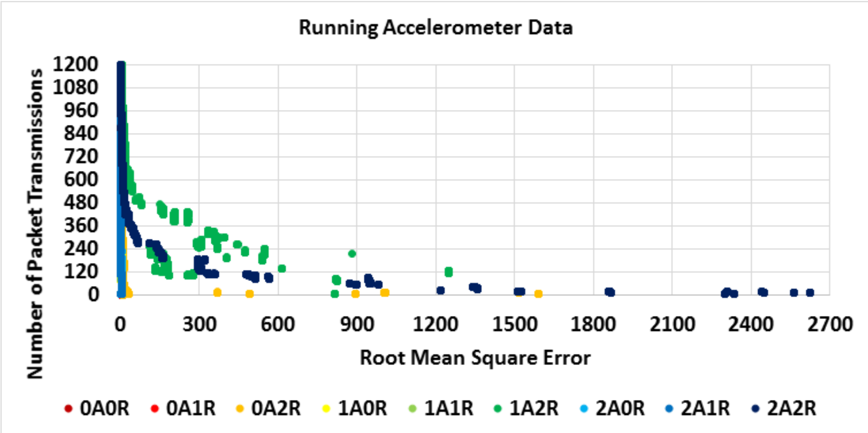

(d) Root mean square error vs. number of packet transmissions where

$$NoPT_{max} = 1200$$

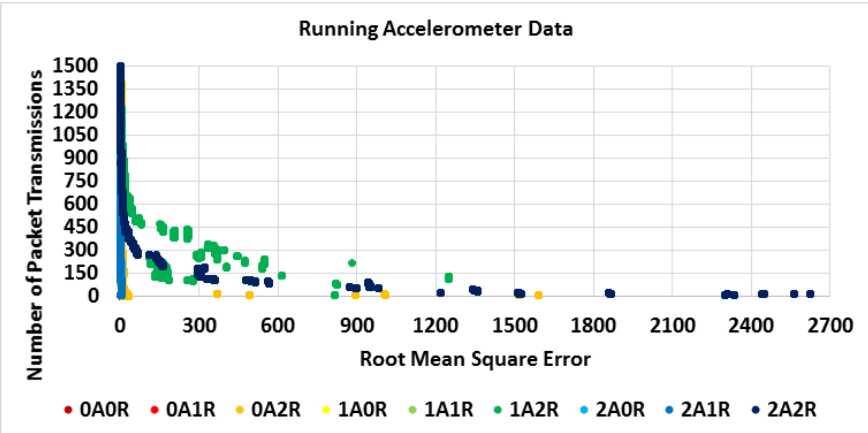

(e) Root mean square error vs. number of packet transmissions where

$$NoPT_{max} = 1500$$

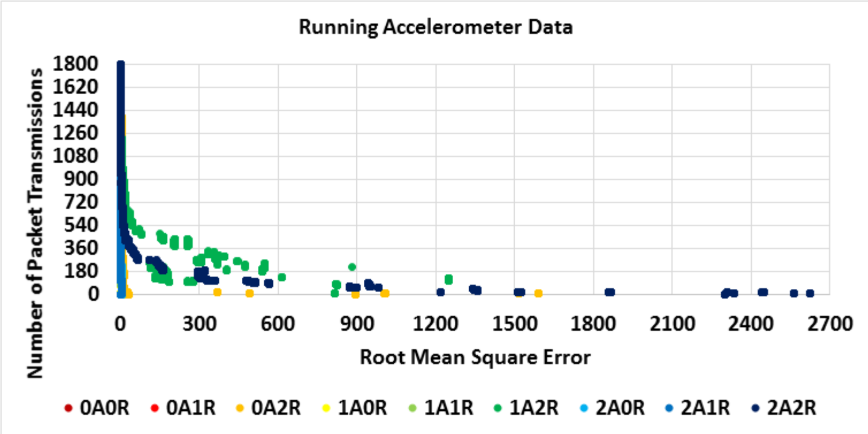

(f) Root mean square error vs. number of packet transmissions where

$$NoPT_{max} = 1800$$

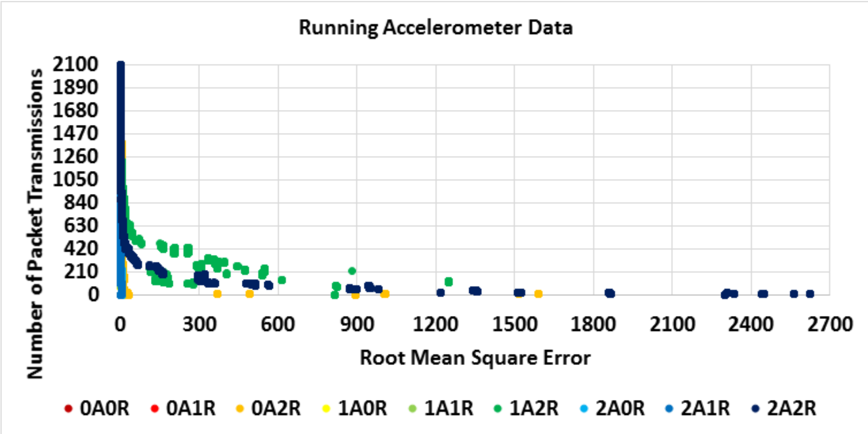

(g) Root mean square error vs. number of packet transmissions where

$$NoPT_{max} = 2100$$

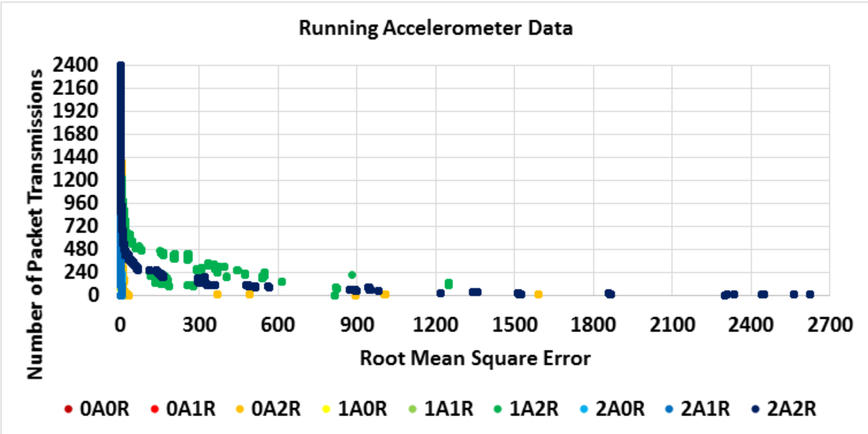

(h) Root mean square error vs. number of packet transmissions where

$$NoPT_{max} = 2400$$

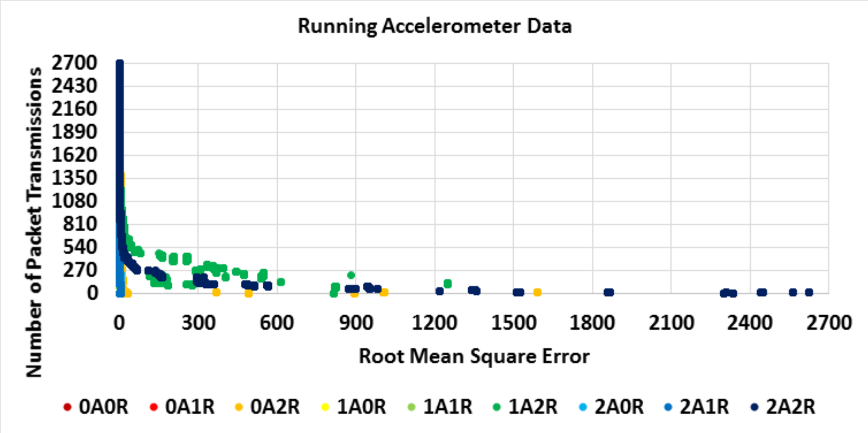

(i) Root mean square error vs. number of packet transmissions where

$$NoPT_{max} = 2700$$

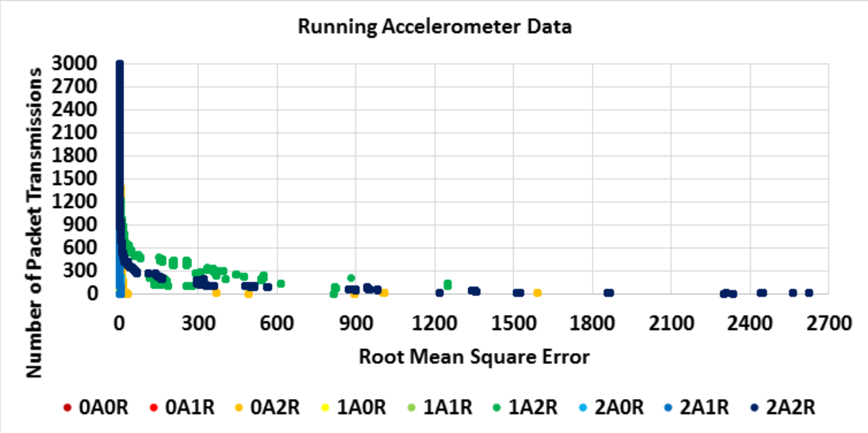

(j) Root mean square error vs. number of packet transmissions where

$$NoPT_{max} = 3000$$

Figure 5.81: Root mean square error vs. number of packet transmissions in running accelerometer data

The results of DAR schemes in running accelerometer data are shown more details in Table 5.60.

Table 5.60: Root Mean Square Error vs. Number of Packet Transmissions in Running Accelerometer Data

NoPT	DAR	$RMSE_{min}$
≤ 2250	0A0R	1.698
	0A1R	0.920
	0A2R	1.495
	1A0R	0.282
	1A1R	0.281
	1A2R	0.460
	2A0R	0.168
	2A1R	0.102
	2A2R	0.129

NoPT = number of packet transmissions
DAR = data abstraction and reformation
0A0R = zeroth-order data abstraction & zeroth-order data reformation
0A1R = zeroth-order data abstraction & first-order data reformation
0A2R = zeroth-order data abstraction & second-order data reformation
1A0R = first-order data abstraction & zeroth-order data reformation
1A1R = first-order data abstraction & first-order data reformation
1A2R = first-order data abstraction & second-order data reformation
2A0R = second-order data abstraction & zeroth-order data reformation
2A1R = second-order data abstraction & first-order data reformation
2A2R = second-order data abstraction & second-order data reformation
$RMSE_{min}$ = minimum root mean square error

From Table 5.60, it is shown that the best DAR schemes in running accelerometer data where $NoPT \leq 2250$ in the terms of root mean square error is 2A1R.

6. Root Mean Square Error vs. Number of Data Transmitted

The comparisons of root mean square error against number of data transmitted are shown in Figure 5.82.

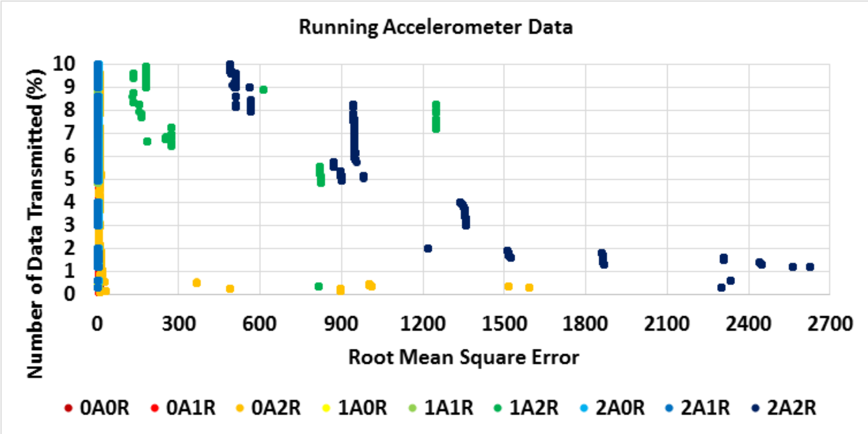

(a) Root mean square error vs. number of data transmitted where

$NoDT_{max} = 10\%$

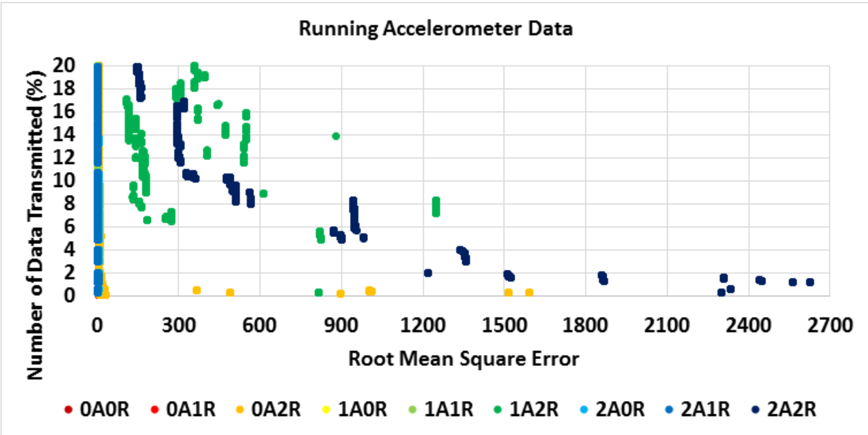

(b) Root mean square error vs. number of data transmitted where

$NoDT_{max} = 20\%$

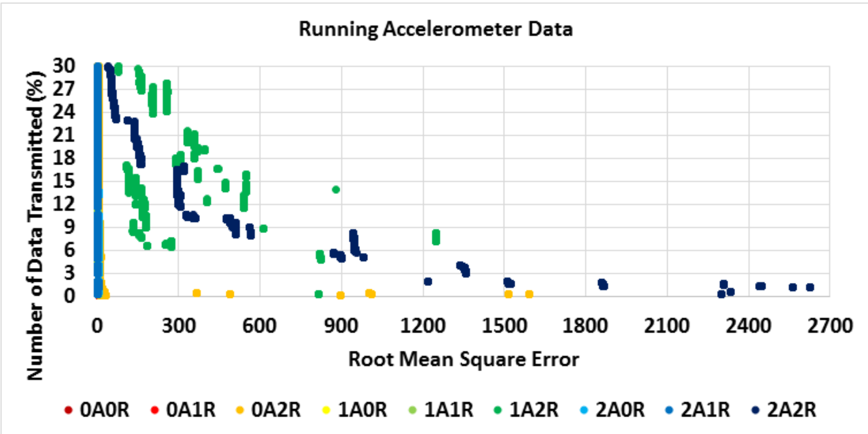

(c) Root mean square error vs. number of data transmitted (%) where

$NoDT_{max} = 30\%$

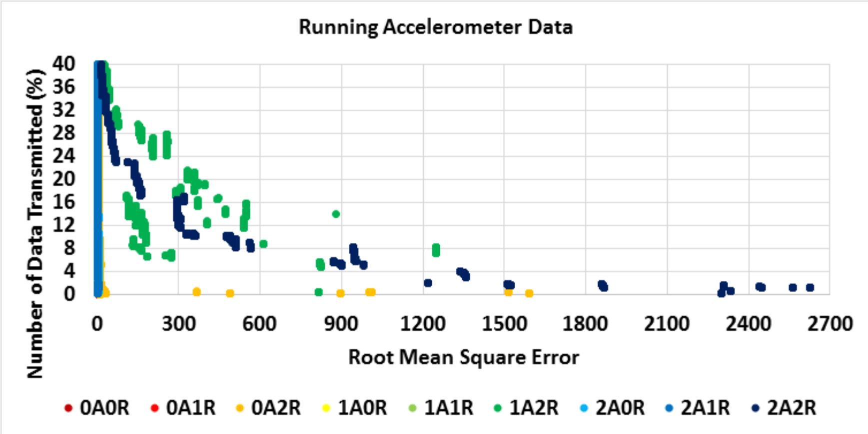

(d) Root mean square error vs. number of data transmitted where

$$NoDT_{max} = 40\%$$

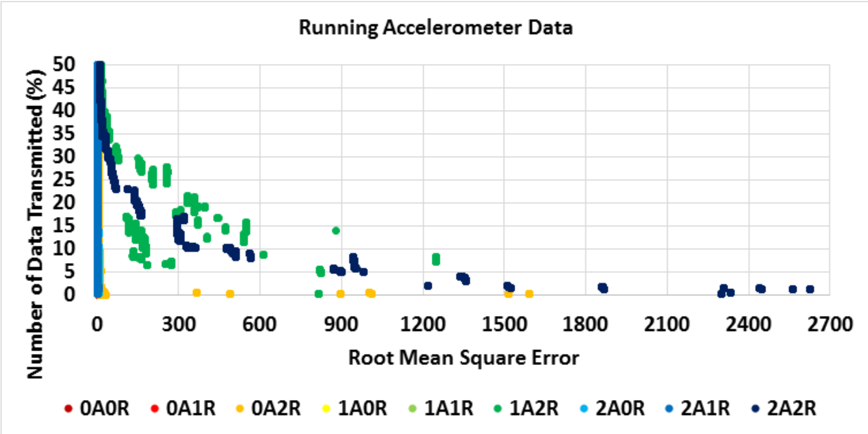

(e) Root mean square error vs. number of data transmitted where

$$NoDT_{max} = 50\%$$

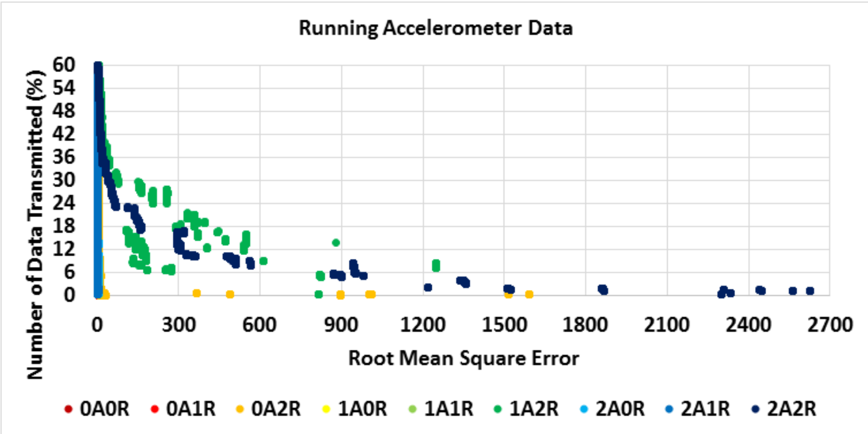

(f) Root mean square error vs. number of data transmitted where

$$NoDT_{max} = 60\%$$

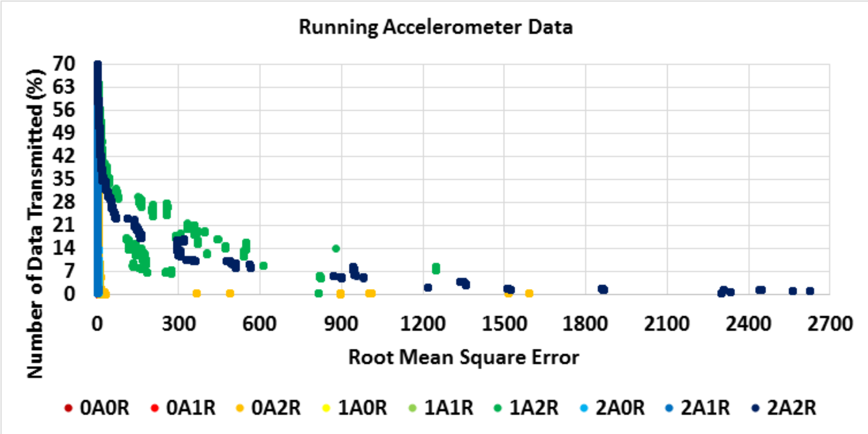

(g) Root mean square error vs. number of data transmitted where

$\boldsymbol{NoDT_{max}} = \mathbf{70\%}$

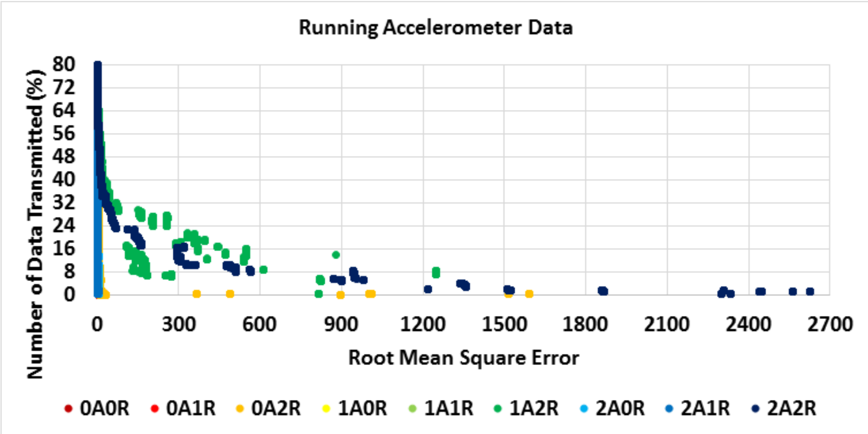

(h) Root mean square error vs. number of data transmitted where

$\boldsymbol{NoDT_{max}} = \mathbf{80\%}$

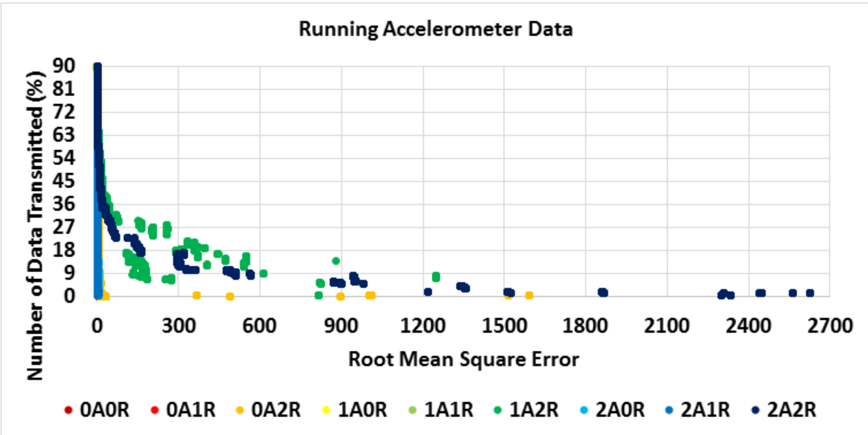

(i) Root mean square error vs. number of data transmitted where

$\boldsymbol{NoDT_{max}} = \mathbf{90\%}$

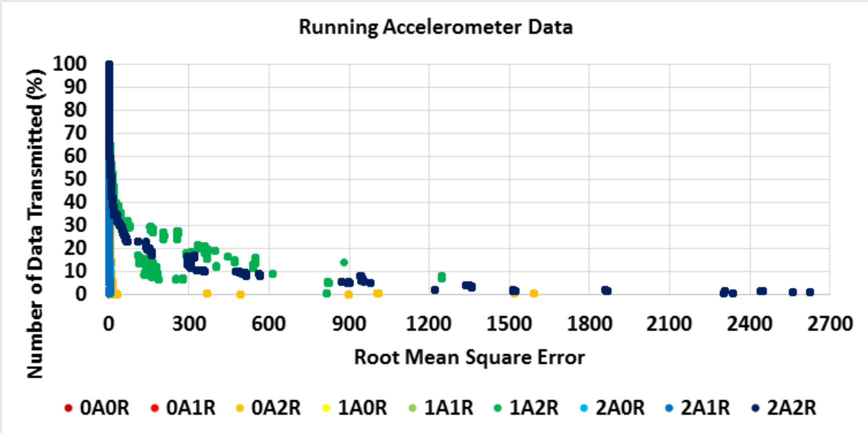

(j) Root mean square error vs. number of data transmitted where

$$NoDT_{max} = 100\%$$

Figure 5.82: Root mean square error vs. number of data transmitted in running accelerometer data

The results of DAR schemes in running accelerometer data are shown more details in Table 5.61.

Table 5.61: Root Mean Square Error vs. Number of Data Transmitted in Running Accelerometer Data

NoDT	DAR	$RMSE_{min}$
≤ 75%	0A0R	1.698
	0A1R	0.920
	0A2R	1.495
	1A0R	0.824
	1A1R	0.825
	1A2R	1.505
	2A0R	1.112
	2A1R	0.996
	2A2R	1.702

NoDT = number of data transmitted
DAR = data abstraction and reformation
0A0R = zeroth-order data abstraction & zeroth-order data reformation
0A1R = zeroth-order data abstraction & first-order data reformation
0A2R = zeroth-order data abstraction & second-order data reformation
1A0R = first-order data abstraction & zeroth-order data reformation
1A1R = first-order data abstraction & first-order data reformation
1A2R = first-order data abstraction & second-order data reformation
2A0R = second-order data abstraction & zeroth-order data reformation
2A1R = second-order data abstraction & first-order data reformation
2A2R = second-order data abstraction & second-order data reformation
$RMSE_{min}$ = minimum root mean square error

From Table 5.61, it is shown that the best DAR schemes in running accelerometer data where $NoDT \leq 75\%$ in the terms of root mean square error is 1A0R.

7. Mean Absolute Percentage Error vs. Number of Packet Transmissions

The comparisons of mean absolute percentage error against number of packet transmissions are shown in Figure 5.83.

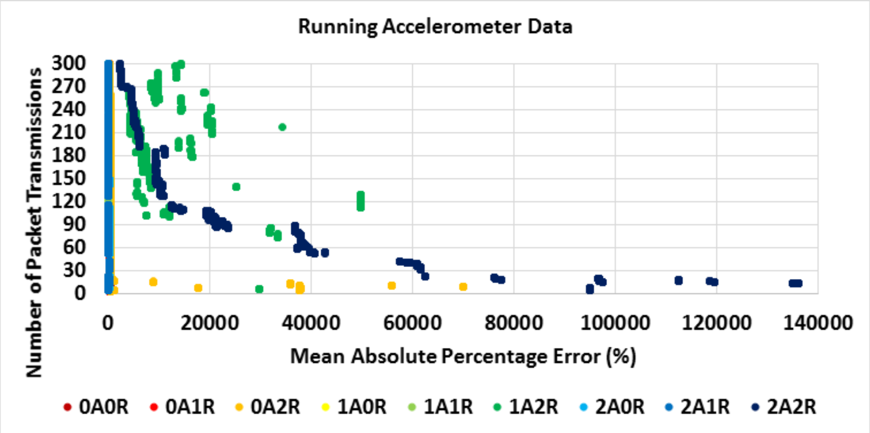

(a) Mean absolute percentage error vs. number of packet transmission where $NoPT_{max} = 300$

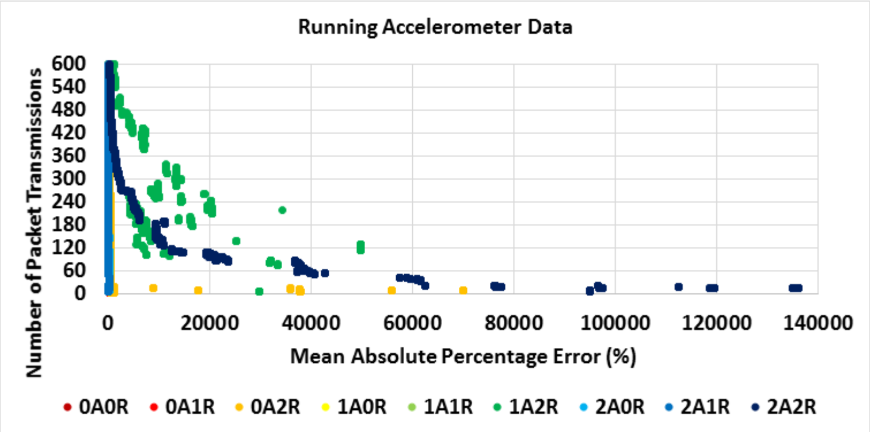

(b) Mean absolute percentage error vs. number of packet transmission where $NoPT_{max} = 600$

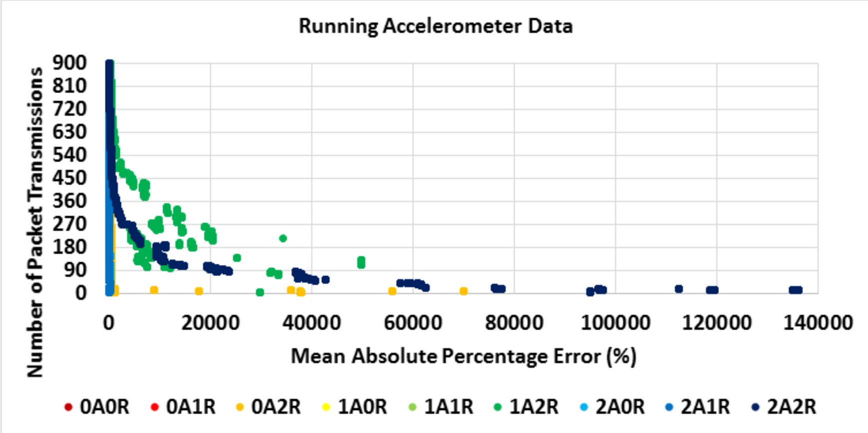

(c) Mean absolute percentage error vs. number of packet transmission where $NoPT_{max} = 900$

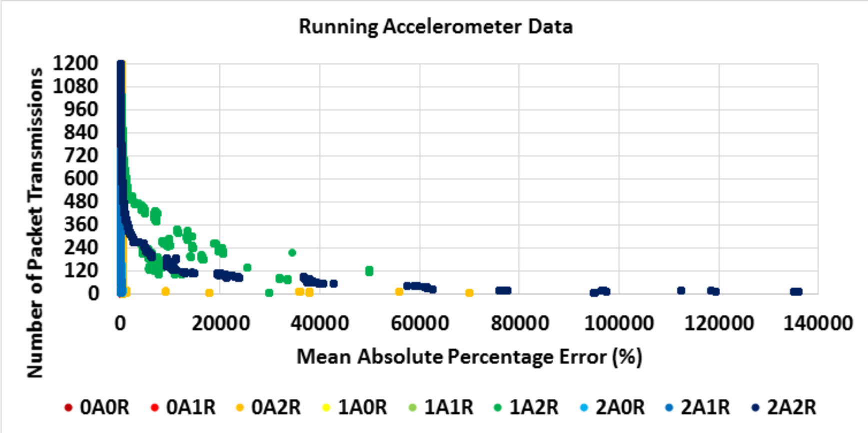

(d) Mean absolute percentage error vs. number of packet transmission where $NoPT_{max} = 1200$

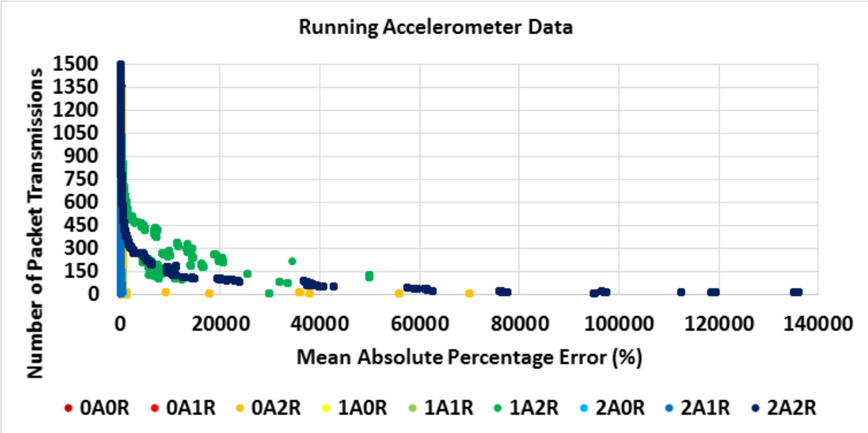

(e) Mean absolute percentage error vs. number of packet transmission where $NoPT_{max} = 1500$

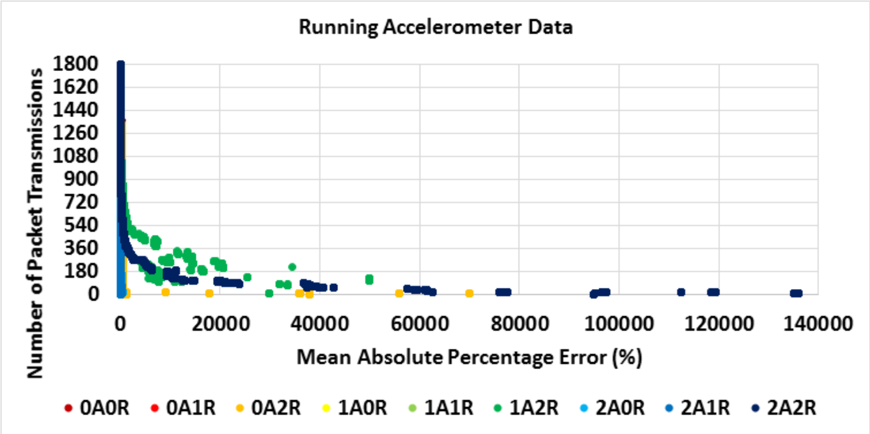

(f) Mean absolute percentage error vs. number of packet transmission

where $NoPT_{max} = 1800$

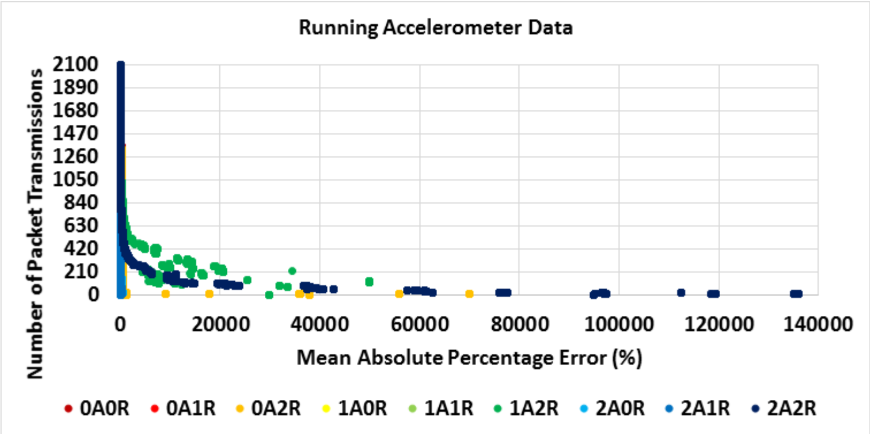

(g) Mean absolute percentage error vs. number of packet transmission

where $NoPT_{max} = 2100$

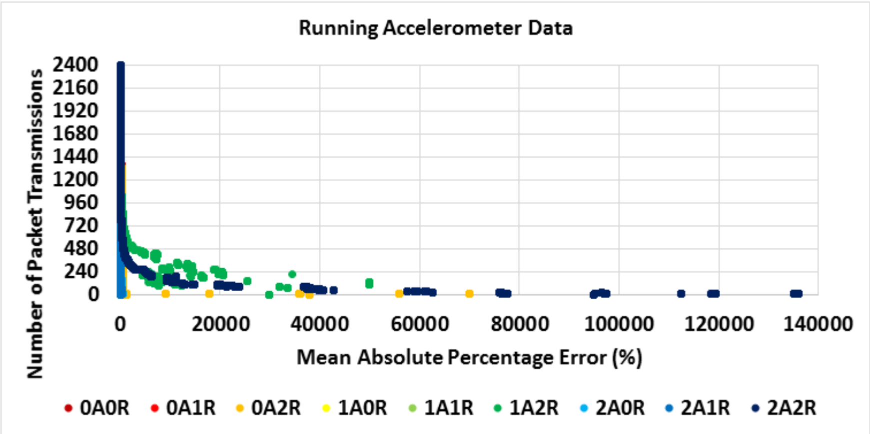

(h) Mean absolute percentage error vs. number of packet transmission

where $NoPT_{max} = 2400$

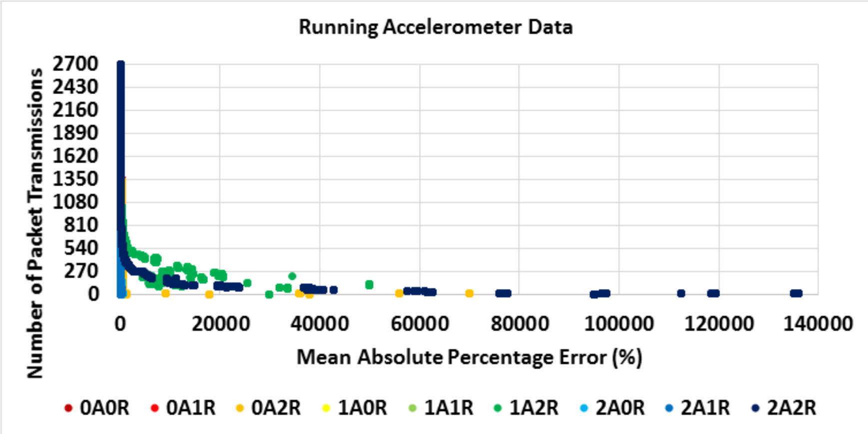

(i) Mean absolute percentage error vs. number of packet transmission where $NoPT_{max} = 2700$

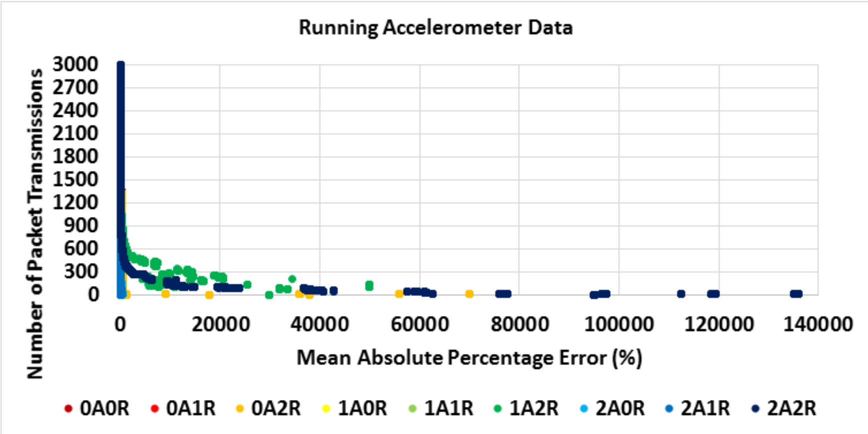

(j) Mean absolute percentage error vs. number of packet transmission where $NoPT_{max} = 3000$

Figure 5.83: Mean absolute percentage error vs. number of packet transmissions in running accelerometer data

The results of DAR schemes in running accelerometer data are shown more details in Table 5.62.

Table 5.62: Mean Absolute Percentage Error vs. Number of Packet Transmissions in Running Accelerometer Data

NoPT	DAR	$MAPE_{min}$ (%)
≤ 2250	0A0R	92.703
	0A1R	49.600
	0A2R	73.653
	1A0R	4.544
	1A1R	5.013
	1A2R	7.469
	2A0R	2.287
	2A1R	2.019
	2A2R	2.240

NoPT = number of packet transmissions
DAR = data abstraction and reformation
0A0R = zeroth-order data abstraction & zeroth-order data reformation
0A1R = zeroth-order data abstraction & first-order data reformation
0A2R = zeroth-order data abstraction & second-order data reformation
1A0R = first-order data abstraction & zeroth-order data reformation
1A1R = first-order data abstraction & first-order data reformation
1A2R = first-order data abstraction & second-order data reformation
2A0R = second-order data abstraction & zeroth-order data reformation
2A1R = second-order data abstraction & first-order data reformation
2A2R = second-order data abstraction & second-order data reformation
$MAPE_{min}$ = minimum mean absolute percentage error

From Table 5.62, it is shown that the best DAR schemes in running accelerometer data where $NoPT \leq 2250$ in the terms of mean absolute percentage error is 2A1R.

8. Mean Absolute Percentage Error vs. Number of Data Transmitted

The comparisons of mean absolute percentage error against number of data transmitted are shown in Figure 5.84.

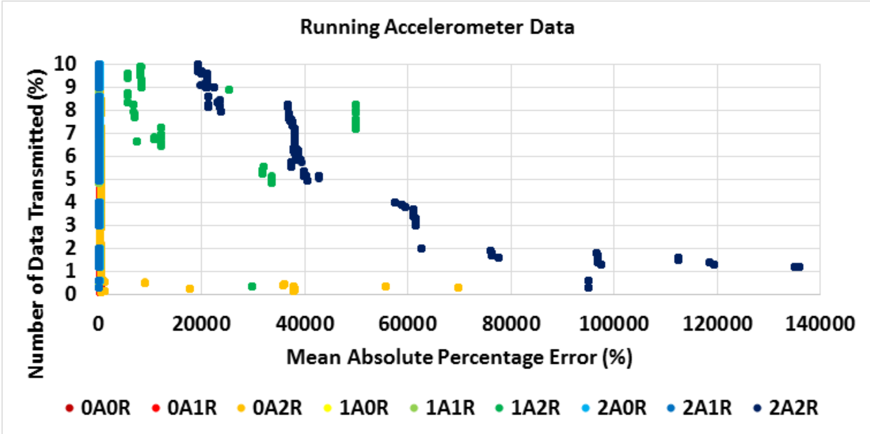

(a) Mean absolute percentage error vs. number of data transmitted where

$$NoDT_{max} = 10\%$$

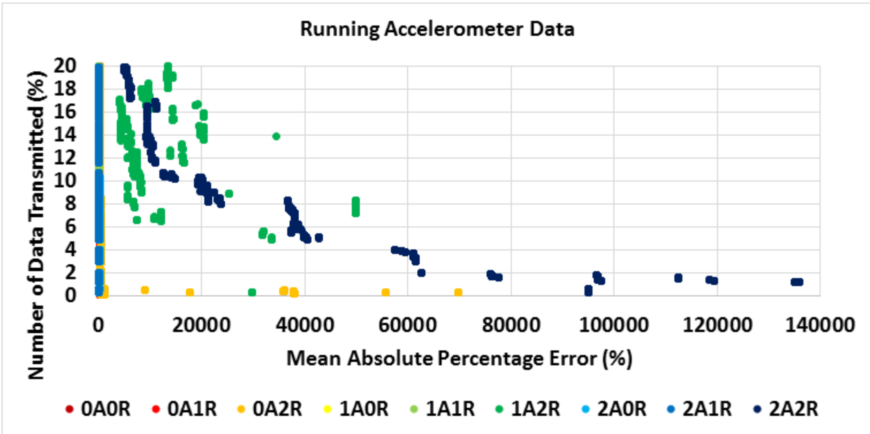

(b) Mean absolute percentage error vs. number of data transmitted where

$$NoDT_{max} = 20\%$$

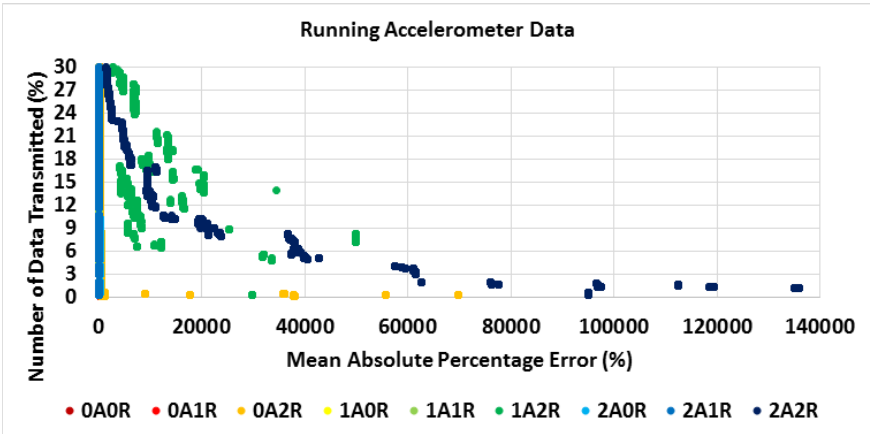

(c) Mean absolute percentage error vs. number of data transmitted where

$$NoDT_{max} = 30\%$$

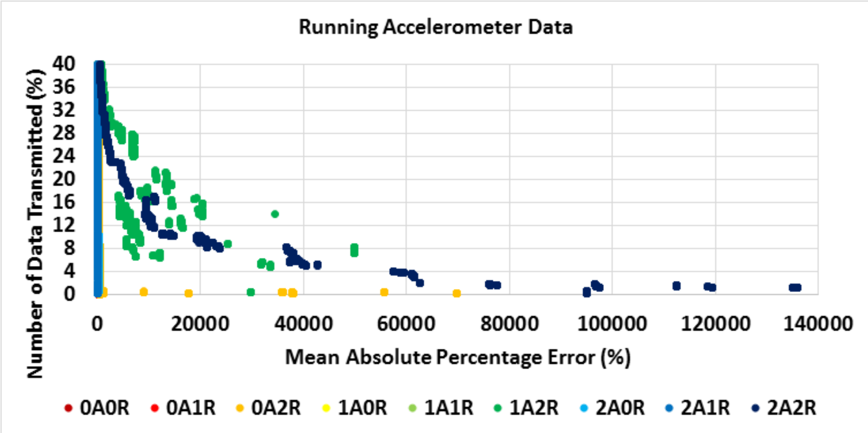

(d) Mean absolute percentage error vs. number of data transmitted where

$\boldsymbol{NoDT_{max} = 40\%}$

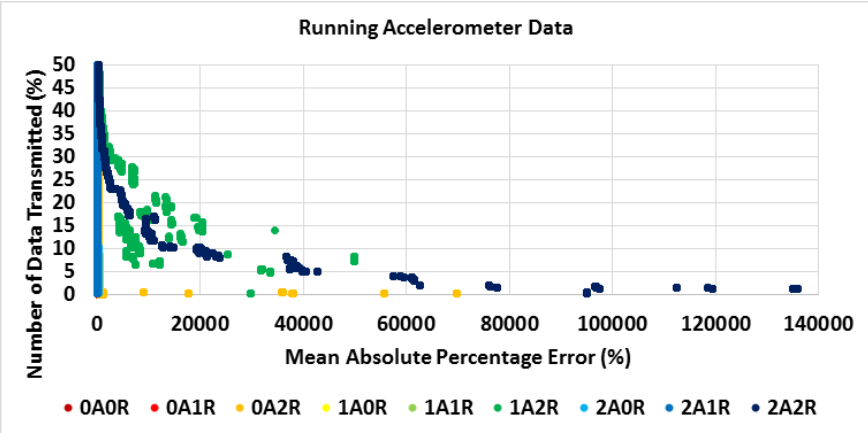

(e) Mean absolute percentage error vs. number of data transmitted where

$\boldsymbol{NoDT_{max} = 50\%}$

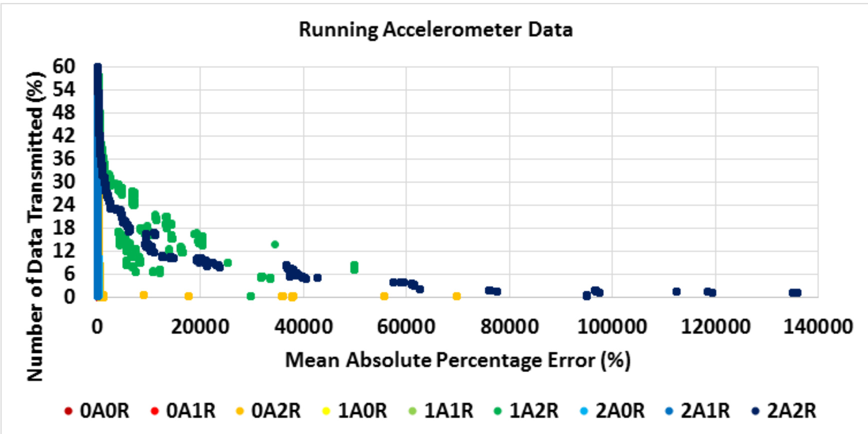

(f) Mean absolute percentage error vs. number of data transmitted where

$\boldsymbol{NoDT_{max} = 60\%}$

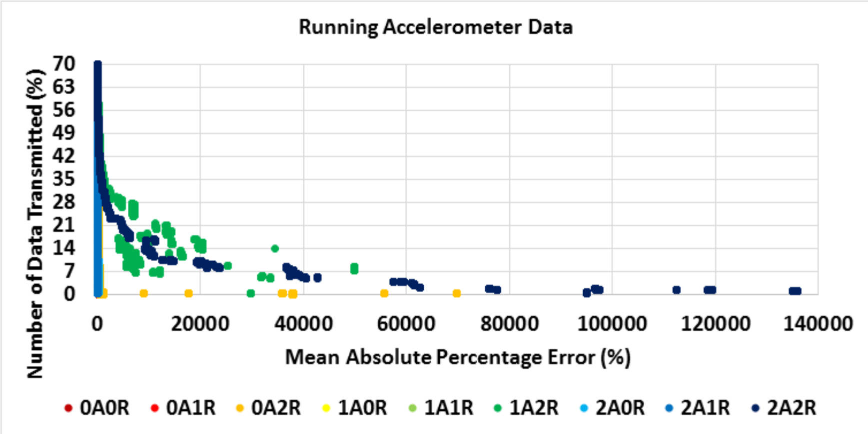

(g) Mean absolute percentage error vs. number of data transmitted where

$NoDT_{max} = 70\%$

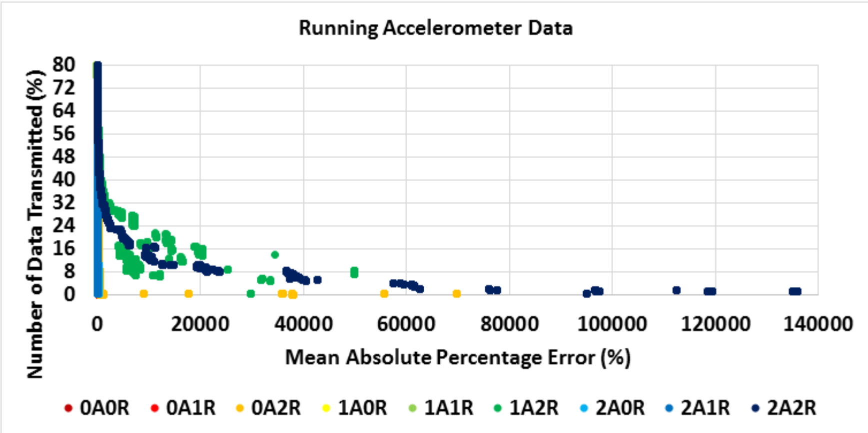

(h) Mean absolute percentage error vs. number of data transmitted where

$NoDT_{max} = 80\%$

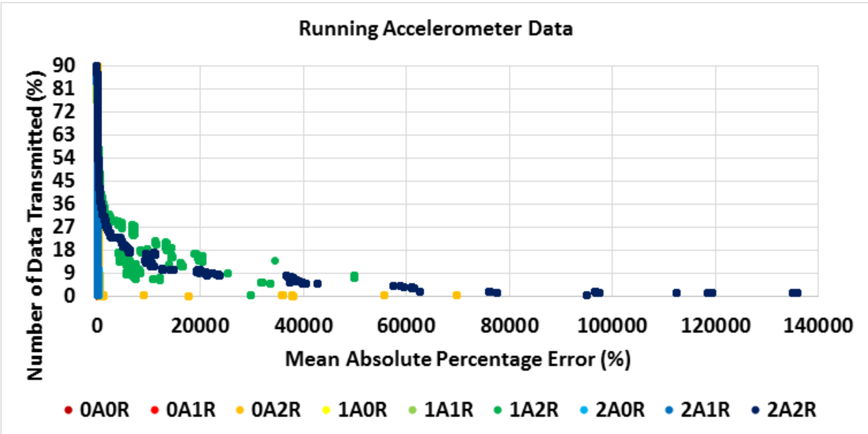

(i) Mean absolute percentage error vs. number of data transmitted where

$NoDT_{max} = 90\%$

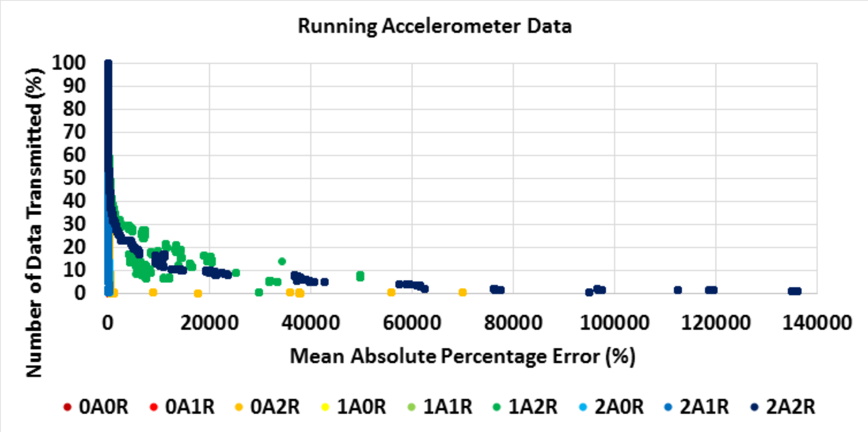

(j) Mean absolute percentage error vs. number of data transmitted (%) where $NoDT_{max}$ = 100%

Figure 5.84: Mean absolute percentage error vs. number of data transmitted in running accelerometer data

The results of DAR schemes in running accelerometer data are shown more details in Table 5.63.

Table 5.63: Mean Absolute Percentage Error vs. Number of Data Transmitted in Running Accelerometer Data

NoDT	DAR	$MAPE_{min}$ (%)
≤ 75%	0A0R	92.703
	0A1R	49.600
	0A2R	73.653
	1A0R	21.690
	1A1R	20.605
	1A2R	41.997
	2A0R	37.562
	2A1R	30.925
	2A2R	54.397

NoDT = number of data transmitted
DAR = data abstraction and reformation
0A0R = zeroth-order data abstraction & zeroth-order data reformation
0A1R = zeroth-order data abstraction & first-order data reformation
0A2R = zeroth-order data abstraction & second-order data reformation
1A0R = first-order data abstraction & zeroth-order data reformation
1A1R = first-order data abstraction & first-order data reformation
1A2R = first-order data abstraction & second-order data reformation
2A0R = second-order data abstraction & zeroth-order data reformation
2A1R = second-order data abstraction & first-order data reformation
2A2R = second-order data abstraction & second-order data reformation
$MAPE_{min}$ = minimum mean absolute percentage error

From Table 5.63, it is shown that the best DAR schemes in running accelerometer data where $NoDT \leq 75\%$ in the terms of mean absolute percentage error is 1A1R.

9. Conclusion

From Table 5.56 – 5.63, it is concluded in Table 5.64, that the best DAR schemes in running accelerometer data is 2A1R.

Table 5.64: Results of DAR Schemes in Running Accelerometer Data

(a) Best DAR Schemes in Running Accelerometer Data where the $NoPT \leq 2250$ and $NoDT \leq 75\%$

DAR	Th	NoPT	NoDT(%)	RMSE	MAPE(%)
0A0R	1.413	2250	75.000	1.698	92.703
0A1R	1.413	2250	75.000	0.920	49.600
0A2R	1.413	2250	75.000	1.495	73.653
1A0R	2.738	1477	74.933	0.825	20.605
1A1R	2.738	1477	74.933	0.825	20.605
1A2R	2.738	1477	74.933	1.505	41.997
2A0R	5.646	1154	74.933	1.117	37.522
2A1R	5.642	1156	75.000	0.996	30.925
2A2R	5.642	1156	75.000	1.702	54.397

(b) Best DAR Schemes in Running Accelerometer Data where the $RMSE \leq 0.25$ and $MAPE \leq 2.5\%$

DAR	Th	NoPT	NoDT(%)	RMSE	MAPE(%)
0A0R	0.084	2995	99.833	0.068	1.631
0A1R	0.124	2992	99.733	0.060	2.278
0A2R	0.084	2995	99.833	0.025	0.809
1A0R	1.244	2438	95.500	0.184	2.497
1A1R	1.095	2546	96.933	0.135	2.491
1A2R	1.017	2605	97.533	0.204	2.485
2A0R	2.382	2228	98.100	0.182	2.476
2A1R	2.420	2206	97.733	0.129	2.487
2A2R	2.401	2217	97.967	0.140	2.426

DAR = data abstraction and reformation
Th = threshold
NoPT = number of packet transmissions
NoDT = number of packet transmitted
RMSE = root mean square error
MAPE = mean absolute percentage error

5.4 Discussions

5.4.1 Number of Data Transmitted and Number of Packet Transmissions

As mentioned earlier that the number of packet transmission and the number of data transmitted is not necessary identical. This happens because different orders of data abstraction will transmit different number of data in one packet. The relationships of number of data transmitted and number of packet transmissions are shown in Table 5.65.

Table 5.65: Relationships of Number of Data Transmitted and Number of Packet Transmissions

Order of Data Abstraction	Relationship
Zeroth	Number of data transmitted = number of packet transmissions
First	Number of data transmitted < 2 x number of packet transmissions
Second	Number of data transmitted < 3 x number of packet transmissions

5.4.2 $RMSE$ and $MAPE$

Again, $RMSE$ and $MAPE$ is the level of accuracy in data reformation. Logically, the number of data transmitted will affect the value of $RMSE$ and $MAPE$ (higher number of data transmitted will resulted in lower $RMSE$ and $MAPE$). However, this does not happen in incremental and decremental temperature data especially in 1A1R. This resulted in conclusions that:

1. In zeroth-order data abstraction, higher value of threshold (th_{value}) will always resulted in lower number of packet transmissions.
2. In first-order data abstraction, the number of packet transmissions will increase when th_{rate} is increasing if there is any $\Delta a_i = th_{rate}$and $\Delta a_i < th_{rate+1}$.
3. In second-order data abstraction, the number of packet transmissions will increase when th_{accel} is increasing if there is any $\Delta^2 a_i = th_{accel}$ and $\Delta^2 a_i < th_{accel+1}$.
4. Higher number of packet transmissions will not always resulted in lower $RMSE$ and $MAPE$.
5. Therefore, the lower value of th_{rate} and th_{accel} will not always resulted in lower $RMSE$ and .
6. In 1A1R, $RMSE$ always smaller than or equals to th_{rate}. In other words, $RMSE \leq th_{rate}$. Therefore in the implementation of 1A1R, the value of th_{rate} can be specifically set to the application requirement's accuracy of the reformed data in the term of $RMSE$.
7. When $RMSE$ increased, $MAPE$ will be increased as well and vice versa.

CHAPTER 6

CONCLUSIONS

6.1 Conclusions

In this dissertation, the author has studied several methods to reduce the energy consumption in WSN. This study focusing on collecting sensor data from sensor nodes to a base station with minimum energy consumption by reducing the number of transmission and the reliability in the reformation of the non-received values. In application/attribute with low sampling rate, the scheme is applied in temperature monitoring application and in application/attribute with abrupt sampling rate, the scheme is applied in movement monitoring application.

The author proposed Data Abstraction and Reformation (DAR) schemes. Generally, DAR schemes can be divided into two major portions, which are data abstraction and data reformation. Data abstraction is to filter sensed value at a sensor node based on some pre-determined criteria, select only the significant data and send them back to the base station; while data reformation is to reconstruct the received values at the base station based on the received data and certain set of principles. Less data transmission will result in less energy consumption in the communication, and thus extending the life of WSNs.

From the result, it shows that DAR schemes is able to minimize energy consumption and increase the reliability in the reformation of the non-received values.

Different orders of DAR schemes have been proposed. There are 9 (nine) combinations of the scheme. They are 0A0R, 0A1R, 0A2R, 1A0R, 1A1R, 1A2R, 2A0R, 2A1R, and 0A2R. From the overall performance, 1A1R can provide satisfactory results for low changing data rate with significant energy saving and data reformation's accuracy; and 2A1R can provide satisfactory results for abrupt changing data rate with significant energy saving and data reformation's accuracy.

In conclusion, through 1A1R scheme, application with low sampling rate can save up to 98% over single data transmissions with 100% of data accuracy; and through 2A1R scheme, application with abrupt sampling rate can save up to 27% over single data transmissions with 97.5% of data accuracy. Therefore, the saving of transmissions can directly be translated to the extension of the lifetime of a wireless sensor network.

6.2 Evaluations

From the objectives in section 1.4, which are:

1. To propose Data Abstraction scheme at sensor nodes that can efficiently filter significant data for transmission in order to minimize communications in the network. This objective has been achieved through zeroth-, first-, and second-order data abstraction and discussed in Chapter 5.
2. To propose Data Reformation scheme at the base station that can effectively reconstruct the full set of data without compromising the

quality of information. This objective has been achieved through zeroth-, first-, and second-order data reformation has been achieved and discussed in Chapter 5.

3. To evaluate the performance of different combinations of DAR. This objective has been achieved through 0A0R, 0A1R, 0A2R, 1A0R, 1A1R, 1A2R, 2A0R, 2A1R, and 2A2R; and discussed in Chapter 5.

6.3 Future Works

For the future work, as the current DAR schemes is based on the single hop (peer-to-peer) network architecture, it is recommended that for the future work:

1. The scheme must not be limited to single hop topology, multi-hop network architecture can be considered for future study.
2. Improving the accuracy in the reformation of the non-received values.

REFERENCES

Aderohunmu, F.A. et al., 2013. Trade-offs of forecasting algorithm for extending WSN lifetime in a real-world deployment. *2013 IEEE International Conference on Distributed Computing in Sensor Systems (DCOSS)*, 20 – 23 May 2013 Cambridge, Massachusetts, USA: IEEE, pp. 283-285.

Aderohunmu, F.A., Brunelli, D., Deng, J.D. and Purvis, M.K., 2015. A data acquisition protocol for a reactive wireless sensor network monitoring application. *Sensors*, 15(5), pp. 10221 - 10254.

Arima, M., Omoto, R., Higuchi, K. and Maenaka, K., 2012. Development of a human monitoring system. *World Automation Congress*, 24 – 28 June 2012 Puerto Vallarta, Mexico: IEEE, pp. 1 – 5.

Azevedo, J.A.R and Santos F.E.S., 2012. Energy harvesting from wind and water for autonomous wireless sensor nodes. *IET Circuits, Devices & Systems*, 6(6), pp. 413 – 420.

Bagree, R., Jain, V.R., Kumar, A. and Ranjan, P., 2010. TigerCENSE: wireless image sensor network to monitor tiger movement. In: Marron, P.J., Voigt, T., Corke, P. and Mottola, L. (eds.). *Real-world wireless sensor networks*. Berlin, Heidelberg: Springer, pp. 13 – 34.

Baine, N.A., Desai, P. and Rattan, K.S., 2011. INS aided by an acoustic wireless sensor network and magnetometer. *SPIE Proceedings 8061*, 25 April 2011, Orlando, Florida, USA: SPIE.

Berlin, E. and Laerhoven, K.V., 2010. An on-line piecewise linear approximation technique for wireless sensor networks. *IEEE 35th Conference on Local Computer Networks*, 10 – 14 October 2010 Denver, CO: IEEE, pp. 905 – 912.

Booranawong, A., Teerapabkajorndet, W. and Limsakul, C., 2013. Energy consumption and control response evaluations of AODV routing in WSANs for building-temperature control. *Sensors*, 13(7), pp. 8303 – 8330.

Chebbi, W., Benjeema, M., Kamoun, L., Jabloun, M. and Sahli, A., 2011. Development of a WSN integrated weather station node for an irrigation alert program under Tunisian conditions. *8th International Multi-Conference on Systems, Signals and Devices*, 22 – 25 March 2011, Sousse: IEEE, pp. 1 – 6.

Chien, T.V., Chan, H.N. and Huu, T.N., 2012. A comparative study on hardware platforms for wireless sensor networks. *International Journal on Advanced Science, Engineering and Information Technology*, 2(1), pp. 70 – 74.

Cosar, E.I., 2009. *A wireless toolkit for monitoring applications*. Master thesis, Helsinki University of Technology, Finland.

Crossbow Technology, Inc., n.d.. *MICA2*. [online] San Jose, California. Available at: <http://www.eol.ucar.edu/isf/facilities/isa/internal/CrossBow/DataSheets/mica2.pdf> [Accessed 27 February 2014].

Crossbow Technology, Inc., n.d.. *MICA2DOT*. [online] San Jose, California. Available at: <http://www.eol.ucar.edu/isf/facilities/isa/internal/CrossBow/DataSheets/mica2dot.pdf> [Accessed 27 February 2014].

Crossbow Technology, Inc., n.d.. *MICAz*. [online] San Jose, California. Available at: <http://www.openautomation.net/uploadsproductos/micaz_datasheet.pdf> [Accessed 27 February 2014].

Crossbow Technology, Inc., n.d.. *STARGATE*. [online] San Jose, California. Available at: <http://www.eol.ucar.edu/isf/facilities/isa/internal/CrossBow/DataSheets/stargate.pdf> [Accessed 27 February 2014].

Crossbow Technology, Inc., 2007. *Stargate NetBridge*. [online] San Jose, California. Available at: <http://www.xbow.jp/sluggo_easy_manual.pdf> [Accessed 27 February 2014].

Crossbow Technology, Inc., n.d.. *TELOSB*. [online] San Jose, California. Available at: <http://www.willow.co.uk/TelosB_Datasheet.pdf> [Accessed 27 February 2014].

Damaso, A., Freitas, D., Rosa, N., Silva, B. and Maciel, P., 2013. Evaluating the power consumption of wireless sensor network applications using models. *Sensors*, 13(3), pp. 3473 – 3500.

de Bree, H. and Wind, J.W., 2011. The acoustic vector sensor: a versatile battlefield acoustics sensor. *SPIE Proceedings 8047*, 23 May 2011, Orlando, Florida, USA: SPIE.

de la Piedra, A., Benitez-Capistros, F., Dominguez, F. and Touhafi, A., 2013. Wireless sensor networks for environmental research: a survey on limitation and challenges. *IEEE EUROCON*, 1 – 4 July 2013 Zagreb: IEEE, pp. 267 – 274.

Dulski, R. et al., 2011. Concept of data processing in multisensory system for perimeter protection. *SPIE Proceedings 8019*, 25 April 2011, Orlando, Florida, USA: SPIE.

Dynastream Innovations Inc, 2014, *ANT+* [Online]. Available at: http://www.thisisant.com/ [Accessed: 27 February 2014].

Faaroq, M.O. and Kunz, T., 2011. Operating systems for wireless sensor networks: a survey. *Sensors*, 11(6), pp. 5900 – 5930.

Goh, H.G., Liew, S.Y., Kwong, K.H., Michie, C. and Andonovic, I., 2012. Abstract reporting and reformation schemes for wireless sensor networks. In: Senac, P., Ott, M. and Seneviratne, A. (eds.). *Wireless Communications and Applications.* Berlin, Heidelberg: Springer, pp. 69 – 74.

Handziski, V., 2005, *The eyesIFX platform* [Online]. Available at: www.tinyos.net/ttx-02-2005/platforms/ttx2005-eyesIFX.ppt [Accessed: 27 February 2014].

Herlien, R. et al., 2010. An ocean observatory sensor network application. *IEEE Sensors*, 1 – 4 November 2010 Kona, HI: IEEE, pp. 1837 – 1842.

Hormann, L.B., Glatz, P.M., Steger, C. and Weiss, R., 2010. A wireless sensor node for river monitoring using MSP430® and energy harvesting. *Fourth European Education and Research Conference*, 1 – 2 December 2010 Nice: IEEE, pp. 140 – 144.

Huang, J. et al., 2010. Rapid prototyping for wildlife and ecological monitoring. *IEEE Systems Journal*, 4(2), pp. 198 – 209.

Jin, N., Ma, R., Lv, Y., Lou, X. and Wei, Q., 2010. A novel design of water environment monitoring system based on WSN. *International Conference on Computer Design and Applications*, 25 – 27 June 2010 Qunhuangdao: IEEE, pp. V2-593 – V2-597.

Kionix, 2010., *KXSD9 Series*. [online] Ithaca, NY. Available at <http://www.kionix.com/sites/default/files/KXSD9%20Product%20Brief.pdf> [Accessed 27 February 2014].

Lajara, R., Alberola, J. and Pelegri-Sebastia, J., 2011. A solar energy powered autonomous wireless actuator node for irrigation systems. *Sensors*, 11(1), pp. 329 – 340.

Lajara, R., Pelegri-Sebastia, J. and Solano, J.J.P., 2010. Power consumption analysis of operating systems for wireless sensor networks. *Sensors*, 10(6), pp. 5809 – 5826.

Lee, H., Banerjee, A., Fang, Y., Lee, B. and King C., 2010. Design of a multifunctional wireless sensor for in-situ monitoring of debris flows. *IEEE Transactions on Instrumentation and Measurement,* 59(11), pp. 2958 – 2967.

LORD Corporation, 2013., *V-Link® -LXRS®*. [online] Williston, VT. Available at <http://aesensors.nl/module/Products/downloadFile/V-Link_LXRS_datasheet.pdf?id=329> [Accessed 27 February 2014].

Lotf, J.J., Nazhad, S.H.H. and Alguliev, R.M., 2011. A survey of wireless sensor networks. *5th International Conference on Application of Information and Communication Technologies*, 12 – 14 October 2011 Baku: IEEE, pp. 1 – 6.

McGarry, S. and Knight, C., 2012. Development and successful application of a tree movement energy harvesting device, to power a wireless sensor node. *Sensors*, 12(9), pp. 12110 – 12125.

MEMSIC Inc., n.d.. *IRIS*. [online] San Jose, California. Available at: <http://www.memsic.com/userfiles/files/Datasheets/WSN/IRIS_Datasheet.pdf> [Accessed 27 February 2014].

Moteiv Corporation, 2006., *tmote sky*. [online] San Francisco, CA. Available at <http://www.eecs.harvard.edu/~konrad/projects/shimmer/references/tmote-sky-datasheet.pdf> [Accessed 27 February 2014].

Nachman, L., n.d., *Imote*[2] [Online]. Available at: www.tinyos.net/ttx-02-2005/platforms/ttx05-imote2.ppt [Accessed: 27 February 2014].

Nasirudin, M.A., Za'bah, U.N. and Sidek, O., 2011. Fresh water real-time monitoring system based on wireless sensor network and GSM. *IEEE Conference on Open Systems*, 25 – 28 September 2011 Langkawi: IEEE, pp. 354 – 357.

National Instruments Corporation, 2010., *NI WSN-3202*. [online] North Mopac Expressway, Austin, Texas. Available at <http://www.ni.com/pdf/manuals/372775e.pdf> [Accessed 27 February 2014].

Naz, P., Hengy, S. and Hamery, P., 2012. Soldier detection using unattended acoustic and seismic sensors. *SPIE Proceedings 8389*, 23 April 2012, Baltimore, Maryland, USA: SPIE.

O'Connor, E., Smeaton, A.F. and O'Connor N.E., 2011. A multi-modal event detection system for river and coastal marine monitoring applications. *IEEE – Spain OCEANS*, 6 – 9 June 2011 Santander: IEEE, pp. 1 – 10.

Patil, M. and Biradar, R.C., 2012. A survey on routing protocols in wireless sensor networks. *18th IEEE International Conference in Networks*, 12 – 14 December 2012 Singapore: IEEE, pp. 86 – 91.

Perez, C.A. et al., 2011. A system for monitoring marine environments based on wireless sensor networks. *IEEE – Spain OCEANS*, 6 – 9 June 2011 Santander: IEEE, pp. 1 – 6.

Potdar, V., Sharif, A. and Chang, E., 2009. Wireless sensor networks: a survey. *International Conference on Advanced Information Networking and Applications Workshops,* 26 – 29 May 2009 Bradford: IEEE, pp. 636 – 641.

Raza, U., Camerra, A., Murphy, A. L., Palpanas, T. and Picco, G.P., 2012. What does model-driven data acquisition really achieve in wireless sensor networks? *2012 IEEE International Conference on Pervasive Computin and Communications (PerCom)*, 19 – 23 May 2012 Lugano, Switzerland: IEEE.

Renterghem, T.V. et al., 2010. Towards an extensive noise and air quality measurement network. *Inter-Noise 2010*, 15 – 16 June 2010 Lisbon, Portugal: I-INCE, pp. 1 – 6.

Reyes, C., Hilaire, T., Paul, S. and Mecklenbrauker, C.F., 2010. Evaluation of the root mean square error performance of the PAST-Consensus algorithm. *International ITG Workshop on Smart Antennas*, 23 – 24 February 2010 Bremen: IEEE, pp. 156 – 160.

Saleh, A.M.S., Ali, B.M., Rasid, M.F.A. and Ismail, A., 2012. A self-optimizing scheme for energy balanced routing in wireless sensor networks using SensorAnt. *Sensors*, 12(8), pp. 11307 – 11333.

Sanchez-Azofeifa, G.A., Rankine, C., Santo, M.E., Fatland, R. and Garcia, M., 2011. Wireless sensing networks for environmental monitoring: two case studies from tropical forests. *IEEE 7th International Conference on E-Science*, 5 – 8 December 2011 Stockholm: IEEE, pp. 70 -76.

Sang, G. and Song, L., 2010. The design and implementation of a farmland monitoring wireless sensor network. *Second Pacific-Asia Conference on Circuits, Communications and System,* 1 – 2 August 2010 Beijing: IEEE, pp. 355 – 358.

Sensicast Systems, Inc., 2006., *Temperature & Humidity Smart Sensor TEHU-1121*. [online] Needham, MA. Available at <http://adaptive-wireless.co.uk/wp-content/uploads/2008/09/tehu-1121.pdf> [Accessed 27 February 2014].

Sieber, A., Karnapke, R., Nolte, J. and Martschei, T., 2011. Using sensor technology to protect an endangered species: a case study. *IEEE 36th Conference on Local Computer Networks*, 4 – 7 October 2011 Bonn: IEEE, pp. 1044 – 1047.

Stellwagen, E., 2016., *Forecasting 101: A Guide to Forecast Error Measuremen Statistics and How to Use Them*. [online] Available at <http://www.forecastpro.com/Trends/forecating101August2011.html> [Accessed 1 November 2016].

Tufail, A., Qamar, A., Khan, A.M., Baig, W.A. and Kim, K., 2013. WEAMR – a weighted energy aware multipath reliable routing mechanism for hotline-based WSNs. *Sensors*, 13(5), pp. 6295 – 6318.

Vijayakumar, S. and Rosario, J.N., 2011. Preliminary design for crop monitoring involving water and fertilizer conservation using wireless sensor networks. *IEEE 3rd International Conference on Communication Software and Networks*, 27 – 29 May 2011 Xi'an: IEEE, pp. 662 – 666.

Wang, Y., Zhang, J. and Xu, H., 2012. The design of data collection methods in wireless sensor networks based on formal concept analysis. In: Jin, D. and Lin, S. (eds.) *Advances in computer science and information engineering*, Berlin, Heidelberg: Springer, pp. 33 – 38.

Wei, Z., Yong, H., Fei, L., Congcong, M. and Yuewei, C., 2011. The fuzzy decision-making method of irrigation amount based on ET and soil water potential. *International Conference on Electronics, Communications and Control*, 9 – 11 September 2011 Ningbo: IEEE, pp. 2927 – 2931.

Xiao-peng, H. and Xiao-liang, H., 2011. Hardware design of river flow velocity monitoring system. *Third International Conference on Measuring Technology and Mechatronics Automation*, 6 – 7 January 2011 Shangshai: IEEE, pp. 304 – 307.

Xue, Y., Ramamurthy, B. and Burbach, M., 2010. A two-tier wireless sensor network infrastructure for large-scale real-time groundwater monitoring. *IEEE 35th Conference on Local Computer Networks*, 10 – 14 October 2010 Denver, CO: IEEE, pp. 874 – 881.

Yang, J., Zhang, D. and Zhang, Y., 2009. An energy-efficient data gathering protocol for wireless sensor networks. *Eighth IEEE/ACIS International Conference on Computer and Information Science*, 1 – 3 June 2009 Shanghai: IEEE, pp. 780 – 785.

Zhuang, W., Costa, M., Cheong, P. and Tam, K., 2011. Flood monitoring of distribution substation in low-lying areas using wireless sensor network. *International Conference on System Science and Engineering*, 8 – 10 June 2011

Macao: IEEE, pp. 601 – 604.

APPENDIX A

LIST OF PUBLICATIONS

1. **Toni**, Goh, H.G. and Liew, S.Y., 2013. Energy Saving Data Abstraction and Reformation Algorithms for Human Movement Monitoring. *The 1st International Workshop on Internet of Things Technologies (IoTT 2013)*, 15 – 18 December 2013 Seoul, South Korea.
2. Goh, H.G., **Toni**, Kwong, K.H., Teoh, S.K., Gan, M.L., Yau, K.L. and Liew, S.Y., 2013. Design of Precision Farming for Smart Villages using Wireless Sensor and Wi-Fi Mesh Networks. *The 2013 International Seminar on Communication, Electronics and Information Technology (ISCEIT 2013)*, 7 – 10 May 2013 Suranaree University of Technology NakhonRatchasima, Thailand. [Abstract].
3. **Toni**, Goh, H.G. and Liew, S.Y., 2012. Performance Study of Zeroth-, First- and Second-order Data Abstraction and Reformation Algorithms for Wireless Sensor Networks, *The IET International Conference on Wireless Communications and Applications (ICWCA 2012)*, 8 – 10 October 2013 Kuala Lumpur, Malaysia.
4. Goh, H.G., **Toni**, Lee, H.Y., Leong, C.F., Kuek, C.S., Liew, S.Y. and Kwong, K.H., 2012. Practical Implementation of Self-powered Wireless Sensor Networks for Paddy Field Monitoring, *The IET International Conference on Wireless Communications and Applications (ICWCA 2012)*, 8 – 10 October 2013 Kuala Lumpur, Malaysia.